

Scuola di Dottorato in Fisica, Astrofisica e Fisica Applicata

Dipartimento di Fisica, Via Celoria 16, 20133, Milano

Corso di Dottorato in Fisica, Astrofisica e Fisica Applicata

Ciclo XXX

# Resummations of Transverse Momentum Distributions

Settore Scientifico Disciplinare FIS/02

Supervisor: Professor Stefano Forte

Tesi di Dottorato di:

Claudio Muselli

Anno Accademico 2016/2017

**Commission of the final examination:**

External Referees:

Pier Francesco Monni, Giovanni Ridolfi

External Members:

Fabrizio Caola, Giulia Zanderighi

Internal Members:

Giancarlo Ferrera, Stefano Forte

**Final examination:**

Date 1/12/2017

Università degli Studi di Milano, Dipartimento di Fisica, Milano, Italy

**Cover illustration:**

The Higgs Boson - A Tales from the Road Comic

*To Giuliapaola*



## Abstract

This thesis arises in the context of precise phenomenology at the Large Hadron Collider, LHC. In the searching for New Physics, an accurate theoretical prediction of many Standard Model processes is crucial to be able to distinguish the desired discrepancy from the known background. After the failure of LHC Run I in the detection of any trace of new physics, experimental search is moving from inclusive cross sections to more exclusive shapes and distributions. In this context, primary importance is covered by transverse momentum distributions. The objective of this thesis is to provide a general study about possible resummation theories which can be applied on transverse momentum distributions. In particular, the known transverse momentum resummation and threshold resummation formalism are reviewed and improved, being able to unify all this information in a unique combined expression. Moreover in the context of high energy resummation, several new ingredients are introduced in this thesis:  $LLx$  resummation is performed for the double differential distribution, and first steps in the extension of this formalism to jets are discussed. As phenomenological applications, a combined resummed result is shown for the Higgs boson transverse momentum distribution; furthermore the impact of quark mass corrections on this spectrum at LHC 13 TeV is analysed, using an high energy expansion.



# Contents

<b>Introduction</b>	<b>1</b>
<b>1 Quantum Chromo-dynamics</b>	<b>9</b>
1.1 The Lagrangian of QCD	10
1.2 The Parton Model and Collinear Factorization	15
1.3 Application: NLO Higgs Boson Production	27
1.4 Resummations in a nutshell: ideas and notations	37
<b>2 Collinear and Threshold Resummation</b>	<b>45</b>
2.1 Which regions do we actually resum?	46
2.2 Factorization in the soft and collinear limit	47
2.3 Threshold Resummation at fixed $p_T$	59
2.4 Transverse Momentum Resummation	61
2.5 Consistent Transverse Momentum Resummation	66
2.6 Combined Resummation for Transverse distributions	78
2.7 Application: EFT Higgs boson at Threshold.	79
<b>3 High Energy Resummation</b>	<b>93</b>
3.1 $k_T$ -factorization	94
3.2 Transverse Momentum Distribution at High Energy	109
3.3 Double differential distribution at high energy.	116
3.4 Application: EFT Higgs boson at high energy	121
<b>4 Phenomenology</b>	<b>131</b>
4.1 Combined Resummation for Higgs at LHC13	132
4.2 Higgs Quark Mass Effects at High Energy	141
<b>Conclusions and Outlooks</b>	<b>157</b>

---

<b>A PDF DGLAP Evolution</b>	<b>159</b>
A.1 Running Coupling evolution	159
A.2 DGLAP Equations	162
A.3 General Solution	165
<b>B Integral Transforms and Special Functions</b>	<b>169</b>
B.1 Fourier and Hankel Transform	169
B.2 Laplace and Mellin Transform	171
B.3 Plus distribution	173
B.4 Special Functions	177
B.5 Mellin Transform of Harmonic Polylogarithms (HPL)	183
<b>C Analytical Expressions</b>	<b>205</b>
C.1 Collinear and Threshold Region	205
C.2 High Energy Region	213
<b>Acknowledgments</b>	<b>225</b>
<b>Bibliography</b>	<b>229</b>

# Introduction

The LHC is probably one of the wonders of the modern world. Its performance has far outstripped every expectations. It is now collecting data with a rate higher even than its designed value. Moreover the experimental community is succeeding in making the systematic error lower and lower every year, with genial solutions and a better electronics. Therefore, increasing the statistics, the overall experimental error at LHC is approaching in many measurements the incredible relative precision of percent, which is remarkably low taking into account the complexity of the whole experiment. The delivered luminosity of LHC during all the working years is shown in Fig. 1

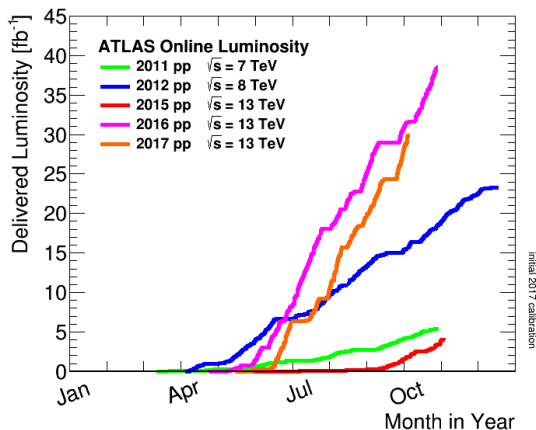


**Figure 1.** Delivered luminosity in the different working years of LHC as a function of months.

If on one hand this is an important result making LHC the most powerful machine ever built, on the other hand this is a continue challenge for theory. Indeed, to produce 5% accurate predictions, the phenomenology community is forced to improve their general understanding about strong and weak interactions which are taking place in the Large Hadron Collider.

The theory which explains collisions at LHC is the Standard Model. This theory was formalized in 60s-70s [1,2] and it permits to describe three of the four fundamental forces, the strong interaction, the weak interaction and the electromagnetic interaction. It is

based on the non-abelian gauge symmetry

$$SU(3)_c \times SU(2)_L \times U(1)_Y$$

and, after a spontaneous symmetry breaking procedure, it permits to describe three fundamental forces: the strong or colour interaction, the weak interaction and the electromagnetic interaction.

The particles which form the standard model are divided into two groups, quarks and leptons, depending on their behaviour under the colour force. The six quarks are subject to the strong interaction, while the six leptons are not. Different types of quarks are distinguished according to their *flavours* and they are respectively *up*, *down*, *charm*, *strange*, *top*, *bottom*: three (*up*, *charm*, *top*) own  $+2/3e$  as electric charge while the others (*down*, *strange*, *bottom*)  $-1/3e$ . Even leptons can be subdivided into two groups: the charged leptons (*electron*, *muon*, and *tau*) characterized by a negative electric charge  $-e$ ; and the neutrinos, which in SM are massless and neutral.

In addition to all these fermion particles which describe the matter, Standard Model predicts four types of additional vector bosons which mediate various forces: the *gluons* for strong interaction, *W* and *Z* bosons for weak interactions, and the *photon* for the electromagnetic force. However, the particle which is central of all the Standard Model, is the Higgs boson *H*, which is responsible for the spontaneous symmetry breaking of the theory and which permits to the boson *W* and *Z* and to all the fermions to acquire a mass throughout their interaction with the Higgs field.

All the particles of Standard Model just presented are contained in Fig. 2; we refer the interested reader to general quantum field theory book [5] for a more detailed description about SM and its dynamic. In this thesis we mainly concentrate on the theory of strong interaction, the Quantum-Chromo Dynamics (QCD), since it constitutes the main contribution to any LHC experiments.

During its activity LHC has widely tested all the predictions of Standard Model: in fact its first discovery was the confirmation of Higgs' existence in 2012. In Fig. 3 we report the most recent measurement which reinforce the experimental evidence of Higgs boson. It shows the di-photon invariant mass spectrum, which is one of the cleanest Higgs decay channels. You can see the Higgs resonance around 125 GeV. The Standard Model always passes all the ever more stringent tests of the LHC; the overall agreement of Figs. 4 between SM predictions and experimental measurements is incredible.

So, where is the problem? The problem is that we have evidences in other fields of physics such as neutrino physics, astrophysics or cosmology that Standard Model can not be the end of the story. It has to be an approximation, a part of a more general theory, the up to now unknown *Theory of Everything*. Therefore we are searching at the LHC for small deviations from Standard Model predictions which could be an hint of this more general theory, an hint of *New Physics*.

However, as you can appreciate from Figs. 4, up to now the search is proving unsuccessful: no deviations have been confirmed in all the measurements. New Physics is hard to see. Hence, the collider community is increasing the spectrum of measurements in order to be able to catch even the most weak signal. From measurement of inclusive rate of productions, the so-called *total cross sections*, we are moving to the measurement of exclusive shapes and distributions, which of course contains more data and more informa-

## Standard Model of Elementary Particles

		three generations of matter (fermions)						
		I	II	III				
mass		$\approx 2.4 \text{ MeV}/c^2$	$\approx 1.275 \text{ GeV}/c^2$	$\approx 172.44 \text{ GeV}/c^2$	0	$\approx 125.09 \text{ GeV}/c^2$		
charge		$2/3$	$2/3$	$2/3$	0	0		
spin		$1/2$	$1/2$	$1/2$	1	0		
		<b>u</b> up	<b>c</b> charm	<b>t</b> top	<b>g</b> gluon	<b>H</b> Higgs		
	<b>QUARKS</b>	$\approx 4.8 \text{ MeV}/c^2$	$\approx 95 \text{ MeV}/c^2$	$\approx 4.18 \text{ GeV}/c^2$	0			
		$-1/3$	$-1/3$	$-1/3$	0			
		$1/2$	$1/2$	$1/2$	1			
		<b>d</b> down	<b>s</b> strange	<b>b</b> bottom	<b><math>\gamma</math></b> photon			
	<b>LEPTONS</b>	$\approx 0.511 \text{ MeV}/c^2$	$\approx 105.67 \text{ MeV}/c^2$	$\approx 1.7768 \text{ GeV}/c^2$	$\approx 91.19 \text{ GeV}/c^2$			
		-1	-1	-1	0			
		$1/2$	$1/2$	$1/2$	1			
		<b>e</b> electron	<b><math>\mu</math></b> muon	<b><math>\tau</math></b> tau	<b>Z</b> Z boson			
		$< 2.2 \text{ eV}/c^2$	$< 1.7 \text{ MeV}/c^2$	$< 15.5 \text{ MeV}/c^2$	$\approx 80.39 \text{ GeV}/c^2$			
		0	0	0	$\pm 1$			
		$1/2$	$1/2$	$1/2$	1			
		<b><math>\nu_e</math></b> electron neutrino	<b><math>\nu_\mu</math></b> muon neutrino	<b><math>\nu_\tau</math></b> tau neutrino	<b>W</b> W boson			
							<b>SCALAR BOSONS</b>	
								<b>GAUGE BOSONS</b>

Figure 2. Table of particles predicted by Standard Model.

tion, but are more difficult to analyse. Some physicists have called this step as *exclusive revolution*.

The exclusive revolution is a challenge both for the experimental community, which has to face difficulties as detector acceptance, detector efficiency, coverage in angle and so on, and for the theoretical community, since the exclusive requirement brings a lot of problems in dealing with strong interactions. Any calculation in QCD requires a suitable definition of the observable to be finite. A more extensive discussion about this point is contained in Chap. 1.

Exclusive predictions in QCD, the field theory which studies strong interactions, are extremely cumbersome. Colour interaction is tackled in all the collider experiments using perturbative expansion: the complete result is expanded in power of the coupling constant  $\alpha_s$  and the series is then truncated at an higher enough order.

However, perturbative expansion is not the end of the story. Most of the exclusive observables which are interesting from the phenomenological side would depend on several scales of energies. When the process is multi-scale, our perturbative expansion would contain logarithms of the ratios between these scales. In the kinematic conditions where these ratios become large, the perturbative expansion is ruined and only the whole series is meaningful. In these regions of phase space, we need a theory able to sum at all orders

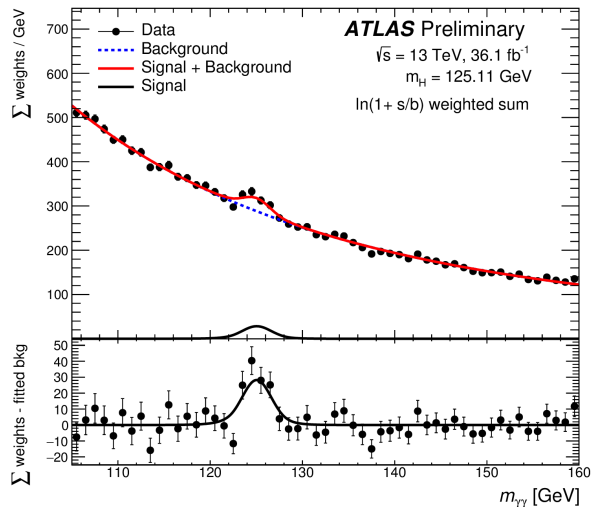


**Figure 3.**  $H \rightarrow \gamma\gamma$  mass invariant distribution with data of LHC Run II at 13 TeV. The Higgs peak is appearing from the background.

these logarithmic contributions. This theory is called resummation.

In conclusion, a complete analysis of an exclusive observable in general deserves both of the fixed order computation and of the resummation to properly describe experimental data. This thesis is inserted in this work stream, and it wants to study resummation properties for a very important exclusive distribution, the transverse momentum distribution.

Before proceeding, we want to highlight the fact that resummation could be used also to help fixed order evaluation. Indeed, due to technical and computational limitations, only the evaluation of the first two or three terms of the perturbative expansion is up to now available for most of the observables and processes. However, especially for exclusive distributions, the experimental precision is now approaching theoretical precision. Hence to further improve predictions for exclusive observables, several roads have to be explored. One of these is to exploit a by-product of resummation theory. Indeed the expansion of the resummed series could be used to provide approximations or checks about the unknown higher orders in perturbative expansion, when fixed order evaluation is not available for computational limitations. We are going to see in this thesis also an example of this particular application.

This thesis is mainly concentrated on the study of the transverse momentum distribution. The transverse momentum spectrum is the distribution of the modulus of the transverse components of the studied system's three-momentum. The transverse plane is defined with respect to the beam direction. It is a very important observable in collider analysis since very often a transverse momentum lower cut can discriminate the interesting signal from the noise and the background of the LHC experiment.

As we have already introduced, resummation is a branch of quantum field theory which studies the possibility to re-sum the whole perturbative series in some particular kinematic regions. By limiting ourselves to some particular kinematic regime, leading

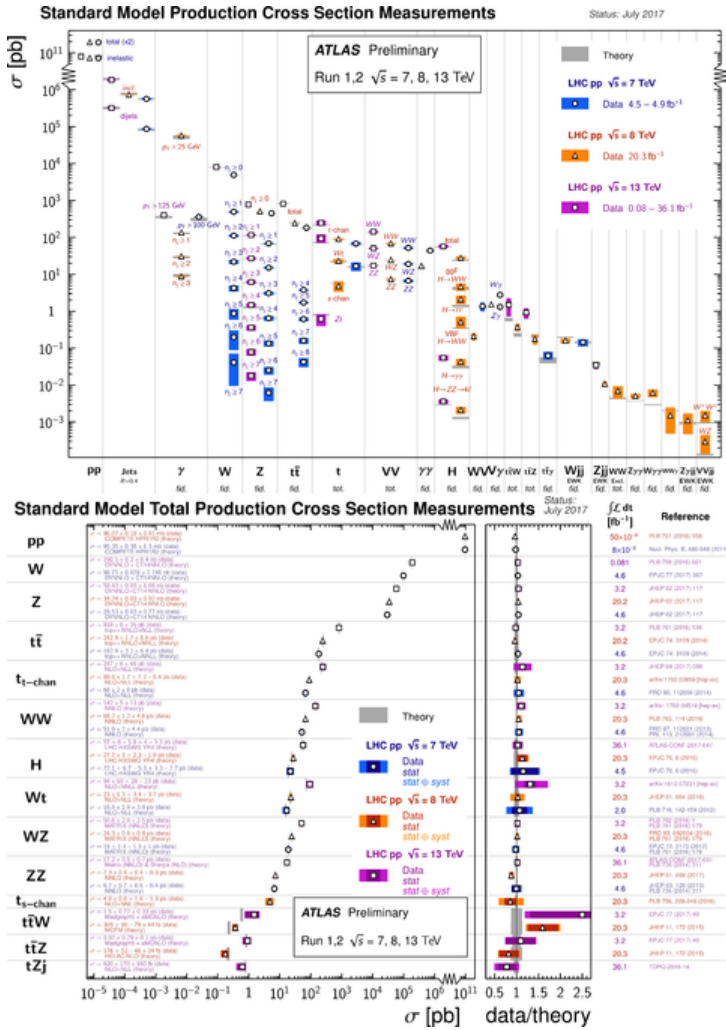


**Figure 4.** ATLAS summary of several Standard Model total production cross section measurements compared to the corresponding theoretical expectations

components can be predicted and summed at all orders in  $\alpha_s$ .

It is a completely different perspective with respect to fixed order evaluation and we want to give you an example. Consider the production of a colour-singlet particle in the final state (Higgs boson or  $W$ ,  $Z$  bosons) whose total cross section is going to depend on a particular kinematic variable called  $z = \frac{Q^2}{s}$  where  $Q^2$  for simplicity is the mass squared of the boson and  $\sqrt{s}$  is the energy in the centre-of-mass frame. For this observable, it will be shown later that leading behaviour in the limit  $z \rightarrow 1$  is of logarithmic type like

$$\frac{\ln^k(1-z)}{1-z}.$$

	LL	NLL	...	Regular
LO	$C_{\text{LO,LL}} \alpha_s \frac{\ln(1-z)}{1-z}$	$C_{\text{LO,NLL}} \alpha_s \frac{1}{1-z}$	0	$\alpha_s R_{\text{LO}}(z)$
NLO	$C_{\text{NLO,LL}} \alpha_s^2 \frac{\ln^3(1-z)}{1-z}$	$C_{\text{NLO,NLL}}^{(3,2)} \alpha_s^2 \frac{\ln^{2,1}(1-z)}{1-z}$	...	$\alpha_s^2 R_{\text{NLO}}(z)$
...	...	...	...	...

**Table 1.** Division of different perturbative coefficients into various terms according to their behaviour in the limit  $z \rightarrow 1$ . In the typical log counting of this resummation the LL log power is  $2n$  at order  $\alpha_s^n$ , the NLL log powers are the ones from  $2n - 1$  till  $n - 1$  and so on. The regular part contain any term which does not diverge in the considered limit.

Then different coefficients of the perturbative series can be organized as in Tab. 1.

As you can appreciate, fixed order evaluation computes the rows of Tab. 1: first row is the so-called Leading Order (LO) prediction, second row the Next-to-Leading Order (NLO) contribution and so on. Instead resummation technique focus its attention on the columns of this table: the so-called Leading Log (LL) prediction takes into account at all the orders in  $\alpha_s$  the most singular contribution in the  $z \rightarrow 1$  limit, the Next-to-Leading Log (NLL) the second column and so on.

If  $z$  is far from one all the coefficients in Tab. 1 can be considered of the same order of magnitude; in this case perturbative approach is perfectly legal and the knowledge of only the first rows of the table will properly approximate the whole result. On the contrary if  $z$  approaches one,

$$(\alpha_s \ln(1-z))^k \sim 1 \quad (0.0.1)$$

leading to a new hierarchy among the terms of Tab. 1. The expansion now has to be performed with respect to the columns, hence in power of  $\alpha_s$  but at fixed  $\alpha_s \ln(1-z)$ . The evaluation of the first term in this new expansion is call LL resummation, the computation of the first and second terms is call NLL resummation and so on.

The double logarithmic behaviour of Tab. 1 is typical of some resummation theories (such as threshold resummation of this example) and it is due to the fact that this logarithmic expansion is usually performed after an exponentiation procedure at the exponent. The observable is then written as

$$\sigma \sim \exp \left[ \frac{1}{\alpha_s} f_1(\alpha_s \ln \lambda) + f_2(\alpha_s \ln \lambda) + \alpha_s f_3(\alpha_s \ln \lambda) + \dots \right] \quad (0.0.2)$$

where  $\lambda$  is the general logarithmic ratio we are resumming and  $f_1$  resums leading logarithmic contribution,  $f_2$  the NLL,  $f_3$  the NNLL and so on. We will come back on this concept in the main text. While individual rows of Tab. 1 are singular when  $z \rightarrow 1$  the resummed result is not, since it takes into account all singular components at any order in  $\alpha_s$ . This is the power of resummation and this is the reason why it is so important in these particular kinematic limits.

From the example just presented you can also appreciate a second possible application of a resummed computation. If enough columns of Tab. 1 are known, it becomes possible to approximate the first unknown row simply by performing an  $\alpha_s$  expansion of the resummed computation. However, resummation has not to be considered as an alternative

to fixed order evaluation but as a support to it, since resummation is able to provide checks and hints about nature and size of higher order corrections.

This thesis mainly concentrates on the study of possible resummations for the transverse momentum distribution in the context of QCD. Therefore, we decide to limit ourselves to one important collider observable and to study the main resummations for this case. We improve in this thesis current knowledge about all these resummation theories, both in the collinear-soft limit and in the high energy limit.

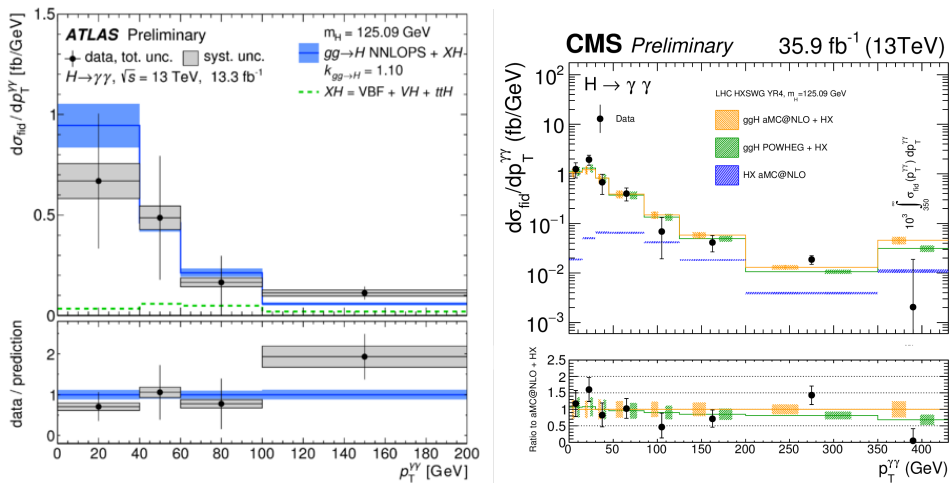


**Figure 5.** ATLAS (2016) and CMS (2017) latest measurements of the Higgs transverse momentum distribution at LHC Run II 13 TeV.

Furthermore, even if all the theoretical discussion is left quite general with respect to the particular process we are interested in, all the examples and applications which are included in this thesis will mainly concentrate on the study of the Higgs boson transverse momentum distribution. The Higgs boson was discovered in 2012, during LHC Run I [3, 4]. However, experimental program of the current LHC Run II is mainly devoted to the study of the properties of the Higgs boson (spin, mass, couplings...). In order to extract this information from data, we need to focus our attention on Higgs distributions. The Higgs boson transverse momentum distribution plays a key role in this derivation, and it is at the centre of many recent research activities. The most recent measurement of ATLAS and CMS at LHC 13 TeV are depicted in Fig. 5.

Summarizing, we have chosen Higgs boson production as application of our studies since it is one of the main research topics at current LHC Run II program.

The thesis will be organized as follow: first, in Chap. 1, a general introduction to the theory of strong interactions, the Quantum Chromo-Dynamics (QCD), is presented, together with a general overview about resummation theories and about notations we are going to use in the rest of the text; then Chap. 2 and Chap. 3 constitute the main body of this work and they are devoted to the two interesting limits where resummation theories can be develop. In particular resummations for transverse momentum distributions in the soft and collinear limit will be the main subject of Chap. 2, while Chap. 3 will concentrate

on the high energy limit. These chapters contain all the theoretical improvement with respect to the current state of the art which we derived. Finally, in Chap. 4 we will show you some phenomenological applications of our studies, mainly concentrated on the case of Higgs boson production. Conclusions and outlooks close then the main text.

We add at the end several appendices where further results are shown and where all the explicit expressions for our formulas and coefficients are listed. In this way, the reader could in principle reproduce all the results which are contained in this thesis.

Before starting our discussion about resummations of transverse momentum distributions, we want to close this introduction with a remark. This thesis is constructed to be self-consistent and to be understood by a master graduated student. However, if you are not familiar with quantum field theory of strong interactions, please read carefully next chapter, since it will constitute the basis for all the subsequent analysis. Normal textbooks, such as Ref. [5,6], can also help you cover the topics which, for lack of space, are left aside in this thesis.

# 1

# Quantum Chromo-dynamics

## Contents

---

<b>1.1</b>	<b>The Lagrangian of QCD</b> . . . . .	<b>10</b>
1.1.1	Asymptotic Freedom and Confinement	13
<b>1.2</b>	<b>The Parton Model and Collinear Factorization</b> . . . . .	<b>15</b>
1.2.1	Collinear Factorization Theorem	16
1.2.2	Generalized Ladder Expansion	21
1.2.3	PDF Evolution: DGLAP Equations	26
<b>1.3</b>	<b>Application: NLO Higgs Boson Production</b> . . . . .	<b>27</b>
1.3.1	Leading order	28
1.3.2	Virtual Contribution	30
1.3.3	Real Contribution	32
1.3.4	NLO transverse momentum distribution and total cross section	34
<b>1.4</b>	<b>Resummations in a nutshell: ideas and notations</b> . . . . .	<b>37</b>
1.4.1	Collinear Factorization in Conjugate Space	40

---

In this first chapter we are going to review some basics of QCD, the Quantum Chromo-dynamics, i.e. the theory describing strong interactions. We start in Sec. 1.1 by summarizing the Lagrangian and the Feynman Rules which control this theory, then we move in Sec. 1.2 to the description of the so-called parton model and collinear factorization both for inclusive cross sections and for differential distributions. The Collinear Factorization Theorem is fundamental to properly understand any perturbative calculation in QCD at high energy; hence, we enunciate this theorem in Sec. 1.2.1, then we provide a general proof in Sec. 1.2.2 and finally in Sec. 1.2.3 we focus our attention on the effects of this factorization in perturbation theory and in the computation of radiative corrections in QCD.

In order to make less theoretical all the discussion, we continue this chapter in Sec. 1.3 by presenting an explicit evaluation of the first QCD radiative correction for a simple process: pointlike Higgs boson production in gluon fusion at NLO. In this simple process the Higgs is directly coupled to the initial state gluons throughout an effective interaction (see Sec. 1.3). That will be the opportunity to see all the framework described in previous

sections at work, and to extensively explain all the technicalities which are behind any calculation in perturbative QCD.

After this explicit application, we decide to insert a last section 1.4 in order to introduce general ideas about the main topic of this thesis: resummations. Moreover this section will be also the right place to specify notations and definitions we are going to extensively use in the next chapters. The aim of this section is also to close this general introduction about QCD and to open the main topic of this thesis, resummation in perturbation theory.

It is important to understand this chapter would not to be a complete treatment of the QCD theory, but only a brief summary of the hypothesis and the important results which are going to be useful in the following chapters. The reader interested in a more exhaustive description should refer to general textbooks such as [5, 6].

## 1.1 The Lagrangian of QCD

The Quantum Chromo-dynamics is a non-abelian gauge theory constructed on the colour gauge group,  $SU(3)_c$ . However, as usually performed in literature, we are going to present a more general theory based on a  $SU(N_c)_c$  symmetry. The fields of QCD are  $N_f$  spin- $\frac{1}{2}$  fields in fundamental representation  $\psi_i(x)$ , called quarks, and a spin-1 gauge field, called gluon.

The required local gauge invariance with respect to  $SU(N_c)_c$  implies the invariance of the Lagrangian under the following infinitesimal fields transformations:

$$\hat{\psi}_i(x) = (1 - i\omega^a(x)t^a)\hat{\psi}_i(x) \quad (1.1.1a)$$

$$A_a^\mu = (\delta_a^c + f_{ab}^c\omega^b(x))A_c^\mu + \partial^\mu\omega^a(x) \quad (1.1.1b)$$

where we define  $t^a$  as a set of  $N_c^2 - 1$  matrices forming a basis of the algebra of  $SU(N_c)_c$ ,  $i = 1, \dots, N_f$  as the index running on the number of active flavours and the structure constants  $f_{abc}$  as

$$[t_a, t_b] = if_{abc}t^c. \quad (1.1.2)$$

It is important to note that the gluon field transforms under the local transformations of the group itself through an inhomogeneous transformation. This situation is quite often in standard gauge theories and it is completely equal to the abelian case of QED (Quantum Electro-Dynamics).

We are now ready to write the complete Lagrangian of QCD:

$$\mathcal{L}_{\text{QCD}} = -\frac{1}{2}\text{Tr}(G_{\mu\nu}G^{\mu\nu}) + \sum_{j=1}^{N_f} \bar{\psi}_j(i\gamma^\mu D_\mu - m_j)\psi_j \quad (1.1.3)$$

with the trace performed on the gauge group  $SU(N_c)_c$ , the gluon field tensor  $G_{\mu\nu}$  defined as

$$G_{\mu\nu} = \sum_a t^a G_{\mu\nu}^a = \partial_\mu A_\nu^a - \partial_\nu A_\mu^a + g_s f_{abc} A_\mu^b A_\nu^c \quad (1.1.4)$$

and the covariant derivative given by

$$D_\mu = \partial_\mu - ig_S t_a A_\mu^a. \quad (1.1.5)$$

In previous equations, we denote with  $g_S$  the strong coupling constant and, as usual, sum is implicit over repeated indexes. The gluon tensor  $G_{\mu\nu}$  transforms under the gauge group according to its adjoint representation.

We conclude this section by summarizing the Feynman Rules of QCD, which will turn out to be useful to evaluate amplitudes and cross sections in the perturbative limit of the theory.

The derivation from *Lagrangian* (1.1.3) of the desired Feynman Rules is possible only once we have decided a particular gauge choice. The gauge-fixing condition is imposed at the level of the Lagrangian by adding to Eq. (1.1.3) a *gauge-fixing* term. Then, in a particular gauge, the gluon propagator can be extracted using Faddeev-Popov procedure [5], in analogy with QED. However, in the case of a non-abelian gauge theory, this process leads to the introduction of a new fictitious type of particle, with general characteristics linked to the particular gauge choice. These new *gauge-dependent* pseudo-particles take the name of *ghosts* of the theory and they are involved in the calculation of radiative corrections.

Their existence is necessary in order to impose the unitarity of the scattering matrix and to verify the optic theorem. Their nature turns out to be strictly connected with the invariance of the Lagrangian Eq. (1.1.3) with respect to the BRST transformation. We refer the reader to Ref. [5] for a general treatment about this symmetry and its relation with *ghosts*.

By choosing a particular gauge fixing condition, the final QCD *Lagrangian* becomes:

$$\mathcal{L} = \mathcal{L}_{\text{QCD}} + \mathcal{L}_{\text{gauge-fixing}} + \mathcal{L}_{\text{ghost}}. \quad (1.1.6)$$

There are many possible choice for the gauge fixing and ghost components. We are going to limit ourselves to the two classes of gauge fixing condition most present in literature.

The first one is the so-called *covariant* class defined as

$$\mathcal{L}_{\text{gauge-fixing}} = -\frac{1}{2\lambda} (t_a \partial^\mu A_\mu^a)^2, \quad \mathcal{L}_{\text{ghost}} = \bar{\eta}^a (-\partial^2 \delta^{ac} - g_S \partial^\mu f^{abc} A_\mu^b) \eta^c, \quad (1.1.14)$$

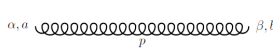
where  $\lambda$  is a arbitrary gauge parameter and  $\eta$  is a complex scalar field in the adjoint representation of the  $SU(N_c)_c$  group. However, the ghost particle, even if it is described by a scalar field, obeys to the Fermi-Dirac statistics. The gluon propagator in the covariant gauge is given by

$$\Delta_{\mu\nu}^{ab}(p) = \delta^{ab} \frac{i}{p^2} \left( -g_{\mu\nu} + (1 - \lambda) \frac{p_\mu p_\nu}{p^2} \right); \quad (1.1.15)$$

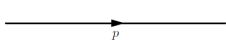
in the particular case with  $\lambda = 1$ , Eq. (1.1.15) returns a particular simple expression for the gluon propagator. This gauge is usually called Feynman Gauge in literature.

Another convenient gauge class (especially in deriving general properties of the theory) is the one of *axial* gauges, which are defined through

$$\mathcal{L}_{\text{gauge-fixing}} = -\frac{1}{2\lambda} (t_a n^\mu A_\mu^a)^2 \quad \mathcal{L}_{\text{ghost}} = 0 \quad (1.1.16)$$



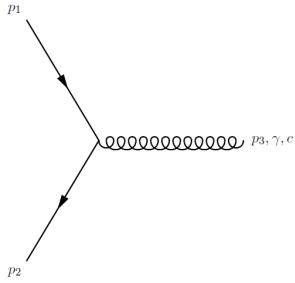
$$\frac{-ig^{\alpha\beta}\delta^{ab}}{p^2 + i\epsilon} \quad (1.1.7)$$



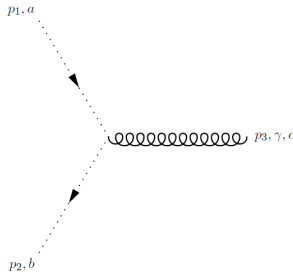
$$\frac{i}{\not{p} - m + i\epsilon} \quad (1.1.8)$$



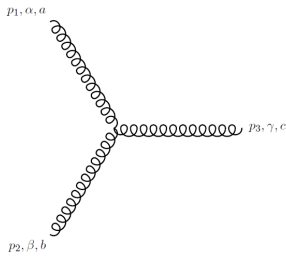
$$\frac{i\delta^{ab}}{p^2 + i\epsilon} \quad (1.1.9)$$



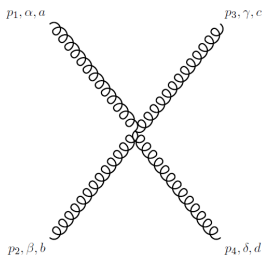
$$-igt^a\gamma^\alpha \quad (1.1.10)$$



$$gf^{abc}p_3^\gamma \quad (1.1.11)$$



$$-gf^{abc} \left[ (p_1 - p_2)^\gamma g^{\alpha\beta} + (p_2 - p_3)^\alpha g^{\beta\gamma} + (p_3 - p_1)^\beta g^{\gamma\alpha} \right] \quad (1.1.12)$$



$$-ig^2 \left[ f^{eac} f^{ebd} (g^{\alpha\beta} g^{\gamma\delta} - g^{\alpha\delta} g^{\beta\gamma}) + f^{ead} f^{ebc} (g^{\alpha\beta} g^{\gamma\delta} - g^{\alpha\gamma} g^{\beta\delta}) + f^{eab} f^{acd} (g^{\alpha\gamma} g^{\beta\delta} - g^{\alpha\delta} g^{\beta\gamma}) \right] \quad (1.1.13)$$

Figure 1.1. Feynman Rules of QCD

where  $\lambda$  is an arbitrary parameter, and  $n$  an arbitrary four-vector. The important property of the axial gauges is not to exhibit any ghost fields. On the contrary, the particular expression for the gluon propagator turn out to be more complicated than in covariant gauges:

$$\Delta_{\mu\nu}^{ab}(p) = \delta^{ab} \frac{i}{p^2} \left( -g_{\mu\nu} + \frac{n_\mu p_\nu + n_\nu p_\mu}{(n \cdot p)} - \frac{(n^2 + \lambda p^2) p_\mu p_\nu}{(n \cdot p)^2} \right) \quad (1.1.17)$$

Even in this case we can simplify previous expression by a proper tuning of the arbitrary parameters. The more common choice in literature is called *light-cone* gauge which corresponds to an axial gauge with  $n^2 = 0$  and  $\lambda = 0$ .

We are now ready to present the Feynman Rules for QCD. For simplicity, we are going to write them in the Feynman Gauge. Feynman Rules are summarized in Fig. 1.1, considering all the momenta as incoming.

### 1.1.1 Asymptotic Freedom and Confinement

Now we want to focus on two important properties of QCD, its asymptotic freedom and the issue of confinement respectively. Calculations, usually, in a quantum field theory are performed in the framework of perturbation theory. A general observable  $\sigma$  is expanded in powers of the coupling constant  $\alpha_s = \frac{g_s^2}{4\pi}$  and the computations of the first orders is considered to be an approximation of the exact result. However, such procedure is reliable only if  $\alpha_s < 1$  to assure the convergence, at least asymptotically, of the perturbative series.

In general, any expanded adimensionless observable  $\sigma$  is going to depend on a set of dimensionless parameters  $\{y\}$  and on a single hard scale  $Q$ , by hypothesis much bigger than all the other dimensional parameters of the theory (e.g. the masses of the particles). If  $Q^2$  is higher enough we can consider to neglect all the various masses of the particles; under this assumption, dimensional analysis suggests that  $\sigma$  should be independent of  $Q$ .

However, in the computation of the radiative corrections of the theory, renormalization must be applied to get rid of the UV divergences from perturbative calculations. This procedure obliges to introduce a new mass scale  $\mu_R$  called renormalization scale, forcing our general observable to acquire a residue dependence on  $Q$  via the ratio  $\frac{Q^2}{\mu_R^2}$ . Nevertheless,  $\mu_R$  being an arbitrary parameter, physical observables such as  $\sigma$  cannot depend on it. This statement is reflected in a renormalized quantum field theory by the requirement that our observable must fulfil the so-called Callan-Symanzik equation:

$$\mu_R^2 \frac{d}{d\mu_R^2} \sigma \left( \frac{Q^2}{\mu_R^2}, \alpha_s, \{y\} \right) = \left[ \mu_R^2 \frac{\partial}{\partial \mu_R^2} + \beta(\alpha_s) \frac{\partial}{\partial \alpha_s} \right] \sigma \left( \frac{Q^2}{\mu_R^2}, \alpha_s, \{y\} \right) = 0 \quad (1.1.18)$$

where we define the *beta function*

$$\beta(\alpha_s) = \mu_R^2 \frac{\partial \alpha_s}{\partial \mu_R^2}. \quad (1.1.19)$$

The most general solution  $\sigma$  of Eq. (1.1.18) is given by

$$\sigma \left( \frac{Q^2}{\mu_R^2}, \alpha_s, \{y\} \right) = \sigma \left( 1, \alpha_s(Q^2), \{y\} \right) \quad (1.1.20)$$

having defined the *running coupling constant* according to

$$\mu_{\text{R}}^2 \frac{\partial \alpha_s(\mu_{\text{R}}^2)}{\partial \mu_{\text{R}}^2} = \beta(\alpha_s), \quad \alpha_s(\mu_{\text{R}}^2) = \alpha_s. \quad (1.1.21)$$

Eq. (1.1.20) states that all the dependence of our observable on the ratio  $\frac{Q^2}{\mu_{\text{R}}^2}$  can be recast in the computation of a new coupling which however evolves with the energy scale according to Eq. (1.1.21). Physically, the running coupling constant  $\alpha_s(Q^2)$  gives the effective strength of the interaction as a function of the energy scale at which it is observed.

If also the particle masses are inserted in our computation, situation becomes more complicated since also these new quantities have to be regularized during higher order computation. This leads to regularized running masses  $m(Q^2)$  and to extra  $\sigma$  dependence on the ratio  $\frac{Q^2}{m^2}$ . However, we are going to leave aside this problem from now on since we are going to focus our attention on single-massive particle final state

The evolution of the coupling constant in Eq. (1.1.21) is completely controlled by the  $\beta$  function, which admits itself a perturbative expansion in power of  $\alpha_s$ . In a  $SU(N_c)_c$  gauge theory with  $N_f$  fermions in the fundamental representation the leading term of the  $\beta$  function is found to be [5]

$$\beta(\alpha_s) = -\beta_0 \alpha_s^2 + \mathcal{O}(\alpha_s^3), \quad \beta_0 = \frac{11N_c - 2N_f}{12\pi}. \quad (1.1.22)$$

In the case of QCD, since  $N_c = 3$ ,  $\beta_0 > 0$  until  $N_f < 17$ . It follows that the QCD running coupling constant  $\alpha_s$  becomes weaker and weaker as the energy scale becomes large. This property of quantum field theory such as QCD is called *asymptotic freedom* and it permits the perturbative analysis at least in the high energy regime. The short-distance behaviour is then solvable by means of Feynman diagram methods.

As long as  $\alpha_s(Q^2)$  or  $\alpha_s(\mu_{\text{R}}^2)$  are in the perturbative regime, it makes sense to truncate the  $\beta$  function to solve perturbatively Eq. (1.1.21). However, even if the renormalization group predicts exactly the scaling of the running coupling, an experimental input is needed to fix its absolute value. The most common convention in the determination of the strong coupling  $\alpha_s$  is to measure it at a scale which is large enough to enter the perturbative regime, as for instance the mass of the  $Z^0$  boson.

Lowering the energy scale,  $\alpha_s$  becomes larger till we exit from the perturbative regime and any predictions relies in principle on the computation of the full series. The value of energy where the perturbative picture is seriously ruined by non-perturbative corrections is found to be comparable with the masses of the lightest hadrons, roughly  $Q \approx 1 \text{ GeV}$ .

For energies lower than this limit, QCD exhibits a striking behaviour, not totally understood, known as *colour confinement*: the only finite-energy asymptotic states of the theory are those that transform trivially under the  $SU(3)$  colour group. Colour charged states, such as quarks and gluons, can only exist in the context of singlet bound states and thus cannot be directly observed. An analytic proof of confinement in QCD is still missing, even if numerical simulations in the so-called Lattice QCD<sup>1</sup> show that colour charged states indeed turn out to be confined for sufficiently strong coupling.

<sup>1</sup>Lattice QCD is an approximated method in which green functions of QCD are derived exactly by replacing the continuum theory by a discrete lattice system.

Therefore, a critical point in the evaluation of observables in QCD is the necessity to link our computations, performed in the perturbative regime in terms of the fundamental constituents of the theory, quarks and gluons, with the hadronic asymptotic states we effectively have in the initial and final state. The solution is achieved by exploiting important factorization properties of perturbative QCD, which will be the subject of the next section.

## 1.2 The Parton Model and Collinear Factorization

In the previous section, we have observed that a perturbative analysis of strong interactions is actually possible, thanks to the asymptotic freedom of QCD. At high energy, the coupling becomes small and we can study interactions between the fundamental fields of the theory, i.e. quarks and gluons, using the Feynman Diagrams approach.

However, the short-distance scattering between particles of QCD can not be observed; indeed, due to confinement, in any measurement we are forced also to deal with long-distance contributions, which convert quarks and gluons into the hadrons we really see. Unfortunately, perturbative approach can not be applied on such hadronization contributions and at first sight the application of QCD on scattering experiments seems doomed to fail.

The entire picture is saved by the so-called *Parton Model*<sup>2</sup>. The basic assumptions of Parton Model are:

- at high energy, the interactions between a probe and a hadron is in fact a scattering between the probe and various constituents of the hadron (called precisely *partons*) which can be considered as pointlike and freely moving;
- any probe interacts with only one parton, and multiple scattering is completely negligible.

Under these assumptions, a scattering involving a hadron can be seen as the product between the probability to find a particular parton inside the hadron times the scattering involving that parton, summed over all the possible partons inside the hadron. By identifying these partons with the fundamental quarks and gluons of QCD, we are able to separate the long-distance contributions, controlling the distribution of partons into hadrons, from the parton scattering amplitude, which is perturbative calculable, since it is linked only to a short-distance dynamics.

The same procedure can be applied also in the final state. The distribution of an hadron can be seen as the product of the distribution of a parton times the probability for the parton to fragmentate into the desired hadron, summed over all the possible partons in the final state. Even in this case we separate the short-distance dynamics, controlling the partonic distribution, from the long-distance dynamics, controlling the *fragmentation function*. In the following we will concentrate on the initial state problem, and we leave aside the discussion about fragmentation functions and hadrons in the final

---

<sup>2</sup>first postulated by Bjorken [7] and Feynman [8]

state. However, the following discussion can be straightforwardly applied also in this case, and we refer the interested reader to Ref. [6] for a more general treatment.

Moreover, in the rest of the thesis, we are going to focus ourselves on hadron-hadron scattering rather than photon-hadron or lepton-hadron scattering. In the same assumptions, the Parton Model states that the hadron-hadron scattering observable can be obtained at high-energy by the product between the probability to find two particular partons into the hadrons and the scattering observable computed with the two partons in the initial state, summed over all the possible couples of partons in the hadrons.

Now, in addition to briefly sketch a proof of the Parton Model, we want to present other two important properties of this construction: first of all, it can be proved for inclusive enough observables that probability distributions, now called PDFs, parton distribution functions, are universal and not correlated with short-distance dynamics; second, for them, we can properly define finite radiative corrections at any orders in the strong coupling.

The Parton Model, together with the two further properties we have just mentioned, forms the so-called *Collinear Factorization Theorem* of QCD, which represents the theoretical ground for any perturbative computation of strong interactions. Last part of this section is devoted to a general proof of this theorem, together with explicit application of the construction.

### 1.2.1 Collinear Factorization Theorem

We start by presenting an heuristic proof of the Parton Model in the context of hadron-hadron scattering [9]. For a complete and general proof, we refer the reader to Ref. [10–12].

Parton Model mechanism can be easily understood with the following physical argument: consider the centre of mass frame of the pair of hadrons; since we are at high energy two important things happen to our particle in this frame. First, it is Lorentz contracted in the direction of the collision, and second its internal interactions are time dilated. Hence, since we want to consider hadrons as formed by virtual interacting partons, at high energy we can consider the lifetime of any virtual partonic state as lengthened.

On the contrary the time it takes one hadron to transverse the other is shortened. In the case, when the latter is much shorter than the former, each hadron will be in a single virtual state characterized by a definite number of partons during the whole interaction. Since partons inside the same hadron do not interact during this time, we can think each one as carrying a definite fraction  $x_1$  and  $x_2$  of the hadrons  $h_1$  and  $h_2$  momenta in the centre of mass frame. Since the interaction is highly boosted, we expect  $x_1, x_2$  to satisfy  $0 < x_i < 1$ , since otherwise one or more partons would have to move in the opposite direction with respect to the hadron they form. It now makes sense to talk about interactions between two particular partons of definite momentum, rather than between two hadrons as a whole. Moreover, if we require the momentum transfer between the interacting partons to be very high, we are assuming that the virtual particles which mediate parton-parton scattering can not travel far. Then, if the density of partons is not too high, any partons will be able to interact with only another single parton, and multiple scattering is negligible. For the same reason, also interactions which occur in the final state, after the hard scattering, are assumed to occur on time scales too long to

interfere with it<sup>3</sup>.

Under these assumptions, the high energy scattering process becomes essentially classical and incoherent. The cross section for hadron scattering may thus be computed combining probabilities, rather than amplitudes. In the case of a total cross section for a process characterized by a transferred momentum  $Q^2$ , we can write:

$$\sigma_{h_1, h_2}(\tau, Q^2) = \sum_{i \in h_1, j \in h_2} \int_{\tau}^1 dx_1 f_i(x_1) \int_{\frac{\tau}{x_1}}^1 dx_2 f_j(x_2) \hat{\sigma}_{i,j} \left( x = \frac{\tau}{x_1 x_2}, Q^2 \right) \quad (1.2.1)$$

where  $f_i(x)$  ( $f_j(x)$ ) is the parton distribution function, PDF, i.e. the probability of finding the parton  $i$  ( $j$ ) in the hadron  $h_1$  ( $h_2$ ) with momentum fraction  $x$  of the hadron momentum, while  $\hat{\sigma}$  is the *partonic cross section*. We are going to come back on Eq. (1.2.1) after the inclusion of radiative corrections of QCD into  $\hat{\sigma}_{i,j}$ .

Using Parton Model we have defined a factorized expression for a general hadronic observable (for example the total cross section as in Eq. (1.2.1)), implicitly in formulas:

$$\mathcal{O} = \mathcal{L} \otimes \hat{\mathcal{O}} \quad (1.2.2)$$

where we call  $\mathcal{O}$ ,  $\hat{\mathcal{O}}$  the selected observable with hadrons and partons respectively in the initial state, and  $\mathcal{L}$  the convolution of the PDFs, which is called in literature parton density luminosity. The symbol  $\otimes$  stands for a multiplicative convolution over the momentum fraction of the partons, as in Eq. (1.2.1). Now, merging Parton Model with QCD, we come to the conclusion that  $\hat{\mathcal{O}}$ , since it describes the hard interaction between quarks and gluons, it has to admit a perturbative expansion in the strong coupling. We thus write:

$$\hat{\mathcal{O}} = \hat{\mathcal{O}}^{(0)} + \hat{\mathcal{O}}^{(1)} \alpha_s + \hat{\mathcal{O}}^{(2)} \alpha_s^2 + \dots \quad (1.2.3)$$

where  $\hat{\mathcal{O}}^{(0)}$  stands for the LO contribution<sup>4</sup>, while the following terms represent radiative corrections to the observable.

As usual, in quantum field theory the corrections  $\hat{\mathcal{O}}^{(i)}$  with  $i > 0$  are computed by evaluating loop Feynman Diagrams. QCD loop diagrams, however, show both UV and IR divergences and, while the former are treated with renormalization techniques, no renormalization procedure can get rid of the latter. The meaning of infra-red singularities is the following: they state that the cross section is sensitive to long distance effects, like fermion masses, hadronization mechanism and so on. This behaviour is linked to the two general properties of QCD we introduced, the confinement and the asymptotic freedom. When the energy becomes soft, the radiation energy scale approaches the critical scale  $\Lambda$ , the Landau pole, where the running coupling explodes. Moreover, at this scale other IR singularities arise from our ignorance about QCD at low energy, in the non-perturbative regime. While the first case is present also in QED, the second is typical of QCD. This fact increases the general difficulty of the fixed order computations in QCD.

In the following we focus our attention on colour singlet production process, since this is the application we have in mind in the rest of the thesis. Similar considerations

<sup>3</sup>This hypothesis is almost trivial in computing total cross section since we integrate over all possible final state; however, it turn out to be very important if we want to study more exclusively the final state dynamics (Parton Shower or Jets) [16–18]

<sup>4</sup>Typically, in literature, we refer to *naïve parton model* if the partonic observable is computed at LO, *improved parton model* if also radiative corrections are included

apply for jet observables. However, situation is slightly different if we consider hadrons in the final state; for a general discussion about *fragmentation functions* and this type of observables we refer the reader to Ref. [6].

Colour singlet production is a general process as

$$h_1 + h_2 \rightarrow \mathcal{S} + X \quad (1.2.4)$$

with  $\mathcal{S}$ , the final state we are interested in, which we want to be not strong interacting, and  $X$  the possible extra radiation. In this process IR divergences arise from loop virtual diagrams, and from integration of phase space in the real emission diagrams with one more particle in the final state.

By inspecting the nature of these IR divergences, it is easy to divide them in two classes:

- *Soft singularities*: divergences obtained in the region when the energy of the extra gluon goes to zero.
- *Collinear singularities*: divergences obtained in the region when the angle with respect to the emitted leg of the extra gluon or quark goes to zero.

By summing virtual and real contributions some cancellations take place. In particular all the soft singularities and all the collinear singularities coming from final state radiations exactly cancel between virtual and real diagrams. Therefore, while considering a process in QCD with a fixed number of particles in the final state is sensitive to long distance contributions, the "inclusive" measurement in which we admit the possible emission of new quarks and gluons is only short-distance dominated. We are going to be more precise about the meaning of "inclusive" measurement in a while. The physical interpretation is rather simple. Since we collide hadrons in the initial state, we are not able to distinguish the radiation of new partons from the rest of partons already in the initial state but not involved in the hard interaction (*spectator partons*), without a detailed description of the structure of the hadron itself. For this reason, the process with a fixed number of partons in the final state is sensitive to long-distance dynamics while the sum is not.

This cancellation is a consequence of the *Kinoshita-Lee-Nauenberg theorem* [13, 14]. Roughly speaking, this theorem deals with divergences that arise because of degeneracy in the final state. In both cases, the final state with an extra gluon or quark is nearly degenerate with the state with no new partons at all. Hence the theorem states that the cross section obtained by summing up over degenerate states is not divergent.

We have understood that an observable that sums over an infinite number of configurations with more and more partons in the final state, is finite as regards final state radiation. Of course, completely inclusive observables, as total cross sections, where all the configurations are taken into account are finite but is also possible to study perturbatively some more exclusive observables, such as angular or rapidity distributions of  $\mathcal{S}$ ?

We have the following statement: cancellations of divergences in the final state occurs for any *infra-red and collinear safe observables* [15]. The definition of an infra-red and collinear safe observable is the following: given an observable

$$V(p_1, \dots, p_n) \quad (1.2.5)$$

defined as a function of all the momenta in the process, it must fulfil

$$V(p_1, \dots, p_i, \dots, p_n) = V(p_1, p_2, \dots, p_{i-1}, p_{i+1}, \dots, p_n) \quad \text{if } p_i^0 \rightarrow 0 \quad (1.2.6a)$$

$$V(p_1, \dots, p_i, \dots, p_j, \dots, p_n) = V(p_1, p_2, \dots, p_i + p_j, \dots, p_n) \quad \text{if } p_i \parallel p_j. \quad (1.2.6b)$$

Eqs. (1.2.6) state that our observable to be perturbative calculable must be insensitive to any extra emission which is soft and/or collinear.

Rapidity distribution of  $\mathcal{S}$  is an example of a more exclusive infra-red and collinear safe observable while the pseudorapidity<sup>5</sup> and transverse momentum distribution is an example of observable always sensitive to long-distance dynamics since it does not fulfil the first requirement of Eqs. (1.2.6). On the contrary the single differential distribution in transverse momentum or the double differential rapidity and transverse momentum distribution are correct infra-red and collinear safe observables. The study of this type of observables in colour singlet production process will be the main subject of this thesis.

We reach the conclusion that any strong radiative contribution in the final state is finite if we limit to consider *infra-red and collinear safe observables*. We move now to initial state radiation. Here the situation is slightly more difficult. Indeed, even if soft divergences still cancel between real and virtual contributions, a collinear singularity persists. We try now to explain why.

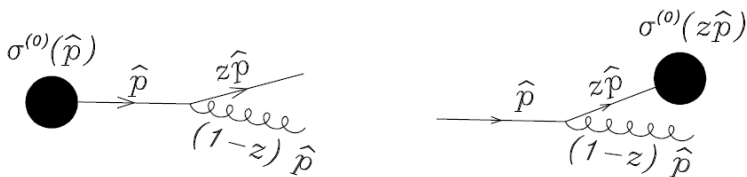


**Figure 1.2.** Single real gluon emission from a general process, in the final state (left) and in the initial state (right) respectively [18].

Look at the Fig. 1.2; it shows the emission of one more gluon with respect to the Born cross section, appearing in the final (left) or in the initial state (right). The main difference between the two cases is related to the Born cross section,  $\hat{\sigma}^{(0)}$ . In both cases, it is a function of the momenta entering or exiting the blob. Hence, there is a difference between the left panel and the right panel of Fig. 1.2: if the new parton is radiated in the final state, the correction multiplies  $\hat{\sigma}^{(0)}(p)$ ; instead, if the new parton is radiated in the initial state, the Born cross section appears as  $\hat{\sigma}^{(0)}(zp)$ . This is an important difference, because one loop virtual corrections share the same kinematics of the Born level and appear in the divergent region multiplied by  $\sigma^{(0)}(p)$ .

Therefore, while in the final state we have total cancellation, in the initial state a residue proportional to  $\sigma^{(0)}(zp) - \sigma^{(0)}(p)$  still remains. This is a totally collinear contribution, since in the soft region  $z \rightarrow 1$ , we recover exact cancellation. How are we able to get rid also of this extra divergence?

<sup>5</sup>The pseudo-rapidity is the variable used for describing angular spectrum. It is defined as

$$\eta = -\ln \tan \frac{\theta}{2} \quad (1.2.7)$$

with  $\theta$  the angle of the studied final state with respect to the beam direction

The way we treat these divergences is analogue to what happens in renormalization: since, in the parton model formula, Eq. (1.2.1) or Eq. (1.2.2), PDFs are quantities which should be measured, we can imagine that in the naïve formulation of the parton model they are bare objects, and that they can be redefined in such a way to reabsorb all collinear divergences: the new PDFs we obtain are what we actually measure and then they have to be finite.

Schematically we have the following situation. We can write our hadronic observable as

$$\mathcal{O} = \mathcal{L} \otimes \Gamma^{\text{div}}(\mu_{\text{F}}^2) \otimes \hat{\mathcal{O}}(\mu_{\text{F}}^2) \quad (1.2.8)$$

where still the symbol  $\otimes$  means a multiplicative convolution, we call  $\Gamma^{\text{div}}$  the collinear divergent part of  $\hat{\mathcal{O}}$  and we introduce a new energy scale  $\mu_{\text{F}}^2$ , emerging in the regularization process (as in dimensional regularization for example). We are now able to redefine our Luminosity according to

$$\mathcal{L}(\mu_{\text{F}}^2) = \Gamma^{\text{div}}(\mu_{\text{F}}^2) \otimes \mathcal{L} \quad (1.2.9)$$

and to associate to  $\mathcal{L}(\mu_{\text{F}}^2)$  the PDFs we actually measure. We end up with a complete finite definition for our *infra-red and collinear safe observable*:

$$\mathcal{O} = \mathcal{L}(\mu_{\text{F}}^2) \otimes \hat{\mathcal{O}}(\mu_{\text{F}}^2). \quad (1.2.10)$$

The process of regularization of divergences brings the PDFs and our partonic cross section to acquire a dependence on a new fictitious energy scale  $\mu_{\text{F}}^2$ , the scale where the PDFs are actually measured. It must be set near the hard scale of the process, as the renormalization scale, in order not to introduce large logarithms in our perturbative expansion.

However, in performing this construction, we have tacitly assumed three important facts:

- the divergent part in the partonic observable factorizes;
- the divergent part is independent of the observable and of the process;
- the factorized expression assumed in the parton model still holds after the inclusion of QCD corrections; this means that diagrams with additional lines connecting the partonic part of the process directly to the non-perturbative hadronic part do not count.

In the following sections we are going to prove the first two assumptions while for a general demonstration of the third fact, which is based on OPE (Operator Product Expansion) expansion we refer the interested reader to Ref. [10].

In conclusion, in this section we present two main ingredients that permits perturbative calculations in QCD: parton model and factorization theorem. First, our hadronic observable can be factorized at the level of probability, rather than amplitudes, into a product of a long-distance object, the PDF luminosity, and a short-distance observable. Moreover, inclusion of QCD radiative corrections into the partonic observable can be performed regularizing all IR and UV singularities. To avoid divergences, however, we need:

- to limit our study to observables which are *infra-red and collinear safe*.
- to redefine our PDFs luminosity, by absorbing all initial state collinear divergences, and to acquire in the PDFs and in the partonic observable a new dependence from the factorization energy scale,  $\mu_F^2$ .

Nevertheless, final factorized result, Eq. (1.2.10), permits us to produce predictions in the high energy limit for strong interacting processes. Collider experiments prove that this entire picture works extremely well, permitting us to evaluate many observables with the incredible precision of even less than 5%.

Time is ripe to present a general proof of Factorization Theorem in the context of hadron-hadron scattering. This will be the subject of the next subsection.

## 1.2.2 Generalized Ladder Expansion

In the previous section, we understood how to introduce QCD radiative corrections in the environment of the Parton Model. When we have to deal with hadrons in the initial state, a residual collinear divergence remains even if we consider a *infra-red and collinear safe* observable.

However, *collinear factorization theorem* states that such divergences are universal and factorizable into *bare* parton distribution functions, leaving at the end all finite objects. As for renormalization, remaining objects, even if finite, acquire a new dependence from an arbitrary scale, in this case called *factorization scale*. We are going to come back about the factorization scale dependence of PDFs and observables in the next section where PDFs evolution will be discussed.

Now, the rest of the section is devoted to present a possible general proof of the *collinear factorization theorem* in the case of hadron-hadron scattering. Our derivation follows very closely the demonstration of Ref. [19, 23], and we refer the interested reader to these references for further details.

Our starting point is the naïve Parton Model factorization, i.e the convolution of two universal *bare* parton distributions  $f_i^{(0)}$  and  $f_j^{(0)}$  with a process-dependent unsubtracted partonic observable  $\hat{\mathcal{O}}_{ij}^{(0)}$ :

$$\mathcal{O} = \sum_{ij} f_i^{(0)} \otimes f_j^{(0)} \otimes \hat{\mathcal{O}}_{ij}^{(0)} \quad (1.2.11)$$

where  $\otimes$  symbol indicates, as before, standard multiplicative convolution in  $x$  space (see Eq. (B.2.16) for definition).

This expression at this point presents mass singularities (IR) both in  $\hat{\mathcal{O}}_{ij}^{(0)}$  and in  $f_i^{(0)}$ . Let us regulate them by means of the dimensional regularization technique; indeed, in the massless theory in  $d = 4 - 2\epsilon$  dimensions, infra-red singularities should appear as poles in  $\epsilon$ .

Now the general strategy, to achieve the factorization of singularities, consists in a reorganization of the perturbative series which goes under the name of generalized ladder expansion (GLE). In order to deal only with physical degrees of freedom, we are going to work in the *light-cone gauge* (axial gauge  $n_\mu A^\mu = 0, \lambda = 0, n^2 = 0$ ), thus ignoring

any *ghost* contribution. First proposed in Ref. [19] for DIS, we shall present it in hadro-production case. The partonic observable  $\hat{\mathcal{O}}_{ij}^{(0)}$  for the subprocess  $p_i(k_1) + p_j(k_2) \rightarrow X(q)$ , with  $X$  denoting any possible final state, can be evaluated by cutting all the diagrams for the forward scattering amplitude  $p_i(k_1) + p_j(k_2) \rightarrow p_i(k_1) + p_j(k_2)$  (using optical theorem, whose realization in perturbative QCD is based on the Cutkosky rules).

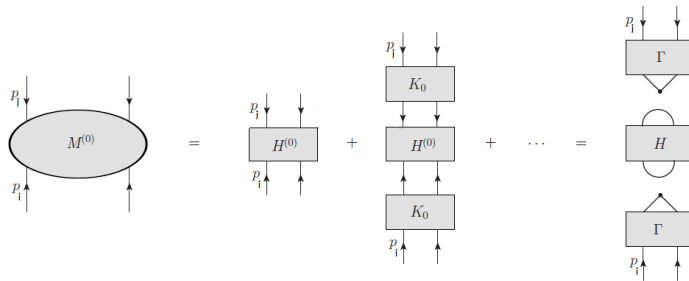


**Figure 1.3.** Generalized ladder expansion subtraction for a single external initial line. The squared matrix element is view as an 2PI hard part dressed by a entire sum of singular  $K_0$  emission kernels.

In Ref. [24], two important results are shown: first, the all-order perturbative series of the cut diagrams can be rewritten as a 2PI hard-interaction contribution  $H_0$  where any of the four external parton lines are consecutively "dressed" with 2PI kernels  $K_0$ , as shown in Fig. 1.3; second, any diagram containing a line which connects kernels belonging to different parton lines of  $H_0$  is finite, i.e. does not carry any extra residual collinear divergences. Regarding the singularity structure, we can think recasting our cut diagrams as a connection between a process-dependent hard part, which contain the Born level, and two ladders of kernels  $K_0$ . Kernel  $K_0$  and the hard part  $H_0$  are formed by a proper combination of 2PI topologies in the  $t$ -channel. With this term, we indicate topologies for which their top cannot be disconnected from the bottom by cutting only two lines; at least three lines must be cut. Examples of such topologies are included in Fig. (1.4) where a possible decomposition for  $K_0$  is sketched.



**Figure 1.4.** Examples of 2PI topologies for the ladder kernel  $K_0$ . The lines and vertices are of any type allowed by the theory.

Note that in Fig. 1.3 external lines connecting two kernels represent full momentum integration, and kernels themselves are sums of cut diagrams. It can be proved [19] that in axial gauge the single 2PI kernel is finite, as long as the integration over the external legs is detained. Hence, all collinear singularities arise from these integrations over the momenta flowing in the lines connecting consecutive kernels. Moreover, it is important to note that hard part  $H_0$  and kernels  $K_0$  carry in principle two pairs of Lorentz indices

and depend on two momenta. They carry in many cases also colour components, but we can strip off all colour dependence diagram by diagram using standard techniques (see Ref. [18, 25, 26] for a general treatment). Therefore we are going to work only with colourless amplitudes and diagrams.

To simplify notations, we shall suppress in the rest of the section all indices and dependences. However, any product in the following formulas has to be intended as

$$C_{\mu\nu}^{\alpha\beta}(q_1, q_2) = \int \frac{d^n l}{(2\pi)^n} A_{\gamma\eta}^{\alpha\beta}(q_1, l) B_{\mu\nu}^{\gamma\eta}(l, q_2) \quad (1.2.12)$$

even if it will be denoted in a more compact way as  $C = AB$ .

Given all these assumptions, the generalized ladder expansion (GLE) of the unsubtracted observable  $\hat{O}_{ij}^{(0)}$  can be written as

$$\begin{aligned} \hat{O}_{ij}^{(0)} &= (H_0)_{ij} \left( 1 + K_0^{(i)} + \left(K_0^{(i)}\right)^2 + \dots \right)_i \left( 1 + K_0^{(j)} + \left(K_0^{(j)}\right)^2 + \dots \right)_j \\ &= (H_0)_{ij} \left( \frac{1}{1 - K_0^{(i)}} \right) \left( \frac{1}{1 - K_0^{(j)}} \right) = (H_0)_{ij} \left( \Gamma_0^{(i)} \right) \left( \Gamma_0^{(j)} \right). \end{aligned} \quad (1.2.13)$$

At first sight, Eq. (1.2.13) could seem the desired factorization:  $H_0$ , being a 2PI kernel, is finite and all mass singularities are contained in the ladder parts  $\Gamma_0$ . Nevertheless  $(H_0)_{ij}$  and  $\left(\Gamma_0^{(i)}\right)$ ,  $\left(\Gamma_0^{(j)}\right)$  are still coupled by both the momentum integration and Lorentz structure, as shown by Eq. (1.2.12). The particular form of the kernel depends only on the type of parton  $i$  to which is connected in  $H_0$ .

Full factorization is achieved using a suitable projector for the parton  $k$   $\mathbb{P}^{(k)}$  to decouple  $H_0$  and  $K_0^{(k)}$  in momentum and spinor space, thus extracting singular part of the integrations. It is convenient to separate the action of the projector in spinor and momentum space  $\mathbb{P}_s^{(k)}$  and  $\mathbb{P}_\epsilon$  respectively, thus permitting us to rewrite full projector implicitly as  $\mathbb{P}^{(k)} = \mathbb{P}_s^{(k)} \mathbb{P}_\epsilon$ . However, since the explicit action of  $\mathbb{P}_s^{(k)}$  on a general kernel is not essential to understand factorization, we do not report it in this section, referring the interested reader to the original papers [19, 23]. Instead, we define the action of  $\mathbb{P}_\epsilon$  projector: when it acts on a generic function  $F$ , it selects just its poles:

$$\mathbb{P}_\epsilon F = \sum_{n>0} \frac{1}{\epsilon^n} \left( \lim_{\epsilon \rightarrow 0} \epsilon^n F \right). \quad (1.2.14)$$

The following steps are rather straightforward, given all the due technicalities we gave ourselves. We proceed with an iterative factorization of the collinear singularities in Eq. (1.2.13). First, we factorize the singular part of the last kernel  $K_0^{(i)}$  on the parton  $i$ :

$$\begin{aligned} \hat{O}_{ij}^{(0)} &= (H_0)_{ij} \left( \sum_{k'=0}^{\infty} \left(K_0^{(j)}\right)^{k'} \right) \left( \sum_{k=0}^{\infty} \left(K_0^{(i)}\right)^k \right) = \mathcal{H}_0 \left( \sum_{k=0}^{\infty} \left(K_0^{(i)}\right)^k \right) \\ &= \mathcal{H}_0 \left[ 1 + \sum_{k=1}^{\infty} \left(K_0^{(i)}\right)^{k-1} \mathbb{P}^{(i)} K_0^{(i)} + \sum_{k=1}^{\infty} \left(K_0^{(i)}\right)^{k-1} \left(1 - \mathbb{P}^{(i)}\right) K_0^{(i)} \right] \end{aligned}$$

$$= \mathcal{H}_0 \left[ 1 + \sum_{k=0}^{\infty} \left( K_0^{(i)} \right)^k \left( 1 - \mathbb{P}^{(i)} \right) K_0^{(i)} \right] + \hat{\mathcal{O}}_{ij}^{(0)} \mathbb{P}^{(i)} K_0 \quad (1.2.15)$$

where we define the object  $\mathcal{H}_0 = (H_0)_{ij} \left( \sum_{k'=0}^{\infty} \left( K_0^{(j)} \right)^{k'} \right)$ .

Bringing last term in Eq. (1.2.15) to the left-hand side of equation gives:

$$\hat{\mathcal{O}}_{ij}^{(0)} \left( 1 - \mathbb{P}^{(i)} K_0^{(i)} \right) = \mathcal{H}_0 \left[ 1 + \sum_{k=0}^{\infty} \left( K_0^{(i)} \right)^k \left( 1 - \mathbb{P}^{(i)} \right) K_0^{(i)} \right]. \quad (1.2.16)$$

We now go on with the iterative factorization, by isolating singular part of  $K_0^{(i)} \left( 1 - \mathbb{P}^{(i)} \right) K_0^{(i)}$  on the right-hand side of Eq. (1.2.16):

$$K_0^{(i)} \left( 1 - \mathbb{P}^{(i)} \right) K_0^{(i)} = \left( 1 - \mathbb{P}^{(i)} \right) \left[ K_0^{(i)} \left( 1 - \mathbb{P}^{(i)} \right) K_0^{(i)} \right] + \mathbb{P}^{(i)} \left[ K_0^{(i)} \left( 1 - \mathbb{P}^{(i)} \right) K_0^{(i)} \right] \quad (1.2.17)$$

Substituting last equation into Eq. (1.2.16) gives:

$$\begin{aligned} \hat{\mathcal{O}}_{ij}^{(0)} \left( 1 - \mathbb{P}^{(i)} K_0^{(i)} \right) &= \mathcal{H}_0 \left[ 1 + \left( 1 - \mathbb{P}^{(i)} \right) K_0^{(i)} + \sum_{k=0}^{\infty} \left( K_0^{(i)} \right)^{k+1} \left( 1 - \mathbb{P}^{(i)} \right) K_0^{(i)} \right] \\ &= \mathcal{H}_0 \left[ 1 + \left( 1 - \mathbb{P}^{(i)} \right) K_0^{(i)} \right. \\ &\quad \left. + \sum_{k=0}^{\infty} \left( K_0^{(i)} \right)^k \left( 1 - \mathbb{P}^{(i)} \right) \left[ K_0^{(i)} \left( 1 - \mathbb{P}^{(i)} \right) K_0^{(i)} \right] \right] \\ &\quad + \hat{\mathcal{O}}_{ij} \mathbb{P}^{(i)} \left[ K_0^{(i)} \left( 1 - \mathbb{P}^{(i)} \right) K_0^{(i)} \right]. \end{aligned} \quad (1.2.18)$$

We again move last term on the left-hand side of Eq. (1.2.18) to obtain:

$$\begin{aligned} \hat{\mathcal{O}}_{ij}^{(0)} \left( 1 - \mathbb{P}^{(i)} K_0^{(i)} - \mathbb{P}^{(i)} \left[ K_0^{(i)} \left( 1 - \mathbb{P}^{(i)} \right) K_0^{(i)} \right] \right) &= \\ \mathcal{H}_0 \left[ 1 + \left( 1 - \mathbb{P}^{(i)} \right) K_0^{(i)} + \sum_{k=0}^{\infty} \left( K_0^{(i)} \right)^k \left( 1 - \mathbb{P}^{(i)} \right) \left[ K_0^{(i)} \left( 1 - \mathbb{P}^{(i)} \right) K_0^{(i)} \right] \right]. \end{aligned} \quad (1.2.19)$$

By iterating infinite times this procedure, we end up with the following series

$$\hat{\mathcal{O}}_{ij}^{(0)} \left[ 1 - \mathbb{P}^{(i)} \left( \sum_{k=0}^{\infty} K_0^{(i)} \left[ \left( 1 - \mathbb{P}^{(i)} \right) K_0^{(i)} \right]^k \right) \right] = \mathcal{H}_0 \left( \sum_{k=0}^{\infty} \left[ \left( 1 - \mathbb{P}^{(i)} \right) K_0^{(i)} \right]^k \right) \quad (1.2.20)$$

which can formally be recast in a more compact form

$$\hat{\mathcal{O}}_{ij}^{(0)} \left[ 1 - \mathbb{P}^{(i)} \left( K_0^{(i)} \frac{1}{1 - \left( 1 - \mathbb{P}^{(i)} \right) K_0^{(i)}} \right) \right] = \mathcal{H}_0 \frac{1}{1 - \left( 1 - \mathbb{P}^{(i)} \right) K_0^{(i)}} \quad (1.2.21)$$

by defining the kernel  $\frac{1}{1-(1-\mathbb{P}^{(i)})K_0^{(i)}}$  as the series expansion in which  $(1-\mathbb{P}^{(i)})$  acts on the full expression on the right:

$$\frac{1}{1-(1-\mathbb{P}^{(i)})K_0^{(i)}} = 1 + (1-\mathbb{P}^{(i)})K_0^{(i)} + (1-\mathbb{P}^{(i)})\left[K_0^{(i)}(1-\mathbb{P}^{(i)})K_0^{(i)}\right] + \dots \quad (1.2.22)$$

Eq. (1.2.21) can now be manipulated to isolate  $\hat{\mathcal{O}}_{ij}^{(0)}$  on the left-side, giving

$$\hat{\mathcal{O}}_{ij}^{(0)} = \left( \mathcal{H}_0 \frac{1}{1-(1-\mathbb{P}^{(i)})K_0^{(i)}} \right) \otimes \left( \frac{1}{1-\mathbb{P}^{(i)}K^{(i)}} \right) \quad (1.2.23)$$

where we define

$$K^{(i)} = K_0^{(i)} \frac{1}{1-(1-\mathbb{P}^{(i)})K_0^{(i)}}. \quad (1.2.24)$$

Please pay attention than now in Eq. (1.2.23), to achieve an expression which is as compact as possible we defined the term  $\frac{1}{1-\mathbb{P}^{(i)}K^{(i)}}$  by the series expansion in which the projector acts only on the adjacent  $K^{(i)}$  on the right:

$$\frac{1}{1-\mathbb{P}^{(i)}K^{(i)}} = 1 + \mathbb{P}^{(i)}K^{(i)} + \left(\mathbb{P}^{(i)}K^{(i)}\right)\left(\mathbb{P}^{(i)}K^{(i)}\right). \quad (1.2.25)$$

Now in Eq. (1.2.23), all the singularities associated to parton  $i$  have been factorized; we can extract parton  $j$  collinear singularities from  $\mathcal{H}_0$  following similar steps. We come to:

$$\begin{aligned} \hat{\mathcal{O}}_{ij}^{(0)} &= \left( (H_0)_{ij} \frac{1}{1-(1-\mathbb{P}^{(i)})K_0^{(i)}} \frac{1}{1-(1-\mathbb{P}^{(j)})K_0^{(j)}} \right) \\ &\quad \otimes \left( \frac{1}{1-\mathbb{P}^{(i)}K_0^{(i)}} \right) \otimes \left( \frac{1}{1-\mathbb{P}^{(j)}K_0^{(j)}} \right) \\ &= \hat{\mathcal{O}}_{ij} \otimes \Gamma^{(i)} \otimes \Gamma^{(j)}. \end{aligned} \quad (1.2.26)$$

Eq. (1.2.26) is our desired factorized expression: we end up with a modified hard-interaction part  $\hat{\mathcal{O}}_{ij}$  free of collinear singularities, which have all been moved into universal objects  $\Gamma^{(i)}$  and  $\Gamma^{(j)}$ .

The cross dots between the  $\Gamma$  and  $\mathcal{O}$  is now only in the form of a normal one dimension convolution. Using Parton Model factorization, Eq. (1.2.11), we can rewrite the hadronic observable as

$$\mathcal{O} = \sum_{ij} f_i^{(0)} \otimes f_j^{(0)} \otimes \hat{\mathcal{O}}_{ij}^{(0)} = \sum_{ij} \left( f_i^{(0)} \otimes \Gamma^{(i)} \right) \otimes \left( f_j^{(0)} \otimes \Gamma^{(j)} \right) \otimes \hat{\mathcal{O}}_{ij} = \sum_{ij} f_i \otimes f_j \otimes \hat{\mathcal{O}}_{ij} \quad (1.2.27)$$

where

$$\hat{\mathcal{O}}_{ij} = \left( (H_0)_{ij} \frac{1}{1-(1-\mathbb{P}^{(i)})K_0^{(i)}} \frac{1}{1-(1-\mathbb{P}^{(j)})K_0^{(j)}} \right) \quad (1.2.28)$$

and

$$f_i = f_i^{(0)} \otimes \left( \frac{1}{1-\mathbb{P}^{(i)}K^{(i)}} \right) \quad (1.2.29)$$

are now by construction finite, and therefore we can finally set  $\epsilon = 0$ .

Finally, we end this section with two important remarks; first when we introduce dimensional regularization, in order to maintain dimensionless all the various quantities we need to introduce a new arbitrary scale of energy, the *factorization scale*. Therefore our final objects  $\hat{O}_{ij}$  and  $\Gamma^{(i)}$  (and  $f_j$ ) will in fact depend also on  $\mu_F^2$ . Then, in the factorization construction it is important to remember there is some arbitrariness in the choice of how much of the finite contributions is to be absorbed into the redefinition of the PDFs. Such a freedom, as for renormalization, takes the name of *factorization scheme* choice. The subtraction scheme is uniquely fixed by the exact definition of the action of the  $\epsilon$  projector  $\mathbb{P}_\epsilon$ . As an example, the projector given by Eq. (1.2.12) subtracts only the pure pole part, thus defining the MS scheme. However, a more common choice, which will be used throughout this thesis, is the so-called  $\overline{\text{MS}}$  scheme where also terms proportional to  $\gamma_E + \ln(4\pi)$  coming from angular integrations are systematically subtracted. This is achieved using the following definition for  $\mathbb{P}_\epsilon$ :

$$\mathbb{P}_\epsilon^{\overline{\text{MS}}} F = \sum_{n>0} \frac{1}{\epsilon^n} \left( \lim_{\epsilon \rightarrow 0} \epsilon^n F \right) \exp[\epsilon(-\gamma_E + \ln(4\pi))]. \quad (1.2.30)$$

In conclusion, in this section we have presented an heuristic demonstration of collinear factorization in the case of hadron-hadron collision at any order in  $\alpha_s$ , based on general ladder expansion (GLE). We proved that we can construct finite *infra-red and collinear safe* observable by factorizing into *bare* PDFs all the residual collinear singularities emerging from initial state radiation.

As well as providing solid grounds to Parton Model and Collinear Factorization Theorem, the same construction will be applied in Chap. 3 to resum leading logarithmic contribution in the high energy regime.

The last topic we need to describe about collinear factorization is the factorization scale dependence. This arbitrary scale was introduced in the process of regularization of collinear divergences and controls the hadron structure at different scale of distance. PDFs evolution will be the subject of the following subsection, which concludes our discussion about collinear factorization at high energy in QCD.

### 1.2.3 PDF Evolution: DGLAP Equations

In the previous sections, we describe how to introduce QCD radiative corrections inside the picture of Parton Model. In order to factorize all the divergences we have to introduce, in addition to renormalization scale, another arbitrary scale, the factorization one. Since it is an arbitrary scale we need to require that hadron observables should be independent from such a scale.

The requirement of scale independence for any hadronic observable brings to renormalization group equations also for PDFs. However, a general treatment of Callan-Symanzik equation in the context of factorization requires a general treatment about OPE expansion, and it will be beyond general scope of this thesis. Hence we are going to limit ourselves to present final results, referring interested reader to Refs. [10, 12].

The condition

$$\mu_F^2 \frac{\partial \mathcal{O}}{\partial \mu_F^2} = 0 \quad (1.2.31)$$

can be fulfilled by requiring that PDFs solve the following set of  $N_f + 1$  equations, known in literature as *Dokshitzer-Gribov-Lipatov-Altarelli-Parisi equations* (DGLAP) [20–22]:

$$\mu_F^2 \frac{\partial}{\partial \mu_F^2} \begin{pmatrix} q_i(x, \mu_F^2) \\ g(x, \mu_F^2) \end{pmatrix} = \int_0^1 \frac{d\xi}{\xi} \begin{pmatrix} P_{q_i, q_j} \left( \frac{x}{\xi}, \alpha_s(\mu_F^2) \right) & P_{q_i, g} \left( \frac{x}{\xi}, \alpha_s(\mu_F^2) \right) \\ P_{g, q_j} \left( \frac{x}{\xi}, \alpha_s(\mu_F^2) \right) & P_{g, g} \left( \frac{x}{\xi}, \alpha_s(\mu_F^2) \right) \end{pmatrix} \begin{pmatrix} q_j(\xi, \mu_F^2) \\ g(\xi, \mu_F^2) \end{pmatrix} \quad (1.2.32)$$

where the various  $P_{ij}$  composing the  $(N_f + 1) \times (N_f + 1)$  matrix are called *inclusive splitting functions* and control the universal collinear splitting of a parton  $i$  into a parton  $j$  and anything else. They admit a perturbative expansion in power of  $\alpha_s$ , leading to a perturbative solution of DGLAP equation. Expansion of the splitting function at leading order  $\mathcal{O}(\alpha_s)$  permits to recover the highest logarithm of the factorization scale in the PDFs (and hence in the partonic observable) at any order in  $\alpha_s$ . The introduction of further orders in the splitting functions permits to recover subleading logarithmic contributions.

It is important to note that the evolution of PDFs mixes the flavour of the partons. Hence talking about different partonic channels is meaningful only specifying the energy scale we are considering. It is only by taking the sum over all the possible flavours that we can be sure to have a subleading factorization scale dependence.

The explicit perturbative solution of Eq. (1.2.32), together with the expression for the leading order of the splitting function are collected in Appendix A.

However, up to now this remains only a theoretical discussion; we want now to present in the next section an explicit evaluation of the first radiative correction to a particular observable. Our desire is to see all this procedure at work, and to highlight cancellation of divergences in an explicit calculation.

## 1.3 Application: NLO Higgs Boson Production

Our aim in this section is to present in detail the computation of the first radiative correction to the Higgs Boson gluon fusion production process in the effective theory approach. This is the main production mechanism at LHC for the Higgs and we will come back to this particular process also in other applications through the thesis.

In the Standard Model, Higgs boson is mainly produced in gluon fusion through a quark loop as in Fig. 1.5 (left); since quark-Higgs coupling is proportional to the mass of the quark, major contribution comes from diagram where top quark circulates in the loop. We are now going to focus on the limit in which we can consider  $m_{\text{top}}^2 \gg m_{\text{H}}^2$ ; in this limit the loop shrinks to a point and we can write an effective pointlike interaction, as depicted in Fig. 1.5 (right). The interaction is controlled by the following effective Lagrangian:

$$\mathcal{L}_{\text{int}}^{\text{eff}} = \frac{\alpha_s}{12\pi v} C_W H G_{\mu\nu}^a G_a^{\mu\nu} \quad (1.3.1)$$

with  $C_W = 1 + \mathcal{O}(\alpha_s)$  Wilson coefficient of the effective interaction,  $H$  the Higgs field in unitary gauge and  $G_{\mu\nu}^a$  the gluon field tensor, Eq. (1.1.4). We summarize the new

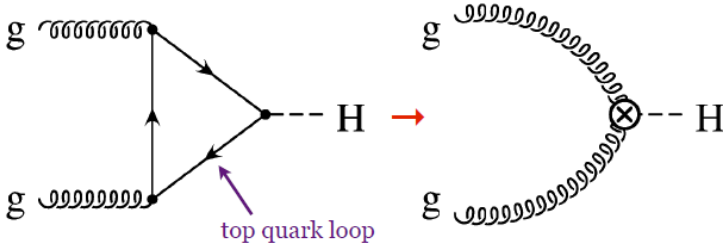


**Figure 1.5.** Feynman Diagrams contributing to gluon fusion Higgs production LO cross section, in Standard Model (left) and in EFT approach (right)

Feynman Rules, which arise from this effective interaction in Fig. 1.6<sup>6</sup>.

### 1.3.1 Leading order

We start our computation from leading order in  $\alpha_s$ . Since it will be useful for NLO computation, we are going to write it in  $d$  dimensions. At this order only one diagram contributes and it is depicted in Fig. 1.7.

The invariant matrix element is simply given by the effective vertex; then we can write:

$$\mathcal{M}_{\text{LO}} = i \frac{\alpha_s}{3\pi v} \epsilon_\alpha^a(p_1) \epsilon_\beta^b(p_2) \left( (p_1 \cdot p_2) g^{\alpha\beta} - p_1^\beta p_2^\alpha \right) \delta^{ab}. \quad (1.3.5)$$

Now, we square the matrix element and we perform the sum and the average over colour and polarizations of the initial states. In performing the sum we have to remember that in QCD

$$\sum \epsilon_\mu^m(p) \epsilon_\nu^n(\bar{p}) = \left( -g^{\mu\nu} + \frac{p^\mu \bar{p}^\nu + p^\nu \bar{p}^\mu}{(p \cdot \bar{p})} \right) \delta^{mn} \quad (1.3.6)$$

with  $p^\mu = (|\mathbf{p}|, \mathbf{p})$ ,  $\bar{p}^\mu = (|\mathbf{p}|, -\mathbf{p})$ .

We thus obtain in this case

$$\frac{1}{256(1-\epsilon)^2} \sum |\mathcal{M}_{\text{LO}}|^2 = \frac{\alpha_s^2}{9\pi^2 v^2} \frac{1}{256(1-\epsilon)^2} 16(1-\epsilon)(p_1 \cdot p_2)^2 = \frac{\alpha_s^2}{576\pi^2 v^2 (1-\epsilon)} s^2 \quad (1.3.7)$$

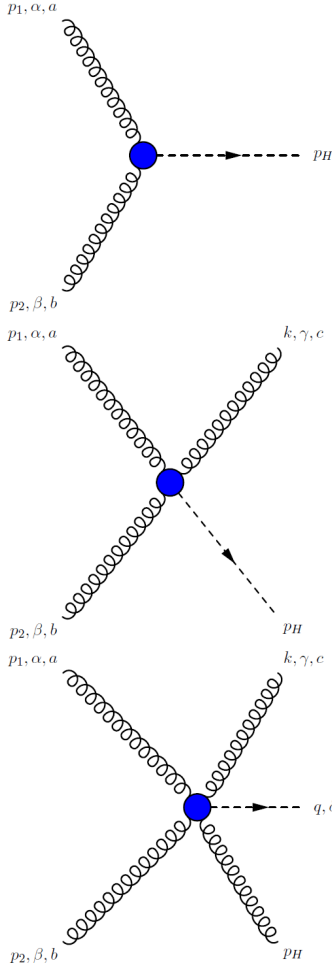
where in the second step we use the definition of the Mandelstam variable  $s = (p_1 + p_2)^2$ .

The phase space for this process turns out to be trivial, since it is a  $2 \rightarrow 1$  process:

$$d\Phi = \frac{d^{d-1} p_H}{(2\pi)^{d-1} 2m_H} (2\pi)^d \delta^{(d)}(p_1 + p_2 - p - H) = \frac{\pi}{m_H} \delta(\sqrt{s} - m_H) = \frac{2\pi}{s} \delta(1 - \hat{\tau}), \quad (1.3.8)$$

with  $\hat{\tau} = \frac{m_H^2}{s}$ .

<sup>6</sup>all momenta are supposed as incoming



$$-i \frac{\alpha_s}{3\pi v} \left( (p_1 \cdot p_2) g^{\alpha\beta} - p_1^\beta p_2^\alpha \right) \delta^{ab} \quad (1.3.2)$$

$$\frac{\alpha_s \sqrt{4\pi\alpha_s}}{3\pi v} f^{abc} \left[ (p_1 - p_2)^\gamma g^{\alpha\beta} + (p_2 - k)^\alpha g^{\beta\gamma} + (k - p_1)^\beta g^{\alpha\gamma} \right] \quad (1.3.3)$$

$$-i \frac{4\alpha_s^2}{3v} \left[ f_{eab} f_{ecd} (g^{\alpha\gamma} g^{\beta\delta} - g^{\alpha\delta} g^{\beta\gamma}) + f_{eac} f_{ebd} (g^{\alpha\beta} g^{\gamma\delta} - g^{\alpha\delta} g^{\beta\gamma}) + f_{ead} f_{ebc} (g^{\alpha\beta} g^{\gamma\delta} - g^{\alpha\gamma} g^{\beta\delta}) \right] \quad (1.3.4)$$

**Figure 1.6.** Effective Feynman Rules when  $m_{\text{top}}$  is integrated out.

Adding the matrix element of Eq. (1.3.7) and the flux factor, we come to the final expression for the Higgs boson production cross section at LO:

$$\sigma_{\text{LO}}(\hat{\tau}) = \frac{\alpha_s^2}{576\pi v^2 (1 - \epsilon)} \delta(1 - \hat{\tau}) = \sigma_0 \delta(1 - \hat{\tau}). \quad (1.3.9)$$

which reduces in four dimension to

$$\sigma_{\text{LO}}(\hat{\tau}) = \frac{\alpha_s^2}{576\pi v^2} \delta(1 - \hat{\tau}) \quad (1.3.10)$$

Now we want to move to the computation of the first radiative correction, the NLO contribution. In this case we have to evaluate separately virtual and real diagrams in a particular regularization scheme in order to highlight divergences. We decide to proceed in the next subsections working in dimensional regularization, which is one of the most common regularization procedures applied in literature.

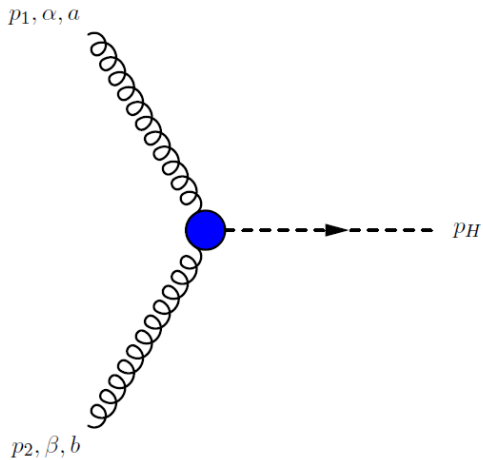


**Figure 1.7.** Feynman Diagram which contributes to LO EFT Higgs boson production

At NLO, other partonic channels start to contribute to the total cross section, the quark-gluon and the quark-antiquark channels. However, since the singularity structure of these new partonic contributions is almost trivial, we will concentrate only on the pure gluonic channel leaving to the interested reader the computation of the other terms. Explicit results can be found for example in the original Ref. [27].

### 1.3.2 Virtual Contribution

We start our NLO computation from the one-loop virtual contribution to the process  $gg \rightarrow H$ , the only non-zero channel at LO.

One-loop diagrams which contribute at this order are depicted in Fig. 1.8. Associated matrix elements are the following:

$$\begin{aligned} \mathcal{M}_{\text{tri}} = & \frac{4\alpha_s^3}{3v} C_A \epsilon_\alpha^a(p_1) \epsilon_\beta^b(p_2) \delta^{ab} \int \frac{d^d k}{(2\pi)^d} \frac{1}{(p_1 + k)^2 (p_2 - k)^2 k^2} \\ & \left[ (2p_1 + k)^\lambda g^{\alpha\mu} - (2k + p_1)^\alpha g^{\mu\lambda} + (k - p_1)^\mu g^{\alpha\lambda} \right] \\ & \left[ (2p_2 - k)_\lambda g^{\beta\nu} + (2k - p_2)^\beta g_\lambda^\nu - (k + p_2)_\nu g_\lambda^\beta \right] \\ & \left[ ((p_1 + k) \cdot (p_2 - k)) g_{\mu\nu} - (p_1 + k)_\nu (p_2 - k)_\mu \right], \end{aligned} \quad (1.3.11)$$

$$\begin{aligned} \mathcal{M}_{\text{bub}} = & \frac{4\alpha_s^2}{3v} C_A \epsilon_\alpha^a(p_1) \epsilon_\beta^b(p_2) \delta^{ab} \int \frac{d^d k}{(2\pi)^d} \frac{1}{k^2 (p_1 + p_2 - k)^2} \\ & \left[ 2g^{\alpha\beta} g^{\gamma\delta} - g^{\alpha\delta} g^{\beta\gamma} - g^{\alpha\gamma} g^{\beta\delta} \right] \\ & \left[ (k \cdot (p_1 + p_2 - k)) g_{\delta\gamma} - k_\delta (p_1 + p_2 - k)_\delta \right]. \end{aligned} \quad (1.3.12)$$

By performing a few simplifications and the decomposition of the tensor integrals appearing in the amplitudes, we can express the result in terms of the following two scalar

integrals

$$\mu^{2\epsilon} \int \frac{d^d k}{(2\pi)^d} \frac{1}{k^2 (k - p_1 - p_2)^2} = (4\pi)^\epsilon \frac{\Gamma(1+\epsilon) \Gamma(1-\epsilon)^2}{\Gamma(1-2\epsilon)} \left(\frac{\mu^2}{m_H^2}\right)^\epsilon \left(\frac{1}{\epsilon} + 2\right) \quad (1.3.13)$$

$$\mu^{2\epsilon} \int \frac{d^d k}{(2\pi)^d} \frac{1}{k^2 (p_1 + k)^2 (k - p_2)^2} = (4\pi)^\epsilon \frac{\Gamma(1+\epsilon) \Gamma(1-\epsilon)^2}{\Gamma(1-2\epsilon)} \frac{1}{2m_H^2} \left(\frac{\mu^2}{m_H^2}\right)^\epsilon \left(\frac{2}{\epsilon^2} - \pi^2\right); \quad (1.3.14)$$

then taking the interference between these virtual corrections and the Born diagram, we come to the following results for the two contributions

$$\begin{aligned} \hat{\sigma}_{\text{tri}} &= \sigma_0 \delta(1 - \hat{\tau}) \left[ \frac{\alpha_s}{2\pi} C_A \left(\frac{4\pi\mu^2}{m_H^2}\right)^\epsilon \frac{\Gamma(1+\epsilon) \Gamma(1-\epsilon)^2}{\Gamma(1-2\epsilon)} \left(-\frac{2}{\epsilon^2} + \frac{10}{3\epsilon} + \frac{179}{36} + \pi^2\right) \right], \\ \hat{\sigma}_{\text{bub}} &= \sigma_0 \delta(1 - \hat{\tau}) \left[ \frac{\alpha_s}{2\pi} C_A \left(\frac{4\pi\mu^2}{m_H^2}\right)^\epsilon \frac{\Gamma(1+\epsilon) \Gamma(1-\epsilon)^2}{\Gamma(1-2\epsilon)} \left(-\frac{10}{3\epsilon} - \frac{179}{36}\right) \right] \end{aligned} \quad (1.3.15)$$

with  $\sigma_0$  coefficient of the Born cross section in  $d$  dimension defined in Eq. (1.3.9).

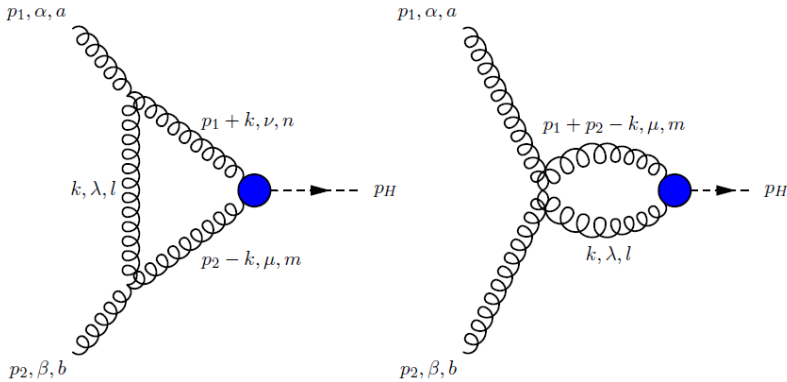


**Figure 1.8.** NLO virtual contribution to the LO gluon fusion process.

Summing over the diagrams, we obtain the following result for the virtual contribution:

$$\hat{\sigma}_{\text{virt}} = \sigma_0 \delta(1 - \hat{\tau}) \left[ \frac{\alpha_s}{2\pi} C_A \left(\frac{4\pi\mu^2}{m_H^2}\right)^\epsilon \frac{\Gamma(1+\epsilon) \Gamma(1-\epsilon)^2}{\Gamma(1-2\epsilon)} \left(-\frac{2}{\epsilon^2} + \pi^2\right) \right]. \quad (1.3.16)$$

As we expect, virtual contribution alone is divergent in  $d = 4$  dimension. The double pole in  $\epsilon$  we found means we are hitting the soft and collinear divergence of the process. In our general discussion of Sec. 1.2.1, we have learned these singularities have to cancel against real contribution as stated by the *Kinoshita-Lee-Nauenberg theorem*. We are going to prove this statement by computing in the next subsection real emission correction for this process.

### 1.3.3 Real Contribution

So far we have considered the virtual NLO contribution to the gluon fusion Higgs production process. We have found it divergent; this is understood and expected, since we have to consider also the real emission of a new parton. Hence we are going to compute at the first not trivial order the following partonic process:

$$g(p_1) + g(p_2) \rightarrow g(k) + H(p_H). \quad (1.3.17)$$

Even this contribution we know to be divergent when the emitted gluon becomes soft and/or collinear. General analysis presented in Sec. 1.2.1 states it is only the sum between the real and the virtual contribution which turns out to be finite. For this reason we are going to perform all the calculations in  $d$  dimensions, using dimensional regularization, as already done in virtual computation.

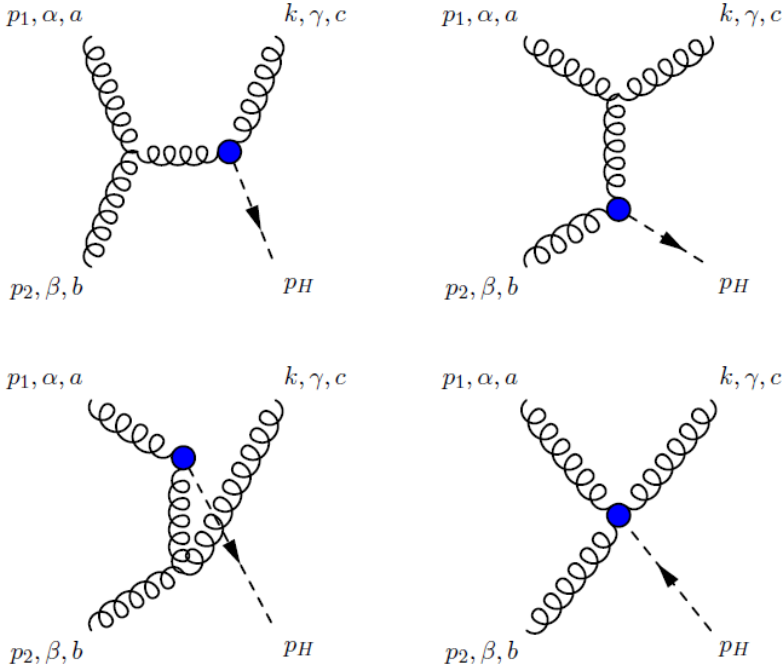


**Figure 1.9.** Feynman Diagram real contributions to  $g + g \rightarrow H + g$

Diagrams which contribute at this order are depicted in Fig. 1.9. The associated invariant matrix elements are the following:

$$\begin{aligned} \mathcal{M}_s = \frac{2\alpha_s^{\frac{3}{2}}}{3\sqrt{\pi}sv} f^{abc} & \left[ -p_2^\gamma \left( t g^{\alpha\beta} + 2k^\alpha p_1^\beta \right) + p_2^\alpha \left( (t+u) g^{\beta\gamma} + 2k^\beta (p_1^\gamma + p_2^\gamma) \right) \right. \\ & \left. + p_1^\gamma \left( u g^{\alpha\beta} - 2k^\alpha p_1^\beta \right) - (t+u) p_1^\beta g^{\alpha\gamma} \right] \epsilon_\alpha^a(p_1) \epsilon_\beta^b(p_2) \epsilon_\gamma^c(k) \quad (1.3.18a) \end{aligned}$$

$$\mathcal{M}_t = \frac{2\alpha_s^{\frac{3}{2}}}{3\sqrt{\pi}tv} f^{abc} \left[ p_1^\gamma \left( (s+u) g^{\alpha\beta} + 2p_2^\alpha \left( k^\beta - p_1^\beta \right) \right) + k^\alpha \left( (s+u) g^{\beta\gamma} + 2p_2^\gamma \left( k^\beta - p_1^\beta \right) \right) \right]$$

$$-g^{\alpha\gamma} \left( sk^\beta + up_1^\beta \right) \left] \epsilon_\alpha^a(p_1) \epsilon_\beta^b(p_2) \epsilon_\gamma^c(k) \quad (1.3.18b)$$

$$\begin{aligned} \mathcal{M}_u = \frac{2\alpha_s^{\frac{3}{2}}}{3\sqrt{\pi}uv} f^{abc} & \left[ k^\alpha \left( sg^{\beta\gamma} - 2 \left( k^\beta p_1^\gamma + p_1^\beta p_2^\gamma \right) \right) + p_2^\alpha \left( tg^{\beta\gamma} + 2k^\beta p_1^\gamma + 2p_1^\beta p_2^\gamma \right) \right. \\ & \left. - (s+t) \left( k^\beta g^{\alpha\gamma} + p_2^\gamma g^{\alpha\beta} \right) \right] \epsilon_\alpha^a(p_1) \epsilon_\beta^b(p_2) \epsilon_\gamma^c(k) \quad (1.3.18c) \end{aligned}$$

$$\begin{aligned} \mathcal{M}_x = \frac{2\alpha_s^{\frac{3}{2}}}{3\sqrt{\pi}v} f^{abc} & \left[ -g^{\alpha\gamma} \left( k^\beta + p_1^\beta \right) + g^{\beta\gamma} \left( k^\alpha + p_2^\alpha \right) + g^{\alpha\beta} \left( p_1^\gamma - p_2^\gamma \right) \right] \\ & \epsilon_\alpha^a(p_1) \epsilon_\beta^b(p_2) \epsilon_\gamma^c(k) \quad (1.3.18d) \end{aligned}$$

with Mandelstam variables defined as

$$s = (p_1 + p_2)^2 \quad t = (p_1 - k)^2 \quad u = (p_2 - k)^2, \quad (1.3.19)$$

and momentum conservation imposed by the requirement  $s + t + u = m_H^2$ .

Now summing over final polarizations, and averaging over initial polarizations, we write the square modulus of  $\mathcal{M} = \mathcal{M}_s + \mathcal{M}_t + \mathcal{M}_u + \mathcal{M}_x$  as

$$\begin{aligned} \frac{1}{256(1-\epsilon)^2} \sum |\mathcal{M}|^2 &= \frac{\alpha_s^3 C_A}{72\pi v^2 (1-\epsilon)^2} \\ & \left[ \frac{M^8 + s^4 + t^4 + u^4}{stu} (1-2\epsilon) + \frac{\epsilon}{2} \frac{(M^4 + s^2 + t^2 + u^2)^2}{stu} \right] \quad (1.3.20) \end{aligned}$$

where we define the dimension  $d = 4 - 2\epsilon$  as in virtual computation.

The phase space for the real emission is a two-body phase space, which takes the form in  $d$  dimension

$$\begin{aligned} d\Phi_2(p_1, p_2, p_H, k) &= \frac{d^{d-1}p_H}{(2\pi)^{d-1} 2E_H} \frac{d^{d-1}k}{(2\pi)^{d-1} 2k} (2\pi)^d \delta^{(d)}(p_1 + p_2 - p_H - k) \\ &= \left( \frac{4\pi\mu^2}{m_H^2} \right)^\epsilon \frac{\hat{\tau}(\xi_p)^{-\epsilon} d\xi_p}{4\pi\Gamma(1-\epsilon) \sqrt{(1-\hat{\tau})^2 - 4\hat{\tau}\xi_p}} \quad (1.3.21) \end{aligned}$$

where we parametrize the kinematics w.r.t. the following dimensionless ratios,  $\hat{\tau} = \frac{m_H^2}{s}$  and  $\xi_p = \frac{p_T^2}{m_H^2}$  ( $p_T^2$  is the Higgs transverse momentum).

Now we are ready to write the real contribution to the total cross section. We thus write:

$$\begin{aligned} d\sigma_{\text{real}} &= \sigma_0 \left( \frac{\alpha_s}{2\pi} C_A \left( \frac{4\pi\mu^2}{m_H^2} \right)^\epsilon \frac{\Gamma(1+\epsilon)\Gamma(1-\epsilon)^2}{\Gamma(1-2\epsilon)} \right) \frac{1}{\xi_p^{1+\epsilon} \sqrt{(1-\hat{\tau})^2 - 4\hat{\tau}\xi_p}} \\ & \left[ 4(1-\hat{\tau}+\hat{\tau}^2)^2 - 8\xi_p\hat{\tau}(1-\hat{\tau})^2 + 4\xi_p^2\hat{\tau}^2 - 8\xi_p\hat{\tau}^2\epsilon - 8\xi_p\hat{\tau}^2\epsilon^2 \right] d\xi_p + \mathcal{O}(\epsilon^3) \quad (1.3.22) \end{aligned}$$

Now, after the computation of virtual and real contributions, we are going to combine these results to form our final prediction for the NLO term. We have preferred not to

perform  $\xi_p$  integration yet, since cancellation of divergences at differential level is, in some sense tricky and we want to present it explicitly. Furthermore, this permits us to show a very important point for the discussion we are going to take in Chap. 2 about threshold limit at differential level. We are going to present explicit expressions both for the total cross section and for the transverse momentum distribution in the next subsection.

### 1.3.4 NLO transverse momentum distribution and total cross section

Next-to-leading order results are achieved by combining real and virtual contributions. We start from the transverse momentum distribution and we will recover the total cross section at the end by performing integration over  $p_T^2$  (hence  $\xi_p$ ). We obtain in  $d = 4 - 2\epsilon$  dimension:

$$\begin{aligned} \frac{d\sigma^{\text{NLO}}}{d\xi_p}(\hat{\tau}, \xi_p) &= \sigma_0 \left( \frac{\alpha_s}{\pi} C_A \left( \frac{4\pi\mu^2}{m_H^2} \right)^\epsilon \frac{\Gamma(1+\epsilon)\Gamma(1-\epsilon)^2}{\Gamma(1-2\epsilon)} \right) \\ &\quad \left\{ \delta(1-\hat{\tau})\delta(\xi_p) \left[ -\frac{1}{\epsilon^2} + 3\zeta_2 \right] + \frac{2(1-\hat{\tau}+\hat{\tau}^2)^2 - 4\xi_p\hat{\tau}(1-\hat{\tau})^2 + 2\xi_p^2\hat{\tau}^2}{\xi_p^{1+\epsilon}\sqrt{(1-\hat{\tau})^2 - 4\hat{\tau}\xi_p}} \right\} \\ &\quad + \mathcal{O}(\epsilon) \end{aligned} \tag{1.3.23}$$

where we ignore terms proportional to  $\epsilon\xi_p$  since they do not contribute to the final result.

Now we are ready to take in Eq. (1.3.23) the limit  $\epsilon \rightarrow 0$ ; the choice of the transverse momentum to parametrize our kinematics, however, makes this expansion highly non-trivial. Indeed our expression Eq. (1.3.23) is soft and collinear divergent in the  $\xi_p^{1+\epsilon}$  factor but also threshold divergent due to the presence of the square root. At first sight, square root may seem integrable but this is not the case. In fact when the Higgs boson becomes collinear or soft, an extra threshold divergence in  $\hat{\tau} \rightarrow 1$  arises at denominator. This makes the  $\epsilon \rightarrow 0$  expansion highly not trivial and moreover it leaves us the following important message: the pure threshold and the soft-collinear limit for transverse momentum distributions are intrinsically different, since threshold divergences may be screened by the finite value of  $p_T$  (or  $\xi_p$ ).

To reach our desired NLO correction, we need to highlight threshold divergence before taking the limit  $\epsilon \rightarrow 0$ . Therefore, we exploit Eq. (B.3.11) to highlight the soft and collinear divergence

$$\frac{1}{\sqrt{(1-\hat{\tau})^2 - 4\hat{\tau}\xi_p}} = \frac{1}{\left[ \sqrt{(1-\hat{\tau})^2 - 4\hat{\tau}\xi_p} \right]_+^a} + \frac{1}{2}\delta(a(\xi_p) - \hat{\tau})[-\ln\xi_p + \ln(1+\xi_p)] \tag{1.3.24}$$

with  $a(\xi_p) = (\sqrt{1+\xi_p} - \sqrt{\xi_p})^2$ , and we rewrite Eq. (1.3.23) as

$$\frac{d\sigma^{\text{NLO}}}{d\xi_p}(\hat{\tau}, \xi_p) = \sigma_0 \left( \frac{\alpha_s}{\pi} C_A \left( \frac{4\pi\mu^2}{m_H^2} \right)^\epsilon \frac{\Gamma(1+\epsilon)\Gamma(1-\epsilon)^2}{\Gamma(1-2\epsilon)} \right)$$

$$\begin{aligned}
& \left\{ \delta(1-\hat{\tau}) \delta(\xi_p) \left[ -\frac{1}{\epsilon^2} + 3\zeta_2 \right] + \frac{2(1-\hat{\tau} + \hat{\tau}^2)^2 - 4\xi_p \hat{\tau} (1-\hat{\tau})^2 + 2\xi_p^2 \hat{\tau}^2}{\xi_p^{1+\epsilon} \left[ \sqrt{(1-\hat{\tau})^2 - 4\hat{\tau}\xi_p} \right]_+^a} \right. \\
& \left. - \delta(a(\xi_p) - \hat{\tau}) a(\xi_p)^2 (1 + 8\xi_p + 9\xi_p^2) \left[ \frac{\ln \xi_p}{\xi_p^{1+\epsilon}} - \frac{\ln(1+\xi_p)}{\xi_p} \right] \right\} \\
& + \mathcal{O}(\epsilon). \tag{1.3.25}
\end{aligned}$$

The  $\epsilon \rightarrow 0$  limit can now be taken using the following expansion

$$\frac{1}{\xi_p^{1+\epsilon}} = -\frac{1}{\epsilon} \delta(\xi_p) + \left[ \frac{1}{\xi_p} \right]_+ + \mathcal{O}(\epsilon), \tag{1.3.26a}$$

$$\frac{\ln \xi_p}{\xi_p^{1+\epsilon}} = -\frac{1}{\epsilon^2} \delta(\xi_p) + \left[ \frac{\ln \xi_p}{\xi_p} \right]_+ + \mathcal{O}(\epsilon), \tag{1.3.26b}$$

with plus distribution defined as in Eq. (B.3.1) with  $\xi_{\max} = \frac{(1-\hat{\tau})^2}{4\hat{\tau}}$ . More details about plus distribution properties are collected in Appendix B. Inserting Eqs. (1.3.26) into Eq. (1.3.25) we obtain:

$$\begin{aligned}
\frac{d\sigma^{\text{NLO}}}{d\xi_p}(\hat{\tau}, \xi_p) &= \sigma_0 \left( \frac{\alpha_s}{\pi} \left( \frac{4\pi\mu^2}{m_H^2} \right)^\epsilon \right) \left\{ \delta(\xi_p) \left[ -\frac{1}{\epsilon} \frac{2C_A (1-\hat{\tau} + \hat{\tau}^2)^2}{(1-\hat{\tau})_+^z} + 3C_A \zeta_2 \delta(1-\hat{\tau}) \right] \right. \\
&+ \frac{2C_A (1-\hat{\tau} + \hat{\tau}^2)^2}{\left[ \sqrt{(1-\hat{\tau})^2 - 4\hat{\tau}\xi_p} \right]_+^a} \left[ \frac{1}{\xi_p} \right]_+ - \frac{4C_A \hat{\tau} (1-\hat{\tau})^2 - 2C_A \xi_p \hat{\tau}^2}{\sqrt{(1-\hat{\tau})^2 - 4\hat{\tau}\xi_p}} \\
&\left. - \delta(a(\xi_p) - \hat{\tau}) a(\xi_p)^2 C_A (1 + 4\xi_p)^2 \left[ \left[ \frac{\ln \xi_p}{\xi_p} \right]_+ - \frac{\ln(1+\xi_p)}{\xi_p} \right] \right\} \\
&+ \mathcal{O}(\epsilon). \tag{1.3.27}
\end{aligned}$$

As we expect, the double pole directly cancels between virtual and real contributions; instead a single collinear pole remains in our final result which has to be factorized into the gluon PDF. Applying  $\overline{\text{MS}}$  subtraction, we add to our NLO correction the following Altarelli-Parisi term

$$\frac{d\sigma_{\text{AP}}^{\text{NLO}}}{d\xi_p}(\hat{\tau}, \xi_p) = \sigma_0 \frac{\alpha_s(m_H^2)}{\pi} \hat{\tau} P_{gg}^{(0)}(\hat{\tau}) \frac{1}{\epsilon} \left( \frac{4\pi\mu^2}{m_H^2} \right)^\epsilon \tag{1.3.28}$$

with  $P_{gg}^{(0)}$  given by Eq. (A.2.8); furthermore we change in Eq. (1.3.27) fixed coupling  $\alpha_s$  with running coupling  $\alpha_s(m_H^2)$

$$\alpha_s = \alpha_s(m_H^2) \left( 1 - \frac{\alpha_s(m_H^2)}{\pi} \left( \frac{\mu^2}{m_H^2} \right)^\epsilon \frac{\beta_0}{\epsilon} \right). \tag{1.3.29}$$

For simplicity we have set factorization and renormalization scale equal to the hard scale  $m_H^2$ . All poles now cancel and we can set  $\epsilon = 0$  to reach the final result for the first

radiative correction to the EFT Higgs boson production process

$$\begin{aligned} \frac{d\sigma^{\text{NLO}}}{d\xi_p}(\hat{\tau}, \xi_p) = \sigma_0 \frac{\alpha_s(m_H^2)}{\pi} \left\{ 3C_A \zeta_2 \delta(\xi_p) \delta(1 - \hat{\tau}) \right. \\ + \frac{2C_A (1 - \hat{\tau} + \hat{\tau}^2)^2}{\left[ \sqrt{(1 - \hat{\tau})^2 - 4\hat{\tau}\xi_p} \right]_+^a} \left[ \frac{1}{\xi_p} \right]_+ - \frac{4C_A \hat{\tau} (1 - \hat{\tau})^2 - 2C_A \xi_p \hat{\tau}^2}{\sqrt{(1 - \hat{\tau})^2 - 4\hat{\tau}\xi_p}} \\ \left. - \delta(a(\xi_p) - \hat{\tau}) a(\xi_p)^2 C_A (1 + 4\xi_p)^2 \left[ \left[ \frac{\ln \xi_p}{\xi_p} \right]_+ - \frac{\ln(1 + \xi_p)}{\xi_p} \right] \right\}. \quad (1.3.30) \end{aligned}$$

We have concluded our calculation. We proved in a concrete example that the cancellation of collinear and soft divergences really occurs as long as we factorized single collinear initial state divergence into renormalized PDF. The result we have just obtained constitutes the NLO correction to the Higgs boson production in the parton channel gluon-gluon. Let us remind you that in order to reach the complete NLO correction to the EFT Higgs boson production process, one should add also the other two parton channel contributions: the quark-gluon and the quark-antiquark. Their expressions can be found for example in Ref. [27].

In Chap. 2 and Chap. 3 we are going to write for the gluon-gluon parton channel of this process, all order expressions in the limits  $\hat{\tau} \rightarrow a(\xi_p)$ <sup>7</sup>,  $\xi_p \rightarrow 0$  and  $\hat{\tau} \rightarrow 0$ : you can any time check that NLO expansion should coincide with corresponding limit of Eq. (1.3.30).

Before ending our discussion about NLO EFT Higgs boson production in gluon fusion, we want to write the corresponding correction for the total cross section. We then integrate Eq. (1.3.30) over  $\xi_p$  obtaining

$$\begin{aligned} \sigma_{\text{NLO}}(\hat{\tau}) = \sigma_0 \frac{\alpha_s(m_H^2)}{\pi} \left\{ 2C_A \zeta_2 \delta(1 - \hat{\tau}) + 4C_A (1 - \hat{\tau} + \hat{\tau}^2)^2 \left( \frac{\ln(1 - \hat{\tau})}{1 - \hat{\tau}} \right)_+^z \right. \\ \left. - \frac{2C_A (1 - \hat{\tau} + \hat{\tau}^2)^2 \ln \hat{\tau}}{1 - \hat{\tau}} - \frac{11}{6} C_A (1 - \hat{\tau})^3 \right\}, \quad (1.3.31) \end{aligned}$$

which clearly turns out to be equal to the one evaluated in literature, for example in Ref. [27]. To reach Eq. (1.3.31) we use the following result

$$\begin{aligned} \int_0^{\frac{(1-\hat{\tau})^2}{4\hat{\tau}}} d\xi_p \left\{ \frac{1}{\left[ \sqrt{(1 - \hat{\tau})^2 - 4\xi_p \hat{\tau}} \right]_+^a} \left[ \frac{1}{\xi_p} \right]_+ - \frac{1}{2} \delta(a(\xi_p) - \hat{\tau}) \left[ \left[ \frac{\ln \xi_p}{\xi_p} \right]_+ - \frac{\ln(1 + \xi_p)}{\xi_p} \right] \right\} \\ = -\frac{\zeta_2}{2} \delta(1 - \hat{\tau}) + 2 \left( \frac{\ln(1 - \hat{\tau})}{1 - \hat{\tau}} \right)_+^z - \frac{\ln \hat{\tau}}{1 - \hat{\tau}}, \quad (1.3.32) \end{aligned}$$

which can be proved using plus distribution properties described in Appendix B.

<sup>7</sup>which means  $x \rightarrow 1$  with  $x$  defined as in Eq. (1.4.10)

We conclude our general introduction to perturbative QCD; we have explained in detail why perturbation theory can be applied at high energy even for a strong interacting theory, and what are the ground rules of such calculations. Moreover, we have presented one of this calculation for an important process in modern collider physics.

Last section of this chapter wants to be an introduction to all the other topics of this thesis. We are going to present base notations and definitions we are going to extensively use, together with general ideas which are behind resummation theories in general.

## 1.4 Resummations in a nutshell: ideas and notations

The main topic of this thesis is resummation, and in particular resummation for transverse momentum distributions. Therefore, we want now to highlight the reason why we study these theories, and the general ideas and approaches in this field.

In Sec. 1.1.1, we presented asymptotic freedom of QCD: at high energies the strong coupling becomes weaker and weaker, thus permitting the convergence, at least asymptotically, of the perturbative series.

However, it turns out that any perturbation series in QCD is only asymptotically convergent; this means that higher orders provide great corrections to the final result and the knowledge of only one or two terms of the series is not enough to properly approximate observables. On one hand, computations of radiative corrections is necessary in QCD to obtain reliable predictions for the processes we are interested in; on the other hand, since we need to be rather "inclusive" in our evaluation to cancel all the IR divergences, the evaluation of QCD series terms is in many cases very cumbersome, since we have to deal with an enormous amount of diagrams.

In recent years, great efforts have been made in order to automatize Feynman diagrams calculations, and now all the important processes in collider physics are known at NNLO accuracy, thus including the first two radiative correction to Born level.

Unfortunately, technical difficulties of fixed order calculations are not the only problem we must concerns ourselves with in providing predictions in QCD.

Consider the perturbation series for a general observable:

$$\mathcal{O} = \mathcal{O}^{(0)} + \alpha_s \mathcal{O}^{(1)} + \alpha_s^2 \mathcal{O}^{(2)} + \dots \quad (1.4.1)$$

Any perturbative coefficient  $\mathcal{O}^{(i)}$  is going to depend on the various scales of energy characterizing the process and the observable (centre of mass energy, invariant mass of the final state, quark masses, transverse momentum...). Usually, in considering exclusive observables such as transverse momentum distribution, more than one scales of energy is involved. In this situation, perturbative coefficients show a logarithmic dependence from the ratios of these different scales, order by order in  $\alpha_s$ . We have already seen two example of this behaviour: to deal with divergences in loop calculations, we are forced to introduce two new arbitrary scales of energy, the *renormalization and factorization scales*. At the end, perturbative coefficients acquire exactly a logarithmic dependence like  $\ln \frac{\mu_R^2}{Q^2}$  or  $\ln \frac{\mu_F^2}{Q^2}$  with  $Q^2$  a common hard scale of the process.

Moreover, we have already presented an example in the introduction regarding provide colour singlet production

$$h_1 + h_2 \rightarrow \mathcal{S} + X. \quad (1.4.2)$$

Let us remind the main points. This process is characterized in general by three scales of energy, the centre of mass energy  $s$ , the invariant mass of the system  $\mathcal{S}$ ,  $Q^2$ , and  $E_r$ . an energy scale associated to the extra radiation  $X$ . Therefore, at any order in  $\alpha_s$ , perturbative coefficients are going to show logarithms of the following ratios:

$$\frac{Q^2}{s} \qquad \frac{E_r}{s}. \quad (1.4.3)$$

This consideration highlights a problem in our perturbative expansion. Referring to this last example, you can easily convince yourself that there are some particular kinematic configurations where these logarithms become large, so large that the product

$$\alpha_s \ln R \sim 1 \qquad \text{if } R \rightarrow 0 \text{ or } R \rightarrow \infty \quad (1.4.4)$$

becomes of order 1 thus destroying our perturbative expansion. In Eq. (1.4.4), we call  $R$  one of the two ratios presented in Eq. (1.4.3).

In such cases, only a prediction which takes into account all these contributions at all orders in  $\alpha_s$  can provide a reliable approximation for the exact result. Theories which permits to predict and evaluate the sum of logarithmic divergent contributions at any order in  $\alpha_s$  for a particular observable are called *resummation theories*.

In general, a resummation theory studies a particular limit of a particular observable and permits to resum an unique class of logarithms. However, general technique exists to derive a new resummation prescription. To perform a resummation of some components, we need some sort of *re-factorization*. It must be true, in the limit we are interested in, that partonic observable presents a new factorization property (in addition to standard collinear factorization), which permits to divide  $\hat{\mathcal{O}}_{ij}$  into the product of a process dependent part (normally called *hard part*) and universal factors which controls dynamics of the divergent contributions.

There are in literature different approaches to derive a *re-factorization*. We can essentially group all existing resummation theories in three different approaches:

- Conjugate space approach,
- Effective Theory approach,
- Monte Carlo approach.

These three approaches differ in the way the observable factorization is derived from matrix element factorization, which must be a prerequisite for any resummation theory.

In the first approach, factorization is shown directly by computing phase space measure for a general process with  $n$  new emitted partons in the final state. A general recursive condition is then found for the whole observable, both matrix element and phase space. This recursion relates complicate diagrams to combination of simpler configurations. Examples of such approach in deriving resummation theories could be found in

Refs. [28–32]. This will be the approach we are going to follow in all the rest of the thesis and we will see that can be applied in many different situations. The most important point of this approach is the requirement of factorization of both matrix elements and phase space; in particular, phase space factorization usually require the definition of appropriate transformation to factorize momentum delta conservation (Fourier transform, Laplace transform...). Resummation is thus performed in conjugate space and final result is then obtained by performing the inverse transform. Inverse transformation of resummed result is far to be trivial and it requires some care; this will be one of the subjects of Chap. 4, where phenomenological consequences are derived.

Main advantage of this technique is the production of a total analytic result and the rather compact expression of the latter. Furthermore, since the analytic structure is totally under control, analytic continuation can extend the goodness of the resummation even outside the kinematic region where it is truly derived. On the contrary, disadvantages are the requirement of a final inverse transform to obtain the real prediction, and the necessity to reformulate factorization for any different observables and limits.

In the second approach, factorization is performed using effective field theory [33–38] which approximates QCD in the limit we are studying. EFT permits to separate regions and modes which contributes in a particular process and are very powerful tools to derive factorization properties. On the contrary, they need to introduce arbitrary parameters which separate various scale of energies. The impact of subleading effects due to these different scales is not totally understood and under control. However, among other theories, *Soft-Collinear-Effective Theory* (SCET) has reached important results, and confirmed in many cases the effects already derived in conjugate space.

The main advantage of SCET is the possibility to study with relative ease multi-scale problem with high multiplicity, and to derive results directly in momentum space. On the contrary, final result turn out to depend from many different arbitrary scale. This fact may increase the error due to subleading contributions. We are going to mention for any resummation presented in this thesis, th parallel derivation, if any, performed in SCET; however, we will refer to original papers and we will not enter in the discussion of this alternative proof.

Very recently [39–44] a different idea was proposed to tackle problem of factorization. For some observables which fulfil particular condition about the kinematic limit we are going to study<sup>8</sup>, is possible to divide total phase space of radiation in two regions: a resolved region and an unresolved one. Complete analytic resummation turn out to be necessary in this approach only in the unresolved region where, however, we can use a phase space of totally uncorrelated emission, thus preventing us to use conjugate space definition to factorize it. Factorization is then trivial to these observable in the unresolved region, and analytic resummation is possible for this type of radiation directly in momentum space. Instead in the resolved region we do not need any factorization at all and radiation can be studied using Monte Carlo methods. Radiation is generated using a Monte Carlo algorithm which integrates over all the energies down to the unresolved region. At the end the combination of these two results produce a numerical resummed prediction for the observable.

---

<sup>8</sup>This condition is called *recursive infra-red collinear safety* and please refer to Refs. [39] for the complete definition

Main advantage of this approach is the possibility to prevent from a complete factorization of the phase space and hence to apply the same construction to very different observables with minimal changes. However, the final result is achieved only numerically, even if directly in momentum space.

After this general introduction, we want to concentrate on the Conjugate space approach. Since we are going to perform our resummations using this technique is of primary importance to present collinear factorization of partonic observables in conjugate space. In particular we focus our attention on the two observables which we are going to study in the other chapters: transverse momentum distribution and inclusive cross section. These two observables are the most important in colour singlet production, which is the main application of the work of this thesis. Discussion about collinear factorization in conjugate space permits us also to introduce important notations we will extensively use in next pages.

### 1.4.1 Collinear Factorization in Conjugate Space

Our starting point is the *improved parton model* i.e. the framework of the parton model with the partonic cross section evaluated by introducing radiative corrections of QCD.

We want to write collinear factorization for the transverse momentum distribution for the colour singlet production process

$$h_1 + h_2 \rightarrow \mathcal{S} + X \quad (1.4.5)$$

where we decide to call  $p_T^2$  and  $Q^2$  transverse momentum and invariant mass of the system  $\mathcal{S}$ , respectively. Requiring  $M_X^2 > 0$  the invariant mass of the extra radiation  $X$  to be positive, we come to the following equation for the improved parton model:

$$\begin{aligned} \frac{d\sigma}{d\xi_p}(\tau, \xi_p, \alpha_s(\mu_R^2), \mu_F^2) &= \sum_{ij} \int_{\tau(\sqrt{1+\xi_p}+\sqrt{\xi_p})^2}^1 dx_1 f_i(x_1, \mu_F^2) \\ &\int_{\frac{\tau(\sqrt{1+\xi_p}+\sqrt{\xi_p})^2}{x_1}}^1 dx_2 f_j(x_2, \mu_F^2) \frac{d\bar{\sigma}_{ij}}{d\xi_p} \left( \frac{\tau}{x_1 x_2}, \xi_p, \alpha_s(\mu_R^2), \mu_F^2 \right) \end{aligned} \quad (1.4.6)$$

where we define

$$\tau = \frac{Q^2}{S} \quad \xi_p = \frac{p_T^2}{Q^2} \quad \frac{\tau}{x_1 x_2} = \hat{\tau} = \frac{Q^2}{s} \quad (1.4.7)$$

and  $\sqrt{S}$ ,  $\sqrt{s}$  to be the hadronic and the partonic centre of mass energy, respectively.

Our desire in this section is to find proper transformations which permit us to write the convolution of Eq. (1.4.6) as ordinary product between an universal object formed by PDFs and a conjugate version of the partonic differential distribution. This is done in order to be able to study resummation of the partonic observable ignoring convolution over PDFs and resumming modes directly at partonic level. Moreover we will see that there is a strong connection between the transformation which decouples the long-distance interaction of PDFs and the transformation which factorizes the phase space measure of multiple emissions.

Eq. (1.4.6) can be recast in a different way as

$$\frac{d\sigma}{d\xi_p}(\tau, \xi_p, \alpha_s(\mu_R^2), \mu_F^2) = \tau' \sum_{ij} \int_{\tau'}^1 \frac{dx}{x} \mathcal{L}_{ij}\left(\frac{\tau'}{x}, \mu_F^2\right) \frac{1}{x} \frac{d\hat{\sigma}_{ij}}{d\xi_p}(x, \xi_p, \alpha_s(\mu_R^2), \mu_F^2), \quad (1.4.8)$$

defining

$$\tau' = \tau \left( \sqrt{1 + \xi_p} + \sqrt{\xi_p} \right)^2, \quad (1.4.9)$$

$$x = \hat{\tau} \left( \sqrt{1 + \xi_p} + \sqrt{\xi_p} \right)^2 \quad (1.4.10)$$

$$\mathcal{L}_{ij}(z, \mu_F^2) = \int_z^1 \frac{dy}{y} f_i(y, \mu_F^2) f_j\left(\frac{z}{y}, \mu_F^2\right). \quad (1.4.11)$$

and

$$\frac{d\hat{\sigma}_{ij}}{d\xi_p}(x, \xi_p, \alpha_s(\mu_R^2), \mu_F^2) = \frac{d\bar{\sigma}_{ij}}{d\xi_p}\left(\frac{x}{(\sqrt{1 + \xi_p} + \sqrt{\xi_p})^2}, \xi_p, \alpha_s(\mu_R^2), \mu_F^2\right). \quad (1.4.12)$$

Now Eq. (1.4.8) is in the form of multiplicative convolution. The multiplicative convolution can be turned into product using Mellin Transform. General properties and important results about Mellin Transform and Fourier Transform - we are going to use the second transformation in Chap. 2 - are collected in Appendix B. Here we are going to limit ourselves to the definition of this Mellin transformation.

Mellin transform is defined in general as

$$F(N) = \int_0^1 dz z^{N-1} F(z) \quad (1.4.13a)$$

$$F(z) = \frac{1}{2\pi i} \int_{N_0-i\infty}^{N_0+i\infty} dN z^{-N} F(N) \quad (1.4.13b)$$

where throughout the thesis we are going to use the same letter both for the function and its transform, using the argument to distinguish between the two. In the inverse definition,  $N_0$  must be a convergent abscissa, hence a value of the real axis at the right of all the singularities of  $F(N)$ . The existence of the direct Mellin transform, as in the Laplace transform case, assures the existence of such  $N_0$ .

Due to this definition, taking Mellin transform w.r.t.  $\tau'$  of Eq. (1.4.8) leads to the following factorized expression:

$$\frac{d\sigma}{d\xi_p}(N, \xi_p, \alpha_s(\mu_R^2), \mu_F^2) = \sum_{ij} \mathcal{L}_{ij}(N, \mu_F^2) \frac{d\hat{\sigma}_{ij}}{d\xi_p}(N, \xi_p, \alpha_s(\mu_R^2), \mu_F^2) \quad (1.4.14)$$

with

$$\frac{d\sigma}{d\xi_p}(N) = \int_0^1 d\tau' \tau'^{N-1} \frac{1}{\tau'} \frac{d\sigma}{d\xi_p}(\tau'), \quad (1.4.15)$$

$$\frac{d\hat{\sigma}}{d\xi_p}(N) = \int_0^1 dx x^{N-1} \frac{1}{x} \frac{d\hat{\sigma}}{d\xi_p}(x). \quad (1.4.16)$$

Eq. (1.4.14) will be the starting point for the next chapters where we are going to focus our attention on resummation of divergent components in  $\frac{d\hat{\sigma}_{ij}}{d\xi_p}$ . Another important topic, especially in Chap. 2, will be the relation between transverse momentum distribution and inclusive cross section. Clearly in momentum space we recover the latter by integration of the former over  $\xi_p$ . However, situation is more complicated in Mellin space, since  $\tau'$ , the variable conjugated to  $N$ , depends intrinsically on  $\xi_p$ .

In general, improved parton model for inclusive cross section takes the form

$$\sigma(\tau, \alpha_s(\mu_R^2), \mu_F^2) = \sum_{ij} \tau \int_{\tau}^1 \frac{dx}{x} \mathcal{L}_{ij}\left(\frac{\tau}{x}, \mu_F^2\right) \hat{\sigma}_{ij}(x, \alpha_s(\mu_R^2), \mu_F^2) \quad (1.4.17)$$

which factorizes into product by taking Mellin transform with respect to  $\tau$  rather than to  $\tau'$  as for transverse momentum distribution.

It can be proved [45], that following relation holds in Mellin space, relating the two partonic objects:

$$\hat{\sigma}_{ij}(N) = \int_0^{\infty} d\xi_p \left(\sqrt{1+\xi_p} - \sqrt{\xi_p}\right)^{2N} \frac{d\hat{\sigma}_{ij}}{d\xi_p}(N, \xi_p), \quad (1.4.18)$$

thus permitting us to relate the total cross section and the transverse momentum distribution directly in conjugate space at partonic level, without concerning ourselves with PDFs.

We want to end this section and this chapter with an important remark for the next chapter. During our discussion about resummation in the soft and collinear limit, we are going to use also Fourier Transform to factorize transverse momentum delta constraint. The two-dimensional Fourier Transform is defined as

$$F(b) = \frac{1}{2\pi} \int_{\mathbb{R}_2} d^2p_{\text{T}} e^{-i\vec{b}\cdot\vec{p}_{\text{T}}} F(p_{\text{T}}) \quad (1.4.19)$$

$$F(p_{\text{T}}) = \frac{1}{2\pi} \int_{\mathbb{R}_2} d^2b e^{i\vec{b}\cdot\vec{p}_{\text{T}}} F(b). \quad (1.4.20)$$

It is interesting to observe that we are free to take simultaneous the Mellin and Fourier transform thanks to the fact that we define the Mellin transform with respect to the scaling variable  $\tau'$ , according to Eq. (1.4.13). Indeed, the variable  $\tau'$  ranges from  $0 \leq \tau' \leq 1$  for all  $p_{\text{T}}^2$ , and  $p_{\text{T}}^2$  ranges from  $0 \leq p_{\text{T}}^2 \leq \infty$  for all  $\tau'$ . Situation is totally different if we would have decided to parametrize kinematics using  $p_{\text{T}}^2$  and scaling variable  $\tau$  Eq. (1.4.7). In that case, for fixed  $p_{\text{T}}^2$ ,  $\tau$  has a  $p_{\text{T}}$ -dependent upper bound

$$0 \leq \tau \leq \left(\sqrt{1+\xi_p} - \sqrt{\xi_p}\right)^2. \quad (1.4.21)$$

Conversely, for fixed  $\tau$ ,  $p_{\text{T}}$  has a  $\tau$ -dependent range, most easily expressed in terms of the dimensionless variable  $\xi_p$ :

$$0 \leq \xi_p \leq \frac{(1-\tau)^2}{4\tau}. \quad (1.4.22)$$

In conclusion, it is not possible to take a Mellin transform with respect to  $\tau$  of the  $p_{\text{T}}$  distribution, or a Fourier transform with respect to  $p_{\text{T}}$  at fixed  $\tau$ , without extending the integration range outside the physical region.

---

We end our preliminary introduction about QCD, and we are ready to start our discussion about resummation for transverse momentum distributions. In the next chapter, we are going to focus on the soft and collinear limit while in Chapter 3 we will study behaviour of the transverse momentum distribution in the high energy regime.



# 2 Collinear and Threshold Resummation

## Contents

---

2.1	<b>Which regions do we actually resum?</b>	46
2.2	<b>Factorization in the soft and collinear limit</b>	47
2.2.1	Matrix Elements Factorization	47
2.2.2	Phase Space Factorization at Threshold	52
2.2.3	Phase Space Factorization at small- $p_T$	56
2.3	<b>Threshold Resummation at fixed <math>p_T</math></b>	59
2.4	<b>Transverse Momentum Resummation</b>	61
2.5	<b>Consistent Transverse Momentum Resummation</b>	66
2.5.1	Resummed Expression	71
2.6	<b>Combined Resummation for Transverse distributions</b>	78
2.7	<b>Application: EFT Higgs boson at Threshold</b>	79

---

This chapter is devoted to the resummation of soft and collinear divergences in transverse momentum distributions. After a brief introduction about the state of the art in this field, we are going to present in Sec. 2.2 the main factorization properties which permit resummation in these kinematic limits. We are going to focus our attention both on the invariant matrix and on the phase space.

However, the factorization of the phase space has to be performed in different way, according to the kinematic region we are interested in. Hence, we are going to study separately the threshold region in Sec. 2.2.2, when  $p_T$  is large but energy is closed to its minimum, and the collinear region in Sec. 2.2.3, when  $p_T$  is much smaller than the centre-of mass energy. This initial analysis will bring us to derive two known resummation theories: *threshold resummation at fixed  $p_T$*  in Sec. 2.3 and *transverse momentum resummation* in Sec. 2.4.

In the last part of the chapter then we try to merge information coming from these two regions. First of all, we relax the constraint of the collinear region, pretending only

$p_T$  to be small, with no condition on  $\hat{s}$ . The resummation theory, we are able to construct with these new assumptions, is called *consistent or joint resummation* and Sec. 2.5 will be devoted to its derivation. Then we are going to combine threshold resummation at large  $p_T$  with consistent resummation in a unique formula in Sec. 2.6 where final considerations will also be drawn.

Finally, as an application, we are going to apply the whole machinery in Sec. 2.7 to our test case, the effective field theory Higgs boson production in gluon fusion. We will derive all the explicit expressions at NNLL accuracy and we will explicitly shown that our final formula owns all the desired properties we required.

## 2.1 Which regions do we actually resum?

This section is meant to be a sort of introduction about the whole rest of the thesis. We focus our attention on transverse momentum distributions and we parametrize the partonic phase space using two sets of variables:  $\hat{\tau}$  and  $\xi_p$  or  $x$  and  $\xi_p$  (see Eq. (1.4.7) or Eq. (1.4.9) for  $\hat{\tau}$  and  $x$  definition). Physical boundaries in these two sets are the following

$$0 \leq \hat{\tau} \leq 1 \quad 0 \leq \xi_p \leq \frac{(1 - \hat{\tau})^2}{4\hat{\tau}}, \quad (2.1.1)$$

$$0 \leq x \leq 1 \quad \xi_p > 0 \quad (2.1.2)$$

and the available phase space is depicted in Fig. 2.1, in the two cases.

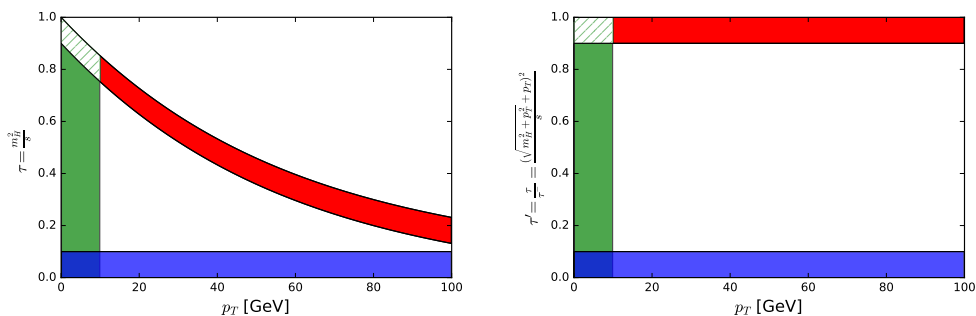


**Figure 2.1.** Available phase space for the production of an object of invariant mass  $Q^2$  and transverse momentum  $p_T$ , parametrized as a function of  $\hat{\tau}$  and  $\xi_p$  (left) or  $x$  and  $\xi_p$  (right).

In Fig. 2.1, moreover, we colour various regions where resummation is up to now available. They are respectively:

- **Threshold Limit:** when the centre of mass energy approach its minimum  $s_{\min} = \left(\sqrt{Q^2 + p_T^2} + p_T\right)^2$ . This region correspond to  $\hat{\tau} \rightarrow \hat{\tau}_{\max} = \left(\sqrt{1 + \xi_p} - \sqrt{\xi_p}\right)^2$  or  $x \rightarrow 1$ .
- **Collinear Limit:** when transverse momentum is small comparing to  $Q^2$ , hence  $p_T^2$  or  $\xi_p \rightarrow 0$ . In this limit, according to  $x$  and  $\hat{\tau}$  definitions, we have  $\hat{\tau} \approx x$ .

- **High Energy Limit:** when the centre of mass energy is large comparing to  $Q^2$ , hence  $s \rightarrow \infty$  and  $x$  or  $\hat{\tau}$  tends to 0. As in the collinear case, the difference between  $x$  and  $\hat{\tau}$  definition is meaningless in this limit.

This Chapter will be devoted to the study of the first two limits while high energy region will be described in detail in Chap. 3. It is important to note that the regions just mentioned overlap. The overlay regions have to be studied separately since the hierarchy of scales changes. We recognize in Fig. 2.1 two overlap areas, when we are both at threshold and collinear, and when we are collinear but at high energy. We are going to study the first case in Sec. 2.5 while we refer to Ref. [46] for a detailed description about how to adapt collinear resummation of Sec. 2.4 and high energy resummation of Sec. 3.2 in the joint region.

Now, after this brief introduction we are ready to study the threshold and collinear limit in the rest of the chapter. Next section will be devoted to factorization both of matrix element in Sec. 2.2.1 and of phase space in Sec. 2.2.2 and Sec. 2.2.3. Then we move to present in detail in Sec. 2.3 and 2.4, resummation in the threshold region, called in literature *threshold resummation at fixed  $p_T$* , and resummation in the collinear region, hence *transverse momentum resummation* or *Collins-Soper-Sterman resummation*.

## 2.2 Factorization in the soft and collinear limit

In this section, we will describe factorization properties which constitute the basis of both transverse momentum resummation and threshold resummation at fixed  $p_T$ . We are going to consider a general  $2 \rightarrow m + n$  process with  $n$  partons characterized by a small value of the transverse momentum, and we will focus on the collinear singular region. While derivation for the matrix elements is common for both the resummation theories, phase space factorization greatly differs. For this reason next part of the section will be divided in three subsections: first we are going to discuss in detail the matrix element factorization, then we will focus on the phase space structure at threshold and finally we conclude with the phase space analysis in the small- $p_T$  limit.

### 2.2.1 Matrix Elements Factorization

We start from the invariant matrix of a process like

$$p(p_1) + p(p_2) \rightarrow \mathcal{S}(q_1, \dots, q_m) + g(k_1) + \dots + g(k_n) \quad (2.2.1)$$

where two generic partons of momenta  $p_1$  and  $p_2$  generate a studied system composed by  $m$  hard particles of momenta  $q_1, \dots, q_m$  plus  $n$  collinear gluons with momenta  $k_1, \dots, k_n$ . All the transverse momenta  $k_{T_1}, k_{T_2}, \dots, k_{T_n}$  are considered smaller compared to  $Q^2$ , invariant mass of system  $\mathcal{S}$ .

In this limit, retaining only the most singular contribution, matrix element factorizes as

$$|\mathcal{M}(p_1, p_2, q_1, \dots, q_m, k_1, \dots, k_n)|^2 = |\mathcal{M}(p_1, p_2, q_1, \dots, q_m)|^2 \frac{1}{n!} |\mathcal{M}(k_1)|^2 \dots |\mathcal{M}(k_n)|^2, \quad (2.2.2)$$

with single splitting term  $|\mathcal{M}(k)|^2$  defined as

$$|\mathcal{M}(k)|^2 = \frac{|\mathcal{M}(p_1, p_2, p_S, k)|^2}{|\mathcal{M}(p_1, p_2, p_S)|^2}, \quad (2.2.3)$$

and  $p_S$  indicating the whole set of system particles momenta  $q_1, \dots, q_m$ . The combinatorial factor  $\frac{1}{n!}$  takes into account indistinguishability of emitted partons in the final state. We are limiting ourself to the case where multiple gluons are emitted from a quark line. Extension to the case when a quark is emitted is very straightforward and it will be left to the reader.

Eq. (2.2.2) states that when the transverse momenta of all the extra emitted gluons becomes small, matrix element factorizes in the Born level times a product of universal splitting kernels one for any emitted collinear parton.

In the next part of this subsection we are going to prove Eq. (2.2.2) for a singular gluon emission from a quark line. Multiple gluon case directly follows as a straightforward generalization.

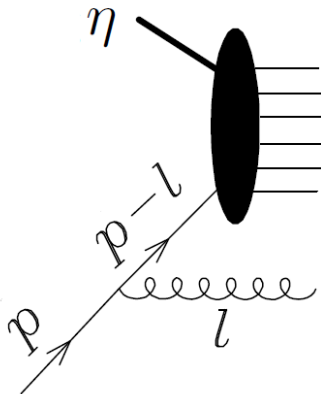


**Figure 2.2.** Single gluon emission from a external quark line. The black bulk represent the invariant matrix for the remaining process [18].

We start by considering the emission depicted in Fig. 2.2; a singular gluon radiation from an initial quark line. Final state radiation from any coloured external line  $q$  in  $\mathcal{S}$  shares the same behaviour due to crossing symmetry. Invariant matrix in this case turn out to be

$$i\mathcal{M}(p, \eta, p_S) = ig_S \mathcal{M}(p-l, \eta, p_S) \frac{\not{p}-\not{l}}{(p-l)^2} \gamma^\mu t^a u(p) \epsilon_\mu(l) \quad (2.2.4)$$

where  $\epsilon_\mu(l)$  is the polarization vector of the emitted gluon,  $u(p)$  is the polarization vector of the incoming quark while  $\mathcal{M}(p-l, p_2, p_S)$  states for the Born matrix element stripped of the polarization vector of  $p-l$ .

Then we select the following parametrization for the different momenta

$$p = \frac{\sqrt{s}}{2} (1, 0, 0, 1) \quad (2.2.5a)$$

$$\eta = \frac{\sqrt{s}}{2} (1, 0, 0, -1) \quad (2.2.5b)$$

$$l = (1 - z)p + \mathbf{1}_T + \xi\eta \quad (2.2.5c)$$

and we are going to simplify Eq. (2.2.4) retaining only leading terms in the limit  $l_T \rightarrow 0$ . On-shell condition on the gluon fixes  $\xi$  value

$$\xi = \frac{l_T^2}{2(p \cdot \eta)(1 - z)} \quad (2.2.6)$$

and then by substituting momenta parametrization Eqs. (2.2.5) into Eq. (2.2.4) we obtain:

$$i\mathcal{M}(p, \eta, p_S) = ig_S \mathcal{M}(p - l, \eta, p_S) \frac{(1 - z)(\not{p} - \not{l})}{-l_T^2} \gamma^\mu t^a u(p) \epsilon_\mu(l). \quad (2.2.7)$$

The trick now to reach the desired result is the following. First, we rewrite momentum  $p$  as

$$p = \frac{l - \mathbf{1}_T - \xi\eta}{(1 - z)} \quad (2.2.8)$$

and then we ignore  $\xi$  components since it is suppressed by a power of  $l_T^2$ . Retaining thus only the singular behaviour in  $l_T^2 \rightarrow 0$  we write Eq. (2.2.7) as

$$\begin{aligned} i\mathcal{M}(p, \eta, p_S) &= ig_S \mathcal{M}(p - l, \eta, p_S) \frac{z\not{l} - \not{\mathbf{1}}_T}{-l_T^2} \gamma^\mu t^a u(p) \epsilon_\mu(l) \\ &= ig_S \mathcal{M}(p - l, \eta, p_S) \frac{z\gamma^\mu \not{l} - \not{\mathbf{1}}_T \gamma^\mu}{-l_T^2} t^a u(p) \epsilon_\mu(l) \\ &= ig_S \mathcal{M}(p - l, \eta, p_S) \frac{z\gamma^\mu ((1 - z)\not{p} - \not{\mathbf{1}}_T) - \not{\mathbf{1}}_T \gamma^\mu}{-l_T^2} t^a u(p) \epsilon_\mu(l) \\ &= ig_S \mathcal{M}(p - l, \eta, p_S) \frac{-2z l_T^\mu - (1 - z)\not{\mathbf{1}}_T \gamma^\mu}{-l_T^2} t^a u(p) \epsilon_\mu(l), \end{aligned} \quad (2.2.9)$$

where in the second step we use gluon transversality,  $l^\mu \epsilon_\mu(l) = 0$ , while in the last one we make use of Dirac equations and of  $\not{\mathbf{1}}_T$  and  $\gamma^\mu$  anticommutator.

We are now ready to take the square modulus together with the sum over polarizations to obtain

$$\begin{aligned} |\mathcal{M}(p, \eta, p_S)|^2 &= g_S^2 \frac{1}{3} \text{Tr}(t^a t^b) \frac{1}{l_T^4} \mathcal{M}(p - l, \eta, p_S) \not{p} \\ &\quad \left(4z^2 + 4z(1 - z) + 2(1 - z)^2\right) l_T^2 \mathcal{M}^\dagger(p - l, \eta, p_S) \\ &= g_S^2 C_F \frac{(1 + z^2)}{l_T^2} |\mathcal{M}_B|^2 \end{aligned} \quad (2.2.10)$$

with colour factor  $C_F = \frac{4}{3}$  and the squared Born matrix element  $|\mathcal{M}_B|^2$  defined in this case as

$$|\mathcal{M}_B|^2 = \sum_{\bar{}} |u(p - l) \mathcal{M}(p - l, \eta, p_S)|^2 = \mathcal{M}(p - l, \eta, p_S) \not{p} \mathcal{M}^\dagger(p - l, \eta, p_S). \quad (2.2.11)$$

Eq. (2.2.10) represents our desired result, comparing it with Eq. (2.2.2), we find explicit expression for

$$|\mathcal{M}(l)|_{q\bar{q}}^2 = \alpha_s C_F \frac{(1+z^2)}{l_T^2}. \quad (2.2.12)$$

Subscript  $q\bar{q}$  was inserted to remind you that the previous evaluation was for a quark line emitting a gluon. In general for any possible splitting we have

$$|\mathcal{M}(l)|_{ij}^2 = \alpha_s \frac{p_{ij}(z)}{l_T^2} \quad (2.2.13)$$

with

$$p_{ij} = (1-z) P_{ij}^{(0)}, \quad (2.2.14)$$

being the numerator of the LO Altarelli-Parisi splitting function  $P_{ij}^{(0)}$ .

We have just proved that in the small- $k_T$  limit, with  $k$  momentum of the emitted gluon from line  $p$ , matrix element factorizes into product of an universal splitting controlled by Eq. (2.2.13), and the matrix element of the remaining process with momentum of line  $p$  modified in  $p+k$ . Procedure can be iterated to completely factorize matrix element from any extra collinear radiation, coming to desired Eq. (2.2.2).

However, before proceeding, some remarks are fundamental:

- The factorization Eq. (2.2.2) is true only for the most singular contribution in the collinear limit. This permits to derive transverse momentum resummation and threshold resummation for transverse momentum distributions strictly speaking only at LL. In fact also NLL can be achieved with the same construction, since extra correlated contributions can be inserted in a inclusive way. Splitting matrix elements, Eq. (2.2.13), have to contain NLO numerator of Altarelli-Parisi splitting function and we have to set factorization and renormalization scale in radiation kernel to proper central scales ( $k_T$  in this case). From NNLL forward, instead, first exclusive correlations between different emissions have to be taken into account. A complete discussion about these corrections is contained in Ref. [44] and we will highlight main points in the last part of this subsection.
- Eq. (2.2.13) represents the universal LO collinear splitting in 4 dimension. However, in this number of dimensions, it diverges when also phase space is taken into account. For this reason, it is useful to compute Eq. (2.2.13) in  $d = 4 - 2\epsilon$  dimension to regularize its behaviour.  $\mathcal{O}(\epsilon)$  terms in splitting kernels are important to derive resummation beyond LL.

Derivation just exposed represents an heuristic proof about matrix element factorization which is behind resummation in soft and collinear limit. As just said, it is strictly valid only at LL, but it contains all the important messages to understand the resummed structures of Sec. 2.4, and of Sec. 2.3. In the next part of this subsection we want to formalize better this concept, following analysis of Ref. [39, 42, 43]. However we stress the reader that this is not mandatory to understand the rest of the discussion of this chapter.

The plain infrared and collinear safety requires that for any value  $v$  of the observable, there exists a scale  $\epsilon_v$  such that emissions at scales lower than  $\epsilon_v$  (hence very *soft* or/and

very *collinear*) do not change the value of the observable. Now a useful way to formalize matrix element factorization and to understand the hierarchy among different correlations is to strengthen previous requirement, thus introducing the concept of *recursive infrared and collinear safety*. Recursive infra-red and collinear safety states that the value of  $\epsilon$  have to be independent on the particular value of the observable  $v$ . Any radiation emitted at scales lower than  $\epsilon v$  do not modify the value of the observable. Collinear and soft scaling is then linear at all orders even after the introduction of the various perturbative corrections.

It is important to note that all global observables for which a resummation is in fact present, are rIRC safe: transverse momentum distribution is one of the possible example. We are now ready to present matrix element factorization beyond LL accuracy.

First of all we conveniently decomposed renormalised squared amplitude for  $n$  real emissions ( $pp \rightarrow \mathcal{S} + n$  gluons) as

$$\begin{aligned}
|\mathcal{M}(p_1, p_2, p_S, k_1, \dots, k_n)|^2 &= |\mathcal{M}_B(p_1, p_2, p_S)|^2 \left\{ \frac{1}{n!} \left[ \prod_{i=1}^n |\mathcal{M}(k_i)|^2 \right] \right. \\
&+ \left[ \sum_{a>b} \frac{1}{(n-2)!} \left[ \prod_{\substack{i=1 \\ i \neq a, b}} |\mathcal{M}(k_i)|^2 \right] |\mathcal{M}(k_a, k_b)|^2 \right. \\
&+ \sum_{a>b} \sum_{\substack{c>d \\ c, d \neq a, b}} \frac{1}{(n-4)!2!} \left[ \prod_{\substack{i=1 \\ i \neq a, b, c, d}} |\mathcal{M}(k_i)|^2 \right] |\mathcal{M}(k_a, k_b)|^2 |\mathcal{M}(k_c, k_d)|^2 + \dots \left. \right] \\
&+ \left. \left[ \sum_{a>b>c} \frac{1}{(n-3)!} \left[ \prod_{\substack{i=1 \\ i \neq a, b, c}} |\mathcal{M}(k_i)|^2 \right] |\mathcal{M}(k_a, k_b, k_c)|^2 + \dots \right] \right\} \quad (2.2.15)
\end{aligned}$$

where we have defined the  $n$ -particle correlated matrix elements squared  $|\mathcal{M}(k_a, \dots, k_n)|^2$  recursively as follows:

$$|\mathcal{M}(k_a)|^2 = \frac{|\mathcal{M}(p_1, p_2, p_S, k_a)|^2}{|\mathcal{M}_B(p_1, p_2, p_S)|^2} \quad (2.2.16a)$$

$$|\mathcal{M}(k_a, k_b)|^2 = \frac{|\mathcal{M}(p_1, p_2, p_S, k_a, k_b)|^2}{|\mathcal{M}_B(p_1, p_2, p_S)|^2} - \frac{1}{2} |\mathcal{M}(k_a)|^2 |\mathcal{M}(k_b)|^2 \quad (2.2.16b)$$

$$\begin{aligned}
|\mathcal{M}(k_a, k_b, k_c)|^2 &= \frac{|\mathcal{M}(p_1, p_2, p_S, k_a, k_b, k_c)|^2}{|\mathcal{M}_B(p_1, p_2, p_S)|^2} - \frac{1}{3!} |\mathcal{M}(k_a)|^2 |\mathcal{M}(k_b)|^2 |\mathcal{M}(k_c)|^2 \\
&- |\mathcal{M}(k_a, k_b)|^2 |\mathcal{M}(k_c)|^2 - |\mathcal{M}(k_c, k_b)|^2 |\mathcal{M}(k_a)|^2 \\
&- |\mathcal{M}(k_a, k_c)|^2 |\mathcal{M}(k_b)|^2 \quad (2.2.16c)
\end{aligned}$$

The decomposition just written can be extended to the case in which the radiated parton is in fact a quark rather than a gluon by properly changing the multiplicity factors of each term. Now we want to link decomposition Eq. (2.2.15) to the accuracy order. The

generic  $n$ - correlated squared amplitudes admit a perturbative expansion [44]

$$|\mathcal{M}(k_1, \dots, k_n)|^2 = \sum_{j=0}^{\infty} \left( \frac{\alpha_s(\mu_R)}{2\pi} \right)^{n+j} n\text{PC}^{(j)} \quad (2.2.17)$$

where  $\alpha_s$  is the strong coupling in the  $\overline{\text{MS}}$  scheme, and notation  $n\text{PC}$  stands for  $n$ -particle correlated.

The important observation which concludes our general analysis is that rIRC safety guarantees a hierarchy between different blocks in the decomposition Eq. (2.2.17), in the sense that, generally correlated blocks with  $n$  particles start contributing at one logarithmic order higher than correlated blocks with  $n - 1$  particles [39, 43]. At LL for instance only  $1\text{PC}^{(0)}$  blocks enters, thus reconstructing our previous naïve derivation where only the singular components have been considered. NLL accuracy is then controlled also by  $1\text{PC}^{(1)}$  and  $2\text{PC}^{(0)}$ ; as said before, however, such terms can be entirely encoded using a modified version of the  $1\text{PC}^{(0)}$  block where NLO Altarelli-Parisi and running coupling contributions are inserted. From NNLL, the factorization of matrix elements is more complicated and we have to take into account first particle exclusive correlations. This does not mean that resummation is ruined, since even now the evaluation a small number of objects (the blocks of Eq. (2.2.17)) permits the prediction of a whole tower of logarithms. However analysis of the single emission block is no longer enough and the complete decomposition Eq. (2.2.15), and Eq. (2.2.17) have to be taken into account.

After this discussion about factorization properties of matrix elements we want to focus our attention on the phase space and we want to prove its factorization in the kinematic limits we are interested in.

## 2.2.2 Phase Space Factorization at Threshold

In previous section, we prove that it is possible to construct a hierarchy in the different configurations which enter at any logarithmic order in the matrix element. However, this is not enough to reach resummation. Indeed, if we want to use renormalization group arguments [31, 47] to derive exponentiation and then resummation, we need also complete factorization of the phase space.

We will see that we are going to reach the factorization of phase space using two different strategies in the threshold and in the collinear limit. Hence we decide to divide the two cases in two different subsections. This subsection will be devoted to the study of the phase space in the threshold limit while following subsection will described the small- $p_T$  one.

First of all, we want to specify better the limit we are working in. Since at threshold the centre-of-mass energy approaches its minimum, the energy is right enough to create the desired final state  $\mathcal{S}$  with its invariant mass  $Q^2$  and its transverse momentum  $p_T$ . Hence the invariant mass of any extra radiation has to approach zero. The threshold condition can then be reformulated as

$$W = \sum_{i>j}^n |k_i| |k_j| (1 - \cos \theta_{ij}) \rightarrow 0 \quad (2.2.18)$$

with  $W$  the invariant mass of the bunch of extra emitted partons  $k_1, \dots, k_n$ . In Eq. (2.2.18),  $|k_i|$  stands for the modulus of the three-momentum, and  $\theta_{ij}$  is the angle between directions of momenta  $k_i$  and  $k_j$ . You can easily convince yourself that in order to fulfil Eq. (2.2.18), only one parton owns a non-zero transverse momentum that has to balance the  $p_T$  of  $\mathcal{S}$ .

Therefore the situation is the following. A general process

$$p_i(p_1) + p_j(p_2) \rightarrow \mathcal{S}(p_S) + X(k_1, \dots, k_n) \quad (2.2.19)$$

can be viewed as the born process

$$p_i(p_1) + p_j(p_2) \rightarrow \mathcal{S}(p_S) + p_k(k_1) \quad (2.2.20)$$

dressed by collinear and soft radiation of small transverse momenta. This means that the factorization of matrix elements derived in Sec. 2.2.1 works also in this case for all the emitted radiation except for the hard recoiling parton  $p_k$ .

To conclude our analysis we want to prove factorization of phase space in this limit; we will closely follow similar derivation of Ref. [31, 47].

The phase space factorization of Refs. [31, 47] is based on the iterative reduction of the  $n + 1$ -body phase space  $d\Phi$  for the process Eq. (2.2.19) into an  $n$ -body and a two-body phase space, which eventually leads to expressing it in terms of  $n$  two-body phase spaces, connected by integrations over intermediate virtual particle masses. Physically, this corresponds to iteratively writing the phase space in terms of the momentum of the last radiated particle, and the system containing the previous  $n - 1$  final-state ones:

$$\begin{aligned} d\Phi(p_1, p_2; k_1, \dots, k_n, p) &= \frac{dP_n^2}{2\pi} d\Phi(p_1, p_2; k_n, P_n) \frac{dP_{n-1}^2}{2\pi} d\Phi(P_n; k_{n-1}, P_{n-1}) \\ &\dots \frac{dP_2^2}{2\pi} d\Phi(P_3; k_2, P_2) d\Phi(P_2; k_1, p), \end{aligned} \quad (2.2.21)$$

where each of the intermediate particle's invariant masses  $P_i^2$  ranges between

$$Q^2 \leq P_i^2 \leq P_{i+1}^2 \quad (2.2.22)$$

and  $P_{n+1}^2 \equiv \hat{s}$  is the total centre-of-mass energy squared.

The result is then simplified taking advantage of the Lorentz invariance of each two-body phase space, in order to rewrite it in the rest frame of its incoming momentum  $P_i$ : in  $d = 4 - 2\epsilon$  dimensions

$$\begin{aligned} d\Phi(P_i; k_j, P_j) &= \frac{(2\pi)^{2-d}}{4} \frac{d^{d-1}k_j}{|\vec{k}_j| \sqrt{|\vec{k}_j|^2 + P_j^2}} \delta\left(\sqrt{P_i^2} - \sqrt{|\vec{k}_j|^2 + P_j^2} - |\vec{k}_j|\right) \\ &= \frac{(4\pi)^{2\epsilon-2}}{2} (P_i^2)^{-\epsilon} \left(1 - \frac{P_j^2}{P_i^2}\right)^{1-2\epsilon} (\sin\theta_j)^{1-2\epsilon} d\theta_j d\Omega_{2-2\epsilon}^j \end{aligned} \quad (2.2.23)$$

$$= \frac{(2\pi)^{2\epsilon-2}}{8} \left(k_{Tj}^2\right)^{-\epsilon} \frac{dk_{Tj}^2 d\Omega_{2-2\epsilon}^j}{\sqrt{P_i^2} \sqrt{\frac{P_i^2}{4} \left(1 - \frac{P_j^2}{P_i^2}\right)^2 - k_{Tj}^2}}, \quad (2.2.24)$$

where the angular integral is written in terms of a  $(1 - 2\epsilon)$ -dimensional azimuthal integration over  $d\Omega_{2-2\epsilon}^i$ , and, equivalently, either a polar integral over  $\theta_i$  in Eq. (2.2.23), or the modulus square of the transverse momentum in Eq. (2.2.24). In the latter case, the square-root factor in the denominator of Eq. (2.2.24) is the Jacobian related to this new choice of integration variable.

Using this result the  $d$ -dimensional phase space Eq. (2.2.21) becomes

$$\begin{aligned}
d\Phi &= (4\pi)^{2\epsilon-3} (P_{n+1}^2)^{-\epsilon} \left(1 - \frac{P_n^2}{P_{n+1}^2}\right)^{1-2\epsilon} (\sin \theta_n)^{1-2\epsilon} d\theta_n d\Omega_{2-2\epsilon}^n dP_n^2 \\
&\times (4\pi)^{2\epsilon-3} (P_n^2)^{-\epsilon} \left(1 - \frac{P_{n-1}^2}{P_n^2}\right)^{1-2\epsilon} (\sin \theta_{n-1})^{1-2\epsilon} d\theta_{n-1} d\Omega_{2-2\epsilon}^{n-1} dP_{n-1}^2 \\
&\dots \\
&\times (4\pi)^{2\epsilon-3} (P_3^2)^{-\epsilon} \left(1 - \frac{P_2^2}{P_3^2}\right)^{1-2\epsilon} (\sin \theta_2)^{1-2\epsilon} d\theta_2 d\Omega_{2-2\epsilon}^2 dP_2^2 \\
&\times \frac{(2\pi)^{2\epsilon-2}}{8} \frac{(p_{\text{T}}^2)^{-\epsilon}}{\sqrt{P_2^2} \sqrt{\frac{P_2^2}{4} \left(1 - \frac{Q^2}{P_2^2}\right)^2 - p_{\text{T}}^2}} d\Omega_{2-2\epsilon}^1 dp_{\text{T}}^2, \tag{2.2.25}
\end{aligned}$$

where, in view of the fact that we are interested in the transverse momentum spectrum of the  $(n + 1)$ -th system  $\mathcal{S}(p)$ , we have parametrized its phase space in terms of  $p_{\text{T}}$  using Eq. (2.2.24), while the identification of  $p_{\text{T}}$  with the transverse momentum in the centre-of-mass frame of the hadronic collision, as well as the reason why all other phase spaces are parametrized in terms of  $\theta_i$  in Eq. (2.2.23), will be clear shortly.

The domain of integration over  $p_{\text{T}}^2$  in Eq. (2.2.25) is

$$0 \leq p_{\text{T}}^2 \leq \frac{P_2^2}{4} \left(1 - \frac{Q^2}{P_2^2}\right)^2, \tag{2.2.26}$$

so that the overall domain of integration Eqs. (2.2.22), (2.1.1) over the  $n$  dimensional variables which characterizes the  $n$  emissions is ordered, with the upper limit of integration of  $p_{\text{T}}^2$  being set by  $P_2^2$ , and then each of the integrations over  $P_i^2$  with  $i \geq 2$  being limited from above by  $P_{i+1}^2$ , with the aforementioned identification  $P_{n+1}^2 = \hat{s}$ .

However, in order to consider instead the case in which  $p_{\text{T}}$  is kept fixed, the integration region can be re-expressed by taking  $p_{\text{T}}$  as outer integration variable. In this case the integration range over  $p_{\text{T}}$  is only limited from above according to Eq. (2.1.1), while the integration over all  $P_i^2$  is now in the range

$$\left(\sqrt{Q^2 + p_{\text{T}}^2} + p_{\text{T}}\right)^2 \leq P_i^2 \leq P_{i+1}^2. \tag{2.2.27}$$

The final simplification of the phase space Eq. (2.2.25) is achieved by rewriting it in terms of the dimensionless variables

$$z_i = \frac{P_i^2}{P_{i+1}^2}, \tag{2.2.28}$$

along with  $x$  Eq. (1.4.9) and  $\xi_p$  Eq. (1.4.7). We thus arrive to our final expression for the phase space:

$$\begin{aligned}
d\Phi &= x (4\pi)^{2\epsilon-3} Q^{2-2\epsilon} x^{\epsilon-1} (1-z_n)^{1-2\epsilon} (\sin\theta_n)^{1-2\epsilon} d\theta_n d\Omega_{2-2\epsilon}^n \frac{dz_n}{z_n} \\
&\times (4\pi)^{2\epsilon-3} Q^{2-2\epsilon} \left(\frac{x}{z_n}\right)^{\epsilon-1} (1-z_{n-1})^{1-2\epsilon} (\sin\theta_{n-1})^{1-2\epsilon} d\theta_{n-1} d\Omega_{2-2\epsilon}^{n-1} \frac{dz_{n-1}}{z_{n-1}} \\
&\dots \\
&\times (4\pi)^{2\epsilon-3} Q^{2-2\epsilon} \left(\frac{x}{z_n \dots z_3}\right)^{\epsilon-1} (1-z_2)^{1-2\epsilon} (\sin\theta_2)^{1-2\epsilon} d\theta_2 d\Omega_{2-2\epsilon}^2 \frac{dz_2}{z_2} \\
&\times \frac{(2\pi)^{2\epsilon-2}}{4} \left(\frac{\xi_p}{(\sqrt{1+\xi_p} + \sqrt{\xi_p})^2}\right)^{-\epsilon} \\
&\quad \frac{Q^{2-2\epsilon}}{\sqrt{\left(1 - \frac{x}{z_n \dots z_2}\right) \left(1 - (\sqrt{1+\xi_p} - \sqrt{\xi_p})^4 \frac{x}{z_n \dots z_2}\right)}} d\Omega_{2-2\epsilon}^1 d\xi_p.
\end{aligned} \tag{2.2.29}$$

For fixed  $p_T$ , the integration over the set of  $n-1$  dimensional variables  $P_i^2$  with  $2 \leq i \leq n$  now becomes the integral over the  $n-1$  variables  $z_i$ ,  $2 \leq i \leq n$ . Its range is

$$\frac{x}{z_n z_{n-1} \dots z_{i+1}} \leq z_i \leq 1. \tag{2.2.30}$$

We note that the phase space Eq. (2.2.29), integrated over the range Eq. (2.2.30) has the structure of a multiple convolution, and thus it factorizes upon taking a Mellin transform with respect to  $x$ , with  $n-1$  identical factors depending on momenta  $k_i$ ,  $2 \leq i \leq n$ , and one factor depending on the two-body phase space of the leading-order process in which a single parton with momentum  $p_T$  recoils against the heavy state  $\mathcal{S}(p)$ . When comparing to the phase-space factorization of Refs. [31, 47] it should be kept in mind that Eq. (2.2.29) holds at the differential level in  $p_T$  because  $x$  Eq. (1.4.10) is  $p_T$  dependent.

The structure of the phase space Eq. (2.2.29), together with factorization of matrix element Eq. (2.2.2) will be the basis for threshold resummation at fixed  $p_T$  of Sec. 2.3.

Note that this factorization is allowed thanks to the choice of parametrizing momenta  $k_i$  in terms of the polar angles  $\theta_i$ : had we chosen to also parametrize them in terms of their transverse component, the Jacobian factors would have spoiled the convolution structure. It is important however to remember that this factorization has been obtained thanks to the choice Eqs. (2.2.23), (2.2.24) of writing each two-body phase space in the respective centre-of-mass frame. Now, in the infra-red limit in which the energy of all emitted partons vanishes, all these reference frames coincide: this is the same mechanism which underlies standard CFP factorization [19], and leads to the factorization in the eikonal limit [31]. But for generic momenta, this phase-space factorization is not useful because it only follows by choosing a different reference frame for each emission.

This is the reason why factorization Eq. (2.2.29) can not be applied in the collinear limit where it is no longer true that all radiation is soft, but we have also to deal with hard-collinear radiation. A different factorization will then be achieved in the next subsection for the small- $p_T$  limit, and it will be performed in Fourier space.

### 2.2.3 Phase Space Factorization at small- $p_T$

In order to study the small  $p_T$  limit we need a factorization of phase space which holds even when longitudinal momenta are not small: this can be done by separating the longitudinal and transverse momentum integrations.

We start from the general form for the phase-space for process Eq. (2.2.19) in  $d = 4 - 2\epsilon$  dimensions:

$$d\Phi_{n+1}(p_1, p_2; p, k_1, \dots, k_n) = \frac{d^{3-2\epsilon} p}{(2\pi)^{3-2\epsilon} 2\sqrt{Q^2 + |\vec{p}|^2}} \frac{d^{3-2\epsilon} k_1}{(2\pi)^{3-2\epsilon} 2E_1} \cdots \frac{d^{3-2\epsilon} k_n}{(2\pi)^{3-2\epsilon} 2E_n} \\ (2\pi)^{4-2\epsilon} \delta^{(4-2\epsilon)}(p_1 + p_2 - p - k_1 - \cdots - k_n). \quad (2.2.31)$$

Representing the transverse momentum constraint as a Fourier transform with respect to an impact parameter  $\vec{b}$  conjugated to  $\vec{p}_T$  we get

$$d\Phi_{n+1}(p_1, p_2, p; k_1, \dots, k_n) = (2\pi)^2 \int d^{2-2\epsilon} b \frac{(p_T^2)^{-\epsilon} dp_T^2 dp_z d\Omega_{2-2\epsilon} e^{i\vec{b} \cdot \vec{p}_T}}{4 (2\pi)^{3-2\epsilon} \sqrt{Q^2 + |\vec{p}|^2}} \\ \frac{|k_{T_1}|^{-2\epsilon} d|k_{T_1}^2| dE_1 d\Omega_{2-2\epsilon} e^{i\vec{b} \cdot \vec{k}_{T_1}}}{4 (2\pi)^{3-2\epsilon} \sqrt{E_1^2 - |k_{T_1}^2|}} \cdots \frac{|k_{T_n}|^{-2\epsilon} d|k_{T_n}^2| dE_n d\Omega_{2-2\epsilon} e^{i\vec{b} \cdot \vec{k}_{T_n}}}{4 (2\pi)^{3-2\epsilon} \sqrt{E_n^2 - |k_{T_n}^2|}} \\ \delta(\sqrt{\hat{s}} - \sqrt{Q^2 + |\vec{p}|^2} - E_1 - \cdots - E_n) \delta(p_z + k_{1z} + \cdots + k_{nz}), \quad (2.2.32)$$

where we have also traded the integral over the longitudinal momentum component for an integral over energy.

In order to separate the transverse and longitudinal momentum dependence, it is convenient to adopt the parametrization<sup>1</sup>

$$k_i = \alpha_i \frac{p_1 + p_2}{2} + \beta_i \frac{p_1 - p_2}{2} + k_{T_i}, \quad (2.2.33)$$

with  $p_1 \cdot k_{T_i} = p_2 \cdot k_{T_i} = 0$ . In the centre-of-mass frame we have

$$E_i = \frac{\sqrt{\hat{s}}}{2} \alpha_i; \quad k_{iz} = \frac{\sqrt{\hat{s}}}{2} \beta_i, \quad (2.2.34)$$

and therefore  $\alpha_i \geq 0$ , while  $\beta_i$  can take either sign. The soft emission limit is  $\alpha_i \rightarrow 0$ .

The mass shell conditions

$$k_i^2 = -|k_{T_i}^2| + \frac{\hat{s}}{4} (\alpha_i^2 - \beta_i^2) = 0 \quad (2.2.35)$$

give

$$|\beta_i| = \sqrt{\alpha_i^2 - \frac{4|k_{T_i}^2|}{\hat{s}}} = \sqrt{\alpha_i^2 - 4\hat{\tau}\xi_i} = \alpha_i + \mathcal{O}(\xi_i), \quad (2.2.36)$$

<sup>1</sup>Please note that the parametrization proposed here is slightly different from the one exposed in the original Ref. [45]; derivation is completely equivalent and we decide to adopt this slightly different parametrization since it permits immediately the separation of the integration ranges; same steps need an extra change of variables in the original parametrization of Ref. [45]

where we have defined  $\xi_i = \frac{|k_{T_i}^2|}{Q^2}$  in analogy to  $\xi_p$ . Furthermore, we have

$$\frac{dE_i}{\sqrt{E_i^2 - k_{T_i}^2}} = \frac{d\alpha_i}{\sqrt{\alpha_i^2 - 4\hat{\tau}\xi_i}}. \quad (2.2.37)$$

In the large  $b$  (small  $p_T$ ) limit we get

$$\begin{aligned} d\Phi_{n+1}(p_1, p_2; p, k_1, \dots, k_n) &= (2\pi)^2 \int d^{2-2\epsilon} b \frac{(p_T^2)^{-\epsilon} dp_T^2 dp_z d\Omega_{2-2\epsilon} e^{i\vec{b}\cdot\vec{p}_T}}{4(2\pi)^{3-2\epsilon} \sqrt{Q^2 + |\vec{p}|^2}} \\ &\frac{|k_{T_1}|^{-2\epsilon} d|k_{T_1}^2| d\alpha_1 d\Omega_{2-2\epsilon} e^{i\vec{b}\cdot\vec{k}_{T_1}}}{4(2\pi)^{3-2\epsilon} \sqrt{\alpha_1^2 - 4\hat{\tau}\xi_1}} \dots \frac{|k_{T_n}|^{-2\epsilon} d|k_{T_n}^2| d\alpha_n d\Omega_{2-2\epsilon} e^{i\vec{b}\cdot\vec{k}_{T_n}}}{4(2\pi)^{3-2\epsilon} \sqrt{\alpha_n^2 - 4\hat{\tau}\xi_n}} \\ &\delta\left(\sqrt{\hat{s}} - \sqrt{Q^2 + p_z^2} - \frac{\sqrt{\hat{s}}}{2} \sum_i \alpha_i\right) \delta\left(p_z + \frac{\sqrt{\hat{s}}}{2} \sum_i \beta_i\right) + \mathcal{O}\left(\frac{1}{b}\right) \end{aligned} \quad (2.2.38)$$

where we have changed integration variables from  $E_i$  to  $\alpha_i$  and we have denoted by  $\mathcal{O}\left(\frac{1}{b}\right)$  neglected terms which lead to power suppressed contributions in the small  $p_T$  limit. Note that we have kept the  $k_{T_i}^2$  dependence in the square-root factors, even though it is also  $\mathcal{O}\left(\frac{1}{b}\right)$ , for reasons to be discussed shortly.

We now perform the  $p_z$  integration with the help of the last delta function. This gives

$$p_z = -\frac{\sqrt{\hat{s}}}{2} \sum_{i=1}^n \beta_i \quad (2.2.39)$$

which implies that  $p_z \ll Q$  in the soft limit  $\alpha_i \rightarrow 0$ , because of Eq. (2.2.36).

The final expression for the phase space is obtained by introducing new variables  $z_i$  through

$$\alpha_1 = 1 - z_1; \quad \alpha_i = z_1 \dots z_{i-1} (1 - z_i), \quad i \geq 2 \quad (2.2.40)$$

with  $0 \leq z_i \leq 1$ , so that  $z_i \rightarrow 1$  in the soft limit, and

$$\sum_{i=1}^n \alpha_i = 1 - z_1 \dots z_n. \quad (2.2.41)$$

The argument of the energy-conservation delta function becomes

$$\begin{aligned} \sqrt{\hat{s}} - \sqrt{Q^2 + p_z^2} - \frac{\sqrt{\hat{s}}}{2} \sum_{i=1}^n \alpha_i &= \sqrt{\hat{s}} \left(1 - \sqrt{\hat{\tau}} - \frac{1}{2}(1 - z_1 \dots z_n)\right) + \mathcal{O}\left((1 - z_i)^2\right) \\ &= -\frac{\sqrt{\hat{s}}}{2} (\hat{\tau} - z_1 \dots z_n) + \mathcal{O}\left((1 - z_i)^2\right) + \mathcal{O}\left((1 - \hat{\tau})^2\right), \end{aligned} \quad (2.2.42)$$

and

$$\prod_{i=1}^n \frac{d\alpha_i}{\sqrt{\alpha_i^2 - 4\hat{\tau}\xi_i}} = \prod_{i=1}^n \frac{dz_i}{\sqrt{(1 - z_i)^2 - \frac{4\hat{\tau}\xi_i}{z_1^2 \dots z_{i-1}^2}}}. \quad (2.2.43)$$

The angular integrations can be performed by

$$\int d\Omega_{2-2\epsilon} e^{i\vec{b}\cdot\vec{k}_T} = (bk_T)^\epsilon (2\pi)^{1-\epsilon} J_{-\epsilon}(bk_T), \quad (2.2.44)$$

where  $J_{-\epsilon}$  is implicitly defined by Eq. (2.2.44) and it reduces to the Bessel function  $J_0$  when  $\epsilon \rightarrow 0$ . We get

$$\begin{aligned} d\Phi_{n+1}(p_1, p_2; p, k_1, \dots, k_n) &= \frac{8\pi^{3-\epsilon} Q^{2n}}{[4(2\pi)^{2-\epsilon}]^{n+1}} \frac{\hat{\tau}}{\Gamma(1-\epsilon)} d\xi_p \int db^2 (bp_T)^{-\epsilon} b^{2n\epsilon} J_{-\epsilon}(bp_T) \\ & J_{-\epsilon}(bk_{T_1}) \frac{(bk_{T_1})^{-\epsilon} d\xi_1 dz_1}{\sqrt{(1-z_1)^2 - 4\xi_1 \hat{\tau}}} \dots J_{-\epsilon}(bk_{T_n}) \frac{(bk_{T_n})^{-\epsilon} d\xi_n dz_n}{\sqrt{(1-z_n)^2 - \frac{4}{z_1^2 \dots z_{n-1}^2} \xi_n \hat{\tau}}} \\ & \delta(\hat{\tau} - z_1 \dots z_n) + \mathcal{O}\left(\frac{1}{b}\right). \end{aligned} \quad (2.2.45)$$

The integration range over transverse momenta is

$$0 \leq \xi_i \leq \frac{z_1^2 \dots z_{i-1}^2 (1-z_i)^2}{4\hat{\tau}}, \quad (2.2.46)$$

while all  $z_i$  range from  $0 \leq z_i \leq 1$ .

The expression of the phase space Eq. (2.2.45) would have the structure of a convolution, and thus factorizes upon Mellin transformation with respect to  $\hat{\tau}$ , were it not for the  $\xi_i$  terms in the denominator. Up to  $\mathcal{O}\left(\frac{1}{b}\right)$  corrections, these can be simplified by letting all  $\xi_i \rightarrow 0$ . This then leads to a factorized form of phase space which, when combined with a suitably factorized and renormalization-group improved form of the amplitude, Eq. (2.2.2) or Eq. (2.2.15), leads to the transverse momentum resummation of Sec. 2.4.

By ignoring term proportional to  $\xi_i$  w.r.t.  $(1-z_i)^2$  term we are implicitly assuming a particular hierarchy of scales, assuming that  $p_T$ , and hence in Fourier space all the  $\xi_i$ s are smaller than all the other energy scales. Looking to coloured region of Fig. 2.1, this is true in the green region when  $p_T$  is small but  $x$  is far from 1 while it is no longer true when we are both collinear and at threshold. In this overlap area we do not have any longer the following hierarchy but energy and  $p_T$ , even if both small with respect to  $Q^2$ , could be comparable in size. Transverse momentum resummation hence undergoes modifications in order to deal also with this kinematic situation, and a resummation of different type of logs arises. To this new *consistent or joint resummation* will be devoted Sec. 2.5 and we are going to come back on this point in that section.

From now on till Sec. 2.5, we are going to assume  $\xi_p$  to be the smallest scale of the process and we simplify Eq. (2.2.45), using the following equality

$$\lim_{\xi \rightarrow 0} \frac{1}{\sqrt{(1-z)^2 - 4a\xi}} = \left(\frac{1}{1-z}\right)_+ - \frac{1}{2} \ln \xi \delta(1-z) \quad (2.2.47)$$

valid in a distributional sense, coming to:

$$d\Phi_{n+1}(p_1, p_2; p, k_1, \dots, k_n) = \frac{8\pi^{3-\epsilon} Q^{2n}}{[4(2\pi)^{2-\epsilon}]^{n+1}} \frac{\hat{\tau}}{\Gamma(1-\epsilon)} d\xi_p \int db^2 (bp_T)^{-\epsilon} b^{2n\epsilon} J_{-\epsilon}(bp_T)$$

$$\begin{aligned}
& J_{-\epsilon}(bk_{T_1})(bk_{T_1})^{-\epsilon} d\xi_1 dz_1 \left[ \left( \frac{1}{1-z_1} \right)_+ - \delta(1-z_1) \frac{1}{2} \ln \xi_1 \right] \\
& \dots J_{-\epsilon}(bk_{T_n})(bk_{T_n})^{-\epsilon} d\xi_n dz_n \left[ \left( \frac{1}{1-z_n} \right)_+ - \delta(1-z_n) \frac{1}{2} \ln \xi_n \right] \\
& \delta(\hat{\tau} - z_1 \dots z_n) + \mathcal{O}\left(\frac{1}{b}\right)
\end{aligned} \tag{2.2.48}$$

where now the integration range over transverse momenta is

$$0 \leq \xi_i \leq \infty \tag{2.2.49}$$

for all  $\xi_i$ s.

Eq. (2.2.48) represents the factorized form of the phase space we are going to use in Sec. 2.4 to formulate transverse momentum resummation, together with the matrix element expressions derived in Sec. 2.2.1.

In conclusion, in this section, we prove factorization of matrix element and phase space both in the threshold limit and in the collinear limit. From NNLL, matrix element factorization occurs in the collinear limit in a more complicated form and single emission is no longer enough to describe the whole process. Phase space instead could be factorized both in the threshold and collinear limit, but in different ways, as shown in Sec. 2.2.2 and 2.2.3. These results are enough to present both the original transverse momentum resummation and the threshold resummation at fixed  $p_T$ . The presentation of these theories in next sections will be more or less a collection of known results [28, 30, 48–51], but they form the background for the new original works of this thesis which are contained in Sec. 2.5 and Sec. 2.6.

## 2.3 Threshold Resummation at fixed $p_T$

In this section we will summarize general theory of threshold resummation at fixed  $p_T$  for transverse momentum distributions. This threshold resummation was derived in general in Ref. [48, 52] at NLL and extended at NNLL in Ref. [45] using results of Refs. [53, 54].

Using renormalization group arguments of Ref. [31, 47], factorized matrix element Eq. (2.2.2) and factorized phase space Eq. (2.2.29) in  $N$  space associated to  $x$ , we can write a resummed expression for  $\frac{d\hat{\sigma}_{ij}}{d\xi_p}$  as

$$\frac{d\hat{\sigma}_{ij}}{d\xi_p} = \sigma_0 (C_0(N, \xi_p))_{ij} (g_0)_{ij}(\xi_p) \exp[\mathcal{G}(N, \xi_p)] \tag{2.3.1}$$

with

$$\mathcal{G}(N, \xi_p) = \Delta_i(N) + \Delta_j(N) + J_k(N) + S(N, \xi_p) \tag{2.3.2}$$

and  $i, j, k = q, g$  the type of the initial partons and of the hard parton recoiling against the studied system  $\mathcal{S}$ . In Eq. (2.3.1) we are assuming that the system  $\mathcal{S}$  does not interact strongly, as in the case of Drell-Yan or Higgs boson production. Therefore not colour

correlations are present and we can define Sudakov exponent components as

$$\Delta_i(N) = \int_0^1 dz \frac{z^{N-1} - 1}{1-z} \int_{\bar{Q}^2}^{\bar{Q}^2(1-z)^2} \frac{dq^2}{q^2} A_i^{\text{th}}(\alpha_s(q^2)) \quad (2.3.3)$$

$$J_k(N) = \int_0^1 dz \frac{z^{N-1} - 1}{1-z} \int_{\bar{Q}^2(1-z)^2}^{\bar{Q}^2(1-z)} \frac{dq^2}{q^2} A_k^{\text{th}}(\alpha_s(q^2)) + B_k^{\text{th}}(\alpha_s(\bar{Q}^2(1-z))) \quad (2.3.4)$$

$$S(N, \xi_p) = - \int_0^1 dz \frac{z^{N-1} - 1}{1-z} A_k^{\text{th}}(\alpha_s(\bar{Q}^2(1-z)^2)) \ln \frac{(\sqrt{1+\xi_p} + \sqrt{\xi_p})^2}{\xi_p}, \quad (2.3.5)$$

where  $\bar{Q}^2 = Q^2(\sqrt{1+\xi_p} + \sqrt{\xi_p})^2$  and  $A_i^{\text{th}}(\alpha_s)$ ,  $B_i^{\text{th}}(\alpha_s)$  are power series in  $\alpha_s$  with numerical coefficients.

$\Delta_i(N)$ ,  $J_k(N)$  and  $S(N, \xi_p)$  embody the different origins of large logarithms in our factorized form. In the threshold limit, the squared amplitude Eq. (2.2.2) and Eq. (2.2.13) has infrared and collinear singularities respectively proportional to  $(1-z_i)^{-2}$  and  $(\sin \theta_i)^{-2}$ ,<sup>2</sup> which, when combined with the phase space Eq. (2.2.29), lead each to a simple pole in  $\epsilon$  upon integration over the emitted particle's momenta. When these poles interfere with the  $(1-z)^{-2\epsilon}$  contained in the phase space Eq. (2.2.29), they originate logarithmic contributions which are resummed in the Sudakov exponential  $\Delta$  for the initial state and in the Jet exponential  $J$  for the final state. Resummation for the final state turn out to be difference since it is originated by the parton recoiling against  $\mathcal{S}$  which owns a non-zero value of transverse momentum. Finally,  $S$  is seen to originate from the Jacobian factor

$$\left( \frac{\xi_p}{(\sqrt{1+\xi_p} + \sqrt{\xi_p})^2} \right)^{-\epsilon} \quad (2.3.6)$$

present in the phase space (2.2.29): this factor is thus due to interference between this large-angle radiation, and the  $\epsilon$  poles due to soft emission. To clarify better various types of contributions we sketch factorization structure of Eq. (2.3.1) in Fig. 2.3.

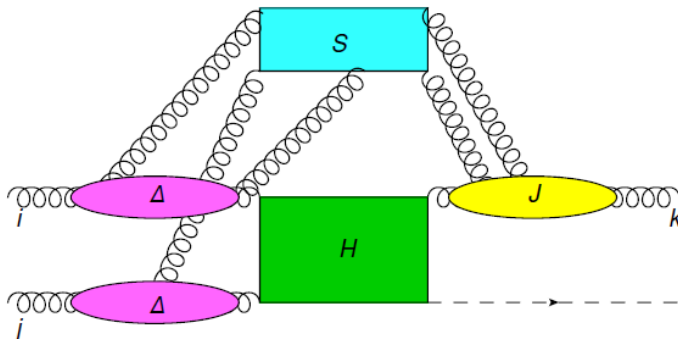


**Figure 2.3.** Factorization structure at threshold; large-angle soft contributions connect different hard Born lines.

<sup>2</sup>Remember that in this kinematics  $k_T = (1-z)\sin \theta$

Furthermore, in order to conclude our description of resummed structure Eq. (2.3.1),  $\sigma_0$  represents the inclusive LO total cross section,  $C_0$  represents the LO transverse momentum distribution normalized to the total cross section and  $(g_0)_{ij}$  takes into account virtual contributions proportional to  $\delta(1-x)$  and hence constant in  $N$ .

It is important to observe, due to the factorization properties highlighted in Sec. 2.2, that  $\Delta$  and  $J$  are universal and depend only on the type of emitting line (quark or gluon line). Instead, large angle soft contribution  $S$  depends on the observable (in this case transverse momentum distribution) and on the number  $m$  of strong interacting particles at the Born level [52, 53]. This is due to the fact that large angle soft contributions connect different hard lines, as depicted in Fig. 2.3. It can be proved that colour dependence is diagonal in the fundamental representation if  $m = 2, 3$ . For  $m \geq 4$  the soft components  $S$  becomes a matrix in colour space (see Ref. [55, 56] for an example).

The anomalous dimension  $A_i^{\text{th}}(\alpha_s)$  is normally denominated *cusplike anomalous dimension* and it coincides with the limit

$$A_i^{\text{th}}(\alpha_s) = \lim_{z \rightarrow 1} p_{ii}(z, \alpha_s) = \lim_{z \rightarrow 1} (1-z) P_{ii}(z, \alpha_s) \quad (2.3.7)$$

of the diagonal components of the Altarelli Parisi splitting functions ( $P_{ij}$  with  $i \neq j$  turn out to be regular in  $z \rightarrow 1$ ). The relation between  $p_{ij}$  contained in Eq. (2.2.13), the Altarelli-Parisi splitting functions and the cusplike anomalous dimension will be very important in Sec. 2.5 for the construction of the *consistent transverse momentum resummation*.

The explicit expressions for the universal anomalous dimension  $A^{\text{th}}$  up to  $\mathcal{O}(\alpha_s^3)$  and  $B^{\text{th}}$  up to  $\mathcal{O}(\alpha_s^2)$ , in order to reach NNLL accuracy are reported in Appendix C, Eqs. (C.1.1) and Eqs. (C.1.2).

We have concluded our general analysis about threshold resummation at fixed  $p_T$ . We now move to the other important resummation theory in the soft and collinear limit, transverse momentum resummation.

## 2.4 Transverse Momentum Resummation

Transverse momentum resummation predicts at any order in  $\alpha_s$  singular components as  $\frac{\ln^k \xi_p}{\xi_p}$  in the transverse momentum distributions.

It was proposed long ago in the seminar paper [28] at NLL using conjugate space formalism, and then formalized and extended in principle at any logarithmic order by Refs. [30, 49–51, 57, 58]. Due to its importance, it was extensively studied also in the context of soft-collinear-effective-theory, for example, in Refs. [34, 36, 59]. Very recently, new Monte-Carlo approach of Ref. [43, 44] permits the first NNNLL resummation directly in momentum space [44]. In this section, we are going to summarize general formulas and ideas behind transverse momentum resummation in conjugate space.

Resummation is performed in Mellin-Fourier space with Mellin transform taken with respect to  $x$  (or  $\hat{\tau}$  since the difference is subleading in the limit  $\xi_p \ll (1-\hat{\tau})^2$ ) and Fourier Transform taken with respect to  $\xi_p$  as

$$\frac{d\hat{\sigma}}{d\xi_p}(N, b) = \int_0^\infty d\xi_p J_0(\hat{b}\sqrt{\xi_p}) \frac{d\hat{\sigma}}{d\xi_p}(N, \xi_p) \quad (2.4.1a)$$

$$\frac{d\hat{\sigma}}{d\xi_p}(N, \xi_p) = \int_0^\infty d\hat{b} \frac{\hat{b}}{2} J_0(\hat{b}\sqrt{\xi_p}) \frac{d\hat{\sigma}}{d\xi_p}(N, b) \quad (2.4.1b)$$

where  $\hat{b} = bQ^2$  is the conjugate variable to  $\sqrt{\xi_p}$ ,  $b$  the conjugate variable to  $p_T$  and  $J_0$  is the Bessel Function  $J$  of order 0.

Please remember that by defining Mellin transform with respect to  $x$  rather than to  $\hat{\tau}$ , kinematic limits Eq. (2.1.2) permit to extend  $\xi_p$  integration range till infinity without exiting from the physical region. Even if such difference is subleading in this context, it will become important in Sec. 2.5 when  $\xi_p \approx (1 - \hat{\tau})^2$  region will be inspected.

Using factorized matrix elements, Eq. (2.2.2), and factorized phase space, Eq. (2.2.48), we come to the following resummed expression:

$$\frac{d\hat{\sigma}_{ij}}{d\xi_p}(N, b, \alpha_s(Q^2), Q^2) = (\sigma_0)_c \sum_{k,l} \mathcal{H}_{cc \rightarrow kl}(N, \alpha_s(Q^2)) \Gamma(N, \hat{b})_{ki} \Gamma(N, \hat{b})_{lj} \exp[\mathfrak{S}(N, \hat{b})] \quad (2.4.2)$$

with

$$\Gamma(N, \hat{b}) = P \exp \left[ \int_0^1 dz z^{N-1} \int_0^\infty d\xi J_0(\hat{b}\sqrt{\xi}) \left\{ \left[ \frac{\mathbf{p}(z, \alpha_s(Q^2\xi))}{\xi} \right]_+ \frac{1}{[1-z]_+} - \frac{1}{2} \left[ \frac{A_c^{\text{th}}(\alpha_s(Q^2\xi)) \ln \xi}{\xi} \right]_+ \delta_c^i \delta(1-z) \right\} \right] \quad (2.4.3)$$

and  $\mathfrak{S}(N, \hat{b})$  written as

$$\begin{aligned} \mathfrak{S}(N, \hat{b}) &= \int_0^1 dz z^{N-1} \int_0^\infty d\xi J_0(\hat{b}\sqrt{\xi}) \\ &\quad \left\{ \left[ \frac{\mathcal{D}_c^{\text{PT}}(\alpha_s(Q^2\xi))}{\xi} \right]_+ \frac{1}{[1-z]_+} - \frac{1}{2} \left[ \frac{\mathcal{D}_c^{\text{PT}}(\alpha_s(Q^2\xi)) \ln \xi}{\xi} \right]_+ \delta(1-z) \right\} \\ &\quad + \int_0^1 dz z^{N-1} \int_0^\infty d\xi J_0(\hat{b}\sqrt{\xi}) \left[ \frac{\tilde{B}_c^{\text{PT}}(\alpha_s(Q^2\xi))}{\xi} \right]_+ \delta(1-z) \\ &\quad + \int_0^1 dz z^{N-1} \int_0^\infty d\xi J_0(\hat{b}\sqrt{\xi}) \left[ \frac{\mathcal{C}_{ij}(z, \alpha_s(Q^2\xi))}{\xi} \right]_+. \end{aligned} \quad (2.4.4)$$

In Eq. (2.4.2), indexes  $i, j$  stand for the different partonic channel we are considering in the initial scale while  $k, l = q, g$  represent the flavour of the intermediate partons resulting after collinear radiation.  $\mathcal{H}_{cc \rightarrow kl}$  takes into account virtual  $\delta(\xi_p)$  contributions,  $\Gamma(N, \hat{b})$  embodies all the LL and NLL terms, while  $\mathfrak{S}$  takes into account all NNLL and beyond terms coming from the more complicated correlated structure of the matrix element. In Eq. (2.4.3), the notation  $P$  in front of the exponential stands for path-ordering since the

exponential is in this case a matrix in flavour space, due to the presence of Altarelli-Parisi splitting function numerator  $\mathbf{p}$ . Altarelli-Parisi splitting function numerator originates from matrix element Eq. (2.2.13), while the extra plus distribution in  $(1-z)$  comes from the first term in phase space decomposition, Eq. (2.2.48). Together they form Altarelli-Parisi splitting function but deprived of delta terms in  $P_{gg}$  and  $P_{q\bar{q}}$ . Then, as in Sec. 2.3,  $A_c^{\text{th}}$  indicates the *cusp anomalous dimension*, hence the limit  $z \rightarrow 1$  of  $p_{cc}$ . Transverse Momentum Resummation separates two classes of process: quark-antiquark initiated and gluon initiated. The index  $c = q, g$  defines this distinction. In Eq. (2.4.2), we fix renormalization and factorization scale to  $Q^2$  for simplicity.

As said before, Eq. (2.4.4) includes extra NNLL terms coming from the more complicated correlated structure of the matrix element. In Eq. (2.4.4), they have been separated according to their  $z \rightarrow 1$  behaviour, divergent ( $\mathcal{D}_c^{\text{pr}}$ ), constant ( $\tilde{B}_c$ ) or suppressed ( $\mathcal{C}_{ij}$ ).

Eq. (2.4.2) is the most suitable form to understand relation with our phase space and matrix element factorization but it is not the most common description of Refs. [28, 30, 58]. We are going to relate the two expressions by solving integrals present in Eq. (2.4.3) and (2.4.4). First of all we rewrite Eq. (2.4.3) and (2.4.4) by solving Mellin integral obtaining

$$\Gamma(N, \hat{b}) = \int_0^\infty d\xi J_0(\hat{b}\sqrt{\xi}) \left\{ \left[ \frac{\gamma(N, \alpha_s(Q^2\xi))}{\xi} \right]_+ - \frac{1}{2} \left[ \frac{A_c^{\text{th}}(\alpha_s(Q^2\xi)) \ln \xi}{\xi} \right]_+ \right\} \quad (2.4.5)$$

$$\begin{aligned} \mathfrak{S}(N, \hat{b}) = & \int_0^\infty d\xi J_0(\hat{b}\sqrt{\xi}) \\ & \left\{ \left[ \frac{\mathcal{D}_c^{\text{pr}}(\alpha_s(Q^2\xi))}{\xi} \right]_+ D_0(N) - \frac{1}{2} \left[ \frac{\mathcal{D}_c^{\text{pr}}(\alpha_s(Q^2\xi)) \ln \xi}{\xi} \right]_+ \right\} \\ & + \int_0^\infty d\xi J_0(\hat{b}\sqrt{\xi}) \left\{ \left[ \frac{B_c(\alpha_s(Q^2\xi))}{\xi} \right]_+ + \left[ \frac{\mathcal{C}_{ij}(N, \alpha_s(Q^2\xi))}{\xi} \right]_+ \right\}, \quad (2.4.6) \end{aligned}$$

where

$$D_0(N) = \int_0^1 dz z^{N-1} \left( \frac{1}{1-z} \right)_+ = \mathcal{M} \left[ \left( \frac{1}{1-z} \right)_+ \right], \quad (2.4.7)$$

$\gamma(N, \alpha_s)$  are now the complete Altarelli-Parisi anomalous dimension and in order to form them we change  $\delta(1-z)$  term  $\tilde{B}_c(\alpha_s)$  accordingly

$$B_c(\alpha_s) = \tilde{B}_c(\alpha_s) - \delta P_{cc}(\alpha_s) \quad (2.4.8)$$

with  $\delta P_{cc}(\alpha_s)$  the  $\delta(1-z)$  term in the diagonal splitting function  $P_{cc}(z, \alpha_s)$ . An explicit expression for  $D_0(N) = -S_1^{\text{H}}(N-1)$  can be found in Appendix B, Eq. (B.5.4).

Crucial trick is now the following: running coupling evolution expresses  $\alpha_s(Q^2\xi)$  in terms of  $\alpha_s(Q^2)$  and  $\ln^k \xi$ , but now  $\xi$  integral relates  $\ln^k \xi$  with  $\ln^k b$  in the following way

$$\int_0^\infty d\xi J_0(\hat{b}\sqrt{\xi}) \left[ \frac{\ln^k \xi}{\xi} \right]_+ = - \int_{\frac{b_0^2}{b^2}}^{Q^2} dq^2 \frac{\ln^k \frac{q^2}{Q^2}}{q^2} + \mathcal{O}(\text{NNNLL}). \quad (2.4.9)$$

with  $b_0 = 2e^{-\gamma_E}$ . At NNNLL extra term proportional to  $\zeta_3$  arise and anomalous dimension have to be changed from  $\xi_p$  form to  $b$  form accordingly [44]. For our scope, since we are interested in presenting expressions up to NNLL, we rewrite exponentials as

$$\Gamma(N, b) = P \exp \left[ - \int_{\frac{b_0}{b^2}}^{Q^2} \frac{dq^2}{q^2} \left( \gamma(N, \alpha_s(q^2)) + \frac{1}{2} A_c^{\text{th}}(\alpha_s(q^2)) \ln \frac{Q^2}{q^2} \right) \right], \quad (2.4.10)$$

$$\begin{aligned} \mathfrak{S}(N, b) = & - \int_{\frac{b_0}{b^2}}^{Q^2} \frac{dq^2}{q^2} \left[ \mathcal{D}_c^{p\text{T}}(\alpha_s(q^2)) D_0(N) + \frac{1}{2} \mathcal{D}_c^{p\text{T}}(\alpha_s(q^2)) \ln \frac{Q^2}{q^2} \right] \\ & - \int_{\frac{b_0}{b^2}}^{Q^2} \frac{dq^2}{q^2} [B_c(\alpha_s(q^2)) + \mathcal{C}_{ij}(N, \alpha_s(q^2))] \end{aligned} \quad (2.4.11)$$

without any change in the anomalous dimensions.

Last step is a reorganization of the resummed expression. First term in  $\Gamma$  can be viewed as the evolution of PDFs from a soft scale  $\frac{b_0^2}{b^2}$  to the hard scale  $Q^2$ . Moreover we can rewrite virtual contribution in Eq. (2.4.2) as

$$\mathcal{H}_{cc \rightarrow ij}(N, \alpha_s(Q^2)) = H_c(\alpha_s(Q^2)) C_{ci}(N, \alpha_s(Q^2)) C_{cj}(N, \alpha_s(Q^2)) \quad (2.4.12)$$

where all the  $N$  dependence is contained into coefficient function  $C$ . It can be proved [28, 30, 58] that all the  $N$  dependence in the exponent  $\mathfrak{S}$  can be adsorbed into  $\mathcal{H}$  simply by evaluating coefficient function  $C$  at the soft scale  $\frac{b_0^2}{b^2}$ .

This means that  $\mathcal{D}_c^{p\text{T}}$  and  $\mathcal{C}_{ij}$  can be related in a simple way with  $\mathcal{H}_{cc \rightarrow i,j}$ . In particular,  $\mathcal{D}_c^{p\text{T}}$  is given by the  $N \rightarrow \infty$  limit of  $\mathcal{H}_{cc \rightarrow cc}$ ; defining

$$\mathcal{H}_{cc \rightarrow cc}(N, \alpha_s) = D_c^{p\text{T}}(\alpha_s) D_0(N) + \mathcal{O}(1) \quad (2.4.13)$$

we have that

$$\mathcal{D}_c^{p\text{T}}(\alpha_s) = \frac{\beta(\alpha_s)}{\alpha_s} \frac{d \ln D_c^{p\text{T}}(\alpha_s)}{d \ln \alpha_s} \quad (2.4.14)$$

where  $\beta(\alpha_s)$  is the QCD beta function defined, for example in Appendix A

$$\beta(\alpha_s) = -\alpha_s^2 (\beta_0 + \alpha_s \beta_1 + \dots). \quad (2.4.15)$$

On the contrary,  $\mathcal{C}_{ij}$  is related to the evolution of the suppressed part in the coefficient function  $C$ . At NNLL, in our case coefficient function  $C$  will contain only at least  $\mathcal{O}\left(\frac{1}{N}\right)$  terms. In this case, at this level of accuracy the relation between  $\mathcal{C}_{ij}$  and the product  $C_{ci}C_{cj}$  is the following:

$$\mathcal{C}_{ij} = \frac{\beta(\alpha_s)}{\alpha_s} \frac{d(\ln C_{c,i}(\alpha_s) + \ln C_{c,j}(\alpha_s))}{d \ln \alpha_s}. \quad (2.4.16)$$

Using these results, we thus obtain the following final expression for the hadronic transverse momentum distribution:

$$\frac{d\sigma}{d\xi_p}(N, b, \alpha_s) = (\sigma_0)_c H_c(\alpha_s(Q^2)) C_{ci}\left(N, \alpha_s\left(\frac{b_0^2}{b^2}\right)\right) C_{cj}\left(N, \alpha_s\left(\frac{b_0^2}{b^2}\right)\right)$$

$$\exp[S_c(b)] f_i\left(N, \frac{b_0^2}{b^2}\right) f_j\left(N, \frac{b_0^2}{b^2}\right) \quad (2.4.17)$$

with

$$S_c(b) = - \int_{\frac{b_0^2}{b^2}}^{Q^2} \frac{dq^2}{q^2} \left[ A_c^{pT}(\alpha_s(q^2)) \ln \frac{Q^2}{q^2} + B_c(\alpha_s(q^2)) \right]. \quad (2.4.18)$$

and  $A_c^{pT}(\alpha_s) = A_c^{\text{th}}(\alpha_s) + \frac{1}{2} \mathcal{D}_c^{pT}(\alpha_s)$ .

Eq. (2.4.17) is the common resummed expression for the transverse momentum distribution presented in literature. However, it gives back directly the hadronic distribution summed over all the partonic channels. If we want to separate different channel contributions we need to come back to Eq. (2.4.2) and to evaluate the path-ordering exponential up to some logarithmic accuracy. Evolution of PDFs up to some logarithmic order is presented in detail in Appendix A, where general perturbative solution of DGLAP equation is derived.

A possible expression for the  $ij$  partonic contribution can be written using definition of **U** Eq. (A.3.12) and **L** Eq. (A.3.8) of Appendix A as

$$\begin{aligned} \frac{d\hat{\sigma}_{ij}}{d\xi_p}(N, b, \alpha_s(\mu_R^2), \mu_F^2) &= (\sigma_0)_c H_c(\alpha_s(\mu_R^2)) \exp[S_c(b)] \\ &C_{ca}\left(N, \alpha_s\left(\frac{b_0^2}{b^2}\right)\right) C_{cb}\left(N, \alpha_s\left(\frac{b_0^2}{b^2}\right)\right) \\ &U_{al}\left(N, \alpha_s\left(\frac{b_0^2}{b^2}\right)\right) L_{lk}(N, b, \mu_F^2) U_{ki}(N, \alpha_s(\mu_F^2)) \\ &U_{br}\left(N, \alpha_s\left(\frac{b_0^2}{b^2}\right)\right) L_{rw}(N, b, \mu_F^2) U_{wj}(N, \alpha_s(\mu_F^2)) \end{aligned} \quad (2.4.19)$$

where  $S_c(b)$  is defined as in Eq. (2.4.18) and  $C_{ca}\left(N, \alpha_s\left(\frac{b_0^2}{b^2}\right)\right) U_{al}\left(N, \alpha_s\left(\frac{b_0^2}{b^2}\right)\right)$  have to be then evolved as

$$\begin{aligned} C_{ca}\left(N, \alpha_s\left(\frac{b_0^2}{b^2}\right)\right) U_{al}\left(N, \alpha_s\left(\frac{b_0^2}{b^2}\right)\right) &= C_{ca}(N, \alpha_s(\mu_R^2)) U_{al}(N, \alpha_s(\mu_R^2)) \\ \exp\left[- \int_{\frac{b_0^2}{b^2}}^{Q^2} \frac{dq^2}{q^2} \frac{\beta(\alpha_s(q^2))}{\alpha_s(q^2)} \left[ \frac{d \ln C_{ca}(N, \alpha_s(q^2))}{d \ln \alpha_s(q^2)} + \frac{d \ln U_{al}(N, \alpha_s(q^2))}{d \ln \alpha_s(q^2)} \right] \right] &. \end{aligned} \quad (2.4.20)$$

At the end all running coupling  $\alpha_s(q^2)$  in the different exponents has to be evolved till  $\alpha_s(\mu_R^2)$  and PDFs are supposed to be evaluated at the factorization scale  $\mu_F^2$ . Sum is implicitly assumed over repeated indexes.

Eq. (2.4.19) is a very suitable form to take under control all the logarithmic contributions and to prevent to insert subleading effects in our result.

In all this thesis, the studied logarithmic accuracy in soft and collinear limit is NNLL. To achieve this accuracy we need cusp anomalous dimension up to three loops,  $B_c^{pT}(\alpha_s)$  at two loops and hard-collinear function  $\mathcal{H}_{cc \rightarrow ij}$  up to order  $\alpha_s^2$  to derive  $D_c^{pT}(\alpha_s)$  at two loops. Moreover we need  $C$  decomposition at one loop to properly define suppressed large  $N$  evolution at NNLL.

It is worth mentioning that while suppressed large- $N$  terms and singular large- $N$  terms are fixed by evolution factor  $\mathcal{D}$  and  $\mathcal{C}$  in Eq. (2.4.2), there is a sort of freedom regarding the position of constant  $N$  terms in Eq. (2.4.17). Inclusion of constant  $N$  terms can be done in  $H_c$  or in  $C$  in any possible combination; this brings to a different definition of the Sudakov exponent in the  $B_c(\alpha_s)$  term. Such invariance is called in literature *resummation scheme invariance* and it has been largely studied in Ref. [50]. We are going to refer the interested reader to this reference for further information. In the rest of the thesis we are going to make a particular resummation scheme choice, pretending to have  $C$  free of constant terms which are all included into  $H_c$ . This resummation choice is called *hard scheme* [50] and all the explicit results of Sec. 2.7 and Appendix C will be presented in this particular scheme.

In conclusion, in this section we summarized the standard transverse momentum resummation in conjugate space up to NNLL. We linked the resummation structure to our factorize phase space and matrix elements, producing our first form Eq. (2.4.2). Then we simplify this expression to match with the standard formula present in literature. At the end, Eq. (2.4.19) shows also a possible implementation of the resummed expression which takes into account, explicitly, different partonic channel contributions and renormalization/factorization scale dependence.

## 2.5 Consistent Transverse Momentum Resummation

In previous section, the original derivation of transverse momentum resummation in Mellin-Fourier space [28, 30, 58] was derived. It is important to remember that the final expression Eq. (2.4.17) is valid only when  $p_T^2$  or  $\xi_p$  is the smallest scale of the process. We used this condition to factorize phase space when we took the limit Eq. (2.2.47). In Mellin-Fourier space we are studying the region

$$b \rightarrow \infty \qquad \text{at fixed } N. \qquad (2.5.1)$$

It is easy to convince yourself that this situation will become troublesome at threshold when also  $s$  is approaching its minimum and it could become of the same order of  $\xi_p$ . In  $b$ - $N$  space we are in the situation where both  $b$  and  $N$  are growing to infinity with no particular pre-definite direction.

In this section we want to overcome this problem and to derive a new resummation theory, which we are going to call *consistent transverse momentum resummation*, valid in the region

$$\xi_p \approx (1 - \hat{\tau})^2 \ll 1. \qquad (2.5.2)$$

Moreover we will see that with a little efforts we could extend our new resummation procedure in order to include the original transverse momentum resummation of Sec. 2.4 as a by-product. All presentation works at NNLL and we will closely follow for all the section the derivation of Ref. [45].

Before starting, we want to highlight the reason of this theoretical study. Several works on threshold resummation for inclusive cross section [60, 64, 65] highlight the fact that threshold dynamics at inclusive level was totally dominated by small- $p_T$  limit at differential level. This suggests the idea that from the pure knowledge of transverse

momentum resummation for single differential transverse momentum distribution, the threshold resummation for total cross section should be derived by simply performing integration over  $\xi_p$ .

However, using original derivation of Sec. 2.4 this is not the case; the situation is even worse, because, strictly speaking, the integral over  $\xi_p$  of the resummed expression Eq. (2.4.17) is divergent. Several solutions have been proposed in literature to overcome this problem, by introducing properly subleading contributions which, without touching the large  $b$  limit, permits to obtain a finite value for the integral. The most common prescription used in literature is the so-called *unitarity constraint* [30, 51, 58]: we fix the integral of the resummed and matched expression to be the inclusive cross section of the fixed order result used in the matching procedure.

In Refs. [60–62], it was shown for the first time that proper subleading contributions could be included at NLL in Eq. (2.4.17) in order to fix integral over  $\xi_p$  to be equal to the NLL threshold resummed inclusive cross section. However, the extension of this formalism to NNLL is particularly cumbersome and first attempt of Ref. [63] showed that ad hoc corrections have to be included in the extension.

In this section, instead, following Ref. [45] we want to present a particular simple derivation which permits to reformulate transverse momentum resummation in order to deal also with region (2.5.2). Being our final expression valid for small- $p_T$  at all energies, it is clear from analysis of Ref. [31, 64] that its integral over  $p_T$  must coincide with a threshold resummed inclusive cross section. In Ref. [45] this occurrence was explicitly checked in general up to NNLL. We will present in this thesis an explicit check of this property in Sec. 2.7 for our test process, EFT Higgs boson production in gluon fusion.

It is important to note that the extension we are going to present is not a  $\xi_p$  extension; we will not derived an expression which is valid even for larger  $p_T$ . Instead, it is an "energy" extension, meaning that we resum leading small- $p_T$  contributions at any value of the centre-of-mass energy, even at threshold. This means that our final formula would not include threshold resummation at fixed  $p_T$  of Sec. 2.3 which still remains a different theory, performed in a disjointed region. We will come back on the relation between consistent small- $p_T$  resummation and threshold resummation at fixed  $p_T$  in Sec. 2.6 where a proper combination of the two will be proposed.

We are ready to start; we want to retrace derivation of the original transverse momentum resummation focusing on the steps where we used condition  $\xi_p \ll (1 - \hat{\tau})^2$ .

In the double limit  $\xi_p \rightarrow 0$ ,  $x \rightarrow 1$  matrix element factorization occurs as in Sec. 2.2.1. Up to NLL, this can be easily appreciated since the derivation works in the small- $\xi_p$  limit for any  $x$  (and hence  $z$ ); beyond NLL situation become more difficult due to correlation presence. In Ref. [45], it was proved that no modification in matrix element occurs even at NNLL; however, a general prove at any logarithmic order is up to now not available.

Hence, up to NNLL, modifications with respect to original derivation of Sec. 2.4 appears only in the phase space. In particular, we make use of condition  $\xi_p \ll (1 - \hat{\tau})^2$  in moving from Eq. (2.2.45) to the factorized phase space expression Eq. (2.2.48).

Therefore, we are going to come back to Eq. (2.2.45) and we are going to search another procedure to reach factorization. In particular we want to use the fact that in

the region of interest Eq. (2.5.2) we have

$$z_1 \approx z_2 \approx \dots \approx z_n \approx \hat{\tau} \approx 1; \quad (2.5.3)$$

they are all of the same size. Then we rewrite square root present in Eq. (2.2.45) as

$$\frac{1}{\sqrt{(1-z_i)^2 - 4\frac{\tau}{z_1^2 \dots z_{i-1}^2} \xi}} \approx \frac{1}{\sqrt{(1-z_i)^2 - 4z_i \xi}} \quad (2.5.4)$$

thus introducing subleading contributions both at threshold and at small- $p_T$ . Clearly Eq. (2.5.4) is one of the possible equivalent form for the original square root but, as highlighted in Ref. [45], subsequent steps turn out to be simpler using this particular modification. We thus reach the following form for the phase space

$$\begin{aligned} d\Phi_{n+1}(p_1, p_2; p, k_1, \dots, k_n) &= \frac{8\pi^{3-\epsilon} Q^{2n}}{[4(2\pi)^{2-\epsilon}]^{n+1}} \frac{\hat{\tau}}{\Gamma(1-\epsilon)} d\xi_p \int db^2 (bp_T)^{-\epsilon} b^{2n\epsilon} J_{-\epsilon}(bp_T) \\ &J_{-\epsilon}(bk_{T_1}) \frac{(bk_{T_1})^{-\epsilon} d\xi_1 dz_1}{\sqrt{(1-z_1)^2 - 4z_1 \xi_1}} \dots J_{-\epsilon}(bk_{T_n}) \frac{(bk_{T_n})^{-\epsilon} d\xi_n dz_n}{\sqrt{(1-z_n)^2 - 4z_n \xi_n}} \\ &\delta(\hat{\tau} - z_1 \dots z_n) + \mathcal{O}\left(\frac{1}{b}\right) + \mathcal{O}\left(\frac{1}{N}\right). \end{aligned} \quad (2.5.5)$$

Phase space of Eq. (2.5.5) is now factorized. However, we need a little more care to highlight  $\epsilon$  pole origin. First of all we have to disentangle various  $\xi_i$  and  $z_i$  interactions. Due to modification Eq. (2.5.4), now the integration limits are

$$0 \leq z_i \leq 1 \quad 0 \leq \xi_i \leq \frac{(1-z_i)^2}{4z_i}. \quad (2.5.6)$$

By performing the following change of variable

$$z'_i = z_i \left( \sqrt{1+\xi_i} + \sqrt{\xi_i} \right)^2 \quad (2.5.7)$$

we reach a totally decoupled situation

$$0 \leq z'_i \leq 1 \quad \xi_i \geq 0. \quad (2.5.8)$$

We are now ready to use the following equality between distributions to highlight threshold divergence hidden into the square root

$$\begin{aligned} \frac{1}{\sqrt{(1-z)^2 - 4z\xi}} &= \frac{1}{\sqrt{(1-z') \left( 1 - (\sqrt{1+\xi} - \sqrt{\xi})^4 z' \right)}} \\ &= \left( \frac{1}{\sqrt{(1-z') \left( 1 - (\sqrt{1+\xi} - \sqrt{\xi})^4 z' \right)}} \right)_+^z \end{aligned}$$

$$+ \frac{1}{2} \frac{1}{(\sqrt{1+\xi} - \sqrt{\xi})^2} (\ln(1+\xi) - \ln \xi) \delta(1-z') \quad (2.5.9)$$

with  $z$  plus distribution defined as

$$\int_0^1 dz g(z) [f(z)]_+^z = \int_0^1 dz (g(z) - g(1)) f(z) \quad (2.5.10)$$

in order to come to the following phase space factorized expression:

$$\begin{aligned} d\Phi_{n+1}(p_1, p_2; p, k_1, \dots, k_n) &= \frac{8\pi^{3-\epsilon} Q^{2n}}{[4(2\pi)^{2-\epsilon}]^{n+1}} \frac{\hat{\tau}}{\Gamma(1-\epsilon)} d\xi_p \int db^2 (bp_{\text{T}})^{-\epsilon} b^{2n\epsilon} J_{-\epsilon}(bp_{\text{T}}) \\ J_{-\epsilon}(bk_{\text{T}_1}) (bk_{\text{T}_1})^{-\epsilon} d\xi_1 dz'_1 &\left[ \left( \frac{1}{\sqrt{(1-z'_1) \left(1 - (\sqrt{1+\xi_1} - \sqrt{\xi_1})^4 z'\right)}} \right)_+^z \right. \\ &\quad \left. + \frac{1}{2} \frac{1}{(\sqrt{1+\xi_1} - \sqrt{\xi_1})^2} (\ln(1+\xi_1) - \ln \xi_1) \delta(1-z'_1) \right] \dots \\ J_{-\epsilon}(bk_{\text{T}_n}) (bk_{\text{T}_n})^{-\epsilon} d\xi_n dz'_n &\left[ \left( \frac{1}{\sqrt{(1-z'_n) \left(1 - (\sqrt{1+\xi_n} - \sqrt{\xi_n})^4 z'\right)}} \right)_+^z \right. \\ &\quad \left. + \frac{1}{2} \frac{1}{(\sqrt{1+\xi_n} - \sqrt{\xi_n})^2} (\ln(1+\xi_n) - \ln \xi_n) \delta(1-z'_n) \right] \\ \delta\left(x \left(\sqrt{1+\xi_p} - \sqrt{\xi_p}\right)^2 - z_1 \dots z_n \left(\sqrt{1+\xi_1} - \sqrt{\xi_1}\right)^2 \dots \left(\sqrt{1+\xi_n} - \sqrt{\xi_n}\right)^2\right) & \\ + \mathcal{O}\left(\frac{1}{b}\right) + \mathcal{O}\left(\frac{1}{N}\right). & \quad (2.5.11) \end{aligned}$$

In conclusion, consistent transverse momentum resummation is now performed as original transverse momentum resummation using the factorized expression for the matrix element  $\mathcal{M}$  Eq. (2.2.2), or (2.2.15) and for the phase space Eq. (2.5.11) rather than Eq. (2.2.45).

In doing this, we also need to pay attention to the actual definition of Mellin and Fourier transform. Indeed, it is no longer possible to ignore upper limit of integration of  $\xi_p$ , since when  $\hat{\tau} \rightarrow 1$ ,  $\xi_p^{\text{max}} \rightarrow 0$ . We thus have to take Mellin transform with respect to  $x$  and use delta constraint to solve it.

Before writing resummed expression in the consistent case it is interesting to understand which actual contributions we are inserting using Eq. (2.5.11) rather than Eq. (2.2.45). The situation is clearer in Mellin-Fourier space; by expanding at small- $\xi$  the square root and then by computing Fourier Mellin transform order by order, we obtain [45]:

$$\int_0^1 dz' z'^{N-1} \int_0^\infty d\xi \frac{(\sqrt{1+\xi} - \sqrt{\xi})^{2N} J_0(b\sqrt{\xi})}{\sqrt{(1-z) \left(1 - (\sqrt{1+\xi_p} - \sqrt{\xi_p})^4 z\right)}} = \frac{2}{b^2} \left(1 - \frac{4N^2}{b^2} + \frac{16N^4}{b^4} + \dots\right). \quad (2.5.12)$$

Thus we are ignoring terms which are suppressed by powers of  $b$  but which are enhanced by the same powers of  $N$ . Clearly, these terms become important when both  $N$  and  $b$  are becoming large. In conclusion, consistent transverse momentum resummation, performed using Eq. (2.5.11) rather than Eq. (2.2.45), considers a slightly different limit in Mellin-Fourier space with respect to the original transverse momentum resummation [45]:

$$b \rightarrow \infty \quad \text{at fixed } \frac{N}{b} \text{ ratio} \quad (2.5.13)$$

rather than

$$b \rightarrow \infty \quad \text{at fixed } N \quad (2.5.14)$$

as in the original Collins-Soper-Sterman work [28]. By considering Eq. (2.5.13) limit, indeed, all the series of contribution coming from the square root Eq. (2.5.12) are taken into account.

However, this is not the only advantage of consistent resummation form. Indeed it is easy to convince yourself that the entire expansion Eq. (2.5.12) is meaningless at integrated level, since all the terms diverge for  $b = 0$ . We can clarify better this concept working directly in momentum space. The integral over  $\xi$  of the square root performed term by term in small- $\xi$  expansion,

$$\int_0^{\frac{(1-z)^2}{4z}} d\xi \frac{1}{\sqrt{(1-z)^2 - 4z\xi}} = \frac{1}{1-z} \int_0^{\frac{(1-z)^2}{4z}} d\xi \left(1 + \frac{2\xi z}{(1-z)^2} + \frac{6\xi^2 z^2}{(1-z)^4} + \dots\right) = \frac{(1-z)}{4z} \left(1 + \frac{1}{4} + \frac{1}{8} + \dots\right), \quad (2.5.15)$$

turns out to be an infinite sum of contributions of the same order. Therefore the entire square root has to be retained in order to catch the correct  $\xi_p$  integral of the resummed expression.

In order to match properly with threshold resummation at inclusive level, even a different logarithmic power counting has to be used. We will see in a while that in the limit Eq. (2.5.13), large-logarithms will be organized using two different scales,  $N$ , and  $\chi = \bar{N}^2 + \frac{b^2}{b_0^2}$ . The logarithmic accuracy will be defined looking at the sum of the power of  $\ln N$  and the power of  $\ln \chi$ . Terms like  $\ln N \ln^{k-1} \chi$  and  $\ln^k \chi$  will be then considered of the same logarithmic order. This different logarithmic counting is linked to our requirement on the integral. Indeed in the example just mentioned both the terms contribute to the  $\ln^k N$  coefficient after  $\xi_p$  integration.

In the next subsection we will see that consistent resummation permits to formulate a resummed expression which coincides in Eq. (2.5.14) region with original transverse momentum resummation, differs in general for  $\frac{N}{b}$  terms but reduces to threshold resummed inclusive cross section when  $b = 0$ .

### 2.5.1 Resummed Expression

Consistent transverse momentum resummation for  $\frac{d\hat{\sigma}}{d\xi_p}$  takes the following form

$$\frac{d\hat{\sigma}_{ij}^{\text{cons}}}{d\xi_p}(N, b, \alpha_s(Q^2), Q^2) = (\sigma_0)_c \sum_{k,l} \mathcal{H}_{cc \rightarrow kl}(N, \alpha_s(Q^2)) \Gamma(N, \hat{b})_{ki} \Gamma(N, \hat{b})_{lj} \exp[\mathfrak{S}(N, \hat{b})] \quad (2.5.16)$$

with

$$\begin{aligned} \Gamma(N, \hat{b}) = & P \exp \left[ \int_0^1 dz' z'^{N-1} \int_0^\infty d\xi J_0(\hat{b}\sqrt{\xi}) (\sqrt{1+\xi} - \sqrt{\xi})^{2N} \right. \\ & \left. \left\{ \left[ \frac{A_c^{\text{th}}(\alpha_s(Q^2\xi))}{\xi} \right]_+ \left[ \frac{1}{\sqrt{(1-z') (1 - (\sqrt{1+\xi} - \sqrt{\xi})^4 z)}} \right]_+^z \right. \right. \\ & + \frac{1}{2} \frac{1}{(\sqrt{1+\xi} - \sqrt{\xi})^2} \\ & \left. \left[ 2 \frac{A_c^{\text{th}}(\alpha_s(Q^2\xi)) \ln(1+\xi)}{\xi} - \left[ \frac{A_c^{\text{th}}(\alpha_s(Q^2\xi)) \ln \xi}{\xi} \right]_+ \right] \delta_c^i \delta(1-z') \right. \\ & \left. + \left[ \frac{\mathbf{p}^{\text{reg}}(z, \alpha_s(Q^2\xi))}{\xi} \right]_+ \right\}, \end{aligned} \quad (2.5.17)$$

$\mathbf{p}^{\text{reg}}$  defined from  $\mathbf{p}$  as

$$p_{ij}^{\text{reg}}(z, \alpha_s) = \frac{p_{ij}(z, \alpha_s) - \delta_{ij} A_i^{\text{th}}(\alpha_s)}{1-z} \quad (2.5.18)$$

and  $\mathfrak{S}(N, \hat{b})$  written as

$$\begin{aligned} \mathfrak{S}(N, \hat{b}) = & \int_0^1 dz' z'^{N-1} \int_0^\infty d\xi J_0(\hat{b}\sqrt{\xi}) (\sqrt{1+\xi} - \sqrt{\xi})^{2N} \\ & \left\{ \left[ \frac{\mathcal{D}_c^{\text{PT}}(\alpha_s(Q^2\xi))}{\xi} \right]_+ \left[ \frac{1}{\sqrt{(1-z') (1 - (\sqrt{1+\xi} - \sqrt{\xi})^4 z)}} \right]_+^z \right. \\ & + \frac{1}{2} \frac{1}{(\sqrt{1+\xi} - \sqrt{\xi})^2} \\ & \left. \left[ 2 \frac{\mathcal{D}_c^{\text{PT}}(\alpha_s(Q^2\xi)) \ln(1+\xi)}{\xi} - \left[ \frac{\mathcal{D}_c^{\text{PT}}(\alpha_s(Q^2\xi)) \ln \xi}{\xi} \right]_+ \right] \delta(1-z') \right\} \\ & + \int_0^1 dz'' z''^{N-1} \int_0^\infty d\xi J_0(\hat{b}\sqrt{\xi}) (\sqrt{1+\xi} - \sqrt{\xi})^{2N} \left[ \frac{\tilde{B}_c^{\text{PT}}(\alpha_s(Q^2\xi))}{\xi} \right]_+ \delta(1-z') \end{aligned}$$

$$+ \int_0^1 dz'' z'^{N-1} \int_0^\infty d\xi J_0(\hat{b}\sqrt{\xi}) \left(\sqrt{1+\xi} - \sqrt{\xi}\right)^{2N} \left[ \frac{\mathcal{C}_{ij}(z', \alpha_s(Q^2\xi))}{\xi} \right]_+ . \quad (2.5.19)$$

In Eq. (2.5.17) and in Eq. (2.5.19) we make use of the  $z$  plus distribution defined in Eq. (2.5.10). Moreover, changing in phase space is applied only to divergent contribution in  $z \rightarrow 1$  since the difference is effective at small- $p_T$  only at threshold. Hence, in Eq. (2.5.17) and (2.5.19), we change the term proportional to  $\mathcal{C}$  and to the regular part of the splitting function  $\mathbf{p}^{\text{reg}}$  only re-expressing its dependence as function of  $z'$  rather than  $z$ . However, such change turn out to be subleading in the limit Eq. (2.5.13) and then it was performed in Eq. (2.5.19) only for symmetry with other components. Special remark is needed for the  $\tilde{B}$  delta term. In principle this term could receive extra contribution when the small- $p_T$  limit is taken at threshold. However, in Ref. [45] it was proved that no extra contribution arises at NNLL. It is important to note however that no all order proof of this fact exists. Even for the delta contribution at NNLL, difference between  $z'$  and  $z$  turns out to be subleading in limit Eq. (2.5.13).

As for original transverse momentum case, Eq. (2.5.16) is not the most simple expression for the consistent resummed case and a more compact form can be in fact derived. However, we still prefer to start again with a formula like Eq. (2.5.16) to explicit the relation between this resummed expression and phase space analysis of Sec. 2.5.

By using running coupling evolution, all integrals in Eq. (2.5.16) can be expressed as a combination of the following two types:

$$\begin{aligned} G_{k,1}(N, b) &= \int_0^\infty d\xi \left(\sqrt{1+\xi} - \sqrt{\xi}\right)^{2N} J_0(bQ\sqrt{\xi}) \int_0^1 dz z^{N-1} \\ &\quad \left( \left( \frac{\ln^k \xi}{\xi} \right)_+ \left( \frac{1}{\sqrt{(1-z)(1-(\sqrt{1+\xi}-\sqrt{\xi})^4 z)}} \right)^z \right. \\ &\quad \left. + \delta(1-z) \frac{1}{2(\sqrt{1+\xi}-\sqrt{\xi})^2} \left( \frac{\ln(1+\xi)\ln^k \xi}{\xi} - \left( \frac{\ln^{k+1} \xi}{\xi} \right)_+ \right) \right) \end{aligned} \quad (2.5.20)$$

$$G_{k,2}(N, b) = \int_0^\infty d\xi \left(\sqrt{1+\xi} - \sqrt{\xi}\right)^{2N} J_0(bQ\sqrt{\xi}) \left( \frac{\ln^k \xi}{\xi} \right)_+ , \quad (2.5.21)$$

where the integrals  $G_{k,1}$  and  $G_{k,2}$  appear in the terms proportional to  $A$ ,  $D$  and  $\tilde{B}$ ,  $C$  respectively. We need to evaluate these integrals in the limit Eq. (2.5.13).

This can be done by defining two generating functions,  $\mathcal{G}_1(N, b, \epsilon)$  and  $\mathcal{G}_2(N, b, \epsilon)$  such that

$$\begin{aligned} G_{k,1}(N, b) &= \left. \frac{d^k}{d\epsilon^k} \mathcal{G}_1(N, b, \epsilon) \right|_{\epsilon=0} \\ G_{k,2}(N, b) &= \left. \frac{d^k}{d\epsilon^k} \mathcal{G}_2(N, b, \epsilon) \right|_{\epsilon=0} . \end{aligned} \quad (2.5.22)$$

These admit the integral representation

$$\mathcal{G}_1(N, b, \epsilon) = \int_0^1 dz z^{N-1} \int_0^{\frac{(1-z)^2}{4z}} d\xi J_0(bQ\sqrt{\xi}) \frac{\xi^{-1+\epsilon}}{\sqrt{(1-z)^2 - 4z\xi}} - \frac{1}{2\epsilon^2} - \frac{1}{\epsilon} \int_0^1 dz z^{N-1} \left( \frac{1}{1-z} \right)_+ \quad (2.5.23)$$

$$\mathcal{G}_2(N, \epsilon) = \int_0^\infty d\xi \left[ \left( \sqrt{1+\xi} - \sqrt{\xi} \right)^{2N} J_0(bQ\sqrt{\xi}) - 1 \right] \xi^{-1+\epsilon}. \quad (2.5.24)$$

Expanding the Bessel function in powers of its argument

$$J_0(bQ\sqrt{\xi}) = \sum_{p=0}^{\infty} \frac{(-1)^p}{\Gamma^2(p+1)} \left( \frac{b^2 Q^2}{4} \right)^p \xi^p \quad (2.5.25)$$

and integrating term by term we get

$$\mathcal{G}_1(N, b, \epsilon) = \sum_{p=0}^{\infty} \left[ \frac{(-1)^p}{\Gamma^2(p+1)} \left( \frac{b^2 Q^2}{4} \right)^p \frac{\Gamma(N-p-\epsilon)\Gamma^2(p+\epsilon)}{2\Gamma(N+p+\epsilon)} \right] - \frac{1}{2\epsilon^2} + \frac{1}{\epsilon} (\psi(N) + \gamma_E) \quad (2.5.26)$$

$$\mathcal{G}_2(N, b, \epsilon) = \sum_{p=0}^{\infty} \left[ \frac{(-1)^p}{\Gamma^2(p+1)} \left( \frac{b^2 Q^2}{4} \right)^p \frac{N\Gamma(N-p-\epsilon)\Gamma(2(p+\epsilon))}{2^{2p+2\epsilon-1}\Gamma(N+1+p+\epsilon)} \right] - \frac{1}{\epsilon}. \quad (2.5.27)$$

We can now take the large- $b$  limit at fixed  $\frac{N}{b}$ . Because the  $\Gamma$  functions do not depend on  $b$ , this limit can be taken using the asymptotic expansion

$$\frac{\Gamma(N-p-\epsilon)}{\Gamma(N+p+\epsilon)} = \left( \frac{1}{N^2} \right)^{p+\epsilon} \left( 1 + \mathcal{O}\left(\frac{1}{N}\right) \right). \quad (2.5.28)$$

By inserting Eq. (2.5.28) into Eqs. (2.5.26), (2.5.27) and performing the sum on  $p$  we obtain

$$\mathcal{G}_1(N, b, \epsilon) = \frac{1}{2} \left( \frac{1}{N^2} \right)^\epsilon \Gamma^2(\epsilon) {}_2F_1\left(\epsilon, \epsilon, 1, -\frac{b^2 M^2}{4N^2}\right) - \frac{1}{2\epsilon^2} + \frac{1}{\epsilon} (\ln N + \gamma_E) + \mathcal{O}\left(\frac{1}{b}\right) \quad (2.5.29)$$

$$\mathcal{G}_2(N, b, \epsilon) = 2^{1-2\epsilon} \left( \frac{1}{N^2} \right)^\epsilon \Gamma(2\epsilon) {}_2F_1\left(\epsilon, \frac{1}{2} + \epsilon, 1, -\frac{b^2 M^2}{4N^2}\right) - \frac{1}{\epsilon} + \mathcal{O}\left(\frac{1}{b}\right). \quad (2.5.30)$$

These provide us with the desired expressions of the generating functions at leading order in the  $b \rightarrow \infty$  limit, for fixed  $\frac{N}{b}$ .

The derivatives of the generating functions Eqs. (2.5.29)- (2.5.30) could be performed using recent results [66, 67] for the expansion of hypergeometric function in powers of  $\epsilon$ . However, very compact closed-form expressions could either be obtained by replacing the

generating functions Eqs. (2.5.29)- (2.5.30) with suitable expressions which only differ by them by subleading terms. Indeed, because powers of  $\ln \xi$  are obtained by differentiation with respect to  $\epsilon$  according to Eq. (2.5.22), an expression of the generating functions which reproduces transverse momentum resummation up to  $N^k\text{LL}$  accuracy can be obtained by expanding the hypergeometric functions in powers of  $\epsilon$ , and at each order in  $\epsilon$  evaluating its large  $b$  limit and retaining the  $k + 1$  highest powers of  $\ln b$ . Furthermore, because of the prefactor of  $N^{-2\epsilon}$  in Eqs. (2.5.29)- (2.5.30) an expression of the generating functions which reproduces inclusive threshold momentum resummation up to  $N^j\text{LL}$  accuracy can be obtained by letting  $b = 0$  and then expanding the hypergeometric functions in powers of  $\epsilon$  and retaining the first  $j$  orders of the expansion. Hence, any function which reproduces these two behaviours of the original generating functions will lead to the same resummed results to the desired accuracy: up to NNLL this requires  $k = j = 2$ .

For  $\mathcal{G}_1$ , we do this by noting that the hypergeometric function  ${}_2F_1$  has the following expansion for large  $z$

$${}_2F_1(\epsilon, \epsilon, 1, -z) = \frac{z^{-\epsilon}}{\Gamma(\epsilon)\Gamma(1-\epsilon)} (\ln z - \psi(1-\epsilon) - \psi(\epsilon) - 2\gamma_E) + \mathcal{O}\left(\frac{1}{z}\right), \quad (2.5.31)$$

and the Taylor expansion

$${}_2F_1(\epsilon, \epsilon, 1, -z) = 1 + \epsilon^2 \text{Li}_2(-z) + \mathcal{O}(\epsilon^3). \quad (2.5.32)$$

We can easily combine these two behaviours by first, letting  $z \rightarrow 1+z$  on the right-hand side of Eq. (2.5.31): this leads to an expression which coincides with Eq. (2.5.31) as  $z \rightarrow \infty$  up to  $\mathcal{O}\left(\frac{1}{z}\right)$  corrections, but is regular as  $z \rightarrow 0$ . Next, we expand the result in powers of  $\epsilon$  and we match to the expansion Eq. (2.5.32). Namely, we note that

$$\frac{(1+z)^{-\epsilon}}{\Gamma(\epsilon)\Gamma(1-\epsilon)} (\ln(1+z) - \psi(1-\epsilon) - \psi(\epsilon) - 2\gamma_E) = 1 - \epsilon^2 \left[ \frac{1}{2} \ln^2(1+z) + \zeta_2 \right] + \mathcal{O}(\epsilon^3). \quad (2.5.33)$$

But

$$\text{Li}_2(-z) + \frac{1}{2} \ln^2(1+z) + \zeta_2 = \text{Li}_2\left(\frac{1}{1+z}\right) - (\ln(1+z) - \ln(z)) \ln(1+z). \quad (2.5.34)$$

Hence it is enough to add the left-hand side of Eq. (2.5.34) to the right-hand side of Eq. (2.5.31) after having performed in it the  $z \rightarrow 1+z$  shift, to get an interpolation of the hypergeometric function which, if substituted in Eq. (2.5.29), leads to the same result up to subleading power corrections in the small  $p_T$  limit and up to  $N^3\text{LL}$  corrections in the threshold limit at the integrated level. This can be increased to  $N^j\text{LL}$  by including the expansion in powers of  $\epsilon$  in Eqs. (2.5.32), (2.5.33) up to  $j-1$ -th order.

The second term on the right-hand side of Eq. (2.5.34) can be dropped, as it is  $O(z)$  as  $z \rightarrow 0$  and  $O\left(\frac{1}{z}\right)$  as  $z \rightarrow \infty$ , and so we end up with the result

$$\begin{aligned} {}_2F_1(\epsilon, \epsilon, 1, -z) &= \frac{(1+z)^{-\epsilon}}{\Gamma(1-\epsilon)\Gamma(\epsilon)} (\ln(1+z) - 2\gamma_E - \psi(1-\epsilon) - \psi(\epsilon)) \\ &\quad + \epsilon^2 \text{Li}_2\left(\frac{1}{1+z}\right) + \mathcal{O}(\text{NNNLL}), \end{aligned} \quad (2.5.35)$$

where the order of the correction means that using Eq. (2.5.35) in the expression Eq. (2.5.29) of the generating function  $\mathcal{G}_1$  leads to a resummed expression which preserves the original accuracy in the small  $p_T$  limit, and which is NNLL accurate in the threshold limit upon integration over  $p_T$ .

For  $\mathcal{G}_2$  we use the expansion

$${}_2F_1\left(\epsilon, \frac{1}{2} + \epsilon, 1, -z\right) = \frac{\sqrt{\pi} 2^{-2\epsilon} z^{-\epsilon}}{\Gamma\left(\frac{1}{2} + \epsilon\right) \Gamma(1 - \epsilon)} + \mathcal{O}\left(\frac{1}{z}\right). \quad (2.5.36)$$

We note furthermore that  $\mathcal{G}_2$  generates the integrals which enter in the terms proportional to  $\mathcal{C}$ ,  $\bar{B}$  in the resummed expression Eq. (2.5.19). These start at least at NLL, hence, up to NNLL accuracy, it is sufficient to perform the expansion in powers of  $\epsilon$  up to first order, rather than second order as in Eq. (2.5.32). Furthermore, we note that the  $\mathcal{O}(\epsilon)$  term in this expansion only receives a contribution from  $\mathcal{C}$ , which vanishes in the threshold limit  $N \rightarrow \infty$ . It follows that is enough to reproduce the expansion

$${}_2F_1\left(\epsilon, \frac{1}{2} + \epsilon, 1, -z\right) = 1 + \mathcal{O}(\epsilon). \quad (2.5.37)$$

This is automatically the case if we simply perform the shift  $z \rightarrow 1 + z$  on the right-hand side of Eq. (2.5.31). We thus end up with the result

$${}_2F_1\left(\epsilon, \frac{1}{2} + \epsilon, 1, -z\right) = \frac{\sqrt{\pi} 2^{-2\epsilon} (1+z)^{-\epsilon}}{\Gamma\left(\frac{1}{2} + \epsilon\right) \Gamma(1 - \epsilon)} + \mathcal{O}(\text{NNNLL}), \quad (2.5.38)$$

where again the order of the correction means that using this result in Eq. (2.5.30) leads to a resummed expression which preserves the original accuracy in the small  $p_T$  limit, and which is NNLL accurate in the threshold limit upon integration over  $p_T$ .

By inserting interpolations Eqs. (2.5.35), (2.5.38) into Eqs. (2.5.29), (2.5.30) and by taking  $k$  derivatives with respect to  $\epsilon$  retaining only terms up to NNLL, we obtain for  $G_{1,k}$  and  $G_{2,k}$  the following expression:

$$G_{k,1}(N, b) = \frac{(-1)^k}{2} \left[ -\frac{1}{k+2} \ln^{k+2} \chi + \frac{\ln \bar{N}^2}{k+1} \ln^{k+1} \chi + \ln^k \bar{N}^2 \text{Li}_2\left(\frac{\bar{N}^2}{\chi}\right) + \mathcal{O}\left(\ln^j \bar{N}^2 \ln^{k-1-j} \chi\right) \right] \quad (2.5.39)$$

$$G_{k,2}(N, b) = -\frac{(-1)^k}{k+1} \ln^{k+1} \chi + \mathcal{O}\left(\ln^{k-1} \chi\right) \quad (2.5.40)$$

with

$$\bar{N} = N e^{\gamma_E} \quad (2.5.41)$$

$$\chi = \bar{N}^2 + \frac{\hat{b}^2}{b_0^2} \quad (2.5.42)$$

$$b_0 = 2e^{-\gamma_E}. \quad (2.5.43)$$

Last simplification we can achieved is based on the following NNLL equality

$$(-1)^k \frac{\ln^k \chi}{k} = - \int_{\frac{Q^2}{\chi}}^{Q^2} \frac{dq^2}{q^2} \ln^{k-1} \left( \frac{q^2}{Q^2} \right) \quad (2.5.44)$$

and consists in rewriting  $\ln \chi$  components as the result of a running coupling evolution from a new soft joint scale  $\frac{Q^2}{\chi}$  to the hard scale  $Q^2$ .

Performing analogue steps as for the construction of the original transverse momentum resummation, Eq. (2.4.17), we can recast Eq. (2.5.16) as

$$\begin{aligned} \frac{d\sigma^{\text{cons}}}{d\xi_p}(N, b, \alpha_s) &= (\sigma_0)_c \bar{H}_c \left( \frac{\bar{N}^2}{\chi}, \alpha_s(Q^2) \right) C_{ci} \left( N, \alpha_s \left( \frac{Q^2}{\chi} \right) \right) C_{cj} \left( N, \alpha_s \left( \frac{Q^2}{\chi} \right) \right) \\ &\exp [S_c(\chi, N)] f_i \left( N, \frac{Q^2}{\chi} \right), f_j \left( N, \frac{Q^2}{\chi} \right). \end{aligned} \quad (2.5.45)$$

In this case the Sudakov exponential is given by two different integrals

$$\begin{aligned} S_c(\chi, N) &= - \int_{\frac{Q^2}{\chi}}^{Q^2} \frac{dq^2}{q^2} \left[ A_c^{pT}(\alpha_s(q^2)) \ln \frac{Q^2}{q^2} + B_c(\alpha_s(q^2)) \right] \\ &+ \int_{\frac{Q^2}{\bar{N}^2}}^{Q^2} \frac{dq^2}{q^2} \mathfrak{G}_c \left( \frac{\bar{N}^2}{\chi} \right) (\alpha_s(q^2)) \end{aligned} \quad (2.5.46)$$

with  $A_c^{pT}(\alpha_s) = A_c^{\text{th}}(\alpha_s) + \frac{1}{2} \mathcal{D}_c^{pT}(\alpha_s)$ ,  $\mathfrak{G} \left( \frac{\bar{N}^2}{\chi} \right) = \beta_0 A_c^{pT, (1)} \text{Li}_2 \left( \frac{\bar{N}^2}{\chi} \right) \alpha_s^2 + \mathcal{O}(\alpha_s^3)$  up to NNLL. We note that consistent derivation, in addition to change the soft scale from  $\frac{b_0^2}{b^2}$  to  $\frac{Q^2}{\chi}$ , produces pure soft contributions in the Sudakov exponent which are fundamental, as we will see, to reproduce the soft resummed inclusive  $\xi_p$  integral.

Moreover, in Eq. (2.5.45), we change the constant  $H$  to  $\bar{H}$  to reabsorb into the hard function all the not logarithmic contributions in the Sudakov exponent. Up to NNLL, we thus have :

$$\bar{H}_c \left( \frac{\bar{N}^2}{\chi}, \alpha_s \right) = H_c(\alpha_s) + A_c^{pT, (1)} \text{Li}_2 \left( \frac{\bar{N}^2}{\chi} \right) \alpha_s + \mathcal{O}(\alpha_s^3). \quad (2.5.47)$$

It is important to stress that  $C(N, \alpha_s)$ ,  $H(\alpha_s)$  definition is completely equal to the original transverse momentum case up to the logarithmic accuracy we are working since no corrections are imposed on  $N$  dependence of not threshold enhanced terms.

As for Eq. (2.4.17), Eq. (2.5.45) gives back directly the hadronic distribution summed over all the partonic channels. Moreover, it is expressed with no dependence from factorization and renormalization scales which are set for simplicity equal to the hard scale  $Q^2$ . If we want to separate different channel contributions and we want to deal with scale variation we need to perform, as before, PDFs evolution up to NNLL logarithmic order<sup>3</sup>.

<sup>3</sup>In fact, NNLL evolution operator can be retained only in its large- $N$  singular part (see closure remark of Appendix A)

Hence a possible expression for the  $ij$  partonic channel contribution can be written using results of Appendix A, Eq. (A.3.8) and Eq. (A.3.12) as

$$\begin{aligned}
\frac{d\hat{\sigma}_{ij}^{\text{cons}}}{d\xi_p}(N, b, \alpha_s(\mu_R^2), \mu_F^2) &= (\sigma_0)_c \bar{H}_c \left( \frac{\bar{N}^2}{\chi}, \alpha_s(\mu_R^2) \right) \\
&\exp[S_c(\chi, N)] C_{ca} \left( N, \alpha_s \left( \frac{Q^2}{\chi} \right) \right) C_{cb} \left( N, \alpha_s \left( \frac{Q^2}{\chi} \right) \right) \\
&U_{al}^{\text{joint}} \left( N, \alpha_s \left( \frac{Q^2}{\chi} \right) \right) L_{lk}^{\text{joint}}(N, \chi, \mu_F^2) U_{ki}^{\text{joint}}(N, \alpha_s(\mu_F^2)) \\
&U_{br}^{\text{joint}} \left( N, \alpha_s \left( \frac{Q^2}{\chi} \right) \right) L_{rw}^{\text{joint}}(N, \chi, \mu_F^2) U_{wj}^{\text{joint}}(N, \alpha_s(\mu_F^2))
\end{aligned} \tag{2.5.48}$$

where  $S_c(\chi, N)$  is defined as in Eq. (2.5.46) and  $C_{ca} \left( N, \alpha_s \left( \frac{Q^2}{\chi} \right) \right) U_{al}^{\text{joint}} \left( N, \alpha_s \left( \frac{b_0^2}{b^2} \right) \right)$  have to be then evolved as

$$\begin{aligned}
C_{ca} \left( N, \alpha_s \left( \frac{Q^2}{\chi} \right) \right) U_{al}^{\text{joint}} \left( N, \alpha_s \left( \frac{Q^2}{\chi} \right) \right) &= C_{ca}(N, \alpha_s(\mu_R^2)) U_{al}^{\text{joint}}(N, \alpha_s(\mu_R^2)) \\
\exp \left[ - \int_{\frac{Q^2}{\chi}}^{Q^2} \frac{dq^2}{q^2} \frac{\beta(\alpha_s(q^2))}{\alpha_s(q^2)} \left[ \frac{d \ln C_{ca}(N, \alpha_s(q^2))}{d \ln \alpha_s(q^2)} + \frac{d \ln U_{al}^{\text{joint}}(N, \alpha_s(q^2))}{d \ln \alpha_s(q^2)} \right] \right] &.
\end{aligned} \tag{2.5.49}$$

The superscript joint has been used to indicate that in consistent resummation to take into account the different counting of logarithms with respect to original transverse momentum resummation, evolution of PDFs has to be performed in a slightly different way. In brief, while to reach  $\ln b$  NNLL accuracy we need NLL complete Altarelli-Parisi evolution, in consistent resummation to reach NNLL accuracy, since we both need to control  $\ln N$  and  $\ln \chi$  contributions, we need NNLL evolution with  $\mathcal{O}(\alpha_s^3)$  anomalous dimension  $\gamma_{ij}^{(2)}$  substituted by their large- $N$  asymptotic behaviour  $\gamma_{ij}^{(2),div}$ . A more extensive discussion about this fact is contained in Appendix A, where also all the explicit expressions are reported.

Eq. (2.5.45) and Eq. (2.5.48) represent the main results of this section. All the phenomenological consequences contained in Chap. 4, regarding consistent resummation, are produced throughout an implementation of Eq. (2.5.48). Consistent resummation correctly sums all the leading contributions in the limit Eq. (2.5.13) up to NNLL. It is easy to convince yourself that Eq. (2.5.45) reduces to Eq. (2.4.17) by taking the limit Eq. (2.5.14), since

$$\chi \rightarrow \frac{\hat{b}^2}{b_0^2} \quad \text{Li}_2 \left( \frac{\bar{N}^2}{\chi} \right) \rightarrow 0. \tag{2.5.50}$$

In this sense, consistent resummation is an extension at threshold of the original transverse momentum resummation. Moreover, we will see in Sec 2.7, where the whole machinery will be applied to our test case, that by taking the integral over  $\xi_p$  of Eq. (2.5.45), the threshold resummed inclusive cross section is correctly reproduced.

However, before moving to an explicit application, let's highlight the fact that even if consistent resummation corrects threshold behaviour in the small- $p_T$  limit, giving sense to  $\xi_p$  integral, it does not reproduce correctly threshold behaviour at fixed- $p_T$ . Indeed, as threshold resummation at fixed- $p_T$  does not reproduce small- $p_T$  resummation, lacking of collinear but not soft contributions, consistent small- $p_T$  resummation does not include threshold resummation at fixed- $p_T$  lacking of soft large-angle terms.

Hence if we are interested to produce a unique formula able to catch the leading behaviour at threshold for all the  $p_T$  we need to properly combine the two resummations just presented. This will be the topic of the next section.

## 2.6 Combined Resummation for Transverse distributions

As presented in the previous section, the small- $p_T$  limit changes dramatically the large- $N$  behaviour of transverse momentum distribution, revealing extra threshold divergences, before screened by the finite value of the transverse momentum. For this reason, threshold resummation at fixed  $p_T$  and consistent small- $p_T$  resummation reproduce different threshold behaviour which are correct in the  $\xi_p$  region where they live but spoil the whole picture if they are extended in a larger  $\xi_p$  range.

Using Collins-Soper-Sterman transverse momentum resummation we meet the same problem since in order not to spoil the fixed order result is matched on, we are forced to turn off resummation at some large  $\xi_p$ . Of course the value of  $\xi_p$  which can be considered the "boundary" of the small- $\xi_p$  region is completely arbitrary and can have a phenomenologically impact in the mid-large  $\xi_p$  range.

Our idea is to switch between our threshold resummed predictions in a continuous way, using a profile matching function. In this way we do not have to define a boundary but we only introduce terms which are subleading in both the regions.

We then define a *combined resummation* as

$$\begin{aligned} \frac{d\hat{\sigma}_{ij}}{d\xi_p}(N, \xi_p, \alpha_s(\mu_R^2), \mu_F^2) &= (1 - T(N, \xi_p)) \frac{d\hat{\sigma}_{ij}^{\text{cons}}}{d\xi_p}(N, \xi_p, \alpha_s(\mu_R^2), \mu_F^2) \\ &+ T(N, \xi_p) \frac{d\hat{\sigma}_{ij}^{\text{th}}}{d\xi_p}(N, \xi_p, \alpha_s(\mu_R^2), \mu_F^2). \end{aligned} \quad (2.6.1)$$

with the matching profile function satisfying

$$\lim_{N \rightarrow \infty} T(N, \xi_p) = 1 \quad \text{at fixed } \xi_p, \quad (2.6.2a)$$

$$\lim_{\xi_p \rightarrow 0} T(N, \xi_p) = 0 \quad \text{at fixed } N, \quad (2.6.2b)$$

$\frac{d\hat{\sigma}_{ij}^{\text{cons}}}{d\xi_p}$  given by Eq. (2.5.48) and  $\frac{d\hat{\sigma}_{ij}^{\text{th}}}{d\xi_p}$  given by Eq. (2.3.1). Of course several possible matching profile functions exist; however, phenomenological studies on our test case show that the dependence of the combined resummed result from the particular form of the matching function is very mild if the consistent small- $p_T$  resummation is used instead of Collins-Soper-Sterman approach.

In the phenomenological application of Chap. 4 we use a profile function of the form

$$T_{k,m}(N, \xi_p) = \frac{N^m \xi_p^k}{1 + N^m \xi_p^k} \quad (2.6.3)$$

with different choice for the  $k, m$  integers.

Using our combined formula Eq. (2.6.1) we are able to resum threshold contributions in the whole  $\xi_p$  spectrum up to NNLL logarithmic accuracy. Moreover due to the properties of our consistent small- $p_T$  resummation, the original transverse momentum resummation is achieved in the limit, Eq. (2.5.14) and resummed threshold behaviour of inclusive cross section is given by integration of Eq. (2.6.1) over  $p_T$ . Indeed the integral of any term multiplying the profile function is suppressed at least as  $\mathcal{O}(\frac{1}{N})$  after  $\xi_p$  integration.

It is important to note that Eq. (2.6.1) contains an inverse Fourier transform in the consistent part. The evaluation of this inverse Fourier transform at resummed level is far to be trivial due to the presence of the Landau pole. We are going to come back on this point in Chap. 4, where resummed phenomenological results for the Higgs boson production process will be presented.

In the next section, we move to an explicit application. Combined Resummation will be written explicitly for the EFT Higgs boson production process and threshold resummed inclusive cross section will be derived after  $\xi_p$  integration.

## 2.7 Application: EFT Higgs boson at Threshold

In this section, we want to write all the explicit expressions for the consistent and combined resummation in the case of EFT Higgs boson production. Moreover we analytically check that threshold resummation for inclusive cross section is reproduced after integration over  $p_T$ .

We start from consistent resummation and in particular from Eq. (2.5.48). At LO, Higgs boson is produced via gluon fusion: we thus have to set index  $c$  to  $g$  in Eq. (2.5.48). Moreover, we can set the hard scale  $Q^2$  to be the mass of the Higgs  $m_H^2$  and we can perform all the implicit sums over repeated indexes to derive explicit formula for each partonic channel. Retaining contributions up to NNLL, we obtain

$$\begin{aligned} \frac{d\hat{\sigma}_{ij}}{d\xi_p}(N, \xi_p, \alpha_s(\mu_R^2), \mu_R^2, \mu_F^2) &= \int_0^\infty db \frac{b}{2} J_0(b m_H^2 \sqrt{\xi_p}) \left( \sqrt{1 + \xi_p} - \sqrt{\xi_p} \right)^{-2N} \\ &\sigma_0(\alpha_s(\mu_R^2)) \tilde{\mathcal{H}}_{gg \rightarrow ij}(N, \chi, \alpha_s(\mu_R^2), \mu_R^2, \mu_F^2) \exp[S_g(N, \chi, \mu_R^2)] \end{aligned} \quad (2.7.1)$$

with

$$\begin{aligned} \tilde{\mathcal{H}}_{gg \rightarrow gg}(N, \chi, \alpha_s(\mu_R^2), \mu_R^2, \mu_F^2) &= (L_{gg}(N, \chi, \mu_F^2))^2 (R_{gg}(N, \chi))^2 \\ &+ \alpha_s(\mu_R^2) \left( 2\mathcal{H}_{gg \rightarrow gq}^{(1)}(N) R_{gg}(N, \chi) R_{gq}(N, \chi) L_{gg}(N, \chi, \mu_F^2) L_{qg}(N, \chi, \mu_F^2) \right. \\ &\quad + \bar{\mathcal{H}}_{gg \rightarrow gg}^{(1)}(N) (R_{gg}(N, \chi))^2 (L_{gg}(N, \chi))^2 \\ &\quad \left. + 2U_{gq}^{\text{joint},(1)}(N) R_{gq}(N, \chi) R_{gg}(N, \chi) L_{gg}(N, \chi, \mu_F^2) L_{qg}(N, \chi, \mu_F^2) \right) \end{aligned}$$

$$\begin{aligned}
& - 2U_{gg}^{\text{joint},(1)}(N) (R_{gg}(N, \chi))^2 L_{gg}(N, \chi, \mu_F^2) L_{qq}(N, \chi, \mu_F^2) \\
& - 2 (R_{gg}(N, \chi))^2 (L_{gg}(N, \chi, \mu_F^2))^2 \beta_0 \ln \frac{m_H^2}{\mu_R^2} \Big) \\
& + \alpha_s^2(\mu_R^2) (L_{gg}(N, \chi, \mu_F^2))^2 \left( \bar{\mathcal{H}}_{gg \rightarrow gg}^{(2)} - 3\beta_0 \bar{\mathcal{H}}_{gg \rightarrow gg}^{(1)} \ln \frac{m_H^2}{\mu_R^2} - 2\beta_1 \ln \frac{m_H^2}{\mu_R^2} + 3\beta_0^2 \ln^2 \frac{m_H^2}{\mu_R^2} \right), \tag{2.7.2a}
\end{aligned}$$

$$\begin{aligned}
\tilde{\mathcal{H}}_{gg \rightarrow gq}(N, \chi, \alpha_s(\mu_R^2), \mu_R^2, \mu_F^2) &= (R_{gg}(N, \chi))^2 L_{gg}(N, \chi, \mu_F^2) L_{qq}(N, \chi, \mu_F^2) \\
& + \alpha_s(\mu_R^2) \left( \mathcal{H}_{gg \rightarrow gq}^{(1)}(N) R_{gg}(N, \chi) R_{qq}(N, \chi) L_{gg}(N, \chi, \mu_F^2) L_{qq}(N, \chi, \mu_F^2) \right. \\
& + \bar{\mathcal{H}}_{gg \rightarrow gg}^{(1)}(N) (R_{gg}(N, \chi))^2 L_{gg}(N, \chi, \mu_F^2) L_{qq}(N, \chi, \mu_F^2) \\
& + U_{gg}^{\text{joint},(1)}(N) (R_{gg}(N, \chi))^2 L_{gg}(N, \chi, \mu_F^2) L_{qq}(N, \chi, \mu_F^2) \\
& - U_{qq}^{\text{joint},(1)}(N) (R_{gg}(N, \chi))^2 (L_{gg}(N, \chi, \mu_F^2))^2 \\
& + U_{qq}^{\text{joint},(1)}(N) R_{gg}(N, \chi) R_{qq}(N, \chi) L_{gg}(N, \chi, \mu_F^2) L_{qq}(N, \chi, \mu_F^2) \\
& - U_{qq}^{\text{joint},(1)}(R_{gg}(N, \chi))^2 (L_{qq}(N, \chi, \mu_F^2))^2 \\
& - U_{qq}^{\text{joint},(1)}(R_{gg}(N, \chi))^2 L_{gg}(N, \chi, \mu_F^2) L_{qq}(N, \chi, \mu_F^2) \\
& \left. - 2 (R_{gg}(N, \chi))^2 L_{gg}(N, \chi, \mu_F^2) L_{qq}(N, \chi, \mu_F^2) \beta_0 \ln \frac{m_H^2}{\mu_R^2} \right) \\
& + \alpha_s^2(\mu_R^2) L_{gg}(N, \chi, \mu_F^2) L_{qq}(N, \chi, \mu_F^2) \left( \mathcal{H}_{gg \rightarrow gq}^{(2)} - \mathcal{H}_{gg \rightarrow gq}^{(1)} \beta_0 \ln \frac{\mu_F^2}{\mu_R^2} - 2\mathcal{H}_{gg \rightarrow qq}^{(1)} \beta_0 \ln \frac{m_H^2}{\mu_R^2} \right) \tag{2.7.2b}
\end{aligned}$$

$$\begin{aligned}
\tilde{\mathcal{H}}_{gg \rightarrow qq}(N, \chi, \alpha_s(\mu_R^2), \mu_R^2, \mu_F^2) &= (R_{gg}(N, \chi))^2 (L_{qq}(N, \chi, \mu_F^2))^2 \\
& + 2\alpha_s(\mu_R^2) \left( \mathcal{H}_{gg \rightarrow qq}^{(1)}(N) R_{gg}(N, \chi) R_{qq}(N, \chi) L_{qq}(N, \chi, \mu_F^2) L_{qq}(N, \chi, \mu_F^2) \right. \\
& + \bar{\mathcal{H}}_{gg \rightarrow gg}^{(1)}(N) (R_{gg}(N, \chi))^2 (L_{qq}(N, \chi, \mu_F^2))^2 \\
& + U_{gg}^{\text{joint},(1)}(N) (R_{gg}(N, \chi))^2 (L_{qq}(N, \chi, \mu_F^2))^2 \\
& - U_{qq}^{\text{joint},(1)}(N) (R_{gg}(N, \chi))^2 L_{gg}(N, \chi, \mu_F^2) L_{qq}(N, \chi, \mu_F^2) \\
& + U_{qq}^{\text{joint},(1)}(N) R_{gg}(N, \chi) R_{qq}(N, \chi) L_{qq}(N, \chi, \mu_F^2) L_{qq}(N, \chi, \mu_F^2) \\
& - U_{qq}^{\text{joint},(1)}(N) (R_{gg}(N, \chi))^2 (L_{qq}(N, \chi, \mu_F^2))^2 \\
& \left. - 2 (R_{gg}(N, \chi))^2 (L_{qq}(N, \chi, \mu_F^2))^2 \beta_0 \ln \frac{m_H^2}{\mu_R^2} \right) \\
& + \alpha_s^2(\mu_R^2) (L_{qq}(N, \chi, \mu_F^2))^2 \mathcal{H}_{gg \rightarrow qq}^{(2)}, \tag{2.7.2c}
\end{aligned}$$

and  $S_g(N, \chi, \mu_R^2)$  given by

$$S_g(N, \chi, \mu_R^2) = \frac{1}{\alpha_s} g_1(\lambda_\chi, ) + g_2(\lambda_\chi) + \alpha_s g_3(\lambda_\chi, \lambda_{\bar{N}}, \mu_R^2) + \mathcal{O}(\alpha_s^4), \tag{2.7.3}$$

$$g_1(\lambda_\chi) = \frac{A_g^{pT,(1)}}{\beta_0^2} (\lambda_\chi + \ln(1 - \lambda_\chi)), \quad (2.7.4)$$

$$g_2(\lambda_\chi, \mu_R^2) = \frac{A_g^{pT,(1)} \beta_1}{\beta_0^3} \left[ \frac{\lambda_\chi + \ln(1 - \lambda_\chi)}{1 - \lambda_\chi} + \frac{1}{2} \ln(1 - \lambda_\chi)^2 \right] \\ - \frac{A_g^{pT,(2)}}{\beta_0^2} \frac{\lambda_\chi + (1 - \lambda_\chi) \ln(1 - \lambda_\chi)}{1 - \lambda_\chi} + \frac{B_g^{pT,(1)}}{\beta_0} \ln(1 - \lambda_\chi) \\ + \frac{A_g^{pT,(1)}}{\beta_0} \frac{\lambda_\chi + (1 - \lambda_\chi) \ln(1 - \lambda_\chi)}{1 - \lambda_\chi} \ln \frac{m_H^2}{\mu_R^2}, \quad (2.7.5)$$

$$g_3(\lambda_\chi, \lambda_{\bar{N}}, \mu_F^2) = \frac{A_g^{pT,(1)} \beta_1^2}{2\beta_0^4} \left[ \frac{\lambda_\chi + \ln(1 - \lambda_\chi)}{(1 - \lambda_\chi)^2} (\lambda_\chi + (1 - 2\lambda_\chi) \ln(1 - \lambda_\chi)) \right] \\ + \frac{A_g^{pT,(1)} \beta_2}{\beta_0^3} \left[ \frac{(2 - 3\lambda_\chi) \lambda_\chi}{2(1 - \lambda_\chi)^2} + \ln(1 - \lambda_\chi) \right] \\ - \frac{A_g^{pT,(2)} \beta_1}{\beta_0^3} \left[ \frac{(2 - 3\lambda_\chi) \lambda_\chi}{2(1 - \lambda_\chi)^2} + \frac{(1 - 2\lambda_\chi) \ln(1 - \lambda_\chi)}{(1 - \lambda_\chi)^2} \right] \\ + \frac{B_g^{pT,(1)} \beta_1}{\beta_0} \frac{\lambda_\chi + \ln(1 - \lambda_\chi)}{1 - \lambda_\chi} - \frac{A_g^{pT,(3)}}{2\beta_0^2} \frac{\lambda_\chi^2}{(1 - \lambda_\chi)^2} - \frac{B_g^{pT,(2)}}{\beta_0} \frac{\lambda_\chi}{1 - \lambda_\chi} \\ + A_g^{pT,(1)} \text{Li}_2 \left( \frac{\bar{N}^2}{\chi} \right) \frac{\lambda_{\bar{N}}}{1 - \lambda_{\bar{N}}} + B_g^{pT,(1)} \frac{\lambda_\chi}{1 - \lambda_\chi} \ln \frac{m_H^2}{\mu_R^2} + \frac{A_g^{pT,(2)}}{\beta_0} \frac{\lambda_\chi^2}{(1 - \lambda_\chi)^2} \ln \frac{m_H^2}{\mu_R^2} \\ + \frac{A_g^{pT,(1)} \beta_1}{\beta_0^2} \left[ \frac{\lambda_\chi (1 - \lambda_\chi) + (1 - 2\lambda_\chi) \ln(1 - \lambda_\chi)}{(1 - \lambda_\chi)^2} \right] \ln \frac{m_H^2}{\mu_R^2} \\ - \frac{A_g^{pT,(1)}}{2} \frac{\lambda_\chi^2}{(1 - \lambda_\chi)^2} \ln^2 \frac{m_H^2}{\mu_R^2}, \quad (2.7.6)$$

$\lambda_\chi = \alpha_s \beta_0 \ln \chi$  and  $\lambda_{\bar{N}} = \alpha_s \beta_0 \ln \bar{N}^2$ . Moreover in Eq. (2.7.2) we introduce the evolution factor  $R_{ij}$  defined as

$$R_{ij}(N, \chi, \mu_F^2) = \frac{C_{ik}(N, \alpha_s \left(\frac{Q^2}{\chi}\right)) U_{kj}^{\text{joint}}(N, \alpha_s \left(\frac{Q^2}{\chi}\right))}{C_{ik}(N, \alpha_s(\mu_F^2)) U_{kj}^{\text{joint}}(N, \alpha_s(\mu_F^2))}; \quad (2.7.7)$$

its  $gg$  and  $gq$  components turn out to be in the Higgs boson production case up to NNLL

$$R_{gg}(N, \chi, \mu_F^2) = \exp \left[ \alpha_s \left( U_{gg}^{\text{joint}}(N) \left( \frac{\lambda_\chi}{1 - \lambda_\chi} - \alpha_s \beta_0 \ln \frac{m_H^2}{\mu_F^2} \right) \right. \right. \\ + \left. \left( \frac{A_g^{pT,(1)} \beta_1^2}{2\beta_0^4} - \frac{A_g^{pT,(1)} \beta_2}{2\beta_0^3} - \frac{A_g^{pT,(2)} \beta_1}{2\beta_0^3} + \frac{A_g^{pT,(3)}}{2\beta_0^2} \right) \frac{(2 - \lambda_\chi) \lambda_\chi \lambda_{\bar{N}}}{2(1 - \lambda_\chi)^2} \right. \\ \left. - \left( \frac{A_g^{pT,(2)} \beta_1}{\beta_0^3} - \frac{A_g^{pT,(1)} \beta_1^2}{\beta_0^4} \right) \frac{\lambda_{\bar{N}} \ln(1 - \lambda_\chi)}{2(1 - \lambda_\chi)^2} - \frac{D_g^{pT,(2)}}{4\beta_0} \lambda_{\bar{N}} \right]$$

$$+ \left( \frac{A_g^{p\text{T},(2)}}{\beta_0} - \frac{A_g^{p\text{T},(1)}\beta_1}{\beta_0^2} \right) \frac{(2 - \lambda_\chi)\lambda_{\bar{N}}\lambda_\chi}{2(1 - \lambda_\chi)^2} \ln \frac{m_{\text{H}}^2}{\mu_{\text{R}}^2} \Bigg], \quad (2.7.8)$$

$$R_{gq}(N, \chi, \mu_{\text{F}}^2) = \exp[-\ln(1 - \lambda_\chi)]. \quad (2.7.9)$$

The other components entering hard function Eq. (2.7.2) are: the PDFs evolution operators  $L^{\text{joint}}$  and  $U^{\text{joint}}$  which are derived from results in Appendix A, Eq. (A.3.8), Eq. (A.3.12); the  $\mathcal{H}_{gg \rightarrow ij}$  components which are the same as in Collins-Soper-Sterman resummation [49], except for  $\bar{\mathcal{H}}_{gg \rightarrow gg}^{(1)}$  which receives the extra contribution of Eq. (2.5.47) and  $\bar{\mathcal{H}}_{gg \rightarrow gg}^{(2)}$  which is defined from  $\mathcal{H}_{gg \rightarrow gg}^{(2)}$  as

$$\bar{\mathcal{H}}_{gg \rightarrow gg}^{(2)} = \mathcal{H}_{gg \rightarrow gg}^{(2)} + \alpha_s^2 D_g^{p\text{T},(2)} \ln \bar{N}. \quad (2.7.10)$$

Their expressions are given in Appendix C, Eqs. (C.1.22) and Eqs. (C.1.23).

This concludes our presentation about consistent transverse momentum resummation for the EFT Higgs boson production process. We now want to prove analytically that previous expressions reduce to Collins-Soper-Sterman transverse momentum resummation in the limit Eq. (2.5.14), and to threshold resummation for inclusive cross section once integration over  $\xi_p$  is performed.

The first comparison is trivial since when  $b \rightarrow \infty$  at fixed  $N$ ,  $\chi \rightarrow \frac{b^2}{b_0^2}$  and any correction proportional to the dilogarithm vanishes. Eq. (2.7.2) or Eq. (2.7.3) could be checked against the results of Ref. [30], obtaining full agreement. The situation is little more complicated if we now want to perform the  $\xi_p$  integration. We are interested to crosscheck our expression against threshold resummation at inclusive level. Therefore, before performing the integral, we can simplify previous expressions by retaining only leading contribution in the  $N \rightarrow \infty$  limit at fixed  $\chi$ . At large- $N$  evolution of PDFs is diagonal; we thus have

$$L_{ij}^{\text{joint}} \rightarrow 0 \quad U_{ij}^{\text{joint},(1)} \rightarrow 0 \quad \text{if } i \neq j. \quad (2.7.11)$$

Taking the large  $N$  limit for the  $gg$  diagonal components (unique component surviving the limit) of Eq. (A.3.8), Eq. (A.3.12) and Eq. (2.7.7), we obtain:

$$\begin{aligned} L_{gg}^{\text{joint,div}}(N, \chi, \mu_{\text{F}}^2) = \exp \Bigg[ & -\frac{1}{\alpha} \frac{A_g^{p\text{T},(1)}}{2\beta_0^2} \lambda_{\bar{N}} \ln(1 - \lambda_\chi) \\ & - \frac{A_g^{p\text{T},(1)}\beta_1}{\beta_0^3} \frac{\lambda_{\bar{N}} \ln(1 - \lambda_\chi)}{2(1 - \lambda_\chi)} + \frac{\delta P_{gg}^{(1)}}{\beta_0} \ln(1 - \lambda_\chi) \\ & - \frac{A_g^{p\text{T},(1)}}{\beta_0} \frac{\lambda_{\bar{N}}\lambda_\chi}{2(1 - \lambda_\chi)} \ln \frac{m_{\text{H}}^2}{\mu_{\text{R}}^2} - \frac{A_g^{p\text{T},(1)}}{\beta_0} \frac{\lambda_{\bar{N}}}{2} \ln \frac{m_{\text{H}}^2}{\mu_{\text{F}}^2} \\ & + \alpha(\mu_{\text{R}}^2) \left( -\frac{A_g^{p\text{T},(1)}\beta_1^2}{\beta_0^4} \frac{\lambda_{\bar{N}}(2\lambda_\chi - 2\ln(1 - \lambda_\chi) + \ln^2(1 - \lambda_\chi))}{4(1 - \lambda_\chi)^2} \right. \\ & \left. + \frac{A_g^{p\text{T},(1)}\beta_2}{\beta_0^3} \frac{\lambda_{\bar{N}}\lambda_\chi}{2(1 - \lambda_\chi)^2} \right) \end{aligned}$$

$$\begin{aligned}
& + A_g^{p_T,(1)} \frac{\lambda_{\bar{N}}}{4(1-\lambda_\chi)^2} \ln^2 \frac{m_H^2}{\mu_R^2} - A_g^{p_T,(1)} \frac{\lambda_{\bar{N}}}{4} \ln^2 \frac{\mu_F^2}{\mu_R^2} \\
& + \frac{A_g^{p_T,(1)} \beta_1}{\beta_0^2} \frac{\lambda_{\bar{N}} (\lambda_\chi - 2) \lambda_\chi + \ln(1-\lambda_\chi)}{2(1-\lambda_\chi)^2} \ln \frac{m_H^2}{\mu_R^2} \\
& - \frac{A_g^{p_T,(1)} \beta_1}{\beta_0^2} \frac{\lambda_{\bar{N}}}{2} \ln \frac{m_H^2}{\mu_F^2} \\
& + \frac{\delta P_{gg}^{(1)} \beta_1}{\beta_0^2} \frac{\ln(1-\lambda_\chi)}{1-\lambda_\chi} + \delta P_{gg}^{(1)} \frac{\lambda_\chi}{1-\lambda_\chi} \ln \frac{m_H^2}{\mu_R^2} + \delta P_{gg}^{(1)} \ln \frac{m_H^2}{\mu_F^2} \Big), \tag{2.7.12}
\end{aligned}$$

$$U_{gg}^{\text{joint,(1),div}}(N) = \frac{1}{\alpha} \left( \frac{A_g^{p_T,(2)}}{\beta_0^2} - \frac{A_g^{p_T,(1)} \beta_1}{\beta_0^3} \right) \frac{\lambda_{\bar{N}}}{2} + \frac{\delta P_{gg}^{(1)} \beta_1}{\beta_0^2} - \frac{\delta P_{gg}^{(2)}}{\beta_0}. \tag{2.7.13}$$

and

$$\begin{aligned}
R_{gg}^{\text{div}}(N, \chi, \mu_F^2) = & \exp \left[ \left( \frac{A_g^{p_T,(2)}}{\beta_0^2} - \frac{A_g^{p_T,(1)} \beta_1}{\beta_0^3} \right) \frac{\lambda_{\bar{N}} \lambda_\chi}{2(1-\lambda_\chi)} \right. \\
& + \alpha_s \left( \left( \frac{A_g^{p_T,(1)} \beta_1^2}{2\beta_0^4} - \frac{A_g^{p_T,(1)} \beta_2}{2\beta_0^3} - \frac{A_g^{p_T,(2)} \beta_1}{2\beta_0^3} + \frac{A_g^{p_T,(3)}}{2\beta_0^2} \right) \frac{(2-\lambda_\chi) \lambda_\chi \lambda_{\bar{N}}}{2(1-\lambda_\chi)^2} \right. \\
& - \left( \frac{A_g^{p_T,(2)} \beta_1}{\beta_0^3} - \frac{A_g^{p_T,(1)} \beta_1^2}{\beta_0^4} \right) \frac{\lambda_{\bar{N}} \ln(1-\lambda_\chi)}{2(1-\lambda_\chi)^2} - \frac{D_g^{p_T,(2)}}{4\beta_0} \lambda_{\bar{N}} \\
& + \frac{\delta P_{gg}^{(1)} \beta_1}{\beta_0^2} \frac{\lambda_\chi}{1-\lambda_\chi} - \frac{\delta P_{gg}^{(2)}}{\beta_0} \frac{\lambda_\chi}{1-\lambda_\chi} \\
& + \left( \frac{A_g^{p_T,(2)}}{\beta_0} - \frac{A_g^{p_T,(1)} \beta_1}{\beta_0^2} \right) \frac{(2-\lambda_\chi) \lambda_{\bar{N}} \lambda_\chi}{2(1-\lambda_\chi)^2} \ln \frac{m_H^2}{\mu_R^2} \\
& \left. \left. + \left( \frac{A_g^{p_T,(1)} \beta_1}{\beta_0} - A_g^{p_T,(2)} \right) \frac{\lambda_{\bar{N}}}{2} \ln \frac{m_H^2}{\mu_F^2} \right) \right]. \tag{2.7.14}
\end{aligned}$$

Putting all this information together, we can rewrite  $gg$  component - the only singular at large  $N$  - of Eq. (2.7.1) as

$$\begin{aligned}
\frac{d\hat{\sigma}_{gg}^{\text{large-}N}}{d\xi_p} (N, \xi_p, \alpha_s(\mu_R^2), \mu_R^2, \mu_F^2) = & \int_0^\infty db \frac{b}{2} J_0(b m_H^2 \sqrt{\xi_p}) \left( \sqrt{1+\xi_p} - \sqrt{\xi_p} \right)^{-2N} \\
& \sigma_0(\alpha_s(\mu_R^2)) \bar{H}_g(\alpha_s(\mu_R^2)) \exp[G_g^{\text{joint}}(N, \chi, \mu_R^2, \mu_F^2)] \tag{2.7.15}
\end{aligned}$$

with

$$G_g^{\text{joint}}(N, \chi, \mu_R^2, \mu_F^2) = S_g(N, \chi, \mu_R^2) + 2 \ln R_{gg}(N, \chi, \mu_F^2) + 2 \ln L_{gg}^{\text{joint,div}}(N, \chi, \mu_F^2). \tag{2.7.16}$$

The complete exponent at large- $N$  turn out to be

$$G_g(N, \chi, \mu_R^2, \mu_F^2) = \frac{1}{\alpha_s} g_1^{\text{div}}(\lambda_\chi, \lambda_{\bar{N}}) + g_2^{\text{div}}(\lambda_\chi, \lambda_{\bar{N}}, \mu_R^2, \mu_F^2) + \alpha_s g_3^{\text{div}}(\lambda_\chi, \lambda_{\bar{N}}, \mu_R^2, \mu_F^2), \quad (2.7.17)$$

$$g_1^{\text{div}}(\lambda_\chi, \lambda_{\bar{N}}) = \frac{A_g^{\text{PT},(1)}}{\beta_0^2} (\lambda_\chi + \ln(1 - \lambda_\chi)) - \frac{A_g^{\text{PT},(1)}}{\beta_0^2} \lambda_{\bar{N}} \ln(1 - \lambda_\chi), \quad (2.7.18)$$

$$\begin{aligned} g_2^{\text{div}}(\lambda_\chi, \lambda_{\bar{N}}, \mu_R^2, \mu_F^2) &= \frac{A_g^{\text{PT},(1)} \beta_1}{\beta_0^3} \left[ \frac{\lambda_\chi + \ln(1 - \lambda_\chi)}{1 - \lambda_\chi} + \frac{1}{2} \ln(1 - \lambda_\chi)^2 \right] \\ &\quad - \frac{A_g^{\text{PT},(2)}}{\beta_0^2} \frac{\lambda_\chi + (1 - \lambda_\chi) \ln(1 - \lambda_\chi)}{1 - \lambda_\chi} \\ &\quad - \frac{A_g^{\text{PT},(1)} \beta_1 \lambda_{\bar{N}} (\lambda_\chi + \ln(1 - \lambda_\chi))}{\beta_0^3 (1 - \lambda_\chi)} + \frac{A_g^{\text{PT},(2)} \lambda_{\bar{N}} \lambda_\chi}{\beta_0^2 (1 - \lambda_\chi)} \\ &\quad + \frac{A_g^{\text{PT},(1)} \lambda_\chi + (1 - \lambda_\chi) \ln(1 - \lambda_\chi)}{\beta_0 (1 - \lambda_\chi)} \ln \frac{m_H^2}{\mu_R^2} \\ &\quad - \frac{A_g^{\text{PT},(1)} \lambda_{\bar{N}} \ln \chi}{\beta_0 (1 - \lambda_\chi)} \ln \frac{m_H^2}{\mu_R^2} - \frac{A_g^{\text{PT},(1)}}{\beta_0} \lambda_{\bar{N}} \ln \frac{m_H^2}{\mu_F^2}, \end{aligned} \quad (2.7.19)$$

$$\begin{aligned} g_3(\lambda_\chi, \lambda_{\bar{N}}, \mu_F^2) &= \frac{A_g^{\text{PT},(1)} \beta_1^2}{2\beta_0^4} \left[ \frac{\lambda_\chi + \ln(1 - \lambda_\chi)}{(1 - \lambda_\chi)^2} (\lambda_\chi + (1 - 2\lambda_\chi) \ln(1 - \lambda_\chi)) \right] \\ &\quad + \frac{A_g^{\text{PT},(1)} \beta_2}{\beta_0^3} \left[ \frac{(2 - 3\lambda_\chi) \lambda_\chi}{2(1 - \lambda_\chi)^2} + \ln(1 - \lambda_\chi) \right] \\ &\quad - \frac{A_g^{\text{PT},(2)} \beta_1}{\beta_0^3} \left[ \frac{(2 - 3\lambda_\chi) \lambda_\chi}{2(1 - \lambda_\chi)^2} + \frac{(1 - 2\lambda_\chi) \ln(1 - \lambda_\chi)}{(1 - \lambda_\chi)^2} \right] \\ &\quad - \frac{A_g^{\text{PT},(3)}}{2\beta_0^2} \frac{\lambda_\chi^2}{(1 - \lambda_\chi)^2} - \frac{\tilde{B}_g^{\text{PT},(2)}}{\beta_0} \frac{\lambda_\chi}{1 - \lambda_\chi} \\ &\quad + A_g^{\text{PT},(1)} \text{Li}_2 \left( \frac{\bar{N}^2}{\chi} \right) \frac{\lambda_{\bar{N}}}{1 - \lambda_{\bar{N}}} - \frac{A_g^{\text{PT},(1)} \beta_1^2 \lambda_{\bar{N}} (\lambda_\chi^2 + \ln^2(1 - \lambda_\chi))}{\beta_0^4 4(1 - \lambda_\chi)^2} \\ &\quad + \frac{A_g^{\text{PT},(1)} \beta_2}{\beta_0^3} \frac{\lambda_{\bar{N}} \lambda_\chi^2}{2(1 - \lambda_\chi)^2} - \frac{A_g^{\text{PT},(2)} \beta_1 \lambda_{\bar{N}} (\lambda_\chi (2 - \lambda_\chi) + 2 \ln(1 - \lambda_\chi))}{\beta_0^3 2(1 - \lambda_\chi)} \\ &\quad + \frac{A_g^{\text{PT},(3)} \lambda_{\bar{N}} (2 - \lambda_\chi) \lambda_\chi}{\beta_0^2 2(1 - \lambda_\chi)^2} - \frac{D_g^{\text{PT},(2)}}{4\beta_0} \lambda_{\bar{N}} \\ &\quad + \frac{A_g^{\text{PT},(1)} \beta_1}{\beta_0^2} \left[ \frac{\lambda_\chi (1 - \lambda_\chi) + (1 - 2\lambda_\chi) \ln(1 - \lambda_\chi)}{(1 - \lambda_\chi)^2} \right] \ln \frac{m_H^2}{\mu_R^2} \\ &\quad + \frac{A_g^{\text{PT},(2)}}{\beta_0} \frac{\lambda_\chi^2}{(1 - \lambda_\chi)^2} \ln \frac{m_H^2}{\mu_R^2} - \frac{A_g^{\text{PT},(1)}}{2} \frac{\lambda_\chi^2}{(1 - \lambda_\chi)^2} \ln^2 \frac{m_H^2}{\mu_R^2} \\ &\quad + A_g^{\text{PT},(1)} \frac{\lambda_{\bar{N}}}{2(1 - \lambda_\chi)^2} \ln^2 \frac{m_H^2}{\mu_R^2} - A_g^{\text{PT},(1)} \frac{\lambda_{\bar{N}}}{2} \ln^2 \frac{\mu_F^2}{\mu_R^2} \end{aligned}$$

$$\begin{aligned}
& + \frac{A_g^{\text{PT},(1)} \beta_1 \lambda_{\bar{N}} (2\lambda_\chi (\lambda_\chi - 2) + \ln(1 - \lambda_\chi))}{\beta_0^2 (1 - \lambda_\chi)^2} \\
& + \frac{A_g^{\text{PT},(2)} \lambda_{\bar{N}} \lambda_\chi (2 - \lambda_\chi)}{\beta_0 (1 - \lambda_\chi)^2} \ln \frac{m_{\text{H}}^2}{\mu_{\text{R}}^2} - A_g^{\text{PT},(2)} \lambda_{\bar{N}} \ln \frac{m_{\text{H}}^2}{\mu_{\text{F}}^2} + \delta P_{gg}^{(1)} \ln \frac{m_{\text{H}}^2}{\mu_{\text{F}}^2}, \quad (2.7.20)
\end{aligned}$$

while the hard function  $\bar{H}_g$  at first orders is given by

$$\begin{aligned}
\bar{H}_g(\alpha_s) &= 1 + \alpha_s \left( \bar{H}_g^{(1)} - 2\beta_0 \ln \frac{m_{\text{H}}^2}{\mu_{\text{R}}^2} \right) \\
& + \alpha_s^2 \left( \bar{H}_g^{(2)} - 3\beta_0 \bar{H}_g^{(1)} \ln \frac{m_{\text{H}}^2}{\mu_{\text{R}}^2} - 2\beta_1 \ln \frac{m_{\text{H}}^2}{\mu_{\text{R}}^2} + 3\beta_0^2 \ln^2 \frac{m_{\text{H}}^2}{\mu_{\text{R}}^2} \right) + \mathcal{O}(\alpha_s^3), \quad (2.7.21)
\end{aligned}$$

with  $H_g^{(i)}$  as in Eq. (C.1.17) of Appendix C.

To conclude our analytic check in the Higgs boson production case we need to integrate Eq. (2.7.15) over  $\xi_p$ . In Fourier space this corresponds to set  $b = 0$ . The factor  $(\sqrt{1 + \xi_p} - \sqrt{\xi_p})^{-2N}$  takes automatically into account different Mellin definition in collinear factorization between transverse momentum distribution and inclusive cross section.

Hence we have the following relation

$$\hat{\sigma}_{gg}(N, \alpha_s(\mu_{\text{R}}^2), \mu_{\text{R}}^2, \mu_{\text{F}}^2) = \sigma_0(\alpha_s(\mu_{\text{R}}^2)) g_0(\alpha_s(\mu_{\text{R}}^2)) \exp[G_g(N, \mu_{\text{R}}^2, \mu_{\text{F}}^2)] \quad (2.7.22)$$

with

$$g_0(\alpha_s(\mu_{\text{R}}^2)) = \bar{H}_g(\mu_{\text{R}}^2) \Big|_{\text{Li}_2(\frac{\bar{N}^2}{x}) \rightarrow \zeta_2} \quad (2.7.23)$$

$$G_g(N, \mu_{\text{R}}^2, \mu_{\text{F}}^2) = G_g^{\text{joint}}(N, \chi, \mu_{\text{R}}^2, \mu_{\text{F}}^2) \Big|_{\text{Li}_2(\frac{\bar{N}^2}{x}) \rightarrow \zeta_2, \lambda_\chi \rightarrow \lambda_{\bar{N}}} . \quad (2.7.24)$$

We crosscheck our result against NNLL threshold resummation for inclusive Higgs boson production cross section of Ref. [65].  $g_1, g_2, g_3$  coincide with corresponding threshold components, including factorization and renormalization scale dependence, if and only if the following relations between transverse momentum anomalous dimension and threshold anomalous dimension hold

$$A_g^{\text{PT},(3)} + \beta_0 D_g^{\text{PT},(2)} = A_g^{\text{th},(3)} \quad (2.7.25)$$

$$D_g^{\text{PT},(2)} + 2\tilde{B}_g^{\text{PT},(2)} + 2A_g^{\text{PT},(1)} \zeta_2 \beta_0 = D_g^{\text{th},(2)} \quad (2.7.26)$$

$$H_g^{(1)} + A_g^{\text{PT},(1)} \zeta_2 = g_0^{\text{th},(1)} = \frac{4C_A \zeta_2}{\pi}. \quad (2.7.27)$$

You can easily check yourself using the explicit expressions for these coefficients contained in Appendix C, that all these relations hold.

Our consistent construction reconstructs threshold resummation at inclusive level up to NNLL in the exponent and up to  $g_0^{(1)}$  in the constant, starting from a NNLL resummation of the transverse momentum distribution in the small- $p_{\text{T}}$  limit. However, it does not

reproduce correctly  $g_0^{(2)}$  and this is understood since  $\alpha_s^2$  constant receive contributions from NNNLL  $g_4$  which is not under our control. Further studies are needed to push all the construction one order higher, in particular to understand joint structure of correlations in the matrix elements from NNLL and beyond.

In moving from consistent resummation alone to combined resummation we add two more ingredients: threshold resummation at fixed  $p_T$ , and the profile matching function.

Explicit formula for threshold resummation at fixed  $p_T$  in the Higgs boson production case can be deduced by general expression (2.3.1):

$$\begin{aligned} \frac{d\hat{\sigma}_{gg}}{d\xi_p}(N, \xi_p, \alpha_s(\mu_R^2), \mu_R^2, \mu_F^2) &= \sigma_0(C_0(N, \xi_p, \alpha_s(\mu_R^2)))_{gg} \\ &\quad (g_0)_{gg}(\xi_p, \alpha_s(\mu_R^2), \mu_R^2, \mu_F^2) \exp[G_{gg \rightarrow gH}(N, \xi_p, \mu_R^2, \mu_F^2)] \end{aligned} \quad (2.7.28a)$$

$$\begin{aligned} \frac{d\hat{\sigma}_{gg}}{d\xi_p}(N, \xi_p, \alpha_s(\mu_R^2), \mu_R^2, \mu_F^2) &= \sigma_0(C_0(N, \xi_p, \alpha_s(\mu_R^2)))_{gg} \\ &\quad (g_0)_{gq}(\xi_p, \alpha_s(\mu_R^2), \mu_R^2, \mu_F^2) \exp[G_{gq \rightarrow qH}(N, \xi_p, \mu_R^2, \mu_F^2)] \end{aligned} \quad (2.7.28b)$$

$$\begin{aligned} \frac{d\hat{\sigma}_{qq}}{d\xi_p}(N, \xi_p, \alpha_s(\mu_R^2), \mu_R^2, \mu_F^2) &= \sigma_0(C_0(N, \xi_p, \alpha_s(\mu_R^2)))_{qq} \\ &\quad (g_0)_{qq}(\xi_p, \alpha_s(\mu_R^2), \mu_R^2, \mu_F^2) \exp[G_{qq \rightarrow gH}(N, \xi_p, \mu_R^2, \mu_F^2)] \end{aligned} \quad (2.7.28c)$$

with

$$\begin{aligned} G_{gg \rightarrow gH}(N, \xi_p, \mu_R^2, \mu_F^2) &= \frac{1}{\alpha_s} (g_1)_{gg}(\lambda_{\bar{N}}) + (g_2)_{gg}(\lambda_{\bar{N}}, \xi_p, \mu_R^2, \mu_F^2) \\ &\quad + \alpha_s (g_3)_{gg}(\lambda_{\bar{N}}, \xi_p, \mu_R^2, \mu_F^2) + \mathcal{O}(\alpha_s^2) \end{aligned} \quad (2.7.29a)$$

$$(g_1)_{gg} = \frac{A_g^{\text{th},(1)}}{\beta_0^2} \left( \lambda_{\bar{N}} + \frac{1 - \lambda_{\bar{N}}}{2} \ln(1 - \lambda_{\bar{N}}) + \left(1 - \frac{\lambda_{\bar{N}}}{2}\right) \ln\left(1 - \frac{\lambda_{\bar{N}}}{2}\right) \right), \quad (2.7.29b)$$

$$\begin{aligned} (g_2)_{gg} &= -\frac{A_g^{\text{th},(1)} \beta_1}{\beta_0^3} \\ &\quad \left( \lambda_{\bar{N}} + \frac{1}{2} \ln(1 - \lambda_{\bar{N}}) + \frac{1}{4} \ln^2(1 - \lambda_{\bar{N}}) + \ln\left(1 - \frac{\lambda_{\bar{N}}}{2}\right) + \frac{1}{2} \ln^2\left(1 - \frac{\lambda_{\bar{N}}}{2}\right) \right) \\ &\quad - \frac{A_g^{\text{th},(2)}}{\beta_0^2} \left( \frac{1}{2} \ln(1 - \lambda_{\bar{N}}) + \lambda_{\bar{N}} + \ln\left(1 - \frac{\lambda_{\bar{N}}}{2}\right) \right) + \frac{B_g^{\text{th},(1)}}{\beta_0} \ln\left(1 - \frac{\lambda_{\bar{N}}}{2}\right) \\ &\quad - \frac{A_g^{\text{th},(1)}}{\beta_0} \frac{1}{2} \ln(1 - \lambda_{\bar{N}}) \ln \frac{(\sqrt{1 + \xi_p} + \sqrt{\xi_p})^2}{\xi_p} \\ &\quad + \frac{A_g^{\text{th},(1)}}{\beta_0} \left( \frac{1}{2} \ln(1 - \lambda_{\bar{N}}) + \lambda_{\bar{N}} + \ln\left(1 - \frac{\lambda_{\bar{N}}}{2}\right) \right) \ln \frac{W^2}{\mu_R^2} - 2 \frac{A_g^{\text{th},(1)}}{\beta_0} \lambda_{\bar{N}} \ln \frac{W^2}{\mu_F^2}, \end{aligned} \quad (2.7.29c)$$

$$(g_3)_{gg} = \frac{A_g^{\text{th},(1)}}{4\beta_0^4(1 - \lambda_{\bar{N}})(2 - \lambda_{\bar{N}})}$$

$$\begin{aligned}
& \left( \lambda_{\bar{N}}^2 (3 - 2\lambda_{\bar{N}}) + 2(2 - \lambda_{\bar{N}})\lambda_{\bar{N}}(1 - \lambda_{\bar{N}}) + (2 - \lambda_{\bar{N}})\ln^2(1 - \lambda_{\bar{N}}) \right. \\
& \quad \left. + 4(1 - \lambda_{\bar{N}})\lambda_{\bar{N}}\ln\left(1 - \frac{\lambda_{\bar{N}}}{2}\right) + 4(1 - \lambda_{\bar{N}})\ln^2\left(1 - \frac{\lambda_{\bar{N}}}{2}\right) \right) \\
& + \frac{A_g^{\text{th},(1)}\beta_2}{4\beta_0^3} \left( \frac{\lambda_{\bar{N}}(8 - 9\lambda_{\bar{N}} + 2\lambda_{\bar{N}}^2)}{(2 - \lambda_{\bar{N}})(1 - \lambda_{\bar{N}})} + 2\ln(1 - \lambda_{\bar{N}}) + 4\ln\left(1 - \frac{\lambda_{\bar{N}}}{2}\right) \right) \\
& + \frac{A_g^{\text{th},(2)}\beta_1}{4\beta_0^3(1 - \lambda_{\bar{N}})(2 - \lambda_{\bar{N}})} \\
& \left( \lambda_{\bar{N}}(2\lambda_{\bar{N}}^2 + 3\lambda_{\bar{N}} - 8) - 2(2 - \lambda_{\bar{N}})\ln(1 - \lambda_{\bar{N}}) - 8(1 - \lambda_{\bar{N}})\ln\left(1 - \frac{\lambda_{\bar{N}}}{2}\right) \right) \\
& + \frac{A_g^{\text{th},(3)}}{4\beta_0^2} \frac{(3 - 2\lambda_{\bar{N}})\lambda_{\bar{N}}^2}{(1 - \lambda_{\bar{N}})(2 - \lambda_{\bar{N}})} - \frac{B_g^{\text{th},(1)}\beta_1}{\beta_0^2} \frac{\lambda_{\bar{N}} + 2\ln\left(1 - \frac{\lambda_{\bar{N}}}{2}\right)}{2 - \lambda_{\bar{N}}} - \frac{B_g^{\text{th},(2)}}{\beta_0} \frac{\lambda_{\bar{N}}}{2 - \lambda_{\bar{N}}} \\
& + \frac{A_g^{\text{th},(1)}\beta_1}{\beta_0^2} \frac{\lambda_{\bar{N}} + \ln(1 - \lambda_{\bar{N}})}{1 - \lambda_{\bar{N}}} \ln \frac{(\sqrt{1 + \xi_p} + \sqrt{\xi_p})^2}{\xi_p} \\
& + \frac{A_g^{\text{th},(2)}}{\beta_0} \frac{\lambda_{\bar{N}}}{1 - \lambda_{\bar{N}}} \ln \frac{(\sqrt{1 + \xi_p} + \sqrt{\xi_p})^2}{\xi_p} - A_g^{\text{th},(1)}\zeta_2 \frac{3 - 2\lambda_{\bar{N}}}{(1 - \lambda_{\bar{N}})(2 - \lambda_{\bar{N}})} \\
& + \frac{A_g^{\text{th},(1)}}{4} \frac{(3 - 2\lambda_{\bar{N}})\lambda_{\bar{N}}^2}{(1 - \lambda_{\bar{N}})(2 - \lambda_{\bar{N}})} \ln^2 \frac{W^2}{\mu_{\text{R}}^2} - A_g^{\text{th},(1)}\lambda_{\bar{N}} \ln^2 \frac{W^2}{\mu_{\text{F}}^2} \\
& + \frac{A_g^{\text{th},(1)}\beta_1}{2\beta_0(1 - \lambda_{\bar{N}})(2 - \lambda_{\bar{N}})} \\
& \left( (4 - 3\lambda_{\bar{N}})\lambda_{\bar{N}} + (2 - \lambda_{\bar{N}})\ln(1 - \lambda_{\bar{N}}) + 4(1 - \lambda_{\bar{N}})\ln\left(1 - \frac{\lambda_{\bar{N}}}{2}\right) \right) \ln \frac{W^2}{\mu_{\text{R}}^2} \\
& + 2A_g^{\text{th},(1)}\lambda_{\bar{N}} \ln \frac{W^2}{\mu_{\text{F}}^2} \ln \frac{W^2}{\mu_{\text{R}}^2} - \frac{A_g^{\text{th},(2)}}{2\beta_0} \frac{(3 - 2\lambda_{\bar{N}})\lambda_{\bar{N}}^2}{(1 - \lambda_{\bar{N}})(2 - \lambda_{\bar{N}})} \ln \frac{W^2}{\mu_{\text{R}}^2} \\
& + 2\frac{A_g^{\text{th},(2)}}{\beta_0}\lambda_{\bar{N}} \ln \frac{W^2}{\mu_{\text{F}}^2} + B_g^{\text{th},(1)} \frac{\lambda_{\bar{N}}}{2 - \lambda_{\bar{N}}} \ln \frac{W^2}{\mu_{\text{R}}^2} \\
& + A_g^{\text{th},(1)} \frac{\lambda_{\bar{N}}}{1 - \lambda_{\bar{N}}} \ln \frac{(\sqrt{1 + \xi_p} + \sqrt{\xi_p})^2}{\xi_p} \ln \frac{W^2}{\mu_{\text{R}}^2}; \tag{2.7.29d}
\end{aligned}$$

$$\begin{aligned}
G_{gq \rightarrow qH}(N, \xi_p, \mu_{\text{R}}^2, \mu_{\text{F}}^2) &= \frac{1}{\alpha_s} (g_1)_{gq}(\lambda_{\bar{N}}) + (g_2)_{gq}(\lambda_{\bar{N}}, \xi_p, \mu_{\text{R}}^2, \mu_{\text{F}}^2) \\
&\quad + \alpha_s (g_3)_{gq}(\lambda_{\bar{N}}, \xi_p, \mu_{\text{R}}^2, \mu_{\text{F}}^2) + \mathcal{O}(\alpha_s^2) \tag{2.7.30a}
\end{aligned}$$

$$\begin{aligned}
(g_1)_{gq} &= \frac{A_g^{\text{th},(1)}}{2\beta_0^2} \left( \lambda_{\bar{N}} + (1 - \lambda_{\bar{N}})\ln(1 - \lambda_{\bar{N}}) \right) \\
&+ \frac{A_q^{\text{th},(1)}}{2\beta_0^2} \left( \lambda_{\bar{N}} - (2 - \lambda_{\bar{N}})\ln\left(1 - \frac{\lambda_{\bar{N}}}{2}\right) \right), \tag{2.7.30b}
\end{aligned}$$

$$\begin{aligned}
(g_2)_{gq} &= -\frac{A_g^{\text{th},(1)}\beta_1}{4\beta_0^3}(2\lambda_{\bar{N}} + \ln(1 - \lambda_{\bar{N}})(2 + \ln(1 - \lambda_{\bar{N}}))) \\
&+ \frac{A_q^{\text{th},(1)}\beta_1}{2\beta_0^3}\left(\lambda_{\bar{N}} + 2\ln\left(1 - \frac{\lambda_{\bar{N}}}{2}\right) + \ln^2\left(1 - \frac{\lambda_{\bar{N}}}{2}\right)\right) \\
&- \frac{A_g^{\text{th},(2)}}{2\beta_0^2}(\lambda_{\bar{N}} + \ln(1 - \lambda_{\bar{N}})) - \frac{A_q^{\text{th},(2)}}{2\beta_0^2}\left(\lambda_{\bar{N}} + 2\ln\left(1 - \frac{\lambda_{\bar{N}}}{2}\right)\right) \\
&+ \frac{B_q^{\text{th},(1)}}{\beta_0}\ln\left(1 - \frac{\lambda_{\bar{N}}}{2}\right) - \frac{A_q^{\text{th},(1)}}{2\beta_0}\ln(1 - \lambda_{\bar{N}})\ln\frac{(\sqrt{1 + \xi_p} - \sqrt{\xi_p})^2}{\xi_p} \\
&+ \frac{A_g^{\text{th},(1)}}{2\beta_0}(\lambda_{\bar{N}} + \ln(1 - \lambda_{\bar{N}}))\ln\frac{W^2}{\mu_{\text{R}}^2} - \frac{A_g^{\text{th},(1)}}{\beta_0}\lambda_{\bar{N}}\ln\frac{W^2}{\mu_{\text{F}}^2} \\
&+ \frac{A_q^{\text{th},(1)}}{2\beta_0}\left(\lambda_{\bar{N}} + 2\ln\left(1 - \frac{\lambda_{\bar{N}}}{2}\right)\right)\ln\frac{W^2}{\mu_{\text{R}}^2} - \frac{A_q^{\text{th},(1)}}{\beta_0}\lambda_{\bar{N}}\ln\frac{W^2}{\mu_{\text{F}}^2}, \tag{2.7.30c} \\
(g_3)_{gq} &= \frac{A_g^{\text{th},(1)}\beta_1^2(\lambda_{\bar{N}} + \ln(1 - \lambda_{\bar{N}}))^2}{4\beta_0^4(1 - \lambda_{\bar{N}})} \\
&+ \frac{A_g^{\text{th},(1)}\beta_2(2 - \lambda_{\bar{N}})\lambda_{\bar{N}} + 2(1 - \lambda_{\bar{N}})\ln(1 - \lambda_{\bar{N}})}{4\beta_0^3(1 - \lambda_{\bar{N}})} \\
&+ \frac{A_q^{\text{th},(1)}\beta_1^2\left(\lambda_{\bar{N}} + 2\ln\left(1 - \frac{\lambda_{\bar{N}}}{2}\right)\right)^2}{4\beta_0^4(2 - \lambda_{\bar{N}})} \\
&+ \frac{A_q^{\text{th},(1)}\beta_2(4 - \lambda_{\bar{N}})\lambda_{\bar{N}} + 4(2 - \lambda_{\bar{N}})\ln\left(1 - \frac{\lambda_{\bar{N}}}{2}\right)}{4\beta_0^3(2 - \lambda_{\bar{N}})} \\
&- \frac{A_g^{\text{th},(2)}\beta_1\lambda_{\bar{N}}(2 + \lambda_{\bar{N}}) + 2\ln(1 - \lambda_{\bar{N}})}{4\beta_0^3(1 - \lambda_{\bar{N}})} \\
&- \frac{A_q^{\text{th},(2)}\beta_1\lambda_{\bar{N}}(4 + \lambda_{\bar{N}}) + 8\ln\left(1 - \frac{\lambda_{\bar{N}}}{2}\right)}{4\beta_0^3(2 - \lambda_{\bar{N}})} \\
&+ \frac{A_g^{\text{th},(3)}\lambda_{\bar{N}}^2}{4\beta_0^2(1 - \lambda_{\bar{N}})} + \frac{A_q^{\text{th},(3)}\lambda_{\bar{N}}^2}{4\beta_0^2(2 - \lambda_{\bar{N}})} \\
&- \frac{B_q^{\text{th},(1)}\beta_1\lambda_{\bar{N}} + 2\ln\left(1 - \frac{\lambda_{\bar{N}}}{2}\right)}{\beta_0^2(2 - \lambda_{\bar{N}})} - \frac{B_q^{\text{th},(2)}\lambda_{\bar{N}}}{\beta_0(2 - \lambda_{\bar{N}})} \\
&+ \frac{A_q^{\text{th},(1)}\beta_1\lambda_{\bar{N}} + \ln(1 - \lambda_{\bar{N}})}{\beta_0^2(1 - \lambda_{\bar{N}})}\ln\frac{(\sqrt{1 + \xi_p} + \sqrt{\xi_p})^2}{\xi_p} \\
&+ \frac{A_q^{\text{th},(2)}\lambda_{\bar{N}}}{\beta_0(1 - \lambda_{\bar{N}})}\ln\frac{(\sqrt{1 + \xi_p} + \sqrt{\xi_p})^2}{\xi_p} \\
&- A_g^{\text{th},(1)}\zeta_2\frac{1}{1 - \lambda_{\bar{N}}} + \frac{A_g^{\text{th},(1)}\lambda_{\bar{N}}^2}{4(1 - \lambda_{\bar{N}})}\ln^2\frac{W^2}{\mu_{\text{R}}^2} - \frac{A_g^{\text{th},(1)}}{2}\lambda_{\bar{N}}\ln^2\frac{W^2}{\mu_{\text{F}}^2} \\
&- A_q^{\text{th},(1)}\zeta_2\frac{1}{2 - \lambda_{\bar{N}}} + \frac{A_q^{\text{th},(1)}\lambda_{\bar{N}}^2}{4(2 - \lambda_{\bar{N}})}\ln^2\frac{W^2}{\mu_{\text{R}}^2} + \frac{A_q^{\text{th},(1)}}{2}\lambda_{\bar{N}}\ln^2\frac{W^2}{\mu_{\text{F}}^2}
\end{aligned}$$

$$\begin{aligned}
& + \frac{A_g^{\text{th},(1)} \beta_1}{2\beta_0^2} \frac{\lambda_{\bar{N}} + \ln(1 - \lambda_{\bar{N}})}{1 - \lambda_{\bar{N}}} \ln \frac{W^2}{\mu_R^2} + \frac{A_q^{\text{th},(1)} \beta_1}{\beta_0^2} \frac{\lambda_{\bar{N}} + 2 \ln\left(1 - \frac{\lambda_{\bar{N}}}{2}\right)}{2 - \lambda_{\bar{N}}} \\
& + A_g^{\text{th},(1)} \lambda_{\bar{N}} \ln \frac{W^2}{\mu_R^2} \ln \frac{W^2}{\mu_F^2} - \frac{A_g^{\text{th},(2)}}{2\beta_0} \frac{\lambda_{\bar{N}}^2}{1 - \lambda_{\bar{N}}} \ln \frac{W^2}{\mu_R^2} - \frac{A_q^{\text{th},(2)}}{\beta_0} \lambda_{\bar{N}} \ln \frac{W^2}{\mu_F^2} \\
& + A_q^{\text{th},(1)} \lambda_{\bar{N}} \ln \frac{W^2}{\mu_R^2} \ln \frac{W^2}{\mu_F^2} - \frac{A_q^{\text{th},(2)}}{2\beta_0} \frac{\lambda_{\bar{N}}^2}{2 - \lambda_{\bar{N}}} \ln \frac{W^2}{\mu_R^2} - \frac{A_q^{\text{th},(2)}}{\beta_0} \lambda_{\bar{N}} \ln \frac{W^2}{\mu_F^2} \\
& + B_q^{\text{th},(1)} \frac{\lambda_{\bar{N}}}{2 - \lambda_{\bar{N}}} \ln \frac{W^2}{\mu_R^2} - A_q^{\text{th},(1)} \frac{\lambda_{\bar{N}}}{1 - \lambda_{\bar{N}}} \ln \frac{(\sqrt{1 + \xi_p} + \sqrt{\xi_p})^2}{\xi_p} \ln \frac{W^2}{\mu_R^2};
\end{aligned} \tag{2.7.30d}$$

and

$$\begin{aligned}
G_{qq \rightarrow gH}(N, \xi_p, \mu_R^2, \mu_F^2) &= \frac{1}{\alpha_s} (g_1)_{qq}(\lambda_{\bar{N}}) + (g_2)_{qq}(\lambda_{\bar{N}}, \xi_p, \mu_R^2, \mu_F^2) \\
&+ \alpha_s (g_3)_{qq}(\lambda_{\bar{N}}, \xi_p, \mu_R^2, \mu_F^2) + \mathcal{O}(\alpha_s^2)
\end{aligned} \tag{2.7.31a}$$

$$\begin{aligned}
(g_1)_{qq} &= \frac{A_q^{\text{th},(1)}}{\beta_0^2} \left( \lambda_{\bar{N}} + (1 - \lambda_{\bar{N}}) \ln(1 - \lambda_{\bar{N}}) \right) \\
&+ \frac{A_g^{\text{th},(1)}}{2\beta_0^2} \left( (2 - \lambda_{\bar{N}}) \ln\left(1 - \frac{\lambda_{\bar{N}}}{2}\right) - (1 - \lambda_{\bar{N}}) \ln(1 - \lambda_{\bar{N}}) \right),
\end{aligned} \tag{2.7.31b}$$

$$\begin{aligned}
(g_2)_{qq} &= \frac{A_g^{\text{th},(1)} \beta_1}{4\beta_0^3} \\
&\left( \ln(1 - \lambda_{\bar{N}}) (2 + \ln(1 - \lambda_{\bar{N}})) - 2 \ln\left(1 - \frac{\lambda_{\bar{N}}}{2}\right) \left(2 + \ln\left(1 - \frac{\lambda_{\bar{N}}}{2}\right)\right) \right) \\
&- \frac{A_q^{\text{th},(1)} \beta_1}{2\beta_0^3} (2\lambda_{\bar{N}} + 2 \ln(1 - \lambda_{\bar{N}}) + \ln^2(1 - \lambda_{\bar{N}})) \\
&- \frac{A_g^{\text{th},(2)}}{2\beta_0^2} \left( \ln(1 - \lambda_{\bar{N}}) - 2 \ln\left(1 - \frac{\lambda_{\bar{N}}}{2}\right) \right) - \frac{A_q^{\text{th},(2)}}{\beta_0^2} (\lambda_{\bar{N}} + \ln(1 - \lambda_{\bar{N}})) \\
&+ \frac{B_g^{\text{th},(1)}}{\beta_0} \ln\left(1 - \frac{\lambda_{\bar{N}}}{2}\right) - \frac{A_g^{\text{th},(1)}}{2\beta_0} \ln(1 - \lambda_{\bar{N}}) \ln \frac{(\sqrt{1 + \xi_p} - \sqrt{\xi_p})^2}{\xi_p} \\
&- \frac{A_g^{\text{th},(1)}}{2\beta_0} \left( \ln(1 - \lambda_{\bar{N}}) - 2 \ln\left(1 - \frac{\lambda_{\bar{N}}}{2}\right) \right) \ln \frac{W^2}{\mu_R^2} \\
&+ \frac{A_q^{\text{th},(1)}}{\beta_0} (\lambda_{\bar{N}} + \ln(1 - \lambda_{\bar{N}})) \ln \frac{W^2}{\mu_R^2} - 2 \frac{A_q^{\text{th},(1)}}{\beta_0} \lambda_{\bar{N}} \ln \frac{W^2}{\mu_F^2},
\end{aligned} \tag{2.7.31c}$$

$$\begin{aligned}
(g_3)_{qq} &= \frac{A_q^{\text{th},(1)} \beta_1^2}{2\beta_0^4} \frac{(\lambda_{\bar{N}} + \ln(1 - \lambda_{\bar{N}}))^2}{1 - \lambda_{\bar{N}}} \\
&+ \frac{A_q^{\text{th},(1)} \beta_2}{2\beta_0^3} \frac{(2 - \lambda_{\bar{N}}) \lambda_{\bar{N}} + 2(1 - \lambda_{\bar{N}}) \ln(1 - \lambda_{\bar{N}})}{1 - \lambda_{\bar{N}}} \\
&+ \frac{A_g^{\text{th},(1)} \beta_1^2}{4\beta_0^4 (1 - \lambda_{\bar{N}}) (2 - \lambda_{\bar{N}})}
\end{aligned}$$

$$\begin{aligned}
& \left( \lambda_{\bar{N}}^2 + 2(2 - \lambda_{\bar{N}}) \lambda_{\bar{N}} \ln(1 - \lambda_{\bar{N}}) + (2 - \lambda_{\bar{N}}) \ln^2(1 - \lambda_{\bar{N}}) \right. \\
& \quad \left. + 4(1 - \lambda_{\bar{N}}) \lambda_{\bar{N}} \ln\left(1 - \frac{\lambda_{\bar{N}}}{2}\right) + 4(1 - \lambda_{\bar{N}}) \ln^2\left(1 - \frac{\lambda_{\bar{N}}}{2}\right) \right) \\
& + \frac{A_g^{\text{th},(1)} \beta_2}{4\beta_0^3 (1 - \lambda_{\bar{N}}) (2 - \lambda_{\bar{N}})} \\
& \quad \left( \lambda_{\bar{N}}^2 + 2(2 - \lambda_{\bar{N}}) (1 - \lambda_{\bar{N}}) \ln(1 - \lambda_{\bar{N}}) - 4(2 - \lambda_{\bar{N}}) (1 - \lambda_{\bar{N}}) \ln\left(1 - \frac{\lambda_{\bar{N}}}{2}\right) \right) \\
& - \frac{A_q^{\text{th},(2)} \beta_1 \lambda_{\bar{N}} (2 + \lambda_{\bar{N}}) + 2 \ln(1 - \lambda_{\bar{N}})}{4\beta_0^3} - \frac{A_g^{\text{th},(2)} \beta_1}{4\beta_0^3 (1 - \lambda_{\bar{N}}) (2 - \lambda_{\bar{N}})} \\
& \quad \left( 3\lambda_{\bar{N}}^+ 2(2 - \lambda_{\bar{N}}) \ln(1 - \lambda_{\bar{N}}) - 8(1 - \lambda_{\bar{N}}) \ln\left(1 - \frac{\lambda_{\bar{N}}}{2}\right) \right) \\
& + \frac{A_g^{\text{th},(3)}}{4\beta_0^2} \frac{\lambda_{\bar{N}}^2}{(1 - \lambda_{\bar{N}}) (2 - \lambda_{\bar{N}})} + \frac{A_q^{\text{th},(3)}}{2\beta_0^2} \frac{\lambda_{\bar{N}}^2}{1 - \lambda_{\bar{N}}} \\
& - \frac{B_g^{\text{th},(1)} \beta_1 \lambda_{\bar{N}} + 2 \ln\left(1 - \frac{\lambda_{\bar{N}}}{2}\right)}{\beta_0^2} \frac{\lambda_{\bar{N}}}{2 - \lambda_{\bar{N}}} - \frac{B_g^{\text{th},(2)}}{\beta_0} \frac{\lambda_{\bar{N}}}{2 - \lambda_{\bar{N}}} \\
& + \frac{A_g^{\text{th},(1)} \beta_1 \lambda_{\bar{N}} + \ln(1 - \lambda_{\bar{N}})}{\beta_0^2} \frac{1 - \lambda_{\bar{N}}}{1 - \lambda_{\bar{N}}} \ln \frac{(\sqrt{1 + \xi_p} + \sqrt{\xi_p})^2}{\xi_p} \\
& + \frac{A_g^{\text{th},(2)}}{\beta_0} \frac{\lambda_{\bar{N}}}{1 - \lambda_{\bar{N}}} \ln \frac{(\sqrt{1 + \xi_p} + \sqrt{\xi_p})^2}{\xi_p} \\
& - 2A_q^{\text{th},(1)} \zeta_2 \frac{1}{1 - \lambda_{\bar{N}}} + \frac{A_q^{\text{th},(1)}}{2} \frac{\lambda_{\bar{N}}^2}{1 - \lambda_{\bar{N}}} \ln^2 \frac{W^2}{\mu_{\text{R}}^2} - A_q^{\text{th},(1)} \lambda_{\bar{N}} \ln^2 \frac{W^2}{\mu_{\text{F}}^2} \\
& + A_g^{\text{th},(1)} \zeta_2 \frac{1}{(1 - \lambda_{\bar{N}}) (2 - \lambda_{\bar{N}})} - \frac{A_g^{\text{th},(1)}}{4} \frac{\lambda_{\bar{N}}^2}{(1 - \lambda_{\bar{N}}) (2 - \lambda_{\bar{N}})} \ln^2 \frac{W^2}{\mu_{\text{R}}^2} \\
& - \frac{A_g^{\text{th},(1)} \beta_1}{2\beta_0^2 (1 - \lambda_{\bar{N}}) (2 - \lambda_{\bar{N}})} \\
& \quad \left( \lambda_{\bar{N}}^2 + (2 - \lambda_{\bar{N}}) \ln(1 - \lambda_{\bar{N}}) - 4(1 - \lambda_{\bar{N}}) \ln\left(1 - \frac{\lambda_{\bar{N}}}{2}\right) \right) \ln \frac{W^2}{\mu_{\text{R}}^2} \\
& + \frac{A_q^{\text{th},(1)} \beta_1 \lambda_{\bar{N}} + \ln(1 - \lambda_{\bar{N}})}{\beta_0^2} \frac{1 - \lambda_{\bar{N}}}{1 - \lambda_{\bar{N}}} \ln \frac{W^2}{\mu_{\text{R}}^2} \\
& - \frac{A_g^{\text{th},(2)}}{2\beta_0} \frac{\lambda_{\bar{N}}^2}{(1 - \lambda_{\bar{N}}) (2 - \lambda_{\bar{N}})} \ln \frac{W^2}{\mu_{\text{R}}^2} + 2A_q^{\text{th},(1)} \lambda_{\bar{N}} \ln \frac{W^2}{\mu_{\text{R}}^2} \ln \frac{W^2}{\mu_{\text{F}}^2} \\
& - \frac{A_q^{\text{th},(2)}}{\beta_0} \frac{\lambda_{\bar{N}}^2}{1 - \lambda_{\bar{N}}} + 2 \frac{A_q^{\text{th},(2)}}{\beta_0} \lambda_{\bar{N}} \ln \frac{W^2}{\mu_{\text{F}}^2} \\
& + B_g^{\text{th},(1)} \frac{\lambda_{\bar{N}}}{2 - \lambda_{\bar{N}}} \ln \frac{W^2}{\mu_{\text{R}}^2} - A_g^{\text{th},(1)} \frac{\lambda_{\bar{N}}}{1 - \lambda_{\bar{N}}} \ln \frac{(\sqrt{1 + \xi_p} + \sqrt{\xi_p})^2}{\xi_p} \ln \frac{W^2}{\mu_{\text{R}}^2}.
\end{aligned} \tag{2.7.31d}$$

Explicit expressions for all the anomalous dimension coefficients can be found in Appendix C, Eq. (C.1.1), Eq. (C.1.2) while LO cross section and NLO matching constant  $g_0$  in the case of Higgs boson production are given by Eq. (C.1.4) and Eq. (C.1.5).

This second resummation does not spoil our previous result about inclusive integrals thanks to the particular form we choose for the profile matching function. Indeed, due to properties Eqs. (2.6.2), we can prove the following result: if  $T(N, \xi_p) f(N, \xi_p) \rightarrow 0$  when  $\xi_p \rightarrow 0$ , then

$$\left[ \int_0^\infty d\xi_p T(N, \xi_p) f(N, \xi_p) \right] \rightarrow 0 \quad \text{as } N \rightarrow \infty. \quad (2.7.32)$$

In this sense, the  $\xi_p$  integral of the combined resummation coincides with the  $\xi_p$  integral of the consistent transverse momentum resummation alone, that we prove to be equal to the threshold resummed inclusive cross section.

In conclusion, we prove that our final formula owns all the properties we are searching for. It reduces to the original transverse momentum resummation at small- $p_T$ ; it takes into account threshold components at all  $p_T$  both at small- $p_T$  and at fixed- $p_T$ ; its integral coincides at large- $N$  with the NNLL threshold resummation for inclusive cross section. This remark ends this chapter; we are going to study more in detail the phenomenological impact of this resummation in Chap. 4, by comparing it with standard transverse momentum resummation.



# 3 High Energy Resummation

## Contents

---

<b>3.1</b>	<b><math>k_T</math>-factorization.</b>	<b>94</b>
3.1.1	LL $x$ Resummation using BFKL equation	99
3.1.2	LL $x$ Resummation using Generalized Ladder Expansion	104
<b>3.2</b>	<b>Transverse Momentum Distribution at High Energy</b>	<b>109</b>
3.2.1	Quark-initiated channels	112
3.2.2	Coloured Final State	113
<b>3.3</b>	<b>Double differential distribution at high energy</b>	<b>116</b>
<b>3.4</b>	<b>Application: EFT Higgs boson at high energy</b>	<b>121</b>
3.4.1	Check against fixed order evaluation	124

---

In this third chapter we are going to discuss in detail the high energy resummation of transverse momentum distribution and other observables. High energy resummation has a long story and it is based on  $k_T$ -factorization, a factorization property [29,68], known for a long time for inclusive cross-sections. This theory was originally applied to the photo- and lepto-production of heavy quarks, and subsequently also derived for deep-inelastic scattering [69,70], heavy quark hadro-production [71], Higgs boson production [72,73], Drell-Yan production [74], and prompt-photon production [75]. A recent new approach to high energy resummation, which is also the basis of the original work contained in this chapter, permits to extend this framework to rapidity distribution [76], and now also to transverse momentum distribution [77].

This chapter shall be organized as follows: the first section 3.1 is devoted to  $k_T$ -factorization and to a general proof of it; then we are going to present the original approach to high energy resummation, based on BFKL and DGLAP duality in Sec. 3.1.1. Then we focus our attention on the high energy resummation of transverse momentum distribution in Sec. 3.2. To reach this result we are going to briefly sketch the alternative derivation of high energy resummation based on the generalized ladder expansion in Sec. 1.2.2.

Finally, the last part of this chapter will be devoted to generalize the theory presented in previous sections to other important cases: the analysis of quark-initiated channels and the analysis of coloured final state. Moreover Sec. 3.3 will be the proper conclusion of this

research project: we will unify resummation for rapidity distributions and resummation for transverse momentum distributions in a unique formula, thus reaching high energy resummation for the complete differential distribution of colour singlet production. Application to our test process, EFT Higgs boson production, closes the chapter in Sec. 3.4, providing also checks about the whole derivation of the chapter.

### 3.1 $k_T$ -factorization

In this section we will summarize the factorization property which constitutes the basis for any approach to high energy resummation:  $k_T$ -factorization. We are going to present this factorization for a general production process of a state  $\mathcal{S}$  in hadron-hadron scattering, characterized by a hard scale  $Q$ . Up to now we limit ourselves (without loss of generality of the subsequent argument) to a gluon initiated process, like Higgs production:

$$g(p) + g(n) \rightarrow \mathcal{S} + X, \quad (3.1.1)$$

with  $g(p)$  and  $g(n)$  initial-state gluons of momentum  $p$  and  $n$  respectively.

The starting point is the observation [29, 79] that in axial gauge leading contributions in the high energy limit come from cut diagrams which are at least two-gluon-irreducible (2GI) in the  $t$ -channel. Moreover, it can be proved [24], with power counting arguments, that any radiation connecting the two initial legs is suppressed by powers of the centre-of-mass energy  $s$ . It follows that any (dimensionless) infra-red safe partonic observable  $\hat{O}$  can be written in terms of a process dependent *hard part*  $H^{\mu\nu\bar{\mu}\bar{\nu}}$  and two universal *ladders* of emission  $L_{\mu\nu}$ :

$$\hat{O} \left( \frac{Q^2}{s}, \{v\}, \frac{\mu_F^2}{Q^2}, \frac{\mu_R^2}{Q^2} \right) = \int \frac{Q^2}{2s} H^{\mu\nu\bar{\mu}\bar{\nu}} (n_L, p_L, \{v\}, \mu_R^2, \mu_F^2, \alpha_s) \\ L_{\mu\nu} (p_L, p, \mu_R^2, \mu_F^2, \alpha_s) L_{\bar{\mu}\bar{\nu}} (n_L, n, \mu_R^2, \mu_F^2, \alpha_s) [dp_L] [dn_L], \quad (3.1.2)$$

where  $Q^2$  is the hard scale of the process (typically the invariant mass of  $\mathcal{S}$ ),  $\{v\}$  denotes the set of variables which characterize the desired observable of the final state  $\mathcal{S}$ , and  $[dp_L]$  and  $[dn_L]$  are the integration measures over the momenta connecting the hard part to the two ladders. Furthermore, in Eq. (3.1.2),  $\frac{1}{2s}$  is a flux factor, and the phase space is included in the hard part. Partonic observable will be chosen by a particular constraint, such as

$$\delta(\{v\} - \{v(q_1, \dots, q_n)\}) \quad (3.1.3)$$

which in Eq. (3.1.2) is supposed to be included in the hard part.

However, for all the subsequent discussion, we are going to suppose that all the momenta entering in the constraint definition, Eq (3.1.3), are contained in the hard part, and no condition is going to link gluons emitted in the ladders with particles in the final hard state. This requirement is of fundamental importance for our derivation, which needs to be inclusive over all the ladders phase space. However, it is a great limitation for example in jet analysis, and first steps to a more exclusive high energy description are now under investigation (see for example Ref. [78, 145]); we are going to come back briefly on this topic in the last part of this chapter, Sec. 3.2.2.

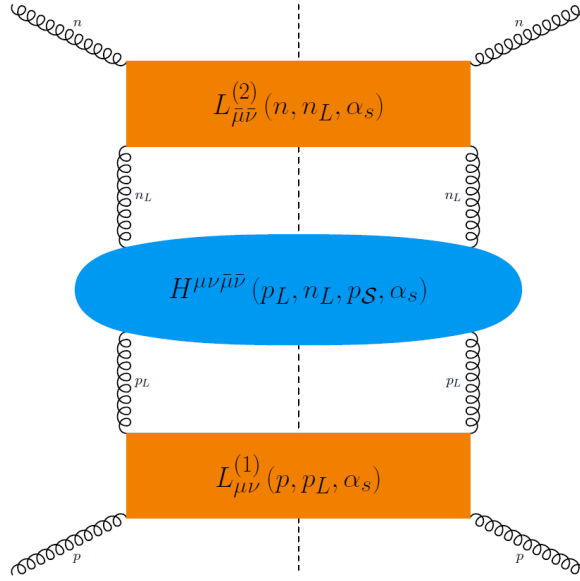


**Figure 3.1.** Hard-ladders decomposition of a general partonic observable in  $k_T$ -factorization

Under these assumptions, the partonic observable is factorized as written in Eq. (3.1.2), and as depicted in Fig. 3.1; however, factorization is up to now not complete since hard part and ladders are still connected by Lorentz index contraction. We are going to tackle this problem in a while.

First, we point out that both hard part and ladders are ultraviolet and collinear divergent; then renormalization and factorization will introduce a dependence on the renormalization and factorization scales  $\mu_R^2$  and  $\mu_F^2$ . In fact, because running coupling effects are logarithmic subleading at LL $x$ , we can ignore  $\mu_R^2$  dependence, which only goes through the coupling  $\alpha_s(\mu_R^2)$  at this level of accuracy. Moreover, to simplify our demonstration, we will assume the hard part to be two-particle irreducible rather than two-gluon irreducible. In this case, hard part is free of collinear singularities [79, 80] and it is thus independent from  $\mu_F^2$ . The extension of the following derivation to the case in which hard part is not collinear safe, such as Drell-Yan production, is not trivial [69, 73], but since it does not affect our argument, it will not be considered here.

To disentangle Lorentz structure of Eq. (3.1.2) we start to write the most general structure of the hard part and the ladders, fulfilling Lorentz invariance and QCD Ward identities:

$$\begin{aligned}
 H^{\mu\nu\bar{\mu}\bar{\nu}}(n_L, p_L, \alpha_s) &= \left( -g^{\mu\nu} + \frac{p_L^\mu p_L^\nu}{p_L^2} \right) \left( -g^{\bar{\mu}\bar{\nu}} + \frac{n_L^{\bar{\mu}} n_L^{\bar{\nu}}}{n_L^2} \right) H_{\perp, \perp} \\
 &+ H_{\perp, \parallel} \left[ n_L^2 \left( -g^{\mu\nu} + \frac{p_L^\mu p_L^\nu}{p_L^2} \right) \left( \frac{n_L^{\bar{\mu}}}{n_L^2} - \frac{p_L^{\bar{\mu}}}{(n_L \cdot p_L)} \right) \left( \frac{n_L^{\bar{\nu}}}{n_L^2} - \frac{p_L^{\bar{\nu}}}{(n_L \cdot p_L)} \right) \right. \\
 &\left. + p_L^2 \left( \frac{p_L^\mu}{p_L^2} - \frac{n_L^\mu}{(n_L \cdot p_L)} \right) \left( \frac{p_L^\nu}{p_L^2} - \frac{n_L^\nu}{(n_L \cdot p_L)} \right) \left( -g^{\bar{\mu}\bar{\nu}} + \frac{n_L^{\bar{\mu}} n_L^{\bar{\nu}}}{n_L^2} \right) \right]
 \end{aligned}$$

$$\begin{aligned}
& + p_L^2 n_L^2 \left( \frac{p_L^\mu}{p_L^2} - \frac{n_L^\mu}{(n_L \cdot p_L)} \right) \left( \frac{p_L^\nu}{p_L^2} - \frac{n_L^\nu}{(n_L \cdot p_L)} \right) \\
& \quad \left( \frac{n_L^{\bar{\mu}}}{n_L^2} - \frac{p_L^{\bar{\mu}}}{(n_L \cdot p_L)} \right) \left( \frac{n_L^{\bar{\nu}}}{n_L^2} - \frac{p_L^{\bar{\nu}}}{(n_L \cdot p_L)} \right) H_{\parallel, \parallel} \\
& + R^{\mu\nu\bar{\mu}\bar{\nu}} H_{\text{mixed}}
\end{aligned} \tag{3.1.4a}$$

$$\begin{aligned}
L^{\mu\nu}(p_L, p, \mu_F^2, \alpha_s) &= \frac{1}{p_L^2} \left( -g^{\mu\nu} + \frac{p_L^\mu p_L^\nu}{p_L^2} \right) L_{\perp}^{(1)} \\
& + \left( \frac{p_L^\mu}{p_L^2} - \frac{p^\mu}{(p \cdot p_L)} \right) \left( \frac{p_L^\nu}{p_L^2} - \frac{p^\nu}{(p \cdot p_L)} \right) L_{\parallel}^{(1)}
\end{aligned} \tag{3.1.4b}$$

$$\begin{aligned}
L^{\bar{\mu}\bar{\nu}}(n_L, n, \mu_F^2, \alpha_s) &= \frac{1}{n_L^2} \left( -g^{\bar{\mu}\bar{\nu}} + \frac{n_L^{\bar{\mu}} n_L^{\bar{\nu}}}{n_L^2} \right) L_{\perp}^{(2)} \\
& + \left( \frac{n_L^{\bar{\mu}}}{n_L^2} - \frac{n^{\bar{\mu}}}{(n \cdot n_L)} \right) \left( \frac{n_L^{\bar{\nu}}}{n_L^2} - \frac{n^{\bar{\nu}}}{(n \cdot n_L)} \right) L_{\parallel}^{(2)},
\end{aligned} \tag{3.1.4c}$$

in terms of dimensionless scalar form factors

$$H_{\text{mixed}} = H_{\text{mixed}} \left( \frac{Q^2}{(n_L \cdot p_L)}, \frac{-p_L^2}{Q^2}, \frac{-n_L^2}{Q^2}, \{v\}, \alpha_s \right) \tag{3.1.5a}$$

$$H_{\{\perp, \parallel\}, \{\perp, \parallel\}} = H_{\{\perp, \parallel\}, \{\perp, \parallel\}} \left( \frac{Q^2}{(n_L \cdot p_L)}, \frac{-p_L^2}{Q^2}, \frac{-n_L^2}{Q^2}, \{v\}, \alpha_s \right) \tag{3.1.5b}$$

$$L_{\{\perp, \parallel\}}^{(1)} = L_{\{\perp, \parallel\}}^{(1)} \left( \frac{-p_L^2}{(p \cdot p_L)}, \frac{\mu_F^2}{-p_L^2}, \alpha_s \right) \tag{3.1.5c}$$

$$L_{\{\perp, \parallel\}}^{(2)} = L_{\{\perp, \parallel\}}^{(2)} \left( \frac{-n_L^2}{(n \cdot n_L)}, \frac{\mu_F^2}{-n_L^2}, \alpha_s \right), \tag{3.1.5d}$$

where we indicate with the notation  $\{\perp, \parallel\}$  that either of the two values can be chosen. Tensor  $R^{\mu\nu\bar{\mu}\bar{\nu}}$  contains all terms which mix contributions coming from the two legs: despite its lengthy expression, it turns out to require only a single further scalar form factor. To come to Eq. (3.1.4) we impose symmetry of hard part and ladders under exchange of the indices  $\mu \leftrightarrow \nu$  and  $\bar{\mu} \leftrightarrow \bar{\nu}$ , plus following Ward identities, valid in axial gauge:

$$p_L^\mu L_{\mu\nu} = p_L^\nu L_{\mu\nu} = 0 \tag{3.1.6a}$$

$$n_L^{\bar{\mu}} L^{\bar{\mu}\bar{\nu}} = n_L^{\bar{\nu}} L^{\bar{\mu}\bar{\nu}} = 0 \tag{3.1.6b}$$

$$p_L^\mu H_{\mu\nu\bar{\mu}\bar{\nu}} = p_L^\nu H_{\mu\nu\bar{\mu}\bar{\nu}} = n_L^{\bar{\mu}} H_{\mu\nu\bar{\mu}\bar{\nu}} = n_L^{\bar{\nu}} H_{\mu\nu\bar{\mu}\bar{\nu}} = 0. \tag{3.1.6c}$$

It is important to point out that Eqs. (3.1.6) are fulfilled only in axial gauge where ghost contributions are absent. On the contrary, we are not requiring Ward identities for external gluons to be fulfilled by only ladders or hard part. In general, looking to decomposition Eqs. (3.1.4), contraction with momentum  $p^\mu, p^\nu$  or  $n^\mu, n^\nu$  gives zero only when the product of the hard and ladders part is considered. The same applies on any final state external gluons which are contained in the hard part.

In particular, to treat final state radiation and coloured particles in the hard part, we need more care to properly define a gauge invariant hard part. We are going to come back on this point, talking about gluons and quarks in the hard part in Sec. 3.2.2. For the rest

of the analysis of this section, we assume to work in the axial gauge, where Eqs. (3.1.4) are properly defined.

Eqs. (3.1.4) greatly simplify in the high energy limit. To perform this limit we recall definition given in Sec. 1.4.1 of Chap. 1

$$\hat{\tau} = \frac{Q^2}{s} \quad (3.1.7)$$

and we introduce a Sudakov parametrization for the two off-shell momenta  $p_L$  and  $n_L$ :

$$p_L = zp - \mathbf{k} - \frac{k_T^2}{s(1-z)}n = \left( \sqrt{\frac{s}{2}}z, -\frac{k_T^2}{\sqrt{2s}(1-z)}, -\mathbf{k}_T \right) \quad (3.1.8a)$$

$$n_L = \bar{z}n - \bar{\mathbf{k}} - \frac{\bar{k}_T^2}{s(1-\bar{z})}p = \left( -\frac{\bar{k}_T^2}{\sqrt{2s}(1-\bar{z})}, \sqrt{\frac{s}{2}}\bar{z}, -\bar{\mathbf{k}}_T \right) \quad (3.1.8b)$$

with  $\mathbf{k}$  and  $\bar{\mathbf{k}}$  purely transverse spacelike four-vectors,  $\mathbf{k}^2 = -k_T^2 < 0$  and  $\bar{\mathbf{k}}^2 = -\bar{k}_T^2 < 0$ , and  $s = 2(p \cdot n)$ . Using this parametrization, integration measures  $[dp_L]$  and  $[dn_L]$  are

$$[dp_L] = \frac{dz}{2(1-z)}d^2\mathbf{k}; \quad [dn_L] = \frac{d\bar{z}}{2(1-\bar{z})}d^2\bar{\mathbf{k}}. \quad (3.1.9)$$

The high energy limit is the limit in which  $\hat{\tau} \rightarrow 0$ : since we are interested in a LL $x$  resummation, we wish to determine the dominant power of  $\hat{\tau}$  contributing to  $\hat{\mathcal{O}}$ , with terms proportional to the highest power of  $\ln \hat{\tau}$  included to all orders in  $\alpha_s$ .

We then note that, since the integration over  $z$  and  $\bar{z}$  ranges from  $\hat{\tau}$  to 1, terms enhanced at small- $\hat{\tau}$  should come from the small  $z$  and  $\bar{z}$  region. Moreover, the moduli of the transverse momentum  $k_T^2$  and  $\bar{k}_T^2$  have to be of the order of the hard scale  $Q^2$ ; hence, at high energy they satisfy  $\frac{k_T^2}{s} \ll 1$  and  $\frac{\bar{k}_T^2}{s} \ll 1$ .

The high energy regime is then controlled by the following region

$$z \ll 1, \quad \frac{k_T^2}{s} \ll 1; \quad \bar{z} \ll 1, \quad \frac{\bar{k}_T^2}{s} \ll 1, \quad (3.1.10)$$

and subleading terms in  $z$ ,  $\bar{z}$ ,  $\frac{k_T^2}{s}$  or  $\frac{\bar{k}_T^2}{s}$  lead upon integration to power-suppressed  $\mathcal{O}(\hat{\tau})$  contributions.

We are now ready to simplify Eqs. (3.1.4). First, recalling one of the initial observation [79], the interference between emissions from different legs is power-suppressed in  $s$ . Then we conclude that  $H_{\text{mixed}}$  Eq. (3.1.4a) is subleading. Moreover, in the high energy limit, the dependence of the remaining scalar functions can be simplified:

$$H_{\{\perp, \parallel\}} \left( \frac{Q^2}{(n_L \cdot p_L)}, \frac{-p_L^2}{Q^2}, \frac{-n_L^2}{Q^2}, \alpha_s \right) = H_{\{\perp, \parallel\}} \left( \frac{\hat{\tau}}{z\bar{z}}, \frac{k_T^2}{Q^2}, \frac{\bar{k}_T^2}{Q^2}, \alpha_s \right) (1 + \mathcal{O}(z, \bar{z})) \quad (3.1.11)$$

$$L_{\{\perp, \parallel\}}^{(1)} \left( \frac{-p_L^2}{(p \cdot p_L)}, \frac{\mu_F^2}{-p_L^2}, \alpha_s \right) = L_{\{\perp, \parallel\}}^{(1)} \left( \frac{\mu_F^2}{k_T^2}, \alpha_s \right) (1 + \mathcal{O}(z)) \quad (3.1.12)$$

$$L_{\{\perp, \parallel\}}^{(2)} \left( \frac{-n_L^2}{(n \cdot n_L)}, \frac{\mu_F^2}{-n_L^2}, \alpha_s \right) = L_{\{\perp, \parallel\}}^{(2)} \left( \frac{\mu_F^2}{\bar{k}_T^2}, \alpha_s \right) (1 + \mathcal{O}(\bar{z})) \quad (3.1.13)$$

retaining terms up to  $\mathcal{O}(1)$  in  $z$  and  $\bar{z}$  expansion. Finally, power counting arguments [24, 29], lead to the conclusion that the transverse scalar function and the longitudinal ones share the same power behaviour in  $\hat{\tau} \rightarrow 0$ .

All these considerations lead to the following factorized expression for our partonic observable, permitting us to rewrite Eq. (3.1.2) as:

$$\begin{aligned} \hat{\mathcal{O}}\left(\hat{\tau}, \{v\}, \frac{\mu_F^2}{Q^2}, \alpha_s\right) &= \int \left[ \frac{\hat{\tau}}{2z\bar{z}} H_{\parallel, \parallel} \left( \frac{\hat{\tau}}{z\bar{z}}, \frac{k_T^2}{Q^2}, \frac{\bar{k}_T^2}{Q^2}, \{v\}, \alpha_s \right) \right] \\ &\quad \left[ 2\pi L_{\parallel}^{(1)} \left( \frac{\mu_F^2}{k_T^2}, \alpha_s \right) \right] \left[ 2\pi L_{\parallel}^{(2)} \left( \frac{\mu_F^2}{\bar{k}_T^2}, \alpha_s \right) \right] \\ &\quad \frac{dz d\bar{z} dk_T^2 d\bar{k}_T^2 d\theta d\bar{\theta}}{z \bar{z} k_T^2 \bar{k}_T^2 2\pi 2\pi} + \mathcal{O}(z, \bar{z}) \end{aligned} \quad (3.1.14)$$

with  $\theta$  and  $\bar{\theta}$  azimuthal angles of the transverse momenta  $\mathbf{k}$  and  $\bar{\mathbf{k}}$ , and the partonic observable considered  $\mu_{\bar{\text{r}}}^2$ -independent, since  $\alpha_s$  is fixed at LLx.

Some remarks about  $k_T$ -factorization of Eq. (3.1.14) are necessary; please note that the dependence on  $\theta$  and  $\bar{\theta}$  is entirely contained in the hard part. Moreover, in the high-energy limit longitudinal components of  $H$  can be selected via the following projectors [29]

$$\mathcal{P}^{\mu\nu} = \frac{k_T^\mu k_T^\nu}{k_T^2} \quad \mathcal{P}^{\bar{\mu}\bar{\nu}} = \frac{\bar{k}_T^{\bar{\mu}} \bar{k}_T^{\bar{\nu}}}{\bar{k}_T^2}. \quad (3.1.15)$$

We can thus rewrite the cross-section Eq. (3.1.14) in terms of a generalized coefficient function

$$\begin{aligned} C_{\hat{\mathcal{O}}}\left(\frac{\hat{\tau}}{z\bar{z}}, \frac{k_T^2}{Q^2}, \frac{\bar{k}_T^2}{Q^2}, \{v\}, \alpha_s\right) &\equiv \int \frac{d\theta d\bar{\theta}}{2\pi 2\pi} \frac{\hat{\tau}}{2z\bar{z}} H_{\parallel, \parallel} \left( \frac{\hat{\tau}}{z\bar{z}}, \frac{k_T^2}{Q^2}, \frac{\bar{k}_T^2}{Q^2}, \alpha_s \right) \\ &\quad \delta(v_i - v_i(p_L, n_L, q_1, \dots, q_n)) \\ &\equiv \int \frac{d\theta d\bar{\theta}}{2\pi 2\pi} \frac{\hat{\tau}}{2z\bar{z}} [\mathcal{P}^{\mu\nu} \mathcal{P}^{\bar{\mu}\bar{\nu}} H_{\mu\nu\bar{\mu}\bar{\nu}}] \\ &\quad \delta(v_i - v_i(p_L, n_L, q_1, \dots, q_n)), \end{aligned} \quad (3.1.16)$$

where we decide to explicit the delta constraint which defines the observable. As said before, this constraint has to depend only from momenta  $p_L, n_L$  and final external momenta contained in the hard part  $q_i$ .

Physically, it is rather simple to recognize in the coefficient function Eq. (3.1.16) the infra-red and collinear safe observable for the partonic process

$$g^*(q) + g^*(r) \rightarrow \mathcal{S}(q_1, \dots, q_n) \quad (3.1.17)$$

with two incoming off-shell gluons with momenta

$$q = zp + k \quad q^2 = -k_T^2 \quad (3.1.18)$$

$$r = \bar{z}n + \bar{k} \quad r^2 = -\bar{k}_T^2, \quad (3.1.19)$$

and where the projectors Eq. (3.1.15) are viewed as a polarization sum prescription

$$\frac{1}{2} \sum_s \mathbf{e}^\mu(k) \mathbf{e}^{\nu*}(k) = \frac{k_T^\mu k_T^\nu}{k_T^2} \quad (3.1.20)$$

for the off-shell gluon polarization vectors  $\epsilon$ . Due to the gauge invariance of the observable, this factorization, originally derived in axial gauge, still holds for any other gauge choice, as long as hard and ladders part are evaluated in the same gauge. In particular computation of ladders will be derived using Feynman gauge in the following sections.

The coefficient function Eq. (3.1.16) represents the process dependent part of the factorized partonic observable  $\hat{\mathcal{O}}$ . Ladders, instead, turn out to be universal and to contain all high energy singularities. Indeed, because hard part is at least 2GI, it have to be regular in the  $\hat{\tau} \rightarrow 0$  limit.

After this presentation of  $k_T$ -factorization, we are going to resum logarithms of  $\hat{\tau}$  contained in the ladders using two different approaches. First of all we will use in Sec. 3.1.1, the original derivation of Refs. [29, 68] where ladders are viewed as gluon Green functions, which solve at the same time collinear evolution (controlled by DGLAP equation), and high energy evolution (controlled by BFKL equation). Instead in Sec. 3.1.2, we will present the different analysis of Ref. [76, 77] where generalized ladder expansion is used to resum high energy contributions. The latter derivation is closer to standard collinear factorization and thus more suitable for observables different from inclusive cross section. Then we are going to use this second approach to derive the general theory of high energy resummation for transverse momentum distributions in Sec. 3.2.

### 3.1.1 LLx Resummation using BFKL equation

In this subsection we want to perform the high energy resummation of Eq. (3.1.14) using evolution equations solved by gluon green function when  $\hat{\tau} \rightarrow 0$ . However, all this formalism, for reasons that will become clear in a while, apply only on inclusive cross section and hence we are going to limit to this observable.

Recalling collinear factorization of total cross section Eq. (1.4.17) and using also  $k_T$ -factorization Eq. (3.1.14) for partonic cross section we are able to write:

$$\begin{aligned} \sigma \left( \tau, \frac{\mu_F^2}{Q^2}, \alpha_s \right) &= \int_{\tau}^1 dx_1 f_g(x_1, \mu_F^2) \int_{\frac{\tau}{x_1}}^1 dx_2 f_g(x_2, \mu_F^2) \\ &\int \frac{dz}{z} \frac{d\bar{z}}{z} \frac{dk_T^2}{k_T^2} \frac{d\bar{k}_T^2}{\bar{k}_T^2} C \left( \frac{\hat{\tau}}{z\bar{z}}, \frac{k_T^2}{Q^2}, \frac{\bar{k}_T^2}{Q^2}, \alpha_s \right) \mathfrak{L} \left( z, \frac{\mu_F^2}{k_T^2}, \alpha_s \right) \mathfrak{L} \left( \bar{z}, \frac{\mu_F^2}{\bar{k}_T^2}, \alpha_s \right) \end{aligned} \quad (3.1.21)$$

where we define

$$\mathfrak{L} \left( \frac{\mu_F^2}{k_T^2}, \alpha_s \right) = 2\pi L_{\parallel}^{(1)} \left( \frac{\mu_F^2}{k_T^2}, \alpha_s \right) \quad (3.1.22)$$

$$\mathfrak{L} \left( \frac{\mu_F^2}{\bar{k}_T^2}, \alpha_s \right) = 2\pi L_{\parallel}^{(2)} \left( \frac{\mu_F^2}{\bar{k}_T^2}, \alpha_s \right). \quad (3.1.23)$$

Up to now we limit ourselves to the gluon gluon contribution discarding into Eq. (3.1.21) the sum over the parton flavours. This was done since, at high energy, resummation of all the other channels can be derived from gluon-gluon one with a very straightforward calculation which will be discussed in detail in Sec. 3.2.1. Up to now, let us assume we have only one type of parton in our hadrons, and this type is the gluon.

Now, we can turn convolution with PDFs into product by taking usual Mellin transform w.r.t  $\tau$  obtaining:

$$\sigma \left( N, \frac{\mu_F^2}{Q^2}, \alpha_s \right) = \int \frac{dk_T^2}{k_T^2} \frac{d\bar{k}_T^2}{\bar{k}_T^2} C \left( N, \frac{k_T^2}{Q^2}, \frac{\bar{k}_T^2}{Q^2}, \alpha_s \right) f_g(N+1, \mu_F^2) \mathfrak{L} \left( \frac{\mu_F^2}{k_T^2}, \alpha_s \right) f_g(N+1, \mu_F^2) \mathfrak{L} \left( \frac{\mu_F^2}{\bar{k}_T^2}, \alpha_s \right). \quad (3.1.24)$$

Then we define the *unintegrated transverse gluon PDF* as

$$\overline{\mathcal{G}}(N, k_T^2, \mu_F^2) = f_g(N+1, \mu_F^2) \mathfrak{L} \left( \frac{\mu_F^2}{k_T^2}, \alpha_s \right) \quad (3.1.25)$$

thus rewriting Eq. (3.1.24) as

$$\sigma \left( N, \frac{\mu_F^2}{Q^2}, \alpha_s \right) = \int \frac{dk_T^2}{k_T^2} \frac{d\bar{k}_T^2}{\bar{k}_T^2} C \left( N, \frac{k_T^2}{Q^2}, \frac{\bar{k}_T^2}{Q^2}, \alpha_s \right) \overline{\mathcal{G}}(N, k_T^2, \mu_F^2) \overline{\mathcal{G}}(N, \bar{k}_T^2, \mu_F^2). \quad (3.1.26)$$

By inspecting Eq. (3.1.26), you can easily convince yourself that it has the form of a multiplicative convolution over the transverse momenta of the incoming gluons. Hence it would be possible to convert it into product by using some sort of Mellin transform. Defining

$$C(N, M_1, M_2, \alpha_s) = \int_0^\infty \frac{dk_T^2}{k_T^2} \left( \frac{k_T^2}{Q^2} \right)^{M_1} \int_0^\infty \frac{d\bar{k}_T^2}{\bar{k}_T^2} \left( \frac{\bar{k}_T^2}{Q^2} \right)^{M_2} \int_0^1 dz z^{N-1} C \left( z, \frac{k_T^2}{Q^2}, \frac{\bar{k}_T^2}{Q^2}, \alpha_s \right) \quad (3.1.27)$$

$$\mathcal{G}(N, M) = \int_0^\infty \frac{dk_T^2}{k_T^2} \left( \frac{\mu_F^2}{k_T^2} \right)^M \int_0^1 dz z^{N-1} \mathcal{G}(z, k_T^2, \mu_F^2), \quad (3.1.28)$$

we have

$$\sigma \left( \tau, \frac{\mu_F^2}{Q^2}, \alpha_s \right) = \int_{M_0-i\infty}^{M_0+i\infty} dM_1 \left( \frac{\mu_F^2}{Q^2} \right)^{-M_1} \int_{M_0-i\infty}^{M_0+i\infty} dM_2 \left( \frac{\mu_F^2}{Q^2} \right)^{-M_2} \int_{N_0-i\infty}^{N_0+i\infty} dN \tau^{-N} \Sigma(N, M_1, M_2, \alpha_s, \mu_F^2) \quad (3.1.29)$$

with

$$\Sigma(N, M_1, M_2, \alpha_s, \mu_F^2) = C(N, M_1, M_2, \alpha_s) \overline{\mathcal{G}}(N, M_1, \mu_F^2) \overline{\mathcal{G}}(N, M_2, \mu_F^2). \quad (3.1.30)$$

Resummation is now performed in  $\Sigma$ , Eq. (3.1.30), by exploiting evolution equations for  $\mathcal{G}(N, M, \mu_F^2)$ . The first equation we want to write controls the small- $\hat{\tau}$  behaviour of this object, which corresponds in  $N$  Mellin space to the small- $N$  region ( $N \rightarrow 0$ ). This equation is called *Balitsky-Fadin-Kuraev-Lipatov equation (BFKL)* [81] and takes the form

$$\frac{\partial \mathcal{G}(z, M, \mu_F^2)}{d\zeta} = \chi(\alpha_s, M) \mathcal{G}(z, M, \mu_F^2) \quad (3.1.31)$$

where  $\chi(\alpha_s, M)$  is called *BFKL kernel* [81] and  $\zeta = \ln \frac{1}{z}$ . First orders in  $\alpha_s$  of such kernel are known for a long time [81] and they are reported for example in Refs. [70, 84]. However, Eq. (3.1.31) alone is not enough to resum LL $x$  contributions contained into  $\Sigma$ . We need another constraint.

The second equation we want to use at the same time is the known DGLAP equation which controls the collinear limit, which corresponds in  $M$  Mellin space to the small- $M$  region ( $M \rightarrow 0$ ). By exploiting both the equation at the same time we end up with an important duality relation between DGLAP and BFKL evolution which is the basis of this approach to high energy resummation.

However,  $\mathcal{G}(N, k_T^2, \mu_F^2)$  does not have to fulfil DGLAP, since it is a transverse momentum dependent PDF (it contains also ladders emission). Fortunately, it is possible to relate this object with normal DGLAP PDF. First of all we define the *integrated PDF* as:

$$G(N, \mu_F^2) = \int_0^{Q^2} \frac{dk_T^2}{k_T^2} \mathcal{G}(N, k_T^2, \mu_F^2). \quad (3.1.32)$$

The Mellin transform w.r.t  $\mu_F^2$  of the integrated PDF

$$G(N, M) = \int_0^\infty \frac{d\mu_F^2}{\mu_F^2} \left( \frac{\mu_F^2}{Q^2} \right)^M G(N, \mu_F^2) \quad (3.1.33)$$

and the Mellin transform w.r.t.  $k_T^2$  of the unintegrated PDF, Eq. (3.1.28) are strictly connected. Indeed, we have

$$\begin{aligned} G(N, \mu_F^2) &= \int_{M_0-i\infty}^{M_0+i\infty} dM \left( \frac{\mu_F^2}{Q^2} \right)^{-M} G(N, M) \\ &= \int_0^{Q^2} \frac{dk_T^2}{k_T^2} \int_{M_0-i\infty}^{M_0+i\infty} dM \left( \frac{\mu_F^2}{k_T^2} \right)^{-M} \mathcal{G}(N, k_T^2, \mu_F^2) \\ &= \int_{M_0-i\infty}^{M_0+i\infty} dM \left( \frac{\mu_F^2}{Q^2} \right)^{-M} \frac{1}{M} \mathcal{G}(N, M, \mu_F^2) \end{aligned} \quad (3.1.34)$$

resulting in

$$G(N, M) = \frac{1}{M} \mathcal{G}(N, M, \mu_F^2). \quad (3.1.35)$$

In Eq. (3.1.34) in the last step we use the following result

$$\int_0^{Q^2} \frac{dk_T^2}{k_T^2} \left( \frac{\mu_F^2}{k_T^2} \right)^{-M} = \frac{1}{M} \left( \frac{\mu_F^2}{Q^2} \right)^{-M}. \quad (3.1.36)$$

Now it can be proved [79, 80, 82] that  $\mu_F^2$  evolution of the integrated PDF  $G(N, \mu_F^2)$  solves DGLAP equation with a small- $\hat{\tau}$  resummed anomalous dimension:

$$\frac{\partial G(N, t)}{\partial t} = \gamma(\alpha_s, N) G(N, t) \quad (3.1.37)$$

where  $t = \ln \frac{Q^2}{\mu_F^2}$  and we decide, with a slightly abuse of notation, to indicate with the same letter the function of  $\mu_F^2$  and  $t$ .

Anomalous dimension  $\gamma$  appearing in Eq. (3.1.37) resums at all orders in  $\alpha_s \ln^k z$  contributions (which corresponds in Mellin space to poles into  $N = 0$ ) contained into splitting functions. We will see that  $\gamma$  in Eq. (3.1.37) and  $\chi$  in Eq. (3.1.31) are related by an important duality relation. By exploiting this duality we are going to be able to write explicit expressions for both.

Now, we want to relate Eq. (3.1.37) with Eq. (3.1.31). We write both in double Mellin space for  $G(N, M)$  obtaining this set of algebraic equations:

$$NG(N, M) = \chi(\alpha_s, M)G(N, M) + \bar{G}_0(M) \quad (\text{BFKL equation}) \quad (3.1.38a)$$

$$MG(N, M) = \gamma(\alpha_s, N)G(N, M) + G_0(N) \quad (\text{DGLAP equation}) \quad (3.1.38b)$$

where  $G_0(N)$  and  $\bar{G}_0(M)$  are non-perturbative boundary conditions. Eqs. (3.1.38) can now be solved to find  $G(N, M)$

$$G(N, M) = \frac{1}{N - \chi(\alpha_s, M)} \bar{G}_0(M) = \frac{1}{M - \gamma(\alpha_s, N)} G_0(N). \quad (3.1.39)$$

Now we perform inverse  $M$  Mellin transform,

$$\begin{aligned} G(N, \mu_F^2) &= \int_{M_0 - i\infty}^{M_0 + i\infty} dM \left( \frac{\mu_F^2}{Q^2} \right)^{-M} \frac{1}{M - \gamma(\alpha_s, N)} G_0(N) \\ &= \left( \frac{\mu_F^2}{Q^2} \right)^{-\gamma(\alpha_s, N)} G_0(N) + \mathcal{O}\left( \frac{\mu_F^2}{Q^2} \right) \end{aligned} \quad (3.1.40)$$

thanks to the residue theorem. At leading twist, we can ignore power corrections in the factorization scale and we end up with the following pole condition

$$M = \gamma(\alpha_s, N). \quad (3.1.41)$$

However, relation Eq. (3.1.39) requires also that at leading twist

$$N = \chi(\alpha_s, M) \quad (3.1.42)$$

and then the consistency between Eq. (3.1.41) and Eq. (3.1.42) implies the following *duality relations*

$$N = \chi(\alpha_s, \gamma(\alpha_s, N)) \quad (3.1.43a)$$

$$M = \gamma(\alpha_s, \chi(\alpha_s, M)). \quad (3.1.43b)$$

These equalities can be exploited to derive the explicit resummed expressions both for  $\chi$  and for  $\gamma$  starting from known fixed order result for the other kernel.

As a last comment about the BFKL kernel and the DGLAP anomalous dimension, let us highlight the fact, which we have not time to discuss in detail, that duality Eqs. (3.1.43) is usually called naïve duality since it is performed at  $LLx$  accuracy discarding for example  $NLLx$  running coupling effects. Unfortunately some effects beyond  $LLx$  are in fact important to obtain stable expansion and resummation of high energy effects into PDFs evolution. For a complete treatment about this problem and the possible solutions adopted in literature we refer the interested reader to Refs. [70, 82–84].

Duality relations (3.1.43) permit us also to reach our desired result, high energy resummation of inclusive cross section. Indeed, coming back to Eq. (3.1.30), using Eq. (3.1.35) and taking inverse Mellin transform with respect to  $M_1$  and  $M_2$  we obtain:

$$\sigma\left(N, \frac{\mu_F^2}{Q^2}, \alpha_s\right) = \int_{M_0-i\infty}^{M_0+i\infty} dM_1 \left(\frac{\mu_F^2}{Q^2}\right)^{-M_1} \int_{M_0-i\infty}^{M_0+i\infty} dM_2 \left(\frac{\mu_F^2}{Q^2}\right)^{-M_2} M_1 M_2 C(N, M_1, M_2, \alpha_s) G(N, M_1) G(N, M_2). \quad (3.1.44)$$

Now using pole condition at leading twist, Eq. (3.1.41) we come to:

$$\sigma\left(N, \frac{\mu_F^2}{Q^2}, \alpha_s\right) = \left(\frac{\mu_F^2}{Q^2}\right)^{-2\gamma(\alpha_s, N)} \gamma(\alpha_s, N)^2 C(N, \gamma(\alpha_s, N), \gamma(\alpha_s, N), \alpha_s) G_0(N) G_0(N). \quad (3.1.45)$$

Last step is to identify  $G_0(N)$ . Here we use explicitly that this observable is an inclusive cross section. Indeed, coefficient function Eq. (3.1.16) for this observable always reduces to partonic LO cross section at first not trivial order in  $\alpha_s$ ; this is not true as we will see for other observables such as transverse momentum distribution.

At LO we thus have (considering  $\mu_F^2 = Q^2$  for simplicity):

$$\sigma_{\text{LO}}(N, \alpha_s) = \hat{\sigma}_{\text{LO}}(N, \alpha_s) G_0(N) G_0(N) \quad (3.1.46)$$

which implies that  $M = 0$  boundary condition have to be equal at leading twist at LL $x$  with normal PDF in  $N$  space:

$$G_0(N) = f_g(N+1, Q^2). \quad (3.1.47)$$

We have almost concluded our analysis about LL $x$  resummation using BFKL evolution. We need to make two final comments:

- all the construction works in a particular subtraction scheme called  $Q_0$  scheme. If we want to use a different scheme such as  $\overline{\text{MS}}$  we need to introduce in Eq. (3.1.45) an extra scheme term called in literature  $R(\alpha_s, \gamma(\alpha_s, N))$  [85]. We include its explicit expression, together with some information about its computation, in Sec. C.2 of Appendix C.
- we work in a framework where only the gluon exists. If also quarks are included two modifications of the present derivation occur. First the anomalous dimension  $\gamma(\alpha_s, N)$  coupled with the BFKL kernel turns out to be  $\gamma_+(\alpha_s, N)$  where  $\gamma_+(\alpha_s, N)$  is the largest eigenvalue of the anomalous dimension matrix in the singlet sector, Eq. (A.3.7), since this is the only component which contains small- $N$  singularities<sup>1</sup>. Second we need to add other channel contributions. We are going to tackle this other problem in Sec. 3.2.1.

In conclusion, this derivation permits to resum inclusive cross sections but since boundary condition can be easily derived only in this case, it is not very suitable to any extension

<sup>1</sup>For a complete definition of the singlet sector please refer to Appendix A

to more exclusive observables. We thus move to present an analogue derivation of high energy resummation based on generalized ladder expansion. The generalized ladder expansion is strictly connected with DGLAP dynamics permitting us to control in a more complete way kinematics in the context of standard collinear factorization. For this reason it is rather simple to move from inclusive observable to some differential distributions.

As a matter of notation we introduce an important quantity that we are going to use through all the rest of the chapter, the so-called *impact factor*, defined as

$$h\left(N, M_1, M_2, \frac{\mu_F^2}{Q^2}, \alpha_s\right) = M_1 M_2 R(\alpha_s, M_1) R(\alpha_s, M_2) C(N, M_1, M_2, \alpha_s) \left(\frac{\mu_F^2}{Q^2}\right)^{-M_1 - M_2}. \quad (3.1.48)$$

Owing to this definition, the partonic LL $x$  resummed cross section turns out to be

$$\hat{\sigma}\left(0, \frac{\mu_F^2}{Q^2}, \alpha_s\right) = h\left(0, \gamma(\alpha_s, N), \gamma(\alpha_s, N), \frac{\mu_F^2}{Q^2}, \alpha_s\right) \quad (3.1.49)$$

where we set to 0 the  $N$  dependence of the impact factor since subleading contributions do not enter at LL $x$ .

This final result will be useful in the next section to relate the two approaches to high energy resummation. In many cases we will ignore  $\mu_F^2$  dependence by setting  $\mu_F^2 = Q^2$  since residual dependence on the ratio  $\frac{\mu_F^2}{Q^2}$  is in fact subleading at LL $x$ .

### 3.1.2 LL $x$ Resummation using Generalized Ladder Expansion

The BFKL technique to derive high energy resummation, even if really powerful to derive small- $\hat{\tau}$  evolution of PDFs at all the order in  $\alpha_s$ , it is not particularly well-suited to be extended to differential observable, since it does not follow standard collinear factorization.

Hence, we are going to present an alternative derivation of high energy resummation based on the generalized ladder expansion of Sec. 1.2.2. Our starting point is again  $k_T$ -factorization for our differential observable, Eq. (3.1.14). Limiting ourselves to the case in which the hard part is 2PI, collinear singularities are only contained in the ladder parts. The generalized Ladder expansion permits us to regularize and factorize them in an iterative way. Such a procedure leads also to the LL $x$  small- $\hat{\tau}$  resummation, as explained in Ref. [76].

We will present the derivation for a general partonic observable, even if we will highlight the step in which we are forced to further specify the type of observable we are studying, in order to proceed. In the generalized ladder expansion, ladders  $L_{\parallel}^{(1)}$  and  $L_{\parallel}^{(2)}$  are computed as a multiple insertion of a 2GI kernel  $K(p_i, p_{i-1}, \mu_F^2, \alpha_s)$  or  $K(n_i, n_{i-1}, \mu_F^2, \alpha_s)$  with  $i = 1, 2, \dots, n$ , connected by a pair of  $t$ -channel gluons (see Fig. 3.2). Collinear factorization requires transverse momenta of the gluons to be ordered,  $k_{T_1}^2 < k_{T_2}^2 < \dots < k_{T_n}^2 = k_T^2$  (and  $\bar{k}_{T_1}^2 < \bar{k}_{T_2}^2 < \dots < \bar{k}_{T_m}^2 = \bar{k}_T^2$ ) and the high energy resummation is only achieved if kernels  $K$  are computed at LL $x$  to all orders in  $\alpha_s$ .

We will present now the derivation in detail. First of all, we write a regularized version of the  $k_T$ -factorization Eq. (3.1.14) for the partonic observable, using also definition of the coefficient function  $C_{\hat{O}}$ , Eq. (3.1.16):

$$\begin{aligned} \hat{O} \left( \hat{\tau}, \{v\}, \frac{\mu_F^2}{Q^2}, \alpha_s; \epsilon \right) &= (\mu_F)^{2\epsilon} \int C_{\hat{O}} \left( \frac{\hat{\tau}}{z\bar{z}}, \frac{k_T^2}{Q^2}, \frac{\bar{k}_T^2}{Q^2}, \{v\}, \alpha_s; \epsilon \right) \\ &\quad \left[ 2\pi L_{\parallel}^{(1)} \left( z, \left( \frac{\mu_F^2}{k_T^2} \right)^\epsilon, \alpha_s; \epsilon \right) \right] \left[ 2\pi L_{\parallel}^{(2)} \left( \bar{z}, \left( \frac{\mu_F^2}{\bar{k}_T^2} \right)^\epsilon, \alpha_s; \epsilon \right) \right] \\ &\quad \frac{dz d\bar{z}}{z \bar{z}} \frac{dk_T^2}{(k_T^2)^{1+\epsilon}} \frac{d\bar{k}_T^2}{(\bar{k}_T^2)^{1+\epsilon}}, \end{aligned} \quad (3.1.50)$$

where we are using dimensional regularization in  $d = 4 - 2\epsilon$  dimension to regularize IR and UV divergences, and the dependence on  $z$  and  $\bar{z}$  in the ladders is  $\mathcal{O}(\epsilon)$  [76].

We factorize, as usual, convolutions using Mellin transformation (see Eq. (1.4.13))

$$\begin{aligned} \hat{O} \left( N, \{v\}, \frac{\mu_F^2}{Q^2}, \alpha_s; \epsilon \right) &= \int_0^\infty \frac{d\xi}{\xi^{1+\epsilon}} \int_0^\infty \frac{d\bar{\xi}}{\bar{\xi}^{1+\epsilon}} C_{\hat{O}} \left( N, \xi, \bar{\xi}, \{v\}, \alpha_s; \epsilon \right) \\ &\quad \left[ 2\pi L_{\parallel}^{(1)} \left( N, \left( \frac{\mu_F^2}{Q^2\xi} \right)^\epsilon, \alpha_s; \epsilon \right) \right] \left[ 2\pi L_{\parallel}^{(2)} \left( N, \left( \frac{\mu_F^2}{Q^2\bar{\xi}} \right)^\epsilon, \alpha_s; \epsilon \right) \right], \end{aligned} \quad (3.1.51)$$

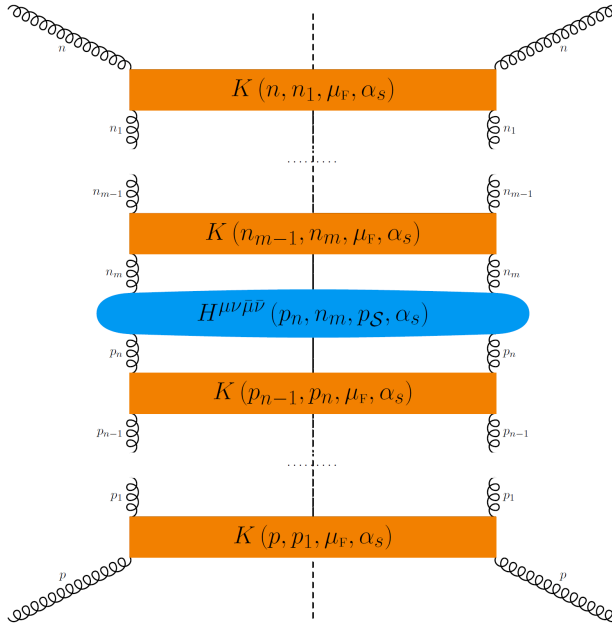


**Figure 3.2.** Schematically computation of ladders as multiple insertion of the Kernel  $K$

with the following definition for the dimensionless variables

$$\xi = \frac{k_{\text{T}}^2}{Q^2} \qquad \bar{\xi} = \frac{\bar{k}_{\text{T}}^2}{Q^2}. \quad (3.1.52)$$

Please keep in mind that the dependence from  $Q^2$  in the ladders is in fact fictitious, as  $\frac{\mu_{\text{F}}^2}{Q^2 \xi} = \frac{\mu_{\text{F}}^2}{k_{\text{T}}^2}$ .

The Kernel  $K$  in this formalism performs the same task of collinear kernel in Sec. 1.2.2, Chap. 1; it thus subtracts collinear singularities from the amplitude. They in fact coincide with the only difference that in this case, to achieve high energy resummation, we need to resum  $K$  at LL $x$  to all orders in  $\alpha_s$ . We call this resummed regularized kernel in  $N$  space, the anomalous dimension  $\gamma$  of this formalism:

$$K \left( N, \left( \frac{\mu_{\text{F}}^2}{Q^2 \xi} \right)^\epsilon, \alpha_s; \epsilon \right) = \gamma \left( N, \left( \frac{\mu_{\text{F}}^2}{Q^2 \xi} \right)^\epsilon, \alpha_s; \epsilon \right). \quad (3.1.53)$$

Inserting ladder  $L^{(1,2)}$  expansions at LL $x$  in Eq. (3.1.51), we obtain:

$$\begin{aligned} \hat{O}^{n,m} \left( N, \{v\}, \frac{\mu_{\text{F}}^2}{Q^2}, \alpha_s; \epsilon \right) &= \int_0^\infty \left[ \gamma \left( N, \left( \frac{\mu_{\text{F}}^2}{Q^2 \xi_n} \right)^\epsilon, \alpha_s; \epsilon \right) \right] \frac{d\xi_n}{\xi_n^{1+\epsilon}} \times \\ &\times \int_0^\infty \left[ \gamma \left( N, \left( \frac{\mu_{\text{F}}^2}{Q^2 \bar{\xi}_m} \right)^\epsilon, \alpha_s; \epsilon \right) \right] \frac{d\bar{\xi}_m}{\bar{\xi}_m^{1+\epsilon}} C_{\hat{O}} \left( N, \xi, \bar{\xi}, \{v\}, \alpha_s; \epsilon \right) \times \\ &\times \int_0^{\xi_n} \left[ \gamma \left( N, \left( \frac{\mu_{\text{F}}^2}{Q^2 \xi_{n-1}} \right)^\epsilon, \alpha_s; \epsilon \right) \right] \frac{d\xi_{n-1}}{\xi_{n-1}^{1+\epsilon}} \times \cdots \times \int_0^{\xi_2} \left[ \gamma \left( N, \left( \frac{\mu_{\text{F}}^2}{Q^2 \xi_1} \right)^\epsilon, \alpha_s; \epsilon \right) \right] \frac{d\xi_1}{\xi_1^{1+\epsilon}} \times \\ &\times \int_0^{\bar{\xi}_m} \left[ \gamma \left( N, \left( \frac{\mu_{\text{F}}^2}{Q^2 \bar{\xi}_{m-1}} \right)^\epsilon, \alpha_s; \epsilon \right) \right] \frac{d\bar{\xi}_{m-1}}{\bar{\xi}_{m-1}^{1+\epsilon}} \times \cdots \times \int_0^{\bar{\xi}_2} \left[ \gamma \left( N, \left( \frac{\mu_{\text{F}}^2}{Q^2 \bar{\xi}_1} \right)^\epsilon, \alpha_s; \epsilon \right) \right] \frac{d\bar{\xi}_1}{\bar{\xi}_1^{1+\epsilon}}. \end{aligned} \quad (3.1.54)$$

We cannot proceed further without specifying better the nature of our observable. If the particular fixed value of the set  $\{v\}$  does not depend on the number of gluon emissions occurring in the ladders (hence in Eq. (3.1.54) on the values of  $n$  and  $m$ ), the iterative subtraction can be performed without problem since any subsequent emission can be treated as independent from the others. Inclusive cross section and transverse momentum distribution belong to this category. However, if this is not the case, as for rapidity distribution, we need to factorize delta constraint by using proper integral transform. An example of this second type of observable is rapidity distribution of Ref. [76] or double differential rapidity and transverse momentum distribution which will be the last application of this chapter, Sec. 3.3.

For the rest of this preliminary derivation, since our main application is high energy resummation of transverse momentum distribution we limit ourselves to the first class of observables. Under these assumptions, the factorization of collinear singularities is performed by requiring Eq. (3.1.54) to be finite after each  $\xi_i$  or  $\bar{\xi}_j$  integration. This leaves a single  $n + m$ -th order  $\epsilon$  pole in the observable that can be subtracted using standard  $\overline{\text{MS}}$  prescription (as explained in Sec. 1.2.2 in standard collinear factorization). After this

iterative subtraction of the first  $n - 1$ ,  $m - 1$  singularities, we get [23, 76, 77]:

$$\begin{aligned}
\hat{O}^{n,m} \left( N, \{v\}, \frac{\mu_F^2}{Q^2}, \alpha_s; \epsilon \right) &= \left[ \gamma \left( N, \left( \frac{\mu_F^2}{Q^2} \right)^\epsilon, \alpha_s; \epsilon \right) \right]^2 \\
&\times \int_0^\infty \frac{d\xi_n}{\xi_n^{1+\epsilon}} \int_0^\infty \frac{d\bar{\xi}_m}{\bar{\xi}_m^{1+\epsilon}} C_{\hat{O}} \left( N, \xi_n, \bar{\xi}_m, \{v\}, \alpha_s; \epsilon \right) \times \\
&\times \frac{1}{(n-1)!} \frac{1}{\epsilon^{n-1}} \left[ \sum_j \frac{\tilde{\gamma}_j(N, \alpha_s; 0)}{j} \left( 1 - \left( \frac{\mu_F^2}{Q^2 \xi_n} \right)^{j\epsilon} \frac{\tilde{\gamma}_i(N, \alpha_s; \epsilon)}{\tilde{\gamma}_i(N, \alpha_s; 0)} \right) \right]^{n-1} \times \\
&\times \frac{1}{(m-1)!} \frac{1}{\epsilon^{m-1}} \left[ \sum_l \frac{\tilde{\gamma}_l(N, \alpha_s; 0)}{l} \left( 1 - \left( \frac{\mu_F^2}{Q^2 \bar{\xi}_m} \right)^{l\epsilon} \frac{\tilde{\gamma}_i(N, \alpha_s; \epsilon)}{\tilde{\gamma}_i(N, \alpha_s; 0)} \right) \right]^{m-1}. \quad (3.1.55)
\end{aligned}$$

where we have introduced the expansion

$$\gamma \left( N, \left( \frac{\mu_F^2}{Q^2 \xi} \right)^\epsilon, \alpha_s; \epsilon \right) = \sum_{j=0}^{\infty} \tilde{\gamma}_j(N, \alpha_s; \epsilon) \left( \frac{\mu_F^2}{Q^2 \xi} \right)^{j\epsilon}. \quad (3.1.56)$$

Summing over all the possible  $n, m$  emissions, collinear singularities exponentiate:

$$\begin{aligned}
\hat{O}_{\text{res}} &= \sum_{n,m=0}^{\infty} \sigma^{n,m} = \gamma \left( N, \left( \frac{\mu_F^2}{Q^2} \right)^\epsilon, \alpha_s; \epsilon \right)^2 \int_0^\infty \frac{d\xi}{\xi^{1+\epsilon}} \int_0^\infty \frac{d\bar{\xi}}{\bar{\xi}^{1+\epsilon}} C_{\hat{O}} \left( N, \xi, \bar{\xi}, \{v\}, \alpha_s; \epsilon \right) \times \\
&\times \exp \left[ \frac{1}{\epsilon} \sum_j \frac{\tilde{\gamma}_j(N, \alpha_s; 0)}{j} \left( 1 - \left( \frac{\mu_F^2}{Q^2 \xi} \right)^{j\epsilon} \frac{\tilde{\gamma}_j(N, \alpha_s; \epsilon)}{\tilde{\gamma}_j(N, \alpha_s; 0)} \right) \right] \times \\
&\times \exp \left[ \frac{1}{\epsilon} \sum_l \frac{\tilde{\gamma}_l(N, \alpha_s; 0)}{l} \left( 1 - \left( \frac{\mu_F^2}{Q^2 \bar{\xi}} \right)^{l\epsilon} \frac{\tilde{\gamma}_l(N, \alpha_s; \epsilon)}{\tilde{\gamma}_l(N, \alpha_s; 0)} \right) \right]. \quad (3.1.57)
\end{aligned}$$

The limit  $\epsilon \rightarrow 0$  can then be taken after performing the expansion

$$\tilde{\gamma}_i \equiv \tilde{\gamma}_i(N, \alpha_s) + \epsilon \dot{\tilde{\gamma}}_i(N, \alpha_s) + \epsilon^2 \ddot{\tilde{\gamma}}_i(N, \alpha_s) + \dots, \quad (3.1.58)$$

reaching the following final expression for  $\hat{O}$

$$\begin{aligned}
\hat{O}_{\text{res}} \left( N, \{v\}, \frac{\mu_F^2}{Q^2}, \alpha_s \right) &= \gamma(N, \alpha_s)^2 \mathcal{R}(N, \alpha_s)^2 \\
&\int_0^\infty d\xi \xi^{\gamma(N, \alpha_s) - 1} \int_0^\infty d\bar{\xi} \bar{\xi}^{\gamma(N, \alpha_s) - 1} C_{\hat{O}} \left( N, \xi, \bar{\xi}, \{v\}, \alpha_s \right) \\
&\times \exp \left[ 2\gamma(N, \alpha_s) \ln \frac{Q^2}{\mu_F^2} \right] \quad (3.1.59)
\end{aligned}$$

where we define [76]

$$\mathcal{R}(N, \alpha_s) \equiv \exp \left[ - \sum_i \frac{\dot{\tilde{\gamma}}_i(N, \alpha_s)}{i} \right]. \quad (3.1.60)$$

Equation (3.1.59) is the resummed form at LL $x$  in the  $\overline{\text{MS}}$  scheme of a generic observable whose constraint leaves as independent multiple ladder emissions. Examples of such observable are inclusive cross section and transverse momentum distribution, but also leading jet  $p_T$  or inclusive jet observable. Moreover, as said in Sec. 3.1.1,  $N$  dependence into  $C_{\hat{\mathcal{O}}}$  is subleading at LL $x$  and then we are free to set  $N = 0$  in the hard part without loosing our accuracy.

The factor  $\mathcal{R}$  of Eq. (3.1.59) depends on the choice of factorization scheme [29, 76] but it is not the only source of dependence on  $\overline{\text{MS}}$  subtraction. Further scheme changes depend on the non-commutativity of exponentiation with iterative collinear subtraction [85]; fortunately it can be proved [76, 77, 85] that even this source factorizes in a common prefactor  $\mathcal{N}(N, \alpha_s)$ . Thus, defining

$$R(N, \alpha_s) = \mathcal{R}(N, \alpha_s) \mathcal{N}(N, \alpha_s), \quad (3.1.61)$$

we obtain our final high energy resummed observable in a generic subtraction scheme as

$$\hat{\mathcal{O}}_{\text{res}} \left( N, \{v\}, \frac{\mu_F^2}{Q^2}, \alpha_s \right) = \left( \frac{\mu_F^2}{Q^2} \right)^{-2\gamma(\alpha_s, N)} \gamma(\alpha_s, N)^2 R(\alpha_s, N)^2 \int_0^\infty d\xi \xi^{\gamma(\alpha_s, N)-1} \int_0^\infty d\bar{\xi} \bar{\xi}^{\gamma(\alpha_s, N)-1} C_{\hat{\mathcal{O}}}(0, \xi, \bar{\xi}, \{v\}, \alpha_s). \quad (3.1.62)$$

Explicit expression for the factor  $R$  is contained in Appendix C, Eq. (C.2.1).

As a last comment we need to show a practical way to compute the  $\gamma$  anomalous dimension of this formalism. Then we use the fact that for inclusive cross section we can match derivation of this section, with analogue proof presented in the previous section, Sec. 3.1.1. By comparing Eq. (3.1.62) with Eq. (3.1.45), we come to

$$\gamma(\alpha_s, N) = \gamma_+(\alpha_s, N). \quad (3.1.63)$$

The anomalous dimension in the generalized ladder expansion framework has to coincide with the DGLAP anomalous dimension, inverse of the BFKL kernel, as stated from duality relations (3.1.43). We remember the reader that a practical implementation of  $\gamma_+$  is contained in Refs. [70, 84], together with some information about its derivation.

Eq. (3.1.63) closes the circle, showing immediately the equivalence between the two approaches. However, as said before, the GLE derivation is more suitable to extension to differential distributions and it will be the starting point for any application we are going to present in the next sections. Before moving on, however, we want to define also in this formalism, a general  $\hat{\mathcal{O}}$ -*impact factor* as

$$h_{\hat{\mathcal{O}}} \left( N, M_1, M_2, \{v\}, \frac{\mu_F^2}{Q^2}, \alpha_s \right) = M_1 M_2 R(\alpha_s, M_1) R(\alpha_s, M_2) C_{\mathcal{O}}(N, M_1, M_2, \{v\}, \alpha_s) \left( \frac{\mu_F^2}{Q^2} \right)^{-M_1 - M_2}, \quad (3.1.64)$$

according to which the resummed partonic observable can be derived as

$$\hat{\mathcal{O}}_{\text{res}} \left( N, \{v\}, \frac{\mu_F^2}{Q^2}, \alpha_s \right) = h_{\hat{\mathcal{O}}} \left( 0, \gamma(\alpha_s, N), \gamma(\alpha_s, N), \{v\}, \frac{\mu_F^2}{Q^2}, \alpha_s \right). \quad (3.1.65)$$

We end this preliminary discussion about high energy resummation of a general observable. In Sec. 3.1.1, we have shown original BFKL duality approach of Ref. [29, 69, 71–75] for the resummation of inclusive cross section, then we move on generalized ladder derivation of Ref. [76, 77] for a general observable which, however, continues to treat multiple ladder emissions as independent.

In the next section we are going to prove that transverse momentum distribution belongs to this subgroup and we are going to apply general formalism just derived to this particular example. Then we are going to cover some subtleties we leave apart in this preliminary derivation: initial quarks contributions in Sec. 3.2.1 and coloured final state in Sec. 3.2.2.

## 3.2 Transverse Momentum Distribution at High Energy

The main observable studied in this thesis is the transverse momentum distribution. Hence, in this section we want to apply the whole machinery presented in Sec. 3.1.2 to this observable to resum at leading log small- $\hat{\tau}$  contributions at all orders in  $\alpha_s$ .

As we have described, the high energy resummation for a general partonic observable is performed in Mellin space, with the variable  $N$  conjugate to the variable  $\hat{\tau}$  and the small- $\hat{\tau}$  region mapped into poles in  $N = 0$ . However, we have learned in Chap. 1, Sec. 1.4.1 that PDF convolution for this observable is not converted into product by Mellin transform w.r.t.  $\tau$ , but w.r.t.  $\tau'$ , Eq. (1.4.9). This is a very unlucky situation, since we compute resummation in  $\tau$  conjugate Mellin space, then we need to perform the inverse, and finally to evaluate convolutions with PDFs in momentum space to reach correct hadronic results.

Fortunately, we can prove by looking to definition of  $x$ , Eq. (1.4.10), and  $\hat{\tau}$ , Eq. (1.4.7), that the difference between the two Mellin definitions is beyond LL $x$  and then we can considered them as equivalent at this level of accuracy

$$x = \tau + \mathcal{O}(\tau^2). \quad (3.2.1)$$

Therefore, we are going to compute high energy resummation in Mellin space with usual technique derived in previous section and then we perform the inversion according to

$$\frac{d\sigma}{d\xi_p}(\tau', \xi_p, \alpha_s(\mu_R^2), \mu_F^2) = \sum_{ij} \int_{N_0-i\infty}^{N_0+i\infty} \frac{dN}{2\pi i} (\tau')^{-N} \mathcal{L}_{ij}(N, \mu_F^2) \frac{d\hat{\sigma}_{ij}^{\text{res}}}{d\xi_p}(N, \xi_p, \alpha_s(\mu_R^2), \mu_F^2) \quad (3.2.2)$$

to obtain the hadronic transverse momentum distribution (for the definition of  $\xi_p$  see for example Eq. (1.4.7)).

Moreover, in order to apply derivation of Sec. 3.1.2, we need to prove that the delta constraint contained in our coefficient function definition, Eq. (3.1.16) does not depend on the number of emission in the ladders.

We decide to study the kinematics for this observable. The generic emission diagram with  $n$  insertions in one leg and  $m$  insertions in the other one is depicted in Fig. 3.3. A Sudakov decomposition for the various momenta could be

$$p_1 = z_1 p - \mathbf{k}_1 \quad (3.2.3a)$$

$$q_1 = (1 - z_1)p + \mathbf{k}_1 \quad (3.2.3b)$$

$$p_2 = z_2 z_1 p - \mathbf{k}_2 \quad (3.2.3c)$$

$$q_2 = (1 - z_2) z_1 p + \mathbf{k}_2 - \mathbf{k}_1 \quad (3.2.3d)$$

$$\dots\dots\dots \quad (3.2.3e)$$

$$p_L = z_1 \dots z_n p - \mathbf{k} \quad (3.2.3f)$$

$$q_L = (1 - z_n) z_1 \dots z_{n-1} p + \mathbf{k} - \mathbf{k}_{n-1} \quad (3.2.3g)$$

$$n_1 = \bar{z}_1 p - \bar{\mathbf{k}}_1 \quad (3.2.3h)$$

$$r_1 = (1 - \bar{z}_1) p + \bar{\mathbf{k}}_1 \quad (3.2.3i)$$

$$n_2 = \bar{z}_2 \bar{z}_1 p - \bar{\mathbf{k}}_2 \quad (3.2.3j)$$

$$r_2 = (1 - \bar{z}_2) \bar{z}_1 p + \bar{\mathbf{k}}_2 - \bar{\mathbf{k}}_1 \quad (3.2.3k)$$

$$\dots\dots\dots \quad (3.2.3l)$$

$$n_L = \bar{z}_1 \dots \bar{z}_m n - \bar{\mathbf{k}} \quad (3.2.3m)$$

$$r_L = (1 - \bar{z}_m) \bar{z}_1 \dots \bar{z}_{m-1} n + \bar{\mathbf{k}} - \bar{\mathbf{k}}_{m-1}. \quad (3.2.3n)$$

The crucial observation here is that the transverse momenta  $\mathbf{k}_i$  and  $\bar{\mathbf{k}}_j$  are independent, with the only ordering constraint  $k_{T,1}^2 < k_{T,2}^2 < \dots < k_T^2$  and  $\bar{k}_{T,1}^2 < \bar{k}_{T,2}^2 < \dots < \bar{k}_T^2$ . They can therefore be chosen as in Eq. (3.2.3), and the fixed value of  $p_T^2$  only constrains the transverse momentum of the last emission, i.e., the values of  $q_L$  and  $r_L$ .

We reach our desired conclusion. Transverse momentum constraint does not depend on the particular value of  $n$  and  $m$  ladder emissions but only on the off-shellness of the gluons entering in the hard part. Hence the general derivation of Sec. 3.1.2 can be applied.

High energy resummed partonic transverse momentum distribution is then obtained from a proper  $p_T$ -*impact factor*, defined as in Eq. (3.1.64). In this case we write,

$$h_{p_T}(N, M_1, M_2, \xi_p, \alpha_s) = M_1 M_2 R(\alpha_s, M_1) R(\alpha_s, M_2) C_{p_T}(N, M_1, M_2, \xi_p, \alpha_s), \quad (3.2.4)$$

where we have set in Eq. (3.1.64)  $\mu_F^2 = Q^2$ . Coefficient function  $C_{p_T}(N, \xi, \bar{\xi}, \xi_p, \alpha_s)$  is defined as

$$\begin{aligned} C_{p_T}\left(\frac{x}{z\bar{z}}, \xi, \bar{\xi}, \xi_p, \alpha_s\right) &= \int \frac{d\theta}{2\pi} \frac{d\bar{\theta}}{2\pi} \frac{x}{2z\bar{z}} H_{\parallel,\parallel}\left(\frac{x}{z\bar{z}}, \xi, \bar{\xi}, \Omega_S, \alpha_s\right) \delta\left(\xi_p - \xi - \bar{\xi} - 2\sqrt{\xi\bar{\xi}} \cos\theta\right) \\ &= \int \frac{d\theta}{2\pi} \frac{d\bar{\theta}}{2\pi} \frac{x}{2z\bar{z}} [\mathcal{P}^{\mu\nu} \mathcal{P}^{\bar{\mu}\bar{\nu}} H_{\mu\nu\bar{\mu}\bar{\nu}}] \delta\left(\xi_p - \xi - \bar{\xi} - 2\sqrt{\xi\bar{\xi}} \cos\theta\right) \end{aligned} \quad (3.2.5)$$

and physically represents the transverse momentum distribution for the LO off-shell process

$$g^*(k) + g^*(\bar{k}) \rightarrow \mathcal{S}(p) \quad (3.2.6)$$

with the following definitions

$$\xi = \frac{k_T^2}{Q^2} \quad \bar{\xi} = \frac{\bar{k}_T^2}{Q^2} \quad \xi_p = \frac{p_T^2}{Q^2}. \quad (3.2.7)$$

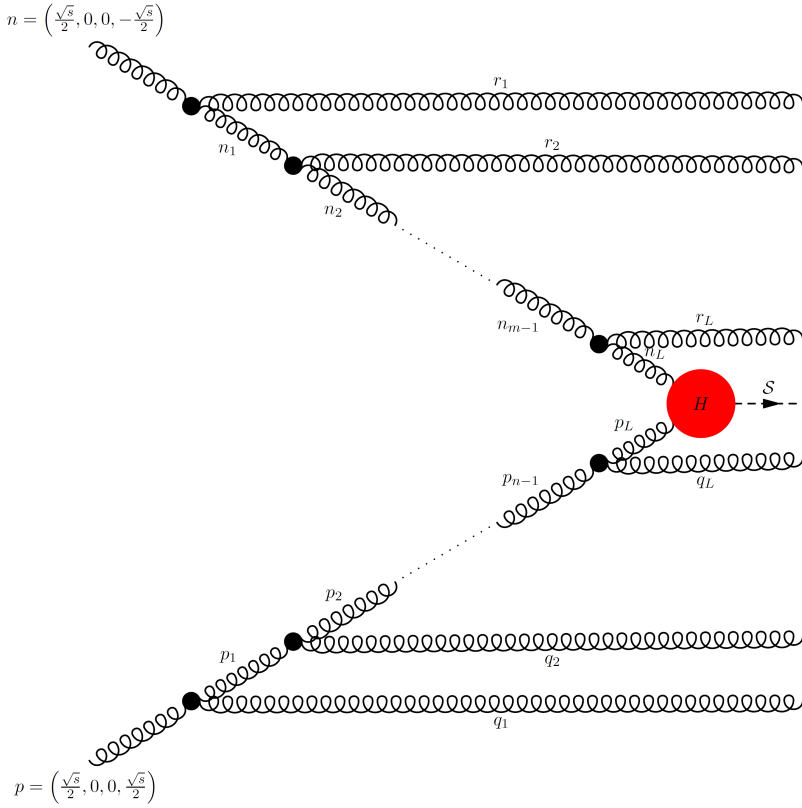


**Figure 3.3.** Kinematics of the ladder

Moreover, its Mellin transformed version can be written as

$$C_{p_T}(N, M_1, M_2, \xi_p, \alpha_s) = \int_0^\infty d\xi \xi^{M_1-1} \int_0^\infty d\bar{\xi} \bar{\xi}^{M_2-1} C_{p_T}(N, \xi, \bar{\xi}, \xi_p, \alpha_s). \quad (3.2.8)$$

Finally from the  $p_T$ -impact factor, Eq. (3.2.4), using general relation Eq. (3.1.65), it is straightforward to derive the resummed expression for the partonic transverse momentum spectrum, up to now in gluon gluon channel:

$$\frac{d\hat{\sigma}_{\text{res}}}{d\xi_p}(N, \xi_p, \alpha_s) = h_{p_T}(0, \gamma(\alpha_s, N), \gamma(\alpha_s, N), \xi_p, \alpha_s). \quad (3.2.9)$$

As you can appreciate by all the discussion in this section, deriving high energy resummation for a generic partonic observable (with some important limitation in the choice of such observable) using generalized ladder expansion permits us to extend this theory with apparent simplicity to transverse momentum distributions.

Even if we have described the high energy resummation for transverse momentum distributions in its general statements, we have left apart some subtleties for a matter

of presentation simplicity. We thus want now to cover these lacks. Then in the next subsections first we are going to tackle quarks initial state and resummation of channels which are different from gluon-gluon one; second we move to study coloured final state, making the first step into the study of jet variables. Finally we want to propose an example of observable for which condition about independence on the number of the emissions is not fulfilled: rapidity and transverse momentum double differential distribution in colour singlet production.

### 3.2.1 Quark-initiated channels

Up to now we consider only gluon-gluon initiated process. We want to discuss briefly modifications occurring when also quarks effects are taken into account at high energy.

First of all, we have already considered the matrix nature of the DGLAP equation, by defining as  $\gamma_+$  rather than  $\gamma_{gg}$  the small- $x$  anomalous dimension which controls the resummation at high energy. What remains to analyse is the effect of quarks in the initial state.

The important observation [68] regards the small- $N$  behaviour of the anomalous dimension; it turns out that only  $\gamma_{qg}$  and  $\gamma_{gg}$  contains high energy singularities while both  $\gamma_{gq}$  and  $\gamma_{q_i q_j}$  are NLL $x$ , thus subleading. Moreover the two divergent components  $\gamma_{qg}$  and  $\gamma_{gg}$  are related one another by colour-charge relation (also known as *Casimir scaling property*)

$$\gamma_{qg} = \frac{C_F}{C_A} \gamma_{gg}. \quad (3.2.10)$$

In conclusion, at LL $x$ , a quark can convert into a gluon but a gluon can not convert into a quark. Therefore, in a quark-initiated process, ladder emissions can be resummed as explained in Sec. 3.2 by substituting kernel  $K$  in the first emission with a colour-charge version  $\frac{C_F}{C_A} K$ . There is also another correction we have to insert: while it is possible at LL $x$  to have an external gluon connected directly to the hard part, in the quark case we have to admit at least one emission in order to convert the quark into gluon. Indeed, no high energy contribution arises from an hard part with a quark external line [68].

Summarizing all these observations in a common prescription, you can easily convince yourself that following expressions give back the correct high energy  $\hat{\mathcal{O}}$ -impact factor in the case of  $gq$  or  $qq$  channels:

$$h_{\hat{\mathcal{O}}}(N, M_1, M_2, \{v\}, \alpha_s)_{gq \rightarrow \mathcal{S}} = \frac{C_F}{C_A} \left( h_{\hat{\mathcal{O}}}(N, M_1, M_2, \{v\}, \alpha_s)_{gg \rightarrow \mathcal{S}} - h_{\hat{\mathcal{O}}}(N, M_1, 0, \{v\}, \alpha_s)_{gq \rightarrow \mathcal{S}} \right), \quad (3.2.11a)$$

$$h_{\hat{\mathcal{O}}}(N, M_1, M_2, \{v\}, \alpha_s)_{qq \rightarrow \mathcal{S}} = \left( \frac{C_F}{C_A} \right)^2 \left( h_{\hat{\mathcal{O}}}(N, M_1, M_2, \{v\}, \alpha_s)_{gg \rightarrow \mathcal{S}} - 2h_{\hat{\mathcal{O}}}(N, M_1, 0, \{v\}, \alpha_s)_{gq \rightarrow \mathcal{S}} + h_{\hat{\mathcal{O}}}(N, 0, 0, \{v\}, \alpha_s)_{gg \rightarrow \mathcal{S}} \right), \quad (3.2.11b)$$

with  $h_{\hat{\mathcal{O}}}(N, M_1, M_2, \{v\}, \alpha_s)_{gg \rightarrow \mathcal{S}}$  the impact factor defined in Eq. (3.1.64).

It is important to note that only the singlet quark component resums at high energy because it is the only component connected to gluons.

### 3.2.2 Coloured Final State

Last subject we want to analyse in this presentation about high energy resummation of transverse momentum distributions is a recent development about the study of coloured final state, and jet observables in general.

The study of jet final states in the context of high energy resummation rises several problems, not all solved up to now, namely:

- Gauge-invariance and hardness of the off-shell evaluation.
- Gluons indistinguishability between hard and ladder parts.
- Jet algorithm problem.

In this section, we are going to tackle and solve the first two problems, following discussion of Ref. [78]. Other correlated works, especially about gauge invariance of off-shell computations are Refs. [86–88]. Jet algorithms constitute a problem in the context of high energy resummation since they require a completely exclusive knowledge of the kinematics of each particle in the final state.  $LLx$  resummation, instead, needs to be inclusive on the ladder phase space to perform both BFKL and GLE approaches.

For some particular jets observables, such as one-jet inclusive cross section or the leading jet  $p_T$  distribution, however, an exclusive knowledge of only the hard part kinematics is enough to produce phenomenological result, and we will describe the reason of this miracle.

It is important to point out that a general theory of high energy resummation of any jet observables is, up to now, not available. Results presenting in this section have to be considered as a sort of introduction into this important topic which is currently under investigation.

We are going to start talking about gauge invariance. First of all, it is important to stress that, from now on, what we actually mean by saying that some  $n$ -gluon amplitude  $\mathcal{M}(\epsilon_1, \dots, \epsilon_n)$ , dependent on the polarization vectors  $\epsilon_i$  with  $i = 1, \dots, n$ , is gauge-invariant is that it satisfies the abelian Ward identities, namely

$$\mathcal{M}(\epsilon_1, \dots, \epsilon_{i-1}, k_i, \epsilon_{i+1}, \dots, \epsilon_n) = 0 \quad \forall i = 1, \dots, n. \quad (3.2.12)$$

Indeed, these are the relations we need to be true in order to be able to exploit the modern and more efficient techniques relying on gauge invariance, such as the helicity formalism (e.g. see Ref. [25]).

This necessity is strictly correlated with computation hardness of processes with jets in the final state. Helicity formalism permits to simplify a lot computations since it naturally work with only physical degrees of freedom. The impossibility to use such a formalism in the context of off-shell computations greatly reduces the number of possible applications, due to the complexity of the calculus with different techniques.

However, in a non-abelian gauge theory Eq. (3.2.12) is verified for process with at most one external off-shell gluon; this means in our  $k_T$ -factorization picture, that Eq. (3.2.12) has to hold for the partonic observable  $\hat{\mathcal{O}}$  but not for separate hard and ladder parts since they are connected by two off-shell external gluon lines. If they do not verify Eq. (3.2.12) separately, we will not be able to apply helicity formalism to any of the two and we will be forced to work in a particular fixed gauge (Feynman gauge for example).

It has been pointed out that, when the final state is coloured, a tree-level scattering amplitude with external off-shell gluon legs – such as the hard coefficient function Eq. (3.1.16) – does not fulfil the Ward identity Eq. (3.2.12) in general, if the calculation is performed by means of the standard QCD Feynman rules (see Refs. [86–88] for instance).

If we do not want to give up gauge invariance and to evaluate the hard part by means of standard technique, making sure to choose the same gauge used in the ladders (namely the Feynman gauge), we could decide to change somehow the definition of the coefficient function Eq. (3.1.16) in order to make it independently gauge-invariant. In this way, we would be able to use modern and efficient helicity techniques in the  $C_{\hat{\mathcal{O}}}$  computation.

In Refs. [86–88] several approaches have been proposed, aiming at restoring gauge invariance of a generic off-shell scattering amplitude. In particular, a possible solutions to this problem is to define a new coefficient function

$$C_{\hat{\mathcal{O}}}\left(\frac{\hat{\tau}}{z\bar{z}}, \frac{k_T^2}{Q^2}, \frac{\bar{k}_T^2}{Q^2}, \{v\}, \alpha_s\right) \equiv \int \frac{d\theta}{2\pi} \frac{d\bar{\theta}}{2\pi} \frac{\hat{\tau}}{2z\bar{z}} [\mathcal{P}^{\mu\nu} \mathcal{P}^{\bar{\mu}\bar{\nu}} \mathcal{H}_{\mu\nu\bar{\mu}\bar{\nu}}] \delta(v_i - v_i(p_L, n_L, q_1, \dots, q_n)), \quad (3.2.13)$$

where  $\mathcal{H}$  is the partonic observable for the process

$$W + W \rightarrow \mathcal{S} \quad (3.2.14)$$

with  $W$  a straight infinite Wilson line which creates the off-shell gluon state. More details about Wilson line, and the new ensuing Feynman rules which control them, are gathered in Ref. [78].

Using these different Feynman Rules to produce off-shell diagrams, contributing to  $\mathcal{C}$  we are able to define a gauge-invariant hard part, and to compute it with modern simple helicity technique. First application to one-jet inclusive cross section of Ref. [78] shows the completely equivalence between Wilson line computation and the standard fixed Feynman gauge computation in this very simple case, namely

$$g^* + g^* \rightarrow g. \quad (3.2.15)$$

Explicit expressions for the off-shell matrix element and for the relevant impact factors have been evaluated for the one-jet inclusive cross section in Ref. [78], and they are collected in Appendix C, Sec. C.2.3.

One jet inclusive cross section case of Ref. [78] gives us the opportunity to point out another important feature of coefficient function (3.1.16) (or Eq. (3.2.13)), which was highlighted only with the new GLE approach. We have already said that the coefficient function is defined to be the partonic observable for the LO off-shell gluon-gluon process

$$g^* + g^* \rightarrow \mathcal{S} \quad (3.2.16)$$

and no restrictions are provided on the on-shell nature of this object.

This is a difference with respect to standard BFKL derivation for inclusive cross section, where the reduction to the LO cross section in the collinear limit is of primary importance. The generalized ladder expansion points out that high energy resummation at LL $x$  is performed for any observable by dressing with ladder emissions the LO off-shell process.

The on-shell (collinear) limit of the coefficient function  $C_{\hat{\mathcal{O}}}(\xi, \bar{\xi} \rightarrow 0)$  could be in principle anything: the LO cross section as for inclusive cross section, a trivial distribution ( $\propto \delta(\xi_p)$ ) as for transverse momentum distribution, even 0 as for the one-jet inclusive cross section Eq. (3.2.15). The only difference is that in the last two cases, final resummed result would own an expansion starting at least one power in  $\alpha_s$  after the order of  $C_{\hat{\mathcal{O}}}$  thus pretending at least one emission in the ladder. However, the high energy resummation is still performed.

Last topic of this subsection will cover modification we have to introduce to generalize the LL $x$  resummation when gluons are considered in the studied final state  $\mathcal{S}$ . When gluons are present in the hard part we need to take into account indistinguishability of them with respect to gluons emitted in the ladders. This means that by considering  $n$  emission from one ladder,  $m$  emission from the other ladder, contribution from this process to the resummed partonic observable should be divided by the combinatorial factor

$$\tilde{\mathcal{O}}^{n,m} = \frac{1}{n+m} \hat{\mathcal{O}}^{n,m}. \quad (3.2.17)$$

A possible way to resum such effect starting from usual  $\hat{\mathcal{O}}$ -impact factor definition, Eq. (3.1.64) is contained in Ref. [78] and we are going to refer to that reference for details. When observable  $\hat{\mathcal{O}}$  is independent from the number of emissions in the ladders as for the one-jet inclusive observable or the leading jet  $p_T$  distribution, the corrected impact factor could be defined as

$$\tilde{h}_{\hat{\mathcal{O}}}(N, \gamma(\alpha_s, N), \gamma(\alpha_s, N), \{v\}, \alpha_s) = -[\chi_0(\gamma(\alpha_s, N))]^m \int_0^{\gamma(\alpha_s, N)} dM' \frac{1}{[\chi_0(M')]^{1+m}} \left( \frac{d\chi_0(M')}{dM'} \right) h_{\hat{\mathcal{O}}}(N, M', M', \{v\}, \alpha_s). \quad (3.2.18)$$

where  $h_{\hat{\mathcal{O}}}(N, M', M', \{v\}, \alpha_s)$  is the usual impact factor defined as in Eq. (3.1.64),  $m$  is the parameter which controls the correction and  $\chi_0$  is the LO BFKL kernel (see Eq. (C.2.2)) in Appendix C).

We have ended our discussion about further generalization of high energy resummation of transverse momentum distributions. We have learned how to define this resummation theory and how to deal with quarks in the initial state and with coloured particle in the final state.

Last comment will be about jet algorithms. To apply a particular jet algorithms completely exclusive final state kinematics has to be known, since we are interested to assign to each particle a value for the transverse momentum, the rapidity and the azimuthal angle. However this is not possible in our context, due to the fact that we have to be inclusive in ladder radiation.

At first sight, it seems that the application of jet algorithms to high energy resummation is doomed to fail but this is not the case. Instead, since subsequent ladder emissions at LL $x$  has to be ordered both in rapidity and in transverse momentum

$$k_{T_1}^2 < k_{T_2}^2 < \dots < k_{T_n}^2 = k_T^2 \quad (3.2.19a)$$

$$y_1 \gg y_2 \gg \dots \gg y_n = y \quad (3.2.19b)$$

$$(3.2.19c)$$

$$\bar{k}_{T_1}^2 < \bar{k}_{T_2}^2 < \dots < \bar{k}_{T_m}^2 = \bar{k}_T^2 \quad (3.2.19d)$$

$$\bar{y}_1 \gg \bar{y}_2 \gg \dots \gg \bar{y}_m = \bar{y}, \quad (3.2.19e)$$

for some jet observables, the pure knowledge of only rapidity and transverse momenta of last emissions, controlled by hard part, is sufficient to completely define the kinematics. For example, please consider the one-jet inclusive case, and the kinematics depicted in Fig. 3.3. Imagine to associate to  $\mathcal{S}$ ,  $q_L$  and  $r_L$  particles a transverse momentum, a rapidity and a azimuthal angle with a distribution which follows the off-shell coefficient function for the process Eq. (3.2.15), and then to use on these three particle an anti- $k_T$  (or a  $k_T$ ) jet algorithm. If these particles does not produce a jet, none of the others would do, because of ordering Eqs. (3.2.19). Therefore we can generate all other radiation inclusively in all the phase space without destroying the logarithmic accuracy.

This opens the possibility to study in the high energy regime some particular jet observable for which Eqs. (3.2.15) assure that any ladders interference is subleading. However, high energy resummed jet phenomenology study is a fledgling field, and more research activity is necessary to understand better all the subtleties.

### 3.3 Double differential distribution at high energy

Surely, a great limitation in all the discussion we made is given by the requirement about the observable  $\hat{O}$  to be independent by the number of emission performed in the ladders. Hence in this section we are going to present an example of observable which does not fulfil this requirement and for which however, high energy resummation is in fact possible: the double differential distribution in rapidity and transverse momentum. Moreover this observable is very important also for jet phenomenology because in many application with jets in the final state it is fundamental to have control at the same time of transverse momentum and rapidity of your studied final state  $\mathcal{S}$ .

As performed in Ref. [89], here we are going to briefly rebuild generalized ladder expansion in this case, trying to highlight main differences and existing solutions. The derivation of course is based on high energy resummation of single differential rapidity distribution of Ref. [76], and of single differential transverse momentum distribution of Ref. [77].

We want to study the transverse momentum and the rapidity of a system  $\mathcal{S}$  in a generic process like

$$h_1 + h_2 \rightarrow \mathcal{S} + X. \quad (3.3.1)$$

The transverse momentum will be parametrized, as before, throughout the dimension-

less variable  $\xi_p$ , Eq. (1.4.7), while the rapidity will be defined as

$$Y = \frac{1}{2} \ln \frac{E_S + p_{z,S}}{E_S - p_{z,S}}. \quad (3.3.2)$$

in the hadronic reference frame. The collinear factorization links hadronic distribution with the partonic one as

$$\frac{d\sigma}{dY d\xi_p} (\tau, \xi_p, Y, \alpha_s (\mu_R^2), \mu_F^2) = \sum_{ij} \int_{x_1^{\min}}^1 dx_1 f_i(x_1, \mu_F^2) \int_{x_2^{\min}}^1 dx_2 f_j(x_2, \mu_F^2) \frac{d\hat{\sigma}}{dy d\xi_p} (\hat{\tau}, \xi_p, y, \alpha_s (\mu_R^2), \mu_F^2) \quad (3.3.3)$$

where we define the partonic rapidity as

$$y = Y - \frac{1}{2} \ln \frac{x_1}{x_2} \quad (3.3.4)$$

and kinematic limits turn out to be, using  $x_1, x_2, \tau, \xi_p, Y, y$  as a set of variables:

$$\begin{aligned} 0 < \tau < 1 & & 0 < \xi_p < \frac{(1-\tau)^2}{4\tau} & & -Y_{\max} < Y < Y_{\max} \\ x_1^{\min} < x_1 < 1 & & x_2^{\min} < x_2 < 1 & & -y_{\max} < y < y_{\max} \end{aligned} \quad (3.3.5)$$

with

$$Y_{\max} = \frac{1}{2} \ln \frac{1 + \sqrt{1 - \frac{4\tau(1+\xi_p)}{(1+\tau)^2}}}{1 - \sqrt{1 - \frac{4\tau(1+\xi_p)}{(1+\tau)^2}}}, \quad (3.3.6)$$

$$x_1^{\min} = \frac{(\sqrt{\tau}\sqrt{1+\xi_p}e^Y - \tau)e^Y}{e^Y - \sqrt{\tau}\sqrt{1+\xi_p}}, \quad (3.3.7)$$

$$x_2^{\min} = \frac{x_1\sqrt{\tau}\sqrt{1+\xi_p} - \tau e^Y}{e^Y(x_1 - \sqrt{\tau}\sqrt{1+\xi_p}e^Y)}, \quad (3.3.8)$$

$$y_{\max} = \frac{1}{2} \ln \frac{1 + \sqrt{1 - \frac{4\hat{\tau}(1+\xi_p)}{(1+\hat{\tau})^2}}}{1 - \sqrt{1 - \frac{4\hat{\tau}(1+\xi_p)}{(1+\hat{\tau})^2}}}. \quad (3.3.9)$$

To perform high energy resummation for  $\frac{d\sigma}{dy d\xi_p}$ , we start by rewriting Eq. (3.1.50) in the case of the double differential cross section:

$$\begin{aligned} \frac{d\sigma}{d\xi_p dy} \left( \hat{\tau}, \xi_p, y, \frac{\mu_F^2}{Q^2}, \alpha_s; \epsilon \right) &= (\mu_F)^{2\epsilon} \int C_{p_T, y} \left( \frac{\hat{\tau}}{z\bar{z}}, \frac{k_T^2}{Q^2}, \frac{\bar{k}_T^2}{Q^2}, \xi_p, y, \alpha_s; \epsilon \right) \\ &\quad \left[ 2\pi L_{\parallel}^{(1)} \left( z, \left( \frac{\mu_F^2}{k_T^2} \right)^\epsilon, \alpha_s; \epsilon \right) \right] \left[ 2\pi L_{\parallel}^{(2)} \left( \bar{z}, \left( \frac{\mu_F^2}{\bar{k}_T^2} \right)^\epsilon, \alpha_s; \epsilon \right) \right] \\ &\quad \frac{dz}{z} \frac{d\bar{z}}{\bar{z}} \frac{dk_T^2}{(k_T^2)^{1+\epsilon}} \frac{d\bar{k}_T^2}{(\bar{k}_T^2)^{1+\epsilon}}, \end{aligned} \quad (3.3.10)$$

with

$$C_{p_T, y} \left( \frac{\hat{\tau}}{z\bar{z}}, \frac{k_T^2}{Q^2}, \frac{\bar{k}_T^2}{Q^2}, \xi_p, y, \alpha_s; \epsilon \right) \equiv \int \frac{d\theta}{2\pi} \frac{d\bar{\theta}}{2\pi} \frac{\hat{\tau}}{2z\bar{z}} [\mathcal{P}^{\mu\nu} \mathcal{P}^{\bar{\mu}\bar{\nu}} H_{\mu\nu\bar{\mu}\bar{\nu}}] \delta \left( \xi_p - \xi - \bar{\xi} - 2\sqrt{\xi\bar{\xi}} \cos \theta \right) \delta \left( y - \frac{1}{2} \ln \frac{z}{\bar{z}} \right),$$

and  $z, \bar{z}, k_T^2$  and  $\bar{k}_T^2$  defined as in Eq. (3.1.8).

By inspecting general ladder kinematics, Eq. (3.2.3) after kernel multiple insertions, you can easily convince yourself that the particular value of  $z, \bar{z}$  contained in the rapidity delta constraint does depend on the number  $n$  and  $m$  of insertion in each leg. Indeed, we have the following relations

$$z = z_1 \dots z_n \quad (3.3.11)$$

$$\bar{z} = \bar{z}_1 \dots \bar{z}_m \quad (3.3.12)$$

and then ladder resummation cannot be performed in exactly the same way as in total cross section or transverse momentum distribution cases. This situation was already solved in the case of single rapidity distribution of Ref. [76] and here we are going to present a similar derivation.

As in Eq. (3.1.51), we expand at LLx ladders  $L^{(1,2)}$  of Eq. (3.3.10) through multiple insertions of a proper kernel  $K$ . The only difference with previous derivation is that we are going to perform such expansion in direct space, rather than in Mellin space. We thus write:

$$\begin{aligned} \frac{d\hat{\sigma}^{n,m}}{dy d\xi_p} \left( \hat{\tau}, \xi_p, y, \frac{\mu_F^2}{Q^2}, \alpha_s; \epsilon \right) &= \int_0^1 dz_n \int_0^\infty \left[ K \left( z_n, \left( \frac{\mu_F^2}{Q^2 \xi_n} \right)^\epsilon, \alpha_s; \epsilon \right) \right] \frac{d\xi_n}{\xi_n^{1+\epsilon}} \times \\ &\times \int_0^1 d\bar{z}_m \int_0^\infty \left[ K \left( \bar{z}_m, \left( \frac{\mu_F^2}{Q^2 \xi_m} \right)^\epsilon, \alpha_s; \epsilon \right) \right] \frac{d\bar{\xi}_m}{\bar{\xi}_m^{1+\epsilon}} \\ C_{p_T, y} \left( \frac{\hat{\tau}}{z\bar{z}}, \xi, \bar{\xi}, \xi_p, y, \alpha_s; \epsilon \right) &\delta \left( \frac{1}{2} \ln \frac{z}{\bar{z}} - \frac{1}{2} \ln \frac{z_1 \dots z_n}{\bar{z}_1 \dots \bar{z}_m} \right) \times \\ &\times \int_0^1 dz_{n-1} \int_0^{\xi_n} \left[ K \left( z_{n-1}, \left( \frac{\mu_F^2}{Q^2 \xi_{n-1}} \right)^\epsilon, \alpha_s; \epsilon \right) \right] \frac{d\xi_{n-1}}{\xi_{n-1}^{1+\epsilon}} \\ &\times \dots \times \int_0^1 dz_1 \int_0^{\xi_2} \left[ K \left( z_1, \left( \frac{\mu_F^2}{Q^2 \xi_1} \right)^\epsilon, \alpha_s; \epsilon \right) \right] \frac{d\xi_1}{\xi_1^{1+\epsilon}} \times \\ &\times \int_0^1 d\bar{z}_{m-1} \int_0^{\bar{\xi}_m} \left[ K \left( \bar{z}_{m-1}, \left( \frac{\mu_F^2}{Q^2 \xi_{m-1}} \right)^\epsilon, \alpha_s; \epsilon \right) \right] \frac{d\bar{\xi}_{m-1}}{\bar{\xi}_{m-1}^{1+\epsilon}} \\ &\times \dots \times \int_0^1 d\bar{z}_1 \int_0^{\bar{\xi}_2} \left[ K \left( \bar{z}_1, \left( \frac{\mu_F^2}{Q^2 \xi_1} \right)^\epsilon, \alpha_s; \epsilon \right) \right] \frac{d\bar{\xi}_1}{\bar{\xi}_1^{1+\epsilon}} \end{aligned} \quad (3.3.13)$$

where we divide rapidity delta constraint

$$\delta \left( y - \frac{1}{2} \ln \frac{z_1 \dots z_n}{\bar{z}_1 \dots \bar{z}_m} \right) = \delta \left( y - \frac{1}{2} \ln \frac{z}{\bar{z}} \right) \delta \left( \frac{1}{2} \ln \frac{z}{\bar{z}} - \frac{1}{2} \ln \frac{z_1 \dots z_n}{\bar{z}_1 \dots \bar{z}_m} \right) \quad (3.3.14)$$

into its hard and ladder parts. We include the hard part delta constraint into  $C_{p_T, y}$  definition in Eq. (3.3.13), according to general  $C_{\mathcal{O}}$  definition, Eq. (3.1.16).

The goal now is reached by performing the right transform which factorizes rapidity delta constraint which is the only part which mix ladders emission throughout various  $z_i$  and  $\bar{z}_i$ . By defining the following Mellin Fourier Transform,

$$\frac{d\hat{\sigma}^{n,m}}{dyd\xi_p} \left( N, \xi_p, b, \frac{\mu_F^2}{Q^2}, \alpha_s; \epsilon \right) = \int_0^1 d\hat{\tau} \hat{\tau}^{N-1} \int_{-\infty}^{\infty} dy e^{-iby} \frac{d\hat{\sigma}^{n,m}}{dyd\xi_p} \left( \hat{\tau}, \xi_p, y, \frac{\mu_F^2}{Q^2}, \alpha_s; \epsilon \right) \quad (3.3.15)$$

we rewrite Eq. (3.3.13) in the following factorized form

$$\begin{aligned} \frac{d\hat{\sigma}^{n,m}}{dyd\xi_p} \left( N, \xi_p, b, \frac{\mu_F^2}{Q^2}, \alpha_s; \epsilon \right) &= \int_0^{\infty} \left[ \gamma \left( N - \frac{ib}{2}, \left( \frac{\mu_F^2}{Q^2 \xi_n} \right)^\epsilon, \alpha_s; \epsilon \right) \right] \frac{d\xi_n}{\xi_n^{1+\epsilon}} \times \\ &\times \int_0^{\infty} \left[ \gamma \left( N + \frac{ib}{2}, \left( \frac{\mu_F^2}{Q^2 \xi_m} \right)^\epsilon, \alpha_s; \epsilon \right) \right] \frac{d\bar{\xi}_m}{\bar{\xi}_m^{1+\epsilon}} C_{p_T, y} \left( N, \xi_n, \bar{\xi}_m, \xi_p, b, \alpha_s; \epsilon \right) \times \\ &\times \int_0^{\xi_n} \left[ \gamma \left( N - \frac{ib}{2}, \left( \frac{\mu_F^2}{Q^2 \xi_{n-1}} \right)^\epsilon, \alpha_s; \epsilon \right) \right] \frac{d\xi_{n-1}}{\xi_{n-1}^{1+\epsilon}} \\ &\times \cdots \times \int_0^{\xi_2} \left[ \gamma \left( N - \frac{ib}{2}, \left( \frac{\mu_F^2}{Q^2 \xi_1} \right)^\epsilon, \alpha_s; \epsilon \right) \right] \frac{d\xi_1}{\xi_1^{1+\epsilon}} \times \\ &\times \int_0^{\bar{\xi}_m} \left[ \gamma \left( N + \frac{ib}{2}, \left( \frac{\mu_F^2}{Q^2 \xi_{m-1}} \right)^\epsilon, \alpha_s; \epsilon \right) \right] \frac{d\bar{\xi}_{m-1}}{\bar{\xi}_{m-1}^{1+\epsilon}} \\ &\times \cdots \times \int_0^{\bar{\xi}_2} \left[ \gamma \left( N + \frac{ib}{2}, \left( \frac{\mu_F^2}{Q^2 \xi_1} \right)^\epsilon, \alpha_s; \epsilon \right) \right] \frac{d\bar{\xi}_1}{\bar{\xi}_1^{1+\epsilon}} \end{aligned} \quad (3.3.16)$$

where we define  $C_{p_T, y}$  in Mellin Fourier space as

$$C_{p_T, y} \left( N, \xi, \bar{\xi}, \xi_p, b, \alpha_s \right) = \int_0^1 dx \hat{\tau} \hat{\tau}^{N-1} \int_{-\infty}^{+\infty} dy e^{-iby} C_{p_T, y} \left( \hat{\tau}, \xi, \bar{\xi}, \xi_p, y, \alpha_s \right). \quad (3.3.17)$$

It is interesting to observe that the Fourier definition Eq. (3.3.15) with physical range of integration does not lead to any further complication in the high energy regime since at LLx

$$y_{\max} \rightarrow \infty \quad \text{as} \quad \hat{\tau} \rightarrow 0. \quad (3.3.18)$$

Since now Eq. (3.3.16) is factorized, following steps to reach the high energy resummation can be performed exactly as in Sec. 3.1.2. Therefore, we require Eq. (3.3.16) to be finite after each  $\xi_i$  or  $\bar{\xi}_j$  integration and we subtract the final single  $n+m$ -th order  $\epsilon$  pole using standard  $\overline{\text{MS}}$  prescription. At the end, by summing also over all possible emissions and by taking  $\epsilon \rightarrow 0$ , we come to

$$\begin{aligned} \frac{d\hat{\sigma}^{\text{res}}}{dyd\xi_p} \left( N, \xi_p, b, \frac{\mu_F^2}{Q^2}, \alpha_s \right) &= \gamma \left( N - \frac{ib}{2}, \alpha_s \right) \gamma \left( N + \frac{ib}{2}, \alpha_s \right) \\ &\mathcal{R} \left( N - \frac{ib}{2}, \alpha_s \right) \mathcal{R} \left( N + \frac{ib}{2}, \alpha_s \right) \end{aligned}$$

$$\int_0^\infty d\xi \xi^{\gamma(N - \frac{ib}{2}, \alpha_s) - 1} \int_0^\infty d\bar{\xi} \bar{\xi}^{\gamma(N + \frac{ib}{2}, \alpha_s) - 1} C_{p_T, y}(N, \xi, \bar{\xi}, \xi_p, b, \alpha_s) \times \exp \left[ \gamma \left( N + \frac{ib}{2}, \alpha_s \right) \ln \frac{Q^2}{\mu_F^2} \right] \exp \left[ \gamma \left( N - \frac{ib}{2}, \alpha_s \right) \ln \frac{Q^2}{\mu_F^2} \right] \quad (3.3.19)$$

where we insert as before the resummation scheme choice factor  $R$ .

Eq. (3.3.19) can be further simplified in the case of colour singlet production, due to the simple  $2 \rightarrow 1$  kinematics of  $C_{p_T, y}$ . In this case we have the following relation:

$$C_{p_T, y}(N, \xi, \bar{\xi}, \xi_p, b, \alpha_s) = C_{p_T}(N, \xi, \bar{\xi}, \xi_p, \alpha_s) \quad (3.3.20)$$

since the rapidity dependence in the hard part is a subleading effect for this kinematics.

In conclusion, the resummation for rapidity and transverse momentum double differential distribution is obtained by applying Eq. (3.3.19) with  $C_{p_T, y}$  in Mellin Fourier space defined as in Eq. (3.3.17). In the case of colour singlet production, high energy resummation can be achieved directly by using  $p_T$ -impact factor defined into Eq. (3.2.4), throughout the substitutions:

$$M_1 = \gamma \left( N - \frac{ib}{2}, \alpha_s \right) \quad (3.3.21)$$

$$M_2 = \gamma \left( N + \frac{ib}{2}, \alpha_s \right), \quad (3.3.22)$$

thus obtaining (with  $\mu_F^2 = Q^2$ )

$$\frac{d\hat{\sigma}^{\text{res}}}{dy d\xi_p}(N, \xi_p, b, \alpha_s) = h_{p_T} \left( 0, \gamma \left( N + \frac{ib}{2}, \alpha_s \right), \gamma \left( N - \frac{ib}{2}, \alpha_s \right), \xi_p, \alpha_s \right), \quad (3.3.23)$$

where again we set  $N = 0$  in the  $p_T$ -impact factor since all other  $N$  dependence is subleading at LL $x$ .

Eq. (3.3.19) and Eq. (3.3.23) are new results of this thesis and permit the high energy resummation for the fully differential colour singlet production case. They have been published in Ref. [89].

Last comment of this section is about relation between the resummation of partonic and hadronic double differential distribution. Although collinear factorization for such observable turn out to be very complicated (see Eq. (3.3.3)), at LL $x$  in Mellin Fourier space it takes a very simple form. We come to the following conclusion

$$\frac{d\sigma^{\text{res}}}{dY d\xi_p}(N, \xi_p, b, \alpha_s) = \sum_{ij} f_i \left( N - \frac{ib}{2} + 1, \alpha_s \right) f_j \left( N + \frac{ib}{2} + 1, \alpha_s \right) \frac{d\hat{\sigma}_{ij}^{\text{res}}}{dy d\xi_p}(N, \xi_p, b, \alpha_s) \quad (3.3.24)$$

where Mellin transform is however defined as in the  $p_T$  case with respect to  $\tau'$  rather than  $\tau$ , Fourier transform is defined as in Eq. (3.3.15) on  $Y$ , and we set  $\mu_F^2 = Q^2$  for simplicity. We remind the reader that we are free to change our Mellin definition and to still use Eq. (3.3.19) or Eq. (3.3.23) for the resummed partonic observable, due to Eq. (3.2.1). Moreover, contributions for channel different from gluon-gluon one are reconstructed using same steps of Sec. 3.2.1 (see Ref. [89]).

Coming to conclusions, in this chapter we summarize very recent results about the high energy resummation for differential observables, focusing our attention in particular on transverse momentum distributions (with or without rapidity dependence). This resummation was achieved by using known results coming from BFKL evolution, described in Sec. 3.1.1, together with an alternative derivation of  $k_T$ -factorization, first exposed in Ref. [76], and here repeated in Sec. 3.1.2.

In the next section, which is the last of this chapter, we are going to present an explicit calculation of the high energy behaviour for our test case, the EFT Higgs boson production. We are going also to check our conclusions against fixed order evaluations, using a technique presented in Ref. [76, 90] to compute the high energy limit of the first terms in the  $\alpha_s$  expansion.

### 3.4 Application: EFT Higgs boson at high energy

This last section will be devoted to the presentation of an explicit application, together with some simple analytic checks. The aim is to verify in a particular process the whole theoretical derivation showed up to now. As in Chap. 1 and in Chap. 2, the process we select to exhibit all the properties of the high energy resummation is the Higgs boson production case in gluon fusion, in the framework of the effective field theory.

We are going to compute the resummation at high energy at  $\text{LL}x$  of the logarithms of  $x$  (see Eq. (1.4.9) for the exact definition of  $x$ ) in the double differential cross section with respect to the Higgs transverse momentum and rapidity. As presented in Sec. 3.3, this resummation is performed in Mellin-Fourier space following Eq. (3.3.23). Moreover due to relation Eq. (3.3.20), for Higgs boson production, the rapidity dependence in the hard part is subleading in conjugate space. Therefore, we are going to show the explicit computation of the  $p_T$ -impact factor, Eq. (3.2.4), in this case.

At the end, the high energy resummation for the Higgs transverse momentum distribution, as well as the high energy resummation for the Higgs rapidity distribution of Ref. [76] or for inclusive cross section of Ref. [72] will be recovered from previous computation following suitable integration over  $y$ ,  $p_T$ , or both.

The transverse momentum distribution  $C_{p_T}(N, \xi, \bar{\xi}, \xi_p, \alpha_s)$  for the off-shell LO process,

$$g^*(p_L) + g^*(n_L) \rightarrow H(p_S) \quad (3.4.1)$$

can be written as [77]

$$\begin{aligned} C_{p_T}(N, \xi, \bar{\xi}, \xi_p, \alpha_s) &= \frac{\alpha_s^2 \sqrt{2} G_F}{288\pi} \int_0^1 d\tau \tau^{N-1} \int_0^{2\pi} \frac{d\theta \cos^2 \theta}{2\pi \tau} \delta\left(\frac{1}{\tau} - 1 - \xi_p\right) \\ &= 2\sigma_0 \int_0^1 d\tau \tau^{N-1} \int_0^{2\pi} \frac{d\theta \cos^2 \theta}{2\pi \tau} \delta\left(\frac{1}{\tau} - 1 - \xi_p\right) \end{aligned} \quad (3.4.2)$$

with  $\sigma_0$  LO EFT total cross section already presented in Sec. 1.3.1, Chap. 1, and  $\tau = \frac{m_H^2}{z\bar{z}s}$  the variable associated to the Mellin definition. We can select  $\tau$  instead of  $x$  because the difference between  $\tau$  and  $x$  is  $\text{NLL}x$ . Moreover,  $\tau$  choice will simplify next steps.

By solving Mellin integration using delta constraint and by inserting Eq. (3.4.2) into the general definition of the  $p_T$ -impact factor, Eq. (3.2.4) we obtain:

$$h_{p_T}(N, M_1, M_2, \xi_p, \alpha_s) = \frac{\sigma_0}{\pi(1+\xi_p)^N} M_1 M_2 R(M_1) R(M_2) \quad (3.4.3)$$

$$\int_0^\infty d\xi \xi^{M_1-1} \int_0^\infty d\bar{\xi} \bar{\xi}^{M_2-1} \int_0^{2\pi} d\theta \cos^2 \theta \delta\left(\xi_p - \xi - \bar{\xi} - 2\sqrt{\xi\bar{\xi}} \cos \theta\right). \quad (3.4.4)$$

Following steps are almost trivial. First we use the  $\delta$  constraint to get rid of  $\theta$  integration,

$$h_{p_T}(N, M_1, M_2, \xi_p, \alpha_s) = \frac{\sigma_0}{\pi(1+\xi_p)^N} M_1 M_2 R(M_1) R(M_2) \quad (3.4.5)$$

$$\int_0^\infty d\xi \xi^{M_1-2} \int_{(\sqrt{\xi_p}-\sqrt{\bar{\xi}})^2}^{(\sqrt{\xi_p}+\sqrt{\bar{\xi}})^2} d\bar{\xi} \bar{\xi}^{M_2-2} \frac{(\xi_p - \xi - \bar{\xi})^2}{\sqrt{2\xi\bar{\xi} + 2\xi\xi_p + 2\bar{\xi}\xi_p - \xi_p^2 - \xi^2 - \bar{\xi}^2}}, \quad (3.4.6)$$

then we perform the following change of variable

$$\xi = \xi_p \xi_1 \quad \bar{\xi} = \xi_p \xi_2, \quad (3.4.7)$$

to factorize into Eq. (3.4.5),  $\xi_p$  dependence. We thus come to

$$h_{p_T}(N, M_1, M_2, \xi_p, \alpha_s) = \sigma_0 \frac{\xi_p^{M_1+M_2-1}}{\pi(1+\xi_p)^N} I(M_1, M_2) \quad (3.4.8)$$

where we define the integral representation  $I$  as

$$I(M_1, M_2) = M_1 M_2 R(M_1) R(M_2) \int_0^\infty d\xi_1 \xi_1^{M_1-2} \int_{(1-\sqrt{\xi_1})^2}^{(1+\sqrt{\xi_1})^2} d\xi_2 \xi_2^{M_2-2} \frac{(1-\xi_1-\xi_2)^2}{\sqrt{2\xi_1\xi_2 + 2\xi_1 + 2\xi_2 - 1 - \xi_1^2 - \xi_2^2}}. \quad (3.4.9)$$

Computation of  $\xi_1$  and  $\xi_2$  integrals in  $I$  is presented in Appendix C. Substituting result Eq. (C.2.11) into Eq. (3.4.8), we write:

$$h_{p_T}(N, M_1, M_2, \xi_p, \alpha_s) = R(M_1) R(M_2) \sigma_0 \frac{\xi_p^{M_1+M_2-1}}{(1+\xi_p)^N} \left[ \frac{\Gamma(1+M_1)\Gamma(1+M_2)\Gamma(2-M_1-M_2)}{\Gamma(2-M_1)\Gamma(2-M_2)\Gamma(M_1+M_2)} \left(1 + \frac{2M_1M_2}{1-M_1-M_2}\right) \right]. \quad (3.4.10)$$

High energy resummation for the rapidity and transverse momentum double differential distribution is now performed; using Eq. (3.3.23) we obtain

$$\frac{d\hat{\sigma}_{gg}}{dy d\xi_p}(N, b, \xi_p, \alpha_s) = h_{p_T}\left(0, \gamma\left(N - \frac{ib}{2}, \alpha_s\right), \gamma\left(N + \frac{ib}{2}, \alpha_s\right), \xi_p, \alpha_s\right) \quad (3.4.11)$$

for the gluon-gluon channel, and

$$\frac{d\hat{\sigma}_{gq}}{dy d\xi_p}(N, b, \xi_p, \alpha_s) = \frac{C_F}{C_A} \left( h_{p_T}\left(0, \gamma\left(N - \frac{ib}{2}, \alpha_s\right), \gamma\left(N + \frac{ib}{2}, \alpha_s\right), \xi_p, \alpha_s\right) \right)$$

$$- h_{p_T} \left( 0, \gamma \left( N - \frac{ib}{2}, 0, \alpha_s \right), 0, \xi_p, \alpha_s \right) \quad (3.4.12)$$

$$\begin{aligned} \frac{d\hat{\sigma}_{gg}}{dyd\xi_p}(N, b, \xi_p, \alpha_s) &= \frac{C_F}{C_A} \left( h_{p_T} \left( 0, \gamma \left( N - \frac{ib}{2}, \alpha_s \right), \gamma \left( N + \frac{ib}{2}, \alpha_s \right), \xi_p, \alpha_s \right) \right. \\ &\quad \left. - h_{p_T} \left( 0, 0, \gamma \left( N + \frac{ib}{2}, \alpha_s \right), 0, \xi_p, \alpha_s \right) \right) \end{aligned} \quad (3.4.13)$$

$$\begin{aligned} \frac{d\hat{\sigma}_{qq}}{dyd\xi_p}(N, b, \xi_p, \alpha_s) &= \left( \frac{C_F}{C_A} \right)^2 \left( h_{p_T} \left( 0, \gamma \left( N - \frac{ib}{2}, \alpha_s \right), \gamma \left( N + \frac{ib}{2}, \alpha_s \right), \xi_p, \alpha_s \right) \right. \\ &\quad \left. - h_{p_T} \left( 0, 0, \gamma \left( N + \frac{ib}{2}, \alpha_s \right), 0, \xi_p, \alpha_s \right) \right. \\ &\quad \left. - h_{p_T} \left( 0, \gamma \left( N - \frac{ib}{2}, \alpha_s \right), 0, 0, \xi_p, \alpha_s \right) + h_{p_T} (0, 0, 0, 0, \xi_p, \alpha_s) \right) \end{aligned} \quad (3.4.14)$$

for the other channel contributions. Resummation is now simply achieved by evaluating LL $x$  anomalous dimension  $\gamma(N, \alpha_s)$ , and by performing inverse Fourier-Mellin transform. A particularly stable implementation for  $\gamma$  is the one presented in Refs. [70, 84] and implemented in the code HELL.

Moreover, the integration over  $\xi_p$  returns the same impact factor used in Ref. [76] for the resummation of the rapidity distribution; integration over  $y$  (achieved in Fourier space setting  $b = 0$ ) reconstructs the known resummation of transverse momentum distribution of Ref. [77]; finally integration over both  $\xi_p$  and  $y$  is consistent with known resummation of Ref. [72] for the inclusive cross section .

Since our aim in this section is to provide explicit analytic checks about our derivation, we will not focus on the resummed result but we are going to expand Eq. (3.4.11) in power of  $\alpha_s$  and to crosscheck first coefficients against fixed order evaluations. The technique we will use to perform this check is the one presented in Ref. [90].

We expand our result in powers of  $\alpha_s$ , using following equalities

$$R(M) = 1 + \frac{8}{3}\zeta_3 M^3 + \mathcal{O}(M^4) \quad (3.4.15)$$

$$\gamma(N, \alpha_s) = \frac{C_A}{\pi} \frac{\alpha_s}{N} + \mathcal{O}(\alpha_s^4), \quad (3.4.16)$$

obtaining:

$$\frac{d\hat{\sigma}_{gg}}{dyd\xi_p}(N, b, \xi_p, \alpha_s) = \sigma_0 \sum_{k=0}^{\infty} \alpha_s^k C_k(N, b, \xi_p) \quad (3.4.17)$$

with

$$C_0(N, b, \xi_p) = \delta(\xi_p), \quad (3.4.18a)$$

$$C_1(N, b, \xi_p) = \frac{C_A}{\pi} \left[ \frac{1}{\xi_p} \right]_+ \left( \frac{1}{N + \frac{ib}{2}} + \frac{1}{N - \frac{ib}{2}} \right), \quad (3.4.18b)$$

$$C_2(N, b, \xi_p) = \left(\frac{C_A}{\pi}\right)^2 \left( \left[ \frac{\ln \xi_p}{\xi_p} \right]_+ \left( \frac{1}{N + \frac{ib}{2}} + \frac{1}{N - \frac{ib}{2}} \right)^2 + \frac{1}{N - \frac{ib}{2}} \frac{1}{N + \frac{ib}{2}} \delta(\xi_p) \right). \quad (3.4.18c)$$

In Eqs. (3.4.18) the plus distribution is defined as in Eq. (B.3.1) with  $\xi_{\max} \rightarrow \infty$ .

We limit ourselves to the gluon-gluon case for simplicity; the interested reader can check also the other channels with similar techniques.

Comparisons with the exact fixed order evaluations for the first coefficient  $C_1$  and  $C_2$  will be performed in the next subsection.

### 3.4.1 Check against fixed order evaluation

In this subsection we want to check the leading log limit of the double differential distribution with respect to the rapidity and the transverse momentum for the Higgs boson production process in gluon fusion. We will follow analogue comparisons performed in Ref. [90] and we are going to compute the high energy limit of the first perturbative order, by explicit computation of relevant Feynman Diagrams. For simplicity, we will use as independent variables  $\hat{\tau}$ ,  $\xi_p$  and  $u = e^{-2y}$ , hence evaluating  $\frac{d\hat{\sigma}}{du d\xi_p}$  rather than  $\frac{d\hat{\sigma}}{dy d\xi_p}$ . We will come back to the set  $x$ ,  $\xi_p$  and  $y$  at the end of the calculus, right before the computation of the Mellin-Fourier transform.

We start from the single emission. Diagrams contributing at LL $x$  are drawn in Fig. 3.1. With the red circle we indicate the  $\overline{\text{MS}}$  collinear counterterm, which occurs to make the sum finite. In computing the square modulus of the amplitude we can ignore interferences between diagrams since they are subleading in the high energy limit.

For the diagrams in the first row of Fig. 3.1, the associated double differential cross section can be written as

$$\begin{aligned} \frac{d\sigma_1}{d\xi_p du} &= \frac{1}{2u} \frac{d\sigma_1}{d\xi_p dy} = \sigma_0 \frac{\bar{z}}{\hat{\tau}} \delta\left(1 - \frac{\bar{z}}{\hat{\tau}} + \bar{\xi}\right) \left[ \bar{\alpha}_s \frac{d\bar{z}}{\bar{z}} \frac{d\bar{\xi}}{\bar{\xi}^{1+\epsilon}} \right] \delta(\xi - \xi_p) \delta(u - \bar{z}) \\ &\quad + \frac{\sigma_0 \bar{\alpha}_s}{\epsilon} \delta(\xi_p) \delta(u - \hat{\tau}). \end{aligned} \quad (3.4.19)$$

where integrations over  $\bar{z}$ ,  $\bar{\xi}$  are implicitly assumed. We are going to use the bar to indicate all the Sudakov components related to the upper leg of the diagrams of Fig. 3.1. Moreover we introduce

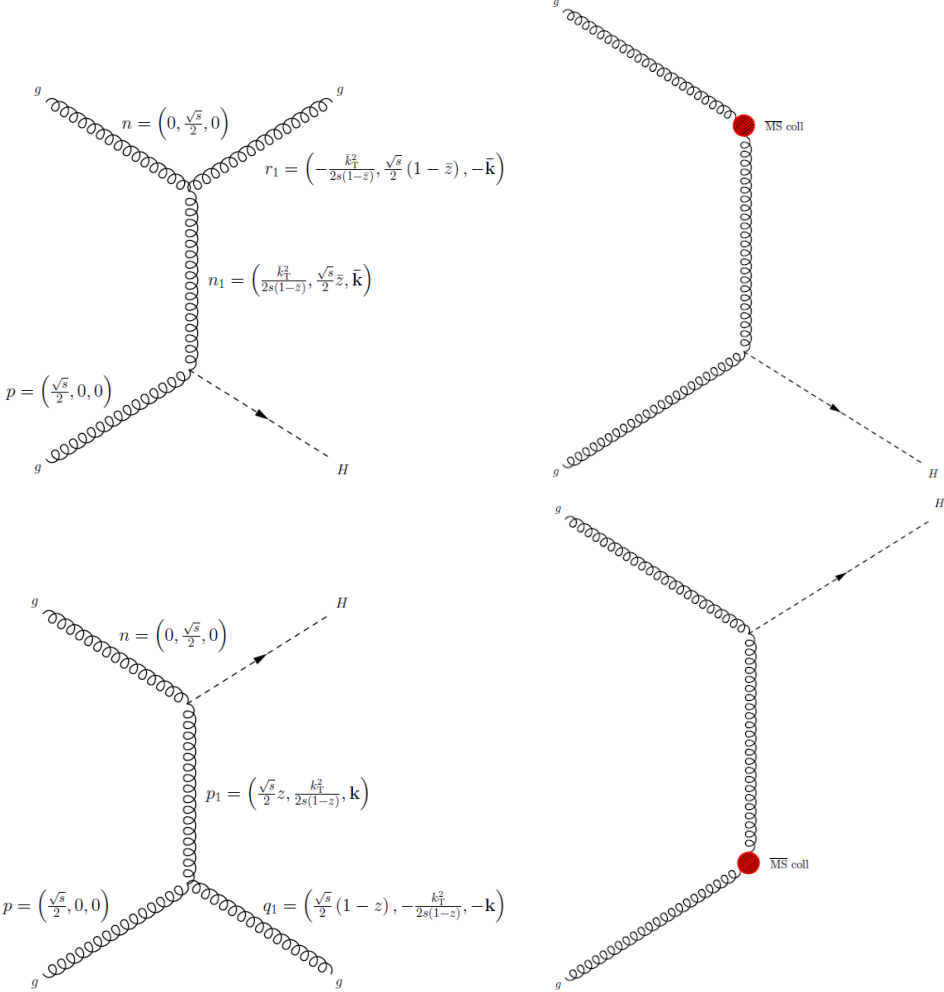
$$\bar{\alpha}_s = \frac{\alpha_s(\mu^2) \mu^{2\epsilon} C_A}{\pi} \quad (3.4.20)$$

with  $\epsilon$  the dimensional regulator, and we ignore all the  $\frac{(4\pi)^\epsilon}{\Gamma(1-\epsilon)}$  terms which are systematically subtracted order by order in  $\overline{\text{MS}}$  scheme.

Kinematic limits for  $\hat{\tau}$ ,  $\xi_p$ ,  $u$ ,  $\bar{z}$ ,  $\bar{\xi}$  in the high energy regime are the following

$$0 < \hat{\tau} < 1, \quad \xi_p > 0, \quad 0 < u < 1, \quad 0 < \bar{z} < 1, \quad \bar{\xi} > 0. \quad (3.4.21)$$

It is important to note that, due to the presence of the collinear counterterm, Eq. (3.4.19) is finite in  $d = 4$  dimension. Now to come to the final result for the single emission we

**Table 3.1.** NLO Feynman Diagrams and  $\overline{\text{MS}}$  subtraction

perform the integration over  $\bar{\xi}$  and  $\bar{z}$  using the two delta constraints. We thus obtain

$$\frac{d\sigma_1}{d\xi_p du} = \sigma_0 \bar{\alpha}_s \left[ \frac{1}{\xi_p^{1+\epsilon}} \delta(u - \hat{\tau}(1 + \xi_p)) + \frac{1}{\epsilon} \delta(\xi_p) \delta(u - \hat{\tau}) \right]. \quad (3.4.22)$$

with now  $\hat{\tau}, \xi_p, u$  running on the following ranges

$$0 < \hat{\tau} < 1, \quad 0 < \xi_p < \frac{1 - \hat{\tau}}{\hat{\tau}}, \quad 0 < u < 1. \quad (3.4.23)$$

In the high energy limit at LL $x$ , two further simplifications on Eq. (3.4.22) occur. First, the delta constraint on the rapidity can be simplified according to

$$\delta(u - \hat{\tau}(1 + \xi_p)) \approx \delta(u - \hat{\tau}); \quad (3.4.24)$$

then, the  $\xi_p$  upper limit can be confused with infinity since  $\hat{\tau} \rightarrow 0$ .

The last step that we need to carry out is the  $\epsilon$  expansion. Using the following expansion into Eq. (3.4.22)

$$\frac{1}{\xi_p^{1+\epsilon}} = -\frac{1}{\epsilon} \delta(\xi_p) + \sum_{j=0}^{\infty} \frac{(-1)^j \epsilon^j}{j!} \left[ \frac{\ln^j \xi_p}{\xi_p} \right]_+ \quad (3.4.25)$$

with the plus distribution defined as in Eq. (B.3.1), we come to

$$\frac{d\sigma_1}{d\xi_p du} = \sigma_0 \bar{\alpha}_s \left[ \frac{1}{\xi_p} \right]_+ \delta(u - \hat{\tau}). \quad (3.4.26)$$

which is our final result. To obtain the complete NLO correction for the EFT Higgs boson production at high energy we need to compute the remaining diagrams of Fig. 3.1. They are obtained from Eq. (3.4.26) by performing the replacement  $y \rightarrow -y$  which means  $u \rightarrow \frac{1}{u}$ . Therefore, the final NLO result turns out to be:

$$\frac{d\sigma_1}{d\xi_p du} = \sigma_0 \bar{\alpha}_s \left[ \frac{1}{\xi_p} \right]_+ \left( \delta(u - \hat{\tau}) + \delta\left(\frac{1}{u} - \hat{\tau}\right) \right) \quad (3.4.27)$$

We now move to the NNLO order. The diagrams contributing at this order are collected in Fig. 3.2 together with the proper collinear subtractions.

We start our computation from the diagrams of the first row. As before the contribution from the second row of diagrams is obtained from the first one by the substitution  $u \rightarrow \frac{1}{u}$ . The double differential cross section in  $d = 4 - 2\epsilon$  dimension can be written as

$$\begin{aligned} \frac{d\sigma_2}{d\xi_p du} = & \sigma_0 \frac{\bar{z}_1 \bar{z}_2}{\hat{\tau}} \delta\left(1 - \frac{\bar{z}_1 \bar{z}_2}{\hat{\tau}} + \bar{\xi}_1\right) \left[ \bar{\alpha}_s \frac{d\bar{z}_2}{\bar{z}_2} \frac{d\bar{\xi}_2}{\bar{\xi}_2^{1+\epsilon}} \right] \left[ \bar{\alpha}_s \frac{d\bar{z}_1}{\bar{z}_1} \frac{d\bar{\xi}_1}{\bar{\xi}_1^{1+\epsilon}} \right] \\ & \delta(\bar{\xi}_1 - \xi_p) \delta(u - \bar{z}_1 \bar{z}_2) \\ & + \sigma_0 \bar{\alpha}_s^2 \left[ \frac{1}{2\epsilon^2} \delta(\xi_p) \delta(u - \hat{\tau}) + \frac{1}{\epsilon} \left[ \frac{1}{\xi_p^{1+\epsilon}} \delta(u - \hat{\tau}(1 + \xi_p)) \right] \right]. \end{aligned} \quad (3.4.28)$$

with the following limits of integrations at high energy for the various quantities

$$0 < \hat{\tau} < 1, \quad \xi_p > 0, \quad 0 < u < 1, \quad 0 < \bar{z}_1, \bar{z}_2 < 1, \quad \bar{\xi}_1 > 0, \quad 0 < \bar{\xi}_2 < \bar{\xi}_1. \quad (3.4.29)$$

Now we solve the integration over  $\bar{\xi}_1, \bar{z}_1$  using the delta constraints contained in Eq. (3.4.28). We thus obtain:

$$\begin{aligned} \frac{d\sigma_2}{d\xi_p du} = & \sigma_0 \bar{\alpha}_s^2 \left[ \frac{d\bar{z}_2}{\bar{z}_2} \frac{d\bar{\xi}_2}{\bar{\xi}_2^{1+\epsilon}} \right] \frac{1}{\xi_p^{1+\epsilon}} \delta(u - \hat{\tau}(1 + \xi_p)) \\ & + \sigma_0 \bar{\alpha}_s^2 \left[ \frac{1}{2\epsilon^2} \delta(\xi_p) \delta(u - \hat{\tau}) + \frac{1}{\epsilon} \left[ \frac{1}{\xi_p^{1+\epsilon}} \delta(u - \hat{\tau}(1 + \xi_p)) \right] \right] \end{aligned} \quad (3.4.30)$$

with now the integration limits given by

$$0 < \hat{\tau} < 1, \quad 0 < \xi_p < \frac{1 - \hat{\tau}}{\hat{\tau}} \approx \infty, \quad 0 < u < 1, \quad u < \bar{z}_2 < 1, \quad 0 < \bar{\xi}_2 < \xi_p. \quad (3.4.31)$$

By performing the integrations over  $\bar{z}_2$  and  $\bar{\xi}_2$  we obtain

$$\begin{aligned} \frac{d\sigma_2}{d\xi_p du} &= \sigma_0 \bar{\alpha}_s^2 \ln \frac{1}{u} \left[ -\frac{1}{\epsilon} \frac{1}{\xi_p^{1+2\epsilon}} \delta(u - \hat{\tau}(1 + \xi_p)) \right] \\ &+ \sigma_0 \bar{\alpha}_s^2 \left[ \frac{1}{2\epsilon^2} \delta(\xi_p) \delta(u - \hat{\tau}) + \frac{1}{\epsilon} \left[ \frac{1}{\xi_p^{1+\epsilon}} \delta(u - \hat{\tau}(1 + \xi_p)) \right] \right]. \end{aligned} \quad (3.4.32)$$

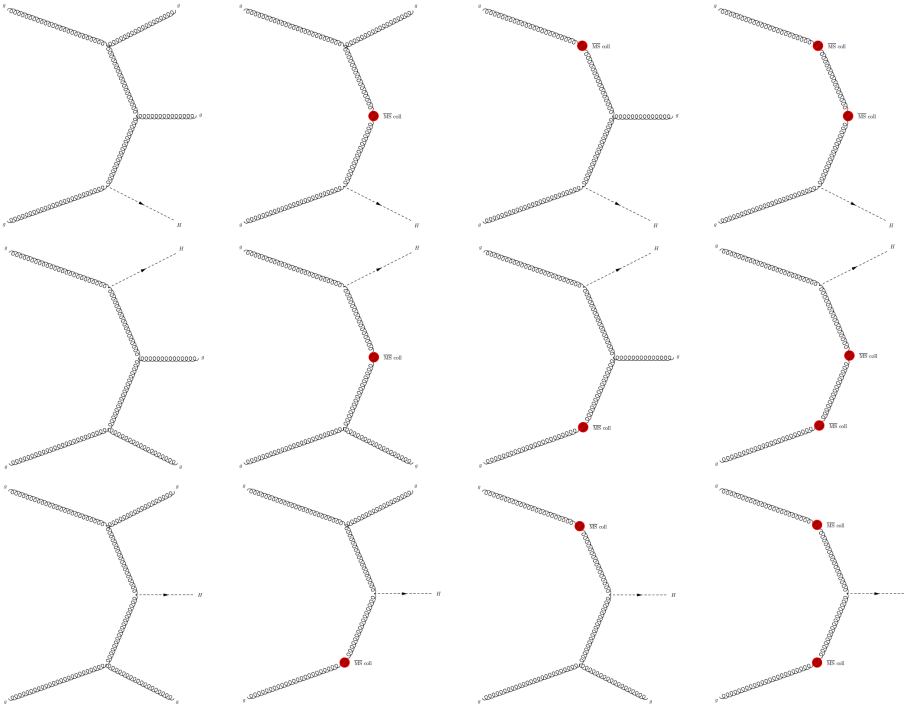
The last step is to use equality Eq. (3.4.25) twice to expand the result around  $\epsilon = 0$ . At the end, we need also to simplify the delta constraint according to Eq. (3.4.24). We write

$$\frac{d\sigma_2}{d\xi_p du} = \sigma_0 \bar{\alpha}_s^2 \ln \frac{1}{u} \left[ \frac{\ln \xi_p}{\xi_p} \right]_+ \delta(u - \hat{\tau}) \quad (3.4.33)$$

which is the final contribution to the double differential cross section from the diagrams of the first row of Fig. 3.2. As said before, the contribution from the second row is obtained from Eq. (3.4.33) by performing the substitution  $u \rightarrow \frac{1}{u}$ .

Then, we have to evaluate graphs of the third row of Fig. 3.2. Their contribution to the double differential cross section in  $d = 4 - 2\epsilon$  dimension at high energy turns out to

**Table 3.2.** NNLO Feynman Diagrams and  $\overline{\text{MS}}$  subtraction



be:

$$\begin{aligned} \frac{d\sigma_2}{d\xi_p du} &= \sigma_0 \frac{z\bar{z}}{\hat{\tau}} \delta\left(1 - \frac{z\bar{z}}{\hat{\tau}} + \xi_p\right) \left[\bar{\alpha}_s \frac{dz}{z} \frac{d\xi}{\xi^{1+\epsilon}}\right] \left[\bar{\alpha}_s \frac{d\bar{z}}{\bar{z}} \frac{d\bar{\xi}}{\bar{\xi}^{1+\epsilon}}\right] \cos^2 \theta \frac{d\theta}{2\pi} \\ &\quad \delta\left(\xi_p - \xi - \bar{\xi} - 2\sqrt{\xi\bar{\xi}} \cos \theta\right) \delta\left(u - \frac{\bar{z}}{z}\right) \\ &\quad + \frac{\sigma_0 \bar{\alpha}_s^2}{u} \left[\frac{1}{\epsilon} \frac{1}{\xi_p^{1+\epsilon}} + \frac{1}{2\epsilon^2} \delta(\xi_p)\right] \end{aligned} \quad (3.4.34)$$

The integration domain is composed by two disjointed regions

$$\begin{aligned} 0 < \hat{\tau} < 1, & & 0 < \hat{\tau} < 1 \\ \hat{\tau} < u < 1, & \cup & 1 < u < \frac{1}{\hat{\tau}} \\ 0 < \xi_p < \frac{u}{\hat{\tau}} - 1, & & 0 < \xi_p < \frac{1}{u\hat{\tau}} - 1. \end{aligned} \quad (3.4.35)$$

and  $\bar{\xi}, \xi > 0$ ,  $0 < z, \bar{z} < 1$ ,  $0 < \theta < 2\pi$ . We are going to compute next steps limiting ourselves to the first region. The complete result is obtained by symmetrizing the final expression with respect to the transformation  $u \rightarrow \frac{1}{u}$ . Moreover, Eq. (3.4.34) is invariant under exchange of  $\xi$  and  $\bar{\xi}$ . We can thus halve the integration region by requiring  $\xi > \bar{\xi}$  and recover the other part by exploiting this symmetry. We then perform the following change of variables:

$$\xi = \xi_p \xi_1, \quad \bar{\xi} = \xi_p w \xi_1, \quad \cos \theta = t, \quad (3.4.36)$$

with

$$\xi_1 > 0, \quad 0 < w < 1, \quad -1 < t < 1. \quad (3.4.37)$$

Using this new set of integration variables and using the delta constraints to eliminate integrations over  $z$  and  $\bar{z}$ , we rewrite Eq. (3.4.34) as:

$$\begin{aligned} \frac{d\sigma_2}{d\xi_p du} &= \frac{2\sigma_0 \bar{\alpha}_s^2}{\pi u} \frac{1}{\xi_p^{1+2\epsilon}} \frac{dw}{w^{1+\epsilon}} \frac{d\xi_1}{\xi_1^{1+2\epsilon}} \frac{t^2 dt}{\sqrt{1-t^2}} \delta(1 - \xi_1 (1 + w + 2\sqrt{wt})) \\ &\quad + \frac{\sigma_0 \bar{\alpha}_s^2}{u} \left[\frac{1}{\epsilon} \frac{1}{\xi_p^{1+\epsilon}} + \frac{1}{2\epsilon^2} \delta(\xi_p)\right]. \end{aligned} \quad (3.4.38)$$

Next step is to use the last delta constraint to solve integration over  $\xi_1$ . Performing the integrations over  $w$  and  $t$  we obtain:

$$\begin{aligned} \frac{d\sigma_2}{d\xi_p du} &= \frac{\sigma_0 \bar{\alpha}_s^2}{\pi u} \frac{1}{\xi_p^{1+2\epsilon}} \left[ \int_{-1}^1 \frac{2t^2 dt}{\sqrt{1-t^2}} \int_0^1 dw \frac{(1+w+2\sqrt{wt})^{2\epsilon} - 1}{w^{1+\epsilon}} - \frac{\pi}{\epsilon} \right] \\ &\quad + \frac{\sigma_0 \bar{\alpha}_s^2}{u} \left[\frac{1}{\epsilon} \frac{1}{\xi_p^{1+\epsilon}} + \frac{1}{2\epsilon^2} \delta(\xi_p)\right] \end{aligned} \quad (3.4.39)$$

$$= \frac{\sigma_0 \bar{\alpha}_s^2}{u} \frac{1}{\xi_p^{1+2\epsilon}} \left[-\frac{1}{\epsilon} - \epsilon + \mathcal{O}(\epsilon^2)\right] + \frac{\sigma_0 \bar{\alpha}_s^2}{u} \left[\frac{1}{\epsilon} \frac{1}{\xi_p^{1+\epsilon}} + \frac{1}{2\epsilon^2} \delta(\xi_p)\right] \quad (3.4.40)$$

Finally we come to the desired final result by expanding in  $\epsilon = 0$  using relation Eq. (3.4.25)<sup>2</sup>. We obtain (recovering also the other region):

$$\frac{d\sigma_2}{d\xi_p du} = \sigma_0 \bar{\alpha}_s^2 \left\{ \left[ \left( \left[ \frac{\ln \xi_p}{\xi_p} \right]_+ + \frac{1}{2} \delta(\xi_p) \right) \frac{\Theta(1-u)}{u} + \left[ u \leftrightarrow \frac{1}{u} \right] \right\}. \quad (3.4.41)$$

Performing the sum we obtain the full NNLO:

$$\begin{aligned} \frac{d\sigma_2}{d\xi_p du} = \sigma_0 \bar{\alpha}_s^2 \left\{ \left[ \ln \frac{1}{u} \left[ \frac{\ln \xi_p}{\xi_p} \right]_+ \delta(u - \hat{\tau}) + \frac{1}{u} \left[ \frac{\ln \xi_p}{\xi_p} \right]_+ \right. \right. \\ \left. \left. + \frac{1}{2u} \delta(\xi_p) \right] \Theta(1-u) + \left[ u \leftrightarrow \frac{1}{u} \right] \right\}. \end{aligned} \quad (3.4.42)$$

Eq. (3.4.27) and Eq. (3.4.42) represent the high energy limit of the NLO and NNLO respectively in momentum space. By taking Mellin-Fourier transform with respect to  $x$  (or  $\hat{\tau}$  since there is no difference at LL $x$ ) and  $y$ , they need to coincide with  $C_1$  and  $C_2$ , Eqs. (3.4.18).

Fourier transform with respect to  $y$  can be rewritten in terms of  $u$  as

$$\int_{-\ln x}^{\ln x} dy e^{-iby} \frac{d\sigma}{dy d\xi_p} = \int_{\frac{1}{x}}^x du u^{-\frac{ib}{2}} \frac{1}{2u} \frac{d\sigma}{dy d\xi_p} = \int_{\frac{1}{x}}^x du u^{-\frac{ib}{2}} \frac{d\sigma}{du d\xi_p}. \quad (3.4.43)$$

With straightforward calculations, we obtain in Mellin-Fourier space

$$\frac{d\sigma_1}{d\xi_p dy}(N, b, \xi_p, \alpha_s) = \sigma_0 \alpha_s \frac{C_A}{\pi} \left[ \frac{1}{\xi_p} \right]_+ \left( \frac{1}{N - \frac{ib}{2}} + \frac{1}{N + \frac{ib}{2}} \right) \quad (3.4.44)$$

for the NLO and

$$\frac{d\sigma_1}{d\xi_p dy}(N, b, \xi_p, \alpha_s) = \sigma_0 \alpha_s^2 \left( \frac{C_A}{\pi} \right)^2 \left\{ \left[ \frac{\ln \xi_p}{\xi_p} \right]_+ \left( \frac{1}{N - \frac{ib}{2}} + \frac{1}{N + \frac{ib}{2}} \right)^2 + \frac{1}{N^2 + \frac{b^2}{4}} \delta(\xi_p) \right\} \quad (3.4.45)$$

for the NNLO. The final results in Mellin-Fourier space are in perfect agreement with our predictions Eqs. (3.4.18), giving in this way a strong cross-check on the whole construction.

Moreover, our final results permit also to check expansions at first orders for the resummed single rapidity or transverse momentum distribution of Refs. [76, 77], or for the resummed total cross section of Ref. [72]. Indeed by integrating over  $y$  - thus setting  $b = 0$  in Fourier space - we recover high energy behaviour of transverse momentum distribution [77]; while performing integration over  $\xi_p$  using Eq. (1.4.18) we obtain

$$\frac{d\sigma_1}{d\xi_p dy}(N, b, \alpha_s) = \sigma_0 \alpha_s \frac{C_A}{\pi} \frac{1}{N} \left( \frac{1}{N - \frac{ib}{2}} + \frac{1}{N + \frac{ib}{2}} \right) + \mathcal{O}\left(\frac{1}{N}\right) \quad (3.4.46)$$

$$\frac{d\sigma_1}{d\xi_p dy}(N, b, \xi_p, \alpha_s) = \sigma_0 \alpha_s^2 \left( \frac{C_A}{\pi} \right)^2 \frac{1}{N^2} \left( \frac{1}{N - \frac{ib}{2}} + \frac{1}{N + \frac{ib}{2}} \right)^2 + \mathcal{O}\left(\frac{1}{N^3}\right) \quad (3.4.47)$$

<sup>2</sup>Note that in high energy limit even in this case  $\xi_p$  upper limit can be confused with  $\infty$

which agrees with predictions of Ref. [76]. It is interesting to note that the second term of Eq. (3.4.42) ( or Eq. (3.4.18c)) which is not subleading at fixed  $\xi_p$ , becomes subleading after  $\xi_p$  integration. This is due to the pointlike nature of the effective interaction.

Finally, the complete integration over  $y$  and  $\xi_p$  clearly recover known result for the total cross section.

In conclusion, in this chapter we cover all recent developments in the theory of high energy resummation. Research efforts have been performed in the last years to extend this resummation theory at  $LLx$  accuracy to more exclusive observables. We have presented the resummation for single transverse momentum distributions and for double differential distributions. Moreover we have discussed analogies and differences when coloured particles appear in the final state. As an example we compute high energy resummation for EFT Higgs boson production in gluon fusion and we crosscheck our prediction against fixed order evaluation up to NNLO.

# 4 Phenomenology

## Contents

---

<b>4.1 Combined Resummation for Higgs at LHC13.</b>	<b>132</b>
4.1.1 Resummation Prescriptions in Literature	133
4.1.2 A Prescription for Combined Resummation	136
4.1.3 Higgs boson resummed transverse momentum distribution	139
<b>4.2 Higgs Quark Mass Effects at High Energy.</b>	<b>141</b>
4.2.1 Standard Model Higgs $p_T$ -Impact Factor	144
4.2.2 Validation of the high-energy approximation	148
4.2.3 Top Mass Effect at NLO on Higgs spectrum	153

---

In this chapter, we are going to describe some phenomenological implications of our studies. In particular we focus our attention on LHC collider physics, by presenting all the results for a proton-proton collider at 13 TeV.

The main applications contained in this chapter are: the combined resummation at NNLL for the Higgs boson production case, and a study, performed through a high energy expansion, about the quark mass impact on the Higgs boson transverse momentum distribution.

For the first application, we point out that the results presenting in this thesis are preliminary and incomplete, since research work is still ongoing. We are going to present resummed results but without any type of matching with a fixed order calculation yet. However, no difficulties are present in principle in the matching procedure and the complete analysis will be published soon. For the same reason also a complete study about the factorization and renormalization scale dependence is absent. Nevertheless, our analytic expressions of Sec. 2 and Appendix C contain all the scale dependent terms and the inclusion of factorization and renormalization scale variation is in fact very straightforward using the results of this thesis.

Even if our phenomenological analysis about combined resummation is still incomplete, the derivation of the resummed transverse momentum distribution is far to be trivial, due to the Landau pole problem. Hence, in the section dedicated to this application we will show you a possible solution to the inversion problem. The final result will

own all the properties we required and some interesting features we are going to highlight in a while.

The Chapter will be divided as follows: in Sec. 4.1, we focus on the combined resummation, on its inversion problem and we present a concrete solution together with phenomenological results for the Higgs boson transverse momentum distribution at LHC13; then in Sec. 4.2, we move to the high- $p_T$  limit of the Higgs spectrum which is now becoming available to experimentalist for the first time at LHC13. In this region, effective field theory approach starts to fail and the inclusion of mass quark effects becomes essential. However, the hardness in fixed order evaluations prevents to calculate the complete process beyond the first not trivial order. A lot of work has been made in this field in the last three years [91–100] to properly approximate higher order mass quark effects; one of the solution proposed [95] is the approximation of these effects using high energy resummation. Phenomenological results of this idea will be exposed in Sec. 4.2.3.

## 4.1 Combined Resummation for Higgs at LHC13

Our objective in this section is to compute the hadronic Higgs boson transverse momentum distribution resummed in the combined soft and collinear region. The resummed expression is given by Eq. (2.6.1) and it is composed by two contributions: the consistent transverse momentum resummation,  $\frac{d\hat{\sigma}_{ij}^{\text{cons}}}{d\xi_p}$ , and the threshold resummation at fixed  $p_T$ ,  $\frac{d\hat{\sigma}_{ij}^{\text{th}}}{d\xi_p}$ . While threshold resummation at fixed  $p_T$  is a function of  $\xi_p$  and  $N$ , consistent transverse momentum resummation presents an extra subtlety, since it is expressed in Eq. (2.5.45) as the inverse Fourier transform of a particular  $N$  and  $b$  expression.

The evaluation of the inverse Mellin (and Fourier) transform is far to be trivial due to the presence of several divergences in our expressions. We are going to present the general problem by looking to threshold resummation at fixed  $p_T$  where the situation is simpler. Resummed expression Eq. (2.3.1) shows two logarithmic branch cuts in the complex plane on the real axis for

$$N > e^{\frac{1}{2\alpha_s\beta_0}}, \quad (4.1.1a)$$

$$N < 0, \quad (4.1.1b)$$

plus single poles for integer value of  $N$  lower than 1 due to the particular form of  $C_0(N, \alpha_s)$ .

Mellin/Laplace inverse exists if and only if it is possible to select a convergence abscissa  $N_0$  to the *right* of all the singularities of the function. For a complete definition of the inverse Mellin (and Fourier) transform, together with all its properties we refer the interested reader to Appendix B. The presence of a logarithmic branch cut extending up to  $N \rightarrow \infty$  on the real axis made impossible the existence of such a  $N_0$ . Therefore the inverse Mellin transform of our resummed expression should not exist.

This is a known problem of resummation theories in general and it is usually called as *Landau pole problem* since the position of the cut is related to the non-perturbative scale  $\Lambda$  of the coupling (see Appendix A, Eq. (A.1.12)). Strictly speaking, this means that our resummed expression is sensitive to non-perturbative effects which are not under

control. Furthermore, it was shown [101] that the computation of the inverse Mellin transform order by order (where Landau pole problem is absent) returns a series which grows factorially. This means that by expanding the resummed result we have thrown away subleading terms that would have compensated the factorial growth. Hence not all the procedures to reach a phenomenological result bring to a meaningful one.

Summarizing, in order to define our desired hadronic resummed observable, we need a *prescription* to evaluate the inverse transform. In defining a prescription, we have to make sure that our procedure is not introducing subleading terms which grow too fast with the order of the perturbative expansion in the final physical result. Otherwise, we are destroying our prediction since it is overwhelmed by non-perturbative effects.

In the next subsection we are going to present two general prescriptions which reproduce analogue and correct results in the case of threshold resummation and standard transverse momentum resummation.

### 4.1.1 Resummation Prescriptions in Literature

The first prescription we are going to present is the most-common used and it is called *Minimal Prescription* [101, 102]. According to *Minimal Prescription*, the integration path for the inverse integral transform<sup>1</sup> has to be chosen to leave to the left all the singularities of the function *except for* the Landau cut, which remains on the right.

In the context of threshold resummation at fixed  $p_T$  this means that the minimal prescription abscissa  $N_{\text{MP}}$  can be chosen in the range

$$1 < N_{\text{MP}} < N_L = e^{\frac{1}{2\alpha_s(\mu_R^2)^{\beta_0}}}, \quad (4.1.2)$$

leading to the following expression for the hadronic transverse momentum distribution

$$\frac{d\sigma^{\text{res}}}{d\xi_p}(\tau, \xi_p, \alpha_s(\mu_R^2), \mu_R^2, \mu_F^2) = \frac{1}{2\pi i} \sum_{ij} \int_{N_{\text{MP}} - i\infty}^{N_{\text{MP}} + i\infty} dN \tau^{-N} \mathcal{L}_{ij}(N, \mu_F^2) \frac{d\hat{\sigma}_{ij}^{\text{th}}}{d\xi_p}(N, \xi_p, \alpha_s(\mu_R^2), \mu_R^2, \mu_F^2) \quad (4.1.3)$$

with  $\frac{d\hat{\sigma}_{ij}^{\text{th}}}{d\xi_p}$  given by Eq. (2.3.1) (or Eq. (2.7.28) in the case of Higgs boson production) and  $\mathcal{L}_{ij}$  the PDFs luminosity.

It can be proved that the minimal result Eq. (4.1.3) owns the following properties [101]:

- The following series

$$\frac{d\sigma_{ij}^{\text{res}}}{d\xi_p}(\tau) = \sum_{k=0}^{\infty} \int_{N_{\text{MP}} - i\infty}^{N_{\text{MP}} + i\infty} dN \tau^{-N} \mathcal{L}_{ij}(N) \Sigma_k(N) \quad (4.1.4)$$

<sup>1</sup>Mellin transform for threshold resummation or Fourier transform for transverse momentum resummation

with

$$\frac{d\hat{\sigma}_{ij}^{\text{th}}}{d\xi_p}(N) = \sum_{k=0}^{\infty} \Sigma_k(N) = \sum_{k=0}^{\infty} h_k \lambda_{\bar{N}}^k \quad (4.1.5)$$

and  $\lambda_{\bar{N}} = \alpha_s \beta_0 \ln \bar{N}^2$  converges asymptotically to the minimal prescription result.

- The coefficients of the series (4.1.4) do not grow factorially.
- If we truncate the series at an order in  $\alpha_s$  where its terms are at the minimum, the difference between the truncate expansion and the full MP result is suppressed by the factor

$$e^{-H(1-\tau)\frac{Q}{\Lambda}} \quad (4.1.6)$$

with  $H$  a slowly varying positive function.

The presence of the Landau pole scale  $\Lambda$  in the factor (4.1.6) reflects the fact that the difference between expanded and resummed expressions probes the non-perturbative dynamics. Our hope is these effects to be small comparing to our perturbative prediction. This is in fact the case since all these non-perturbative effects come suppressed by the factor (4.1.6) which is stronger than any power behaviour.

In conclusion, the Minimal Prescription gives back a resummed hadronic result which catches all the leading logarithmic behaviour without introducing spurious large non-perturbative effects. We have presented the explicit procedure in the case of threshold resummation and inverse Mellin transform but the same prescription can be also extended to transverse momentum resummation and to Fourier transform. We do not wish to go into detail about the particular construction in this case, referring the interested reader to the original Ref. [102].

However, Minimal Prescription is not the only possible solution. In more recent years, a new approach was proposed in Ref. [103, 104] based on the theory of divergent series. Indeed, as we have just seen, the series obtained by expanding in power of  $\lambda_{\bar{N}}$ , Eq. (4.1.4) is divergent. This is a consequence of the Landau pole problem. The Minimal Prescription permits to compute the asymptotic result, the divergent series is tending to. The idea of Ref. [103, 104] is instead to sum the divergent series using the Borel transform formalism. For this reason, the prescription proposed in Ref. [103, 104] is usually called *Borel Prescription*.

Our starting point is the series Eq. (4.1.4). We rewrite it as

$$\begin{aligned} \frac{d\sigma_{ij}^{\text{res}}}{d\xi_p}(\tau) &= \sum_{k=0}^{\infty} \int_{N_0-i\infty}^{N_0+i\infty} dN \tau^{-N} \mathcal{L}_{ij}(N) \Sigma_k(N), \\ &= \sum_{k=0}^{\infty} \int_{N_0-i\infty}^{N_0+i\infty} dN \tau^{-N} \mathcal{L}_{ij}(N) h_k \bar{\alpha}_s^k \ln^k \bar{N} \end{aligned} \quad (4.1.7)$$

where  $\bar{\alpha}_s = \alpha_s \beta_0$  and in the second line we explicit the  $\alpha_s$  dependence of  $\Sigma_k$ .

However, as we have already understood, Eq. (4.1.7) contains a divergent series which is only asymptotic to the desired result.

Nevertheless, the divergence in the series representation Eq. (4.1.7) can be removed by performing a Borel transform with respect to  $\bar{\alpha}_s$ , permitting us to reach a closed form

for our hadronic distribution, even if in Borel space. We are going to call  $w$  the Borel variable associated to  $\bar{\alpha}_s$ . The effect of the divergence of the original series appears again when we want to recover the desired result by performing the inverse Borel transform

$$\frac{d\sigma_{ij}^{\text{res}}}{d\xi_p}(\tau) = \int_0^\infty dw e^{-\frac{w}{\bar{\alpha}_s}} \frac{d\sigma_{ij}^{\text{res}}}{d\xi_p}(\tau, w) \quad (4.1.8)$$

since this integral diverges in the  $w \rightarrow \infty$  limit.

The *Borel prescription* states that a valid resummed expression in  $\tau$  space can be achieved by extending integral of Eq. (4.1.8) only up to some bound  $C$ . In this way we are cutting off the singularity of the Borel integral located at infinity. In formula, the resummed transverse momentum distribution turns out to be:

$$\frac{d\sigma_{ij}^{\text{BP}}}{d\xi_p}(\tau) = \int_0^C dw e^{-\frac{w}{\bar{\alpha}_s}} \frac{d\sigma_{ij}^{\text{res}}}{d\xi_p}(\tau, w) \quad (4.1.9)$$

It can be proved [103, 104] that the Borel prescription result owns the following properties:

- the difference between the divergence series and the Borel prescription result vanishes faster than any power of  $\alpha_s$  as  $\alpha_s \rightarrow 0$ .
- the original series Eq. (4.1.7) is an asymptotic expansion of the final result Eq. (4.1.9).
- the value of the cut-off  $C$  is related to the  $\mathcal{O}\left(\frac{\Lambda^2}{Q^2}\right)$  we are including in the result. In this sense *Borel prescription* is discarding non-perturbative higher twist contributions. Region beyond  $w = C$  is equivalent to including a twist- $t$  contribution to our resummed perturbative expression with

$$t = 2 + 2C \quad (4.1.10)$$

and  $C$  the value of the cut-off.

All these properties state that also *Borel Prescription* is a meaningful prescription to perform the inverse transform without discarding important non-perturbative contributions. Even this time all the discussion just presented is in the context of threshold resummation but the same procedure can be extended to transverse momentum resummation as performed in Ref. [104]

Phenomenological analysis [103, 104] show that the difference between Minimal and Borel prescriptions is in fact very small and only located very close to the singularity. This is a very remarkable result because it assures our resummed construction to be on solid ground and almost independent on non-perturbative effects.

We have presented these two prescriptions because we are going to use both of them to produce a meaningful prescription in the case of combined resummation. To the construction of a meaningful resummed formula in  $x, \xi_p$  space for the combined resummation of Sec. 2.6 will be devoted the next subsection.

## 4.1.2 A Prescription for Combined Resummation

As said in the previous sections, the combined resummation is a proper combination of two different resummations: consistent transverse momentum resummation and threshold resummation at fixed  $p_T$ .

Threshold resummation at fixed  $p_T$ , Eq. (2.3.1) is a function of  $N$  and  $\xi_p$  with divergences in Mellin space only on the real axis. Minimal prescription Eq. (4.1.3) can be applied without any problem by selecting  $N_{\text{MP}}$  in the range Eq. (4.1.2).

The integral inversion of consistent transverse momentum resummation, however, represents a harder task. Indeed,  $\frac{d\hat{\sigma}_{ij}^{\text{cons}}}{d\xi_p}(N, \xi_p)$  is written as the inverse Fourier transform of a particular function  $\frac{d\hat{\sigma}_{ij}^{\text{cons}}}{d\xi_p}(N, b)$  in Mellin-Fourier space. Singularities structure in  $N$ - $b$  space of Eq. (2.5.45) or Eq. (2.5.48) is complicated by the particular form of the function  $\chi$ . In addition to the two Landau pole logarithmic branch cut,

$$\text{Re}(N) > N_L = e^{\frac{1}{2\alpha_s\beta_0}} \quad \text{Im}(N) = 0, \quad (4.1.11)$$

$$\text{Re}\left(N^2 + \frac{b^2}{4}\right) > e^{\frac{1}{\alpha_s\beta_0}} \quad \text{Im}\left(N^2 + \frac{b^2}{4}\right) = 0, \quad (4.1.12)$$

consistent resummation presents an additional logarithmic branch cut,

$$\text{Re}\left(N^2 + \frac{b^2}{4}\right) < 0 \quad \text{Im}\left(N^2 + \frac{b^2}{4}\right) = 0 \quad (4.1.13)$$

due to the existence of the logarithm of the soft scale  $\chi$ .

Unfortunately, here we are no longer able to apply the *Minimal Prescription*, since it does not exist a contour deformation in  $N$ - $b$  space which manages to leave all the singularities on the left and the Landau cuts on the right.

Even if one can think that our resummation is dominated by non-perturbative effects, and thus not meaningful, this will be an incorrect statement. Due to its simplicity, *Minimal Prescription* is often considered as the unique prescription to invert and give sense to a resummed expression in conjugate space; but this is not true and it is not guaranteed that it has to work for all the resummed expressions.

In Refs. [61–63], the authors arrive to similar conclusions for the joint resummation but in order to be able to apply the usual *Minimal Prescription* technique they decide to modify their resummed expression by substituting  $\chi$  with a phenomenological  $\chi_{\text{ph}}$

$$\chi_{\text{ph}}(\eta) = \frac{b}{b_0} + \frac{\bar{N}}{1 + \eta \frac{b}{b_0 \bar{N}}} \quad (4.1.14)$$

with  $\eta$  a phenomenological arbitrary parameter. Singularity structure permits now to deform integration path in order to meet the assumptions of Minimal Prescription. The general prescription adopted is discussed in detail for example in Ref. [61].

We do not agree with this approach. Our general analysis about phase space decomposition in the small- $p_T$  regime at threshold shows that the further contributions we have to resum are combinations of  $\frac{N}{b}$  but only with *even* powers. This is reflected in the

particular form of our  $\chi$ . The phenomenological  $\chi_{\text{ph}}$  introduces instead also spurious *odd* power of the ratio  $\frac{N}{b}$  which are totally non-physical. Even if you can select, as performed in Refs. [62, 63], a value of  $\eta$  which cancels the first spurious term  $\frac{N}{b}$  higher odd powers remains in the final results.

In conclusion, in Ref. [61–63], minimal prescription is applied by inserting spurious perturbative contributions in the resummed expression which permits to deform the integration path accordingly. The size of these spurious effects is now object of investigation.

We decide to select another path. Our idea is not to touch our resummed expression but to change the resummation prescription. In this way we are not introducing perturbative contributions but we are changing only the size of non-perturbative effects which, however, we know to be small. We discard *Minimal Prescription* and we try to apply on our resummed expression *Borel Prescription*.

Our starting point is consistent transverse momentum resummation in  $N$ - $b$  space given by Eq. (2.5.45) (or Eq. (2.7.1) in the case of Higgs boson production) which we can write as a series expansion in  $\lambda_\chi$ . By defining

$$\frac{d\hat{\sigma}_{ij}^{\text{cons}}}{d\xi_p}(N, \xi_p, \alpha_s) = \int_0^\infty db \frac{b}{2} J_0(\hat{b}\sqrt{\xi_p}) \left(\sqrt{1+\xi_p} - \sqrt{\xi_p}\right)^{-2N} \Sigma(N, \lambda_\chi, \alpha_s),$$

$$= \left(\sqrt{1+\xi_p} - \sqrt{\xi_p}\right)^{-2N} \bar{\Sigma}(N, \xi_p, \alpha_s) \quad (4.1.15)$$

$$(4.1.16)$$

where we suppress all the dependence from  $\mu_R$  and  $\mu_F$  for simplicity, we can write the following expansion for  $\Sigma$

$$\Sigma(N, \lambda_\chi, \alpha_s) = \sum_{k=0}^{\infty} h_k(N, \alpha_s) \lambda_\chi^k = \sum_{k=0}^{\infty} h_k(N, \alpha_s) \bar{\alpha}_s \ln^k \chi \quad (4.1.17)$$

with  $h_k(N, \alpha_s)$  expansion coefficients *independent* from  $b$ . This is possible since all the  $b$  dependence in the resummed expression is through the combination  $\chi$ .

Now we perform the inverse Fourier transform of  $\Sigma(N, \lambda_\chi, \alpha_s)$  term by term using the following result:

$$\int_0^\infty db \frac{b}{2} J_0(\hat{b}\sqrt{\xi_p}) \ln^k \left(\bar{N}^2 + \frac{b^2}{b_0^2}\right) = \frac{\partial^k}{\partial \epsilon^k} \int_0^\infty db \frac{b}{2} J_0(\hat{b}\sqrt{\xi_p}) \left(\bar{N}^2 + \frac{b^2}{b_0^2}\right)^\epsilon \Bigg|_{\epsilon \rightarrow 0}$$

$$= \frac{\partial^k}{\partial \epsilon^k} M(N, \xi_p, \epsilon) \Bigg|_{\epsilon \rightarrow 0} \quad (4.1.18)$$

with

$$M(N, \xi_p, \epsilon) = \frac{2N^{1+\epsilon} \xi_p^{-\frac{1}{2}-\frac{\epsilon}{2}} K_{1+\epsilon}(2N\sqrt{\xi_p})}{\Gamma(-\epsilon)} e^{2\gamma_E \epsilon} \quad (4.1.19)$$

and  $K$  modified Bessel function of the second kind. Eq. (4.1.19) has been simplified by using the fact that all the integration path of the Mellin inverse transform lies in the semi-plane  $\text{Re}(N) > 0$ .

We are now ready to switch to Borel space and to perform some tricks to reach our final result. First we take Borel transform with respect to  $\bar{\alpha}_s$  obtaining

$$\bar{\Sigma}(N, \xi_p, \omega, \alpha_s) = \sum_{k=0}^{\infty} h_k(N, \alpha_s) \frac{w^{k-1}}{(k-1)!} \frac{\partial^k}{\partial \epsilon^k} M(N, \xi_p, \epsilon) \Big|_{\epsilon=0}; \quad (4.1.20)$$

then we rewrite partial derivative w.r.t.  $\epsilon$  as a contour integral around the origin, using the result

$$\frac{\partial^k}{\partial \epsilon^k} M(N, \xi_p, \epsilon) \Big|_{\epsilon=0} = \frac{k!}{2\pi i} \oint_H \frac{d\xi}{\xi^{1+k}} M(N, \xi_p, \xi) \quad (4.1.21)$$

with  $H$  a contour which encloses the origin. Finally we perform the inverse Borel transform to reach our final result for  $\bar{\Sigma}(N, \xi_p, \alpha_s)$ , the inverse Fourier transform of  $\Sigma(N, \lambda_\chi, \alpha_s)$ :

$$\begin{aligned} \bar{\Sigma}(N, \xi_p, \alpha_s) &= \frac{1}{2\pi i} \int_0^\infty dw e^{-\frac{w}{\bar{\alpha}_s}} \oint_H \frac{d\xi}{\xi^2} M(N, \xi_p, \xi) \sum_{k=0}^{\infty} k h_k(N, \alpha_s) \left(\frac{w}{\xi}\right)^{k-1} \\ &= \frac{1}{2\pi i} \int_0^\infty dw e^{-\frac{w}{\bar{\alpha}_s}} \oint_H \frac{d\xi}{\xi} \frac{\partial}{\partial w} \Sigma\left(N, \frac{w}{\xi}, \alpha_s\right), \end{aligned} \quad (4.1.22)$$

where in the second step we use

$$\sum_{k=0}^{\infty} k h_k(N, \alpha_s) \left(\frac{w}{\xi}\right)^{k-1} = \xi \frac{\partial}{\partial w} \Sigma\left(N, \frac{w}{\xi}, \alpha_s\right). \quad (4.1.23)$$

Now, a resummed expression for  $\frac{d\hat{\sigma}_{ij}^{\text{cons}}}{d\xi_p}$  in  $N, \xi_p$  space can be obtained following these steps. First we insert Eq. (4.1.22) into Eq. (4.1.16), then we integrate by parts in  $w$  and finally we apply the *Borel Prescription* cutting off  $w$  inverse Borel integral up to some fixed value  $C$ . Last two steps would have been performed in the opposite order, leading to a difference but equivalent Borel prescription [104]. Numerically we have not found differences between the two approaches and then we decide to present results only for one procedure for simplicity.

In formula we obtain:

$$\begin{aligned} \frac{d\hat{\sigma}_{ij}^{\text{cons}}}{d\xi_p}(N, \xi_p, \alpha_s) &= \frac{1}{2\pi i} \int_0^C dw e^{-\frac{w}{\bar{\alpha}_s}} \frac{1}{\bar{\alpha}_s} \left( \sqrt{1 + \xi_p} - \sqrt{\xi_p} \right)^{2N} \\ &\quad \oint_H \frac{d\xi}{\xi} M(N, \xi_p, \xi) \Sigma\left(N, \frac{w}{\xi}\right). \end{aligned} \quad (4.1.24)$$

Our inversion procedure is not concluded yet, since we still need to get rid of the inverse Mellin transform. However, by inspecting singularities of Eq. (4.1.24), we can prove that they are completely equal to the one of threshold resummation at fixed  $p_T$ , Eq. (4.1.1). Therefore, we are now able to construct our combined expression, to add PDFs luminosities and then to use the *Minimal Prescription* on the  $N$  inversion integral to reach the desired final hadronic result.

Summarizing, we have found a possible prescription for our combined resummation, based on a combination of a *Minimal Prescription* in  $N$  space and a *Borel Prescription* in  $b$  space to solve the double inverse transform. This procedure gives back a final hadronic distribution which contains small non-perturbative effects and no spurious perturbative contributions.

In the next subsection, we are going to present numerical results for the Higgs boson transverse momentum distribution at LHC 13 TeV.

### 4.1.3 Higgs boson resummed transverse momentum distribution

We are finally ready to present the resummed Higgs boson transverse momentum distribution at LHC 13 TeV. In Fig. 4.1, we show the hadronic distribution  $\frac{d\sigma}{dp_T}$  resummed at LL, NLL, and NNLL logarithmic accuracy using our combined expression Eq. (2.6.1) (red/dashed line).

We compare our predictions with standard transverse momentum resummation at LL, NLL and NNLL accuracy of Ref. [30] (black/dotted line). In this implementation of Collins-Soper-Sterman resummation, large-medium- $p_T$  range is constructed by imposing the *unitarity constraint* [30]. Therefore the integral of the NNLL CSS resummation is set equal to the integral of its hard part.

In Fig. 4.1, we show also separately the two components which form our combination, consistent transverse momentum resummation (blue/solid line) and threshold resummation at fixed  $p_T$  (orange/dot-dashed line). As you can appreciate, threshold resummation at fixed  $p_T$  starts one order logarithmic after consistent transverse momentum resummation, since  $C_0$  carries an extra power of  $\alpha_s$  in front of the exponential.

All plots are produced with  $\mu_R^2 = \mu_F^2 = m_H^2$  and with the PDF4LHC15 NNLO set of parton distributions PDF4LHC15\_nnlo\_100 [105–111], for the LHC with  $\sqrt{s} = 13$  TeV. We have accessed to PDFs sets, thanks to the general platform LHAPDF6.1 [112].

In comparing consistent small- $p_T$  resummation with original treatment, we see a larger difference at LL and NLL while the difference is almost zero at NNLL. This is well understood since threshold  $\frac{N}{b}$  components are subleading effects which become smaller and smaller by increasing logarithmic order.

Moreover, let us highlight the fact that such a small difference at NNLL is typical of the CSS small- $p_T$  resummation enforced with unitarity constraint. If another regulation of the large- $p_T$  limit, as the one proposed in Ref. [113], is used, larger difference even at NNLL appears in the medium- $p_T$  range (50-100 GeV).

Unlike standard  $p_T$  resummation, consistent small- $p_T$  resummation does not require any regulation procedure to get rid of its medium large- $p_T$  behaviour. This is due to the fact that the  $b = 0$  limit of our resummed expression coincides with the threshold resummed inclusive cross section and this fix the value of the integral of our distribution.

However, the integral of our consistent distribution is fixed up to  $\mathcal{O}\left(\frac{1}{N}\right)$  contributions; the combination of Eq. (2.6.1) with threshold resummation at fixed  $p_T$  deserves to further specify some of these subleading contributions. In medium-large- $p_T$  range our transverse momentum distribution contains the correct large- $N$  behaviour at all orders. We will see that effects of this second type of resummation, due to the matching procedure, starts

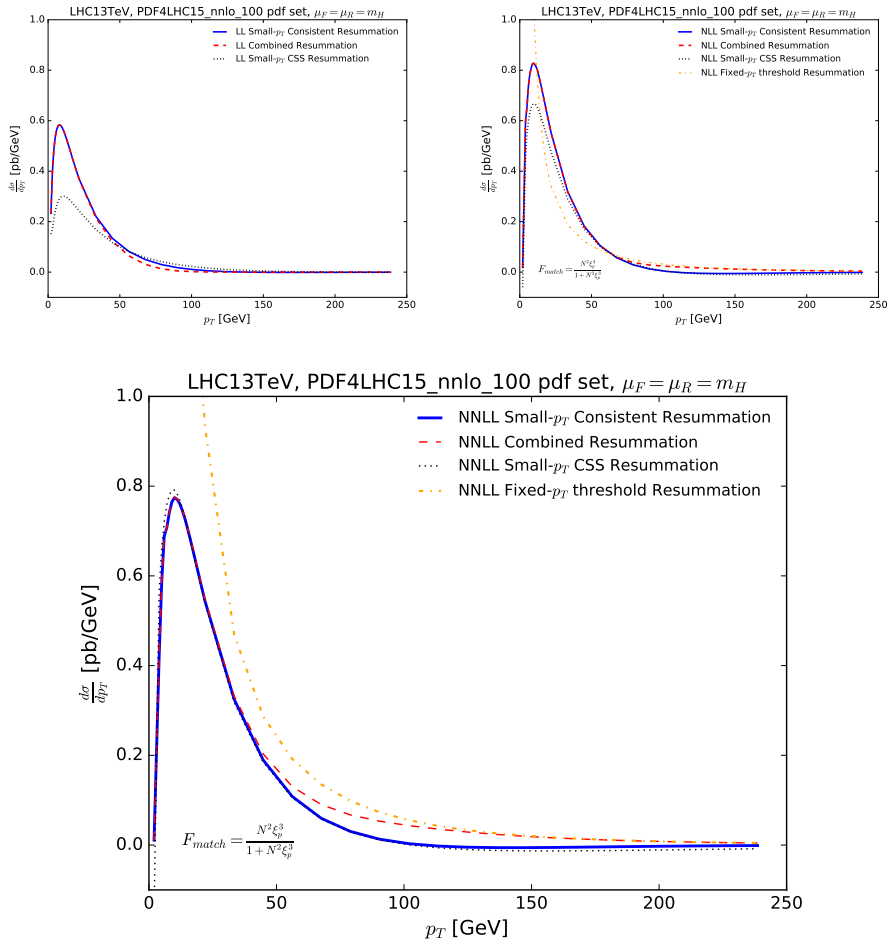


**Figure 4.1.** Plots at LL (upper-left panel), NLL (upper-right panel) and NNLL (bottom panel) of the resummed components in the following cases: consistent small- $p_T$  resummation (blue/solid line), CSS transverse momentum resummation of Ref. [30] (black/dotted line), threshold resummation at fixed  $p_T$  (orange/dot-dashed line) and combined resummation (red/dashed line).

to contribute up to 100 GeV, when consistent resummation is already turned off. The matching function used in Fig. 4.1 is Eq. (2.6.3) with  $m = 2$  and  $k = 3$ . We vary  $m$  and  $k$  value from 2 to 5 requiring only that  $k > m$ : almost no differences appears in the final combined expression. This assures us that our combination is on solid ground and does not depend too much on the particular matching procedure we adopt.

As a last comment, we plot in Fig. 4.2 the whole series LL, NLL, NNLL for the consistent small- $p_T$  resummation (left) and for the standard small- $p_T$  resummation (right). Even if NNLL central values are pretty close each other, consistent series converges better than CSS series. A better convergence of the resummed series brings to a small scale

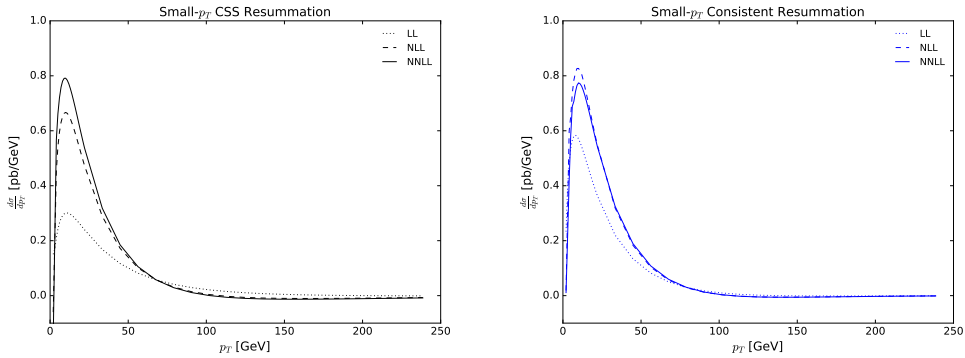


**Figure 4.2.** Whole series behaviour in the CSS case (left) and in the consistent case (right). Consistent small- $p_T$  resummation series shows a better convergence.

variation error for the final NNLL result. However, scale variation analysis is still ongoing and we will not include seven-point variation plot in this thesis.

We have presented our preliminary phenomenological results about combined resummation for the Higgs boson production process. Phenomenological analysis is up to now preliminary and incomplete and research activity is still on-going. Future outlooks include a study of the scale variation error, an analytic comparison with joint resummation of Ref. [61–63] and an extension to Drell-Yan production process. Moreover, we are going to match our result with fixed order calculations in order to produce a new resummed prediction for these processes.

We end our first application about threshold and collinear limit of transverse momentum distribution. Up to now we focus our attention on the  $p_T \lesssim m_H$  region where EFT approximation works very well. We will move in the next section to the high- $p_T$  limit of Higgs spectrum presenting a possible estimate of quark mass effects using high energy resummation.

## 4.2 Higgs Quark Mass Effects at High Energy

Up to now, we focus our attention on the Higgs transverse momentum distribution in the range of  $p_T$  where  $p_T \lesssim m_H$  is at least equal to the hard scale. In this range, Higgs boson production can be studied with reasonable accuracy by exploiting its pointlike limit, thus ignoring quark mass effects coming from the quark loop. Indeed, Higgs boson production is mainly produced at LHC via gluon fusion through the coupling with a heavy quark (top or bottom). When the mass of the quark can be considered larger than the other scale, we can shrink the quark loop by considering the gluons coupled directly with the Higgs through a pointlike interaction. Situation is drawn in Fig. 1.5.

Calculations greatly simplify and fixed order evaluations can be carried on up to even N<sup>3</sup>LO [114] at inclusive level and up to NNLO at fully differential level [115–117]. Quark mass contributions in this framework come up as a overall Wilson coefficient  $|W(\alpha_s)|^2$ ,

which rescales the LO cross section. Up to two loops it turns out to be:

$$W(\alpha_s(\mu^2)) = 1 + W_1 \alpha_s(\mu^2) + W_2 \alpha_s^2(\mu^2) + \mathcal{O}(\alpha_s^3), \quad (4.2.1a)$$

$$W_1 = \frac{11}{4\pi}, \quad (4.2.1b)$$

$$W_2 = \frac{1}{\pi^2} \left[ \frac{2777}{288} + \frac{19}{16} \ln \frac{\mu^2}{m_q^2} + N_f \left( -\frac{67}{96} + \frac{1}{3} \ln \frac{\mu^2}{m_q^2} \right) \right], \quad (4.2.1c)$$

with  $m_q$  the mass of the heavy quark.

Such a rescaled EFT cross section works very well at inclusive level [114], where quark mass effects turn out to be rather small. This is in fact not totally true since top contribution turns out to be about +7% of the N<sup>3</sup>LO correction, while top-bottom contribution comes as a negative contribution of about -5%. The sum over these effects bring to a tiny overall correction, see Tab. 4.1 [114].

$\sigma_{EFT}^{LO}$	15.05 pb	$\sigma_{EFT}^{NLO}$	34.66 pb
$R_{LO} \sigma_{EFT}^{LO}$	16.00 pb	$R_{LO} \sigma_{EFT}^{NLO}$	36.84 pb
$\sigma_{ex;t}^{LO}$	16.00 pb	$\sigma_{ex;t}^{NLO}$	36.60 pb
$\sigma_{ex;t+b}^{LO}$	14.94 pb	$\sigma_{ex;t+b}^{NLO}$	34.96 pb
$\sigma_{ex;t+b+c}^{LO}$	14.83 pb	$\sigma_{ex;t+b+c}^{NLO}$	34.77 pb

**Table 4.1.** Inclusive cross section in the rEFT framework and with full quark mass effects, up to NLO.

This situation can be well understood by looking to the transverse momentum distribution, where the situation is quite different. First of all, this accidental cancellation does not take place since top contribution starts to be important when  $p_T$  scale becomes of the same size of the top mass, while bottom-top interference dominates in the medium  $p_T$  region, between the value of the two heavy quark masses. Moreover, as we will see in a while, high- $p_T$  limit behaviour predicted in the EFT framework or in the full Standard Model (SM from now on) are completely different. This means that when  $p_T$  becomes large, real transverse momentum distribution starts to deviate more and more from its EFT prediction.

Instead at small- $p_T$ , the effects of the heavy quark could be considered as pointlike since the important scale  $p_T$  is effectively much smaller than the heavy quark mass. Hence for example, results of Chap. 2, Sec. 2.7 about combined resummation, computed in the EFT framework can be applied to the full SM case simply by rescaling the LO cross section  $\sigma_0$  by the Wilson coefficient, Eq. (4.2.1).

This behaviour at small- $p_T$  also explains why rescaled EFT prediction works so well for the inclusive cross section. Indeed, it was shown by Ref. [64, 118–120] using saddle point analysis, that the Higgs boson production at LHC is dominated by threshold effects. But in Sec. 2.7, we proved that threshold resummation at inclusive level is completely controlled by the small- $p_T$  region of the transverse spectrum. Therefore since quark mass

effects are tiny in this region of the transverse momentum distribution, they turn out to have a small impact on the inclusive cross section, too.

Quark mass effects on the Higgs boson transverse momentum distribution have been studied extensively in the last years [91–100]. Fixed order evaluation at the first not trivial order is available since a long time [121] but NLO has not been calculated yet, due to the complexity of the two loops virtual corrections. Indeed, this computation is a huge multi-scale process since it involves in addition to  $p_T$  and  $m_H$  also all the masses of heavy quarks,  $m_b$  and  $m_t$ .

Since fixed order precision is up to now unsatisfactory in the high- $p_T$  limit, several different approximated approaches have been proposed. Following sections will treat one of these approaches which exploits high energy resummation to derive all-order considerations about the nature of these corrections. One of the advantage of this technique is the possibility to study the whole series in a regime where quark mass effects are fundamental. The disadvantage is that, since resummation is only at LLx, the overall precision of the approximation is quite low. Therefore, even if it is possible to approximate the size of the NLO contribution, more efforts will be necessary to decrease the error of such a construction. Research activity is on-going and general outlooks will be drawn at the end of this chapter.

In general, different techniques are used to properly approximate NLO effects of only top quark and top-bottom interference, which are the only two sizeable contributions. In the estimate of top mass quark terms at NLO, great accuracy can be achieved by exploiting Monte-Carlo parton shower merging techniques, as performed in Refs. [93, 94]. In this approach, NLO real emissions and one loop virtual-real contributions are evaluated exactly in the full standard model while the lacking two loops contribution is constructed as a rescaled EFT term, weighted using parton shower matching. The interested reader is referred to the original works for a more detailed presentation [93, 94].

However, parton shower approach turns out to be inaccurate to describe the medium- $p_T$  region where bottom interference dominates. In this region, instead, a different analysis can be carried on [97–100]. All virtual and real contributions are approximated in the limit where the mass of the quark is smaller compared to the hard scale, and computation is performed in this limit. This brings to the possibility to derive the singular behaviour in this limit which turns out to be logarithmic in the ratio  $\frac{p_T}{m_q}$  with  $m_q$  the mass of the lighter quark, but suppressed by an overall Yukawa factor  $\frac{m_q}{m_H}$ . The NLO singular approximation of the complete top-bottom interference has been calculated in Ref. [99].

Moreover, this type of logarithmic contribution has been resummed in Refs. [97, 100]. This resummation is incredibly interesting since it is one of the first example of soft but not Sudakov resummation. The origin of this singular component is gluon radiation from internal loop soft quark lines [100]. The soft nature of this logarithms was anticipated also in Ref. [122]. In the same Ref. [122], another collinear origin for possible divergent  $\ln \frac{p_T}{m_q}$  was hypothesised: we will see in the following section that high energy resummation suggests no exponentiation for this other type of contribution.

In conclusion, great interest has been shown in the last years in the estimate of quark mass effects on the Higgs boson transverse momentum distribution. Thanks to these efforts, a general understanding about the size of such contributions has been achieved, at least at NLO. In the high- $p_T$  regime parton shower approach reproduces quite well full

standard model behaviour, while in the medium- $p_T$  regime where interference dominates, the singular approximation of Refs. [98, 99] catches all the sizeable terms.

We are now going to focus in the following subsections on the high energy approach of Ref. [95], which constitutes a general analysis at all orders and can be used to verify approximated conclusion of previous approaches. In particular, we are going to conclude that power behaviour in the  $p_T \rightarrow \infty$  limit is completely controlled by LO cross section. Therefore, parton shower approach of Refs. [93, 94], based on a rescaling of one loop contributions, catches the leading behaviour in the large- $p_T$  region at all the orders. We thus understand from a theoretical point of view the accuracy found in the phenomenological applications. In the same way, high energy analysis shows no exponentiation and logarithmic resummation for the  $\ln \frac{p_T}{m_q}$  contributions coming from collinear evolution. This reinforces the hypothesis that the logarithmic origin found in NLO top-bottom evaluation of Refs. [97, 98] and resummed in Ref. [100] would be the unique logarithmic origin which requires such an all-order treatment.

Following subsections will be organized as follows. In Sec. 4.2.1, general form for the  $p_T$ -impact factor, Eq. (3.2.4) in the case of Higgs boson production with quark mass effects will be presented. Then, in Sec. 4.2.2, we will focus our attention on its partonic expansion, checking the accuracy of this construction at LO (and in some sense even at NLO) both at partonic level and at hadronic level. Finally in Sec. 4.2.3, general results are drawn and conclusions/outlooks are presented.

## 4.2.1 Standard Model Higgs $p_T$ -Impact Factor

To derive the high energy resummation of the Higgs transverse momentum distribution, we will follow the steps presented in our general discussion of Sec. 3.2 of Chap. 3. The object we need to compute is the off-shell transverse momentum distribution  $C_{p_T}$  for the process

$$g^* + g^* \rightarrow H. \quad (4.2.2)$$

Using this result into Eq. (3.2.4), we can derive the particular form for the  $p_T$ -impact factor. In the case of Higgs boson production in full standard model it turns out to be:

$$h_{p_T}(N, M_1, M_2, \xi_p, \{y_i\}) = \sigma_0(\{y_i\}) M_1 M_2 R(M_1) R(M_2) \frac{\xi_p^{M_1+M_2-1}}{(1+\xi_p)^N} \int_0^\infty d\xi_1 \xi_1^{M_1-1} \int_0^\infty d\xi_2 \xi_2^{M_2-1} \int_{-1}^1 \frac{du}{\sqrt{1-u^2}} \frac{2}{\pi} F(\xi_1, \xi_2, \xi_p, \{y_i\}) \delta(1 - \xi_1 - \xi_2 - 2\sqrt{\xi_1 \xi_2} u), \quad (4.2.3)$$

where we have introduced

$$u = \cos \theta, \quad \xi_1 = \frac{\xi}{\xi_p} = -\frac{k_{t,1}^2}{p_T^2}, \quad \xi_2 = \frac{\bar{\xi}}{\xi_p} = -\frac{k_{t,2}^2}{p_T^2} \quad (4.2.4)$$

and  $k_{t,1}^2, k_{t,2}^2$  are the off-shellness of the incoming gluons. The complete derivation of Eq. (4.2.3) is contained in Appendix C, Sec. C.2.2, together with the explicit expressions for the form factor  $F$  and the LO total cross section  $\sigma_0(y_i)$ . All the mass quark dependence of Eq. (4.2.3) has been introduced through Yukawa couplings  $y_i = \frac{m_{q_i}^2}{m_H^2}$ .

Eq. (4.2.3) has to be compared with analogue expression in the EFT case, Eq. (3.4.10). By replacing the LO cross section with the complete SM LO inclusive cross section, we obtain the rEFT prediction for the  $p_T$ -impact factor:

$$h_{p_T}(N, M_1, M_2, \xi_p, \alpha_s) = R(M_1) R(M_2) \sigma_0(y_i) \frac{\xi_p^{M_1+M_2-1}}{(1+\xi_p)^N} \left[ \frac{\Gamma(1+M_1)\Gamma(1+M_2)\Gamma(2-M_1-M_2)}{\Gamma(2-M_1)\Gamma(2-M_2)\Gamma(M_1+M_2)} \left( 1 + \frac{2M_1M_2}{1-M_1-M_2} \right) \right]. \quad (4.2.5)$$

By using the limit expressions of the form factor  $F$  in the small- $p_T$  and high quark mass  $y_i \rightarrow \infty$  limits, Eqs. (C.2.47) it is easily to prove that Eq. (4.2.5) is the correct expression both when the mass of the quark is large compared to the hard scale, both when  $p_T$  is much smaller than the quark mass. We thus prove the statement made in Sec. 4.2, about the region where rEFT approximates well the complete result.

Eq. (4.2.3) can be used to perform LL $x$  high energy resummation for the SM Higgs transverse momentum distribution. As explained in Sec. 3, to reach the resummed result, we need to substitute the Mellin momenta  $M_i$  with the LL $x$  matched and resummed anomalous dimension  $\gamma$ , constructed for example in Refs. [70, 84]. However, the impact of the high energy resummation at LHC is rather mild for the Higgs boson production, and almost the same accuracy could be obtained more directly by expanding Eq. (4.2.3) at first orders in  $\alpha_s$ .

Therefore we decide to study quark mass effects on the Higgs boson transverse momentum distribution by expanding at first orders in  $\alpha_s$  Eq. (4.2.3) and Eq. (4.2.5) and by comparing order by order the two different predictions. To extract from this high energy comparison phenomenological consequences we need to estimate the goodness of the high energy approximation. We will do this by comparing HE LL $x$  behaviour with fixed order results, where available. This will be done in Sec. 4.2.2.

Expanding in power of  $\alpha_s$  means expanding in power of  $M_i$  the  $p_T$ -impact factor. We thus obtain [77, 95]

$$h_{p_T}(N, M_1, M_2, \xi_p, \{y_i\}) = \sigma_0(\{y_i\}) R(M_1) R(M_2) \frac{\xi_p^{M_1+M_2-1}}{(1+\xi_p)^N} \times \left[ c_0(\xi_p, \{y_i\})(M_1+M_2) + \sum_{j \geq k > 0} c_{j,k}(\xi_p, \{y_i\}) \left( M_1^k M_2^j + M_1^j M_2^k \right) \right] \quad (4.2.6)$$

for expansion of Eq. (4.2.3), with explicit expressions of  $c_0$  and  $c_{j,k}$  given in Eq. (C.2.48) and Eq. (C.2.32) of Appendix C, and

$$h_{p_T}^{\text{PL}}(N, M_1, M_2, \xi_p) = \sigma_0(y_i) R(M_1) R(M_2) \frac{\xi_p^{M_1+M_2-1}}{(1+\xi_p)^N} \times \left[ c_0^{\text{PL}}(M_1+M_2) + \sum_{j \geq k > 0} c_{j,k}^{\text{PL}} \left( M_1^j M_2^k + M_1^k M_2^j \right) \right]. \quad (4.2.7)$$

for expansion of Eq. (4.2.5), with the following values for the first  $c_{ij}^{\text{PL}}$  coefficients:

$$c_0^{\text{PL}} = 1, \quad (4.2.8a)$$

$$c_{1,1}^{\text{PL}} = 0, \quad (4.2.8b)$$

$$c_{2,1}^{\text{PL}} = 1. \quad (4.2.8c)$$

Up to NNLO, only coefficients  $c_0$ ,  $c_{1,1}$  and  $c_{2,1}$  enter in the approximation. Comparisons between SM and EFT predictions for these terms are shown in Fig. 4.3.

As expected all the full SM coefficients tend to the corresponding pointlike result as  $p_T \rightarrow 0$ , and they vanish at large  $p_T$ . This is required in order for the inclusive cross section to be free of spurious double energy logarithms [77,95].

This is a very important point and we want to discuss it a little more. It was proved that the inclusive cross section shows a very different behaviour in the high energy regime in the pointlike case and in the full resolved one. In particular,

$$\sigma \underset{x \rightarrow 0}{\sim} \sigma_{\text{LO}} \times \begin{cases} \delta(1-x) + \sum_{k=1}^{\infty} c_k \alpha_s^k \ln^{2k-1} \frac{1}{x}, & \text{pointlike} \\ \delta(1-x) + \sum_{k=1}^{\infty} d_k \alpha_s^k \ln^{k-1} \frac{1}{x}, & \text{resolved.} \end{cases} \quad (4.2.9)$$

the effective theory at high energy leads to spurious double logarithmic singularities which are absent in the full SM case. In Ref. [77], the origin of this fact was found in the different behaviour of the transverse momentum distribution in the large- $p_T$  regime, where quark mass effects dominate. In formula we have

$$\frac{d\sigma}{d\xi_p} \underset{x \rightarrow 0}{\sim} \frac{\sigma_{\text{LO}}}{\xi_p} \times \begin{cases} \sum_{k=1}^{\infty} \alpha_s^k \ln^{k-1} \frac{1}{x} \sum_{n=0}^{k-1} c_{kn} \ln^n \xi_p, & \text{pointlike} \\ \sum_{k=1}^{\infty} d_k(\xi_p) \alpha_s^k \ln^{k-1} \frac{1}{x}, & \text{resolved,} \end{cases} \quad (4.2.11)$$

where in the resolved case  $d_k(\xi_p)$  coefficients vanish at least as a power of  $\xi_p^{-1}$  as  $\xi_p \rightarrow \infty$  so that the integral is finite.

This fact brings to several important consequences. First, it can be proved at LO that the EFT LO transverse momentum distribution [123] scales as  $\frac{1}{\xi_p}$  at large- $p_T$  while the full SM LO transverse momentum distribution [121] scales as  $\frac{1}{\xi_p^2}$ . The HE LO prediction  $c_0(\xi_p)$  scales with the same power law of the full SM LO result. Moreover, by inspecting expansion Eq. (4.2.6), you can easily convince yourself that the leading behaviour at any order in the  $\xi_p \rightarrow \infty$  limit is always controlled by the LO coefficient. Hence at HE at any order, the overall prediction scales at high  $p_T$  as the full LO cross section. Moreover, the fact that also in the opposite limit  $x \rightarrow 1$ , threshold resummation at fixed  $p_T$  Eq. (2.7.28) predicts an high- $p_T$  power behaviour at all the orders equal to the one of the leading order result, suggests that high-energy approximation reproduces the correct high- $p_T$  behaviour of the full result to all orders.

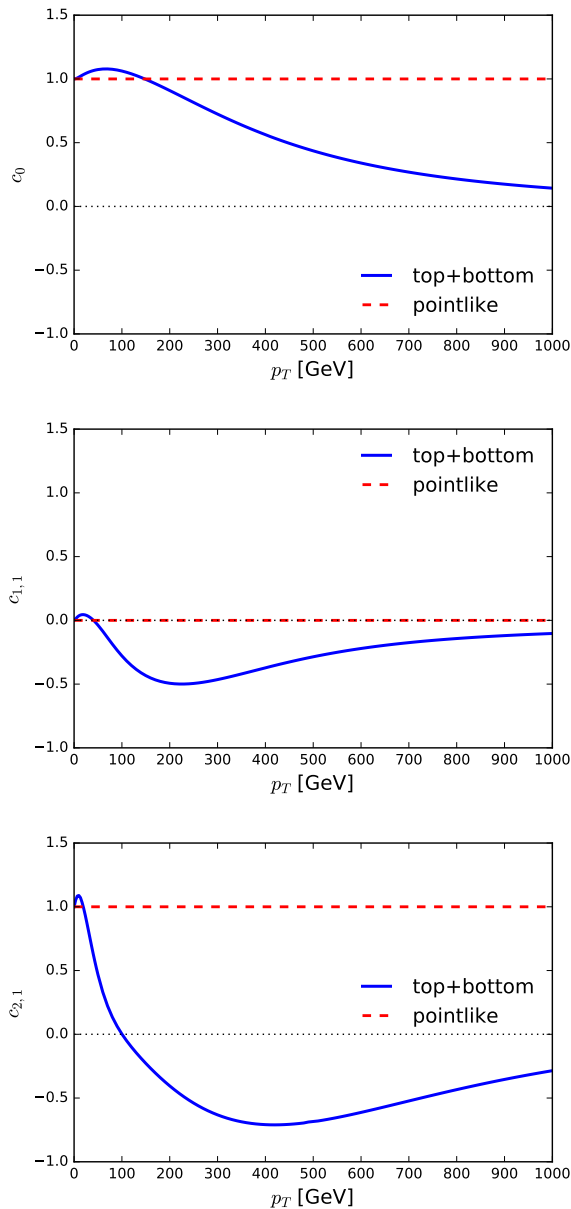


**Figure 4.3.** The first three coefficients  $c_{i,j}$  Eq. (C.2.32) in the expansion of the  $p_T$  impact factor Eq. (4.2.6) with finite top and bottom masses, compared to the pointlike result.

All these considerations confirm from the theoretical point of view, the phenomenological analysis of Refs. [93,94] where LO rescaling was used for higher order corrections. In the light of high energy analysis, it is reasonable to believe that these approaches reproduce quite well top contributions which are important in the large- $p_T$  regime.

Furthermore, in Fig. 4.3, we note that pointlike approximation breaks down for  $p_T \sim m_t$ . In the high-energy limit, one expects the departure from pointlike to become increasingly marked as the perturbative order is raised, because with an increasingly large number of hard emissions more energy flows into the loop which is less well approximated by a pointlike interaction: so higher-order coefficients  $c_{i,j}$  deviate more from their pointlike limit than lower-order ones. On the other hand, the lower order coefficients are enhanced by higher powers of  $\ln \xi_p$ , due to the overall factor  $\xi_p^{M_1+M_2}$ , so low-order coefficients dominate, and the shape of the  $p_T$  distribution remains similar as the perturbative order is increased. We will note this fact also at hadronic level in the Sec. 4.2.2.

In Fig. 4.3, overall impact of top and bottom contributions is shown. We want now to assess the relative impact of the bottom, top and interference contributions. In order to do this, we write each coefficient as

$$c_{j,k}(\xi_p, y_t, y_b) = R^t(y_t, y_b) c_{j,k}^t(\xi_p, y_t) + R^b(y_t, y_b) c_{j,k}^b(\xi_p, y_b) + R^i(y_t, y_b) c_{j,k}^i(\xi_p, y_t, y_b), \quad (4.2.13)$$

where the normalization ratios

$$R^t(y_t, y_b) = \frac{|K(y_t)|^2}{|K(y_t) + K(y_b)|^2} = 1.107 \quad (4.2.14a)$$

$$R^b(y_t, y_b) = \frac{|K(y_b)|^2}{|K(y_t) + K(y_b)|^2} = 0.008 \quad (4.2.14b)$$

$$R^i(y_t, y_b) = \frac{K(y_b)^* K(y_t) + K(y_b) K(y_t)^*}{|K(y_t) + K(y_b)|^2} = -0.115. \quad (4.2.14c)$$

account for the mismatch in normalization between the Wilson coefficients in the form factor Eq. (C.2.25) when both the top and bottom contributions are included.

The separate contributions are compared in Fig. 4.4 to each other and to their sums, already shown in Fig. 4.3, both with and without the normalization coefficients Eq. (4.2.14). It is clear that while in each case the un-normalized coefficients  $c^t$ ,  $c^b$  and  $c^i$  are all of the same order, after multiplying by the Wilson coefficients Eqs. (4.2.14) the top contribution is dominant, while the pure bottom contribution becomes entirely negligible. However, in the region  $m_b \lesssim p_T \lesssim m_t$  and even for somewhat larger  $p_T$  values, the interference contribution provides a small but non-negligible correction.

In Ref. [95], this bottom contribution was studied and logarithmic dependence from  $\frac{p_T}{m_b}$  appears in the resummed result. However it was proved that no resummation occurs at LLx for these contributions. This suggests that hard collinear bottom logarithms does not exponentiate even if a complete prove beyond LLx is up to now not available. We refer to Refs. [95, 122] the interested reader for a more detailed discussion.

After this general presentation about the  $p_T$ -impact factor expansion in the Higgs boson production case, let us move to a parton and hadron level check of the high energy approximation against complete fixed order results.

## 4.2.2 Validation of the high-energy approximation

In this section, we want to compare our LLx approximation (in particular LO and NLO coefficients) against known fixed order results, both at partonic level both at hadronic

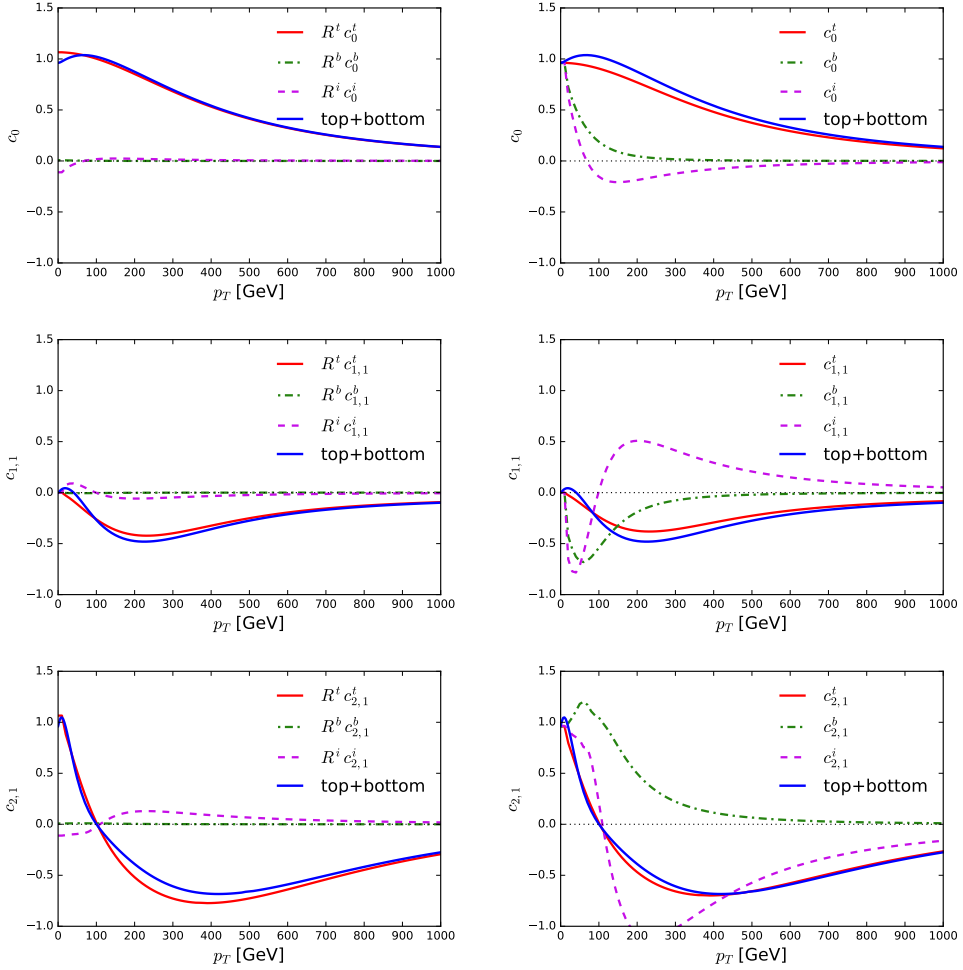


**Figure 4.4.** Contribution from top (red, solid), bottom (green, dot-dashed) and interference (purple, dashed) to the coefficients shown in Fig. 4.3, with their sum also shown as blue line: the three coefficients  $c_0$ ,  $c_{1,1}$  and  $c_{2,1}$  are shown from top to bottom, including (left) or not including (right) the normalization due to the Wilson coefficient Eqs. (4.2.13), (4.2.14).

level.

At partonic level, we compare leading  $\mathcal{O}(\alpha_s)$  prediction with fixed order evaluation of Ref. [121]. At leading  $\mathcal{O}(\alpha_s)$ , Eq. (4.2.6) reduces to

$$\frac{d\hat{\sigma}^{\text{LL}x\text{-LO}}}{d\xi_p} = \sigma_0(y_b, y_t) c_0(\xi_p, y_t, y_b) \frac{2C_A\alpha_s}{\pi} \frac{1}{\xi_p}, \quad (4.2.15)$$

with  $\sigma_0$  given by Eqs. (C.2.20) and  $c_0$ , Eq. (C.2.32); note in particular that it does not depend on  $x$  because the LL $x$  cross section is proportional to  $\sigma_0 \alpha_s^k \ln^{k-1} x$ ,  $k = 1$ . The coefficient  $c_0$  can be determined in fully analytic form, see Eq. (C.2.48) in Appendix C.

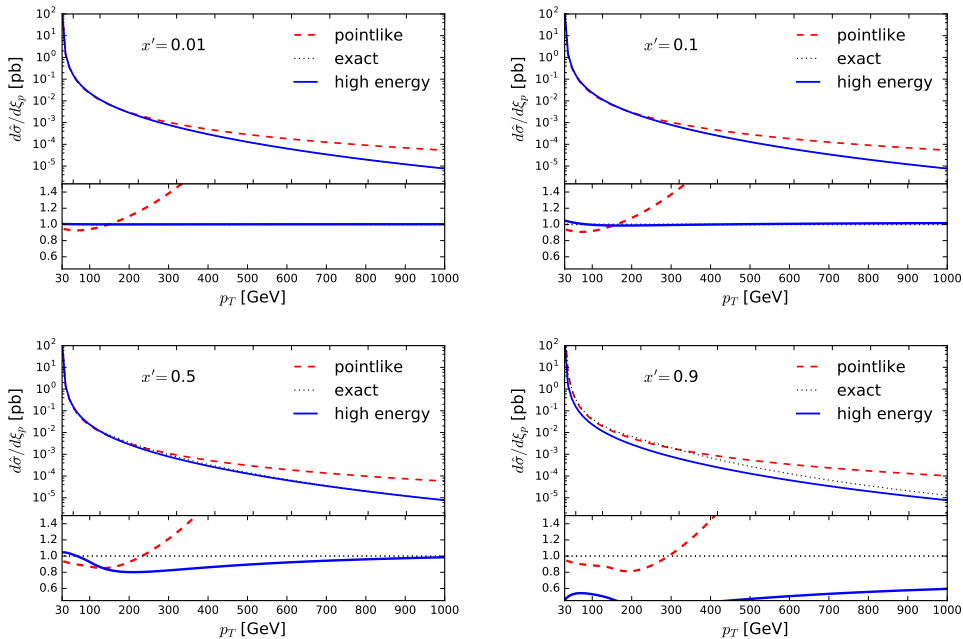


**Figure 4.5.** The partonic leading order transverse momentum distribution in the high-energy limit (blue, solid) compared to the exact result of Ref. [121] (black, dotted). The leading order pointlike result [123] is also shown for comparison (red, dot-dashed). Results are shown for three different values of  $x$  Eq. (1.4.10):  $x = 0.01$  (top left),  $x = 0.1$  (top right),  $x = 0.5$  (bottom left),  $x = 0.9$  (bottom right); in each case, the ratio to the exact result is also plotted.

In Figure 4.5 we compare the exact [121], high-energy and pointlike [123] LO results for four different values of  $x$  (see Eq. (1.4.10) for a definition of  $x$ ). Here and henceforth we only show predictions for large enough  $p_T > 30$  GeV: indeed we learned in Chap. 2 that fixed order prediction ceases to be valid under this value and transverse momentum resummation has to be performed. The relation of the latter to the high-energy approximation was discussed in Ref. [46]. As expected, the pointlike approximation breaks down for  $p_T \gtrsim m_t$  where the finite-mass result drops rather faster; moreover the deficit which is seen in the pointlike result in the region  $m_b \lesssim p_T \lesssim m_t$  is due to top-bottom interference, as shown also in Fig. 4.4. The high-energy approximation appears to be very accurate for  $x \lesssim 0.1$ ; for higher  $x$  values it starts deteriorating and for large  $x \sim 0.5$  it is typically off by 20%. However, the accuracy of the high-energy approximation does not depend on  $p_T$  if  $p_T \gtrsim m_H$ : this is understood since we have just said in the previous subsection that the large- $p_T$  behaviour of the high-energy approximation is qualitatively the same as that of the full result.

The pointlike approximation instead departs from the exact result by an increasingly large amount as  $p_T$  grows: in fact, as  $p_T \rightarrow \infty$ ,  $c_0(\xi_p, y_t, y_b)$  Eq. (4.2.15) drops as  $\frac{1}{p_T^2}$ , while it is constant in the effective theory, so  $\frac{d\sigma^{\text{LL}x-\text{LO}}}{d\xi_p} \underset{p_T \rightarrow \infty}{\sim} \frac{1}{(p_T^2)^a}$  with  $a = 2$  in the

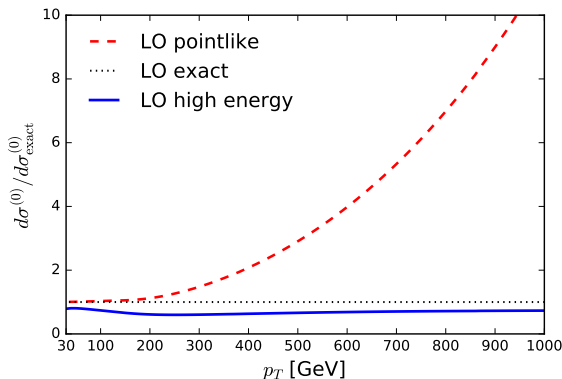


**Figure 4.6.** The ratio of the high-energy approximation (in solid blue) and of the effective theory result (in dotted red) to the full result for the hadron-level transverse momentum distribution at LO plotted as a function of  $p_T$  (GeV) at the LHC 13 TeV.

full theory, and  $a = 1$  in the effective theory. In the opposite limit  $p_T \rightarrow 0$  instead, the high-energy limit becomes pointlike, up to an overall rescaling: it is indeed clear from the plots that in the region  $x \lesssim 0.1$  in which the high-energy approximation holds, as  $p_T \rightarrow 0$  the high-energy and pointlike results coincide.

Now we are going to move to hadronic comparisons. In particular, we validate the high energy approximation at leading and next-to-leading order. As derived at the parton level (see Fig. 4.5), the high energy approximation is mostly relevant in the region  $p_T > m_H$ , where the pointlike approximation fails, while for lower  $p_T$  values the high-energy result rapidly approaches its pointlike limit, and eventually, for low enough  $p_T$ , Sudakov resummation of transverse momentum logs becomes necessary. In the region of interest for this study, as demonstrated in Sect. 4.2.1, the contribution of the bottom quark is entirely negligible. Therefore, in the remainder of this section we will only include the top contribution.

All plots are produced with  $\mu_R^2 = \mu_F^2 = Q^2$  and with the PDF4LHC15 NNLO set of parton distributions PDF4LHC15\_nnlo\_100 [105–111], for the LHC with  $\sqrt{s} = 13$  TeV.

To perform the comparison, we define the NLO transverse momentum distribution

$$\frac{d\sigma}{d\xi_p}(\tau', \xi_p, y_t, \alpha_s) = \alpha_s \frac{d\sigma^{(0)}}{d\xi_p} + \alpha_s^2 \frac{d\sigma^{(1)}}{d\xi_p} + \mathcal{O}(\alpha_s^3), \quad (4.2.16)$$

and the  $K$ -factor

$$K = 1 + \frac{d\sigma^{(1)}/d\xi_p}{d\sigma^{(0)}/d\xi_p}. \quad (4.2.17)$$

In Fig. 4.6 we compare the leading order contribution  $\frac{d\sigma^{(0)}}{d\xi_p}$  computed in the high-energy approximation to the exact result of Ref. [121], and also with the effective-field theory result. It is clear that, as expected, the high-energy approximation is most accurate for  $p_T \sim m_H$  but only slowly deteriorates for larger  $p_T$ : in fact, for all  $0.5 \lesssim p_T \lesssim 1$  TeV the high-energy approximation is about 60% of the full theory LO result. The effective

field theory result instead is driven by the fact that at the parton level it has the wrong large- $p_T$  power behaviour, and is off by an increasingly large factor: at  $p_T \sim 1$  TeV it is in fact too large by about one order of magnitude.

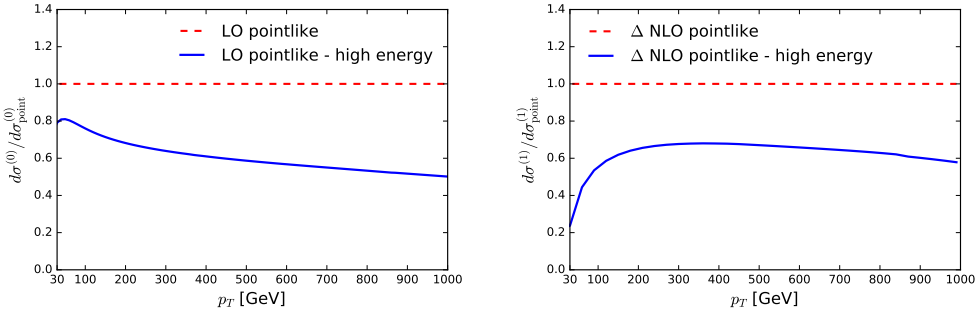


**Figure 4.7.** The ratio of the high-energy approximation to the pointlike result for the hadron-level transverse momentum distribution plotted as a function of  $p_T$  (GeV) at the LHC 13 TeV for the LO, on the left and for the NLO contribution, on the right.

Beyond leading order we do not have any exact result to compare to, as only the effective field theory result is available. We expect a similar pattern to hold, and we can provide some evidence for this by studying the relation between the high-energy approximation and the full result, both determined in the pointlike limit.

This comparison is shown in Fig. 4.7 (left) for the LO contribution  $\frac{d\sigma^{(0)}}{d\xi_p}$ . It is apparent that the quality of the high-energy approximation in the pointlike limit is quite similar to that in the full theory discussed above. The NLO contribution  $\frac{d\sigma^{(1)}}{d\xi_p}$  is also shown in Fig. 4.7 (right): we compare the high-energy pointlike result of Ref. [77] to the full result of Ref. [124]. Again, in the medium-high  $p_T$  region the pattern is quite similar to that seen at LO.

This suggests that the high-energy approximation might remain accurate in a relatively wide kinematic region. In order to test this, we have repeated the comparison of the high-energy to the full result for the NLO term  $\frac{d\sigma^{(1)}}{d\xi_p}$ , both in the pointlike limit, shown in Fig. 4.7, for a wide range of values of  $p_T$  and the collider energy. Results are shown in Fig. 4.8 [90]. As expected, the high-energy approximation becomes better as the center-of-mass energy is increased at fixed  $p_T$ . On the other hand, if  $p_T$  is varied at fixed energy the quality of the approximation remains constant in a wide range of transverse momenta, and it only starts deteriorating when the transverse momentum is larger than say  $\sim 20\%$  of its upper kinematic limit  $\sqrt{s}/2$ . This is expected because the high-energy limit holds when  $\sqrt{s}$  is much larger than all other scales: for instance, at large  $p_T$  there are  $\ln p_T$  contributions which should be resummed to all orders [125], but are increasingly subleading in the high-energy expansion. However, in this region the transverse momentum distribution is tiny, so in practice the high-energy approximation is uniformly accurate throughout the physically relevant region.

Summarizing, we have compared our high energy approximation w.r.t. available fixed order evaluations, both at partonic level and at hadronic level. Results show that HE

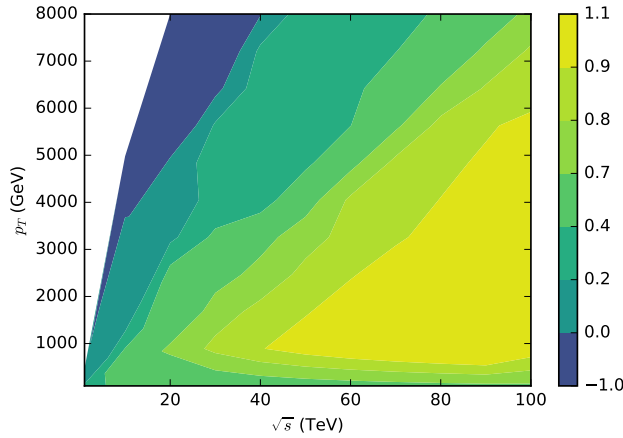


**Figure 4.8.** The ratio of the NLO contribution  $\frac{d\sigma^{(1)}}{d\xi_p}$  in the high-energy approximation to exact result, both computed in the pointlike limit, for the Higgs transverse momentum distribution at a proton-proton collider plotted as a function of the transverse momentum  $p_T$  (in GeV) and the center-of-mass energy  $\sqrt{s}$  (in TeV).

LLx prediction turn out to be off of around 40% both at LO and at NLO at LHC 13 TeV, but with a uniform accuracy throughout the physically relevant region. This accuracy guarantees that all order considerations made in Sec. 4.2.1 for the high-energy prediction should work with reasonable precision also for the complete result.

As a last remark of this section we are going to present in the next subsection possible approximations for the  $p_T$  spectrum of the Higgs boson with finite top mass beyond leading order.

### 4.2.3 Top Mass Effect at NLO on Higgs spectrum

In Fig. 4.9 we propose three different determinations of the  $K$ -factor Eq. (4.2.17) in the high- $p_T$  region we are interested in: using the full pointlike NLO result, the high-energy approximation to it (i.e. pointlike, and high-energy), and the high-energy result, but with full mass dependence. In each case, both the LO and NLO contributions are computed using the same approximation. This plot shows that for  $p_T \gtrsim 200$  GeV all these  $K$ -factors have a similar behaviour, and differ by comparable amounts.

This plot suggests two main conclusions. First, in the only case in which we can compare the high-energy approximation to the full result, namely the pointlike limit, we see that the high-energy approximation is quite good (red vs. green curve in Fig. 4.9), with an accuracy of about 20% or better for all  $p_T \gtrsim 200$  GeV, which does not deteriorate as  $p_T$  increases. Second, even though (recall Sect. 4.2.2) the shape of the distribution at high  $p_T$  differs between the pointlike and massive case (a different power of  $p_T$ ) the  $K$  factors are similar and approximately  $p_T$  independent, at least in the only case in which we can compare the pointlike and massive results, namely the high-energy limit (green

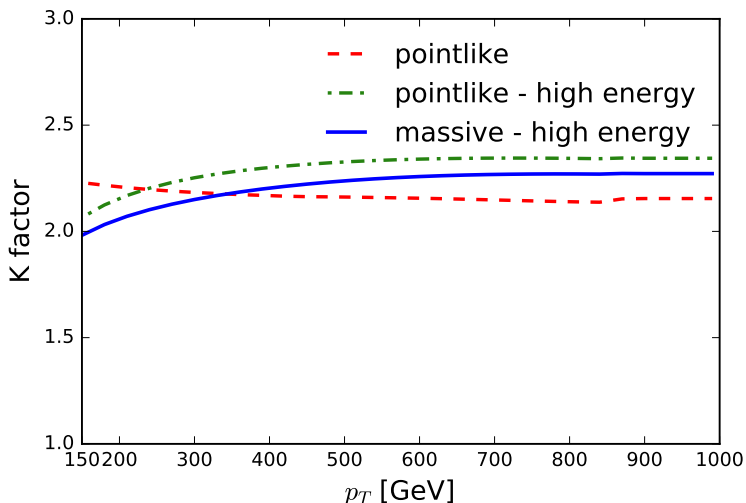


**Figure 4.9.** The NLO  $K$ -factor Eq. (4.2.17) computed using the full result in the pointlike limit (red, dashed), and the high-energy approximation, either with full mass dependence (blue, solid) or in the pointlike limit (green, dot-dashed). In each case, the LO cross-section is computed using the same approximation as the NLO term.

and blue curve).

These two observations, taken together, suggest that the best approximation to the full NLO result can be obtained by combining the full LO result with a  $K$ -factor computed in the high-energy approximation, namely, by multiplying the LO cross-section by the  $K$  factor (blue curve) of Fig. 4.9, corresponding to the high-energy fully massive result. This is our preferred approximation, and it is shown in Fig. 4.10, where it is also compared to the LO exact result and to the NLO pointlike approximation; all results are also shown as ratios to the LO. It is clear that the pointlike result has the wrong power behaviour at large  $p_T$  and thus fails for  $p_T \gtrsim 200$  GeV.

The comparison of  $K$ -factors of Fig. 4.9 suggests that if one wishes to use the NLO pointlike result, rather than the high-energy approximation, a better approximation can be obtained by using the pointlike NLO to compute the  $K$  factor (red curve of Fig. 4.9), and using this  $K$  factor to rescale the full massive leading order. The quality of this approximation is possibly comparable to that of our favourite approximation based on the high-energy limit: indeed, as discussed in Sect. 4.2.1 this approximation captures the leading large  $p_T$  term proportional to  $c_0$ . This curve is also shown in Fig. 4.10: it is seen to be quite close to our favourite approximation in a wide range of  $p_T$  but it starts departing from it only at the largest  $p_T$  where we expect the high-energy approximation to be more accurate.

If our approximation to the  $K$ -factor based on the high-energy limit is used, it is natural to ask what is the associated uncertainty. Having observed that, at the level of  $K$ -factors, the difference between the pointlike and massive cases is somewhat smaller than the difference between the high-energy and full results (see Fig. 4.10), we can con-

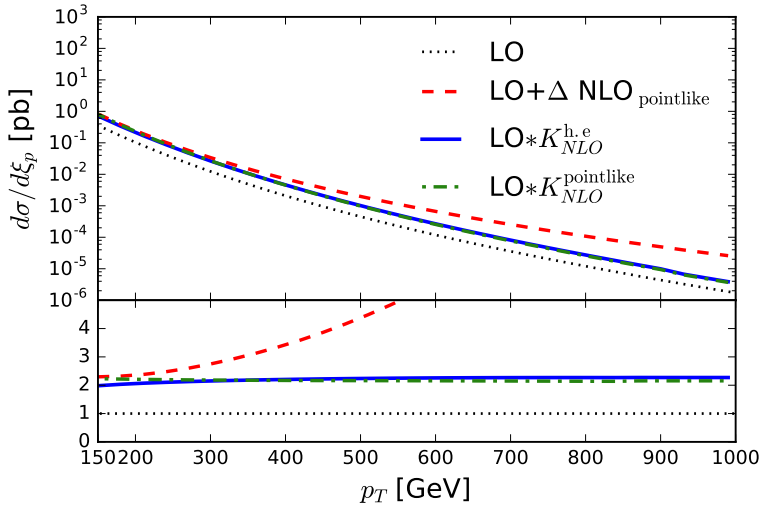


**Figure 4.10.** Various approximations to the NLO Higgs transverse momentum distribution. The curves shown correspond (from top to bottom) to adding the pointlike approximation to the NLO contribution to the full LO result (red, dashed), or to multiplying the full LO result by the  $K$ -factors of Fig. (4.9) computed respectively in the high-energy approximation but with full mass dependence (blue, solid) or in the pointlike approximation (green dot-dashed). The full LO result is also shown for comparison (black, dotted). In the bottom plot all curves are shown as ratios to the exact LO result.

servatively estimate the uncertainty on the high-energy approximation to be given by the percentage discrepancy between high-energy and full results (both pointlike) shown in Fig. 4.8. Of course, this is just the uncertainty related to the high-energy approximation, which will then have to be supplemented with all other sources of uncertainty (missing higher orders,  $\alpha_s$ , PDFs, etc.).

Giving the overall accuracy of about 20% it is natural that high energy approach can not compete in precision with parton shower approaches of Refs. [93, 94]. Nevertheless, central value predictions turn out to be compatible one with each others, and the all order structure of high energy resummed result permits to fulfil general matching matrix element procedure with a theoretical background which holds even beyond NLO. For this reason, a critical comparison between approximations just presented and similar results of Refs. [93, 94, 96] is highly desired. This fact was also highlighted in the last LesHouches Workshop *Physics at TeV* 2017 as a primary topic in Higgs boson research activity.

Even if the high energy resummation could produce meaningful approximation at NLO for top contributions, the same is not true for bottom-top interference. Indeed, high energy resummation does not show the logarithmic non-Sudakov enhancement which was found in the soft regime in Refs. [97–100]. If on one hand this suggests that no logarithmic resummation is needed to deal with pure collinear logs  $\ln \frac{p_T}{m_q}$ , on the other hand this prevent to study medium- $p_T$  region with this technique.

In conclusion, high energy resummation provides a reasonable approximation for top

contribution in the large- $p_T$  range, which has to be compared critically with other approximations presented in literature [93, 94, 96]. To all of them top-bottom interference and resummation of soft bottom logs of Refs. [98, 100] has to be added to increase the precision in the region where  $p_T$  is comparable with the Higgs mass. We acknowledge that the join of all these considerations can provide an approximation of the NLO coefficient in the full theory with an overall error of about 10% throughout the whole  $p_T$  spectrum.

Of course the 20% of accuracy of our final approximation can not satisfy us. Therefore we are working to decrease the error; future outlooks include the will to produce a unique resummation which takes into account high-energy and threshold contribution at the same time, as done for inclusive cross section in Refs. [56, 64, 118]. We believe that a full resummation in all the coloured regions of Fig. 2.1 of Chap. 2, expanded in power of  $\alpha_s$ , can provide high-accurate approximations for the unknown higher order coefficients of transverse momentum distributions. However, more research activity is necessary and this thesis has to be considered as a first step in the construction of a general resummation formula able to resums all the singular behaviours in transverse momentum spectrum.

# Conclusions and Outlooks

We have presented a detailed overview about possible resummations of transverse momentum distributions in different kinematic limits. On the theoretical side, we have obtained several results.

First of all, we have presented a general description about matrix element and phase space factorization in the collinear and soft limit. We have proved that the phase space factorization takes place in different ways in the following three conditions

1.  $p_T \ll 1$        $(1-x) \sim 1$ ;
2.  $p_T \ll 1$        $(1-x) \ll 1$ ;
3.  $p_T \sim 1$        $(1-x) \ll 1$ ;

with  $x$  defined as in Eq. (1.4.10). In each region, a different resummation theory can then be constructed; we proved that original *Collins-Soper-Sterman* transverse momentum resummation resums leading contributions only from the first region. Then we derive a new resummation theory which takes into account at the same time all leading contributions from the first two regions; as a by-product our final resummation formula, called *consistent transverse momentum resummation*, owns a finite  $p_T$  integral which coincides in  $N$  space up to subleading  $\mathcal{O}(\frac{1}{N})$  terms with a threshold resummed inclusive cross section.

Finally as final result we have produced a combined expression which contains also the leading contributions from the third region. Since a unique expression which studies all previous limits at the same time is up to now not available, we decide to introduce a profile matching function which interpolates between consistent transverse momentum resummation and threshold resummation at fixed  $p_T$  of the third region.

Then we move to the high energy limit. In these years, we have improved a lot the state of the art in this field. First we have extended general LL high energy resummation framework from inclusive cross section to transverse momentum distributions; then we moved from transverse momentum distributions to any general observable which is independent from the number of the emissions in the initial legs. For all these observables, we have proved that high energy factorization goes as in the inclusive case as long as the correct LO off-shell quantity is computed.

Several other minor achievements have then been obtained, some of them reported in this thesis, some excluded for lack of space. We joined high energy resummation of single differential transverse momentum or rapidity distribution in a unique high energy

resummation for the double differential distribution. Then we studied a proper extension to coloured final state, producing for the first time an high energy prediction for the one-jet inclusive cross section. Even if this theoretical extension results to be trivial, several important ideas turn out to be necessary in order to overcome the technical difficulty of the actual off-shell computation. Finally, some recent developments we contributed have not been inserted in this thesis. In particular, we concluded the high energy computation of DIS structure functions, considering also the case of weak NC and CC contributions, and we presented a stable numerical implementation of the  $LLx$  resummed and matched DGLAP anomalous dimension  $\gamma$ , currently available in the public code HELL [70].

From the phenomenological point of view, some applications of the new theories we studied in this three years of Ph.D. are still on-going. We have already used high energy resummation to size the impact of quark mass effects on the high- $p_T$  tail of the Higgs boson transverse momentum distribution. This analysis permitted us to deduce some important all-order considerations about the leading behaviour at large- $p_T$  of the SM and EFT distributions respectively; moreover, it permitted us to produce a reasonable NLO approximation for the full SM K factor. In the context of combined resummation, we present in this thesis for the first time a practical way to perform the integral inversion avoiding the problem of the Landau pole. The prescription adopted in this case is particular interesting since for the first time we are forced to use also Borel prescription to reach the final result.

Summarizing, we have presented some important recent achievements in the context of resummations for transverse momentum distributions. Looking to Fig. 2.1, we reach the point where in all the coloured regions a resummation theory is actual available.

However, there is still a lot of work to do. Our final desire is to produce a unique formula able to take into account all the information coming from coloured regions of Fig. 2.1. This means that combined resummation has to be matched with high energy resummation as already done for example for inclusive cross section in Refs. [56, 64, 118]. Phenomenological analysis of consistent transverse momentum resummation and combined resummation has to be concluded. The resummed result presented in this thesis has to be matched with fixed order calculation and a critical comparison between this result and similar results, like CSS transverse momentum resummation or joint resummation has to be performed.

In the context of high energy resummation, our preliminary analysis about  $LLx$  resummation of jet observables has to be extended; in particular, it is important to improve our comprehension about the impact of different jet algorithms in the analysis of our parton result.

In these three years of Ph.D. we try to answer about the possibility to extend known resummation tools for inclusive cross section, to transverse momentum distributions. This procedure delivered many new questions about the relations among these resummation theories and their actual impact on phenomenological predictions.

This is *torment and delight* of the research...

We would like this thesis to be the starting point for other physicists to continue this work, in order to fill the holes and answer the questions that for incompetence or lack of time we left. This is our conclusion, our will, our desire...

# A PDF DGLAP Evolution

## Contents

---

<b>A.1 Running Coupling evolution</b> . . . . .	<b>159</b>
<b>A.2 DGLAP Equations.</b> . . . . .	<b>162</b>
A.2.1 Flavour Decomposition . . . . .	162
<b>A.3 General Solution</b> . . . . .	<b>165</b>

---

In this Appendix, we want to focus our attention on the DGLAP equations: after a detailed presentation of this set of relations, we are going to present a complete perturbative solution up to some logarithmic accuracy in the factorization and hard scales. The application to transverse momentum resummation and consistent transverse momentum resummation will be also discussed in detail, highlighting the main differences in the logarithmic counting. We are going to follow in all the Appendix the approach of Ref. [126]; in this derivation, central role is covered by strong coupling constant  $\alpha_s$ , since  $\mu_F^2$  evolution of PDFs is rewritten as a proper evolution of the anomalous dimension through its  $\alpha_s$  running coupling. Therefore, before entering in the presentation of the Altarelli-Parisi equations, we want to remind how running coupling evolution is usually performed in QCD.

## A.1 Running Coupling evolution

Strong running coupling constant has to fulfil the following renormalization group equation:

$$\mu_R^2 \frac{d}{d\mu_R^2} \alpha_s(\mu_R^2) = \beta(\alpha_s(\mu_R^2)) \quad (\text{A.1.1})$$

where we introduce a beta function  $\beta(\alpha_s)$  which admits the following series expansion:

$$\beta(\alpha_s) = -\beta_0 \alpha_s^2 - \beta_1 \alpha_s^3 - \beta_2 \alpha_s^4 + \mathcal{O}(\alpha_s^5). \quad (\text{A.1.2})$$

The inclusion of extra terms into the beta function permits the prediction of towers of  $\mu_R^2$  logarithms with lower and lower power. Using resummation terminology,  $\beta_0$  resums the

highest logarithm of the renormalization scale at any order,  $\beta_1$  NLL components and so on.

For our scope, a NNLL solution is enough to reproduce all the results of this thesis, and therefore we are going to limit ourselves to this logarithmic accuracy. First of all, we report the explicit expressions of the first three coefficients:

$$\beta_0 = \frac{11C_A - 2N_f}{12\pi} \quad (\text{A.1.3a})$$

$$\beta_1 = \frac{17C_A^2 - (5C_A + 3C_F)N_f}{24\pi^2} \quad (\text{A.1.3b})$$

$$\begin{aligned} \beta_2 = \frac{1}{(4\pi)^3} & \left[ \frac{2857}{54}C_A^3 + \left( C_F^2 - \frac{205}{18}C_FC_A - \frac{1415}{54}C_A^2 \right) N_f \right. \\ & \left. + \left( \frac{11}{9}C_F + \frac{77}{54}C_A \right) N_f^2 \right], \end{aligned} \quad (\text{A.1.3c})$$

which we are going to use in our generic solution.

We start by separating variables into Eq. (A.1.1), rewriting it as:

$$-\frac{d\alpha_s}{\beta_0\alpha_s^2 + \beta_1\alpha_s^3 + \beta_2\alpha_s^4} = \frac{d\mu_R^2}{\mu_R^2}. \quad (\text{A.1.4})$$

Our aim is to predict the NNLL evolution of the running coupling from an initial scale  $\mu_i^2$  to a final scale  $\mu_f^2$ . We prefer not to specify further the values of these scales in order to remain as general as possible. Integrating on each side, we obtain the following implicit equation:

$$\begin{aligned} \left[ \frac{1}{\beta_0\alpha_s} - \frac{2(\beta_1^2 - 2\beta_0\beta_2) \arctan\left(\frac{\beta_1 + 2\alpha_s\beta_2}{\sqrt{4\beta_0\beta_2 - \beta_1^2}}\right)}{2\beta_0^2\sqrt{4\beta_0\beta_2 - \beta_1^2}} \right. \\ \left. + \frac{\beta_1}{\beta_0^2} \ln(\alpha_s) - \frac{\beta_1}{2\beta_0^2} \ln(\beta_0 + \alpha_s\beta_1 + \alpha_s^2\beta_2) \right]_{\alpha_s(\mu_i^2)}^{\alpha_s(\mu_f^2)} = \ln \frac{\mu_f^2}{\mu_i^2}. \end{aligned} \quad (\text{A.1.5})$$

Now using a procedure similar to a general resummed solution, we express  $\alpha_s(\mu_f^2)$  as a NNLL function of  $\alpha_s(\mu_i^2)$ :

$$\alpha_s(\mu_f^2) = \alpha_s(\mu_i^2) f_1(\lambda_{\mu_i}) + \alpha_s(\mu_i^2)^2 f_2(\lambda_{\mu_i}) + \alpha_s(\mu_i^2)^3 f_3(\lambda_{\mu_i}) + \mathcal{O}(\alpha_s^4) \quad (\text{A.1.6})$$

with  $\lambda_{\mu_i} = \alpha_s(\mu_i^2) \beta_0 \ln \frac{\mu_f^2}{\mu_i^2}$ , and we expand Eq. (A.1.5) in power of  $\alpha_s(\mu_i^2)$  at fixed  $\lambda_{\mu_i}$  to find the explicit form of various  $f_i$ .

We obtain:

$$\begin{aligned} \frac{1 - f_1}{\beta_0\alpha_s f_1} + \frac{\beta_1 f_1^2 \ln f_1 - \beta_0 f_2}{\beta_0^2 f_1^2} \\ + \left( \frac{\beta_1^2 - \beta_0\beta_2}{\beta_0^3} + \frac{(\beta_0\beta_2 - \beta_1^2) f_1^4 + \beta_0\beta_1 f_1^2 f_2 + \beta_0^2 f_2^2 - \beta_0^2 f_1 f_3}{\beta_0^3 f_1^3} \right) \alpha_s = \ln \frac{\mu_f^2}{\mu_i^2}, \end{aligned} \quad (\text{A.1.7})$$

where we suppress  $\lambda_{\mu_i}$  dependence of  $f_i$  and  $\mu_i^2$  dependence of  $\alpha_s$  for simplicity.

A comparison performed order by order brings to the following system of equations

$$\frac{1 - f_1}{\beta_0 \alpha_s f_1} = \ln \frac{\mu_f^2}{\mu_i^2}, \quad (\text{A.1.8a})$$

$$\frac{\beta_1 f_1^2 \ln f_1 - \beta_0 f_2}{\beta_0^2 f_1^2} = 0, \quad (\text{A.1.8b})$$

$$\frac{\beta_1^2 - \beta_0 \beta_2}{\beta_0^3} + \frac{(\beta_0 \beta_2 - \beta_1^2) f_1^4 + \beta_0 \beta_1 f_1^2 f_2 + \beta_0^2 f_2^2 - \beta_0^2 f_1 f_3}{\beta_0^3 f_1^3} = 0, \quad (\text{A.1.8c})$$

which permits us to find  $f_1, f_2, f_3$ . Denoting

$$X = 1 + \lambda_{\mu_i} = 1 + \alpha_s (\mu_i^2) \beta_0 \ln \frac{\mu_f^2}{\mu_i^2}, \quad (\text{A.1.9})$$

the explicit expressions for the various  $f_i$  turn out to be:

$$f_1(X) = \frac{1}{X}, \quad (\text{A.1.10a})$$

$$f_2(X) = -\frac{\beta_1 \ln X}{\beta_0 X^2}, \quad (\text{A.1.10b})$$

$$f_3(X) = \frac{1}{X^3} \left[ \frac{\beta_1^2}{\beta_0^2} (\ln^2 X - \ln X - (1 - X)) + \frac{\beta_2}{\beta_0} (1 - X) \right]. \quad (\text{A.1.10c})$$

By substituting Eqs. (A.1.10) into Eq. (A.1.6), we obtain the desired NNLL solution for the running coupling evolution:

$$\begin{aligned} \alpha_s(\mu_f^2) &= \frac{\alpha_s(\mu_i^2)}{X} - \frac{\alpha_s^2(\mu_i^2) \beta_1 \ln X}{\beta_0 X^2} \\ &+ \frac{\alpha_s^3(\mu_i^2)}{X^3} \left[ \frac{\beta_1^2}{\beta_0^2} (\ln^2 X - \ln X - (1 - X)) + \frac{\beta_2}{\beta_0} (1 - X) \right] + \mathcal{O}(\alpha_s^4(\mu_i^2)). \end{aligned} \quad (\text{A.1.11})$$

Before proceeding, please note the presence in our general solution of the Landau Pole at any logarithmic order. At a particular energy scale, the running coupling constant explodes; this critical scale is usually denote  $\Lambda$  and it is given by:

$$\frac{\Lambda}{Q} = e^{\frac{1}{2\alpha_s \beta_0}}. \quad (\text{A.1.12})$$

Running coupling evolution in the context of resummation leads to the same singularity in our resummed formula in conjugate space. We refer the reader to Sec. 4.1 of Chap. 4 or to Ref. [101–104] for a more detailed description about Landau pole problem in the context of resummation in QCD.

With such a result under our belt, we are now ready to move to PDFs evolution and to a general solution for the Altarelli-Parisi equations.

## A.2 DGLAP Equations

In Sec. 1.2.3 of Chap. 1 we understood that in order to make QCD radiative corrections finite in the context of the naïve parton model we need to factorize into *bare* PDFs, the remaining collinear divergences. This procedure leads to a new factorized version of the parton distribution functions which is finite and can then be fitted from experimental data.

However, the scale at which this factorization procedure takes place is totally arbitrary, and final PDFs will depend on this choice of factorization scale,  $\mu_F^2$ . Evolution of PDFs can be derived in the context of perturbative QCD, using renormalization group arguments. This brings to the famous *Dokshitzer-Gribov-Lipatov-Altarelli-Parisi equations* (DGLAP) [20–22]:

$$\mu_F^2 \frac{\partial}{\partial \mu_F^2} \begin{pmatrix} q_i(N, \mu_F^2) \\ g(N, \mu_F^2) \end{pmatrix} = \begin{pmatrix} \gamma_{q_i, q_j}(N, \alpha_s(\mu_F^2)) & \gamma_{q_i, g}(N, \alpha_s(\mu_F^2)) \\ \gamma_{g, q_j}(N, \alpha_s(\mu_F^2)) & \gamma_{g, g}(N, \alpha_s(\mu_F^2)) \end{pmatrix} \begin{pmatrix} q_j(N, \mu_F^2) \\ g(N, \mu_F^2) \end{pmatrix}. \quad (\text{A.2.1})$$

With respect to Eq. (1.2.32), written in the text, we decide to present here the equations directly in Mellin space to convert multiplicative convolutions into normal products. The Mellin transforms of the splitting functions  $P_{ij}$  are called *Altarelli-Parisi anomalous dimensions*.

Our objective in this section is to perturbatively solve previous equation to predict the first towers of logarithms of the factorization scale. We are going to present a general procedure to compute PDFs evolution following the work of Ref. [126].

### A.2.1 Flavour Decomposition

First of all, we need to separate the different quarks components which are linked in Eq. (A.2.1) by the matrix nature of the Altarelli-Parisi anomalous dimension  $\gamma_{ij}$ . It turns out that the  $(N_f + 1) \times (N_f + 1)$  matrix can in fact be block decomposed, in  $N_f - 1$ ,  $1 \times 1$  matrices and a single  $2 \times 2$  matrix which couples a particular quark combination, the *singlet* one, with the gluon. Usually in literature we refer to them as *non-singlet* and *singlet* sectors.

We start from the non-singlet sector; there are three different types of non-singlet quark combination

$$q_{\text{ns},i}^+ = (1 - i)(q_i + \bar{q}_i) + \sum_{j=1}^{i-1} (q_j + \bar{q}_j), \quad (\text{A.2.2a})$$

$$q_{\text{ns},i}^- = (1 - i)(q_i - \bar{q}_i) + \sum_{j=1}^{i-1} (q_j - \bar{q}_j), \quad (\text{A.2.2b})$$

$$q_{\text{ns}}^v = \sum_{j=1}^{N_f} (q_j - \bar{q}_j), \quad (\text{A.2.2c})$$

which evolve with three different one-dimensional anomalous dimension:

$$\gamma_{\text{ns}}^+ = \gamma_{q_i q_i} + \gamma_{q_i \bar{q}_i} = \gamma_{qq} + \gamma_{q\bar{q}}, \quad (\text{A.2.3a})$$

$$\gamma_{\text{ns}}^- = \gamma_{q_i q_i} - \gamma_{q_i \bar{q}_i} = \gamma_{qq} - \gamma_{q\bar{q}}, \quad (\text{A.2.3b})$$

$$\gamma_{\text{ns}}^v = \gamma_{q_i q_i} - \gamma_{q_i \bar{q}_i} + N_f (\gamma_{q_i q_j} - \gamma_{q_i \bar{q}_j}) = \gamma_{qq} - \gamma_{q\bar{q}} + N_f (\gamma_{qQ} - \gamma_{q\bar{Q}}) \quad (\text{A.2.3c})$$

where in the second equality we introduce the shorter notation  $qq$  ( $q\bar{q}$ ) and  $qQ$  ( $q\bar{Q}$ ) to indicate the splitting between quark (anti-quark) of same or different flavour.

It is important to note that only  $\gamma_{qq}$  starts at order  $\alpha_s$ ;  $\gamma_{q\bar{q}}$ ,  $\gamma_{qQ}$  and  $\gamma_{q\bar{Q}}$  instead are of  $\mathcal{O}(\alpha_s^2)$  and a non-vanishing difference between  $\gamma_{qQ}$  and  $\gamma_{q\bar{Q}}$  comes for the first time only at order  $\alpha_s^3$ .

We now move to the singlet sector; the quark combination which is linked to gluon is the following

$$q_s = \sum_{r=1}^{N_f} (q_r + \bar{q}_r) \quad (\text{A.2.4})$$

and the  $2 \times 2$  matrix which controls the evolution turns out to be

$$\gamma_s = \begin{pmatrix} \gamma_{q_s q_s} & \gamma_{q_s g} \\ \gamma_{g q_s} & \gamma_{gg} \end{pmatrix} \quad (\text{A.2.5})$$

with

$$\gamma_{q_s q_s} = \gamma_{q_i q_i} + \gamma_{q_i \bar{q}_i} + N_f (\gamma_{q_i q_j} + \gamma_{q_i \bar{q}_j}) = \gamma_{qq} + \gamma_{q\bar{q}} + N_f (\gamma_{qQ} + \gamma_{q\bar{Q}}), \quad (\text{A.2.6a})$$

$$\gamma_{q_s g} = N_f \gamma_{q_i g} = N_f \gamma_{\bar{q}_i g}, \quad (\text{A.2.6b})$$

$$\gamma_{g q_s} = \gamma_{g q_i} = \gamma_{g \bar{q}_i}. \quad (\text{A.2.6c})$$

In general all the anomalous dimensions presented here have been computed up to two loops. Their expressions can be found in Ref. [127] for the non-singlet sector, and in Ref. [128] for the singlet sector. Here we limit ourselves to report their LO contribution

$$\gamma_{qq}^{(0)}(N) = \frac{C_F}{2\pi} \left[ \frac{3}{2} - \frac{1}{N+1} - \frac{1}{N+2} - 2\psi(N+1) - 2\gamma_E \right], \quad (\text{A.2.7a})$$

$$\gamma_{qg}^{(0)}(N) = \frac{N_f}{2\pi} \left[ \frac{1}{N+1} - \frac{2}{N+2} + \frac{2}{N+3} \right], \quad (\text{A.2.7b})$$

$$\gamma_{gq}^{(0)}(N) = \frac{C_F}{2\pi} \left[ \frac{2}{N} - \frac{2}{N+1} + \frac{1}{N+2} \right], \quad (\text{A.2.7c})$$

$$\gamma_{gg}^{(0)}(N) = \frac{C_A}{\pi} \left[ \frac{1}{N} - \frac{2}{N+1} + \frac{1}{N+2} - \frac{1}{N+3} - \psi(N+1) - \gamma_E \right] + \beta_0, \quad (\text{A.2.7d})$$

together with the corresponding  $z$ -space splitting functions  $P^{(0)}$

$$P_{qq}^{(0)}(z) = \frac{C_F}{2\pi} \frac{1+z^2}{(1-z)_+} + \frac{3C_F}{4\pi} \delta(1-z), \quad (\text{A.2.8a})$$

$$P_{qg}^{(0)}(z) = \frac{N_f}{2\pi} \left[ z^2 + (1-z)^2 \right], \quad (\text{A.2.8b})$$

$$P_{gq}^{(0)}(z) = \frac{C_F}{2\pi} \left[ \frac{1+(1-z)^2}{z} \right], \quad (\text{A.2.8c})$$

$$P_{gg}^{(0)}(z) = \frac{C_A}{\pi} \left[ \frac{z}{(1-z)_+^z} + \frac{1-z}{z} + z(1-z) \right] + \beta_0 \delta(1-z) \quad (\text{A.2.8d})$$

with plus distribution defined as in Eq. (B.3.2) and  $\psi$  the PolyGamma function, Eq. (B.4.8). More properties about plus distributions, and special functions involved in Mellin evaluations are collected in the next Appendix B.

In Eqs. (A.2.7) and Eqs. (A.2.8), we call with the pedix  $qq$  any singlet or non-singlet combination since at LO

$$\gamma_{\text{ns}}^{+, (0)} = \gamma_{\text{ns}}^{-, (0)} = \gamma_{\text{ns}}^{v, (0)} = \gamma_{q_s q_s}^{(0)} = \gamma_{qq}^{(0)}. \quad (\text{A.2.9})$$

As a last comment about flavour decomposition, we want to describe how to relate observables computed in the usual base  $q_i, g$  with their counterparts in the block diagonal base  $q_{\text{ns}}^+, q_{\text{ns}}^-, q_{rmns}^v, q_s, g$ . For simplicity, we are going to present the decomposition for a generic inclusive cross section, but same combinations could be used for any other factorized observable.

The hadronic cross section can be written in the standard base, making explicit the sum over different partonic channel, as:

$$\begin{aligned} \sigma = & \hat{\sigma}_{gg} gg + \hat{\sigma}_{gq} g \sum_{i=1}^{N_f} (q_i + \bar{q}_i) + \hat{\sigma}_{q\bar{q}} \sum_{i=1}^{N_f} (q_i \bar{q}_i + \bar{q}_i q_i) + \hat{\sigma}_{qq} \sum_{i=1}^{N_f} (q_i q_i + \bar{q}_i \bar{q}_i) \\ & + \hat{\sigma}_{qQ} \sum_{i=1}^{N_f} \sum_{j=1}^{N_f} (1 - \delta_{ij}) (q_i q_j + \bar{q}_i \bar{q}_j) + \hat{\sigma}_{q\bar{Q}} \sum_{i=1}^{N_f} \sum_{j=1}^{N_f} (1 - \delta_{ij}) (\bar{q}_i q_j + q_i \bar{q}_j). \end{aligned} \quad (\text{A.2.10})$$

Now switching to the block diagonal base we obtain for the same hadronic quantity,

$$\begin{aligned} \sigma = & \hat{\sigma}_{gg} gg + \hat{\sigma}_{gq} g q_s + \hat{\sigma}_{SS} q_s q_s + \hat{\sigma}_{VV} q_{\text{ns}}^v q_{\text{ns}}^v \\ & + \hat{\sigma}_{++} \sum_{i=2}^{N_f} \frac{1}{i(i-1)} q_{\text{ns}}^+ q_{\text{ns}}^+ + \hat{\sigma}_{--} \sum_{i=2}^{N_f} \frac{1}{i(i-1)} q_{\text{ns}}^- q_{\text{ns}}^- \end{aligned} \quad (\text{A.2.11})$$

resulting in the following equalities:

$$\hat{\sigma}_{SS} = \hat{\sigma}_{qq} + \hat{\sigma}_{q\bar{q}} + \hat{\sigma}_{qQ} + \hat{\sigma}_{q\bar{Q}}, \quad (\text{A.2.12a})$$

$$\hat{\sigma}_{VV} = \hat{\sigma}_{qq} - \hat{\sigma}_{q\bar{q}} + \hat{\sigma}_{qQ} - \hat{\sigma}_{q\bar{Q}}, \quad (\text{A.2.12b})$$

$$\hat{\sigma}_{++} = \frac{N_f - 1}{N_f} (\hat{\sigma}_{qq} + \hat{\sigma}_{q\bar{q}}) - \frac{1}{N_f} (\hat{\sigma}_{qQ} + \hat{\sigma}_{q\bar{Q}}), \quad (\text{A.2.12c})$$

$$\hat{\sigma}_{--} = \frac{N_f - 1}{N_f} (\hat{\sigma}_{qq} - \hat{\sigma}_{q\bar{q}}) - \frac{1}{N_f} (\hat{\sigma}_{qQ} - \hat{\sigma}_{q\bar{Q}}) \quad (\text{A.2.12d})$$

After this discussion about how to link the non-singlet, singlet base with the standard quark flavour base, we can focus our attention on the computation of PDFs evolution up to some logarithmic accuracy in the factorization scale.

## A.3 General Solution

Our scope in this section is to derive the general solution which relates PDFs evaluated at the final scale  $\mu_f^2$  to PDFs evaluated at the initial scale  $\mu_i^2$ , retaining terms up to NNLL in the logarithms  $\ln \frac{\mu_f^2}{\mu_i^2}$ .

We start again from the non-singlet sector; in this case since the evolution of non-singlet components is completely decoupled, we write the Altarelli-Parisi equation for  $q_{\text{ns}}^+$ ,  $q_{\text{ns}}^-$  and  $q_{\text{ns}}^v$  as

$$\mu_F^2 \frac{\partial q_{\text{ns}}^i(N, \mu_F^2)}{\partial \mu_F^2} = \gamma_{\text{ns}}^i(N, \alpha_s(\mu_F^2)) q_{\text{ns}}^i(N, \mu_F^2), \quad (\text{A.3.1})$$

with index  $i = +, -, v$ .

The solution of the differential equation Eq. (A.3.1) can be easily written as

$$q_{\text{ns}}^i(N, \mu_f^2) = g_{\text{ns}}^i(N, \mu_i^2) \exp \left[ \int_{\mu_i^2}^{\mu_f^2} \frac{dq^2}{q^2} \gamma_{\text{ns}}^i(N, \alpha_s(q^2)) \right], \quad (\text{A.3.2})$$

to obtain a NNLL solution we need  $\gamma_{\text{ns}}^i$  up to  $\mathcal{O}(\alpha_s^3)$  and the NNLL solution of the running coupling evolution Eq. (A.1.11). Performing the integral at the exponent and retaining only the first three contributions, we obtain

$$q_{\text{ns}}^i(N, \mu_f^2) = g_{\text{ns}}^i(N, \mu_i^2) \exp \left[ g_{\text{ns}}^{i,(1)}(N, \lambda_{\mu_i}) + \alpha_s(\mu_i^2) g_{\text{ns}}^{i,(2)}(N, \lambda_{\mu_i}) + \alpha_s(\mu_i^2)^2 g_{\text{ns}}^{i,(3)}(N, \lambda_{\mu_i}) \right], \quad (\text{A.3.3})$$

where  $\lambda_{\mu_i}$  is defined as in Eq. (A.1.6), and

$$g_{\text{ns}}^{i,(1)}(N, \lambda_{\mu_i}) = \frac{\gamma_{\text{ns}}^{i,(0)}(N)}{\beta_0} \ln(1 + \lambda_{\mu_i}), \quad (\text{A.3.4a})$$

$$g_{\text{ns}}^{i,(2)}(N, \lambda_{\mu_i}) = \frac{\gamma_{\text{ns}}^{i,(0)}(N) \beta_1}{\beta_0^2} \frac{\ln(1 + \lambda_{\mu_i}) - \lambda_{\mu_i}}{1 + \lambda_{\mu_i}} + \frac{\gamma_{\text{ns}}^{i,(1)}(N)}{\beta_0} \frac{\lambda_{\mu_i}}{1 + \lambda_{\mu_i}}, \quad (\text{A.3.4b})$$

$$g_{\text{ns}}^{i,(3)}(N, \lambda_{\mu_i}) = \frac{\gamma_{\text{ns}}^{i,(0)}(N) \beta_1^2}{2\beta_0^2} \frac{\lambda_{\mu_i}^2 - \ln^2(1 + \lambda_{\mu_i})}{(1 + \lambda_{\mu_i})^2} + \frac{\gamma_{\text{ns}}^{i,(0)}(N) \beta_2}{2\beta_0^2} \frac{\lambda_{\mu_i}^2}{(1 + \lambda_{\mu_i})^2} - \frac{\gamma_{\text{ns}}^{i,(1)}(N) \beta_1}{2\beta_0^2} \frac{\lambda_{\mu_i} (2 + \lambda_{\mu_i}) - 2 \ln(1 + \lambda_{\mu_i})}{(1 + \lambda_{\mu_i})^2} + \frac{\gamma_{\text{ns}}^{i,(2)}(N)}{2\beta_0} \frac{\lambda_{\mu_i} (2 + \lambda_{\mu_i})}{(1 + \lambda_{\mu_i})^2}. \quad (\text{A.3.4c})$$

The time is ripe to tackle the singlet sector. Of course a simple solution as Eq. (A.3.4) is not possible since the evolution of the singlet quark combination is coupled with gluon dynamics. The differential equation, we need to solve, is the following:

$$\mu_F^2 \frac{\partial}{\partial \mu_F^2} \begin{pmatrix} q_s(N, \mu_F^2) \\ g(N, \mu_F^2) \end{pmatrix} = \begin{pmatrix} \gamma_{q_s q_s}(N, \alpha_s(\mu_F^2)) & \gamma_{q_s g}(N, \alpha_s(\mu_F^2)) \\ \gamma_{g q_s}(N, \alpha_s(\mu_F^2)) & \gamma_{g g}(N, \alpha_s(\mu_F^2)) \end{pmatrix} \begin{pmatrix} q_s(N, \mu_F^2) \\ g(N, \mu_F^2) \end{pmatrix}. \quad (\text{A.3.5})$$

The main idea of the general approach of Ref. [126] is: we are going to find logarithmic corrections more and more subleading by solving perturbatively Eq. (A.3.5) around the LO solution. By LO solution we mean the solution of Eq. (A.3.5) found with  $\gamma_s$  computed at first not trivial order.

The LO solution is our starting point; we are going to write it in the following way:

$$\mathbf{p}_s^{\text{LO}}(N, \mu_f^2) = \mathbf{L}(N, \lambda_{\mu_i}) \mathbf{p}_s^{\text{LO}}(N, \mu_i^2) \quad (\text{A.3.6})$$

with  $\mathbf{p}_s^{\text{LO}} = \begin{pmatrix} q_s \\ g \end{pmatrix}$  the singlet doublet and  $\mathbf{L}$  the LO singlet evolution matrix. To evaluate it, we need to diagonalize  $\gamma_s^{(0)}$  the LO singlet anomalous dimension matrix and then apply solution Eq. (A.3.4) to each eigenvector. We call  $\gamma_+^{(0)}$  and  $\gamma_-^{(0)}$  the greater and the smaller eigenvalue of  $\gamma_s^{(0)}$  respectively. Their explicit expressions as a function of the entries of  $\gamma_s^{(0)}$  turn out to be:

$$\gamma_{\pm}^{(0)}(N) = \frac{1}{2} \left[ \gamma_{q_s q_s}^{(0)}(N) + \gamma_{g g}^{(0)}(N) \pm \sqrt{\left( \gamma_{q_s q_s}^{(0)}(N) - \gamma_{g g}^{(0)}(N) \right)^2 + 4 \gamma_{q_s g}^{(0)}(N) \gamma_{g q_s}^{(0)}(N)} \right]. \quad (\text{A.3.7})$$

Clearly the same combination defines other eigenvalues at any order in  $\alpha_s$  of  $\gamma_s$ ; hence it is perfectly meaningful to talk about anomalous dimension  $\gamma_+$  as the series expansion formed by the largest eigenvalue of  $\gamma_s$  at any order in  $\alpha_s$ . For example we have seen in Chap. 3 that it is the largest eigenvalue  $\gamma_+(N, \alpha_s)$  which diverges at any order in the high energy regime and it is the one which is resummed using BFKL duality (see also Ref. [70, 84]).

In conclusion, a general NNLL expression for  $\mathbf{L}(N, \mu_f^2, \mu_i^2)$  can be written as

$$\mathbf{L}(N, \lambda_{\mu_i}) = \mathbf{e}_+(N) \exp[G_+^{\text{LO}}(N, \lambda_{\mu_i})] + \mathbf{e}_-(N) \exp[G_-^{\text{LO}}(N, \lambda_{\mu_i})] \quad (\text{A.3.8})$$

where we define the projector  $\mathbf{e}_{\pm}$  as

$$\mathbf{e}_{\pm}(N) = \frac{1}{\gamma_{\pm}^{(0)}(N) - \gamma_{\mp}^{(0)}(N)} \left[ \gamma_s^{(0)}(N) - \gamma_{\mp}^{(0)}(N) \mathbf{I} \right] \quad (\text{A.3.9})$$

and the exponential  $G_{\pm}^{\text{LO}}$  as

$$\begin{aligned} G_{\pm}^{\text{LO}}(N, \lambda_{\mu_i}) &= \frac{\gamma_{\pm}^{(0)}}{\beta_0} \ln(1 + \lambda_{\mu_i}) + \alpha_s(\mu_i^2) \frac{\gamma_{\pm}^{(0)}(N) \beta_1 \ln(1 + \lambda_{\mu_i}) - \lambda_{\mu_i}}{\beta_0^2 (1 + \lambda_{\mu_i})} \\ &+ \alpha_s(\mu_i^2) \left[ \frac{\gamma_{\pm}^{(0)}(N) \beta_1^2 \lambda_{\mu_i}^2 - \ln^2(1 + \lambda_{\mu_i})}{2\beta_0^2 (1 + \lambda_{\mu_i})^2} + \frac{\gamma_{\pm}^{(0)}(N) \beta_2}{2\beta_0^2} \frac{\lambda_{\mu_i}^2}{(1 + \lambda_{\mu_i})^2} \right]. \end{aligned} \quad (\text{A.3.10})$$

Now, to introduce higher order corrections to  $\gamma_s$ , we search for a particular "rotation"  $\mathbf{U}(N, \alpha_s)$ , by which the general solution can be written as

$$\mathbf{p}_s(N, \mu_f^2) = \mathbf{U}(N, \alpha_s(\mu_f^2)) \mathbf{L}(N, \lambda_{\mu_i}) \mathbf{U}(N, \alpha_s(\mu_i^2))^{-1} \mathbf{p}_s^{\text{LO}}(N, \mu_i^2). \quad (\text{A.3.11})$$

For all the details we refer the interested reader to Ref. [126]. Here we limit ourselves to present a suitable definition of the operator  $\mathbf{U}$  which permits us to reach the desired result. Let us highlight that the general solution of Eq. (A.3.11) was used in Sec. 2.4 and Sec. 2.5 of Chap. 2 to express PDFs at the soft scale as a function of PDFs at the factorization scale.

To end our discussion about a general NNLL solution of DGLAP equations we need to specify the perturbative expansion of the operator  $\mathbf{U}$ . It can be proved [126] that  $\mathbf{U}$  can be found recursively as

$$\mathbf{U}(N, \alpha_s) = 1 + \sum_{k=1}^{\infty} \alpha_s^k \mathbf{U}^{(k)}(N), \quad (\text{A.3.12})$$

with

$$\mathbf{U}^{(k)} = -\frac{1}{k} \left[ \mathbf{e}_- \tilde{\mathbf{R}}_k \mathbf{e}_- + \mathbf{e}_+ \tilde{\mathbf{R}}_k \mathbf{e}_+ \right] + \frac{\mathbf{e}_+ \tilde{\mathbf{R}}_k \mathbf{e}_-}{\frac{1}{\beta_0} (\gamma_-^{(0)} - \gamma_+^{(0)}) - k} + \frac{\mathbf{e}_- \tilde{\mathbf{R}}_k \mathbf{e}_+}{\frac{1}{\beta_0} (\gamma_+^{(0)} - \gamma_-^{(0)}) - k} \quad (\text{A.3.13})$$

where we suppress  $N$  dependence for simplicity and we define

$$\tilde{\mathbf{R}}_k(N) = \mathbf{R}_k(N) + \sum_{i=1}^{k-1} \mathbf{R}_{k-i}(N) \mathbf{U}^{(i)}(N) \quad (\text{A.3.14})$$

and

$$\mathbf{R}_k(N) = \frac{1}{\beta_0} \gamma_s^{(k)}(N) - \sum_{i=1}^k \frac{\beta_i}{\beta_0} \mathbf{R}_{k-i}(N). \quad (\text{A.3.15})$$

For the sake of completeness, we write explicitly the NNLL general solution as a function of  $\mathbf{L}$  and of the first two orders of the operator  $\mathbf{U}$ :

$$\begin{aligned} \mathbf{p}_s^{\text{NNLL}}(N, \mu_f^2) = & \left[ \mathbf{L}(N, \lambda_{\mu_i}) + \alpha_s(\mu_f^2) \mathbf{U}^{(1)}(N) \mathbf{L}(N, \lambda_{\mu_i}) \right. \\ & - \alpha_s(\mu_i^2) \mathbf{L}(N, \lambda_{\mu_i}) \mathbf{U}^{(1)}(N) + \alpha_s^2(\mu_f^2) \mathbf{U}^{(2)}(N) \mathbf{L}(N, \lambda_{\mu_i}) \\ & - \alpha_s(\mu_f^2) \alpha_s(\mu_i^2) \mathbf{U}^{(1)}(N) \mathbf{L}(N, \lambda_{\mu_i}) \mathbf{U}^{(1)}(N) \\ & \left. + \alpha_s^2(\mu_i^2) \mathbf{L}(N, \lambda_{\mu_i}) \left( \left( \mathbf{U}^{(1)}(N) \right)^2 - \mathbf{U}^{(2)}(N) \right) \right] \mathbf{p}_s^{\text{NNLL}}(N, \mu_i^2). \end{aligned} \quad (\text{A.3.16})$$

We are going to end this section with an important remark about logarithmic accuracy in the context of transverse momentum resummation and consistent resummation. In original transverse momentum resummation at NNLL, the evolution of PDFs from scale  $\frac{b_0^2}{\bar{b}^2}$  to factorization scale  $\mu_F^2$  has to be performed at NLL, hence including only operator  $\mathbf{U}^{(1)}$ . However, in consistent resummation this logarithmic accuracy is not enough at NNLL since we are also interested in components  $\ln^{k-3} \chi \ln N$  which are created by NNLL PDFs evolution from scale  $\frac{Q^2}{\chi}$  to factorization scale  $\mu_F^2$ . Therefore, in this case, the evolution is performed at NNLL but with  $\mathbf{U}^{(2)}$  substituted by its leading large- $N$  behaviour. This simplify the whole derivation, since in the large- $N$  limit operator  $\mathbf{U}$  is diagonal.



# B Integral Transforms and Special Functions

## Contents

---

<b>B.1</b>	<b>Fourier and Hankel Transform.</b>	<b>169</b>
B.1.1	Additive Convolution	170
<b>B.2</b>	<b>Laplace and Mellin Transform.</b>	<b>171</b>
B.2.1	Multiplicative Convolutions	173
<b>B.3</b>	<b>Plus distribution</b>	<b>173</b>
B.3.1	Mellin and Fourier transform of plus distribution	175
<b>B.4</b>	<b>Special Functions</b>	<b>177</b>
B.4.1	Euler Gamma and related functions	177
B.4.2	Bessel Function	178
B.4.3	Hypergeometric Function	179
B.4.4	Polylogarithms and Harmonic Polylogarithms (HPL)	180
<b>B.5</b>	<b>Mellin Transform of Harmonic Polylogarithms (HPL)</b>	<b>183</b>
B.5.1	Harmonic Sums ( $S^H$ )	184
B.5.2	Analytic continuation of Harmonic Sums up to fourth order	185

---

In this Appendix, we collect some useful definitions and results concerning Fourier and Mellin transformations. We will also define properties of plus distributions and of some special functions we have extensively used throughout the whole thesis. Last section will be devoted to the computation of Mellin transform of Harmonic Polylogarithms which enter in any fixed order calculations up to NNLO.

## B.1 Fourier and Hankel Transform

*Multidimensional Fourier transform* of a generic function  $g : \mathbb{R}^n \rightarrow \mathbb{R}^n$  is defined as

$$g(\vec{b}) \equiv \mathcal{F}[g(\vec{\xi})] \equiv \frac{1}{(2\pi)^{\frac{n}{2}}} \int_{\mathbb{R}^n} g(\vec{\xi}) e^{-i\vec{b} \cdot \vec{\xi}} d^n \xi, \quad (\text{B.1.1})$$

where another time we distinguish between the function and its transform by the name of the argument.

According to Eq. (B.1.1), the inverse Fourier transform is given by

$$g(\vec{\xi}) \equiv \mathcal{F}^{-1}[g(\vec{b})] \equiv \frac{1}{(2\pi)^{\frac{n}{2}}} \int_{\mathbb{R}^n} g(\vec{b}) e^{i\vec{b} \cdot \vec{\xi}} d^n b. \quad (\text{B.1.2})$$

In collider phenomenology, many times we have to deal with central functions in  $\mathbb{R}^n$ , i.e. dependent only from the radius  $r$

$$g(x_1, \dots, x_n) \equiv g(r). \quad (\text{B.1.3})$$

In this case, Fourier transform Eq. (B.1.1) can be simplified as

$$\begin{aligned} g(b) = \mathcal{F}[g(r)] &= \frac{1}{(2\pi)^{\frac{n}{2}}} \int_{\mathbb{R}^n} g(r) e^{-i\vec{b} \cdot \vec{\xi}} d^n \xi, \\ &= b^{1-\frac{n}{2}} \int_0^\infty dr r r^{\frac{n}{2}-1} f(r) J_{\frac{n}{2}-1}(br) \end{aligned} \quad (\text{B.1.4})$$

with  $J$  the Bessel function of order  $\frac{n}{2} - 1$  (see Sec. B.4.2 for complete definition),  $b$  the modulus of  $\vec{b}$  and of course  $r$  the modulus of  $\vec{\xi}$ .

Due to angular symmetry, inverse Fourier transform of  $g(b)$  can be obtained with Eq. (B.1.4) simply by switching  $b$  with  $r$ .

The case with  $n = 2$  is particular important in literature and in this thesis and it is usually called as *Hankel Transform*:

$$g(b) \equiv \mathcal{H}[g(r)] \equiv \int_0^\infty dr r J_0(br) g(r), \quad (\text{B.1.5a})$$

$$g(r) \equiv \mathcal{H}^{-1}[g(b)] \equiv \int_0^\infty db b J_0(br) g(b). \quad (\text{B.1.5b})$$

## B.1.1 Additive Convolution

Let us define the additive convolution product  $*$ :

$$(f * g)(\xi) = \frac{1}{(2\pi)^{\frac{n}{2}}} \int_{\mathbb{R}^n} d^n y f(\vec{y}) g(\vec{\xi} - \vec{y}), \quad (\text{B.1.6})$$

Looking at definition Eq. (B.1.6), it is clear that it is commutative

$$(f * g) = (g * f). \quad (\text{B.1.7})$$

Now we are going to prove that under Fourier transformation, additive convolution product diagonalizes:

$$\begin{aligned} \mathcal{F}[(f * g)(\xi)] &= \frac{1}{(2\pi)^{\frac{n}{2}}} \int_{\mathbb{R}^n} d^n \xi e^{-i\vec{b} \cdot \vec{\xi}} \frac{1}{(2\pi)^{\frac{n}{2}}} \int_{\mathbb{R}^n} d^n y f(\vec{y}) g(\vec{\xi} - \vec{y}) \\ &= \frac{1}{(2\pi)^{\frac{n}{2}}} \int_0^1 d^n y e^{-i\vec{b} \cdot \vec{y}} f(\vec{y}) \frac{1}{(2\pi)^{\frac{n}{2}}} \int_{\mathbb{R}^n} d^n \xi' e^{-i\vec{b} \cdot \vec{\xi}'} g(\vec{\xi}') = f(\vec{b})g(\vec{b}). \end{aligned} \quad (\text{B.1.8})$$

## B.2 Laplace and Mellin Transform

The Mellin transform is a particular case of Laplace transform. Therefore we decide to start considering some definitions and results about Laplace transform which remain also valid in the case of Mellin transform.

*Laplace transform* of a function  $g(t)$  is given by

$$g(s) \equiv \int_0^{\infty} dt e^{-st} g(t) \quad (\text{B.2.1})$$

where, as usual in this thesis, we distinguish the Laplace transformed function by its argument.

If the function  $g(s)$  is well defined, then it is free of singularities for  $\text{Re } s > c$  for some value  $c$  depending on  $g(t)$ . Indeed, in order for the integral Eq. (B.2.1) to converge, the function  $g(t)$  can grow at most as  $e^{ct}$  as  $t \rightarrow \infty$  and then the transform is free of singularities for  $\text{Re } s > c$ .

The inverse is defined as ( $c_0 > c$ ):

$$g(t) = \frac{1}{2\pi i} \int_{c_0 - i\infty}^{c_0 + i\infty} ds e^{st} g(s). \quad (\text{B.2.2})$$

The proof is trivial:

$$\frac{1}{2\pi i} \int_{c_0 - i\infty}^{c_0 + i\infty} ds e^{st} g(s) = \int_0^{\infty} dt' g(t') \frac{1}{2\pi i} \int_{c_0 - i\infty}^{c_0 + i\infty} ds e^{s(t-t')}, \quad (\text{B.2.3})$$

$$= \int_0^{\infty} dt' g(t') \delta(t - t'), \quad (\text{B.2.4})$$

$$= \begin{cases} g(t) & t \geq 0 \\ 0 & t < 0. \end{cases} \quad (\text{B.2.5})$$

If  $g(t)$  is real, then  $g(s)$  is a real function, i.e. it satisfies

$$g(s^*) = (g(s))^* \quad (\text{B.2.6})$$

with  $*$  indicates complex conjugation. You can immediately verify relation Eq. (B.2.6) from the definition Eq. (B.2.1).

When a function  $g(z)$  is defined in the range  $0 < z < 1$  (this is quite common in QCD collider phenomenology) we can decide to take a Laplace transform by using  $z = e^{-t}$ . The resulting transform is generally called *Mellin transform*,

$$g(N) \equiv \mathcal{M}[g(z)] \equiv \int_0^1 dz z^{N-1} g(z). \quad (\text{B.2.7})$$

Clearly, the inverse, according to Eq. (B.2.2), is defined as

$$g(x) \equiv \mathcal{M}^{-1}[g(N)] \equiv \frac{1}{2\pi i} \int_{N_0 - i\infty}^{N_0 + i\infty} dN z^{-N} g(N) \quad (\text{B.2.8})$$

with  $N_0$  chosen greater than the real part of the rightmost singularity ( $N_0$  must exist, because again  $g(N)$  has a convergence abscissa).

Here a list of some basic properties of the Mellin transform we extensively use throughout the thesis:

1. *Shift operation*

$$\mathcal{M}[z^c g(z)] = g(N + c) = \mathbf{N}_c g(N) \quad (\text{B.2.9})$$

2. *Dilatation* (Hard Scale changing)

$$\mathcal{M}[g(az)\Theta(a-x)] = \int_0^a dz z^{N-1} g(az) = a^N \int_0^1 d\xi \xi^{N-1} g(\xi) = a^N g(N), \quad (\text{B.2.10})$$

with  $0 < a < 1$ .

3. *Logarithm treatment*

$$\mathcal{M}[\ln^k(g(z))] = \frac{\partial^k}{\partial \epsilon^k} \mathcal{M}[(g(z))^\epsilon] = \frac{\partial^k}{\partial \epsilon^k} \mathcal{G}(N, \epsilon) \quad (\text{B.2.11})$$

with  $\mathcal{G}$  usually called *generating function* of  $g(z)$ .

4. *Useful series representation* If  $N$  is limited to integers we can simplify Mellin computation by exploiting the following series representations:

$$\mathcal{M}\left[\frac{g(z)}{1-z}\right] = \sum_{N'=N-1}^{\infty} \int_0^1 dz z^{N'-1} g(z) = \sum_{N'=N-1}^{\infty} g(N'), \quad (\text{B.2.12a})$$

$$\mathcal{M}\left[\frac{g(z)}{1+z}\right] = (-1)^N \sum_{N'=N-1}^{\infty} (-1)^{N'} \int_0^1 dz z^{N'-1} g(z) = (-1)^N \sum_{N'=N-1}^{\infty} g(N'), \quad (\text{B.2.12b})$$

$$\begin{aligned} \mathcal{M}\left[\frac{g(z)}{(1 \pm z)^\alpha}\right] &= \sum_{N'=0}^{\infty} \binom{\alpha}{N'} (\pm)^{N'} \int_0^1 dz z^{N+N'-1} g(z) \\ &= \sum_{N'=0}^{\infty} \binom{\alpha}{N'} (\pm)^{N'} g(N + N'). \end{aligned} \quad (\text{B.2.12c})$$

Usually, at the end, final result is analytic continued to all the complex plane.

Last remark of this section is about actual numerical computation of inverse Mellin transform, Eq. (B.2.8). The integration contour can be deformed at will, as long as it does not cross any singularity (all the singularities must remain at the left of the contour). A typical deformation, since  $x < 1$ , consists in giving a phase to the upper and lower parts of the integration path in such a way that the real part of  $N$  be negative and increasing as its absolute value goes to infinity.

In particular we find pretty useful following manipulations, if  $g(N)$  is a real function (see Eq. (B.2.6)):

$$g(z) = \frac{1}{2\pi i} \int_{N_0-i\infty}^{N_0+i\infty} dN z^{-N} g(N),$$

$$\begin{aligned}
&= \frac{1}{\pi} \operatorname{Im} \left[ \int_{N_0}^{N_0+i\infty} dN z^{-N} g(N) \right], \\
&= \frac{1}{\pi} \operatorname{Im} \left[ \frac{r+I}{\int_0^1 \frac{du}{u}} z^{-N_0+(r+I)\ln u} g(N_0 - (r+I)\ln u) \right], \tag{B.2.13}
\end{aligned}$$

$$= \frac{1}{\pi} \operatorname{Im} \left[ \frac{r-I}{\int_0^1 \frac{du}{u}} z^{-N_0+(r-I)\ln u} g(N_0 - (r-I)\ln u) \right], \tag{B.2.14}$$

where in the last two equalities we perform the following variable change

$$N = N_0 - (r \pm I) \ln u \tag{B.2.15}$$

with  $r > 0$  arbitrary slope. All the numerical Mellin evaluations performed in this thesis have been carried out using the following parametrization for the integrand function.

## B.2.1 Multiplicative Convolutions

Let us define the multiplicative convolution product  $\otimes$ :

$$\begin{aligned}
(f \otimes g)(z) &= \int_z^1 \frac{dy}{y} f(y) g\left(\frac{x}{z}\right), \\
&= \int_0^1 dy \int_0^1 dw f(w) g(y) \delta(z - yw). \tag{B.2.16}
\end{aligned}$$

Looking at the second line of Eq. (B.2.16), it is clear that it is commutative

$$(f \otimes g) = (g \otimes f) \tag{B.2.17}$$

and it can be trivially extended to many functions

$$(g_1 \otimes \cdots \otimes g_n)(z) = \int_0^1 dw_1 \cdots \int_0^1 dw_n g_1(w_1) \cdots g_n(w_n) \delta(z - w_1 \cdots w_n). \tag{B.2.18}$$

Now we are going to prove that under Mellin transformation, multiplicative convolution product diagonalizes:

$$\begin{aligned}
\mathcal{M}[(f \otimes g)(z)] &= \int_0^1 dz z^{N-1} \int_0^1 dy \int_0^1 dw f(y) g(w) \delta(z - yw) \\
&= \int_0^1 dy y^{N-1} f(y) \int_0^1 dw w^{N-1} g(w) = f(N)g(N). \tag{B.2.19}
\end{aligned}$$

## B.3 Plus distribution

In this thesis, we define and use two types of plus distributions which arise from the cancellation of soft divergences.

First, given a function  $f$  divergent in  $\xi \rightarrow 0$  we define the following plus distribution as

$$\int_0^{\xi_{\max}} d\xi [f(\xi)]_+ \phi(\xi) = \int_0^{\xi_{\max}} d\xi f(\xi) [\phi(\xi) - \Theta(1 - \xi)\phi(0)] \tag{B.3.1}$$

with  $\phi$  a Schwartz test function and  $\Theta$  the Heaviside distribution.  $\xi_{\max}$  is the upper limit of the  $\xi$  variable; in almost all our applications it coincides with  $\infty$ .

Another plus distribution we can introduce works for a function  $g$ , defined in the range  $0 < z < a$ , and singular in  $z \rightarrow a$ . We write

$$\int_0^a dz [g(z)]_+^a \phi(z) = \int_0^a dz g(z) [\phi(z) - \phi(a)]. \tag{B.3.2}$$

The most important case in this second group is when  $a = 1$ . We have called in the text this particular plus distribution as  $[g(z)]_+^z = [g(z)]_+^1$ , due to its importance.

From the two definition it follows that, formally

$$[f(\xi)]_+ = f(\xi) - \delta(\xi) \int_0^1 d\xi' f(\xi'), \tag{B.3.3}$$

$$[g(z)]_+^a = g(z) - \delta(a - z) \int_0^a dz' g(z'), \tag{B.3.4}$$

but, since  $f(\xi)$  diverges as  $\xi \rightarrow 0$  and  $g(z)$  as  $z \rightarrow a$ , these expressions make sense only in a regularized form:

$$[f(\xi)]_+ = \lim_{\eta \rightarrow 0^+} \left[ \Theta(\xi - \eta) f(\xi) - \delta(\xi) \int_{\eta}^1 d\xi f(\xi) \right], \tag{B.3.5}$$

$$[g(z)]_+^a = \lim_{\eta \rightarrow 0^+} \left[ \Theta(a - \eta - z) g(z) - \delta(a - z) \int_0^{a-\eta} dz g(z) \right], \tag{B.3.6}$$

where the limit is intended to be performed *after* the integration over the test function  $\phi$ .

Plus distributions, defined in Eq. (B.3.1) and in Eq. (B.3.2) with  $a = 1$ , regularize functions which diverge as  $\xi \rightarrow 0$  or  $z \rightarrow 1$  at most as

$$\xi^{-\alpha} \qquad (1 - z)^{-\alpha} \qquad \alpha < 2 \tag{B.3.7}$$

in the sense that the integral Eq. (B.3.1) (or Eq. (B.3.2)) over any test function  $\phi$  is finite. In particular the usual logarithms

$$\frac{\ln^k \xi}{\xi} \qquad \frac{\ln^k (1 - z)}{1 - z} \tag{B.3.8}$$

are properly regularized.

Some useful identities can be derived directly from the definitions. For plus distribution Eq. (B.3.1), we have

$$[h(\xi)f(\xi)]_+ = h(\xi) [f(\xi)]_+ - \delta(\xi) \int_0^1 d\xi' g(\xi') [f(\xi)]_+, \tag{B.3.9a}$$

$$h(\xi) [f(\xi)]_+ = h(0) [f(\xi)]_+ + [h(\xi) - h(0)] f(\xi) \quad (\text{B.3.9b})$$

with  $h(\xi)$  a regular function in  $\xi \rightarrow 0$ ; instead, for plus distribution Eq. (B.3.2), we can write

$$[q(z)g(z)]_+^a = q(z) [g(z)]_+^a - \delta(a-z) \int_0^a dy q(y) [g(y)]_+, \quad (\text{B.3.10a})$$

$$q(z) [g(z)]_+^a = q(a) [g(z)]_+^a + [q(z) - q(a)] g(z). \quad (\text{B.3.10b})$$

We want also to note that a regular function  $h$  or  $q$  can be *dressed* by plus distribution by adding a proper bound term. In formulas we have

$$h(\xi) = [h(\xi)]_+ + \delta(\xi) \int_0^1 d\xi' h(\xi'), \quad (\text{B.3.11a})$$

$$q(z) = [q(z)]_+^a + \delta(a-z) \int_0^a dy q(y). \quad (\text{B.3.11b})$$

We have used Eq. (B.3.11) in Chap. 1 and in Chap. 2 in Sec. 2.4 and Sec. 2.5 to make explicit the presence of a soft and collinear divergence.

### B.3.1 Mellin and Fourier transform of plus distribution

We want to study the behaviour in  $b$  space (using Fourier/Hankel transform) or in  $N$  space (using Mellin transform) of plus distributions defined in the previous section. For this discussion and in all the following sections we are going to limit Eq. (B.3.2) to the case  $a = 1$ . Therefore we will talk about properties of plus distribution  $[g(z)]_+^z$ .

From the definition Eq. (B.1.5) (with  $\xi = r^2$ ), the Fourier (Hankel) transform of plus distribution Eq. (B.3.1) is given by

$$\mathcal{H} [(f(\xi))_+] = \frac{1}{2} \int_0^\infty d\xi \left[ J_0(b\sqrt{\xi}) - 1 \right] f(\xi). \quad (\text{B.3.12})$$

Analogously, from the definition Eq. (B.2.7), the Mellin transform of plus distribution Eq. (B.3.2) turns out to be

$$\mathcal{M} [(g(z))_+^z] = \int_0^\infty dz [z^{N-1} - 1] g(z). \quad (\text{B.3.13})$$

We want now to prove that the behaviour in  $b$ ,  $N$  space of a plus distribution is qualitatively different from that of an ordinary function. To see this, we recall first the famous *Riemann-Lebesgue Lemma*

**Theorem B.3.1.** *If  $f(\xi)$  is integrable ( $\in L_1$ ), then*

$$\lim_{b \rightarrow \infty} \mathcal{F}[f(\xi)] = 0 \quad (\text{B.3.14})$$

and its generalization to Mellin transform

**Theorem B.3.2.** *If  $g(z)$  is integrable ( $\in L_1$ ), then*

$$\lim_{N \rightarrow \infty} \mathcal{M}[g(z)] = 0. \quad (\text{B.3.15})$$

Therefore any continuous function of  $\xi$  or  $z$  must vanish in the large- $b$  or  $-N$  limit.

This is not true for distributions. For example, the Fourier transform of  $\delta(\xi)$  or the Mellin transform of  $\delta(1-z)$  is 1, hence a constant for all values of  $b$  or  $N$ . In particular, it does not vanish as  $b$  or  $N$  increases.

For the interesting case of plus distributions, Eq. (B.3.1) and Eq. (B.3.2), we can prove the following theorems:

**Theorem B.3.3.** *For real  $b > 1$ , if  $f(\xi)$  is singular in  $\xi = 0$  as  $\xi^{-\alpha}$  with  $\alpha < 2$  then  $|\mathcal{F}[(f(\xi))_+]|$  diverges as  $b \rightarrow \infty$ ;*

*Proof.* Proof is almost trivial; first we note

$$|\mathcal{F}[(f(\xi))_+]| = |\mathcal{H}[(f(\xi))_+]| = \left| \int_0^\infty d\xi, \frac{\xi}{2} [J_0(b\sqrt{\xi}) - 1] f(\xi) \right| \xrightarrow{b \rightarrow \infty} \left| \int_0^\infty d\xi f(\xi) \right| \quad (\text{B.3.16})$$

where in the last step we use Riemann-Lebesgue Lemma. We reach the conclusion since

$$\lim_{b \rightarrow \infty} |\mathcal{F}[(f(\xi))_+]| = \left| \int_0^\infty d\xi f(\xi) \right| \quad (\text{B.3.17})$$

which is divergent. □

**Theorem B.3.4.** *For real  $N > 1$ , if  $g(z)$  is singular in  $z = 1$  as  $(1-z)^{-\alpha}$  with  $\alpha < 2$  then  $|\mathcal{M}[(g(z))_+]|$  diverges as  $N \rightarrow \infty$ ;*

*Proof.* In this case we first note

$$|\mathcal{M}[(g(z))_+]| \leq \int_0^1 dz |(z^{N-1} - 1)| |g(z)| \stackrel{N \geq 1}{=} -\mathcal{M}[|(g(z))_+]| \quad (\text{B.3.18})$$

where the minus sign comes from the fact that  $z^{N-1} - 1 < 0$  for  $N > 1$ . The boundary function  $-\mathcal{M}[|(g(z))_+]|$  is an monotone increasing function for all  $N > 1$ . Then we come to the conclusion using monotone convergence theorem to pass the limit  $N \rightarrow \infty$  under the integral:

$$\lim_{N \rightarrow \infty} |\mathcal{M}[(g(z))_+]| = \left| \int_0^1 dz g(z) \right| \quad (\text{B.3.19})$$

which again is divergent. □

We thus conclude this section with the following message. The difference between the Fourier or Mellin transform of a function and that of a plus distribution of a  $\xi = 0$  or  $z = 1$  singular function is that the first is limited and goes to zero as  $b$  or  $N$  tends to infinity, while the second at some point starts increasing and goes to infinity at large  $b$  or  $N$ .

## B.4 Special Functions

In this section we collect definitions and properties of some special functions which appear in this thesis or which are useful in conjugate transform computations. We will mainly concentrate on those properties which are useful in the context of resummation. This Appendix is *not* intended as a complete overview on the subject.

### B.4.1 Euler Gamma and related functions

The base function of this group is Euler Gamma function which is defined as

$$\Gamma(z) \equiv \int_0^{\infty} dt e^{-t} t^{z-1}; \quad (\text{B.4.1})$$

the integral converges in the half-plane  $\text{Re } z > 0$ . The Gamma function is a real function, i.e. it satisfies

$$\Gamma(z^*) = (\Gamma(z))^*; \quad (\text{B.4.2})$$

in particular,  $\text{Im } \Gamma(z) = 0$  for  $z \in \mathbb{R}$ . Integrating by parts, it is easy to show that  $\Gamma(z)$  satisfy the recursion relation

$$\Gamma(z+1) = z\Gamma(z). \quad (\text{B.4.3})$$

Then, because additionally  $\Gamma(1) = 1$ , for  $z = n \in \mathbb{N}$  we have

$$\Gamma(n+1) = n! \quad (\text{B.4.4})$$

extending the factorial to complex values. Eq. (B.4.3) in reverse allows to analytically extend the Gamma function to the whole complex plane, apart from some singular points. Indeed, the Gamma function has poles for non-positive integer values of its argument; more precisely, for  $n \in \mathbb{N}$ ,  $\Gamma(-n)$  has a simple pole with residue

$$\text{Res}_{z=-n} \Gamma(z) = \frac{(-1)^n}{n!}. \quad (\text{B.4.5})$$

Around one of such poles, the Gamma function satisfies the expansion

$$\Gamma(z-n) = \frac{(-1)^n}{n!} \left[ \frac{1}{z} + \psi(n+1) + \mathcal{O}(z) \right] \quad (\text{B.4.6})$$

where  $\psi$  is the PolyGamma function, defined in Eq. (B.4.8).

Another important property satisfied by Gamma function is the so called *Euler reflection formula*

$$\Gamma(z)\Gamma(1-z) = \frac{\pi}{\sin(\pi z)}, \quad (\text{B.4.7})$$

which is useful to relate the region of convergence of the integral in Eq. (B.4.1), with the region  $\text{Re}(z) < 0$ .

Logarithmic derivatives of the Gamma function are usually called PolyGamma function of order  $k$

$$\psi_k(z) \equiv \frac{d^{k+1}}{dz^{k+1}} \ln \Gamma(z), \quad (\text{B.4.8})$$

with the identification of  $\psi_0(z) = \psi(z)$ , the original polygamma function. From the recursion property of the Euler Gamma, Eq. (B.4.3), we deduce the recursion formula for the  $k$ -order polygamma

$$\psi_n(z+1) \equiv \psi_n(z) + n! (-1)^n \frac{1}{z^{n+1}}. \quad (\text{B.4.9})$$

Our last comment is about the behaviour of polygamma functions at large  $|z|$ . At large  $|z|$  with  $\arg z < \pi$ , only  $\psi(z)$  is divergent

$$\psi(z+1) \approx \ln z + \mathcal{O}\left(\frac{1}{z}\right) \quad (\text{B.4.10})$$

while all the polygammas of higher orders,  $\psi_n$  with  $n \geq 1$ , vanish as  $\frac{1}{z^n}$ .

## B.4.2 Bessel Function

Bessel functions are the canonical solutions  $y(x)$  of Bessel's differential equation:

$$x^2 \frac{d^2 y}{dx^2} + x \frac{dy}{dx} + (x^2 - \alpha^2) y = 0 \quad (\text{B.4.11})$$

for an arbitrary complex number  $\alpha$ , which is usually denoted as the order of the Bessel function.

Because Eq. (B.4.11) is a second-order differential equation, there must be two linearly independent solutions. They are called Bessel functions of first and second kind.

Real values of the order  $\alpha$  define Bessel functions of the first kind  $J_\alpha(x)$  and Bessel functions of the second kind  $Y_\alpha(x)$ . The difference is that  $J_\alpha(x)$  always vanishes for  $x = 0$  and it is a single-valued function, while  $Y_\alpha(x)$  diverges at the origin and it is a multi-value function.

Useful integral representations are in particular

$$J_\alpha(x) = \frac{1}{\pi} \int_0^\pi \cos(\alpha\tau - x \sin \tau) d\tau - \frac{\sin(\alpha x)}{\pi} \int_0^\infty e^{-x \sinh(t) - \alpha t} dt, \quad (\text{B.4.12})$$

$$Y_\alpha(x) = \frac{1}{\pi} \int_0^\pi \sin(x \sin(\tau) - \tau\alpha) d\tau - \frac{1}{\pi} \int_0^\infty e^{-x \sinh(t)} (e^{-\alpha t} \cos(\alpha\pi) + e^{\alpha t}) dt, \quad (\text{B.4.13})$$

while series representations are given by

$$J_\alpha(x) = \sum_{k=0}^{\infty} \frac{(-1)^k}{k! \Gamma(k + \alpha + 1)} \left(\frac{x}{2}\right)^{2k + \alpha}, \quad (\text{B.4.14})$$

$$Y_\alpha(x) = \csc(\pi\alpha) \left( \cos(\alpha\pi) \sum_{k=0}^{\infty} \left[ \frac{(-1)^k}{k! \Gamma(k + \alpha + 1)} \left(\frac{x}{2}\right)^{2k + \alpha} \right] - \sum_{k=0}^{\infty} \left[ \frac{(-1)^k}{k! \Gamma(k - \alpha + 1)} \left(\frac{x}{2}\right)^{2k - \alpha} \right] \right). \quad (\text{B.4.15})$$

We have used both integral and series representation for the function  $J_0$  in Chap. 2.

On the contrary, if  $\alpha$  is purely imaginary, relative solutions of Eq. (B.4.11) are denominated *modified Bessel functions* of first or second kind, and denoted by  $I_\alpha$  and  $K_\alpha$ . They are expressed as a function of  $J_\alpha$  and  $Y_\alpha$  as:

$$I_\alpha(x) = i^{-\alpha} J_\alpha(ix), \quad (\text{B.4.16})$$

$$K_\alpha(x) = \frac{\pi}{2} \frac{I_{-\alpha}(x) - I_\alpha(x)}{\sin(\alpha x)}. \quad (\text{B.4.17})$$

We have employed modified Bessel function of second kind  $K$  in Chap. 4 to invert our consistent transverse momentum resummation.

### B.4.3 Hypergeometric Function

The Hypergeometric functions are a class of very general special functions, which contains many other examples of this Section as special cases. The most general definition can be given in term of the power series, for  $|z| < 1$ :

$${}_pF_q(a_1, \dots, a_p; b_1, \dots, b_q; z) = \sum_{k=0}^{\infty} \frac{(a_1)_k \dots (a_p)_k}{(b_1)_k \dots (b_q)_k} \frac{z^k}{k!}, \quad (\text{B.4.18})$$

where  $(a)_k$  is the Pochhammer symbol

$$(a)_k = \frac{\Gamma(a+k)}{\Gamma(a)} = a(a+1)\dots(a+k-1). \quad (\text{B.4.19})$$

Even if when  $p > q + 1$  the series Eq. (B.4.18) has zero radius of convergence, in some case it is still possible to give sense to these functions by exploiting some analytic relations. In these cases, power series Eq. (B.4.18) has to be interpreted as asymptotic expansion.

Many other ordinary or special functions can be written as Hypergeometric functions of some order. For example

- Exponential Functions

$${}_0F_0(; ; z) = e^z; \quad (\text{B.4.20})$$

- Logarithmic Functions

$$(z-1) {}_2F_1(1, 1; 2; 1-z) = \ln z; \quad (\text{B.4.21})$$

- PolyLogarithmic Functions

$$z_{n+1} F_n(1, 1, 1, \dots, 1; 2, 2, \dots, 2; z) = \text{Li}_n(z); \quad (\text{B.4.22})$$

- Bessel Functions

$$J_\alpha(z) = \frac{1}{\Gamma(\alpha+1)} \left(\frac{z}{2}\right)^\alpha {}_0F_1\left(; \alpha+1; -\frac{z^2}{4}\right), \quad (\text{B.4.23})$$

$$Y_\alpha(z) = -\frac{2^\alpha z^{-\alpha} \Gamma(\alpha)}{\pi} {}_0F_1\left(\ ; \alpha + 1; -\frac{z^2}{4}\right) - \frac{2^{-\alpha} z^\alpha \cos(\alpha\pi) \Gamma(-\alpha)}{\pi} {}_0F_1\left(\ ; \alpha + 1; -\frac{z^2}{4}\right), \quad (\text{B.4.24})$$

$$I_\alpha(z) = \frac{1}{\Gamma(\alpha + 1)} \left(\frac{z}{2}\right)^\alpha {}_0F_1\left(\ ; \alpha + 1; \frac{z^2}{4}\right), \quad (\text{B.4.25})$$

$$K_\alpha(z) = 2^{\alpha-1} z^{-\alpha} \Gamma(\alpha) {}_0F_1\left(\ ; 1 - \alpha; \frac{z^2}{4}\right) + 2^{-\alpha-1} z^\alpha \Gamma(-\alpha) {}_0F_1\left(\ ; \alpha + 1; \frac{z^2}{4}\right); \quad (\text{B.4.26})$$

- Polygamma Functions

$$(-1)^{n+1} n! z^{-n-1} {}_{n+2}F_{n+1}(1, z, z, \dots, z; z+1, z+1, \dots, z+1; 1) = \psi_n(z). \quad (\text{B.4.27})$$

One of the most used Hypergeometric Function is the so-called *Euler Hypergeometric Function*, which is characterized by  $p = 2$  and  $q = 1$ . Its definition is

$${}_2F_1(a, b; c; z) = \sum_{k=0}^{\infty} \frac{(a)_k (b)_k}{(c)_k} \frac{z^k}{k!}. \quad (\text{B.4.28})$$

We have already met this particular special function in Chap. 2, since it appears both in Higgs threshold resummation at fixed  $p_T$  and in consistent transverse momentum resummation. The expansion of this function in powers of  $a, b, c$  has been studied in detail in recent years, see Refs. [66, 67]. General solution was found by using another type of special functions, the Harmonic Polylogarithms (HPL), which are the subject of the next subsection.

## B.4.4 Polylogarithms and Harmonic Polylogarithms (HPL)

The Harmonic Polylogarithms or HPL are another wide class of special functions which are formed by subsequent integration of the basis

$$\frac{1}{1-x}, \quad \frac{1}{x}, \quad \frac{1}{1+x}. \quad (\text{B.4.29})$$

They are extremely useful in analytically solving most of the loop integrals appearing at higher orders; for this reason NNLO analytic computations present in literature are very often written as proper combination of Harmonic Polylogarithms of various order.

They have been widely studied in literature [129–133, 135, 135] and we refer the interested reader to these papers for a more exhaustive treatment of the subject.

In this subsection we limit ourselves to properly define the Harmonic Polylogarithms of weight  $m$  and to list its main properties.

The harmonic polylogarithms of weight  $m$  and argument  $z$  are classified by a set of  $m$  indices, grouped into a  $m$ -dimensional vector  $\vec{\omega}_m$  and are usually indicated by  $H(\vec{\omega}_m, z)$  or  $H_{\vec{\omega}_m}(z)$ . Each entry of the vector  $\vec{\omega}_m$  can assume the values 0, 1,  $-1$ .

They are defined by a recursive procedure. For  $m = 1$ , one states

$$H(0; z) = \int_0^z dx \frac{1}{x} = \ln z, \quad (\text{B.4.30})$$

$$H(1; z) = \int_0^z dx \frac{1}{1-x} = -\ln(1-z), \quad (\text{B.4.31})$$

$$H(-1; z) = \int_0^z dx \frac{1}{1+x} = \ln(1+z) \quad (\text{B.4.32})$$

and higher weight HPL are defined by integration of Harmonic Polylogarithms of lower weight. In particular, let us call  $a$  the last index added to the vector  $\vec{\omega}_m$

$$\vec{\omega}_m = (a, \vec{\omega}_{m-1}); \quad (\text{B.4.33})$$

HPL of weight  $m$  associated to the vector indexed  $\vec{\omega}_m$  is going to be

$$H(\vec{\omega}_m; z) = \int_0^z dx f(a; x) H(\vec{\omega}_{m-1}; x) \quad (\text{B.4.34})$$

with basis function  $f(a; x)$  defined as

$$f(0; x) = \frac{1}{x}, \quad (\text{B.4.35a})$$

$$f(1; x) = \frac{1}{1-x}, \quad (\text{B.4.35b})$$

$$f(-1; x) = \frac{1}{1+x}. \quad (\text{B.4.35c})$$

Harmonic Polylogarithms give back as particular cases both normal Polylogarithms  $\text{Li}_n$  and Nielsen Polylogarithms  $S_{n,p}$ . In particular, we have:

$$\text{Li}_n(z) = \int_0^z \frac{dx}{x} \text{Li}_{n-1}(x) = H(\vec{0}_{n-1}, 1; z), \quad (\text{B.4.36})$$

$$S_{n,p}(z) = \frac{(-1)^{n+p-1}}{(n-1)!p!} \int_0^1 \frac{(\ln t)^{n-1} \ln^p(1-zt)}{t} = H(\vec{0}_n, \vec{1}_p; z) \quad (\text{B.4.37})$$

with  $\text{Li}_1(z) = -\ln(1-z)$ , and  $\vec{0}_n, \vec{1}_m$  vectors of 0s or 1s of length  $n$  or  $m$  respectively.

In many applications in collider physics it is useful to analytically compute the Mellin transform of lengthy expressions written as a function of HPL of different weights. The Mellin transform of HPL can be computed in terms of particular objects denoted as Harmonic Sums. To the Mellin transformation of Harmonic Polylogarithms is devoted the last section of this Appendix. We use these results in the computation of Mellin transform of  $\mathcal{H}$  at two loops in transverse momentum resummation and to expand the Hypergeometric function in the consistent resummation.

However, before moving to Mellin space, we want to list some important general properties of HPL which help to deal with the algebra of this class of functions:

Weight	Full Basis	Minimal Set
2	9	3
3	27	8
4	81	18
5	243	48
6	729	116
7	2187	312
8	6561	810

**Table B.1.** Size of the full base and of the minimal set for the first weights

1. Given a *only-zero*, *only-one*, *only-minus one* vector  $\vec{0}_m, \vec{1}_m, \left(-\vec{1}\right)_m$  we have

$$H\left(\vec{0}_m; z\right) = \frac{1}{m!} \ln^m z, \quad (\text{B.4.38a})$$

$$H\left(\vec{1}_m; z\right) = \frac{(-1)^m}{m!} \ln^m (1-z), \quad (\text{B.4.38b})$$

$$H\left(\left(-\vec{1}\right)_m; z\right) = \frac{1}{m!} \ln^m (1+z). \quad (\text{B.4.38c})$$

2. if  $\vec{\omega}_m \neq \vec{0}_m$  then

$$H\left(\vec{\omega}_m; 0\right) = 0 \quad (\text{B.4.39})$$

3. *Derivative*: if  $\vec{\omega}_m = (a, \vec{\omega}_{m-1})$

$$\frac{d}{dz} H\left(\vec{\omega}_m; z\right) = f(a; z) H\left(\vec{\omega}_{m-1}; z\right) \quad (\text{B.4.40})$$

4. *Reflection Rule*: if  $m_1 \neq 0$  then

$$H\left(\omega_m, \dots, \omega_1; -z\right) = (-1)^m H\left(-\omega_m, \dots, -\omega_1; z\right) \quad (\text{B.4.41})$$

5. *Reduction Rules*: the following two identities permits to express higher order HPL as combination of lower order HPL; they are found by exploiting integration by parts or fraction reduction on definition Eq. (B.4.34). In formulas we have:

$$\begin{aligned} H\left(\omega_1, \dots, \omega_m; z\right) &= H\left(\omega_1; z\right) H\left(\omega_2, \dots, \omega_m; z\right) - H\left(\omega_2, \omega_1; z\right) H\left(\omega_3, \dots, \omega_m; z\right) \\ &+ H\left(\omega_3, \omega_2, \omega_1; z\right) H\left(\omega_4, \dots, \omega_m; z\right) - \dots - (-1)^m H\left(\omega_m, \dots, \omega_1; z\right), \end{aligned} \quad (\text{B.4.42})$$

$$\begin{aligned} H\left(a; z\right) H\left(\omega_m, \dots, \omega_1; z\right) &= H\left(a, \omega_m, \dots, \omega_1; z\right) + H\left(\omega_m, a, \omega_{m-1}, \dots, \omega_1; z\right) \\ &+ H\left(\omega_m, \omega_{m-1}, a, \dots, \omega_1; z\right) + \dots + H\left(\omega_m, \dots, \omega_1, a; x\right). \end{aligned} \quad (\text{B.4.43})$$

Using reduction relations, Eq. (B.4.42), (B.4.43) we can lower the number of independent HPL and construct at any weight  $m$  a set of minimal HPL which permits to reconstruct the whole group. In Table B.1, we report for the first weights the total number of possible Harmonic Polylogarithms and the dimension of the minimal set.

## B.5 Mellin Transform of Harmonic Polylogarithms (HPL)

In many applications, we wonder to compute analytically the Mellin transform of our expressions. This is particularly true in the context of resummation in conjugate space, where the analytic requirement is often necessary to reach the desired factorized expression. However, switching from inclusive cross section to differential observables, explicit expressions of our anomalous dimensions and hard functions tend to become complicated, thus involving even Harmonic Polylogarithms of higher weights. In the applications of this thesis, we face the problem to compute analytically Mellin transform of HPLs of weight four and lower.

Therefore in this section, we want to highlight the procedure we use to evaluate these Mellin transforms. Final results are going to be proper combination of a particular set of special functions called Harmonic Sums. To the numerical computation of Harmonic Sums for complex argument will be devoted next subsection.

We are ready to present the general procedure, we use in the computation of Mellin Transforms of all the Harmonic Polylogarithms [136]. It is constitute by several steps:

1. First of all, we consider  $N$  as a integer value  $n$ , and we compute the solution according to this hypothesis.
2. Looking at the integrand, if there is a power of  $\frac{1}{1-x}$  or  $\frac{1}{1+x}$ , replace it by a sum according to Eqs. (B.2.12).
3. Powers of  $\ln(1-x)$ , if any, have to be treated separately according to

$$\int_0^1 dx x^m \ln^p(1-x) F(x) = \int_0^1 dx x^m \ln^p(1-x) (F(x) - F(1)) + F(1) \int_0^1 dx x^m \ln^p(1-x) \quad (\text{B.5.1})$$

where we call  $F(x)$  the rest of the integrand and it has a finite value at  $x = 1$ . The second term can now be directly integrated.

4. Do a partial integration on the powers of  $x$ . Thanks to the second step, the values at  $x = 0$  and  $x = 1$  never present any problems.
5. If there is only a power of  $x$  left one can integrate and the integration phase is finished. Otherwise one should repeat previous steps until all functions have been broken down.
6. At the end of the integration we end up with terms which may contain nested sums, either to a finite upper limit or to infinity. These sums can all be expressed as combination of proper Harmonic Sums ( $S^H$ ).
7. Analytic continuation of the final result from integers to a generic complex value has to be performed as explained at the end of this appendix in Sec. B.5.2.5.

### B.5.1 Harmonic Sums ( $S^H$ )

Harmonic Sums ( $S^H$ ) of different weights  $m$  are defined on natural number  $n \in \mathbb{N}$  recursively as follows. In the following we define the *weight* of an Harmonic Sums the number of nested sums is forming to; instead, we call the *order* of an Harmonic Sums the sum of the values of its indexes. For weight  $m = 1$  we introduce

$$S_{\omega}^H(n) = \sum_{i=1}^n \frac{1}{i^{\omega}}, \quad (\text{B.5.2a})$$

$$S_{-\omega}^H(n) = \sum_{i=1}^n \frac{(-1)^i}{i^{\omega}}, \quad (\text{B.5.2b})$$

and then for higher weights the following relation holds

$$S_{\omega, j_1, \dots, j_{m-1}}^H(n) = \sum_{i=1}^n \frac{1}{i^{\omega}} S_{j_1, \dots, j_{m-1}}^H(i), \quad (\text{B.5.3a})$$

$$S_{-\omega, j_1, \dots, j_{m-1}}^H(n) = \sum_{i=1}^n \frac{(-1)^i}{i^{\omega}} S_{j_1, \dots, j_{m-1}}^H(i). \quad (\text{B.5.3b})$$

The Harmonic Sums of weight 1 can all be expressed as a proper combination of other known special functions, according to

$$S_1^H(N) = \Psi(N) = \psi_0(N+1) + \gamma_E, \quad (\text{B.5.4a})$$

$$S_k^H(N) = \frac{(-1)^{k-1}}{(k-1)!} \psi_{k-1}(N+1) + \zeta_k, \quad k > 1, \quad (\text{B.5.4b})$$

$$S_{-1}^H(N) = (-1)^N \beta(N+1) - \ln 2, \quad (\text{B.5.4c})$$

$$S_{-k}^H(N) = \frac{(-1)^{-k-1}}{(-k-1)!} (-1)^N \beta^{(-k-1)}(N+1) - \left(1 - \left(\frac{1}{2}\right)^{-k-1}\right) \zeta_{-k}, \quad k > 1; \quad (\text{B.5.4d})$$

On the contrary, no relations are in general present for Harmonic sums of higher weight.

Using Harmonic Sums all the Harmonic Polylogarithms can be analytically Mellin transformed. Up to now this is a standard procedure and many tools exist to perform it automatically. We want only to mention the Mathematica package *MT* [137] and the FORM procedure *SUMMER* [136] which we use during this thesis work to perform Mellin transformations.

Of course, at the end, the result is a function of these special sums and in order to evaluated them, we need a procedure to perform the analytic continuation of definition (B.5.3) from natural numbers to all the complex plane. This is not a totally trivial task. In Refs. [138, 139], a general procedure to perform the analytic continuation of Harmonic Sums up to fourth order was presented and expressions for all the  $S_{j_1, j_2, j_3, j_4}^H$  with  $j_1 + j_2 + j_3 + j_4 = 4$  are written explicitly. Unfortunately, in both the references some typos are present, and moreover the important caveat of Sec. B.5.2.5 is completely absent and some equalities, which seems to be valid for all the complex plane, are in fact

true only for integers<sup>1</sup>.

For this reason we find useful to write again explicitly in the next subsection the expressions of the analytic continuation of the Harmonic Sums up to fourth order, which are the special functions we use in all our applications. Furthermore, we want to specify better the way in which such expressions have to be used in Mellin integral computations. To derive these formulas, we apply a similar technique of the one presented in Refs. [138, 139].

## B.5.2 Analytic continuation of Harmonic Sums up to fourth order

The main idea to perform the analytic continuation of various  $S^H$  is to construct a set of functions, whose Mellin transform is in relation one to one with the minimal set of Harmonic Sums at some fixed order. All the other  $S^H$  are then computed by exploiting the properties listed for example in Ref. [136].

Mellin transform of the selected set of functions is then evaluated using proper polynomial interpolations. We decide to define three sets of coefficients, approximating different classes of functions. Set  $a^{(l)}$  is defined according to

$$\ln^l(1+x) \approx \sum_{k=0}^{8+l} a_k^{(l)} x^{k+1}; \quad (\text{B.5.5})$$

its values up to  $l = 3$  are explicitly (starting from  $k = 0$ ):

$$a^{(1)} = \left\{ 0.999999974532238, -0.499995525889840, 0.333203435557262, \right. \\ \left. -0.248529457782640, 0.191451164719161, -0.137466222728331, \right. \\ \left. 0.0792107412244877, -0.0301109656912626, 0.00538406208663153, \right. \\ \left. 0.0000001349586745 \right\}, \quad (\text{B.5.6a})$$

$$a^{(2)} = \left\{ 0, 0.99999980543793, -0.999995797779624, \right. \\ \left. 0.916516447393493, -0.831229921350708, 0.745873737923571, \right. \\ \left. -0.634523908078600, 0.467104011423750, -0.261348046799178, \right. \\ \left. 0.0936814286867420, -0.0156249375012462 \right\} \quad (\text{B.5.6b})$$

$$a^{(3)} = \left\{ 0, 0, 0.99999989322696, -1.49999722020708, \right. \\ \left. 1.74988008499745, -1.87296689068405, 1.91539974617231, \right.$$

---

<sup>1</sup>In particular, in Ref. [139] we do not agree with Eqs. (62), (72), (124), (134) where typos are present; furthermore in all the equations where coefficients  $c^{(k)}$  are used, their values have been modified to contain also polynomial  $P_1^{(k)}$ . Instead in Ref. [138], for example, Eq. (43) shows two different way to compute the same analytic continuation of the Harmonic Sums  $S_{-1,-1}^H$ . However, this equality does not hold for values of  $N$  which are non-integers. This can be proved simply by performing numerically the Mellin transform of the function  $\left(\frac{\ln(1+x)}{x-1}\right)_+$

$$\left. \begin{aligned} & -1.85963744001295, 1.62987195424434, -1.17982353224299, \\ & 0.628710122994999, -0.211307487211713, 0.0328953352932140 \end{aligned} \right\}. \quad (\text{B.5.6c})$$

Set  $b^{(l)}$  approximates following functions:

$$\frac{\ln^l(1+x) - \ln^l 2}{x-1} \approx \sum_{k=0}^{L(l)} b_k^{(l)} x^k \quad (\text{B.5.7})$$

with  $L(1) = 8$ ,  $L(2) = 9$ ,  $L(3) = 15$ .  $b_k^{(l)}$  values are:

$$\begin{aligned} b^{(1)} = \left\{ & 0.693147166991375, -0.306850436868254, 0.193078041088284, \right. \\ & -0.139403892894644, 0.105269615988049, -0.0746801353858524, \\ & \left. 0.0427339135378207, -0.0161809049989783, 0.00288664611077007 \right\}, \end{aligned} \quad (\text{B.5.8a})$$

$$\begin{aligned} b^{(2)} = \left\{ & 0.480453024731510, 0.480450679641120, -0.519463586324817, \right. \\ & 0.479285947990175, -0.427765744446172, 0.360855321373065, \\ & -0.263827078164263, 0.146927719341510, -0.0525105367350968, \\ & \left. 0.00874144396622167 \right\}, \end{aligned} \quad (\text{B.5.8b})$$

$$\begin{aligned} b^{(3)} = \left\{ & 0.33302465198526926, 0.33302465294458333, 0.33302458698245874, \right. \\ & -0.6669733788751905, 0.8329914797601391, -0.9166248356766676, \\ & 0.9555225313767898, -0.9626278376733954, 0.9315917979228248, \\ & -0.8411435378489305, 0.6749616810627938, -0.4530769450120006, \\ & 0.23754927911496704, -0.08942075739064419, 0.021221995497457305, \\ & \left. -0.00236584329575064 \right\}. \end{aligned} \quad (\text{B.5.8c})$$

Then we are going to use a third set  $c^{(l)}$  with  $l = 1, 2, 3, 4$  to approximate some special functions entering in our computation. In particular we define:

$$\text{Li}_2(x) \approx P_0^{(1)}(x) + P_1^{(1)}(x) \ln(1-x), \quad (\text{B.5.9})$$

$$\text{Li}_3(x) \approx P_0^{(2)}(x) + P_1^{(2)}(x) \ln(1-x), \quad (\text{B.5.10})$$

$$S_{1,2}(x) \approx P_0^{(3)}(x) + P_1^{(3)}(x) \ln(1-x) + P_2^{(3)}(x) \ln^2(1-x), \quad (\text{B.5.11})$$

$$\text{Li}_2^2(x) \approx P_0^{(4)}(x) + P_1^{(4)}(x) \ln(1-x) + P_2^{(4)}(x) \ln^2(1-x), \quad (\text{B.5.12})$$

with

$$P_0^{(1)}(x) = \sum_{k=0}^{11} c_k^{(1)} x^k, \quad (\text{B.5.13a})$$

$$P_1^{(1)}(x) = \frac{11}{6} - 3x + \frac{3}{2}x^2 - \frac{1}{3}x^3 = \sum_{k=0}^3 P_{1,k}^{(1)}x^k; \quad (\text{B.5.13b})$$

$$P_0^{(2)}(x) = \sum_{k=0}^{12} c_k^{(2)}x^k, \quad (\text{B.5.14a})$$

$$P_1^{(2)}(x) = -1 + \frac{5}{2}x - 2x^2 + \frac{1}{2}x^3 = \sum_{k=0}^3 P_{1,k}^{(2)}x^k; \quad (\text{B.5.14b})$$

$$P_0^{(3)}(x) = \sum_{k=0}^9 c_k^{(3)}x^k, \quad (\text{B.5.15a})$$

$$P_1^{(3)}(x) = \frac{205}{144} - \frac{25}{12}x + \frac{23}{24}x^2 - \frac{13}{36}x^3 + \frac{1}{16}x^4 = \sum_{k=0}^4 P_{1,k}^{(3)}x^k, \quad (\text{B.5.15b})$$

$$P_2^{(3)}(x) = -\frac{25}{24} + 2x - \frac{3}{2}x^2 + \frac{2}{3}x^3 - \frac{1}{8}x^4 = \sum_{k=0}^4 P_{2,k}^{(3)}x^k; \quad (\text{B.5.15c})$$

$$P_0^{(4)}(x) = \sum_{k=0}^{12} c_k^{(4)}x^k, \quad (\text{B.5.16a})$$

$$P_1^{(4)}(x) = -\left(\frac{167}{36} - \frac{25}{6}\zeta_2\right) + \left(\frac{235}{18} - 8\zeta_2\right)x - \left(\frac{40}{3} - 6\zeta_2\right)x^2 \\ + \left(\frac{109}{18} - \frac{8}{3}\zeta_2\right)x^3 - \left(\frac{41}{36} - \frac{1}{2}\zeta_2\right)x^4 = \sum_{k=0}^4 P_{1,k}^{(4)}x^k, \quad (\text{B.5.16b})$$

$$P_2^{(4)}(x) = \frac{35}{12} - \frac{26}{3}x + \frac{19}{2}x^2 - \frac{14}{3}x^3 + \frac{11}{12}x^4 = \sum_{k=0}^4 P_{2,k}^{(4)}x^k; \quad (\text{B.5.16c})$$

and

$$c^{(1)} = \left\{ 2.2012182965269744E - 8, 2.833327652357064, -1.8330909624101532, \right. \\ 0.7181879191200942, -0.0280403220046588, -0.181869786537805, \\ 0.532318519269331, -1.07281686995035, 1.38194913357518, \\ \left. -1.11100841298484, 0.506649587198046, -0.100672390783659 \right\}, \quad (\text{B.5.17a})$$

$$c^{(2)} = \left\{ 0, -6.050453690953361E - 6, 2.12530461606213, \right. \\ -1.0523034829446278, 0.160180000661971, -0.351982379713689, \\ \left. 1.41033369447519, -3.53344124579927, 5.93934899678262, \right.$$

$$\left. \begin{aligned} & -6.60019998525006, 4.66330491799074, -1.89825521858848, \\ & 0.339773000152805 \end{aligned} \right\}, \quad (\text{B.5.17b})$$

$$c^{(3)} = \left\{ \begin{aligned} & 0, 1.423616247405256, -0.08001203559240111, \\ & -0.39875367195395994, 0.339241791547134, -0.0522116678353452, \\ & -0.0648354706049337, 0.0644165053822532, -0.0394927322542075, \\ & 0.0100879370657869 \end{aligned} \right\}, \quad (\text{B.5.17c})$$

$$c^{(4)} = \left\{ \begin{aligned} & -1.84461401708802E-8, 2.2150086978693073, -0.9133677154535804, \\ & 3.4783104357500143, -2.823955592989266, 0.992890266001707, \\ & -1.30026190226546, 3.41870577921103, -5.76763902370864, \\ & 6.45554138192407, -4.59405622046138, 1.88510809558304, \\ & -0.340476080290674 \end{aligned} \right\}. \quad (\text{B.5.17d})$$

We need a last set of coefficient  $d^{(l)}$ ,  $l = 1, 2$  to approximate a particular combination of Nielsen Polylogarithms which turn out to be very useful with Harmonic Sums of fourth order. We define the combination

$$I_1(x) = \frac{1}{2}S_{1,2}(x^2) - S_{1,2}(x) - S_{1,2}(-x) \quad (\text{B.5.18})$$

and we approximate  $I_1(x)$  as

$$I_1(x) \approx P_0^I(x) + P_2^I(x) \ln(1-x) \quad (\text{B.5.19})$$

with

$$P_0^I(x) = \sum_{k=0}^9 d_k^{(1)} x^k, \quad (\text{B.5.20a})$$

$$P_2^I(x) = \sum_{k=0}^9 d_k^{(2)} x^k, \quad (\text{B.5.20b})$$

and

$$d^{(1)} = \left\{ \begin{aligned} & 0, -0.822467033400776, 0.0887664705657325, -0.0241549406045162, \\ & 0.00965074750946139, -0.00470587487919749, 0.00246014308378549, \\ & -0.00116431121874067, 0.000395705193848026, -0.0000664699010014505 \end{aligned} \right\}, \quad (\text{B.5.21a})$$

$$d^{(2)} = \left\{ -0.822467033400776, 0.999999974532241, -0.249997762945014, \right.$$

$$\left. \begin{aligned} &0.111067811851394, -0.0621323644338330, 0.0382902328987004, \\ &-0.0229110370338977, 0.0113158200819689, -0.00376387065979726, \\ &0.000598229109013054 \end{aligned} \right\}. \tag{B.5.21b}$$

Let us remind you that all the vectors presented before start with  $k = 0$  as first number.

Using previous approximations, we are now able to compute the Mellin transform of the following set of 39 functions. Then we are going to express the analytic continuation of all the Harmonic Sums up to fourth order as a combination of these transforms.

We explicitly write:

$$g_1(N) = \mathcal{M} \left[ \frac{\ln(1+x)}{1+x} \right] = \frac{1}{2} \left( \ln^2 2 - (N-1) \sum_{k=1}^{10} \frac{a_k^{(2)}}{N+k} \right), \tag{B.5.22}$$

$$g_2(N) = \mathcal{M} \left[ \frac{\ln^2(1+x)}{1+x} \right] = \frac{1}{3} \left( \ln^3 2 - (N-1) \sum_{k=2}^{12} \frac{a_k^{(3)}}{N+k} \right), \tag{B.5.23}$$

$$g_3(N) = \mathcal{M} \left[ \frac{\text{Li}_2(x)}{1+x} \right] = \zeta_2 \ln 2 - \sum_{k=0}^9 a_k^{(1)} \left( \frac{N-1}{N+k} \zeta_2 + \frac{k+1}{(N+k)^2} \Psi(N+k) \right), \tag{B.5.24}$$

$$\begin{aligned} g_4(N) &= \mathcal{M} \left[ \frac{\text{Li}_2(-x)}{1+x} \right] \\ &= -\frac{1}{2} \zeta_2 \ln 2 + \sum_{k=0}^9 a_k^{(1)} \left( \frac{N-1}{N+k} \frac{\zeta_2}{2} + \frac{k+1}{(N+k)^2} (\ln 2 - \beta(N+k+1)) \right), \end{aligned} \tag{B.5.25}$$

$$\begin{aligned} g_5(N) &= \mathcal{M} \left[ \frac{\text{Li}_2(x) \ln x}{1+x} \right] \\ &= -\sum_{k=0}^9 a_k^{(1)} \left( \frac{k+1}{(N+k)^2} \left( \zeta_2 + \psi_1(N+k+1) - 2 \frac{\Psi(N+k)}{N+k} \right) \right), \end{aligned} \tag{B.5.26}$$

$$\begin{aligned} g_6(N) &= \mathcal{M} \left[ \frac{\text{Li}_3(x)}{1+x} \right] \\ &= \zeta_3 \ln 2 - \sum_{k=0}^9 a_k^{(1)} \left( \frac{N-1}{N+k} \zeta_3 + \frac{k+1}{(N+k)^2} \left( \zeta_2 - \frac{\Psi(N+k)}{N+k} \right) \right), \end{aligned} \tag{B.5.27}$$

$$\begin{aligned} g_7(N) &= \mathcal{M} \left[ \frac{\text{Li}_3(-x)}{1+x} \right] = -\frac{3}{4} \zeta_3 \ln 2 \\ &+ \sum_{k=0}^9 a_k^{(1)} \left( \frac{N-1}{N+k} \frac{3}{4} \zeta_3 + \frac{k+1}{(N+k)^2} \frac{1}{2} \zeta_2 - \frac{k+1}{(N+k)^3} (\ln 2 - \beta(N+k+1)) \right), \end{aligned} \tag{B.5.28}$$

$$g_8(N) = \mathcal{M} \left[ \frac{S_{1,2}(x)}{1+x} \right] = \zeta_3 \ln 2$$

$$- \sum_{k=0}^9 a_k^{(1)} \left( \frac{N-1}{N+k} \zeta_3 + \frac{k+1}{(N+k)^2} \frac{1}{2} (\Psi^2(N+k) + \zeta_2 - \psi_1(N+k+1)) \right), \quad (\text{B.5.29})$$

$$g_9(N) = \mathcal{M} \left[ \frac{S_{1,2}(-x)}{1+x} \right] = \frac{1}{8} \zeta_3 \ln 2 - \sum_{k=0}^9 \left[ a_k^{(1)} \frac{N-1}{N+k} \left( \frac{\zeta_3}{8} - \frac{1}{2} \sum_{j=1}^{10} \frac{a_j^{(2)}}{N+k+j+1} \right) \right] - \frac{1}{2} \sum_{i=2}^{12} \frac{a_i^{(3)}}{N+i}, \quad (\text{B.5.30})$$

$$g_{10}(N) = \mathcal{M} \left[ \frac{I_1(x)}{1+x} \right] = -\frac{5}{8} \zeta_3 \ln 2 + \sum_{k=1}^{10} \left[ a_k^{(2)} \frac{\Psi(N+k)}{N+k} \right] + \sum_{k=0}^9 \left[ a_k^{(1)} \frac{N-1}{N+k} \left( \frac{5}{8} \zeta_3 - \sum_{j=0}^9 a_j^{(1)} \frac{\Psi(N+k+j+1)}{N+k+j+1} \right) \right], \quad (\text{B.5.31})$$

$$g_{11}(N) = \mathcal{M} \left[ \frac{\text{Li}_2(x) \ln(1-x)}{1+x} \right] = \sum_{k=0}^{11} \left[ c_k^{(1)} \left( \frac{1}{2} (\ln^2 2 - \zeta_2) - \sum_{j=0}^9 a_j^{(1)} \left( \frac{j+1}{N+k+j} \Psi(N+k+j) - \Psi(j+1) \right) \right) \right] + \sum_{k=0}^3 P_{2,k}^{(1)} \left( \frac{7}{4} \zeta_3 - \zeta_2 \ln 2 + \frac{1}{3} \ln^2 2 + \sum_{j=0}^9 a_j^{(1)} \left( \frac{j+1}{N+k+j} (\Psi^2(N+k+j) + \zeta_2 - \psi_1(N+k+j+1)) - \Psi^2(j+1) - \zeta_2 + \psi_1(j+2) \right) \right), \quad (\text{B.5.32})$$

$$g_{12}(N) = \mathcal{M} \left[ \frac{\text{Li}_2(-x) \ln(1-x)}{1+x} \right] = \sum_{k=0}^9 \frac{a_k^{(1)}}{k+1} \left( \frac{1}{2} \left( \ln^2 2 - \sum_{j=1}^{10} \left[ a_j^{(2)} \frac{N+k}{N+k+j+1} \right] \right) - \left( \beta^{(1)}(N+k) + \beta(N+k) (\Psi(N+k) - \ln 2) \right) \right), \quad (\text{B.5.33})$$

$$g_{13}(N) = \mathcal{M} \left[ \frac{\text{Li}_2(-x) \ln(1+x)}{1+x} \right] = -\frac{1}{4} \zeta_2 \ln^2 2 + \frac{1}{2} \left( \sum_{k=2}^{11} \left[ \frac{a_k^{(3)}}{N+k} \right] + \sum_{k=1}^{10} \left[ a_k^{(2)} \frac{N-1}{N+k} \left( \frac{1}{2} \zeta_2 - \frac{\ln 2 - \beta(N+k+1)}{N+k} \right) \right] \right), \quad (\text{B.5.34})$$

$$g_{14}(N) = \mathcal{M} \left[ -\frac{\ln(1+x)^2 - \ln^2 2}{1-x} \right] = \sum_{k=0}^9 \frac{b_k^{(2)}}{N+k}, \quad (\text{B.5.35})$$

$$g_{15}(N) = \mathcal{M} \left[ -\frac{\text{Li}_2(x) (\ln(1+x) - \ln 2)}{1-x} \right] = \sum_{k=0}^8 \frac{b_k^{(1)}}{N+k} \left( \zeta_2 - \frac{\Psi(N+k)}{N+k} \right), \quad (\text{B.5.36})$$

$$\begin{aligned}
g_{16}(N) &= \mathcal{M} \left[ -\frac{\text{Li}_2(-x)(\ln(1+x) - \ln 2)}{1-x} \right] \\
&= \sum_{k=0}^8 \frac{b_k^{(1)}}{N+k} \left( -\frac{1}{2}\zeta_2 + \frac{\ln 2 - \beta(N+k+1)}{N+k} \right), \tag{B.5.37}
\end{aligned}$$

$$g_{17}(N) = \mathcal{M} \left[ -\frac{\ln x \ln(1+x)^2}{1-x} \right] = \ln^2 2 \psi_1(N) - \sum_{k=0}^9 \frac{b_k^{(2)}}{(N+k)^2}, \tag{B.5.38}$$

$$\begin{aligned}
g_{18}(N) &= \mathcal{M} \left[ -\frac{\text{Li}_2(x) - \zeta_2}{1-x} \right] = \frac{1}{N-1} (\Psi^2(N-1) + \zeta_2 - \psi_1(N)) - \zeta_2 \Psi(N-1) \\
&+ \sum_{k=0}^{11} \left[ c_k^{(1)} \frac{N-1}{N+k-1} \Psi(N+k-1) \right] \\
&- \sum_{k=0}^3 P_{2,k}^{(1)} \frac{N-1}{N+k-1} (\Psi^2(N+k-1) + \zeta_2 - \psi_1(N+k)), \tag{B.5.39}
\end{aligned}$$

$$g_{19}(N) = \mathcal{M} \left[ -\frac{\text{Li}_2(-x) + \frac{\zeta_2}{2}}{1-x} \right] = \frac{1}{2}\zeta_2 \Psi(N-1) - \sum_{k=0}^8 \frac{a_k^{(1)}}{k+1} \Psi(N+k), \tag{B.5.40}$$

$$\begin{aligned}
g_{20}(N) &= \mathcal{M} \left[ -\frac{\text{Li}_3(x) - \zeta_3}{1-x} \right] = \frac{1}{2}\zeta_2^2 - \zeta_3 \Psi(N-1) \\
&+ \sum_{k=0}^{12} \left[ c_k^{(2)} \frac{N-1}{N+k-1} \Psi(N+k-1) \right] - \frac{1}{2} \sum_{k=0}^{12} \left[ c_k^{(4)} \frac{N-1}{N+k-1} \right] \\
&- \sum_{k=0}^3 \left[ P_{2,k}^{(2)} \frac{N-1}{N+k-1} (\Psi^2(N+k-1) + \zeta_2 - \psi_1(N+k)) \right] \\
&+ \frac{N-1}{2} \sum_{k=0}^4 \left[ P_{2,k}^{(4)} \frac{\Psi(N+k-1)}{N+k-1} - P_{3,k}^{(4)} \frac{\Psi^2(N+k-1) + \zeta_2 - \psi_1(N+k)}{N+k-1} \right], \tag{B.5.41}
\end{aligned}$$

$$\begin{aligned}
g_{21}(N) &= \mathcal{M} \left[ -\frac{S_{1,2}(x) - \zeta_3}{1-x} \right] = -\zeta_3 \Psi(N-1) \\
&+ \frac{1}{2(N-1)} (\Psi^3(N-1) + 3\Psi(N-1)(\zeta_2 - \psi_1(N)) + 2\zeta_3 + \psi_2(N)) \\
&+ \sum_{k=0}^9 \left[ c_k^{(3)} \frac{N-1}{N+k-1} \Psi(N+k-1) \right] + \sum_{k=0}^4 \frac{N-1}{N+k-1} \\
&\left( P_{3,k}^{(3)} (\Psi^3(N+k-1) + 3\Psi(N+k-1)(\zeta_2 - \psi_1(N+k))) \right. \\
&\quad \left. + 2\zeta_3 + \psi_2(N+k) \right) - P_{2,k}^{(3)} (\Psi^2(N+k-1) + \zeta_2 - \psi_1(N+k)), \tag{B.5.42}
\end{aligned}$$

$$g_{22}(N) = \mathcal{M} \left[ -\frac{\text{Li}_2(x) \ln x}{1-x} \right] = \sum_{k=1}^{11} \left[ c_k^{(1)} \psi_1(N+k) \right] \\ - \sum_{k=0}^3 P_{2,k}^{(1)} \left( \Psi(N+k-1) \psi_1(N+k) - \frac{1}{2} \psi_2(N+k) \right), \quad (\text{B.5.43})$$

$$g_{23}(N) = \mathcal{M} \left[ -\frac{\text{Li}_3(-x) + \frac{3}{4} \zeta_3}{1-x} \right] = -\frac{1}{2} \zeta_2^2 + \zeta_3 \ln 2 + \frac{3}{4} \zeta_3 \Psi(N-1) - g_6(N) \\ - \sum_{k=0}^8 a_k^{(1)} \frac{N-1}{N+k} \left( \zeta_3 - \frac{\zeta_2}{N+k} - \frac{\zeta_2}{k+1} \right. \\ \left. + \Psi(N+k) \left( \frac{1}{(N+k)^2} + \frac{1}{(k+1)^2} + \frac{1}{k(N+k)} \right) \right), \quad (\text{B.5.44})$$

$$g_{24}(N) = \mathcal{M} \left[ -\frac{I_1(x) + \frac{5}{8} \zeta_3}{1-x} \right] = -2\zeta_3 \ln 2 + 2g_8(N) + \frac{5}{8} \zeta_3 \Psi(N-1) \\ + \sum_{k=0}^8 \left[ a_k^{(1)} \frac{N-1}{N+k} \left( 2\zeta_3 - \frac{\Psi^2(N+k) + \zeta_2 - \psi_1(N+k+1)}{N+k} \right) \right] \\ + \sum_{k=0}^8 \left[ d_k^{(1)} \frac{N-1}{N+k} \Psi(N+k) \right] \\ - \sum_{k=0}^9 \left[ d_k^{(2)} \frac{N-1}{N+k-1} \left( \Psi^2(N+k-1) + \zeta_2 - \psi_1(N+k) \right) \right], \quad (\text{B.5.45})$$

$$g_{25}(N) = \frac{5}{16} \zeta_3 \ln 2 + \frac{1}{2} g_{10}(N) - \frac{1}{8} \zeta_3 \Psi(N-1) \\ + \frac{1}{2} \sum_{k=1}^{10} \left[ \frac{a_k^{(2)}}{k+1} \frac{N-1}{N+k} \Psi(N+k) \right] \\ + \frac{1}{2} \sum_{k=0}^8 \left[ a_k^{(1)} \frac{N-1}{N+k} \left( -\frac{5}{8} \zeta_3 + \sum_{j=0}^8 a_j^{(1)} \frac{\Psi(N+k+j+1)}{N+k+j+1} \right) \right], \quad (\text{B.5.46})$$

$$g_{26}(N) = \mathcal{M} \left[ \frac{\ln^2(1-x)}{1+x} \right] = \frac{7}{4} \zeta_3 - \zeta_2 \ln 2 + \frac{1}{3} \ln^3 2 + \sum_{k=0}^9 a_k^{(1)} \\ \left( \frac{k+1}{N+k} \left( \Psi^2(N+k) + \zeta_2 - \psi_1(N+k+1) \right) \right. \\ \left. - \left( \Psi(k+1) + \zeta_2 - \psi_1(k+2) \right) \right), \quad (\text{B.5.47})$$

$$g_{27}(N) = \mathcal{M} \left[ \frac{\ln(1-x)}{1+x} \right] = \frac{1}{2} (\ln^2 2 - \zeta_2) - \sum_{k=0}^9 a_k^{(1)} \left( \frac{k+1}{N+k} \Psi(N+k) - \Psi(k+1) \right), \quad (\text{B.5.48})$$

$$g_{28}(N) = \mathcal{M} \left[ -\frac{\ln(1+x) - \ln 2}{1-x} \right] = \sum_{k=0}^8 \frac{b_k^{(1)}}{N+k}, \quad (\text{B.5.49})$$

$$\begin{aligned} g_{29}(N) = \mathcal{M} \left[ \frac{\ln^3(1-x)}{1+x} \right] &= -6\text{Li}_2 \left( \frac{1}{2} \right) - \sum_{k=0}^9 a_k^{(1)} \\ &\left( \frac{k+1}{N+k} \left( \Psi^3(N+k) + 3\Psi(N+k)(\zeta_2 - \psi_1(N+k+1)) \right. \right. \\ &+ 2\zeta_3 + \psi_2(N+k+1) \left. \right) - \left( \Psi^3(k+1) + 3\Psi(k+1)(\zeta_2 - \psi_1(k+2)) \right. \\ &\left. \left. + \zeta_2 + \psi_2(k+2) \right) \right) \end{aligned} \quad (\text{B.5.50})$$

$$\begin{aligned} g_{30}(N) = \mathcal{M} \left[ \frac{\ln^3(1+x)}{1+x} \right] &= \ln^4 2 \\ &- \sum_{k=0}^9 \left[ a_k^{(1)} \left( (N-1) \sum_{j=2}^{12} \left[ \frac{a_j^{(3)}}{N+j+k+1} \right] + 3g_2(N+k) \right) \right], \end{aligned} \quad (\text{B.5.51})$$

$$g_{31}(N) = \mathcal{M} \left[ -\frac{\ln^3(1+x) - \ln^3 2}{1-x} \right] = \sum_{k=0}^{15} \frac{b_k^{(3)}}{N+k}, \quad (\text{B.5.52})$$

$$\begin{aligned} g_{32}(N) = \mathcal{M} \left[ -\frac{S_{1,2} \left( \frac{1-x}{2} \right)}{1-x} \right] &= - \sum_{k=1}^{10} \left[ c_k^{(3)} \frac{2^{-k} \Gamma(k) \Gamma(N)}{\Gamma(N+k)} \right] \\ &+ \sum_{k=0}^4 \left[ \left( P_{1,k}^{(3)} - 2 \ln 2 P_{2,k}^{(3)} \right) \sum_{j=0}^8 \left[ b_j^{(1)} \frac{2^{-k} \Gamma[k+1] \Gamma[n+j]}{\Gamma(N+k+j+1)} \right] \right] \\ &+ \sum_{k=0}^4 \left[ P_{2,k}^{(3)} \sum_{j=0}^9 \left[ b_j^{(2)} \frac{2^{-k} \Gamma[k+1] \Gamma[n+j]}{\Gamma(N+k+j+1)} \right] \right], \end{aligned} \quad (\text{B.5.53})$$

$$\begin{aligned} g_{33}(N) = \mathcal{M} \left[ \frac{\text{Li}_3 \left( \frac{1-x}{2} \right)}{1+x} \right] &= - (N-1) \sum_{k=0}^{12} \left[ c_k^{(2)} \left( \sum_{j=0}^8 \left[ a_j^{(1)} \frac{2^{-k} \Gamma(k+1) \Gamma(N+j)}{\Gamma(N+j+k+1)} \right] \right) \right] \\ &+ (N-1) \sum_{k=0}^3 \left[ P_{1,k}^{(2)} \left( \sum_{j=0}^9 \left[ b_j^{(2)} \frac{2^{-k} \Gamma(k+2) \Gamma(N+j-1)}{\Gamma(N+j+k+1)} \right] \right. \right. \\ &\left. \left. - \ln 2 \sum_{j=0}^8 \left[ b_j^{(1)} \frac{2^{-k} \Gamma(k+2) \Gamma(N+j-1)}{\Gamma(N+j+k+1)} \right] \right) \right] \\ &+ \sum_{k=1}^{11} \left[ c_k^{(1)} \left( \sum_{j=0}^8 \left[ a_j^{(1)} \frac{2^{-k} \Gamma(k) \Gamma(N+j+1)}{\Gamma(N+j+k+1)} \right] \right) \right] \\ &- \sum_{k=0}^3 \left[ P_{1,k}^{(1)} \left( \sum_{j=0}^9 \left[ b_j^{(2)} \frac{2^{-k} \Gamma(k+1) \Gamma(N+j)}{\Gamma(N+j+k+1)} \right] \right) \right] \end{aligned}$$

$$- \ln 2 \sum_{j=0}^8 \left[ b_j^{(1)} \frac{2^{-k} \Gamma(k+1) \Gamma(N+j)}{\Gamma(N+j+k+1)} \right] \Bigg), \quad (\text{B.5.54})$$

$$g_{34}(N) = \mathcal{M} \left[ -\frac{\text{Li}_3\left(\frac{1-x}{2}\right)}{1-x} \right] = - \sum_{k=1}^{12} \left[ c_k^{(2)} \frac{2^{-k} \Gamma(k) \Gamma(N)}{\Gamma(N+k)} \right] \\ + \sum_{k=0}^3 \left[ P_{1,k}^{(2)} \left( \sum_{j=0}^8 \left[ b_j^{(1)} \frac{2^{-k} \Gamma(k+1) \Gamma(j+N)}{\Gamma(N+k+j+1)} \right] \right) \right], \quad (\text{B.5.55})$$

$$g_{35}(N) = \mathcal{M} \left[ \frac{S_{1,2}\left(\frac{1-x}{2}\right)}{1+x} \right] = -(N-1) \sum_{k=0}^9 \left[ c_k^{(3)} \left( \sum_{j=0}^8 \left[ a_j^{(1)} \frac{2^{-k} \Gamma(1+k) \Gamma(N+j)}{\Gamma(N+k+j+1)} \right] \right) \right] \\ + (N-1) \sum_{k=0}^4 \left[ P_{1,k}^{(3)} \left( \sum_{j=0}^9 \left[ b_j^{(2)} \frac{2^{-k} \Gamma(k+2) \Gamma(N+j-1)}{\Gamma(N+j+k+1)} \right] \right) \right] \\ - \ln 2 \sum_{j=0}^9 \left[ b_j^{(1)} \frac{2^{-k} \Gamma(k+2) \Gamma(N+j-1)}{\Gamma(N+k+j+1)} \right] \Bigg) \\ + (N-1) \sum_{k=0}^4 \left[ P_{2,k}^{(3)} \left( \sum_{j=0}^{15} \left[ b_j^{(3)} \frac{2^{-k} \Gamma(k+2) \Gamma(N+j-1)}{\Gamma(N+k+j+1)} \right] \right) \right] \\ - 2 \ln 2 \sum_{j=0}^9 \left[ b_j^{(2)} \frac{2^{-k} \Gamma(k+2) \Gamma(N+j-1)}{\Gamma(N+k+j+1)} \right] \\ + \ln^2 2 \sum_{j=0}^8 \left[ b_j^{(1)} \frac{2^{-k} \Gamma(k+2) \Gamma(N+j-1)}{\Gamma(N+k+j+1)} \right] \Bigg) \\ - \frac{1}{2} \left( \sum_{k=0}^{15} \left[ \frac{b_k^{(3)}}{N+k} \right] - 2 \ln 2 \sum_{k=0}^9 \left[ \frac{b_k^{(2)}}{N+k} \right] + \ln^2 2 \sum_{k=0}^8 \left[ \frac{b_k^{(1)}}{N+k} \right] \right), \quad (\text{B.5.56})$$

$$g_{36}(N) = \mathcal{M} \left[ \frac{\text{Li}_2\left(\frac{1-x}{2}\right) \ln(1+x)}{1+x} \right] \\ = -\frac{N-1}{2} \sum_{k=0}^{11} \left[ c_k^{(1)} \left( \sum_{j=0}^{10} \left[ a_j^{(2)} \frac{2^{-k} \Gamma(k+1) \Gamma(N+j)}{\Gamma(N+k+j+1)} \right] \right) \right] \\ + \frac{N-1}{2} \sum_{k=0}^3 \left[ P_{1,k}^{(1)} \left( \sum_{j=0}^{15} \left[ b_j^{(3)} \frac{2^{-k} \Gamma(k+2) \Gamma(N+j-1)}{\Gamma(N+k+j+1)} \right] \right) \right] \\ - \ln 2 \sum_{j=0}^9 \left[ b_j^{(2)} \frac{2^{-k} \Gamma(k+2) \Gamma(N+j-1)}{\Gamma(N+k+j+1)} \right] \Bigg) \\ + \frac{1}{2} \left( \sum_{k=0}^{15} \left[ \frac{b_k^{(3)}}{N+k} \right] - \ln 2 \sum_{k=0}^9 \left[ \frac{b_k^{(2)}}{N+k} \right] \right), \quad (\text{B.5.57})$$

$$g_{37}(N) = \mathcal{M} \left[ \frac{\ln^2(1+x) \ln(1-x)}{1+x} \right] = \sum_{k=0}^{10} a_k^{(2)} g_{27}(N+k), \quad (\text{B.5.58})$$

$$\begin{aligned} g_{38}(N) &= \mathcal{M} \left[ -\frac{\text{Li}_2\left(\frac{1-x}{2}\right) \ln(1-x)}{1-x} \right] \\ &= -\sum_{k=1}^{11} \left[ c_k^{(1)} \frac{2^{-k} \Gamma(k) \Gamma(N) (\Psi(k-1) - \Psi(N+k-1))}{\Gamma(N+k)} \right] \\ &\quad + \sum_{k=0}^3 \left[ P_{1,k}^{(1)} \left( \sum_{j=0}^8 \left[ b_j^{(1)} \frac{2^{-k} \Gamma(k+1) \Gamma(N+j) (\Psi(k) - \Psi(k+N+j))}{\Gamma(N+k+j)} \right] \right) \right], \end{aligned} \quad (\text{B.5.59})$$

$$\begin{aligned} g_{39}(N) &= \mathcal{M} \left[ -\frac{\ln(1-x) (\text{Li}_2\left(\frac{1+x}{2}\right) - \zeta_2)}{1-x} \right] = -g_{38}(N) \\ &\quad - \sum_{k=0}^8 b_k^{(1)} \left( \frac{\Psi^2(N+k) + \zeta_2 - \psi_1(N+k+1)}{N+k} + \frac{\Psi(N+k) \ln 2}{N+k} \right), \end{aligned} \quad (\text{B.5.60})$$

where we use the functions

$$\Psi(x) = \psi_0(x+1) + \gamma_e, \quad (\text{B.5.61})$$

$$\beta(x) = \frac{1}{2} \left( \psi_0\left(\frac{1+x}{2}\right) - \psi_0\left(\frac{x}{2}\right) \right), \quad (\text{B.5.62})$$

in addition to usual Gamma and PolyGamma special functions.

Now we are going to write analytic continuation for all the Harmonic Sums up to four order; we are going to divide them for orders. We recall the fact that all the Harmonic Sums of weight 1 can be expressed as combination of ordinary special functions as given in Eqs. (B.5.4).

Then we are going to use Harmonic Sums of lower order to define the analytic continuation of  $S^H$  of higher order. We are going to use also definitions of functions  $\Psi$ ,  $\beta$  and their derivatives, indicated with the symbol  $f^{(j)}$  in the next formulas.

### B.5.2.1 Harmonic Sums of order 1

$$S_1^H(N) = \Psi(N) = \psi_0(N+1) + \gamma_e, \quad (\text{B.5.63})$$

$$S_{-1}^H(N) = (-1)^N \beta(N+1) - \ln 2, \quad (\text{B.5.64})$$

$$(\text{B.5.65})$$

### B.5.2.2 Harmonic Sums of order 2

$$S_2^H(N) = \zeta_2 - \psi_1(N+1), \quad (\text{B.5.66})$$

$$S_{-2}^H(N) = -(-1)^N \beta^{(1)}(N+1) - \frac{\zeta_2}{2}, \quad (\text{B.5.67})$$

$$S_{-1,-1}^H(N) = \frac{1}{2} \left( (S_{-1}^H(N))^2 + S_2^H(N) \right), \quad (\text{B.5.68})$$

$$S_{-1,1}^H(N) = (-1)^N g_1(N) + S_1^H(N) S_{-1}^H(N) + S_{-2}^H(N) \\ + (S_1^H(N) - S_{-1}^H(N)) \ln 2 - \frac{1}{2} \ln^2 2, \quad (\text{B.5.69})$$

$$S_{1,-1}^H(N) = -(-1)^N g_1(N) - (S_1^H(N) - S_{-1}^H(N)) \ln 2 + \frac{1}{2} \ln^2 2, \quad (\text{B.5.70})$$

$$S_{1,1}^H(N) = \frac{1}{2} \left( (S_1^H(N))^2 + S_2^H(N) \right); \quad (\text{B.5.71})$$

### B.5.2.3 Harmonic Sums of order 3

$$S_3^H(N) = \frac{1}{2} \psi_2(N+1) + \zeta_3, \quad (\text{B.5.72})$$

$$S_{-3}^H(N) = \frac{1}{2} (-1)^N \beta^{(2)}(N+1) - \frac{3}{4} \zeta_3, \quad (\text{B.5.73})$$

$$S_{-2,-1}^H(N) = -g_{19}(N) + \ln 2 (S_2^H(N) - S_{-2}^H(N)) - \frac{5}{8} \zeta_3, \quad (\text{B.5.74})$$

$$S_{-2,1}^H(N) = -(-1)^N g_3(N) + \zeta_2 S_{-1}^H(N) - \frac{5}{8} \zeta_3 + \zeta_2 \ln 2, \quad (\text{B.5.75})$$

$$S_{2,-1}^H(N) = -(-1)^N g_4(N) - \ln 2 (S_2^H(N) - S_{-2}^H(N)) - \frac{1}{2} \zeta_2 S_{-1}^H(N) \\ + \frac{1}{4} \zeta_3 - \frac{1}{2} \zeta_2 \ln 2, \quad (\text{B.5.76})$$

$$S_{2,1}^H(N) = -g_{18}(N) + 2\zeta_3, \quad (\text{B.5.77})$$

$$S_{-1,-2}^H(N) = -S_{-2,-1}^H(N) + S_{-2}^H(N) S_{-1}^H(N) + S_3^H(N), \quad (\text{B.5.78})$$

$$S_{-1,2}^H(N) = -S_{2,-1}^H(N) + S_{-3}^H(N) + S_{-1}^H(N) S_2^H(N), \quad (\text{B.5.79})$$

$$S_{1,-2}^H(N) = -S_{-2,1}^H(N) + S_{-3}^H(N) + S_{-2}^H(N) S_1^H(N), \quad (\text{B.5.80})$$

$$S_{1,2}^H(N) = -S_{2,1}^H(N) + S_3^H(N) + S_2^H(N) S_1^H(N), \quad (\text{B.5.81})$$

$$S_{-1,-1,-1}^H(N) = \frac{1}{6} \left( 2S_{-3}^H(N) + (S_{-1}^H(N))^3 + 3S_{-1}^H(N) S_{-2}^H(N) \right), \quad (\text{B.5.82})$$

$$S_{-1,1,-1}^H(N) = \frac{1}{2} g_{14}(N) + \ln 2 (S_{-1,-1}^H(N) - S_{-1,1}^H(N)) + \frac{1}{2} \ln^2 2 S_{-1}^H(N) \\ + \frac{1}{8} \zeta_3 - \frac{1}{2} \zeta_2 \ln 2 + \frac{1}{3} \ln^3 2, \quad (\text{B.5.83})$$

$$S_{1,1,-1}^H(N) = \frac{1}{2} (-1)^N g_2(N) + \ln 2 (S_{1,-1}^H(N) - S_{1,1}^H(N)) \\ + \frac{1}{2} \ln^2 2 (S_1^H(N) - S_{-1}^H(N)) - \frac{1}{6} \ln^3 2, \quad (\text{B.5.84})$$

$$S_{1,-1,-1}^H(N) = \frac{1}{2} \left( -S_{-1,1,-1}^H(N) + S_{-1}^H(N) S_{1,-1}^H(N) - S_{2,1}^H(N) - S_{-1,-2}^H(N) \\ + S_1^H(N) S_2^H(N) + S_{-1}^H(N) S_{-2}^H(N) + 2S_3^H(N) \right), \quad (\text{B.5.85})$$

$$S_{-1,-1,1}^{\text{H}}(N) = \frac{1}{2} \left( -S_{-1,1,-1}^{\text{H}}(N) + S_{-1}^{\text{H}}(N) S_{-1,1}^{\text{H}}(N) + S_{-1,-2}^{\text{H}}(N) + S_{2,1}^{\text{H}}(N) \right), \quad (\text{B.5.86})$$

$$S_{-1,1,1}^{\text{H}}(N) = S_{1,1,-1}^{\text{H}}(N) - S_1^{\text{H}}(N) S_{1,-1}^{\text{H}}(N) + S_{-2,1}^{\text{H}}(N) + S_{-1,2}^{\text{H}}(N) + \frac{1}{2} \left( (S_1^{\text{H}}(N))^2 S_{-1}^{\text{H}}(N) - S_{-1}^{\text{H}}(N) S_2^{\text{H}}(N) \right) - S_{-3}^{\text{H}}(N), \quad (\text{B.5.87})$$

$$S_{1,-1,1}^{\text{H}}(N) = -2S_{1,1,-1}^{\text{H}}(N) + S_1^{\text{H}}(N) S_{1,-1}^{\text{H}}(N) - S_{-2,1}^{\text{H}}(N) - S_{-1,2}^{\text{H}}(N) + S_1^{\text{H}}(N) S_{-2}^{\text{H}}(N) + S_{-1}^{\text{H}}(N) S_2^{\text{H}}(N) + 2S_{-3}^{\text{H}}(N), \quad (\text{B.5.88})$$

$$S_{1,1,1}^{\text{H}}(N) = \frac{1}{6} \left( (S_1^{\text{H}}(N))^3 + 3S_1^{\text{H}}(N) S_2^{\text{H}}(N) + 2S_3^{\text{H}}(N) \right), \quad (\text{B.5.89})$$

### B.5.2.4 Harmonic Sums of order 4

$$S_4^{\text{H}}(N) = \frac{2}{5} \zeta_2^2 - \frac{1}{6} \psi_3(N+1), \quad (\text{B.5.90})$$

$$S_{-4}^{\text{H}}(N) = -\frac{1}{6} (-1)^N \beta^{(3)}(N+1) - \frac{7}{20} \zeta_2^2, \quad (\text{B.5.91})$$

$$S_{-2,-2}^{\text{H}}(N) = \frac{1}{2} \left( (S_{-2}^{\text{H}}(N))^2 + S_4^{\text{H}}(N) \right), \quad (\text{B.5.92})$$

$$S_{-3,1}^{\text{H}}(N) = (-1)^N g_6(N) + \zeta_2 S_{-2}^{\text{H}}(N) - \zeta_3 S_{-1}^{\text{H}}(N) - \frac{3}{5} \zeta_2^2 + 2\text{Li}_4\left(\frac{1}{2}\right) + \frac{3}{4} \zeta_3 \ln 2 - \frac{1}{2} \zeta_2 \ln^2 2 + \frac{1}{12} \ln^4 2, \quad (\text{B.5.93})$$

$$S_{-2,2}^{\text{H}}(N) = (-1)^N g_5(N) - 2S_{-3,1}^{\text{H}}(N) + 2\zeta_2 S_{-2}^{\text{H}}(N) + \frac{3}{40} \zeta_2^2, \quad (\text{B.5.94})$$

$$S_{2,-2}^{\text{H}}(N) = -S_{-2,2}^{\text{H}}(N) + S_{-4}^{\text{H}}(N) + S_{-2}^{\text{H}}(N) S_2^{\text{H}}(N), \quad (\text{B.5.95})$$

$$S_{2,2}^{\text{H}}(N) = \frac{1}{2} \left( (S_2^{\text{H}}(N))^2 + S_4^{\text{H}}(N) \right), \quad (\text{B.5.96})$$

$$S_{3,-1}^{\text{H}}(N) = (-1)^N g_7(N) - \ln 2 \left( S_3^{\text{H}}(N) - S_{-3}^{\text{H}}(N) \right) - \frac{1}{2} \zeta_2 S_{-2}^{\text{H}}(N) + \frac{3}{4} \zeta_3 S_{-1}^{\text{H}}(N) - \frac{1}{8} \zeta_2^2 + \frac{3}{4} \zeta_3 \ln 2, \quad (\text{B.5.97})$$

$$S_{-3,-1}^{\text{H}}(N) = g_{23}(N) + \ln 2 \left( S_3^{\text{H}}(N) - S_{-3}^{\text{H}}(N) \right) - \frac{1}{2} \zeta_2 S_2^{\text{H}}(N) - 2\text{Li}_4\left(\frac{1}{2}\right) + \frac{11}{10} \zeta_2^2 - \frac{7}{4} \zeta_3 \ln 2 + \frac{1}{2} \zeta_2 \ln^2 2 - \frac{1}{12} \ln^4 2, \quad (\text{B.5.98})$$

$$S_{3,1}^{\text{H}}(N) = \frac{1}{2} g_{22}(N) - \frac{1}{4} S_4^{\text{H}}(N) - \frac{1}{4} (S_2^{\text{H}}(N))^2 + \zeta_2 S_2^{\text{H}}(N) - \frac{3}{20} \zeta_2^2, \quad (\text{B.5.99})$$

$$S_{-1,-3}^{\text{H}}(N) = -S_{-3,-1}^{\text{H}}(N) + S_{-3}^{\text{H}}(N) S_{-1}^{\text{H}}(N) + S_4^{\text{H}}(N), \quad (\text{B.5.100})$$

$$S_{-1,3}^{\text{H}}(N) = -S_{3,-1}^{\text{H}}(N) + S_3^{\text{H}}(N) S_{-1}^{\text{H}}(N) + S_{-4}^{\text{H}}(N), \quad (\text{B.5.101})$$

$$S_{1,-3}^{\text{H}}(N) = -S_{-3,1}^{\text{H}}(N) + S_{-3}^{\text{H}}(N) S_1^{\text{H}}(N) + S_{-4}^{\text{H}}(N), \quad (\text{B.5.102})$$

$$S_{1,3}^{\text{H}}(N) = -S_{3,1}^{\text{H}}(N) + S_3^{\text{H}}(N) S_1^{\text{H}}(N) + S_4^{\text{H}}(N), \quad (\text{B.5.103})$$

$$S_{-2,1,1}^H(N) = -(-1)^N g_8(N) + \zeta_3 S_{-1}^H(N) - \text{Li}_4\left(\frac{1}{2}\right) + \frac{1}{8}\zeta_2^2 + \frac{1}{8}\zeta_3 \ln 2 + \frac{1}{4}\zeta_2 \ln^2 2 - \frac{1}{24} \ln^4 2, \quad (\text{B.5.104})$$

$$S_{-2,1,-1}^H(N) = -g_{25}(N) - \ln 2 (S_{-2,1}^H(N) - S_{-2,-1}^H(N)) + \frac{1}{2} \ln^2 2 (S_{-2}^H(N) - S_2^H(N)) + \frac{3}{40} \zeta_2^2, \quad (\text{B.5.105})$$

$$S_{-2,-1,-1}^H(N) = \frac{1}{2} (-S_{-1,-2,-1}^H(N) + S_{-2,2}^H(N) + S_{3,-1}^H(N) + S_{-1}^H(N) S_{-2,-1}^H(N)), \quad (\text{B.5.106})$$

$$S_{-2,-1,1}^H(N) = \frac{\zeta_2^2}{4} - g_{24}(N) - S_{2,-1,-1}^H(N) + (-S_{2,-1}^H(N) + S_{2,1}^H(N)) \ln 2 - 2\text{Li}_4\left(\frac{1}{2}\right) - \frac{1}{2} S_{-2}^H(N) (\zeta_2 - \ln^2 2) + \frac{1}{2} S_2^H(N) (\zeta_2 - \ln^2 2) + \frac{1}{2} \zeta_2 \ln^2 2 - \frac{1}{12} \ln^3 2 - \frac{7}{4} \zeta_3 \ln 2, \quad (\text{B.5.107})$$

$$S_{2,1,-1}^H(N) = -(-1)^N g_9(N) - \ln 2 (S_{2,1}^H(N) - S_{2,-1}^H(N)) + \frac{1}{2} \ln^2 2 (S_2^H(N) - S_{-2}^H(N)) + \frac{1}{8} \zeta_3 S_{-1}^H(N) + 3\text{Li}_4\left(\frac{1}{2}\right) - \frac{6}{5} \zeta_2^2 + \frac{11}{4} \zeta_3 \ln 2 - \frac{3}{4} \zeta_2 \ln^2 2 + \frac{1}{8} \ln^4 2, \quad (\text{B.5.108})$$

$$S_{1,2,-1}^H(N) = (-1)^N g_{13}(N) - \frac{6}{5} \zeta_2^2 - \frac{1}{2} \zeta_2 S_{1,-1}^H(N) - 2S_{2,1,-1}^H(N) + S_{1,-2}^H(N) \ln 2 - S_{1,2}^H(N) \ln 2 + 2S_{2,-1}^H(N) \ln 2 - 2S_{2,1}^H(N) \ln 2 + \frac{1}{8} \ln^4 2 + \frac{1}{2} \zeta_2 \ln 2 S_{-1}^H(N) - \frac{1}{2} \zeta_2 \ln 2 S_1^H(N) - \zeta_2 \ln^2 2 - \frac{1}{2} S_{-2}^H(N) \ln^2 2 + S_2^H(N) \ln^2 2 + 3\text{Li}_4\left(\frac{1}{2}\right) + \frac{1}{4} S_1^H(N) \zeta_3 + \frac{105}{40} \zeta_3 \ln 2, \quad (\text{B.5.109})$$

$$S_{-1,2,-1}^H(N) = g_{16}(N) - 2S_{-2,1,-1}^H(N) - \frac{1}{2} \zeta_2 S_{-1,-1}^H(N) + \ln^2 2 (S_{-2}^H(N) - S_2^H(N)) - \ln 2 (2(S_{-2,1}^H(N) - S_{-2,-1}^H(N)) + S_{-1,2}^H(N) - S_{-1,-2}^H(N)) - \ln 2 \left( S_{-2,-1}^H(N) - \ln 2 (S_2^H(N) - S_{-2}^H(N)) + \frac{1}{2} \zeta_2 S_1^H(N) \right) + \left( \frac{1}{4} \zeta_3 - \frac{1}{2} \zeta_2 \ln 2 \right) (S_{-1}^H(N) - S_1^H(N)) + \frac{1}{4} \zeta_3 S_1^H(N) + \frac{33}{20} \zeta_2^2 - 4\text{Li}_4\left(\frac{1}{2}\right) - \frac{13}{4} \zeta_3 \ln 2 + \frac{3}{4} \zeta_2 \ln^2 2 - \frac{1}{6} \ln^4 2, \quad (\text{B.5.110})$$

$$S_{-1,2,1}^H(N) = (-1)^N g_{11}(N) + \zeta_2^2 + \zeta_2 S_{-1,1}^H(N) - 2S_{-2,1,1}^H(N) + \frac{1}{4} \zeta_2 \ln^2 2 - \frac{1}{8} \ln^4 2 - 3\text{Li}_4\left(\frac{1}{2}\right) + 2\zeta_3 S_{-1}^H(N), \quad (\text{B.5.111})$$

$$S_{-1,1,-2}^H(N) = -\frac{g_{17}(N)}{2} + \frac{7}{8} \zeta_2^2 - \frac{1}{2} \zeta_2 S_{-1,1}^H(N) - S_{-2,1,-1}^H(N) - S_{-1,2,-1}^H(N)$$

$$\begin{aligned}
& -\frac{1}{2}S_2^{\text{H}}(N)\ln^2 2 - \frac{\ln^4 2}{12} + (S_3^{\text{H}}(N) - S_{-2,1}^{\text{H}}(N) - S_{-1,2}^{\text{H}}(N))\ln 2 \\
& + \frac{1}{2}S_{-2}^{\text{H}}(N)(\ln^2 2 + 2S_{-1}^{\text{H}}(N)\ln 2) - 2\text{Li}_4\left(\frac{1}{2}\right) \\
& + \frac{1}{8}\zeta_3(S_{-1}^{\text{H}}(N) - 21\ln 2) + \frac{5}{4}\zeta_2\ln^2 2, \tag{B.5.112}
\end{aligned}$$

$$S_{2,-1,-1}^{\text{H}}(N) = \frac{1}{2}(-S_{-1,2,-1}^{\text{H}}(N) + S_{-3,-1}^{\text{H}}(N) + S_{-1}^{\text{H}}(N)S_{2,-1}^{\text{H}}(N) + S_{2,2}^{\text{H}}(N)), \tag{B.5.113}$$

$$S_{-1,-1,2}^{\text{H}}(N) = \frac{1}{2}(S_{-1}^{\text{H}}(N)S_{-1,2}^{\text{H}}(N) + S_{-1,-3}^{\text{H}}(N) + S_{2,2}^{\text{H}}(N) - S_{-1,2,-1}^{\text{H}}(N)), \tag{B.5.114}$$

$$S_{2,1,1}^{\text{H}}(N) = -g_{21}(N) + \frac{6}{5}\zeta_2^2, \tag{B.5.115}$$

$$S_{1,2,1}^{\text{H}}(N) = -2S_{2,1,1}^{\text{H}}(N) + S_{3,1}^{\text{H}}(N) + S_1^{\text{H}}(N)S_{2,1}^{\text{H}}(N) + S_{2,2}^{\text{H}}(N), \tag{B.5.116}$$

$$S_{1,1,2}^{\text{H}}(N) = S_{2,1,1}^{\text{H}}(N) + \frac{1}{2}(S_1^{\text{H}}(N)(S_{1,2}^{\text{H}}(N) - S_{2,1}^{\text{H}}(N)) + S_{1,3}^{\text{H}}(N) - S_{3,1}^{\text{H}}(N)), \tag{B.5.117}$$

$$S_{1,-2,1}^{\text{H}}(N) = -2S_{-2,1,1}^{\text{H}}(N) + S_{-3,1}^{\text{H}}(N) + S_1^{\text{H}}(N)S_{-2,1}^{\text{H}}(N) + S_{-2,2}^{\text{H}}(N), \tag{B.5.118}$$

$$\begin{aligned}
S_{1,1,-2}^{\text{H}}(N) &= S_{-2,1,1}^{\text{H}}(N) + S_{-2}^{\text{H}}(N)S_2^{\text{H}}(N) - S_{-2,2}^{\text{H}}(N) \\
&\quad - S_{-2}^{\text{H}}(N)S_{1,1}^{\text{H}}(N) + S_1^{\text{H}}(N)S_{1,-2}^{\text{H}}(N) + S_{1,-3}^{\text{H}}(N) - S_1^{\text{H}}(N)S_{-3}^{\text{H}}(N), \tag{B.5.119}
\end{aligned}$$

$$\begin{aligned}
S_{-1,-2,-1}^{\text{H}}(N) &= 2(-1)^N g_{12}(N) - \zeta_2 S_{-1,1}^{\text{H}}(N) - \frac{3}{2}\zeta_2\ln^2 2 + \frac{1}{3}\ln^4 2 - S_2^{\text{H}}(N)(\zeta_2 - \ln^2 2) \\
&\quad - S_{-2}^{\text{H}}(N)(-\zeta_2 + \ln^2 2 + 2S_{-1}^{\text{H}}(N)\ln 2) - 3\zeta_2^2 - S_{-2,2}^{\text{H}}(N) - S_{3,-1}^{\text{H}}(N) \\
&\quad - 2S_{2,-1,1}^{\text{H}}(N) - 2S_3^{\text{H}}(N)\ln 2 + 2(S_{-2,1}^{\text{H}}(N) + S_{-1,2}^{\text{H}}(N))\ln 2 + 8\text{Li}_4\left(\frac{1}{2}\right) \\
&\quad + \frac{21}{4}\zeta_3\ln 2 - S_{-1}^{\text{H}}(N)S_{-2,-1}^{\text{H}}(N) - \frac{5}{4}\zeta_3 S_{-1}^{\text{H}}(N), \tag{B.5.120}
\end{aligned}$$

$$\begin{aligned}
S_{-1,-2,1}^{\text{H}}(N) &= g_{15}(N) - \frac{19}{40}\zeta_2^2 - S_{-2,-1,1}^{\text{H}}(N) - S_{2,-1,-1}^{\text{H}}(N) + \text{Li}_4\left(\frac{1}{2}\right) \\
&\quad + \frac{1}{2}\zeta_2(S_{-1}^{\text{H}}(N))^2 + \zeta_2 S_2^{\text{H}}(N) - S_{2,-1}^{\text{H}}(N)\ln 2 + \frac{1}{3}\zeta_2\ln^2 2 - \frac{1}{2}S_2^{\text{H}}(N)\ln^2 2 \\
&\quad + \frac{1}{24}\ln^4 2 - \frac{1}{2}S_{-2}^{\text{H}}(N)(\zeta_2 - \ln^2 2) + \frac{1}{4}\zeta_3\ln 2 + S_{-1}^{\text{H}}(N)\zeta_2\ln 2 \\
&\quad - \frac{5}{8}\zeta_3 S_{-1}^{\text{H}}(N), \tag{B.5.121}
\end{aligned}$$

$$\begin{aligned}
S_{2,-1,1}^{\text{H}}(N) &= -S_{1,2,-1}^{\text{H}}(N) - S_{2,1,-1}^{\text{H}}(N) + S_{3,-1}^{\text{H}}(N) \\
&\quad + S_2^{\text{H}}(N)(S_{-1,1}^{\text{H}}(N) + S_{1,-1}^{\text{H}}(N)) + S_{2,-2}^{\text{H}}(N) - S_2^{\text{H}}(N)S_{-2}^{\text{H}}(N) \\
&\quad - S_1^{\text{H}}(N)S_{-1,2}^{\text{H}}(N) + S_1^{\text{H}}(N)S_{-3}^{\text{H}}(N), \tag{B.5.122}
\end{aligned}$$

$$S_{-1,-1,-2}^{\text{H}}(N) = \frac{1}{2}(-S_{-1,-2,-1}^{\text{H}}(N) + S_{2,-2}^{\text{H}}(N) + S_{-1}^{\text{H}}(N)S_{-1,-2}^{\text{H}}(N) + S_{-1,3}^{\text{H}}(N)), \tag{B.5.123}$$

$$S_{1,-1,-2}^H(N) = -S_{-1,-2,1}^H(N) - S_{-1,1,-2}^H(N) + S_{-1,-3}^H(N) + S_{-2,-2}^H(N) + S_1^H(N) S_{-1,-2}^H(N), \quad (\text{B.5.124})$$

$$S_{1,-2,-1}^H(N) = S_{-1,-2,1}^H(N) - S_{-1}^H(N) S_{-2,1}^H(N) - S_{-1,-3}^H(N) + S_{-1}^H(N) S_{-3}^H(N) + S_1^H(N) S_{-2,-1}^H(N) + S_{1,3}^H(N) - S_1^H(N) S_3^H(N), \quad (\text{B.5.125})$$

$$S_{1,-1,2}^H(N) = -S_{1,2,-1}^H(N) - S_{2,1,-1}^H(N) + S_{1,-3}^H(N) + S_{3,-1}^H(N) + S_2^H(N) S_{1,-1}^H(N), \quad (\text{B.5.126})$$

$$S_{-1,1,2}^H(N) = S_{1,2,-1}^H(N) + S_{2,1,-1}^H(N) - S_{-1,2,1}^H(N) + S_{-2,2}^H(N) + S_{-3,1}^H(N) - S_{-4}^H(N) + S_{-1,3}^H(N) - S_{3,-1}^H(N) - S_2^H(N) S_{1,-1}^H(N) + S_1^H(N) S_{-1,2}^H(N) - S_1^H(N) S_{-3}^H(N), \quad (\text{B.5.127})$$

$$S_{-1,-1,-1,-1}^H(N) = \frac{1}{4} S_4^H(N) + \frac{1}{8} (S_2^H(N))^2 + \frac{1}{3} S_{-3}^H(N) S_{-1}^H(N) + \frac{1}{4} S_2^H(N) (S_{-1}^H(N))^2 + \frac{1}{14} (S_{-1}^H(N))^4, \quad (\text{B.5.128})$$

$$S_{-1,1,1,1}^H(N) = -(-1)^N \frac{1}{6} g_{29}(N) - \text{Li}_4\left(\frac{1}{2}\right), \quad (\text{B.5.129})$$

$$S_{-1,1,1,-1}^H(N) = -\frac{1}{6} g_{31}(N) + \frac{12}{30} \zeta_2^2 - S_{-1,1,1}^H(N) \ln 2 + \frac{1}{2} \zeta_2 \ln^2 2 + S_{-1,1,-1}^H(N) \ln 2 - \text{Li}_4\left(\frac{1}{2}\right) - \frac{1}{6} \ln^2 4 - \frac{1}{6} S_{-1}^H(N) \ln^3 2 - \frac{1}{2} (S_{-1,-1}^H(N) - S_{-1,1}^H(N)) \ln^2 2 - \zeta_3 \ln 2, \quad (\text{B.5.130})$$

$$S_{1,-1,1,-1}^H(N) = -\frac{\Pi^4}{720} - g_{32}(N) - S_{1,-1,1}^H(N) \ln 2 - \frac{1}{2} S_{1,-1}^H(N) \ln^2 2 - \frac{1}{6} S_1^H(N) \ln^3 2 - \frac{1}{24} \ln^4 2 + \frac{1}{8} S_1^H(N) \zeta_3 + \frac{1}{2} \zeta_3 \ln 2, \quad (\text{B.5.131})$$

$$S_{-1,1,-1,-1}^H(N) = (-1)^N g_{33}(N) + \frac{1}{8} \zeta_2^2 - S_{-1,1,-1}^H(N) \ln 2 - \frac{1}{4} \ln^2 2 - \frac{1}{6} S_{-1}^H(N) \ln^3 2 + \frac{1}{2} S_{-1,1}^H(N) (\zeta_2 - \ln^2 2) + \frac{1}{2} S_{-1}^H(N) \zeta_2 \ln 2 + \frac{1}{2} \zeta_2 \ln^2 2 - \frac{7}{8} S_{-1}^H(N) \zeta_3 - \frac{7}{8} \zeta_3 \ln 2 - \frac{1}{24} \ln^4 2, \quad (\text{B.5.132})$$

$$S_{-1,-1,1,-1}^H(N) = -(-1)^N g_{35}(N) - \frac{6}{5} \zeta_2^2 - S_{-1,-1,1}^H(N) \ln 2 - \frac{3}{4} \zeta_2 \ln^2 2 - \frac{1}{2} S_{-1,-1}^H(N) \ln^2 2 - \frac{1}{6} S_{-1}^H(N) \ln^3 2 + \frac{1}{12} \ln^4 2 + 3 \text{Li}_4\left(\frac{1}{2}\right) + \frac{1}{8} S_{-1}^H(N) \zeta_3 + \frac{11}{4} \zeta_3 \ln 2, \quad (\text{B.5.133})$$

$$S_{1,1,-1,-1}^H(N) = g_{34}(N) - S_{1,1,-1}^H(N) \ln 2 - \frac{1}{6} S_1^H(N) \ln^3 2 + \frac{1}{2} S_{1,1}^H(N) (\zeta_2 - \ln^2 2) + \frac{1}{2} S_1^H(N) \zeta_2 \ln 2 + \text{Li}_4\left(\frac{1}{2}\right) - \frac{7}{8} S_1^H(N) \zeta_3, \quad (\text{B.5.134})$$

$$S_{1,1,1,-1}^H(N) = -(-1)^N \frac{1}{6} g_{30}(N) + \ln 2 (S_{1,1,-1}^H(N) - S_{1,1,1}^H(N)) + \frac{1}{24} \ln^4 2$$

$$+ \frac{1}{2} (S_{1,1}^{\text{H}}(N) - S_{1,-1}^{\text{H}}(N)) \ln^2 2 - \frac{1}{6} (S_1^{\text{H}}(N) - S_{-1}^{\text{H}}(N)) \ln^3 2, \quad (\text{B.5.135})$$

$$\begin{aligned} S_{1,1,1,1}^{\text{H}}(N) &= \frac{1}{4} S_4^{\text{H}}(N) + \frac{1}{8} (S_2^{\text{H}}(N))^2 + \frac{1}{3} S_3^{\text{H}}(N) S_1^{\text{H}}(N) \\ &\quad + \frac{1}{4} S_2^{\text{H}}(N) (S_1^{\text{H}}(N))^2 + \frac{1}{24} (S_1^{\text{H}}(N))^4, \end{aligned} \quad (\text{B.5.136})$$

$$\begin{aligned} S_{1,-1,-1,-1}^{\text{H}}(N) &= (-1)^N g_{36}(N) - \frac{6}{5} \zeta_2^2 - 2S_{-1,-1,1,-1}^{\text{H}}(N) + \frac{1}{6} \ln^4 2 \\ &\quad + (S_{-1,-1,-1}^{\text{H}}(N) - 2S_{-1,-1,1}^{\text{H}}(N) + S_{1,-1,-1}^{\text{H}}(N)) \ln 2 - \zeta_2 \ln^2 2 \\ &\quad + \frac{1}{6} (S_{-1}^{\text{H}}(N) - S_1^{\text{H}}(N)) \ln^3 2 + \frac{1}{2} (S_1^{\text{H}}(N) - S_{-1}^{\text{H}}(N)) \zeta_2 \ln 2 \\ &\quad + \frac{1}{2} S_{1,-1}^{\text{H}}(N) (\zeta_2 - \ln^2 2) + \frac{1}{4} (S_{-1}^{\text{H}}(N) - S_1^{\text{H}}(N)) \zeta_3 \\ &\quad + 3\text{Li}_4\left(\frac{1}{2}\right) + \frac{23}{8} \zeta_3 \ln 2, \end{aligned} \quad (\text{B.5.137})$$

$$\begin{aligned} S_{1,1,-1,1}^{\text{H}}(N) &= -(-1)^N \frac{g_{37}(N)}{2} - \frac{2}{5} \zeta_2^2 - S_{-1,-1,1,-1}^{\text{H}}(N) - S_{1,-1,-1,-1}^{\text{H}}(N) \\ &\quad + \frac{1}{2} (S_1^{\text{H}}(N) - S_{-1}^{\text{H}}(N)) \zeta_2 \ln 2 - \frac{1}{2} \zeta_2 \ln^2 2 + \frac{1}{6} \ln^4 2 \\ &\quad + (S_{-1,-1,-1}^{\text{H}}(N) - S_{-1,-1,1}^{\text{H}}(N) - S_{1,-1,-1}^{\text{H}}(N) + S_{1,-1,1}^{\text{H}}(N)) \ln 2 \\ &\quad + \frac{1}{2} (S_{-1,-1}^{\text{H}}(N) - S_{-1,1}^{\text{H}}(N)) \ln^2 2 + \frac{1}{3} (S_{-1}^{\text{H}}(N) - S_1^{\text{H}}(N)) \ln^3 2 \\ &\quad + \frac{1}{2} (S_{1,-1}^{\text{H}}(N) - S_{1,1}^{\text{H}}(N)) (\zeta_2 - \ln^2 2) + \text{Li}_4\left(\frac{1}{2}\right) \\ &\quad + \frac{1}{8} (S_{-1}^{\text{H}}(N) - S_1^{\text{H}}(N)) \zeta_3 + \zeta_3 \ln 2, \end{aligned} \quad (\text{B.5.138})$$

$$\begin{aligned} S_{1,-1,1,1}^{\text{H}}(N) &= -S_{-1,1,1,1}^{\text{H}}(N) - S_{1,1,-1,1}^{\text{H}}(N) - S_{1,1,1,-1}^{\text{H}}(N) + \frac{1}{6} S_{-1}^{\text{H}}(N) (S_1^{\text{H}}(N))^3 \\ &\quad + \frac{1}{2} \left( (S_1^{\text{H}}(N))^2 S_{-2}^{\text{H}}(N) + S_{-1}^{\text{H}}(N) S_1^{\text{H}}(N) S_2^{\text{H}}(N) + S_{-2}^{\text{H}}(N) S_2^{\text{H}}(N) \right) \\ &\quad + S_1^{\text{H}}(N) S_{-3}^{\text{H}}(N) + \frac{1}{3} S_{-1}^{\text{H}}(N) S_3^{\text{H}}(N) + S_{-4}^{\text{H}}(N), \end{aligned} \quad (\text{B.5.139})$$

$$\begin{aligned} S_{-1,-1,-1,1}^{\text{H}}(N) &= -S_{1,-1,-1,-1}^{\text{H}}(N) - S_{-1,1,-1,-1}^{\text{H}}(N) - S_{-1,-1,1,-1}^{\text{H}}(N) + S_{-4}^{\text{H}}(N) \\ &\quad + \frac{1}{2} \left( (S_{-1}^{\text{H}}(N))^2 S_{-2}^{\text{H}}(N) + 3S_1^{\text{H}}(N) S_{-1}^{\text{H}}(N) S_2^{\text{H}}(N) + S_{-2}^{\text{H}}(N) S_2^{\text{H}}(N) \right) \\ &\quad + \frac{1}{6} S_1^{\text{H}}(N) (S_{-1}^{\text{H}}(N))^3 + S_{-1}^{\text{H}}(N) S_3^{\text{H}}(N) + \frac{1}{3} S_1^{\text{H}}(N) S_{-3}^{\text{H}}(N), \end{aligned} \quad (\text{B.5.140})$$

$$\begin{aligned} S_{1,-1,-1,1}^{\text{H}}(N) &= \frac{1}{2} g_{39}(N) - \frac{1}{2} S_{1,-1,-1,1}^{\text{H}}(N) - \frac{1}{2} (S_{-1,-1,1}^{\text{H}}(N) + S_{1,-1,-1}^{\text{H}}(N)) \ln 2 \\ &\quad + \frac{1}{12} (S_{-1}^{\text{H}}(N) - S_1^{\text{H}}(N)) \ln^3 2 + \frac{1}{12} \ln^4 2 - \frac{1}{4} S_{1,-1}^{\text{H}}(N) (\zeta_2 + \ln^2 2) \\ &\quad + \frac{1}{4} (S_{-1}^{\text{H}}(N) - S_1^{\text{H}}(N)) \zeta_2 \ln 2 + \frac{3}{2} \text{Li}_4\left(\frac{1}{2}\right) \end{aligned}$$

$$+ \frac{7}{8} (S_1^H(N) - S_{-1}^H(N)) \zeta_3 - \frac{1}{4} \zeta_2 \ln^2 2 + \frac{7}{16} \zeta_3 \ln 2, \quad (\text{B.5.141})$$

$$\begin{aligned} S_{-1,1,-1,1}^H(N) = & -S_{-1,-1,1,1}^H(N) - S_{1,-1,-1,1}^H(N) - S_{1,1,-1,-1}^H(N) - S_{1,-1,1,-1}^H(N) \\ & - S_{-1,1,1,-1}^H(N) + \frac{1}{4} S_2^H(N) S_{-2}^H(N) + \frac{1}{2} (S_{-2}^H(N))^2 + \frac{3}{2} S_4^H(N) \\ & + \frac{1}{4} \left( (S_1^H(N))^2 (S_{-1}^H(N))^2 + (S_1^H(N))^2 S_2^H(N) + (S_{-1}^H(N))^2 S_2^H(N) \right) \\ & + S_{-1}^H(N) S_1^H(N) S_{-2}^H(N) + S_1^H(N) S_3^H(N) + S_{-1}^H(N) S_{-3}^H(N); \end{aligned} \quad (\text{B.5.142})$$

### B.5.2.5 Important Caveat in the use of $S^H$ to solve Mellin Integrals

We need to stress you about an important caveat in using the formulas just listed to solve Mellin integrals using Harmonic Sums. Harmonic Sums are defined for integer value of Mellin argument  $n$ ; the analytic extension to all the complex plane we perform in the previous sections destroy some of the properties of  $S^H$  which are valid for integers. In particular, problems arise in dealing with factors  $(-1)^N$  which are present in our expressions. In particular, if for integer values it is always true

$$(-1)^n (-1)^n = (-1)^{2n} = 1 \quad (\text{B.5.143})$$

this is no longer true in the complex plane.

In general, then, if you apply in your Mellin computations our analytic continuation of  $S^H$  or the results of Ref. [138] (even correcting all the typos) without paying attention, you will probably come to the incorrect result for the integral for complex value of  $N$ . The reason is that in order to express the solution of the integral as a function of Harmonic Sums or in expressing the Harmonic Sums using previous equations we explicitly make use of the fact that  $N$  is in fact integer and we simplify  $(-1)^N$  factor according to Eq. (B.5.143).

The following statement helps us to solve this problem and to compute all the Mellin integrals of HPL using previous equations. It can be proved that in all the Mellin transform results no  $(-1)^N$  factor could appear. They have to cancel between integral representations as function of  $S^H$ , and explicit  $S^H$  expressions of previous sub-subsections.

To reach the correct result the following steps have to be performed *in the following order* during Mellin integral computation<sup>2</sup>

1. We solve the Mellin integral for a general integer value of  $N = n$ ; in this sense, we can use sum rules Eqs. (B.3.11) to express our solution as a function of Harmonic Sums of integer value. In this phase, available routine as Mathematica package *MT* [137] or as SUMMER form procedure [136] could be used.
2. We express the Harmonic Sums of integer values using expressions contained in the previous sub-subsections.

<sup>2</sup>In Refs. [138, 139] there is no indication about this problem; some relations as for example Eq. (43) of Ref. [138] are in fact wrong if you compute both members for a complex value of  $N$ . Moreover if you are going to use results of program ANCONT [139] for  $S^H$  numerical evaluation in computing generic HPL integrals, in many cases you does not obtain the correct value for the integral, for the reason exposed above.

3. We simplify final expression - always for  $n$  integer - using Eq. (B.5.143) to deal with the  $(-1)^n$  factor. If all goes well, we have to observe that the final formula does no longer contain any  $(-1)^n$  term.
4. We consider our final expression as the analytic continuation of the integral in the whole complex plane. We can now compute it as a function of a general  $N$  and our final formula will give back the correct result for any complex value.

We want to clarify better the concept by presenting the computation of the Mellin transform for the function:

$$\frac{\ln(1+z) - \ln 2}{1-z}. \tag{B.5.144}$$

We follow the procedure explained in Sec. B.5 and we limit ourself to an integer  $N = n+1$ . Using Eq. (B.4.43) and Eq. (B.4.42), we write the Mellin transform as

$$\begin{aligned} \int_0^1 dz z^n \frac{\ln(1+z) - \ln 2}{1-z} &= \sum_{n'=n}^{\infty} \int_0^1 dz z^{n'} (\ln(1+z) - \ln 2) \\ &= - \sum_{n'=n}^{\infty} \frac{1}{n'+1} \int_0^1 dz \frac{z^{n'+1}}{1+z} \\ &= - \sum_{n'=n}^{\infty} \frac{(-1)^{n'+1}}{n'+1} \sum_{k=n'+1}^{\infty} \frac{(-1)^k}{k+1} \\ &= \sum_{n''=n+1}^{\infty} \frac{(-1)^{n''}}{n''} \sum_{k'=n''+1}^{\infty} \frac{(-1)^{k'}}{k'} \\ &= \sum_{n''=n+1}^{\infty} \frac{(-1)^{n''}}{n''} \left[ S_{-1}^{\text{H}}(\infty) - \sum_{k'=1}^{n''} \frac{(-1)^{k'}}{k'} \right] \\ &= (S_{-1}^{\text{H}}(\infty))^2 - S_{-1}^{\text{H}}(\infty) S_{-1}^{\text{H}}(n) - S_{-1,-1}^{\text{H}}(\infty) + S_{-1,-1}^{\text{H}}(n) \\ &= S_{-1,-1}^{\text{H}}(n) + S_{-1}^{\text{H}}(n) \ln 2 - \frac{\zeta_2}{2} + \frac{\ln^2 2}{2} \end{aligned} \tag{B.5.145}$$

where in the last step we insert the known results

$$S_{-1}(\infty) = -\ln 2, \tag{B.5.146}$$

$$S_{-1,-1}(\infty) = \frac{\zeta_2}{2} + \frac{\ln^2 2}{2}. \tag{B.5.147}$$

Now to reach the desired solution we substitute expressions for  $S_{-1,-1}^{\text{H}}(n)$  and  $S_{-1}^{\text{H}}(n)$  given in previous sub-subsection for a generic integer  $n$ . We thus obtain

$$\mathcal{M} \left[ \frac{\ln(1+z) - \ln 2}{1-z} \right] = \frac{1}{2} (\beta^2(n+1) - \psi_1(n+1)) \tag{B.5.148}$$

which can be analytical continued in all the complex plane as

$$\mathcal{M} \left[ \frac{\ln(1+z) - \ln 2}{1-z} \right] = \frac{1}{2} (\beta^2(N) - \psi_1(N)) \tag{B.5.149}$$

which is the correct final result.

However, if last two steps are performed in the opposite order (so first we continue the solution to complex plane  $N$  and then substitute expressions for different  $S^H$ ), we will come to the following different result

$$\mathcal{M} \left[ \frac{\ln(1+z) - \ln 2}{1-z} \right] = \frac{1}{2} (\beta^2(N) - \psi_1(N)) + ((-1)^{2N} - 1) \ln^2 2 \quad (\text{B.5.150})$$

which is incorrect for non-integers value of  $N$ .

It is important to note that from the numerical point of view, it is no always simple to perform analytically all the simplifications to get rid of all the  $(-1)^N$  terms and to assure their cancellation. However, we find a trick to reach the correct result in a more efficient way without any simplification: if you substitute in all the expressions, both for the integral you want to compute and for the analytic continuations of  $S^H$  of the previous sub-subsection, all the  $(-1)^N$  factors with  $(-1)^n$  with  $n$  the integer part of  $\text{Re}(N)$ , you will end up with the correct integral value, since all the factors will cancel as in the integer case

Summarizing, even if  $S^H$  expressions of previous sub-subsection are the correct analytic continuation for the Harmonic Sums in the complex plane, they are not the most useful objects to compute Mellin integrals. To reach Mellin integral computation we need to convert all the term  $(-1)^N$  into  $(-1)^n$  with  $n$  the integer counterpart of the Mellin variable  $N$ .

# C

# Analytical Expressions

## Contents

---

<b>C.1 Collinear and Threshold Region</b> . . . . .	<b>205</b>
C.1.1 Threshold resummation at fixed $p_T$	206
C.1.2 Transverse momentum resummation	209
<b>C.2 High Energy Region</b> . . . . .	<b>213</b>
C.2.1 EFT Higgs boson production	214
C.2.2 SM Higgs boson production	216
C.2.3 One-Jet inclusive cross section	222

---

We are going to report in this appendix all the analytical expressions which complete our discussion presented in the text. In particular, here we are going to make explicit all the values of the different anomalous dimensions which have been introduced and used in Chap. 2 and Chap. 3. The unique exceptions will be the  $LLx$  DGLAP resummed anomalous dimension and the NLO BFKL kernel for which we refer the interested reader to specialized references such as Refs. [70, 84]. This is due to the complexity of the derivation of this object.

This appendix will be divided in two section. In the first, we are going to list all the important results which are useful in the soft and collinear region, while in the latter we will focus our attention on the high energy regime, presenting more details about the computation of the different impact factors presented in Chap. 3. Furthermore, each section will be divided in subsections owing to the different application we are presenting.

## C.1 Collinear and Threshold Region

In Chap. 2, we have presented different resummation theories which study different logarithmic contributions in the soft and collinear region. We will thus explicit the important analytical expressions we omit in the text for threshold resummation at fixed  $p_T$  and then for transverse momentum resummation.

### C.1.1 Threshold resummation at fixed $p_T$

We give here explicit expressions of the coefficients which determine threshold resummation at fixed  $p_T$  for a general colour singlet process, like Higgs or Drell-Yan production, hence Eq. (2.3.1).

The cusp anomalous dimensions  $A_g^{\text{th}}(\alpha_s)$  and  $A_q^{\text{th}}(\alpha_s)$  i.e. the contributions which are proportional to a plus distribution in the  $P_{gg}$  and  $P_{qq}$  splitting function respectively, are given by (see e.g. Ref. [65]):

$$A_c^{\text{th}}(\alpha_s) = A_c^{\text{th},(1)}\alpha_s + A_c^{\text{th},(2)}\alpha_s^2 + A_c^{\text{th},(3)}\alpha_s^3 + \mathcal{O}(\alpha_s^4)$$

$$A_c^{\text{th},(1)} = \frac{C_c}{\pi}, \quad (\text{C.1.1a})$$

$$A_c^{\text{th},(2)} = \frac{C_c}{2\pi^2} \left[ C_A \left( \frac{67}{18} - \zeta_2 \right) - \frac{5}{9} N_f \right], \quad (\text{C.1.1b})$$

$$A_c^{\text{th},(3)} = \frac{C_c}{\pi^3} \left[ \left( \frac{245}{96} - \frac{67}{36} \zeta_2 + \frac{11}{8} \zeta_4 + \frac{11}{24} \zeta_3 \right) C_A^2 + \left( -\frac{209}{432} + \frac{5}{18} \zeta_2 - \frac{7}{12} \zeta_3 \right) C_A N_f \right. \\ \left. + \left( -\frac{55}{96} + \frac{1}{2} \zeta_3 \right) C_F N_f - \frac{1}{108} N_f^2 \right], \quad (\text{C.1.1c})$$

with  $C_c = C_A$  if  $c = g$  is a gluon and  $C_c = C_F$  if  $c = q$  is a quark.

Furthermore, in the jet function  $J$ , a second anomalous dimension  $B_c^{\text{th}}$ , controlling final collinear radiation is introduced. Its analytical expression turns out to be

$$B_c^{\text{th}}(\alpha_s) = B_c^{\text{th},(1)}\alpha_s + B_c^{\text{th},(2)}\alpha_s^2 + \mathcal{O}(\alpha_s^3)$$

$$B_q^{\text{th},(1)} = -\frac{3}{4} \frac{C_F}{\pi}, \quad (\text{C.1.2a})$$

$$B_q^{\text{th},(2)} = \frac{1}{16\pi^2} \left[ C_F^2 \left( -\frac{3}{2} + 12\zeta_2 - 24\zeta_3 \right) + C_F C_A \left( -\frac{3155}{54} + \frac{44}{3} \zeta_2 + 40\zeta_3 \right) \right. \\ \left. + C_F N_f \left( \frac{247}{27} - \frac{8}{3} \zeta_2 \right) \right], \quad (\text{C.1.2b})$$

$$B_g^{\text{th},(1)} = -\beta_0 = -\frac{11}{12\pi} C_A + \frac{1}{6\pi} N_f, \quad (\text{C.1.2c})$$

$$B_g^{\text{th},(2)} = \frac{1}{16\pi^2} \left[ C_A^2 \left( -\frac{611}{9} + \frac{88}{3} \zeta_2 + 16\zeta_3 \right) + C_A N_f \left( \frac{428}{27} - \frac{16}{3} \zeta_2 \right) + 2C_F N_f - \frac{20}{27} N_f^2 \right], \quad (\text{C.1.2d})$$

in the quark and gluon cases respectively.

Only the initial state radiation, controlled by  $\Delta$ , Eq. (2.3.3) and final state radiation, controlled by  $J$ , Eq. (2.3.4) are universal.

Soft anomalous dimension depends on the number of coloured particle in the LO Born process. In the context of transverse momentum distribution of colour singlet production processes, we prove it is proportional to the cusp anomalous dimension and then it can be derived using the explicit results just presented, Eq. (C.1.1).

Moreover to specify all the ingredients of the resummed formula Eq. (2.3.1), we need to express the Born level cross section  $\sigma_0 C_0$  and the matching constant  $g_0$ . Of course all these quantities are process dependent: we are going to present explicit results for our test case, hence Higgs boson production in the effective field theory. Analogue results for Drell-Yan production can be found in Ref. [140].

The LO coefficient functions  $C_0(N, \xi_p)$  in Eq. (2.7.28), after factoring the leading-order total cross section

$$\sigma_0 = \frac{\alpha_s^2 \sqrt{2} G_F}{576\pi}. \quad (\text{C.1.3})$$

are given by

$$\begin{aligned} (C_0(N, \xi_p, \alpha_s))_{gg} &= \frac{2\alpha_s C_A}{\pi} \frac{1}{\xi_p} \frac{\Gamma(\frac{1}{2}) \Gamma(N)}{\Gamma(N + \frac{1}{2})} \left( {}_2F_1\left(\frac{1}{2}, N, N + \frac{1}{2}, (\sqrt{1 + \xi_p} - \sqrt{\xi_p})^4\right) \right. \\ &- 2 \frac{1 + \xi_p}{(\sqrt{1 + \xi_p} + \sqrt{\xi_p})^2} \frac{N}{N + \frac{1}{2}} {}_2F_1\left(\frac{1}{2}, N + 1, N + \frac{3}{2}, (\sqrt{1 + \xi_p} - \sqrt{\xi_p})^4\right) \\ &+ \frac{(1 + \xi_p)(3 + \xi_p)}{(\sqrt{1 + \xi_p} + \sqrt{\xi_p})^4} \frac{N(N + 1)}{(N + \frac{1}{2})(N + \frac{3}{2})} {}_2F_1\left(\frac{1}{2}, N + 2, N + \frac{5}{2}, (\sqrt{1 + \xi_p} - \sqrt{\xi_p})^4\right) \\ &- 2 \frac{1 + \xi_p}{(\sqrt{1 + \xi_p} + \sqrt{\xi_p})^6} \frac{N(N + 1)(N + 2)}{(N + \frac{1}{2})(N + \frac{3}{2})(N + \frac{5}{2})} {}_2F_1\left(\frac{1}{2}, N + 3, N + \frac{7}{2}, (\sqrt{1 + \xi_p} - \sqrt{\xi_p})^4\right) \\ &+ \frac{1}{(\sqrt{1 + \xi_p} + \sqrt{\xi_p})^8} \frac{N(N + 1)(N + 2)(N + 3)}{(N + \frac{1}{2})(N + \frac{3}{2})(N + \frac{5}{2})(N + \frac{7}{2})} \\ &\left. {}_2F_1\left(\frac{1}{2}, N + 4, N + \frac{9}{2}, (\sqrt{1 + \xi_p} - \sqrt{\xi_p})^4\right) \right) \end{aligned} \quad (\text{C.1.4a})$$

$$\begin{aligned} (C_0(N, \xi_p, \alpha_s))_{qq} &= \frac{\alpha_s C_F}{\pi} \frac{1}{\xi_p} \frac{\Gamma(\frac{1}{2}) \Gamma(N)}{\Gamma(N + \frac{1}{2})} \left( {}_2F_1\left(\frac{1}{2}, N, N + \frac{1}{2}, (\sqrt{1 + \xi_p} - \sqrt{\xi_p})^4\right) \right. \\ &- \frac{(4 + 3\xi_p)}{(\sqrt{1 + \xi_p} + \sqrt{\xi_p})^2} \frac{N}{N + \frac{1}{2}} {}_2F_1\left(\frac{1}{2}, N + 1, N + \frac{3}{2}, (\sqrt{1 + \xi_p} - \sqrt{\xi_p})^4\right) \\ &+ 3 \frac{1 + \xi_p}{(\sqrt{1 + \xi_p} + \sqrt{\xi_p})^4} \frac{N(N + 1)}{(N + \frac{1}{2})(N + \frac{3}{2})} {}_2F_1\left(\frac{1}{2}, N + 2, N + \frac{5}{2}, (\sqrt{1 + \xi_p} - \sqrt{\xi_p})^4\right) \\ &\left. - \frac{1}{(\sqrt{1 + \xi_p} + \sqrt{\xi_p})^6} \frac{N(N + 1)(N + 2)}{(N + \frac{1}{2})(N + \frac{3}{2})(N + \frac{5}{2})} {}_2F_1\left(\frac{1}{2}, N + 3, N + \frac{7}{2}, (\sqrt{1 + \xi_p} - \sqrt{\xi_p})^4\right) \right) \end{aligned} \quad (\text{C.1.4b})$$

$$\begin{aligned} (C_0(N, \xi_p, \alpha_s))_{qq} &= \frac{2\alpha_s C_F^2}{\pi} \frac{1}{(\sqrt{1 + \xi_p} + \sqrt{\xi_p})^2} \left( {}_2F_1\left(\frac{1}{2}, N, N + \frac{1}{2}, (\sqrt{1 + \xi_p} - \sqrt{\xi_p})^4\right) \right. \\ &- 2 \frac{(1 + \xi_p)}{(\sqrt{1 + \xi_p} + \sqrt{\xi_p})^2} \frac{N}{N + \frac{1}{2}} {}_2F_1\left(\frac{1}{2}, N + 1, N + \frac{3}{2}, (\sqrt{1 + \xi_p} - \sqrt{\xi_p})^4\right) \\ &\left. + \frac{1}{(\sqrt{1 + \xi_p} + \sqrt{\xi_p})^4} \frac{N(N + 1)}{(N + \frac{1}{2})(N + \frac{3}{2})} {}_2F_1\left(\frac{1}{2}, N + 2, N + \frac{5}{2}, (\sqrt{1 + \xi_p} - \sqrt{\xi_p})^4\right) \right) \end{aligned} \quad (\text{C.1.4c})$$

where  ${}_2F_1$  is the Hypergeometric Function, Eq. (B.4.28).

The matching constant,

$$g_{0\ ij}(\xi_p) = 1 + g_0^{(1)\ ij}(\xi_p) \left( \frac{\alpha_s}{\pi} \right) + \mathcal{O}(\alpha_s^2), \quad (\text{C.1.5})$$

instead is given by [45, 48]

$$\begin{aligned} g_0^{(1)\ gg}(\xi_p) &= \frac{67}{36}C_A - \frac{5}{18}N_f + C_A\zeta_2 - \beta_0 \ln \frac{\xi_p}{1 + \xi_p} - \frac{1}{8}C_A \ln^2 \frac{\xi_p}{1 + \xi_p} \\ &+ 2C_A \text{Li}_2 \left( 1 - \frac{\sqrt{\xi_p}}{\sqrt{1 + \xi_p}} \right) + C_A \ln \left( 1 - \frac{\sqrt{\xi_p}}{\sqrt{1 + \xi_p}} \right) \ln \frac{\xi_p}{1 + \xi_p} \\ &- \frac{1}{2}C_A \ln \left( 1 + \frac{\sqrt{\xi_p}}{\sqrt{1 + \xi_p}} \right) \ln \frac{\xi_p}{1 + \xi_p} + \frac{1}{2}C_A \ln^2 \left( 1 + \frac{\sqrt{\xi_p}}{\sqrt{1 + \xi_p}} \right) + 2\beta_0 \ln^2 \left( 1 + \frac{\sqrt{\xi_p}}{\sqrt{1 + \xi_p}} \right) \\ &+ C_A \text{Li}_2 \left( \frac{2\sqrt{\xi_p}}{\sqrt{1 + \xi_p} + \sqrt{\xi_p}} \right) - \frac{(C_A - N_f)(\sqrt{\xi_p}\sqrt{1 + \xi_p}(1 + \xi_p) - 2\xi_p - \xi_p^2)}{6(1 + 8\xi_p + 9\xi_p^2)} \end{aligned} \quad (\text{C.1.6a})$$

$$\begin{aligned} g_0^{(1)\ gq}(\xi_p) &= -\frac{7}{4}C_F + \frac{134}{36}C_A - \frac{20}{36}N_f - 8C_F\zeta_2 + 12C_A\zeta_2 - 4\beta_0 \ln \frac{\xi_p}{1 + \xi_p} + \frac{3}{2}C_F \ln \frac{\xi_p}{1 + \xi_p} \\ &- \frac{1}{2}C_A \ln^2 \frac{\xi_p}{1 + \xi_p} + 4(C_F + C_A) \text{Li}_2 \left( 2, 1 - \frac{\sqrt{\xi_p}}{\sqrt{1 + \xi_p}} \right) \\ &+ \frac{2(C_A - C_F)(1 + 3\xi_p + 3\sqrt{\xi_p}\sqrt{1 + \xi_p})}{2\sqrt{\xi_p}\sqrt{1 + \xi_p} + 1 + 3\xi_p} + 8\beta_0 \ln \left( 1 + \frac{\sqrt{\xi_p}}{\sqrt{1 + \xi_p}} \right) \\ &- 3C_F \ln \left( 1 + \frac{\sqrt{\xi_p}}{\sqrt{1 + \xi_p}} \right) + 2C_F \ln \left( 1 - \frac{\sqrt{\xi_p}}{\sqrt{1 + \xi_p}} \right) \ln \frac{\xi_p}{1 + \xi_p} \\ &+ 2C_A \ln \left( 1 - \frac{\sqrt{\xi_p}}{\sqrt{1 + \xi_p}} \right) \ln \frac{\xi_p}{1 + \xi_p} - 2C_F \ln \left( 1 + \frac{\sqrt{\xi_p}}{\sqrt{1 + \xi_p}} \right) \ln \frac{\xi_p}{1 + \xi_p} \\ &- 2C_F \ln^2 \left( 1 + \frac{\sqrt{\xi_p}}{\sqrt{1 + \xi_p}} \right) + 4C_F \text{Li}_2 \left( \frac{2\sqrt{\xi_p}}{\sqrt{1 + \xi_p} + \sqrt{\xi_p}} \right) \end{aligned} \quad (\text{C.1.6b})$$

$$\begin{aligned} g_0^{(1)\ qq}(\xi_p) &= -\frac{9}{2}C_F + \frac{79}{12}C_A - \frac{5}{6}N_f + 12C_F\zeta_2 - 10C_A\zeta_2 - \frac{(C_F - C_A)\sqrt{1 + \xi_p}}{\sqrt{\xi_p}} \\ &+ 4C_F \text{Li}_2 \left( 1 - \frac{\sqrt{\xi_p}}{\sqrt{1 + \xi_p}} \right) - \frac{3}{4}C_F \ln \frac{\xi_p}{1 + \xi_p} - \beta_0 \ln \frac{\xi_p}{1 + \xi_p} + \frac{1}{4}C_A \ln^2 \frac{\xi_p}{1 + \xi_p} \\ &- \frac{1}{2}C_F \ln^2 \frac{\xi_p}{1 + \xi_p} + 2C_F \ln \left( 1 - \frac{\sqrt{\xi_p}}{\sqrt{1 + \xi_p}} \right) \ln \frac{\xi_p}{1 + \xi_p} + \frac{3}{2}C_F \ln \left( 1 + \frac{\sqrt{\xi_p}}{\sqrt{1 + \xi_p}} \right) \\ &+ 2\beta_0 \ln \left( 1 + \frac{\sqrt{\xi_p}}{\sqrt{1 + \xi_p}} \right) + C_A \ln^2 \left( 1 + \frac{\sqrt{\xi_p}}{\sqrt{1 + \xi_p}} \right) \end{aligned}$$

$$- C_A \ln \left( 1 + \frac{\sqrt{\xi_p}}{\sqrt{1 + \xi_p}} \right) \ln \frac{\xi_p}{1 + \xi_p} + 2C_A \text{Li}_2 \left( \frac{2\sqrt{\xi_p}}{\sqrt{1 + \xi_p} + \sqrt{\xi_p}} \right). \quad (\text{C.1.6c})$$

## C.1.2 Transverse momentum resummation

We collect expressions of the coefficients which determine original and consistent transverse momentum resummation, Eq. (2.4.17) and Eq. (2.5.45) in the context of colour singlet production. The hard function which is process dependent will be specified only for our test case, Higgs boson production, while we refer the reader to Ref. [58, 141] for analogue expressions for Drell-Yan case.

All the expressions we are going to list are based on the results of Refs. [30, 49–51, 58, 142] for the standard transverse momentum resummation and on Ref. [45] for consistent transverse momentum resummation.

The Sudakov exponent Eq. (2.4.18) depends on two anomalous dimensions  $A_c^{p\text{T}}$  and  $B_c^{p\text{T}}$ . Their expansions are given by

$$A_c^{p\text{T}}(\alpha_s) = A_c^{p\text{T},(1)}\alpha_s + A_c^{p\text{T},(2)}\alpha_s^2 + A_c^{p\text{T},(3)}\alpha_s^3 + \mathcal{O}(\alpha_s^4), \quad (\text{C.1.7})$$

with

$$A_c^{p\text{T},(1)} = \frac{C_c}{\pi} \quad (\text{C.1.8})$$

$$A_c^{p\text{T},(2)} = \frac{C_c}{2\pi^2} \left[ C_A \left( \frac{67}{18} - \zeta_2 \right) - \frac{5}{9} N_f \right] \quad (\text{C.1.9})$$

$$\begin{aligned} A_c^{p\text{T},(3)} &= \frac{C_c}{4\pi^3} \left[ C_A^2 \left( \frac{15503}{648} - \frac{67}{9} \zeta_2 - 11\zeta_3 + \frac{11}{2} \zeta_4 \right) + C_F N_f \left( -\frac{55}{24} + 2\zeta_3 \right) \right. \\ &\quad \left. + C_A N_f \left( -\frac{2051}{324} + \frac{10}{9} \zeta_2 \right) - \frac{25}{81} N_f^2 \right]. \end{aligned} \quad (\text{C.1.10})$$

and

$$B_c^{p\text{T}}(\alpha_s) = B_c^{p\text{T},(1)}\alpha_s + B_c^{p\text{T},(2)} + \mathcal{O}(\alpha_s^2), \quad (\text{C.1.11})$$

with

$$B_g^{p\text{T},(1)} = -2\beta_0 = \frac{11C_A - 2N_f}{6\pi}, \quad (\text{C.1.12a})$$

$$B_g^{p\text{T},(2)} = \frac{1}{16\pi^2} \left[ \left( -\frac{64}{3} - 24\zeta_3 \right) C_A^2 + \frac{16}{3} C_A N_f + 4C_F N_f \right] + \frac{\beta_0}{\pi} C_A \zeta_2, \quad (\text{C.1.12b})$$

$$B_q^{p\text{T},(1)} = -\frac{3C_F}{2\pi}, \quad (\text{C.1.12c})$$

$$\begin{aligned} B_q^{p\text{T},(2)} &= \frac{1}{16\pi^2} [-3 + 24\zeta_2 - 48\zeta_3] C_F^2 + \left( -\frac{17}{3} - \frac{88}{3} \zeta_2 + 24\zeta_3 \right) C_F C_A \\ &\quad + \left( \frac{2}{3} + \frac{16}{3} \zeta_2 \right) C_F N_f + \frac{\beta_0}{\pi} C_F \zeta_2. \end{aligned} \quad (\text{C.1.12d})$$

As highlighted in Chap. 2, the two loops contribution to the anomalous dimension  $B^{p_T,(2)}$  depends on the resummation scheme choice. The formula presented above is computed in the *hard scheme* of Ref. [50].

In performing PDFs evolution in consistent transverse momentum resummation we need also the  $\delta(1-x)$  terms of the splitting function  $P_{cc}$  up to two loops. They are given by

$$\delta P_{cc}^{(1)} = -\frac{B_c^{p_T,(1)}}{2}, \quad (\text{C.1.13a})$$

$$\delta P_{cc}^{(2)} = -\frac{B_c^{p_T,(2)} - \frac{\beta_0}{\pi} C_c \zeta_2}{2}. \quad (\text{C.1.13b})$$

Last coefficient which depends only on the LO production mechanism (gluon fusion  $c = g$  or quark annihilation  $c = q$ ) is the large- $N$  behaviour of the hard function, Eq. (2.4.13). Its expansion turns out to be

$$D_c^{p_T}(\alpha_s) = D_c^{p_T,(1)}\alpha_s + D_c^{p_T,(2)}\alpha_s^2 + \mathcal{O}(\alpha_s^3) \quad (\text{C.1.14})$$

with

$$D_g^{p_T,(1)} = 0, \quad (\text{C.1.15a})$$

$$D_g^{p_T,(2)} = \frac{C_c}{\pi} \left[ C_A \left( -\frac{101}{27} + \frac{7}{2}\zeta_3 \right) + \frac{14}{27}N_f \right]. \quad (\text{C.1.15b})$$

Let us remind you that here and in all the previous expressions  $C_c = C_A$  if  $c = g$ , a gluon fusion process, and  $C_c = C_F$  if  $c = q$ , a quark annihilation process.

Now we move to the process dependent part, the hard function. Since it is process dependent, here we limit to present explicit results for our test case, Higgs boson production. The Drell-Yan process hard part can be deduced from Ref. [58, 141].

The function  $\mathcal{H}_{gg \rightarrow ij}(N, \alpha_s)$  in the context of Higgs boson production is given in Refs. [30, 49], and it is defined by factoring out the inclusive cross section Eq. (C.1.3). In Eq. (2.4.17) and Eq. (2.5.45) it is decomposed as

$$\mathcal{H}_{gg \rightarrow ij}(N, \alpha_s) = \sum_{ij} H_g(\alpha_s) [C_{gi}(N, \alpha_s) C_{g,j}(N, \alpha_s) + G_{gi}(N, \alpha_s) G_{gi}(N, \alpha_s)], \quad (\text{C.1.16})$$

where in the hard resummation scheme  $H_g$  contains all the constant terms while  $C$  and  $G$  embody the not trivial  $N$  dependence. Please note that, in those equations, the couplings of  $C$  and  $H$  are evaluated at different scale. However, in the final expressions for the hard part Eqs. (2.7.2) the various coefficients  $\mathcal{H}$  are computed as in Eq. (C.1.16) with the same scale in all the couplings. The difference between the two expressions is taken into account in Eqs. (2.7.2) in the evolution factor  $R$ , Eq. (2.7.7).

Separation of the  $N$  dependent part into two functions  $C$  and  $G$  is due to the presence of spin correlation in gluon initiated processes, as highlighted in Ref. [57]. However, since these contributions due to azimuthal correlations  $G$  start at  $\mathcal{O}(\alpha_s)$ , they only contribute at  $\mathcal{O}(\alpha_s^2)$  in  $\mathcal{H}$ . However, at NNLL, the division of  $\mathcal{H}$  into  $H$ ,  $C$  and  $G$  at  $\mathcal{O}(\alpha_s^2)$  is

subleading; thus we decide in the text, in Eqs. (2.4.17), (2.5.45), and Eqs. (2.4.19), (2.5.48) to ignore this subtlety and to introduce for simplicity a unique function  $C$ .

In the Higgs boson production case, we have:

$$\begin{aligned} H_g(\alpha_s) &= 1 + \frac{\alpha_s}{\pi} 3C_A \zeta_2 \\ &+ \left(\frac{\alpha_s}{\pi}\right)^2 \left( C_A^2 \left( \frac{93}{16} + \frac{67}{12} \zeta_2 - \frac{55}{18} \zeta_3 + \frac{65}{8} \zeta_4 \right) + C_A N_f \left( -\frac{5}{3} - \frac{5}{6} \zeta_2 - \frac{4}{9} \zeta_3 \right) \right) \\ &+ \mathcal{O}(\alpha_s^3), \end{aligned} \quad (\text{C.1.17})$$

up to two loops, for the constant term and

$$C_{gg}(N, \alpha_s) = 1 + \mathcal{O}(\alpha_s^2), \quad (\text{C.1.18})$$

$$C_{gq}(N, \alpha_s) = \alpha_s \frac{C_F}{2\pi} \frac{1}{N+1} + \mathcal{O}(\alpha_s^2), \quad (\text{C.1.19})$$

$$G_{gg}(N, \alpha_s) = \alpha_s \frac{C_A}{\pi} \frac{1}{N(N-1)} + \mathcal{O}(\alpha_s^2), \quad (\text{C.1.20})$$

$$G_{gq}(N, \alpha_s) = \alpha_s \frac{C_F}{\pi} \frac{1}{N(N-1)} + \mathcal{O}(\alpha_s^2), \quad (\text{C.1.21})$$

up to one loop, for the  $N$  dependent part. Plugging all together we derive the one loop expressions for  $\mathcal{H}_{gg \rightarrow ij}^{(1)}$ :

$$\mathcal{H}_{gg \rightarrow gg}^{(1)} = \frac{3C_A \zeta_2}{\pi}, \quad (\text{C.1.22a})$$

$$\mathcal{H}_{gg \rightarrow gq}^{(1)} = \frac{C_F}{2\pi} \frac{1}{N+1}, \quad (\text{C.1.22b})$$

$$\mathcal{H}_{gg \rightarrow qq}^{(1)} = 0. \quad (\text{C.1.22c})$$

As already said, at NNLL, decomposition of Eq. (C.1.16) at  $\mathcal{O}(\alpha_s^2)$  is immaterial; we then decide to present explicit results directly for  $\mathcal{H}_{gg \rightarrow ij}^{(2)}$ . They can be obtained in  $z$  space from Ref. [49]:

$$\mathcal{H}_{gg \rightarrow qq}^{(2)}(z) = -\frac{C_F^2}{\pi^2} \left[ \frac{2(1-z)}{z} + \frac{(2+z)^2}{4z} \ln z \right], \quad (\text{C.1.23a})$$

$$\begin{aligned} \mathcal{H}_{gg \rightarrow gq}^{(2)}(z) &= \frac{1}{\pi^2} \left[ C_F^2 \left( \frac{1}{48} (2-z) \ln^3 z - \frac{1}{32} (3z+4) \ln^2 z + \frac{5}{16} (z-3) \ln z \right. \right. \\ &+ \frac{1}{12} \left( \frac{1}{z} + \frac{z}{2} - 1 \right) \ln^3(1-z) + \frac{1}{16} \left( z + \frac{6}{z} - 6 \right) \ln^2(1-z) \\ &+ \left. \left( \frac{5z}{8} + \frac{2}{z} - 2 \right) \ln(1-z) + \frac{5}{8} - \frac{13}{16} z \right) \\ &+ C_F N_f \left( \frac{1}{24z} (1+(1-z)^2) \ln^2(1-z) + \frac{1}{18} \left( z + \frac{5}{z} - 5 \right) \ln(1-z) \right) \end{aligned}$$

$$\begin{aligned}
& -\frac{14}{27} + \frac{14}{27z} + \frac{13}{108}z \Big) \\
& + C_F C_A \left( -\frac{(1+(1+z)^2)}{2z} \text{Li}_3\left(\frac{1}{1+z}\right) + \left(\frac{1}{2} - \frac{5}{2z} - \frac{5}{4}z\right) \text{Li}_3(z) \right. \\
& - \frac{3}{4z} (1+(1+z)^2) \text{Li}_3(-z) + \left(\frac{z}{4} + \frac{(1+(1+z)^2)}{4z} \ln(z)\right) \text{Li}_2(-z) \\
& + \left(2 - \frac{11}{6z} - \frac{z}{2} + \frac{z^2}{3} + \left(-\frac{1}{2} + \frac{3}{2z} + \frac{3z}{4}\right) \ln z\right) \text{Li}_2(z) \\
& + \frac{(1+(1+z)^2)}{12z} \ln^3(1+z) - \frac{(1+(1-z)^2)}{24z} \ln^3(1-z) \\
& - \frac{1}{24z} \left( (1+(1+z)^2) (3\ln^2 z + \pi^2) - 6z^2 \ln z \right) \ln(1+z) \\
& + \frac{1}{48z} (6(1+(1-z)^2) \ln z - 5z^2 - 22(1-z)) \ln^2(1-z) \\
& + \frac{1}{72z} \left( -152 + 152z - 43z^2 + 6(-22 + 24z - 9z^2 + 4z^3) \ln z \right. \\
& \quad \left. + 9(1+(1-z)^2) \ln^2 z \right) \ln(1-z) - \frac{1}{12} \left(1 + \frac{z}{2}\right) \ln^3 z \\
& + \frac{1}{48} (36 + 9z + 8z^2) \ln^2 z + \left(-\frac{107}{24} - \frac{1}{z} + \frac{z}{12} - \frac{11}{9}z^2\right) \ln z \\
& + \frac{1}{z} \left(4\zeta_3 - \frac{503}{54} + \frac{11}{36}\pi^2\right) + \frac{1007}{108} - \frac{\pi^2}{3} - \frac{5}{2}\zeta_3 + z \left(\frac{\pi^2}{3} + 2\zeta_3 - \frac{133}{108}\right) \\
& \left. + z^2 \left(\frac{38}{27} - \frac{\pi^2}{18}\right) \right] \Big), \tag{C.1.23b}
\end{aligned}$$

$$\begin{aligned}
\mathcal{H}_{gg \rightarrow gg}^{(2)}(z) &= \frac{1}{\pi^2} \left[ \left( \left( -\frac{101}{27} + \frac{7}{2}\zeta_3 \right) C_A^2 + \frac{14}{27} C_A N_f \right) \left( \frac{1}{1-z} \right)_+ \right. \\
& + \left( C_A^2 \left( \frac{93}{16} + \frac{67}{12}\zeta_2 - \frac{55}{18}\zeta_3 + \frac{65}{8}\zeta_4 \right) + C_A N_f \left( -\frac{5}{3} - \frac{5}{6}\zeta_2 - \frac{4}{9}\zeta_3 \right) \right) \delta(1-z) \\
& + C_A^2 \left( \frac{(1+z+z^2)^2}{z(1+z)} \left( 2\text{Li}_3\left(\frac{z}{1+z}\right) - \text{Li}_3(-z) \right) \right. \\
& + \frac{2-17z-22z^2-10z^3-12z^4}{2z(1+z)} \zeta_3 \\
& - \frac{5-z+5z^2+z^3-5z^4+z^5}{z(1-z)(1+z)} (\text{Li}_3(z) - \zeta_3) \\
& + \text{Li}_2(z) \frac{\ln(z)}{1-z} \frac{3-z+3z^2+z^3-3z^4+z^5}{z(1+z)} + \frac{1}{12} z \ln(1-z) \\
& \left. + \frac{(1+z+z^2)^2}{z(1+z)} \left( \ln(z) \text{Li}_2(-z) - \frac{1}{3} \ln^3(1+z) + \zeta_2 \ln(1+z) \right) \right]
\end{aligned}$$

$$\begin{aligned}
& + \frac{1-z}{3z} (11-z+11z^2) \text{Li}_2(1-z) - \frac{1}{6} \frac{\ln^3(z)}{1-z} \frac{(1+z-z^2)^2}{1+z} \\
& + \ln^2(z) \left( \frac{(1-z+z^2)^2}{2z(1-z)} \ln(1-z) \right. \\
& \quad \left. - \frac{(1+z+z^2)^2}{2z(1+z)} \ln(1+z) + \frac{25-11z+44z^2}{24} \right) \\
& + \ln(z) \left( \frac{(1+z+z^2)^2}{z(1+z)} \ln^2(1+z) + \frac{(1-z+z^2)^2}{2z(1-z)} \ln^2(1-z) \right. \\
& \quad \left. - \frac{72+773z+149z^2+536z^3}{72z} \right) + \frac{517}{27} - \frac{449}{27z} - \frac{380z}{27} + \frac{835z^2}{54} \\
& + C_A N_f \left( \frac{1+z}{12} \ln^2(z) + \frac{1}{36} (13+10z) \ln(z) - \frac{z}{12} \ln(1-z) \right. \\
& \quad \left. - \frac{83}{54} + \frac{121}{108z} + \frac{55}{54} z - \frac{139}{108} z^2 \right) \\
& + C_F N_f \left( \frac{1+z}{12} \ln^3(z) + \frac{1}{8} (3+z) \ln^2(z) \right. \\
& \quad \left. + \frac{3}{2} (1+z) \ln(z) - \frac{1-z}{6z} (1-23z+z^2) \right) \Bigg], \tag{C.1.23c}
\end{aligned}$$

where  $\text{Li}_k(z)$  ( $k = 2, 3$ ) are the usual polylogarithm functions,

$$\text{Li}_2(z) = - \int_0^z \frac{dt}{t} \ln(1-t) \quad , \quad \text{Li}_3(z) = \int_0^1 \frac{dt}{t} \ln(t) \ln(1-zt) \quad . \tag{C.1.24}$$

The Mellin transform of Eqs. (C.1.23) can be computed analytically using the Harmonic Sums up to fourth order and the results of Appendix B. Let us conclude this section with a last comment: when expressions Eqs. (C.1.22) and Eqs. (C.1.23) are used in the context of consistent small- $p_T$  resummation,  $\mathcal{H}_{gg \rightarrow gg}$  term has to be changed according to Eq. (2.5.47) and Eq. (2.7.10).

We have presented all the analytical expressions needed for the computation of our final expression Eqs. (2.5.45) and (2.5.48), and of the original transverse momentum resummation Eqs. (2.4.17) and (2.4.19).

## C.2 High Energy Region

In this section we will give you more details about the explicit computation of the various *impact factors* presenting in the text. Moreover, we will include all the analytical expressions for them in Mellin space.

Before starting, we want to briefly discuss the factorization scheme dependence in the context of high energy resummation and to present the explicit expression for the factor

$R(M)$ . We decide to place first this discussion since it is common to all the applications.

In our general derivation of Chap. 3, factorization scheme dependence was produced by subleading  $\epsilon$  correction in the anomalous dimension  $\gamma$ , Eq. (3.1.60). We call this factor  $\mathcal{R}$  in the text. However, as pointed out in Ref. [85] this is not the only factorization scheme dependence of our construction. The second origin is linked to the factorization structure itself which was derived explicitly in the  $\overline{\text{MS}}$  scheme. Ladder exponentiation and collinear subtraction does not commute if another scheme would be selected. In Ref. [85], it was proved that it is possible to take into account this anomalous dimension fluctuation, linked to the non-commutativity of ladder subtraction and exponentiation in a further prefactor, generally called  $\mathcal{N}$ . The product of these two scheme dependent factors forms the  $R$  factor [69, 85] introduced in the text in our general impact factor definition, Eq. (3.1.64).

The explicit expression for the factor  $R(M)$  at LL $x$  turns out to be

$$R(M) = \sqrt{\frac{\Gamma(1-M)\chi_0(M)}{\Gamma(1+M)(-M\chi'_0(M))}} \exp \left[ -M\gamma_E + \int_0^M dM' \frac{\pi}{C_A} \frac{\zeta_2 - \psi_1(1-M')}{\chi_0(M')} \right] \quad (\text{C.2.1})$$

while we refer to Ref. [85] for the separate explicit formulas for factors  $\mathcal{R}$  and  $\mathcal{N}$ . In Eq. (C.2.1), as in the text, we call  $\chi_0$  the LO BFKL kernel [81] which takes the following form

$$\chi_0(M) = -\frac{C_A}{\pi} (2\gamma_E + \psi_0(M) + \psi_0(1-M)). \quad (\text{C.2.2})$$

We have concluded our discussion about the factorization scheme dependence. We are going to present all the results in the  $\overline{\text{MS}}$  scheme; the reader should be able now to switch factorization scheme using Eq. (C.2.1).

We will divide this section in several subsection, one for each treated process. In particular, they are: Higgs boson production, both in the effective field theory framework and in the full standard model, and one-jet inclusive production.

## C.2.1 EFT Higgs boson production

The computation of the  $p_T$ -impact factor in the case of the EFT Higgs boson production was already sketched in the text, in Sec. 3.4 of Chap. 3. From the LO off-shell transverse momentum distribution  $C_{p_T}(N, \xi, \bar{\xi}, \xi_p, \alpha_s)$ , Eq. (3.4.2), the impact factor was found to be given by the following integral

$$h_{p_T}(N, M_1, M_2, \xi_p, \alpha_s) = \sigma_0 \frac{\xi_p^{M_1+M_2-1}}{\pi(1+\xi_p)^N} I(M_1, M_2) \quad (\text{C.2.3})$$

with

$$I(M_1, M_2) = M_1 M_2 R(M_1) R(M_2) \int_0^\infty d\xi_1 \xi_1^{M_1-2} \int_{(1-\sqrt{\xi_1})^2}^{(1+\sqrt{\xi_1})^2} d\xi_2 \xi_2^{M_2-2} \frac{(1-\xi_1-\xi_2)^2}{\sqrt{2\xi_1\xi_2 + 2\xi_1 + 2\xi_2 - 1 - \xi_1^2 - \xi_2^2}}. \quad (\text{C.2.4})$$

To the explicit computation of  $I$  integral will be devoted the rest of this subsection.

We first change variable from  $\xi_2$  to a new variable  $u$ , defined implicitly as

$$\xi_2 = 1 + \xi_1 - 2\sqrt{\xi_1}u \quad (\text{C.2.5})$$

in terms of which, Eq. (C.2.4) becomes

$$I(M_1, M_2) = M_1 M_2 R(M_1) R(M_2) \int_0^\infty d\xi_1 4\xi_1^{M_1} \int_{-1}^1 du \left(1 - \frac{1}{\sqrt{\xi_1}}u\right)^2 (1 + \xi_1)^{M_2-2} \frac{(1 - \sqrt{ru})^{M_2-2}}{\sqrt{1-u^2}}, \quad (\text{C.2.6})$$

where  $r \equiv \frac{4\xi_1}{(1+\xi_1)^2}$ .

With straightforward manipulations, Eq. (C.2.6) can be rewritten in terms of a single integral function

$$F(M_1, M_2) = \int_0^\infty d\xi_1 \xi_1^{M_1} (1 + \xi_1)^{M_2} \int_{-1}^1 du \frac{(1 - \sqrt{ru})^{M_2}}{\sqrt{1-u^2}}, \quad (\text{C.2.7})$$

as

$$I(M_1, M_2) = M_1 M_2 R(M_1) R(M_2) \left[ F(M_1 - 2, M_2 - 2) - 2F(M_1 - 1, M_2 - 2) + F(M_1, M_2 - 2) - 2F(M_1 - 2, M_2 - 1) + 2F(M_1 - 1, M_2 - 1) + F(M_1 - 2, M_2) \right]. \quad (\text{C.2.8})$$

We compute  $F$  by expanding  $(1 - \sqrt{ru})^{M_2}$  in powers of  $u$ , with the result

$$\begin{aligned} F(M_1, M_2) &= \int_0^\infty d\xi_1 \xi_1^{M_1} (1 + \xi_1)^{M_2} \int_{-1}^1 du \frac{(1 - \sqrt{ru})^{M_2}}{\sqrt{1-u^2}} \\ &= \sum_{k=0}^\infty \binom{M_2}{2k} \int_0^\infty d\xi_1 \xi_1^{M_1} (1 + \xi_1)^{M_2} r^k \int_{-1}^1 du \frac{u^{2k}}{\sqrt{1-u^2}} \\ &= \sum_{k=0}^\infty \binom{M_2}{2k} \frac{4^k \sqrt{\pi} \Gamma(\frac{1}{2} + k)}{\Gamma(1+k)} \int_0^\infty d\xi_1 \xi_1^{M_1+k} (1 + \xi_1)^{M_2-2k} \\ &= \sum_{k=0}^\infty \binom{M_2}{2k} \frac{4^k \sqrt{\pi} \Gamma(\frac{1}{2} + k)}{\Gamma(1+k)} \frac{\Gamma(1+k+M_1) \Gamma(k-1-M_1-M_2)}{\Gamma(2k-M_2)}. \quad (\text{C.2.9}) \end{aligned}$$

The sum can then be performed in closed form:

$$F(M_1, M_2) = \frac{\pi \Gamma(1+M_1) \Gamma(1+M_2) \Gamma(-1-M_1-M_2)}{\Gamma(-M_1) \Gamma(-M_2) \Gamma(2+M_1+M_2)}. \quad (\text{C.2.10})$$

Substituting this expression in Eq. (C.2.8) and exploiting the properties of the Euler Gamma function we finally get

$$I(M_1, M_2) = \pi R(M_1) R(M_2) \left[ \frac{\Gamma(1+M_1)\Gamma(1+M_2)\Gamma(2-M_1-M_2)}{\Gamma(2-M_1)\Gamma(2-M_2)\Gamma(M_1+M_2)} \left( 1 + \frac{2M_1M_2}{1-M_1-M_2} \right) \right], \quad (\text{C.2.11})$$

which is the result used in the text to obtain final expression Eq. (3.4.10).

## C.2.2 SM Higgs boson production

In Chap. 4 we have seen that a phenomenology study of quark mass effects on the Higgs boson transverse momentum distribution is possible using high energy resummation. This is due to the fact that the  $p_T$ -impact factor can be computed both in the EFT framework as in Sec. 3.4 and in the full Standard Model, thus retaining all the quark mass dependence.

In Sec. 4.2, however, we focus our attention on phenomenological implications of our high energy analysis and the explicit form of  $p_T$ -impact factor in the SM case was introduced as a known result. In this subsection, we want to fill this lack by presenting more details about the computation of this object. Discussion will follow original derivation of Ref. [95].

We start our derivation from the computation of the LO off-shell transverse momentum distribution  $C_{p_T}$ . Parametrizing the off-shell gluon momenta in terms of longitudinal and transverse components as

$$\begin{aligned} k_1 &= zp_1 + k_{t,1} \\ k_2 &= \bar{z}p_2 + k_{t,2} \end{aligned} \quad (\text{C.2.12})$$

with

$$\begin{aligned} p_i^2 &= 0, \quad p_i \cdot k_{t,j} = 0, \quad i, j = 1, 2 \\ k_1^2 &= k_{t,1}^2 = -\xi m_H^2 < 0, \quad k_2^2 = k_{t,2}^2 = -\bar{\xi} m_H^2 < 0 \quad 2p_1 \cdot p_2 = \hat{s}, \\ k_{t,1} \cdot k_{t,2} &= -\sqrt{\xi\bar{\xi}} m_H^2 \cos\theta. \end{aligned}$$

we can write the coefficient function  $C_{p_T}(N, \xi, \bar{\xi}, \xi_p, \{y_i\})$  as the following Mellin transform

$$C_{p_T}(N, \xi, \bar{\xi}, \xi_p, \{y_i\}) = \int_0^1 d\hat{\tau} \hat{\tau}^{N-1} C_{p_T}(\hat{\tau}, \xi, \bar{\xi}, \xi_p, \{y_i\}) \quad (\text{C.2.14})$$

where

$$\hat{\tau} = \frac{m_H^2}{\hat{s}z\bar{z}}. \quad (\text{C.2.15})$$

Note that Mellin transformation in Eq. (C.2.14) is performed for simplicity with respect to the standard  $p_T$ -independent scaling variable Eq. (1.4.7) as in the inclusive computation of Ref. [73]: as already mentioned in the text, computing the Mellin transform with respect to the variable  $x$ , Eq. (1.4.10), would lead to a result which differs only by subleading terms, and thus to the same final LL $x$  answer.

The quantity  $C_{p_T}(x, \xi, \bar{\xi}, \xi_p, \{y_i\})$  in Eq. (C.2.14) is the transverse momentum distribution

$$C_{p_T}(\hat{\tau}, \xi, \bar{\xi}, \xi_p, \{y_i\}) = \int \frac{1}{2\hat{s}z\bar{z}} \times \left[ \frac{1}{256} \sum_{\text{col, pol}} |M(g^*g^* \rightarrow H)|^2 \right] \times$$

$$\times d\mathcal{P}(k_1 + k_2 \rightarrow p_h) \times \delta\left(\xi_p - \xi - \bar{\xi} - 2\sqrt{\xi\bar{\xi}}\cos\theta\right). \quad (\text{C.2.16})$$

In Eq. (C.2.16)  $d\mathcal{P}$  is the phase space factor

$$d\mathcal{P}(k_1 + k_2 \rightarrow p_h) = \frac{2\pi}{m_H^2} \delta\left(\frac{1}{\hat{\tau}} - 1 - \xi - \bar{\xi} - 2\sqrt{\xi\bar{\xi}}\cos\theta\right) \frac{d\theta}{2\pi}; \quad (\text{C.2.17})$$

the sum over off-shell gluon polarizations is performed using

$$\sum_{\lambda} \epsilon_{\lambda}^{\mu}(k_i) \epsilon_{\lambda}^{\nu*}(k_i) = -2 \frac{k_{t,i}^{\mu} k_{t,i}^{\nu}}{k_{t,i}^2}; \quad (\text{C.2.18})$$

and the flux factor is determined on the surface orthogonal to  $p_{1,2}$ .

After standard algebraic manipulations,  $C_{p_T}$  can be written as

$$C_{p_T}(N, \xi, \bar{\xi}, \xi_p, \{y_i\}) = 2\sigma_0(\{y_i\}) \int_0^1 d\hat{\tau} \hat{\tau}^{N-2} \int_0^{2\pi} \frac{d\theta}{2\pi} \tilde{F}(\xi, \bar{\xi}, \xi_p, \{y_i\}) \delta\left(\frac{1}{x} - 1 - \xi_p\right) \delta\left(\xi_p - \xi - \bar{\xi} - 2\sqrt{\xi\bar{\xi}}\cos\theta\right), \quad (\text{C.2.19})$$

where  $\sigma_0$  is the LO Higgs production cross-section

$$\sigma_0(\{y_i\}) = \sigma_0^{\text{PL}} \left| \sum_{\{y_i\}} K(y_i) \right|^2, \quad (\text{C.2.20})$$

$$\sigma_0^{\text{PL}} = \frac{G_F \sqrt{2} \alpha_s^2}{576\pi}, \quad (\text{C.2.21})$$

$$K(y) = 6y \left(1 - \frac{1}{4}(1 - 4y) \ln^2 \frac{\sqrt{1-4y} - 1}{\sqrt{1-4y} + 1}\right). \quad (\text{C.2.22})$$

In Eq. (C.2.21) (as well as in all the remaining equations in this section) the branch cut in the logarithm should be handled by giving  $y$  a small negative imaginary part.

The rather lengthy explicit formula for the form factor  $\tilde{F}$  is reported in the next subsection, Eq. (C.2.35) together with some limiting cases. Note that the quark mass dependence is contained both in the Born cross-section  $\sigma_0$  and in the form factor  $\tilde{F}$ . Note also that if the exact quark mass dependence is retained, the form factor  $\tilde{F}$  vanishes in the  $\xi, \bar{\xi} \rightarrow \infty$  limit, while it approaches a constant ( $\tilde{F} \rightarrow \cos^2\theta$ ) in the pointlike approximation. This fact leads to a qualitatively different high-energy behaviour in the two cases, which was discussed in detail in Chap. 4, Sec. 4.2.3.

Inserting the expression Eq. (C.2.19) for the coefficient function  $C_{p_T}$  in the general expression for the  $p_T$ -impact factor Eq. (3.2.4) and using one delta function to perform the  $\hat{\tau}$  Mellin integral we obtain

$$h_{p_T}(N, M_1, M_2, \xi_p, \{y_i\}) = \sigma_0(\{y_i\}) M_1 M_2 R(M_1) R(M_2) \frac{\xi_p^{M_1+M_2-1}}{(1+\xi_p)^N} \int_0^{\infty} d\xi_1 \xi_1^{M_1-1}$$

$$\int_0^\infty d\xi_2 \xi_2^{M_2-1} \int_{-1}^1 \frac{du}{\sqrt{1-u^2}} \frac{2}{\pi} F(\xi_1, \xi_2, \xi_p, \{y_i\}) \delta\left(1 - \xi_1 - \xi_2 - 2\sqrt{\xi_1 \xi_2} u\right), \quad (\text{C.2.23})$$

where we have introduced

$$u = \cos \theta, \quad \xi_1 = \frac{\xi}{\xi_p} = -\frac{k_{t,1}^2}{p_T^2}, \quad \xi_2 = \frac{\bar{\xi}}{\xi_p} = -\frac{k_{t,2}^2}{p_T^2} \quad (\text{C.2.24})$$

and defined

$$F(\xi_1, \xi_2, \xi_p, \{y_i\}) = \tilde{F}(\xi, \bar{\xi}, \xi_p, \{y_i\}). \quad (\text{C.2.25})$$

Eq. (C.2.23) represents the integral representation of the  $p_T$ -impact factor in the case of Standard Model Higgs production. If we are interested in a resummed evaluation, we need to perform last integrations numerically, using a numerical form for the LL $x$  resummed anomalous dimension, as already performed for DIS and DY in the program HELL [70, 84].

In Chap. 4, however a perturbative expansion Eq. (C.2.23) was presented and used. Let us comment briefly how this expansion is computed.

For the sake of extracting the first several orders in the expansion of the cross-section in powers of  $\alpha_s$  we are interested in, we need the expansion of the impact factor in powers of  $M_i$ . This task is not entirely straightforward because of the  $1/M_i$  collinear singularities coming from the  $\xi_i^{M_i-1}$  terms. Although the actual singularities are removed by the  $M_i R(M_i)$  factorization terms, they prevent a naive Taylor expansion in  $M_i$ . In Ref. [77] this problem was circumvented by analytically computing the impact factor for arbitrary values of  $M_i$ . In the present case, however, an analytic computation does not appear viable because of the complexity of  $F$  when the full quark mass dependence is retained.

In order to extract the desired coefficients in the expansion of the impact factor we then proceed as follows. First, we note that because of the kinematics in the LL $x$  limit we cannot have collinear singularities in both  $\xi_1$  and  $\xi_2$  at the same time. This is because the transverse momentum of the two incoming off-shell gluons must exactly balance the Higgs transverse momentum, so we cannot have  $\xi_1 = \xi_2 = 0$  and  $\xi_p \neq 0$  at the same time. This is made explicit by the delta constraint in Eq. (C.2.23). It is then natural to split the integration domain in two regions, one with  $\xi_1 > \xi_2$  and another with  $\xi_2 > \xi_1$ . In the first one, we define  $\xi_2 = z\xi_1$  and rewrite Eq. (C.2.23) as

$$h_{p_T}^I(N, M_1, M_2, \xi_p, \{y_i\}) = \sigma_0(\{y_i\}) M_1 M_2 R(M_1) R(M_2) \frac{\xi_p^{M_1+M_2-1}}{(1+\xi_p)^N} \int_0^1 dz z^{M_2-1} \int_{-1}^1 \frac{2du}{\pi\sqrt{1-u^2}} \int_0^\infty d\xi_1 \xi_1^{M_1+M_2-1} F(\xi_1, z\xi_1, \xi_p, \{y_i\}) \delta(1 - \xi_1(1 + 2\sqrt{z}u + z)), \quad (\text{C.2.26})$$

where we have denoted with  $h_{p_T}^I$  the contribution from this first integration region.

We now use the delta function to perform the  $\xi_1$  integration to obtain

$$h_{p_T}^I(N, M_1, M_2, \xi_p, \{y_i\}) = \sigma_0(\{y_i\}) M_1 M_2 R(M_1) R(M_2) \frac{\xi_p^{M_1+M_2-1}}{(1+\xi_p)^N} \int_0^1 dz z^{M_2-1}$$

$$\int_{-1}^1 \frac{2du}{\pi\sqrt{1-u^2}} \left[ \frac{1}{1+2\sqrt{zu}+z} \right]^{M_1+M_2} F \left( \frac{1}{1+2\sqrt{zu}+z}, \frac{z}{1+2\sqrt{zu}+z}, \xi_p, \{y_i\} \right). \quad (\text{C.2.27})$$

Note that in Eq. (C.2.27) the limit  $\xi_1 \rightarrow 0$  is harmless and only the limit  $z \rightarrow 0$  is associated with a collinear singularity. We compute it using the identity

$$z^{M-1} = \frac{1}{M} \delta(z) + \sum_{j=0}^{\infty} \frac{M^{j-1}}{(j-1)!} \left[ \frac{\ln^{j-1} z}{z} \right]_+, \quad (\text{C.2.28})$$

where the plus distribution is defined as in Eq. (B.3.2).

We then rewrite Eq. (C.2.27) as

$$h_{p_T}^I(N, M_1, M_2, \xi_p, \{y_i\}) = \sigma_0(\{y_i\}) M_1 M_2 R(M_1) R(M_2) \frac{\xi_p^{M_1+M_2-1}}{(1+\xi_p)^N} \int_{-1}^1 \frac{2du}{\pi\sqrt{1-u^2}} \times \\ \times \left( \frac{1}{M_2} F(1, 0, \{y_i\}) + \int_0^1 dz \frac{a^{M_1+M_2} F(a, b, \xi_p, \{y_i\}) - F(1, 0, \xi_p, \{y_i\})}{z} z^{M_2} \right) \quad (\text{C.2.29})$$

where we have introduced the notation

$$a = a(z, u) = \frac{1}{1+2\sqrt{zu}+z}, \quad b = b(z, u) = \frac{z}{1+2\sqrt{zu}+z}. \quad (\text{C.2.30})$$

In Eq. (C.2.29) the collinear pole in  $M_2 = 0$  has been isolated explicitly, and the remainder can be Taylor-expanded in  $M_i$ ; Eq. (C.2.29) only involves integrals over compact regions, which can be easily performed numerically. Since  $F$  is symmetric under  $\xi_1 \leftrightarrow \xi_2$  exchange, the result for the second region  $\xi_1 < \xi_2$  can now be obtained from the left hand side of Eq. (C.2.29) via  $M_1 \leftrightarrow M_2$  exchange.

Combining the contributions from the two regions, we find that the expansion of the impact factor Eq. (C.2.23) has the general structure

$$h_{p_T}(N, M_1, M_2, \xi_p, \{y_i\}) = \sigma_0(\{y_i\}) R(M_1) R(M_2) \frac{\xi_p^{M_1+M_2-1}}{(1+\xi_p)^N} \times \\ \times \left[ c_0(\xi_p, \{y_i\}) (M_1 + M_2) + \sum_{j \geq k > 0} c_{j,k}(\xi_p, \{y_i\}) \left( M_1^k M_2^j + M_1^j M_2^k \right) \right] \quad (\text{C.2.31})$$

with

$$c_0(\xi_p, \{y_i\}) = \int_{-1}^1 \frac{2du}{\pi\sqrt{1-u^2}} F(0, 1, \xi_p, \{y_i\}) \quad (\text{C.2.32})$$

$$c_{j,k}(\xi_p, \{y_i\}) = \frac{1}{(j-1)! (k-1)!} \frac{1}{1+\delta_{jk}} \times \\ \int_{-1}^1 \frac{2du}{\pi\sqrt{1-u^2}} \int_0^1 dz \frac{\ln^{j-1} a \ln^{k-1} b F(a, b, \xi_p, \{y_i\}) - \delta_{j,1} \ln^{k-1} z F(1, 0, \xi_p, \{y_i\})}{z} \\ + (j \leftrightarrow k) \quad (\text{C.2.33})$$

and  $a, b$  defined in Eq. (C.2.30). A relatively simple analytic expression for  $c_0$  will be presented in the next subsection, Eq. (C.2.48).

Eq. (C.2.31) was the result used in the text, in Chap. 4, Sec. 4.2 and it concludes the discussion of this section. In the next subsection we limit ourselves to present the analytical expressions for the form factor  $F$  and  $c_0$ .

### C.2.2.1 Form factors and perturbative coefficients

We give here the expressions for the form factor  $F$  used in the previous section in the computation of the  $p_T$ -impact factor. We also provide analytic form of the first LO coefficient of the expansion in power of  $\alpha_s$  of the  $p_T$ -impact factor,  $c_0$ .

The  $p_T$ -impact factor is expressed in Eq. (C.2.23) as a double integral over  $\xi_1$  and  $\xi_2$  of a function  $F(\xi_1, \xi_2, \xi_p, \{y_i\})$ . This function is deduced from the off-shell form factor  $\tilde{F}(\xi, \bar{\xi}, \xi_p, \{y_i\})$  as

$$F(\xi_1, \xi_2, \xi_p, \{y_i\}) = \tilde{F}(\xi_p \xi_1, \xi_p \xi_2, \xi_p, \{y_i\}). \quad (\text{C.2.34})$$

This form factor is given by [73, 143]:

$$\tilde{F}(\xi, \bar{\xi}, \xi_p, \{y_i\}) = \frac{2304\pi^4}{|\sum_i K(y_i)|^2} \left| \sum_i y_i A(\xi, \bar{\xi}, \xi_p, y_i) \right|^2 \quad (\text{C.2.35})$$

with the sum  $i$  which runs over the set  $\{y_i\}$  of quarks circulating in the loop, and

$$\begin{aligned} A(\xi, \bar{\xi}, \xi_p, y) &= \frac{C_0(\xi, \bar{\xi}, y)}{\sqrt{\xi\bar{\xi}}} \\ &= \left[ \left( \frac{2y}{\Delta_3} + \frac{6\xi\bar{\xi}}{\Delta_3^2} \right) ((\xi_p - \xi - \bar{\xi})(1 + \xi + \bar{\xi}) + 4\xi\bar{\xi}) - \frac{\xi_p - \xi - \bar{\xi}}{2} + 2 \frac{\xi\bar{\xi}(1 - \xi_p)}{\Delta_3} \right] \\ &\quad - \frac{1}{\sqrt{\xi\bar{\xi}}} [B_0(-\bar{\xi}, y) - B_0(1, y)] \left[ -\frac{\bar{\xi}}{\Delta_3} (\xi_p - \bar{\xi} + \xi) + \frac{6\xi\bar{\xi}}{\Delta_3^2} (1 + \xi_p)(1 + \xi - \bar{\xi}) \right] \\ &\quad - \frac{1}{\sqrt{\xi\bar{\xi}}} [B_0(-\xi, y) - B_0(1, y)] \left[ -\frac{\xi}{\Delta_3} (\xi_p - \xi + \bar{\xi}) + \frac{6\xi\bar{\xi}}{\Delta_3^2} (1 + \xi_p)(1 + \bar{\xi} - \xi) \right] \\ &\quad + \frac{1}{4\pi^2} \frac{1}{\Delta_3} \frac{1}{\sqrt{\xi\bar{\xi}}} ((\xi_p - \xi - \bar{\xi})(1 + \xi + \bar{\xi}) + \xi\bar{\xi}) \end{aligned} \quad (\text{C.2.36})$$

where  $\Delta_3 = (1 + \xi + \bar{\xi})^2 - 4\xi\bar{\xi}$  and

$$B_0(\rho, y) = -\frac{1}{16\pi^2} \sqrt{\frac{\rho - 4y}{\rho}} \ln \frac{\sqrt{\frac{\rho - 4y}{\rho}} + 1}{\sqrt{\frac{\rho - 4y}{\rho}} - 1} \quad (\text{C.2.37})$$

$$C_0(\xi, \bar{\xi}, y) = \frac{1}{16\pi^2} \frac{1}{\sqrt{\Delta_3}} \left[ \ln(1 - y_-) \ln \left( \frac{1 - y_- \delta_1^+}{1 - y_- \delta_1^-} \right) \right]$$

$$\begin{aligned}
& + \ln(1-x_-) \ln\left(\frac{1-x_- \delta_2^+}{1-x_- \delta_2^-}\right) + \ln(1-z_-) \ln\left(\frac{1-z_- \delta_3^+}{1-z_- \delta_3^-}\right) \\
& + \text{Li}_2(y_+ \delta_1^+) + \text{Li}_2(y_- \delta_1^+) - \text{Li}_2(y_+ \delta_1^-) - \text{Li}_2(y_- \delta_1^-) \\
& + \text{Li}_2(x_+ \delta_2^+) + \text{Li}_2(x_- \delta_2^+) - \text{Li}_2(x_+ \delta_2^-) - \text{Li}_2(x_- \delta_2^-) \\
& + \text{Li}_2(z_+ \delta_3^+) + \text{Li}_2(z_- \delta_3^+) - \text{Li}_2(z_+ \delta_3^-) - \text{Li}_2(z_- \delta_3^-) \Big] \quad (\text{C.2.38})
\end{aligned}$$

with

$$\delta_1 \equiv \frac{-\xi + \bar{\xi} - 1}{\sqrt{\Delta_3}}, \quad \delta_2 \equiv \frac{\xi - \bar{\xi} - 1}{\sqrt{\Delta_3}}, \quad \delta_3 \equiv \frac{\xi + \bar{\xi} + 1}{\sqrt{\Delta_3}}, \quad (\text{C.2.39})$$

$$\delta_i^\pm \equiv \frac{1 \pm \delta_i}{2}, \quad (\text{C.2.40})$$

$$(\text{C.2.41})$$

and

$$x_\pm \equiv -\frac{\bar{\xi}}{2y} \left(1 \pm \sqrt{1 + \frac{4y}{\xi}}\right), \quad (\text{C.2.42})$$

$$y_\pm \equiv -\frac{\xi}{2y} \left(1 \pm \sqrt{1 + \frac{4y}{\xi}}\right), \quad (\text{C.2.43})$$

$$z_\pm \equiv \frac{1}{2y} \left(1 \pm \sqrt{1 - 4y}\right). \quad (\text{C.2.44})$$

The form factor  $A$  can be expressed in terms of standard one-loop scalar integrals [144] by letting

$$C_0(\xi, \bar{\xi}, y_i) = \frac{m_{\text{H}}^2}{16\pi^2} I_3(-\xi m_{\text{H}}^2, -\bar{\xi} m_{\text{H}}^2, m_{\text{H}}^2, m_i^2, m_i^2, m_i^2) \quad (\text{C.2.45})$$

$$B_0(\rho, y) - B_0(1, y) = \frac{1}{16\pi^2} [I_2(\rho m_{\text{H}}^2, m_i^2, m_i^2) - I_2(m_{\text{H}}^2, m_i^2, m_i^2)]. \quad (\text{C.2.46})$$

As already stated in the main text, the analytic continuation of the form factor has to be handled by giving  $y$  a small negative imaginary part.

Using these expressions, we obtain the following limiting cases

$$\lim_{y \rightarrow \infty} F(\xi_1, \xi_2, \xi_p, y) = \frac{(1 - \xi_1 - \xi_2)^2}{4\xi_1 \xi_2} \quad (\text{C.2.47a})$$

$$\lim_{\xi_p \rightarrow 0} F(\xi_1, \xi_2, \xi_p, \{y_i\}) = \frac{(1 - \xi_1 - \xi_2)^2}{4\xi_1 \xi_2}, \quad (\text{C.2.47b})$$

which could be useful to check our computation against known results of Ref. [73, 77]

Finally, we provide an analytic expression for the first expansion coefficient  $c_0$  Eq. (C.2.32) of the perturbative expansion Eq. (C.2.31):

$$c_0(\xi_p, \{y_i\}) = \frac{2304\pi^4}{|\sum_i K(y_i)|^2} \left| \sum_i y_i A(0, \xi_p, \xi_p, y_i) \right|^2 \quad (\text{C.2.48})$$

with

$$\begin{aligned}
A(0, \xi_p, \xi_p, y) = & \frac{1}{32\pi^2} \left( \frac{4y-1-\xi_p}{(1+\xi_p)^2} \left[ \ln^2 \frac{\sqrt{1-4y}-1}{\sqrt{1-4y}+1} - \ln^2 \frac{\sqrt{1+\frac{4y}{\xi_p}}-1}{\sqrt{1+\frac{4y}{\xi_p}}+1} \right] \right. \\
& + \frac{4\xi_p}{(1+\xi_p)^2} \left[ \sqrt{1-4y} \ln \frac{\sqrt{1-4y}+1}{\sqrt{1-4y}-1} - \sqrt{1+\frac{4y}{\xi_p}} \ln \frac{\sqrt{1+\frac{4y}{\xi_p}}+1}{\sqrt{1+\frac{4y}{\xi_p}}-1} \right] \\
& \left. + \frac{4}{1+\xi_p} \right). \tag{C.2.49}
\end{aligned}$$

### C.2.3 One-Jet inclusive cross section

For a sake of completeness, in this section we want to present analytic expressions about the first application of the high energy formalism to a coloured final state, in particular the one-jet inclusive cross section. The objective is the computation of the impact factor for the partonic processes:

$$g + g \rightarrow g + X, \tag{C.2.50}$$

$$g + q \rightarrow g + X, \tag{C.2.51}$$

$$q + q \rightarrow g + X, \tag{C.2.52}$$

$$q + g \rightarrow q + X, \tag{C.2.53}$$

$$q + q \rightarrow q + X. \tag{C.2.54}$$

Using relations (3.2.11), we can reduce the number of impact factors we need to evaluate to only two,

$$g + g \rightarrow g + X, \tag{C.2.55}$$

$$q + g \rightarrow q + X. \tag{C.2.56}$$

As exposed in the text, in Sec. 3.2.2, the computation of these impact factors is based on the evaluation of the off-shell cross section for the LO off-shell processes:

$$g^* + g^* \rightarrow g, \tag{C.2.57}$$

$$g^* + q \rightarrow q. \tag{C.2.58}$$

This calculus was performed by means of the standard QCD Feynman rules in the Feynman gauge, and of two gauge-restoring techniques, namely the prescriptions of Ref. [86] and the Wilson lines technique of Ref. [88], in order to cross-check our results. We do not enter into details about Wilson lines technique and we refer interested reader to original Ref. [78]. Here we limit ourselves to present final results.

The off-shell matrix element for the process Eq. (C.2.57) turns out to be

$$|\bar{\mathcal{M}}|^2 = \alpha_s \frac{C_A \pi}{2} z \bar{z} s \tag{C.2.59}$$

while for the process Eq. (C.2.58) we obtain

$$|\bar{\mathcal{M}}|^2 = \alpha_s \frac{C_F \pi}{2} z \bar{z} s \quad (\text{C.2.60})$$

where we are using the kinematics defined in Eqs. (C.2.13) with the substitution  $m_H \rightarrow p_T^2$  and  $p_T$  the modulus of the transverse momentum of the emitted gluon (quark).

From the off-shell matrix elements, the derivation of the impact factors is very straightforward. We start from the pure gluonic partonic channel. First, by putting together the squared matrix element Eq. (C.2.59), the phase space volume element

$$d\Phi_1 = \frac{2\pi}{p_T^2} \delta\left(\frac{1}{\hat{\tau}} - 1\right), \quad (\text{C.2.61})$$

the flux factor

$$\phi = 2z\bar{z}s, \quad (\text{C.2.62})$$

and extracting an overall factor of  $p_T^2$  we obtain the dimensionless cross section of  $g^*g^* \rightarrow g$

$$\bar{\sigma}|_{g^*g^* \rightarrow g} = p_T^2 \sigma|_{g^*g^* \rightarrow g} = \sigma_0 \delta(1 - \hat{\tau}), \quad (\text{C.2.63})$$

where we have defined

$$\sigma_0 = \frac{C_A \pi^2}{2} \alpha_s. \quad (\text{C.2.64})$$

In Eq. (C.2.61) and Eq. (C.2.63), we define our Mellin variable  $\hat{\tau}$  as

$$\hat{\tau} = \frac{p_T^2}{z\bar{z}s} \quad (\text{C.2.65})$$

in analogy with the Higgs case, Eq. (C.2.15).

Then, the hard coefficient function is obtained by imposing on the dimensionless off-shell cross section Eq. (C.2.63) transverse momentum conservation and then by performing angular integration over the possible direction of incoming transverse momenta:

$$C(\tau, \xi_1, \xi_2, \alpha_s) = \int_0^{2\pi} \frac{d\theta_1}{2\pi} \int_0^{2\pi} \frac{d\theta_2}{2\pi} \bar{\sigma}|_{g^*g^* \rightarrow g} \delta\left(1 - \xi_1 - \xi_2 - 2\sqrt{\xi_1}\sqrt{\xi_2}\cos\theta_1\right), \quad (\text{C.2.66})$$

whose explicit expression in Mellin space reads

$$C(N, \xi_1, \xi_2, \alpha_s) = \frac{\sigma_0}{2\pi} \frac{2}{\sqrt{2\xi_1\xi_2 + 2\xi_1 + 2\xi_2 - 1 - \xi_1^2 - \xi_2^2}}, \quad (\text{C.2.67})$$

where  $N$  is the Mellin variable conjugate to  $\hat{\tau}$ . Variable  $\xi_1$  and  $\xi_2$  are defined in the same way as in previous section C.2.2.

Finally, the impact factor is computed by applying Eq. (3.2.4) on hard coefficient function Eq. (C.2.67) and by performing Mellin integrations. Mellin integrations are completely equivalent to the ones present in the EFT Higgs boson production case of

Sec. C.2.1; the results in that subsection can be used to solve Mellin integrals in this step. The final result reads

$$h(N, M_1, M_2, \alpha_s) \Big|_{gg \rightarrow g} = \sigma_0 M_1 R(M_1) M_2 R(M_2) \frac{\Gamma(M_1) \Gamma(M_2) \Gamma(1 - M_1 - M_2)}{\Gamma(1 - M_1) \Gamma(1 - M_2) \Gamma(M_1 + M_2)}. \quad (\text{C.2.68})$$

Similar steps leads to the following form for the impact factor of the process Eq. (C.2.58)

$$h(N, M, \alpha_s) = \frac{C_F}{C_A} \sigma_0 M R(M) \quad (\text{C.2.69})$$

thus concluding our derivation in the one-jet inclusive case. As already said, the impact factors of all the other partonic channels can be derived from Eq. (C.2.68) or Eq. (C.2.69) using relations Eqs. (3.2.11).

Let us conclude this subsection with an important remark. All the impact factors computed in this section does not take into account indistinguishability of gluons in the final state. Therefore, they have to be corrected using the formula presented in Sec. 3.2.2, Eq. (3.2.18). In particular, each impact factor has to be corrected with a different  $m$ .  $m = 1$  in the  $gg \rightarrow g$  case,  $m = 0$  in the  $gq \rightarrow g$  case,  $m = -1$  in the  $qq \rightarrow g$  case. This difference is due to the presence of quarks in the initial state (see Ref. [78] for details). On the contrary, the impact factors for the processes  $gq \rightarrow q$  and  $qq \rightarrow q$  have not to be corrected since they do not contain gluons in the hard final state.

# Acknowledgments

This is the unique part of this thesis where I am going to use the first person since what I am going to write is extremely personal. And it will be also the unique part where I am going to use the Italian Language, for two reasons: first, in order not to introduce further grammatical errors; second to give the opportunity also to my family and to my friends, which I am going to thank in these lines to understand something in this whole thesis.

Inanzitutto questi ringraziamenti saranno abbastanza lunghi in quanto vorrei riuscire a ringraziare tutte le persone che mi sono state vicine e mi hanno aiutato in questo percorso, che raggiunge per quanto mi riguarda in questo momento il suo compimento. E' stato un cammino lungo e difficile, molto più faticoso di quanto mi aspettassi e per questo sono ancora più orgoglioso della meta raggiunta. Come in una salita in montagna, la difficoltà del percorso aumenta il valore della meta. Sono stati tre anni duri, intensi, e a dispetto di quanto forse si poteva vedere dall'esterno a tratti anche sofferti. Ho imparato in questi tre anni (quattro forse contando la tesi magistrale) cosa vuol dire fare ricerca in fisica, nell'ambito da me scelto così interessante quanto impegnativo. Nonostante i risultati che sono qui contenuti, ottenere ogni singola riga di questa tesi mi è costata fatica e applicazione, sconforto in molte sere e gioia nei momenti delle scoperte. Ogni riga mi è costata innumerevoli errori e innumerevoli idee sballate. Alla fine però ce l'ho fatta e sono orgoglioso di tutto ciò che ho scritto in questa tesi, dal primo punto all'ultima virgola.

Non ce l'avrei mai fatta senza il sostegno continuo del mio Relatore Stefano Forte che voglio qui ringraziare per primo. A Milano mi sono sentito subito accolto e ho trovato in lui un aiuto costante in questa mia attività. Lo ringrazio per le innumerevoli discussioni sui problemi, sulle soluzioni, sulla forma e sulla sostanza. Lo ringrazio per avermi sempre dato la possibilità di svolgere un'attività didattica in parallelo con il tutorato nei corsi di Meccanica Quantistica e Fisica Teorica. Questa attività didattica mi è servita molto spesso per staccare la spina dalla pura ricerca ed è stata una componente importantissima nel mio sviluppo in questi tre anni.

Vorrei ringraziare anche le altre persone con cui ho collaborato durante questo mio dottorato. Il mio professore a Genova inanzitutto Giovanni Ridolfi che sempre mi ispira con la sua infinita conoscenza e la sua esposizione perfetta di ogni argomento e problema. E' sempre stato per me un modello specialmente nell'approccio agli studenti e alla didattica. Rimarrà sempre per me un grande maestro di fisica e di vita.

Poi le altre persone che hanno creduto in me: Simone Marzani, Fabrizio Caola, Pier Francesco Monni e Marco Bonvini, che sempre mi hanno ascoltato, consigliato e dedicato del tempo. In particolare vorrei spendere due parole in più di ringraziamento per Marco, con cui condivido la città di provenienza, Genova. Ho deciso di iscrivermi a fisica proprio grazie a uno stage seguito durante il liceo tenuto dall'allora tutor Marco Bonvini. Nutro per lui un rispetto profondo e nonostante un'incompatibilità di carattere l'ho sempre ritenuto un collaboratore fidato e preparatissimo. Mi scuso con lui per tutte le volte in cui la mia incapacità specialmente nelle questioni informatiche l'hanno deluso o messo in difficoltà: non era mia intenzione (quanto al fatto invece di non usare Mac ma Windows invece non rinnego niente!). Voglio fargli sapere che ho imparato molto da lui in questi tre anni e se ora so scrivere un programma decente e leggibile è sicuramente merito soprattutto suo e lo ringrazio. Anche se questo aumenterà il suo già considerevole ego.

Vorrei ringraziare tutti i ragazzi che hanno fatto le loro tesi magistrali o triennali con me come correlatore: Gherardo Vita, Marco Rossi, Claudio Valletta, Simone Zoia, Ilaria Casati e Gabriele Confalonieri. Mi perdonino se a volte sono stato stressante o poco chiaro o non sono riuscito a essere quello che loro avrebbero voluto. Per me è stato un onore partecipare al loro percorso di formazione e ho cercato di svolgere questa attività sempre al massimo delle mie possibilità. Auguro a tutti loro un fulgido futuro nel campo della fisica; le qualità certo non mancano.

Chiudo questi ringraziamenti lavorativi ringraziando tutto il gruppo di fisica teorica di Milano con cui mi sono sempre trovato benissimo e con cui ho condiviso pranzi e discussioni in questi tre anni; e i miei colleghi di ufficio, che sono stati miei compagni durante i lunghi giorni di lavoro: Marco Rabbiosi, Nicolò Petri, Zahari Kassabov e Marco Antonelli.

A questo punto vorrei ringraziare la mia famiglia che mi è sempre stata accanto e pur senza capirmi fino in fondo mi ha aiutato e sostenuto. Vorrei ringraziare mio padre che è la mia prima guida e il mio primo modello, perché ha condiviso con me la sua esperienza da ricercatore (anche se in un altro ambito) calmandomi nei momenti di sconforto e spingendomi nei momenti di eccitazione. Colgo questa occasione per ringraziarlo una volta per tutte per essere stato sempre al mio fianco in ogni situazione, in ogni condizione, in ogni luogo. Lo so che è mio padre ma ci tengo che rimanga almeno una volta per iscritto.

Vorrei ringraziare mia madre per avermi ascoltato mille volte lamentarmi dei vari conti che non tornavano, dei vari integrali che non convergevano pur senza comprendere veramente quello di cui stavo parlando. Quegli sfoghi mi sono serviti moltissimo e per questo vorrei ringraziarla.

Concludo augurando a mio fratello ogni bene possibile nel suo dottorato di ricerca in matematica che sta per intraprendere, affinché possa essere un'esperienza formativa e gratificante come sono stati per me questi tre anni. Io so che è il migliore e riuscirà a ottenere nella vita tutto ciò che desidera perché le capacità ci sono in abbondanza, anche di più di quello che c'erano nel suo fratello più grande.

Ringrazio in generale tutti (nonni compresi) per la loro vicinanza e la loro spinta durante tutti i miei studi che con questo lavoro raggiungono il loro livello più alto.

Vorrei ringraziare ancora in queste righe tutti i miei amici che con serate giochi, discussioni e altre attività mi hanno aiutato a staccare dallo studio o dal lavoro sia durante i cinque anni di università sia durante questi tre anni di dottorato. In particolare un

grazie a Enrico per essere stato sempre un amico disponibile e in grado di venire anche se avvisato con un preavviso di dieci, venti minuti. E poi un grazie a Matteo, Marco, Edo, Stea, Alice, Nicoletta, Elisa, Federica, Filippo, Claudio, Francesca, Chiara, Sonia, Flavio per tutti questi anni insieme. Nonostante ora la vita ci porti chi più vicino chi più lontano, noi sappiamo di condividere un'amicizia profonda.

Infine concludo questi miei lunghissimi ringraziamenti, rivolgendomi a te, Giuliapaola, a cui dedico questa mia tesi. Non c'è una cosa in particolare per cui ti debba ringraziare se non per esserci, sempre, da otto anni al mio fianco. Con te ho vissuto gioie e tristezze, malattia e salute, entusiasmo e scoraggiamento ma mai mi sono sentito abbandonato. Sei la mia roccia e hai reso la mia vita meravigliosa. E lo sai. Grazie!

I switch again to the English language to close these very lengthy acknowledgements. Thanks to the help of many persons, I'm now concluding this hard path, and I can say that it was worth it. I have a last acknowledgement which is very important to me and it will close this page.

*Last but not least I thank God for many useful discussions!*

A handwritten signature in black ink, appearing to read 'Stefano' followed by a stylized name or initials.



# Bibliography

- [1] S. Weinberg, *A Model of Leptons*, *Phys. Rev. Lett.* **19** (1967) 1264.  
[doi:10.1103/PhysRevLett.19.1264]
- [2] P. W. Higgs, *Broken Symmetries and the Masses of Gauge Bosons*,  
*Phys. Rev. Lett.* **13** (1964) 508. [doi:10.1103/PhysRevLett.13.508]
- [3] G. Aad *et al.* [ATLAS Collaboration], *Observation of a new particle in the search for the Standard Model Higgs boson with the ATLAS detector at the LHC*,  
*Phys. Lett. B* **716** (2012) 1  
doi:10.1016/j.physletb.2012.08.020 [arXiv:1207.7214 [hep-ex]].
- [4] S. Chatrchyan *et al.* [CMS Collaboration], *Observation of a new boson at a mass of 125 GeV with the CMS experiment at the LHC*,  
*Phys. Lett. B* **716** (2012) 30  
doi:10.1016/j.physletb.2012.08.021 [arXiv:1207.7235 [hep-ex]].
- [5] M. Peskin, D. Schoeder *An introduction to quantum field theory*, Addison-Wesley, (1995).
- [6] R. K. Ellis, W. J. Stirling, B. V. Webber *QCD and Collider Physics*, Cambridge University Press, (1996).
- [7] J. D. Bjorken, E. A. Paschos, *Inelastic Electron-Proton and  $\gamma$ -Proton Scattering and the Structure of the Nucleon*, *Phys. Rev.* **185** (1969) 1975.
- [8] R. P. Feynman *Very High-Energy Collisions of Hadrons*, *Phys. Rev. Lett.* **23** (1969) 1415.
- [9] J. C. Collins, D. E. Soper and G. F. Sterman, *Factorization of Hard Processes in QCD*, *Adv. Ser. Direct. High Energy Phys.* **5** (1989) 1  
doi:10.1142/97898145032660001 [hep-ph/0409313].
- [10] S. D. Drell and T. M. Yan, *Massive Lepton Pair Production in Hadron-Hadron Collisions at High-Energies*,  
*Phys. Rev. Lett.* **25** (1970) 316, Erratum: [*Phys. Rev. Lett.* **25** (1970) 902].  
[doi:10.1103/PhysRevLett.25.316]
- [11] S. D. Drell and T. M. Yan, *Partons and their Applications at High-Energies*,  
*Annals Phys.* **66** (1971) 578, [*Annals Phys.* **281** (2000) 450].  
[doi:10.1016/0003-4916(71)90071-6]

- [12] T. M. Yan and S. D. Drell, *The Parton Model and its Applications*, *Int. J. Mod. Phys. A* **29** (2014) 0071, doi:[10.1142/S0217751X14300713](https://doi.org/10.1142/S0217751X14300713) [[arXiv:1409.0051](https://arxiv.org/abs/1409.0051) [hep-ph]].
- [13] T. Kinoshita, *Mass singularities of Feynman amplitudes*, *J.Math.Phys.* **3** (1962) 650–677.
- [14] T. Lee, M. Nauenberg, *Degenerate Systems and Mass Singularities*, [[Phys.Rev. 133 \(1964\) B1549--B1562](https://arxiv.org/abs/1964.01549)].
- [15] G. P. Salam and G. Soyez, *A Practical Seedless Infrared-Safe Cone jet algorithm*, *JHEP* **0705** (2007) 086, doi:[10.1088/1126-6708/2007/05/086](https://doi.org/10.1088/1126-6708/2007/05/086) [[arXiv:0704.0292](https://arxiv.org/abs/0704.0292) [hep-ph]].
- [16] S. Höche, *Introduction to parton-shower event generators*, doi:[10.1142/97898146787660005](https://doi.org/10.1142/97898146787660005), [[arXiv:1411.4085](https://arxiv.org/abs/1411.4085) [hep-ph]].
- [17] R. Atkin, *Review of jet reconstruction algorithms*, *J. Phys. Conf. Ser.* **645** (2015) no.1, 012008. [[doi:10.1088/1742-6596/645/1/012008](https://doi.org/10.1088/1742-6596/645/1/012008)]
- [18] P. Nason, *Introduction to QCD*, *Conf. Proc. C* **9705251** (1997) 94.
- [19] G. Curci, W. Furmanski and R. Petronzio, *Evolution of Parton Densities Beyond Leading Order: The Nonsinglet Case*, *Nucl. Phys. B* **175** (1980) 27. [[doi:10.1016/0550-3213\(80\)90003-6](https://doi.org/10.1016/0550-3213(80)90003-6)]
- [20] Y. L. Dokshitzer, *Sov. Phys. JETP* **46** (1977) 641 [*Zh. Eksp. Teor. Fiz.* **73** (1977) 1216].
- [21] V. N. Gribov, L. N. Lipatov, *Sov. J. Nucl. Phys.* **15** (1972) 438 [*Yad. Fiz.* **15** (1972) 781].
- [22] G. Altarelli, G. Parisi *Asimptotic Freedom in Parton Language*, *Nucl. Phys. B* **126** (1977) 298.
- [23] F. Caola, *High-energy resummation in perturbative QCD: theory and phenomenology*, PhD Thesis.
- [24] R. K. Ellis, H. Georgi, M. Machacek, H. D. Politzer and G. G. Ross, *Perturbation Theory and the Parton Model in QCD*, *Nucl. Phys. B* **152** (1979) 285. [[doi:10.1016/0550-3213\(79\)90105-6](https://doi.org/10.1016/0550-3213(79)90105-6)]
- [25] L. J. Dixon, J. M. Henn, J. Plefka and T. Schuster, *All tree-level amplitudes in massless QCD*, *JHEP* **1101** (2011) 035 doi:[10.1007/JHEP01\(2011\)035](https://doi.org/10.1007/JHEP01(2011)035) [[arXiv:1010.3991](https://arxiv.org/abs/1010.3991) [hep-ph]].
- [26] W. Kilian, T. Ohl, J. Reuter and C. Speckner, *QCD in the Color-Flow Representation*, *JHEP* **1210** (2012) 022 doi:[10.1007/JHEP10\(2012\)022](https://doi.org/10.1007/JHEP10(2012)022) [[arXiv:1206.3700](https://arxiv.org/abs/1206.3700) [hep-ph]].
- [27] S. Dawson, *Radiative corrections to Higgs boson production*, *Nucl. Phys. B* **359** (1991) 283. [[doi:10.1016/0550-3213\(91\)90061-2](https://doi.org/10.1016/0550-3213(91)90061-2)]

- [28] J. C. Collins, D. E. Soper and G. F. Sterman, *Transverse Momentum Distribution in Drell-Yan Pair and W and Z Boson Production*, *Nucl. Phys. B* **250** (1985) 199. [[doi:10.1016/0550-3213\(85\)90479-1](https://doi.org/10.1016/0550-3213(85)90479-1)]
- [29] S. Catani, M. Ciafaloni and F. Hautmann, *High-energy factorization and small  $x$  heavy flavor production*, *Nucl. Phys. B* **366** (1991) 135. [[doi:10.1016/0550-3213\(91\)90055-3](https://doi.org/10.1016/0550-3213(91)90055-3)]
- [30] G. Bozzi, S. Catani, D. de Florian and M. Grazzini, *Transverse-momentum resummation and the spectrum of the Higgs boson at the LHC*, *Nucl. Phys. B* **737** (2006) 73  
[doi:10.1016/j.nuclphysb.2005.12.022](https://doi.org/10.1016/j.nuclphysb.2005.12.022) [[hep-ph/0508068](https://arxiv.org/abs/hep-ph/0508068)].
- [31] S. Forte and G. Ridolfi, *Renormalization group approach to soft gluon resummation*, *Nucl. Phys. B* **650** (2003) 229  
[doi:10.1016/S0550-3213\(02\)01034-9](https://doi.org/10.1016/S0550-3213(02)01034-9) [[hep-ph/0209154](https://arxiv.org/abs/hep-ph/0209154)].
- [32] E. Laenen, L. Magnea, G. Stavenga and C. D. White, *Next-to-eikonal corrections to soft gluon radiation: a diagrammatic approach*, *JHEP* **1101** (2011) 141  
[doi:10.1007/JHEP01\(2011\)141](https://doi.org/10.1007/JHEP01(2011)141) [[arXiv:1010.1860](https://arxiv.org/abs/1010.1860) [[hep-ph](https://arxiv.org/abs/hep-ph)]].
- [33] V. Ahrens, T. Becher, M. Neubert and L. L. Yang, *Renormalization-Group Improved Prediction for Higgs Production at Hadron Colliders*, *Eur. Phys. J. C* **62** (2009) 333  
[doi:10.1140/epjc/s10052-009-1030-2](https://doi.org/10.1140/epjc/s10052-009-1030-2) [[arXiv:0809.4283](https://arxiv.org/abs/0809.4283) [[hep-ph](https://arxiv.org/abs/hep-ph)]].
- [34] T. Becher, M. Neubert and D. Wilhelm, *Electroweak Gauge-Boson Production at Small  $q_T$ : Infrared Safety from the Collinear Anomaly*, *JHEP* **1202** (2012) 124  
[doi:10.1007/JHEP02\(2012\)124](https://doi.org/10.1007/JHEP02(2012)124) [[arXiv:1109.6027](https://arxiv.org/abs/1109.6027) [[hep-ph](https://arxiv.org/abs/hep-ph)]].
- [35] R. Boughezal, X. Liu and F. Petriello, *Power Corrections in the  $N$ -jettiness Subtraction Scheme*, *JHEP* **1703** (2017) 160  
[doi:10.1007/JHEP03\(2017\)160](https://doi.org/10.1007/JHEP03(2017)160) [[arXiv:1612.02911](https://arxiv.org/abs/1612.02911) [[hep-ph](https://arxiv.org/abs/hep-ph)]].
- [36] I. Z. Rothstein and I. W. Stewart, *An Effective Field Theory for Forward Scattering and Factorization Violation*, *JHEP* **1608** (2016) 025  
[doi:10.1007/JHEP08\(2016\)025](https://doi.org/10.1007/JHEP08(2016)025) [[arXiv:1601.04695](https://arxiv.org/abs/1601.04695) [[hep-ph](https://arxiv.org/abs/hep-ph)]].
- [37] M. A. Ebert and F. J. Tackmann, *Resummation of Transverse Momentum Distributions in Distribution Space*, *JHEP* **1702** (2017) 110  
[doi:10.1007/JHEP02\(2017\)110](https://doi.org/10.1007/JHEP02(2017)110) [[arXiv:1611.08610](https://arxiv.org/abs/1611.08610) [[hep-ph](https://arxiv.org/abs/hep-ph)]].
- [38] G. Lusterians, W. J. Waalewijn and L. Zeune, *Joint transverse momentum and threshold resummation beyond NLL*, *Phys. Lett. B* **762** (2016) 447  
[doi:10.1016/j.physletb.2016.09.060](https://doi.org/10.1016/j.physletb.2016.09.060) [[arXiv:1605.02740](https://arxiv.org/abs/1605.02740) [[hep-ph](https://arxiv.org/abs/hep-ph)]].
- [39] A. Banfi, G. P. Salam and G. Zanderighi, *Principles of general final-state resummation and automated implementation*, *JHEP* **0503** (2005) 073  
[doi:10.1088/1126-6708/2005/03/073](https://doi.org/10.1088/1126-6708/2005/03/073) [[hep-ph/0407286](https://arxiv.org/abs/hep-ph/0407286)].

- [40] A. Banfi, G. P. Salam and G. Zanderighi, *Phenomenology of event shapes at hadron colliders*, *JHEP* **1006** (2010) 038  
doi:10.1007/JHEP06(2010)038 [[arXiv:1001.4082](#) [[hep-ph](#)]].
- [41] A. Banfi, P. F. Monni, G. P. Salam and G. Zanderighi, *Higgs and Z-boson production with a jet veto*, *Phys. Rev. Lett.* **109** (2012) 202001  
doi:10.1103/PhysRevLett.109.202001 [[arXiv:1206.4998](#) [[hep-ph](#)]].
- [42] A. Banfi, H. McAslan, P. F. Monni and G. Zanderighi, *A general method for the resummation of event-shape distributions in  $e^+e^-$  annihilation*, *JHEP* **1505** (2015) 102  
doi:10.1007/JHEP05(2015)102 [[arXiv:1412.2126](#) [[hep-ph](#)]].
- [43] P. F. Monni, E. Re and P. Torrielli, *Higgs Transverse-Momentum Resummation in Direct Space*, *Phys. Rev. Lett.* **116** (2016) no.24, 242001  
doi:10.1103/PhysRevLett.116.242001 [[arXiv:1604.02191](#) [[hep-ph](#)]].
- [44] W. Bizon, P. F. Monni, E. Re, L. Rottoli and P. Torrielli, *Momentum-space resummation for transverse observables and the Higgs  $p_\perp$  at  $N^3LL+NNLO$* , [[arXiv:1705.09127](#) [[hep-ph](#)]].
- [45] C. Muselli, S. Forte and G. Ridolfi, *Combined threshold and transverse momentum resummation for inclusive observables*, *JHEP* **1703** (2017) 106  
doi:10.1007/JHEP03(2017)106 [[arXiv:1701.01464](#) [[hep-ph](#)]].
- [46] S. Marzani, *Combining  $Q_T$  and small- $x$  resummations*, *Phys. Rev. D* **93** (2016) no.5, 054047  
doi:10.1103/PhysRevD.93.054047 [[arXiv:1511.06039](#) [[hep-ph](#)]].
- [47] P. Bolzoni, S. Forte and G. Ridolfi, *Renormalization group approach to Sudakov resummation in prompt photon production*, *Nucl. Phys. B* **731** (2005) 85  
doi:10.1016/j.nuclphysb.2005.07.036 [[hep-ph/0504115](#)].
- [48] D. de Florian, A. Kulesza and W. Vogelsang, *Threshold resummation for high-transverse-momentum Higgs production at the LHC*, *JHEP* **0602** (2006) 047  
doi:10.1088/1126-6708/2006/02/047 [[hep-ph/0511205](#)].
- [49] S. Catani and M. Grazzini, *Higgs Boson Production at Hadron Colliders: Hard-Collinear Coefficients at the NNLO*, *Eur. Phys. J. C* **72** (2012) 2013  
Erratum: [*Eur. Phys. J. C* **72** (2012) 2132]  
doi:10.1140/epjc/s10052-012-2013-2, 10.1140/epjc/s10052-012-2132-9 [[arXiv:1106.4652](#) [[hep-ph](#)]].
- [50] S. Catani, L. Cieri, D. de Florian, G. Ferrera and M. Grazzini, *Universality of transverse-momentum resummation and hard factors at the NNLO*, *Nucl. Phys. B* **881** (2014) 414  
doi:10.1016/j.nuclphysb.2014.02.011 [[arXiv:1311.1654](#) [[hep-ph](#)]].
- [51] S. Catani, D. de Florian, G. Ferrera and M. Grazzini, *Vector boson production at hadron colliders: transverse-momentum resummation and leptonic decay*, *JHEP* **1512** (2015) 047  
doi:10.1007/JHEP12(2015)047 [[arXiv:1507.06937](#) [[hep-ph](#)]].

- [52] R. Bonciani, S. Catani, M. L. Mangano and P. Nason, *Sudakov resummation of multiparton QCD cross-sections*, *Phys. Lett. B* **575** (2003) 268  
doi:10.1016/j.physletb.2003.09.068 [[hep-ph/0307035](#)].
- [53] S. M. Aybat, L. J. Dixon and G. F. Sterman, *The Two-loop anomalous dimension matrix for soft gluon exchange*, *Phys. Rev. Lett.* **97** (2006) 072001  
doi:10.1103/PhysRevLett.97.072001 [[hep-ph/0606254](#)].
- [54] E. Gardi and L. Magnea, *Factorization constraints for soft anomalous dimensions in QCD scattering amplitudes*, *JHEP* **0903** (2009) 079  
doi:10.1088/1126-6708/2009/03/079 [[arXiv:0901.1091](#) [hep-ph](#)].
- [55] N. Kidonakis, E. Laenen, S. Moch and R. Vogt, *Sudakov resummation and finite order expansions of heavy quark hadroproduction cross-sections*, *Phys. Rev. D* **64** (2001) 114001  
doi:10.1103/PhysRevD.64.114001 [[hep-ph/0105041](#)].
- [56] C. Muselli, M. Bonvini, S. Forte, S. Marzani and G. Ridolfi, *Top Quark Pair Production beyond NNLO*, *JHEP* **1508** (2015) 076  
doi:10.1007/JHEP08(2015)076 [[arXiv:1505.02006](#) [hep-ph](#)].
- [57] S. Catani and M. Grazzini, *QCD transverse-momentum resummation in gluon fusion processes*, *Nucl. Phys. B* **845** (2011) 297  
doi:10.1016/j.nuclphysb.2010.12.007 [[arXiv:1011.3918](#) [hep-ph](#)].
- [58] G. Bozzi, S. Catani, G. Ferrera, D. de Florian and M. Grazzini, *Transverse-momentum resummation: A Perturbative study of Z production at the Tevatron*, *Nucl. Phys. B* **815** (2009) 174  
doi:10.1016/j.nuclphysb.2009.02.014 [[arXiv:0812.2862](#) [hep-ph](#)].
- [59] S. Mantry and F. Petriello, *Transverse Momentum Distributions from Effective Field Theory*, *Int. J. Mod. Phys. Conf. Ser.* **04** (2011) 106  
doi:10.1142/S2010194511001619 [[arXiv:1108.3609](#) [hep-ph](#)].
- [60] E. Laenen, G. F. Sterman and W. Vogelsang, *Recoil and threshold corrections in short distance cross-sections*, *Phys. Rev. D* **63** (2001) 114018  
doi:10.1103/PhysRevD.63.114018 [[hep-ph/0010080](#)].
- [61] A. Kulesza, G. F. Sterman and W. Vogelsang, *Joint resummation in electroweak boson production*, *Phys. Rev. D* **66** (2002) 014011  
doi:10.1103/PhysRevD.66.014011 [[hep-ph/0202251](#)].
- [62] A. Kulesza, G. F. Sterman and W. Vogelsang, *Joint resummation for Higgs production*, *Phys. Rev. D* **69** (2004) 014012  
doi:10.1103/PhysRevD.69.014012 [[hep-ph/0309264](#)].
- [63] S. Marzani and V. Theeuwes, *Vector boson production in joint resummation*, *JHEP* **1702** (2017) 127  
doi:10.1007/JHEP02(2017)127 [[arXiv:1612.01432](#) [hep-ph](#)].

- [64] R. D. Ball, M. Bonvini, S. Forte, S. Marzani and G. Ridolfi, *Higgs production in gluon fusion beyond NNLO*, *Nucl. Phys. B* **874** (2013) 746  
doi:10.1016/j.nuclphysb.2013.06.012 [[arXiv:1303.3590](#) [hep-ph](#)].
- [65] S. Moch, J. A. M. Vermaseren and A. Vogt, *Higher-order corrections in threshold resummation*, *Nucl. Phys. B* **726** (2005) 317  
doi:10.1016/j.nuclphysb.2005.08.005 [[hep-ph/0506288](#)].
- [66] T. Huber and D. Maitre, *HypExp: A Mathematica package for expanding hypergeometric functions around integer-valued parameters*, *Comput. Phys. Commun.* **175** (2006) 122  
doi:10.1016/j.cpc.2006.01.007 [[hep-ph/0507094](#)].
- [67] T. Huber and D. Maitre, *HypExp 2, Expanding Hypergeometric Functions about Half-Integer Parameters*, *Comput. Phys. Commun.* **178** (2008) 755  
doi:10.1016/j.cpc.2007.12.008 [[arXiv:0708.2443](#) [hep-ph](#)].
- [68] S. Catani, M. Ciafaloni and F. Hautmann, *Gluon Contributions To Small  $x$  Heavy Flavor Production*, *Phys. Lett. B* **242** (1990) 97;
- [69] S. Catani and F. Hautmann, *High-energy factorization and small  $x$  deep inelastic scattering beyond leading order*, *Nucl. Phys. B* **427** (1994) 475  
[[hep-ph/9405388](#)].
- [70] M. Bonvini, S. Marzani and C. Muselli, *Towards parton distribution functions with small- $x$  resummation: HELL 2.0*, [[arXiv:1708.07510](#) [hep-ph](#)].
- [71] R. D. Ball and R. K. Ellis, *Heavy quark production at high-energy*, *JHEP* **0105** (2001) 053 [[hep-ph/0101199](#)].
- [72] F. Hautmann, *Heavy top limit and double logarithmic contributions to Higgs production at  $m_H^2/s$  much less than 1*, *Phys. Lett. B* **535** (2002) 159  
[[hep-ph/0203140](#)].
- [73] S. Marzani, R. D. Ball, V. Del Duca, S. Forte and A. Vicini, *Higgs production via gluon-gluon fusion with finite top mass beyond next-to-leading order*, *Nucl. Phys. B* **800** (2008) 127  
doi:10.1016/j.nuclphysb.2008.03.016 [[arXiv:0801.2544](#) [hep-ph](#)].
- [74] S. Marzani and R. D. Ball, *High Energy Resummation of Drell-Yan Processes*, *Nucl. Phys. B* **814** (2009) 246 [[arXiv:0812.3602](#) [hep-ph](#)].
- [75] G. Diana, *High-energy resummation in direct photon production*, *Nucl. Phys. B* **824** (2010) 154 [[arXiv:0906.4159](#) [hep-ph](#)].
- [76] F. Caola, S. Forte and S. Marzani, *Small  $x$  resummation of rapidity distributions: The Case of Higgs production*, *Nucl. Phys. B* **846** (2011) 167 [[arXiv:1010.2743](#) [hep-ph](#)].
- [77] S. Forte and C. Muselli, *High energy resummation of transverse momentum distributions: Higgs in gluon fusion*, *JHEP* **1603** (2016) 122  
doi:10.1007/JHEP03(2016)122 [[arXiv:1511.05561](#) [hep-ph](#)].

- [78] S. Zoia and C. Muselli, *High Energy Resummation of Jet Observables*, [[arXiv:1710.08416](#) [[hep-ph](#)]].
- [79] R. D. Ball and S. Forte, *Momentum conservation at small  $x$* , *Phys. Lett. B* **359**, 362 (1995) [[hep-ph/9507321](#)].
- [80] G. Altarelli, R. D. Ball and S. Forte, *Resummation of singlet parton evolution at small  $x$* , *Nucl. Phys. B* **575** (2000) 313 [[hep-ph/9911273](#)].
- [81] L. N. Lipatov, *Sov. J. Nucl. Phys.* **23** (1976) 338 [*Yad. Fiz.* **23** (1976) 642].  
V. S. Fadin, E. A. Kuraev, L. N. Lipatov, *Phys. Lett. B* **60** (1975) 50.  
E. A. Kuraev, L. N. Lipatov, V. S. Fadin, *Sov. Phys. JETP* **44** (1976) 443 [*Zh. Eksp. Teor. Fiz.* **71** (1977) 840].  
E. A. Kuraev, L. N. Lipatov, V. S. Fadin, *Sov. Phys. JETP* **45** (1977) 199 [*Zh. Eksp. Teor. Fiz.* **72** (1977) 377].  
I. I. Balitsky, L. N. Lipatov, *Sov. J. Nucl. Phys.* **28** (1978) 822 [*Yad. Fiz.* **28** (1978) 1597].
- [82] G. Altarelli, R. D. Ball and S. Forte, *Small  $x$  resummation and HERA structure function data*, *Nucl. Phys. B* **599** (2001) 383  
doi:10.1016/S0550-3213(01)00023-2 [[hep-ph/0011270](#)].
- [83] M. Ciafaloni, D. Colferai, G. P. Salam and A. M. Stasto, *A Matrix formulation for small- $x$  singlet evolution*, *JHEP* **0708** (2007) 046  
doi:10.1088/1126-6708/2007/08/046 [[arXiv:0707.1453](#) [[hep-ph](#)]].
- [84] M. Bonvini, S. Marzani and T. Peraro, *Small- $x$  resummation from HELL*, *Eur. Phys. J. C* **76** (2016) no.11, 597  
doi:10.1140/epjc/s10052-016-4445-6 [[arXiv:1607.02153](#) [[hep-ph](#)]].
- [85] M. Ciafaloni and D. Colferai, *Dimensional regularisation and factorisation schemes in the BFKL equation at subleading level*, *JHEP* **0509** (2005) 069  
doi:10.1088/1126-6708/2005/09/069 [[hep-ph/0507106](#)].
- [86] A. van Hameren, *Helicity amplitudes for high-energy scattering processes*, *PoS RADCOR* **2013** (2013) 036.
- [87] A. van Hameren, P. Kotko and K. Kutak, *Helicity amplitudes for high-energy scattering*, *JHEP* **1301** (2013) 078,  
doi:10.1007/JHEP01(2013)078 [[arXiv:1211.0961](#) [[hep-ph](#)]].
- [88] P. Kotko, *Wilson lines and gauge invariant off-shell amplitudes*, *JHEP* **1407** (2014) 128,  
doi:10.1007/JHEP07(2014)128 [[arXiv:1403.4824](#) [[hep-ph](#)]].
- [89] C. Muselli, *Double Differential High Energy Resummation*, [[arXiv:1710.09376](#) [[hep-ph](#)]].
- [90] C. Muselli, *High-energy Resummation of Higgs  $p_T$  Distribution*, *Acta Phys. Polon. B* **48** (2017) 1105. [[doi:10.5506/APhysPolB.48.1105](#)]

- [91] R. V. Harlander, T. Neumann, K. J. Ozeren and M. Wiesemann, *Top-mass effects in differential Higgs production through gluon fusion at order  $\alpha_s^4$* , *JHEP* **1208** (2012) 139  
doi:10.1007/JHEP08(2012)139 [[arXiv:1206.0157](#) [[hep-ph](#)]].
- [92] R. V. Harlander and T. Neumann, *Probing the nature of the Higgs-gluon coupling*, *Phys. Rev. D* **88** (2013) 074015  
doi:10.1103/PhysRevD.88.074015 [[arXiv:1308.2225](#) [[hep-ph](#)]].
- [93] M. Buschmann, D. Goncalves, S. Kuttimalai, M. Schonherr, F. Krauss and T. Plehn, *Mass Effects in the Higgs-Gluon Coupling: Boosted vs Off-Shell Production*, *JHEP* **1502** (2015) 038  
doi:10.1007/JHEP02(2015)038 [[arXiv:1410.5806](#) [[hep-ph](#)]].
- [94] R. Frederix, S. Frixione, E. Vryonidou and M. Wiesemann, *Heavy-quark mass effects in Higgs plus jets production*, *JHEP* **1608** (2016) 006  
doi:10.1007/JHEP08(2016)006 [[arXiv:1604.03017](#) [[hep-ph](#)]].
- [95] F. Caola, S. Forte, S. Marzani, C. Muselli and G. Vita, *The Higgs transverse momentum spectrum with finite quark masses beyond leading order*, *JHEP* **1608** (2016) 150  
doi:10.1007/JHEP08(2016)150 [[arXiv:1606.04100](#) [[hep-ph](#)]].
- [96] T. Neumann and C. Williams, *The Higgs boson at high  $p_T$* , *Phys. Rev. D* **95** (2017) no.1, 014004  
doi:10.1103/PhysRevD.95.014004 [[arXiv:1609.00367](#) [[hep-ph](#)]].
- [97] K. Melnikov and A. Penin, *On the light quark mass effects in Higgs boson production in gluon fusion*, *JHEP* **1605** (2016) 172  
doi:10.1007/JHEP05(2016)172 [[arXiv:1602.09020](#) [[hep-ph](#)]].
- [98] K. Melnikov, L. Tancredi and C. Wever, *Two-loop amplitudes for  $q\bar{q} \rightarrow Hq$  and  $q\bar{q} \rightarrow Hg$  mediated by a nearly massless quark*, *Phys. Rev. D* **95** (2017) no.5, 054012  
doi:10.1103/PhysRevD.95.054012 [[arXiv:1702.00426](#) [[hep-ph](#)]].
- [99] J. M. Lindert, K. Melnikov, L. Tancredi and C. Wever, *Top-bottom interference effects in Higgs plus jet production at the LHC*, *Phys. Rev. Lett.* **118** (2017) no.25, 252002  
doi:10.1103/PhysRevLett.118.252002 [[arXiv:1703.03886](#) [[hep-ph](#)]].
- [100] T. Liu and A. A. Penin, *High-Energy Limit of QCD beyond Sudakov Approximation*, [[arXiv:1709.01092](#) [[hep-ph](#)]].
- [101] S. Catani, M. L. Mangano, P. Nason and L. Trentadue, *The Resummation of soft gluons in hadronic collisions*, *Nucl. Phys. B* **478** (1996) 273  
doi:10.1016/0550-3213(96)00399-9 [[hep-ph/9604351](#)].
- [102] E. Laenen, G. F. Sterman and W. Vogelsang, *Higher order QCD corrections in prompt photon production*, *Phys. Rev. Lett.* **84** (2000) 4296  
doi:10.1103/PhysRevLett.84.4296 [[hep-ph/0002078](#)].

- [103] R. Abbate, S. Forte and G. Ridolfi, *A New prescription for soft gluon resummation*, *Phys. Lett. B* **657** (2007) 55  
doi:10.1016/j.physletb.2007.09.060 [[arXiv:0707.2452 \[hep-ph\]](#)].
- [104] M. Bonvini, S. Forte and G. Ridolfi, *Borel resummation of transverse momentum distributions*, *Nucl. Phys. B* **808** (2009) 347  
doi:10.1016/j.nuclphysb.2008.09.041 [[arXiv:0807.3830 \[hep-ph\]](#)].
- [105] J. Butterworth et al., *PDF4LHC recommendations for LHC Run II*, *J. Phys.* **G43** (2016) 023001, [[arXiv:1510.03865](#)].
- [106] **NNPDF** Collaboration, R. D. Ball et al., *Parton distributions for the LHC Run II*, *JHEP* **04** (2015) 040, [[arXiv:1410.8849](#)].
- [107] L. A. Harland-Lang, A. D. Martin, P. Motylinski, and R. S. Thorne, *Parton distributions in the LHC era: MMHT 2014 PDFs*, *Eur. Phys. J.* **C75** (2015), no. 5 204, [[arXiv:1412.3989](#)].
- [108] S. Dulat, T.-J. Hou, J. Gao, M. Guzzi, J. Huston, P. Nadolsky, J. Pumplin, C. Schmidt, D. Stump, and C. P. Yuan, *New parton distribution functions from a global analysis of quantum chromodynamics*, *Phys. Rev.* **D93** (2016), no. 3 033006, [[arXiv:1506.07443](#)].
- [109] S. Carrazza, S. Forte, Z. Kassabov, J. I. Latorre, and J. Rojo, *An Unbiased Hessian Representation for Monte Carlo PDFs*, *Eur. Phys. J.* **C75** (2015), no. 8 369, [[arXiv:1505.06736](#)].
- [110] J. Gao and P. Nadolsky, *A meta-analysis of parton distribution functions*, *JHEP* **07** (2014) 035, [[arXiv:1401.0013](#)].
- [111] G. Watt and R. S. Thorne, *Study of Monte Carlo approach to experimental uncertainty propagation with MSTW 2008 PDFs*, *JHEP* **08** (2012) 052, [[arXiv:1205.4024](#)].
- [112] A. Buckley, J. Ferrando, S. Lloyd, K. Nordström, B. Page, M. Rüfenacht, M. Schönherr and G. Watt, *LHAPDF6: parton density access in the LHC precision era*, *Eur. Phys. J.* **C 75** (2015) 132  
doi:10.1140/epjc/s10052-015-3318-8 [[arXiv:1412.7420 \[hep-ph\]](#)].
- [113] S. Frixione, P. Nason and G. Ridolfi, *Problems in the resummation of soft gluon effects in the transverse momentum distributions of massive vector bosons in hadronic collisions*, *Nucl. Phys. B* **542** (1999) 311  
doi:10.1016/S0550-3213(98)00853-0 [[hep-ph/9809367](#)].
- [114] C. Anastasiou, C. Duhr, F. Dulat, E. Furlan, T. Gehrmann, F. Herzog, A. Lazopoulos and B. Mistlberger, *High precision determination of the gluon fusion Higgs boson cross-section at the LHC*, *JHEP* **1605** (2016) 058  
doi:10.1007/JHEP05(2016)058 [[arXiv:1602.00695 \[hep-ph\]](#)].
- [115] R. Boughezal, F. Caola, K. Melnikov, F. Petriello and M. Schulze, *Higgs boson production in association with a jet at next-to-next-to-leading order*, *Phys. Rev. Lett.* **115** (2015) no.8, 082003  
doi:10.1103/PhysRevLett.115.082003 [[arXiv:1504.07922 \[hep-ph\]](#)].

- [116] R. Boughezal, C. Focke, W. Giele, X. Liu and F. Petriello, *Higgs boson production in association with a jet at NNLO using jetiness subtraction*, *Phys. Lett. B* **748** (2015) 5  
doi:10.1016/j.physletb.2015.06.055 [[\[arXiv:1505.03893 \[hep-ph\]\]](#)].
- [117] X. Chen, J. Cruz-Martinez, T. Gehrmann, E. W. N. Glover and M. Jaquier, *NNLO QCD corrections to Higgs boson production at large transverse momentum*, *JHEP* **1610** (2016) 066  
doi:10.1007/JHEP10(2016)066 [[\[arXiv:1607.08817 \[hep-ph\]\]](#)].
- [118] M. Bonvini, R. D. Ball, S. Forte, S. Marzani and G. Ridolfi, *Updated Higgs cross section at approximate  $N^3LO$* , *J. Phys. G* **41** (2014) 095002 [[\[arXiv:1404.3204 \[hep-ph\]\]](#)].
- [119] M. Bonvini and S. Marzani, *Resummed Higgs cross section at  $N^3LL$* , *JHEP* **1409** (2014) 007 [[\[arXiv:1405.3654 \[hep-ph\]\]](#)].
- [120] M. Bonvini, S. Forte, G. Ridolfi and L. Rottoli, *Resummation prescriptions and ambiguities in SCET vs. direct QCD: Higgs production as a case study*, *JHEP* **1501** (2015) 046 [[\[arXiv:1409.0864 \[hep-ph\]\]](#)].
- [121] U. Baur and E. W. N. Glover, *Higgs Boson Production at Large Transverse Momentum in Hadronic Collisions*, *Nucl. Phys. B* **339** (1990) 38.  
[\[doi:10.1016/0550-3213\(90\)90532-I\]](#)
- [122] A. Banfi, P. F. Monni and G. Zanderighi, *Quark masses in Higgs production with a jet veto*, *JHEP* **1401** (2014) 097  
doi:10.1007/JHEP01(2014)097 [[\[arXiv:1308.4634 \[hep-ph\]\]](#)].
- [123] R. K. Ellis, I. Hinchliffe, M. Soldate, and J. J. van der Bij, *Higgs Decay to  $\tau^+\tau^-$ : A Possible Signature of Intermediate Mass Higgs Bosons at the SSC*, *Nucl. Phys.* **B297** (1988) 221.
- [124] C. J. Glosser and C. R. Schmidt, *Next-to-leading corrections to the Higgs boson transverse momentum spectrum in gluon fusion*, *JHEP* **0212** (2002) 016  
doi:10.1088/1126-6708/2002/12/016 [[\[hep-ph/0209248\]](#)].
- [125] E. L. Berger, J. w. Qiu and X. f. Zhang, *QCD factorized Drell-Yan cross-section at large transverse momentum*, *Phys. Rev. D* **65** (2002) 034006  
doi:10.1103/PhysRevD.65.034006 [[\[hep-ph/0107309\]](#)].
- [126] A. Vogt, *Efficient evolution of unpolarized and polarized parton distributions with QCD-PEGASUS*, *Comput. Phys. Commun.* **170** (2005) 65  
doi:10.1016/j.cpc.2005.03.103 [[\[hep-ph/0408244\]](#)].
- [127] S. Moch, J. A. M. Vermaseren and A. Vogt, *The Three loop splitting functions in QCD: The Nonsinglet case*, *Nucl. Phys. B* **688** (2004) 101  
doi:10.1016/j.nuclphysb.2004.03.030 [[\[hep-ph/0403192\]](#)].
- [128] A. Vogt, S. Moch and J. A. M. Vermaseren, *The Three-loop splitting functions in QCD: The Singlet case*, *Nucl. Phys. B* **691** (2004) 129  
doi:10.1016/j.nuclphysb.2004.04.024 [[\[hep-ph/0404111\]](#)].

- [129] E. Remiddi and J. A. M. Vermaseren, *Harmonic polylogarithms*, *Int. J. Mod. Phys. A* **15** (2000) 725  
doi:10.1142/S0217751X00000367 [[hep-ph/9905237](#)].
- [130] T. Gehrmann and E. Remiddi, *Numerical evaluation of harmonic polylogarithms*, *Comput. Phys. Commun.* **141** (2001) 296  
doi:10.1016/S0010-4655(01)00411-8 [[hep-ph/0107173](#)].
- [131] T. Gehrmann and E. Remiddi, *Numerical evaluation of two-dimensional harmonic polylogarithms*, *Comput. Phys. Commun.* **144** (2002) 200  
doi:10.1016/S0010-4655(02)00139-X [[hep-ph/0111255](#)].
- [132] R. Bonciani, G. Degrossi and A. Vicini, *On the Generalized Harmonic Polylogarithms of One Complex Variable*, *Comput. Phys. Commun.* **182** (2011) 1253  
doi:10.1016/j.cpc.2011.02.011 [[arXiv:1007.1891](#) [[hep-ph](#)]].
- [133] J. Ablinger, J. Blumlein and C. Schneider, *Harmonic Sums and Polylogarithms Generated by Cyclotomic Polynomials*, *J. Math. Phys.* **52** (2011) 102301  
doi:10.1063/1.3629472 [[arXiv:1105.6063](#) [[math-ph](#)]].
- [134] D. Maitre, *HPL, a mathematica implementation of the harmonic polylogarithms*, *Comput. Phys. Commun.* **174** (2006) 222  
doi:10.1016/j.cpc.2005.10.008 [[hep-ph/0507152](#)].
- [135] D. Maitre, *Extension of HPL to complex arguments*, *Comput. Phys. Commun.* **183** (2012) 846  
doi:10.1016/j.cpc.2011.11.015 [[hep-ph/0703052](#)].
- [136] J. A. M. Vermaseren, *Harmonic sums, Mellin transforms and integrals*, *Int. J. Mod. Phys. A* **14** (1999) 2037  
doi:10.1142/S0217751X99001032 [[hep-ph/9806280](#)].
- [137] M. Höschele, J. Hoff, A. Pak, M. Steinhauser and T. Ueda, *MT: A Mathematica package to compute convolutions*, *Comput. Phys. Commun.* **185** (2014) 528  
doi:10.1016/j.cpc.2013.10.007 [[arXiv:1307.6925](#) [[hep-ph](#)]].
- [138] J. Blumlein and S. Kurth, *Harmonic sums and Mellin transforms up to two loop order*, *Phys. Rev. D* **60** (1999) 014018  
doi:10.1103/PhysRevD.60.014018 [[hep-ph/9810241](#)].
- [139] J. Blumlein, *Analytic continuation of Mellin transforms up to two loop order*, *Comput. Phys. Commun.* **133** (2000) 76  
doi:10.1016/S0010-4655(00)00156-9 [[hep-ph/0003100](#)].
- [140] D. de Florian and W. Vogelsang, *Threshold resummation for the inclusive-hadron cross-section in pp collisions*, *Phys. Rev. D* **71** (2005) 114004  
doi:10.1103/PhysRevD.71.114004 [[hep-ph/0501258](#)].
- [141] S. Catani, L. Cieri, D. de Florian, G. Ferrera and M. Grazzini, *Vector boson production at hadron colliders: hard-collinear coefficients at the NNLO*, *Eur. Phys. J. C* **72** (2012) 2195  
doi:10.1140/epjc/s10052-012-2195-7 [[arXiv:1209.0158](#) [[hep-ph](#)]].

- [142] S. Catani, D. de Florian and M. Grazzini, *Universality of nonleading logarithmic contributions in transverse momentum distributions*, *Nucl. Phys. B* **596** (2001) 299  
doi:10.1016/S0550-3213(00)00617-9 [[hep-ph/0008184](#)].
- [143] V. Del Duca, W. Kilgore, C. Oleari, C. Schmidt and D. Zeppenfeld, *Gluon fusion contributions to  $H + 2$  jet production*, *Nucl. Phys. B* **616** (2001) 367  
doi:10.1016/S0550-3213(01)00446-1 [[hep-ph/0108030](#)].
- [144] R. K. Ellis and G. Zanderighi, *Scalar one-loop integrals for QCD*, *JHEP* **0802** (2008) 002  
doi:10.1088/1126-6708/2008/02/002 [[arXiv:0712.1851](#) [[hep-ph](#)]].
- [145] S. Zoia, *High-energy Resummation with Coloured Final States*, Master Thesis.